Université de Strasbourg

Ecole Doctorale des Sciences de la Vie et de la Santé

THESE DE DOCTORAT

présentée en vue d'obtenir le grade de

Docteur de l' Université de Strasbourg

Discipline : Sciences du Vivant

Spécialité : Aspects moléculaires et cellulaires de la biologie

Par

Santiago X. GUERRERO

Role of HIV-1 Vif in viral replication: translational regulation of APOBEC3G and RNA chaperone activity

Soutenue le 25 octobre 2013 devant la commission d'examen :

Dr. Jean-Christophe PAILLART	Directeur de thèse
Dr. Clarisse BERLIOZ-TORRENT	Rapporteur externe
Dr. Théophile OHLMANN	Rapporteur externe
Dr. Olivier ROHR	Rapporteur interne

UPR 9002 du CNRS, Institut de Biologie Moléculaire et Cellulaire, Strasbourg

A mes parents, Anibal et Maria
Personne n'a été encouragé ni aimé de façon
aussi inconditionnelle que je l'ai été par vous.
Je vous aime

A mis padres, Aníbal y María
Nadie ha sido apoyado ni amado de manera
tan incondicional como yo lo he sido por ustedes.
Les amo mucho

ACKNOWLEDGMENTS

Je voudrais tout d'abord remercier les membres du jury, Clarisse Berlioz-Torrent, Théophile Ohlmann et Olivier Rohr qui ont accepté d'évaluer mon travail de thèse.

Je remercie tous les organismes qui m'ont permis de réaliser ce travail : CNRS, SIDACTION, ANRS et SENESCYT.

Merci beaucoup Roland et JC de m'avoir accepté dans un laboratoire où j'ai eu l'opportunité d'apprendre énormément de choses et de grandir scientifiquement. Merci Roland pour tes remarques scientifiques qui ont été indispensables pour la réussite de cette thèse.

JC, j'ai encore ton premier e-mail du 21/07/2010 où tu m'as dit textuellement « je suis sûr que nous allons faire du très bon travail ensemble ». Voilà le résultat, je suis sûr que nous l'avons fait ! Je te remercie de m'avoir fait confiance, d'avoir cru en moi, mais également pour ton encadrement et ta rigueur scientifique. Comme je te le dis tout le temps, tu es le meilleur !

Merci beaucoup à tous les membres de l'équipe. Serena, Catherine et Valérie merci de votre enthousiasme et pour la joie que vous apportez tous les jours à cette équipe. Julien, merci de ton amitié, de ton support, de ton temps et surtout des conseils scientifiques et personnels que tu m'as donné tout au long de ces dernières années. Merci à mon ami de pause, Patrick. Nous avons commencé la thèse ensemble et je tiens à te remercier pour ton amitié et pour ta complicité pendant ces moments importants de la vie doctorale. Red, mon pote, merci de ton support, de tes conseils scientifiques et techniques et d'avoir mis de l'ambiance au laboratoire. Plus qu'un collègue de travail, tu es devenu un de mes meilleurs amis. J'espère qu'un jour nous pourrons travailler de nouveau dans une même équipe. Marie G., Camille et Elodie, merci de votre aide pendant le temps où nous avons partagé les paillasses. Je vous souhaite le meilleur dans vos thèses.

Je tiens à remercier Géraldine, Thomas et Christiane de l'institut de Virologie de Strasbourg pour votre indispensable collaboration dans mon projet de thèse mais aussi pour votre enthousiasme et générosité.

Gaëlle M. je te remercie pour tes conseils et pour les bons moments et discussions à CSHL 2013. Delphine R., je te remercie pour ta gentillesse, de m'avoir appris beaucoup de techniques et pour les bons moments que nous avons passés ensemble avec Red et Patrick.

Je tiens à remercier Guillaume, Philippe et Dominique pour votre amabilité et disponibilité. Vous n'avez jamais hésité à m'aider au laboratoire. Merci à tous les amis de l'IBMC. Paola et Jana merci pour vos conseils scientifiques en salle culture mais aussi pour les bons moments. Sophie P., Noe, Sarah, Cédric R., Delphine P., Arnaud, Vijay, Melodie, Marie C., Hagen, Delphine K., Joelle, Anne-Sophie, Micka, Pierre, Suraya, Romain, Erika et Patryk merci pour tout, pour les verres, les discussions, les fêtes et les pots que nous avons partagés. Merci également à tous les membres de l'UPR 9002 qui m'ont supporté durant ces années.

Merci aux amis de Strasbourg (Bertrand de Faÿ, Gaëlle G., Anthony, Hugo Manda, Fede et Luis) avec lesquels j'ai partagé des moments inoubliables, merci de votre support pendant mon master et ma thèse. Je tiens à remercier Pilar et Cedric pour votre support et amitié. J'aimerais aussi remercier Andres C. pour ton soutien, je suis sûr que nous allons faire des choses importantes pour la recherche scientifique de l'Équateur.

Un grand merci à Mireia, ma copine, tu as été une personne très importante pendant ces longues dernières années de thèse, merci de ton sourire, de ton écoute, de ta bonne humeur et de ta grande patience avec moi. Je t'adore, je ne pourrais pas continuer ma carrière scientifique sans toi, je t'espère encore à mes côtés dans les années à venir.

J'aimerais finalement remercier ma famille (Aníbal, María y Andrés) pour votre support inconditionnel durant toutes ces longues années en France. Vous êtes les personnes les plus importantes de ma vie. Merci d'avoir cru en moi et de m'avoir témoigné tant de fierté. Je tiens aussi à remercier mon meilleur ami Pablo, comme ton père nous l'a dit : tu es mon frère de l'âme, réellement un ami. Merci pour tout.

TABLE OF CONTENTS

LIST OF ABBREVIATIONS

(-) DNA	minus-strand DNA
(-) ssDNA	minus-strand strong-stop DNA
(+) DNA	plus-strand DNA
(+) ssDNA	plus-strand strong-stop DNA
5-PPP	5-triphosphorylated
A1	APOBEC1
AAV	adeno-associated virus
AGS	Aicardi-Goutières syndrome
AID	activation-induced deaminase
AIDS	acquired immunodeficiency syndrome
ALIX	ALG-2-interacting protein X
APOBEC	apolipoprotein B mRNA-editing enzyme,
ATG16L1	autophagy-related gene 16-like 1
BIR	baculovirus inhibitor repeat
CA	capsid
CAML	calcium modulating cyclophilin ligand
CARD	caspase-recruitment domain
CAT	chloramphenicol acetyl transferase
CC domain	coiled-coil domain
CD54	cluster of differentiation 54
CDA domain	cytidine deaminase domain
CDC	Centers for Disease Control
CDK9	cyclin-dependent kinase 9
CTD	C-terminal domain
CMR1	chromosome region maintenance 1
CT	cytoplasmic
CUL4	cullin 4
CycT1	cyclin T1
CypA	cyclophilin A
DC	dentritic cell
DCAF1	cul4-associated factor 1
DDB1	DNA damage-binding protein 1
DDR	DNA-damage-response
dGTP	deoxyguanosine triphosphatase
DNA	deoxyribonucleic acid
DNA-PK	DNA-dependent protein kinase
dNTP	deoxynucleoside triphosphate
dsDNA	double-stranded DNA
EC	extracellular
EIAV	equine infectious anemia virus
eIF	eukaryotic initiation factor
EMCV	encephalomyocarditis virus
ENV	envelope
ER	endoplasmic reticulum
eRF1	eukaryotic translation termination factor 1

eRF3	eukaryotic translation termination factor 3
ESCRT	endosomal sorting complexes required for transport
ESE	exonic splicing enhancer
ESS/ISS	exonic/intronic splicing silencer
FIV	feline immunodeficiency virus
FRET	fluorescence resonance energy transfer
FV	foamy virus
Fv1	friend virus susceptibility factor-1
GDP	guanosine diphosphatase
GFP	green fluorescent protein
gp	glycoprotein
GPI	glycophosphatidylinositol
gRNA	genomic ribonucleic acid
GTP	guanosine triphosphatase
HBV	hepatitis B virus
HEK 293 cell	human embryonic kidney 293 cell
HIV	human immunodeficiency virus type
HLA-II	human leukocyte antigen II
HMG I	high mobility group I
HR1	heptad repeat 1
HR2	heptad repeat 2
Hsp70	70 kilodalton heat shock protein
ICAM-1	intercellular adhesion molecule 1
IFN	interferon
IKKα	inhibitor κB *kinase* α
IKKε	inhibitor κB *kinase* ε
IL	interleukin
IN	integrase
INI1/HSNF5	integrase interactor 1
IRES	internal ribosome entry site
IRF7	interferon regulatory factor 7
ISG	interferon inducible gene
kDa	kilodalton
LEDGF/p75	lens epithelium-derived growth factor/p75
LGP2	laboratory of genetics and physiology 2
LINE	long interspersed nuclear element
LRR	leucine-rich repeat
LRT	late reverse transcript
LTR	long terminal repeat
LysRS	Lysyl-tRNA synthetase
MA	matrix
mAUG	main AUG
MAVS	mitochondrial antiviral signaling protein
MDA5	melanoma differentiation associated gene 5
MLV	murine leukemia virus
MMTV	mouse mammary tumor virus
mORF	major open reading frame
MOV10	Moloney leukemia virus 10
mRNA	messenger ribonucleic acid
MuV	mumps virus
MV	measles virus
MyD88	myeloid differentiation primary response 88
N	nucleus
NACHT	NAIP, CIIA, HET-E and TP1.
NC	nucleoclapsid

NF-κB	nuclear factor kappa-light-chain-enhancer of activated B cells
NLR	NOD-like receptor
NLRC	NOD-like receptor family CARD domain containing
NLRP	NOD-like receptor family PYD-containing
NLS	nuclear localization sequence
NMR	nuclear magnetic resonance
NOD	nucleotide oligomerization domain
NPC	nuclear pore complex
NTD	N-terminal domain
ORF	open reading frame
OvLV	ovine lentivirus
P-TEFb	positive transciption elongation factor b
PAMP	pathogen-associated molecular pattern
PBMC	peripheral blood mononuclear cell
PBS	primer binding site
pDC	plasmacytoid dendritic cell
PIC	pre-integration complex
PPT	polypurine tract
PR	protease
$Pr160^{GagPol}$	precursor 160 GagPol
$Pr55^{Gag}$	precursor 55 Gag
PRR	pattern recognition receptor
PYD	pyrin domain
RanGTP	ran bound to guanosine triphosphatase
Rev	regulator of expression of virion proteins
RIG-I	retinoic acid-inducible gene I
RING	really interesting new gene
RIPK2	receptor-interacting serine-threonine protein kinase 2
RLR	(RIG-I)-like receptor
RNA	ribonucleic acid
RNase H	ribonuclease H
RRE	Rev response element
RSV	respiratory syncytial virus
RT	reverse transcriptase
RTC	reverse transcription complex
SAM	sterile alpha motif
SAMHD1	sterile alpha motif and HD-domain containing protein 1
SDS-PAGE	sodium dodecyl sulfate – polyacrylamide gel electrophoresis
SEM	scanning electron micrograph
Ser	serine
SINE	short interspersed nuclear element
SIP1	smad interacting protein 1
SIV	simian immunodeficiency virus
SIVagmGri	african green monkey grivet SIV
SIVagmTan	african green monkey tantalus SIV
SIVagmVer	african green monkey vervet SIV
SIVcol	mantled guereza SIV
SIVcpz	chimpanzee SIV
SIVcpzPtt	chimpanzee *Pan troglodytes troglodytes* SIV
SIVdeb	de Brazza's monkey SIV
SIVden	Dent's mona monkey SIV
SIVdrl	drill monkey SIV
SIVgor	western gorilla SIV
SIVgsn	greater spot-nosed monkeys SIV
SIVlho	L'Hoest's monkey SIV

SIVmac	rhesus *macaque* SIV
SIVmnd	nandrill SIV
SIVmon	mona monkey SIV
SIVmus	mustached monkey SIV
SIVolc	olive colobus monkey SIV
SIVrcm	red-capped mangabey SIV
SIVsmm	sooty mangabey SIV
SIVsun	sun-tailed monkey SIV
SIVsyk	sykes's monkey SIV
SIVtal	talapoins SIV
SIVtan	tantalus monkey SIV
SIVver	vervet monkey SIV
SIVwrc	western red colobus monkey SIV
SLFN	Schlafen
SMN	survival motor neuron
SMUG1	single-strand selective monofunctional uracil DNA glycosylase
SNP	single-nucleotide polymorphisms
SP1	spacer peptide 1
SP2	spacer peptide 2
ssRNA	single-stranded viral RNA
SUMO1	small ubiquitin-like modifier 1
SUMO2	small ubiquitin-like modifier 2
TAK1	TGF-activated kinase
TAR	viral transactivation response
Tat	transactivator of transcription
TBK1	TANK-binding kinase 1
TGN	trans-Golgi network
TIF	transcript isoform
TIP47	tall-interacting protein of 47 kDa
TIRAP/Mal	TIR domain-containing adaptor protein/MyD88 adapter-like
TLR	toll-like receptor
TM	transmembrane
TOP	terminal oligopyrimidine
TRIF	TIR-domain-containing adapter-inducing interferon-β
TRIM	tripartite motif
TRIM5α	tripartite motif 5 alpha
$tRNA^{Lys-3}$	transfer RNA lysine-3
TSG101	tumor susceptibility gene 101
uAUG	upstream AUG
Ubc9	ubiquitin carrier protein 9
UDG	uracil-DNA glycosylase
UNAIDS	United Nations Programme on HIV and AIDS
UNG2	uracil-DNA glycosylase 2
uORF	upstream open reading frame
UTR	untranslated region
uUGA	upstream UGA
Vif	viral infectivity factor
Vpr	viral protein R
Vpu	viral protein unique
Vpx	viral protein X
WHO	World Health Organization

I. INTRODUCTION

1. Origins of HIV-1 and AIDS Pandemic

Human acquired immunodeficiency syndrome (AIDS) is caused by two lentiviruses of the Retroviridae family, human immunodeficiency viruses types 1 and 2 (HIV-1 and HIV-2). In 1981, AIDS was recognized as a new disease when increasing cases of rare opportunistic infections were reported in young homosexual men (Centers for Disease Control (CDC), 1981, 1982). HIV-1 was subsequently discovered to be the causing agent of this immune system deficiency (Barré-Sinoussi et al., 1983). Three years after the discovery of HIV-1, a morphologically similar but genetically distinct virus, named human immunodeficiency virus type 2 (HIV-2), was discovered in West African patients with AIDS (Clavel et al., 1986). Interestingly, this virus was closely related to a simian retrovirus that caused an immune system deficiency in macaques (Chakrabarti et al., 1987; Guyader et al., 1987). Additional simian immunodeficiency viruses (SIVs) were subsequently discovered in various primates such as chimpanzees, African green monkeys, mandrills and others (Sharp et al., 2013) (Fig.1).

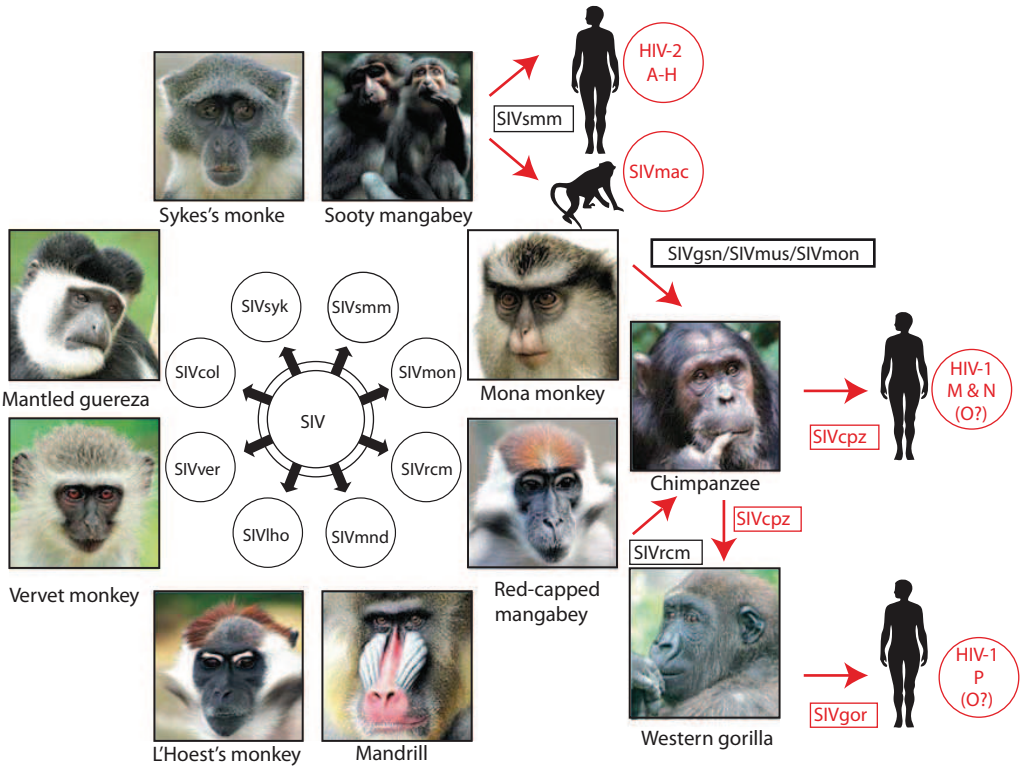

Figure 1. Origins of HIV. HIV-1 and HIV-2 were originated by a cross-species infection involving different primate lentiviruses (Sharp and Hahn, 2011).

Despite the fact that these viruses are closely related with the human and simian AIDS viruses in the lentiviruses phylogeny (Fig. 2), they are non-pathogenic in their natural hosts. Interestingly, HIV-1 has a close phylogenetic relationship with the SIVcpz (Huet et al., 1990), while HIV-2 with SIVsmm (Hirsch et al., 1989). This evidence shows that both macaque and human AIDS was originated by a cross-species infection involving different primate lentiviruses (Sharp and Hahn, 2011). During virus infection, HIV and SIV interact with a large number of host proteins (e.g. host restriction factors) and since the common ancestor of primates existed 25 million years ago, the divergence of these host proteins could be an obstacle to this cross-species infection. Therefore, a number of adaptive events have to be overcome before these lentiviruses can contaminate new species. To date, it is widely accepted that HIV-1 and HIV-2 have emerged from zoonotic events of viruses infecting primates in Africa (Sharp et al., 2013).

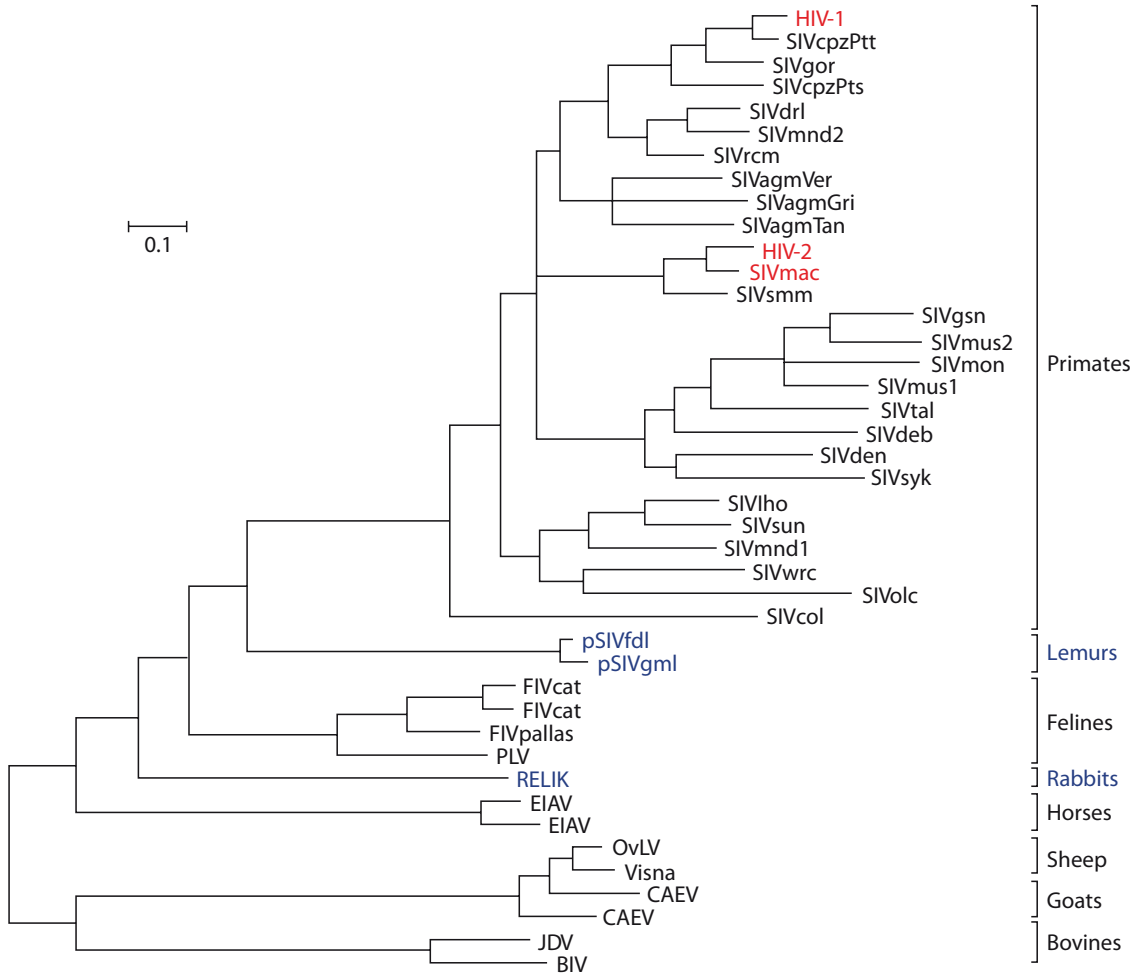

Figure 2. Phylogeny of lentiviruses based on Pol sequence. Endogenous (blue) and Exogenous (black) retrovirus are indicated, with HIV-1, HIV-2 and SIVmac highlighted in red (Sharp and Hahn, 2011).

According to the 2012 UNAIDS and WHO reports, three decades after the discovery of AIDS, the pandemic HIV-1 main (M) group have infected at least 70 million people and caused more than 35 million deaths. Globally, 34.0 million [31.4–35.9 million] people were living with HIV at the end of 2011. In 2011, an estimated 0.8% of adults aged 15-49 years worldwide are living with HIV, although this percentage varies considerably between regions (Fig. 3). Sub-Saharan Africa remains the most severely affected region, with nearly 1 in every 20 adults (4.9%) living with HIV and accounting for 69% of the people living with HIV worldwide. Additionally, 1.7 million people died of AIDS in 2011, a 24% decrease since 2005. This is due in part to antiretroviral treatment (ART) scale-up. Despite the efficiency of this antiretroviral therapy, access to this treatment remains limited, and the development of an effective vaccine is uncertain. Thus, AIDS continues to be an important priority in worldwide public health (McCoy and Weiss, 2013; Sharp and Hahn, 2011).

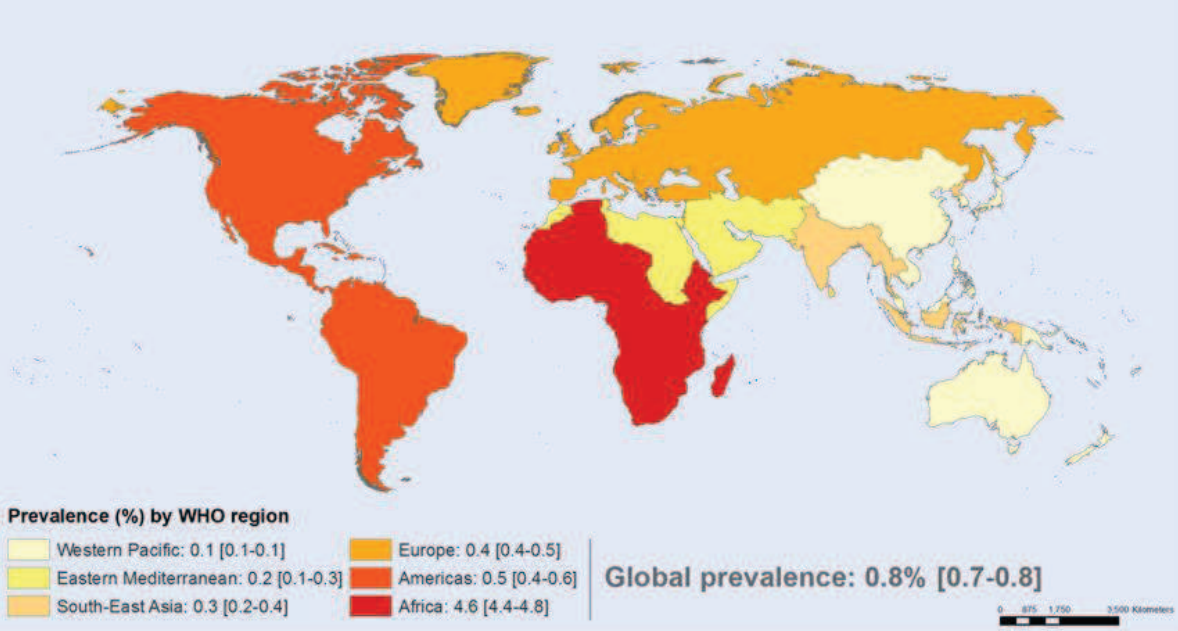

Figure 3. Adult HIV Prevalence Rate by region (2011).

2. Overview of the HIV-1 life cycle

The HIV-1 life cycle can be structured into two phases (Fig. 4): (1) an early phase that begins with the recognition of the target cells, attachment and entry, retro-transcription of the viral genome and integration of the viral DNA into the host cell

genome; (2) a late phase that continues with the viral mRNA biogenesis and transport, synthesis of viral proteins, packaging, assembly, budding and release of viral particles.

2.1 Viral entry

The HIV-1 envelope proteins (ENV) are expressed as a precursor protein, gp160, which transits the Golgi apparatus to complete glycosylation (Swanstrom and Coffin, 2012). The precursor is then cleaved by the cellular protease furin into two proteins, gp120 and gp41 (Hallenberger et al., 1992). These proteins are present on HIV-1 envelope as trimers of gp120-gp41 heterodimers. Cryo-electron microscopy tomography analysis of wild-type HIV-1 virion showed 14 ± 7 trimers per particle (Zhu et al., 2006).

HIV-1 infects $CD4^+$ T cell with an initial interaction between gp120 and the surface receptor CD4 (Fig. 4, step 1).The binding of gp120 to CD4 triggers conformational changes in gp120 that lead to recognition of a co-receptor, a member of the seven-trans-membrane chemokine-receptor family, CCR5 or CXCR4 (Alkhatib et al., 1996). Binding to CCR5 is known as R5 tropism, while binding to CXR4 as X4 tropism. R5-tropic isolates predominates in early infection, whereas X4-tropic isolates are found in late infection (Duncan and Sattentau, 2011). Engagement of this co-receptor releases gp41 from its high energy state leading to the insertion of the fusion peptide, located at the amino terminus of gp41, into the cell membrane. As the fusion peptide inserts into the host cell membrane, gp41 refolds itself through the heptad repeat sequences HR1 and HR2.

This event triggers the formation of a six-helix hairpin structure inducing the fusion (Fig. 4, step 2) of the viral and host cell membranes and further release of the HIV-1 core into the cytoplasm (Swanstrom and Coffin, 2012). Viral entry in the absence of CD4 expression has been reported but the presence of one of the co-receptors is indispensable for the entry process (Reeves et al., 1999).

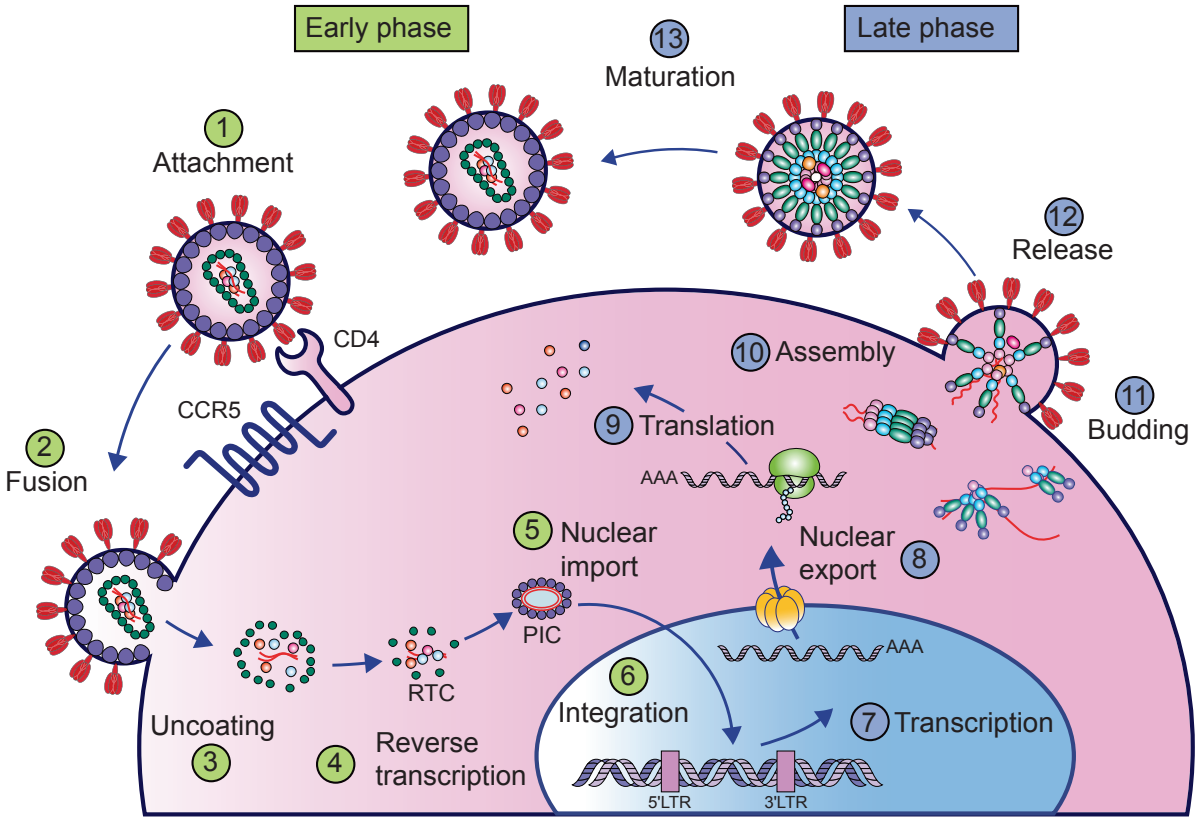

Figure 4. Overview of the HIV-1 life cycle. Early phase initiates with the attachment (1) and finalizes with the integration of the viral DNA into the host genome (6). Late phase continues with transcription of viral DNA (7) and conclude with the release and maturation of the viral particles (13).

2.2 Uncoating and reverse transcription

Once inside the cytoplasm of the infected cell, the HIV-1 core undergoes a partial and progressive disassembly of the viral capsid (CA), known as uncoating (Fig. 4, step 3). This process is still not well understood and several models have been proposed. In a first model, the HIV-1 core remains intact until it reaches the nuclear membrane and uncoating occurs at the nuclear pore after completion of reverse transcription (Arhel, 2010; Arhel et al., 2007). A second model suggests that viral capsid is disassembled immediately following fusion and most CA is dissociated from the nucleoprotein complex (Suzuki and Craigie, 2007). A third model proposes that CA remains intact for some time post-entry and uncoating occurs gradually during transport towards the nucleus (Warrilow et al., 2009).

During the uncoating process, the viral core is rearranged to form the reverse transcription complex (RTC), in which reverse transcription occurs (Fig. 4, step 4). This process is catalyzed by the viral reverse transcriptase (RT). Reverse transcription process has been extensively studied (Le Grice, 2012) and RT is a major target for anti-HIV-1 therapy (Das and Arnold, 2013; Ilina et al., 2012; Lange and van Leeuwen, 2002).

Reverse transcriptase generates a linear DNA duplex *via* a complex and multistep process (Fig. 5). Briefly, reverse transcription begins with minus-strand DNA ((-) DNA) synthesis that is primed from a host-cell transfer RNA ($tRNA^{Lys-3}$). The $tRNA^{Lys-3}$ anneals to the PBS (Fig. 5A) located at the 5' end of the viral RNA genome and the (−) DNA synthesis continues to the 5' end generating a DNA intermediate termed minus-strand strong-stop DNA ((-) ssDNA) (Fig. 5B). This is followed by the first strand transfer step (Fig. 5C), in which (-) ssDNA is transferred from the 5' end to the 3' end R region of the viral genome. After first strand transfer, (−) DNA synthesis continues, accompanied by RNase-H digestion of the template strand except for the polypurine tract region (PPT) that is relatively resistant to RNase-H degradation (Fig. 5D) (Thomas et al., 2007). PPT region serves as a primer for the plus-strand DNA synthesis ((+) DNA). Plus-strand DNA synthesis continues to the 5' of the (−) DNA until it reaches the PBS region generating the plus strand strong stop DNA ((+) ssDNA) (Fig 5E). In order to complete plus-strand DNA synthesis, a second strand transfer step occurs in which (+) ssDNA is transferred to the 3' end of the (−) DNA to form a circular intermediate (Fig 5F). The final product of this complex process is resolved into a linear double-stranded DNA (dsDNA) with duplicated long terminal repeats (LTRs) intermediate (Fig. 5G) (Basu et al., 2008).

2.3 Nuclear Import and integration

Completion of RTC maturation and reverse transcription generates the pre-integration complex (PIC). HIV-1 PIC is composed of the dsDNA associated with the viral proteins RT, the matrix (MA), integrase (IN) and the viral protein R (Vpr) (Miller et al., 1997). Several cellular factors have also been shown to be present in the HIV-1 PIC, such as the high mobility group protein HMG I (Y) and LEDGF/p75 (Llano et al., 2006; Miller et al., 1997).

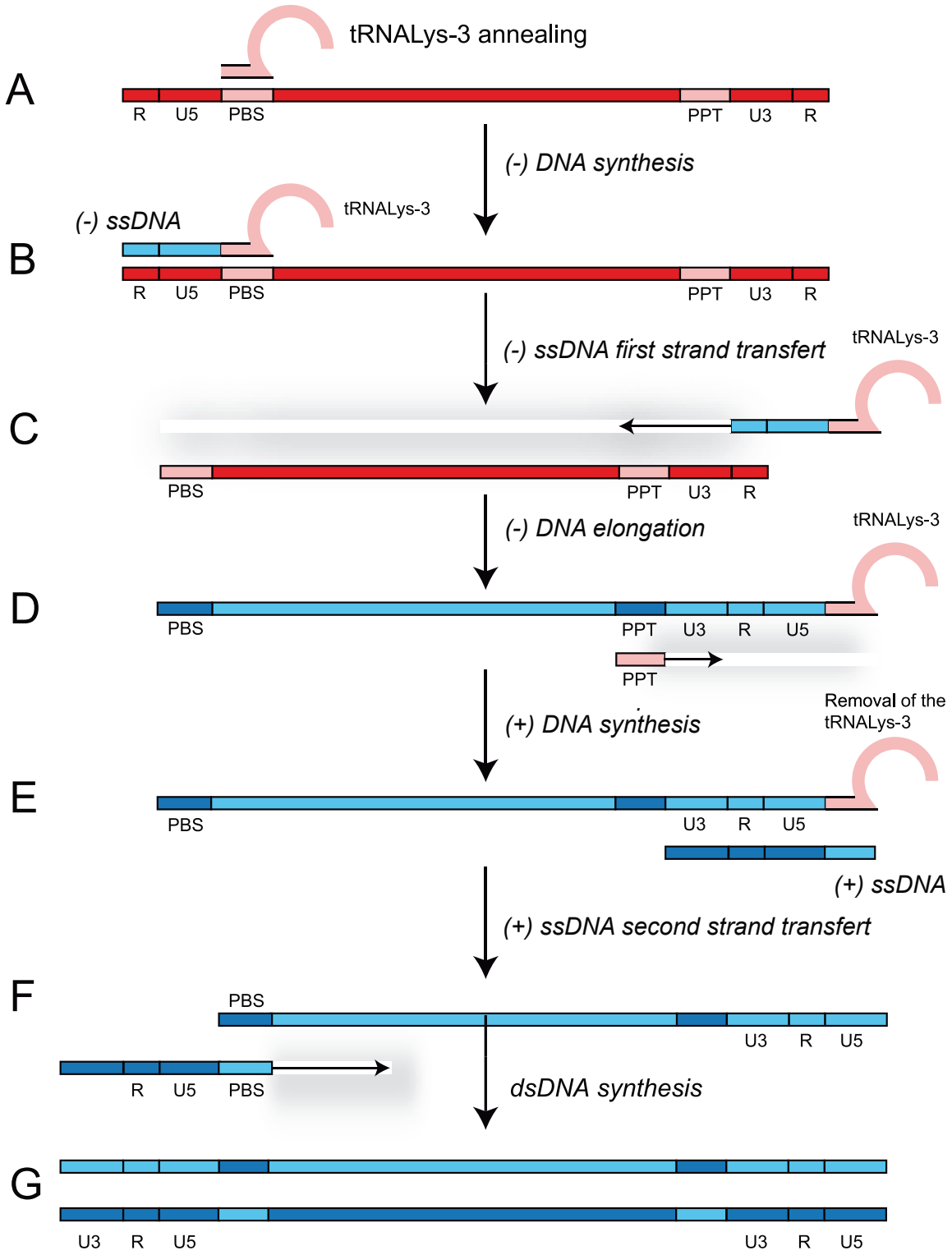

Figure 5. Reverse transcription. This process can be divided in 3 principal steps: 1) (-) DNA synthesis (A to D), 2) (+) DNA synthesis (D to F) and 3) synthesis of the double-stranded viral DNA (dsDNA) (G).

Since the HIV-1 PIC has an estimated diameter of 56 nm and the central channel of the nuclear pore is able to transport macromolecules only up to 39 nm (Panté and Kann, 2002), the PIC can only enter into the cell nucleus by active diffusion ensured by the nuclear import machinery (Fig. 4, step 5). Among the proteins implicated in the import machinery, the importin 7 has been proposed to play an important role in nuclear import of HIV-1 PIC in primary macrophages (Fassati et al., 2003). The viral proteins associated with the HIV-1 PIC play also a significant role in this complex process, although the precise function of each remains undetermined (Suzuki and Craigie, 2007).

Once inside the nucleus, the IN, which is a member of the D,D(35)E transposase/IN superfamily of proteins, mediates integration of the viral DNA (Fig. 4, step 6) into the host genome. Additionally, several cellular DNA binding proteins have been reported to bind the IN and could therefore play a role in the integration process. For example, the integrase interactor 1 (Ini1, also called hSNF5) (Kalpana et al., 1994), the high mobility group protein HMG I (Y) (Miller et al., 1997), the survival motor neuron (SMN) interacting protein 1 (SIP1) (Nishitsuji et al., 2009) or the small ubiquitin-like modifiers (SUMO1 and SUMO2) and their conjugation enzyme Ubc9 (Li et al., 2012b).

Viral dsDNA integration occurs in two well-characterized catalytic steps, named the end-processing reaction and the joining reaction. End processing involves removal of a dinucleotide from the 3’ strand of the U3 and U5 viral DNA LTRs. The endonucleolytic cleavage always occurs at the 3’ of a conserved dinucleotide (CA) and results in exposure of a new hydroxyl group at the 3’ end of the viral dsDNA. This hydroxyl group is used as an attacking nucleophile on the target DNA during the joining reaction, in which the viral DNA is inserted into the cellular DNA (Krishnan and Engelman, 2012). Integration site preferentially occurs in genes highly transcribed by the RNA polymerase II favoring efficient HIV-1 gene expression (Ciuffi, 2008). Recently, Cooper et al (2013) have shown that the integration process triggers the death of $CD4^+$ T cells. This mechanism is activated by a DNA-dependent protein kinase (DNA-PK), a central component of the DNA damage response.

2.4 Viral mRNA biogenesis and splicing

Integration determines the passage from the early to the late phase of HIV-1 replication, in which viral mRNA biogenesis and further protein synthesis occurs followed by the assembly, release and maturation of viral particles. Once the viral genome is integrated, the viral transcription initiates from a complex promoter located within the 5' LTR of the viral genome (Fig. 4, step 7). The HIV-1 LTR promoter contains two Sp1 binding motifs and two nuclear factor NF-κB binding sites which serves to regulate basal HIV-1 transcription (Krishnan and Engelman, 2012; Ocwieja, 2012).

Transcription of the viral genome requires the viral transactivator protein (Tat) which activates RNA polymerase II by recruiting several specific factors. During this process, Tat interacts with the cellular protein positive transcription elongation factor b (P-TEFb), including the cyclin-dependent kinase 9 (CDK9) and cyclin T1 (CycT1) to the viral transactivation response (TAR) element. Subsequent CDK9-mediated phosphorylation of the heptad repeat residues Ser-2 and Ser-5 in the C-terminal domain of the large subunit of RNA polymerase II stimulates transcription elongation (Wagschal et al., 2012).

Viral mRNAs are produced as a variety of alternatively spliced species ensuring the synthesis of all HIV-1 structural and regulatory proteins. More than 40 different viral mRNAs are produced during the infectious cycle by alternative splicing of a single polycistronic pre-mRNA. HIV-1 mRNAs can be divided into three classes: multiply spliced (2 kb), singly spliced (4 kb) and full-length non-spliced mRNAs (9kb) (Leblanc et al., 2013). HIV-1 RNA splicing is regulated by *cis*-acting sequences including suboptimal splice sites (polypyrimidine tracts and branch point sequences), exonic splicing enhancers (ESEs) and the exonic/intronic splicing silencers (ESS／ISS).

2.5 Nuclear export and translation of the viral mRNA

Once the viral mRNA biogenesis is accomplished, the multiply spliced (2 kb) viral mRNAs are exported from the nucleus to the cytoplasm by the endogenous nuclear pathway (Fig. 4, step 8). On the contrary, the singly spliced (4 Kb) and the unspliced full-length (9 Kb) viral RNAs are exported by a mechanism involving the HIV-1 Rev protein (Fernandes et al., 2012; Purcell and Martin, 1993). This protein acts as a linker between the Rev response element (RRE), located within the *env* mRNA coding region, and the host cellular proteins implicated in the mRNA nuclear export process.

Rev recruits the exportin CRM1 (Chromosome Region Maintenance 1) and the nuclear export factor Ran bound to guanosine triphosphatase (RanGTP). The Rev-CRM1-RanGTP complex interacts with the nuclear pore complex (NPC) to be transported through the nuclear pore to the cytoplasm. The hydrolysis of GTP to GDP allows the dissociation of the complex and the redirection of Rev back into the nucleus (Purcell and Martin, 1993; Tazi et al., 2010).

The translation of HIV-1 mRNAs (Fig. 4, step 9) is initiated by the classical cap-dependent mechanism or by internal recruitment of the ribosome through specific RNA regions called IRES (internal ribosome entry site). In the classical model the ribosome initiates translation from the first AUG in a favorable Kozak context after scanning of the 5'UTR (discussed below). In the IRES-dependent mechanism the ribosome is recruited near or at the AUG star codon without a scanning step (Balvay et al., 2009; Chamond et al., 2010).

2.6 Assembly, budding and maturation

The late stages of HIV-1 replication comprise the assembly of virus particles from newly synthesized components at the host cell membrane and the release of progeny virus (Fig. 4, step 10-12). Viral assembly is mediated by the $Pr55^{Gag}$ through a complex network of interactions (Fig. 6). The assembling virion packages the genomic viral RNA, cellular $tRNA^{Lys-3}$, the Gag polyprotein, the viral ENV protein and the three viral enzymes: protease (PR), reverse transcriptase (RT), and integrase (IN) (Sundquist and Kräusslich, 2012). Moreover, other cellular and viral components

are also incorporated including the viral infectivity factor (Vif), the viral protein R (Vpr), and several cellular proteins: Cyp-A, Hsp70, LysRS, TSG101, Ubiquitin, APOBEC3G, INI1/HSNF5, Staufen, UNG2, HLA-II, ICAM-1, CD54, annexins and tetraspanins (Balasubramaniam and Freed, 2011; Ott, 2008; Paxton et al., 1993; Selig et al., 1999).

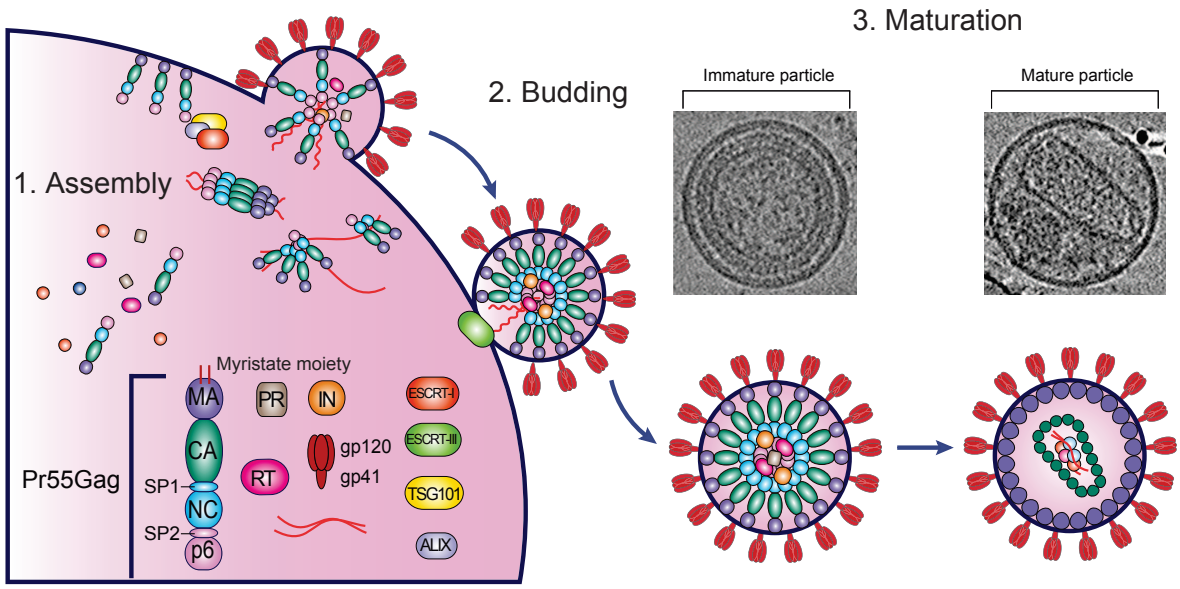

Figure. 6. Late stages in HIV-1 life cycle. Assembly (1) is mediated by the $Pr55^{Gag}$ through a complex network of interactions. The virion packages the genomic RNA and several viral and cellular proteins (see text). After assembly, the host ESCRT machinery is recruited for viral budding (2). Viral maturation (3) starts immediately after budding and is mediated by the viral protease (PR).

Coding for the structural proteins, the precursor, $Pr55^{Gag}$ contains four major domains (MA, CA, nucleocapsid (NC) and p6) and two spacer peptides (SP1 and SP2). The $Pr55^{Gag}$ is myristylated and binds to the plasma membrane through the M myristate moiety while the CA, SP1, and NC domains promote Gag multimerization and assembly. The assembling particle incorporates the cellular $tRNA^{Lys3}$ and the viral genomic RNA through an interaction with NC domain and the $Pr160^{GagPol}$. Two copies of the viral RNA are incorporated into the viral particle by interactions between the $Pr55^{Gag}$ and the encapsidation signal Ψ (Psi) positioned at the leader region of the genomic RNA (Paillart et al., 2004). Concerning the envelope glycoproteins, they are recruited into the budding virions through interactions with MA domain (Sundquist and Kräusslich, 2012). In this process, the cellular cofactor

TIP47 (Tall-Interacting Protein of 47 kDa) is also required for envelope glycoproteins incorporation into HIV particles (Bauby et al., 2008).

After assembly of the viral particles, the host ESCRT (endosomal sorting complexes required for transport) machinery mediates budding of the virion particles from the plasma membrane (Fig. 6). During this process, ESCRT-I is recruited through interactions between viral p6 and host TSG101 and ALIX. This in turn recruits ESCRT-III to initiate membrane fission and virion release (Martin-Serrano and Neil, 2011).

Viral maturation (Fig. 4, step 13 and Fig. 6) begins immediately following the budding process, and is driven by viral PR cleavage of $Pr55^{Gag}$ and $Pr160^{GagPol}$ at different sites, producing the fully processed MA, CA, NC, p6, PR, RT, and IN proteins. During this process, these proteins rearrange orderly: MA remains associated with the viral membrane, NC condenses with the dimeric gRNA, and CA reassembles to form a conical core shell enclosing the NC-RNA complex. This reorganization results in a mature infectious virion that is capable to infect new $CD4^+$ T cell (Dordor et al., 2011; de Marco et al., 2012).

3. Innate immune responses in HIV-1 infection

The innate immune system is the first line of antiviral defense and protects the host by either eliminating the pathogen or by reducing the negative impact of infection on host fitness (Medzhitov et al., 2012). However, regarding endogenous retroviruses, immune responses involve self-preservation mechanisms and not virus elimination strategies since these retroviruses are significantly integrated in the human genome (Griffiths, 2001; Iwasaki, 2012). This notion might be considered to analyze immune response against exogenous retroviruses like HIV-1 (Iwasaki, 2012). Innate immunity facilitates a rapid response by the recognition of evolutionarily conserved elements on pathogens, named pathogen-associated molecular patterns (PAMPs) (Silvin and Manel, 2013). This recognition is mediated by pattern recognition receptors (PRRs), including, the toll-like receptors (TLRs), the (RIG-I)-like receptors (RLRs), and the nucleotide oligomerization domain (NOD)-like receptors (NLRs) (Fig. 7) (Carrington and Alter, 2012).

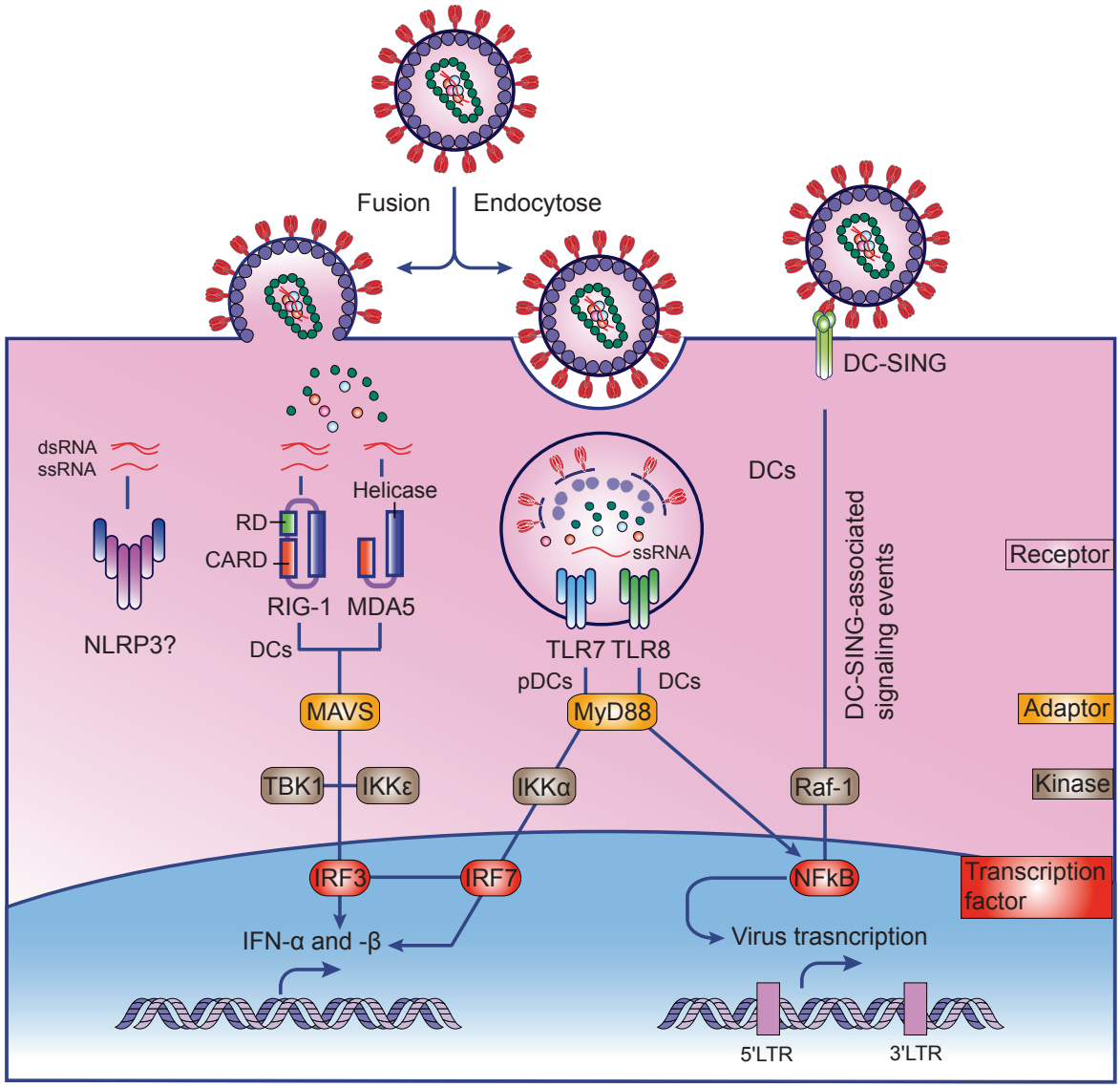

Figure 7. Pattern recognition receptors (PRRs) in HIV-1 infection. Single (ssRNA) and double-stranded HIV-1 viral RNA (dsRNA) are recognized by PRRs to induce IFN response. Thus, TLR7 induce IFN-α/β expression through MyD88 adaptor, IKKα and IRF7 in pDC. In DCs, TLR8 and DC-SIGN signaling promotes HIV-1 transcription through MyD88 adaptor and Raf-1, respectively. RIG-I-like receptors (RIG-1 and MDA5) also promote IFN-α/β production through MAVS adaptor, TBK1, IKKε, IRF3 and IRF7. NLRP3 could also detect HIV-1 RNA.

PAMPs recognition leads to signal transduction, stimulation of transcription factors such as NF-κB and interferon regulatory factors (IRFs), and finalizes with the expression of pro-inflammatory cytokines such as type-1 interferons (IFNs) which activate the expression of several proteins including cellular restriction factors (Jolly, 2011).

3.1 Toll-like receptors

TLRs are expressed in macrophages and dendritic cells. They are named for their similarity to Toll, a receptor first identified in *Drosophila* to have an important role in the immunity of this organism regarding fungal infections (Hoffmann, 2003; Lemaitre et al., 1996). To date, thirteen human and mouse TLRs have been reported. TLRs trigger the NF-κB pathway, which activates cytokine expression, through several protein adaptors, such as MyD88, TRIF and TIRAP/Mal. In addition, other receptors such as type-C lectins and scavenger receptors can also activate TLR-like responses (Poovassery and Bishop, 2012).

During HIV-1 infection, TLR7 mediates the detection of single stranded viral RNAs (ssRNA). TLR7 is constitutively expressed by plasmacytoid dendritic cells (pDC) and B cells (Poovassery and Bishop, 2012; Santana-de Anda et al., 2013). In this mechanism, HIV-1 virus particles are endocytosed by pDCs to generate a proteolytic degradation compartment in which virus components are degraded and the viral RNA is recognized by TLR7. These events induce the expression of IFN-α/β through MyD88 adaptor, IKKα and the interferon regulatory factor 7 (IRF7) (Fig. 7) (Hardy et al., 2007).

Similarly to TRL7, TLR8 also recognizes ssRNA but is expressed in dendritic cells (DCs) (Heil et al., 2004). However, in contrast to the signaling cascade activated by TRL7, TLR8 signals are exploited by HIV-1 to enhance its own transcription in DCs. In this mechanism, HIV-1 ssRNA activates the transcription factor NF-kB through TLR8 to initiate transcription of the integrated provirus. At this point, NF-kB is required for transcription initiation but is not sufficient for elongation. In parallel, the association between gp120 and DC-SIGN induces phosphorylation of the NF-κB through Raf-1, allowing transcription elongation of HIV-1 transcripts. Thus, TLR8 and DC-SIGN signaling promotes HIV-1 transcription (Fig. 7) (Gringhuis et al., 2010; Tremblay, 2010).

3.2 RIG-I-like receptors

Retinoic acid-inducible gene I (RIG-I)-like receptors (RLRs) are expressed in almost all cell types, including epithelial and fibroblastic cells as well as macrophages and

DCs (Kato et al., 2006). RLRs are RNA helicases that specifically detects viral RNA molecules in the cytoplasm (Solis et al., 2011). RLRs contain an N-terminal caspase-recruitment domains (CARDs) and a DExD/H-box helicase domain (Dixit and Kagan, 2013). RLR family has three members: RIG-I, melanoma differentiation associated gene 5 (MDA5) and laboratory of genetics and physiology 2 (LGP2) (Dixit and Kagan, 2013).

During HIV-1 infection, RIG-I and MDA5 detect HIV-1 RNA in the cytoplasm of infected cells. RIG-I recognizes both the dimeric and monomeric forms of the genomic RNA, while MDA5 only detects the dimeric conformation (Solis et al., 2011). RIG-I discriminates viral from cellular RNA by the recognition of 5-triphosphorylated (5-PPP) structures, modifications that are not found on processed cellular RNA (Hornung et al., 2006; Pichlmair et al., 2006).

After detection of HIV-1 RNA, RIG-I and MDA5 interact with the downstream CARD-containing adapter mitochondrial antiviral signaling protein (MAVS) (Kawai et al., 2005). MAVS in turn activates the IKK-related kinases TBK1 and IKKε, which result in the activation of IRF3 and IRF7. The coordinated activation of these factors results in the induction of the IFN-α/β (Fig. 7) (Eisenächer and Krug, 2012). However, HIV-1 depletes RIG-I cytoplasmic levels through the action of the HIV-1 protease (PR). The decrease of cytoplasmic RIG-I was prevented by the lysosomal inhibitor E64, suggesting that PR targets RIG-I to the lysosomes (Solis et al., 2011). Concerning LGP2, this protein does not present any CARDs and was originally reported as a negative regulator of RLR signaling *in vitro*. However, Satoh et al (2010) have shown that LGP2 was required for RIG-I and MDA5-mediated antiviral responses *in vivo*.

3.3 NOD-like receptors

NOD-like receptors (NLRs) are expressed primarily in phagocytes including macrophages and neutrophils (Franchi et al., 2009). NLRs typically contain a central nucleotide-binding domain termed NACHT domain, a C-terminal receptor domain characterized by a series of leucine-rich repeats (LRRs) and a N-terminal binding region that presents protein-protein interaction domains such as the caspase recruitment domain (CARD), pyrin domain (PYD), and baculovirus inhibitor repeat domain (BIR) (Philpott and Girardin, 2010).

To date, 22 members of the human NLR protein family have been reported, which can be distinguished into three subfamilies depending on the basis of their N-terminal region (CARD, PYD or BIR). NLR proteins trigger a number of signal transduction cascades. For example, NOD1 and NOD2 induce the pro-inflammatory NF-κB pathway through the interaction with the receptor-interacting serine-threonine protein kinase 2 (RIPK2) (Monie, 2013). NOD1 and NOD2 also promote autophagy by recruiting the autophagy-related gene 16-like 1 (ATG16L1) to the plasma membrane (Travassos et al., 2010). Finally, NLR family members, NLRP1 (NLR family PYD-containing 1), NLRP3 and NLRC4 (NLR family CARD-containing 4) activate the caspase-1 inflammasome pathway, which leads to the production of interleukin-1β (IL-1β) and IL-18 (Yu and Levine, 2011).

During virus infection, NLRP3, NOD2, NLRX1 and NLRC5 play an important role in virus recognition by activating different signaling pathways (Jacobs and Damania, 2012; Kanneganti, 2010). Among these proteins, only NLRP3 has shown to have a susceptibility to HIV-1 infection. Indeed, a single-nucleotide polymorphisms (SNP) in NLRP3 is associated in HIV-1 infection (Pontillo et al., 2010, 2012). Although no data has shown that HIV-1 genetic material triggers this pathway, NLRP3 could be activated by HIV-1 RNA (Fig. 7) due to its previously reported ability in recognizing viral RNA of influenza A virus (Allen et al., 2009), vaccinia virus Ankara (Delaloye et al., 2009) or encephalomyocarditis virus (EMCV) (Poeck et al., 2010).

3.4 HIV-1 restriction factors

Recognition of HIV-1 RNA by PRRs leads to the induction of type-1 IFNs. IFNs activate interferon inducible genes (ISGs), some of which encode important antiviral proteins capable of counteracting HIV-1 at many diverse steps in the life cycle (Fig. 8). These have been termed restriction factors or intrinsic resistance factors, and they have at least four main characteristics: 1) the expression of the restriction factors is often activated by IFNs, mainly IFN-α; 2) a restriction factor must cause a significant reduction in HIV-1 infectivity; 3) HIV-1 has co-evolved with the restriction factors developing complex defense mechanisms to inhibit their activity. These restriction factors are often counteracted by viral proteins; and 4) restriction factors present hallmarks of positive selection during evolution caused by protein-protein

interactions that often occur between restriction and counter-restriction factors (Fig. 8) (Harris et al., 2012).

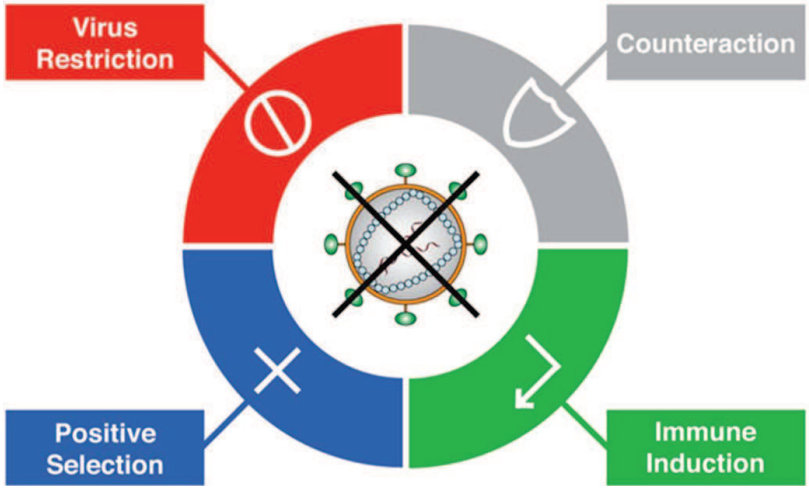

Figure 8. Properties of a HIV-1 restriction factor. A) Four defining characteristics are presented: 1) interferon responsiveness (promoter sign); 2) HIV-1 restriction (no-go sign); 3) Counteraction mechanism (shield sign); and 4) positive selection signatures (plus sign) (Harris et al., 2012).

Historically, Lilly (1967) discovered the first restriction factor against murine leukemia virus (MLV) infection, termed Friend virus susceptibility factor-1 (Fv1). Fv1 gene encodes a Gag-like protein that recognizes the MLV CA protein and blocks infection by mechanism operating after reverse transcription but before integration (Jolicoeur and Rassart, 1980; Kozak and Chakraborti, 1996). Fv1 was subsequently discovered to be a species-specific variant of TRIM5α (see below) (Hatziioannou et al., 2004).

Restrictions factors have been commonly characterized from non-permissive cells that are restrictive for viral replication. This restricting phenotype can be dominant and capable of severely inhibiting virus replication. Consequently, when a non-permissive cell is fused with a permissive cell, the restrictive phenotype is conferred to the resulting heterokaryon. Such cell fusion experiments have led to the discovery of cellular restriction factors counteracted by Vif and Vpu (Madani and Kabat, 1998; Sheehy et al., 2002; Simon et al., 1998; Varthakavi et al., 2003).

3.4.1 APOBEC3G

3.4.1.1 APOBEC3G and other members of the cytidine deaminase family

APOBEC3G (*apo*lipoprotein *B* mRNA-editing enzyme, *c*atalytic polypeptide-like *3G*, also known as CEM15) (Sheehy et al., 2002) belongs to the APOBEC family of putative cytosine-deaminase proteins that includes 11 members located on chromosome 12 (activation-induced deaminase, AID and A1), chromosome 6 (A2), chromosome 22 (A3A, A3B, A3C, A3DE, A3F, A3G, and A3H) and chromosome 1 (A4) (Fig. 9) (Smith et al., 2012).

All APOBEC family members present one (A1, AID, A2, A3A, A3C, A3H and A4) or two cytidine deaminase domains (CDAs) (A3B, A3DE, A3F, A3G) (Smith et al., 2012). Among these two domains, only the C-terminal domain is active, while the N-terminal domain is implicated in different functions such as RNA binding, multimerization or encapsidation. Recently, Uyttendaele et al. (2012) showed that both CDAs of A3G are involved in Vif binding (see below). CDAs of the A3 subfamily are characterized by a conserved zinc(Z)-coordinating DNA cytosine deaminase motif, H-x_1-E-$x_{25–31}$-C-$_{x2–4}$-C (x stands for a non-conserved amino acid).

The A3 Z domains can be divided into three groups (Z1, Z2 and Z3). Z1 and Z2 proteins possess a SW-S/T-C-$x_{2–4}$-C motif, while Z3 proteins have a TW-S-C-x_2-C motif. Z1 and Z2 proteins can be further distinguished by H-x_1-E-x_5- X-V/I and H-x_1-E-x_5-W-F motifs, respectively. Z1 proteins also present a unique isoleucine within a conserved RIY motif located C-terminal to the zinc-coordinating residues (LaRue et al., 2009) (Fig. 9). At least one protein of each Z domains has DNA cytosine deaminase activity; thus, A3F, A3G and A3H have catalytically competent Z2, Z1 and Z3 domains, respectively (LaRue et al., 2009). This enzymatically active site catalyzes the hydrolytic deamination at the C4 position of the C (or dC) base, converting C to U (or dC to dU) (Harris and Liddament, 2004).

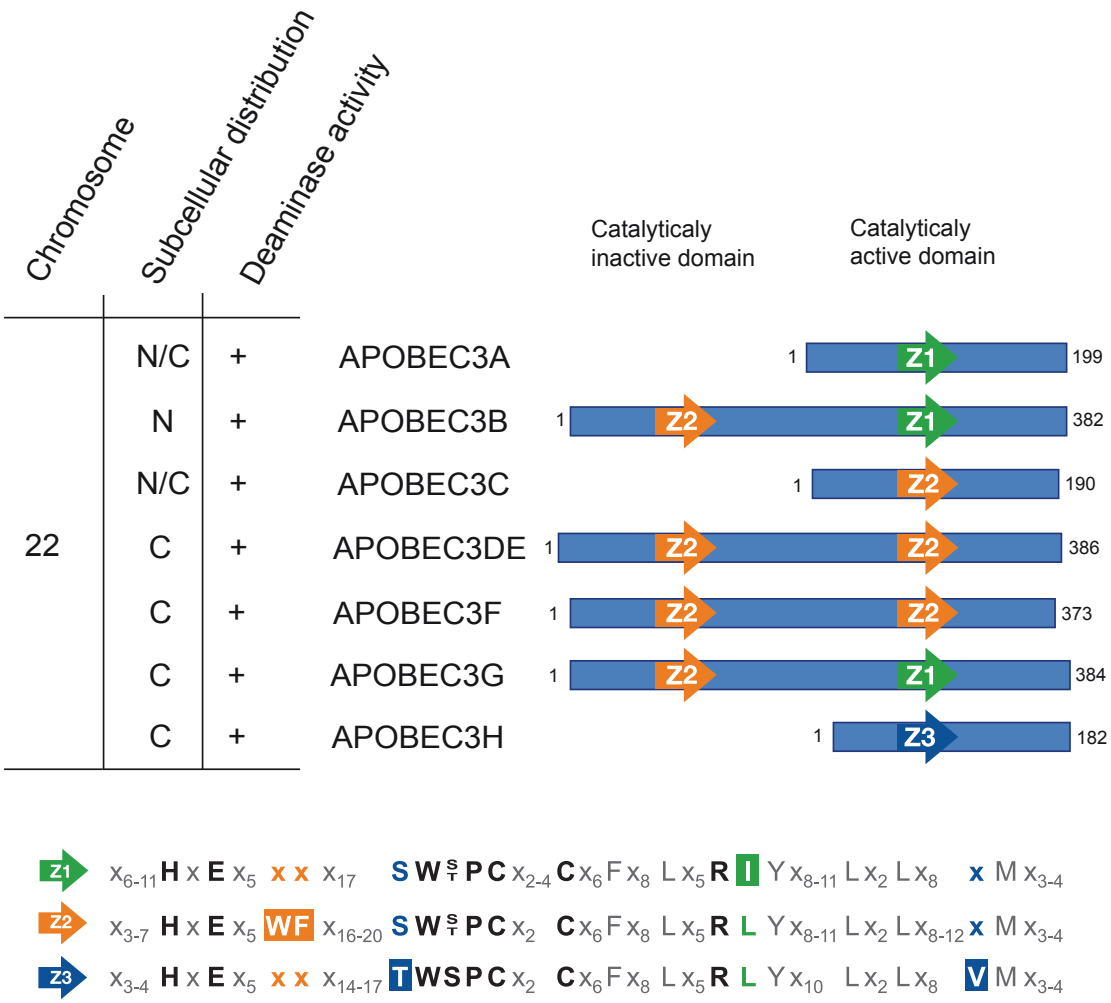

Figure 9. APOBEC3 subfamily. A schematic domain organization of APOBEC3 members is shown. Blue bars indicate APOBEC3 proteins and their relative alignments according to exon junctions. Z1, Z2, and Z3 domains are shown in green, orange and blue, respectively. The subcellular distribution is shown (nucleus, N, cytoplasm, C) and the deaminase activity is indicated by +/-. The conserved zinc (Z)-coordinating DNA cytosine deaminase motif of Z1, Z2 and Z3 is shown (Adapted from Franca et al., 2006, LaRue et al., 2008, 2009 and Smith et al., 2012).

Structural studies of the C-terminal CDA of A3G by nuclear magnetic resonance (NMR) (Chen et al., 2008; Harjes et al., 2009) and X-ray crystallography (Holden et al., 2008; Shandilya et al., 2010) revealed that the CDA is composed of five stranded β-sheet (β1–β5) with six α-helices (α1–α6) with a coordinated zinc ion. Kitamura et al (2012) have confirmed this observation by solving the structure of full-length human A3C (Fig. 10). Recently, the C-terminal CDA of human A3F has been determined (Bohn et al., 2013; Shandilya et al., 2013). This domain also share structural motifs with the C-terminal CDA of A3G reported by Shandilya et al. (2010). However, it seems that these two enzymes present potentially different modes for Vif binding (Shandilya et al., 2013).

APOBEC family members are present only within the vertebrate lineage. The most ancient are AID and APOBEC2. AID is expressed in germinal center B-cells and generates the deamination of DNA cytidine residues in the immunoglobulin genes resulting in the diversification of the adaptive immune system (Wang et al., 2012b). A2 is expressed in cardiac and skeletal muscle and is necessary for normal muscle development and maintenance of fiber-type ratios in skeletal muscle (Sato et al., 2010)

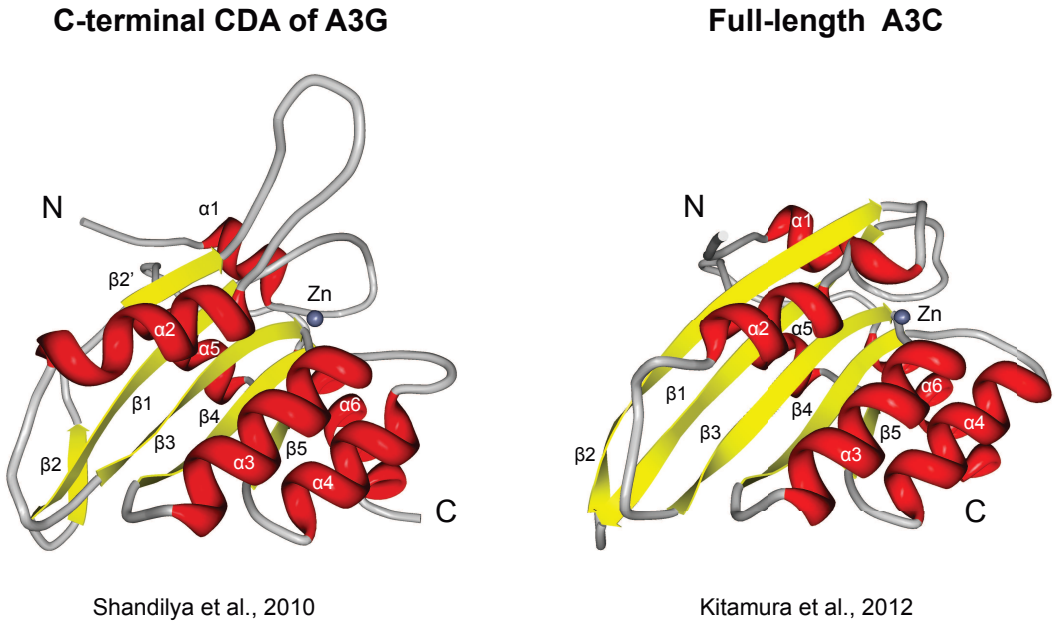

Figure 10. Structure of A3G CDA and full-length A3C. A3G CDA and A3C full-length are composed of five stranded β-sheet (β1–β5) with six α-helices (α1–α6) with a coordinated zinc ion. Adapted from Kitamura et al., 2012 (PDB 3VOW) and Shandilya et al., 2010 (PDB 3IR2).

A1 and A3 are later evolutionary arrivals whose expression is only found in mammals. A1 is expressed in enterocytes and is involved in lipid metabolism (Ashur-Fabian et al., 2010). A3 members participate in innate immunity against exogenous retrovirus, endogenous retroelements, DNA and RNA viruses (Table 1). A4 has been identified in silico and presents orthologues in mammals, birds and amphibians. In mammals, A4 is expressed principally in testis, suggesting a possible role in spermatogenesis (Franca et al., 2006; Rogozin et al., 2005) as measles (MV), mumps (MuV) and human respiratory syncytial virus (RSV).

Table 1. APOBEC3 family members activity against retroviruses

	Exogenous retrovirus					Endogenous retroelements			DNA viruses	
	HIV-1	SIV	EIAV	MLV	FV	LTR	LINES	SINES	HBV	AAV
A3A	+	-	-	+	ND	+	+	+	-	+
A3B	-	-	-	-	-	+	+	+	+	-
A3C	-	-	-	-	-	+	+	+	-	-
A3DE	+	+	-	-	ND	ND	+	+	ND	ND
A3F	+	+	+	-	+	+	+	+	+	-
A3G	+	+	+	+	+	+	-	+	+	-
A3H	+	+	-	-	ND	ND	+	+	-	ND

SIV = Simian Immunodeficiency Virus; EIAV = Equine Infectious Anemia Virus; MLV = murine leukemia viruses; FV = Foamy Virus; LTR = Long Terminal Repeat based endogenous retroviruses; LINEs = Autonomous Long Interspersed Nuclear Elements; SINEs = non-autonomous short interspersed nuclear elements; HBV = Hepatitis B Virus; AAV = Adeno-associated virus; ND = Not Determined. (Adapted from Smith et al., 2012)

3.4.1.2 HIV-1 restriction by APOBEC3G/3F deamination activity

A3G was discovered through efforts to determine the HIV-1 Vif function that is required for the generation of infectious particles by non-permissive cells, particularly $CD4^+$ T cells, but not by permissive cells such as HEK293T (Madani and Kabat, 1998; Sheehy et al., 2002; Simon et al., 1998). Using a cDNA subtraction-based screen between the permissive cell line CEM-SS and the closely related but non-permissive CEM cell line, Sheehy et al (2002) identified A3G (firstly called CEM15) as a restriction factor and Vif as its counter-restriction factor. Indeed, A3G expression in CEM-SS cells is sufficient to render these cells non-permissive to HIV-1ΔVif replication. Additionally, inhibition of HIV-1ΔVif only occurs in the next viral cycle, indicating that A3G is incorporated into the viral particles. Xu et al. (2007) determined that approximately 7 (+/-4) molecules of A3G are incorporated into ΔVif viral particles produced from peripheral blood mononuclear cells (PBMCs) and showed that a few A3G molecules are necessary to inhibit HIV-1 replication. The identification of A3G as the restriction factor was soon followed by the characterization of A3F, which is also a potent retroviral inhibitor counteracted by Vif. A3F can perform its activity independently of A3G, is expressed in many human

tissues alongside with A3G and shows a partial resistance to Vif (Liddament et al., 2004; Wiegand et al., 2004; Zheng et al., 2004). However, A3G restricts HIV-1 to a greater extent than A3F and A3DE (Chaipan et al., 2013).

Concerning the other members of the A3 family, A3A restricts some endogenous retroelements and another DNA virus, but not HIV-1, due to its incapacity to associate with the HIV-1 PIC (Goila-Gaur et al., 2007; Zheng et al., 2012). However, recent studies showed that A3A has an anti-HIV-1 activity associated with a specific A3A protein variant. Indeed, deaminase activity in PBMCs or isolated primary monocyte-derived cells correlated with a variant whose translation initiated with methionine at residue 13 instead of residue 1 after treatment with IFN-α or IFN-α-inducing TLR ligands (Thielen et al., 2010). Furthermore, Berger et al (2011) showed that A3A counteracts HIV-1 replication during reverse transcription and inhibits the spread of replication-competent R5-tropic HIV-1, specifically in differentiated THP-1 cells, primary macrophages and DCs.

Several studies showed that A3B is also able to counteract HIV-1 replication even in the presence of HIV-1 Vif protein. A3B differs from A3G and A3F in that it is incapable to bind Vif protein and is therefore packaged into viral particles regardless the presence of Vif (Bogerd et al., 2007; Doehle et al., 2005). A3B inhibits HIV-1 in a cell type-dependent manner. A3B counteracts HIV-1 in commonly used cell lines (HEK293 and HeLa cells) but not in T cell lines, such as SupT1 and CEM-SS. It is currently thought that A3B may require an unknown A3B-interacting partner to perform its activity in HeLa or HEK293 cell lines. Affinity tag purification mass spectrometry and heterokaryon fusion experiments have yield a number of possible candidates for this unknown partner but it remains indeterminate (Hultquist and Harris, 2013).

Contrary to A3B, A3C possesses a limited cytidine deamination activity in non-permissive cells. This cause insufficient dG → dA substitutions that allows HIV-1 replication; thus, A3C may therefore contribute to HIV-1 diversity (Bourara et al., 2007). Indeed, Smith (2011) suggests that A3 members may produce favorable mutations which generate HIV-1 quasispecies and diversify viral genome. A3DE also counteracts HIV-1 replication in a Vif-sensitive manner although its activity is reduced compared with A3G and A3F (Dang et al., 2006). A3H was initially

characterized to lack antiretroviral activity against HIV-1 due to its low protein expression (Dang et al., 2008; OhAinle et al., 2006). However, in addition to the inactive A3H haplotype I (A3H HapI), several studies showed that other A3H haplotypes exist and some of them (A3H HapII, III, IV and V) are stably expressed and can potently restrict HIV-1 (Chaipan et al., 2013; Harari et al., 2009; Ooms et al., 2013). To summary, A3DE, A3F, and A3G possess the most relevant anti-HIV-1 activity *in vivo* (Refsland et al., 2012), although only A3G and A3F are considered to be the main HIV-1 restriction factors.

A3G/F is packaged into the budding virions by an interaction with the N-terminal domain of the nucleocapsid (NC) of Gag (Alce and Popik, 2004; Zennou et al., 2004; Zheng et al., 2012) (Fig. 11). In fact, HIV-1 virus particles deleted for the NC domain fail to incorporate A3G into the virions (Schäfer et al., 2004). Furthermore, HIV-1 RNA also promotes A3G incorporation into the virions by stabilizing the A3G-NC interaction (Burnett and Spearman, 2007; Khan et al., 2005). In this mechanism, the SL1 hairpin structure of the dimerization initiation site located in the 5'-untranslated region of the HIV-1 RNA is necessary for A3G incorporation (Khan et al., 2005). Additionally, Wang et al. (2007) showed that polymerase III-derived 7SL RNA is involved in A3G packaging. In this mechanism, NC domain of HIV-1 Gag mediates efficient packaging of 7SL RNA, as well as A3G. Reducing 7SL RNA packaging by overexpression of a 7SL RNA-binding protein (SRP19) inhibited 7SL RNA and A3G virion packaging (Wang et al., 2007).

Once packaged into the virion, A3G/F are introduced into the next target cell and perform their antiviral activity (Henriet et al., 2009). In this process, A3G/F remain attached to HIV-1 PIC with different affinity (A3F>A3G>A3C) (Burdick et al., 2013) and execute their cytidine deamination activity during reverse transcription. A3G/F induce a high level of dG → dA mutations (hypermutation) in the (+) DNA. These mutations reflect the previous dC → dU substitutions introduced by the cytidine deaminase activity of A3G/F on the (−) DNA during reverse transcription (Liddament et al., 2004; Zhang et al., 2003) (Fig. 5D and Fig. 11). A3G mutates (−) DNA 5'-CC → 5'CU and causes (+) DNA 5'GG → 5'AG substitutions (Liddament et al., 2004). A3B, A3DE, A3F, and A3H mutate 5'TC → 5'TU and cause 5'GA → 5'AA mutations. A3DE mutates (−) DNA 5'CG → 5'UG and produces 5'-GC → AC mutations (Zheng

et al., 2012). *In vitro* experiments determined that the (−) DNA, in its single-strand conformation, is the preferential substrate of A3G (10% of cytidines are mutated) rather than double-stranded DNA or RNA/DNA hybrids (Harris et al., 2003; Yu et al., 2004).

Recently, Holtz et al. (2013), using *in vitro* FRET-based oligonucleotide assays (fluorescence resonance energy transfer), have shown that the A3G deamination sites are governed by the sequence context surrounding the CC dinucleotide as well as the secondary structure of the ssDNA. A3G activity is enhanced when an A, C or T are present on either side of the CC, but G bases around this dinucleotide limit A3G activity. These results are supported by the fact that HIV-1 sequences recovered from infected individuals showed A3G deamination activity on 40% of 5'-CCCC-3' sequences, 21% of 5'-ACCA-3' sequences, 11% of 5'-TCCT-3' sequences and 0% of 5'-GCCG-3' (Jern et al., 2009). Concerning the structure of the ssDNA, A3G has a lower deamination activity for the CC positioned in ssDNA stem structures or the CC located in three base loops (Holtz et al., 2013). Moreover, the minimal ssDNA substrate length for A3G activity was recently determined to be a pentanucleotide containing the 5'-CCC motif located in the center of this molecule (Solomon et al., 2013).

It was initially proposed that the introduction of dC → dU mutations in the (–) DNA may activate uracil-DNA glycosylases (UDGs). These UDGs can recognize the U-containing (–) DNA generating a basic AP (apurinic/apyrimidinic) site leading to (–) DNA degradation by specific AP-endonucleases (Harris et al., 2003). However, this pathway is now considered improbable (Gillick et al., 2013), principally because decrease in viral cDNA is still observed in the absence of cellular UDGs (UNG2 and SMUG1) (Langlois and Neuberger, 2008). Despite that, dG → dA substitutions in the viral genome might lead to non-functional viral proteins or cause an integration defect of the viral genome (Franca et al., 2006; Harris et al., 2003; Wissing et al., 2010).

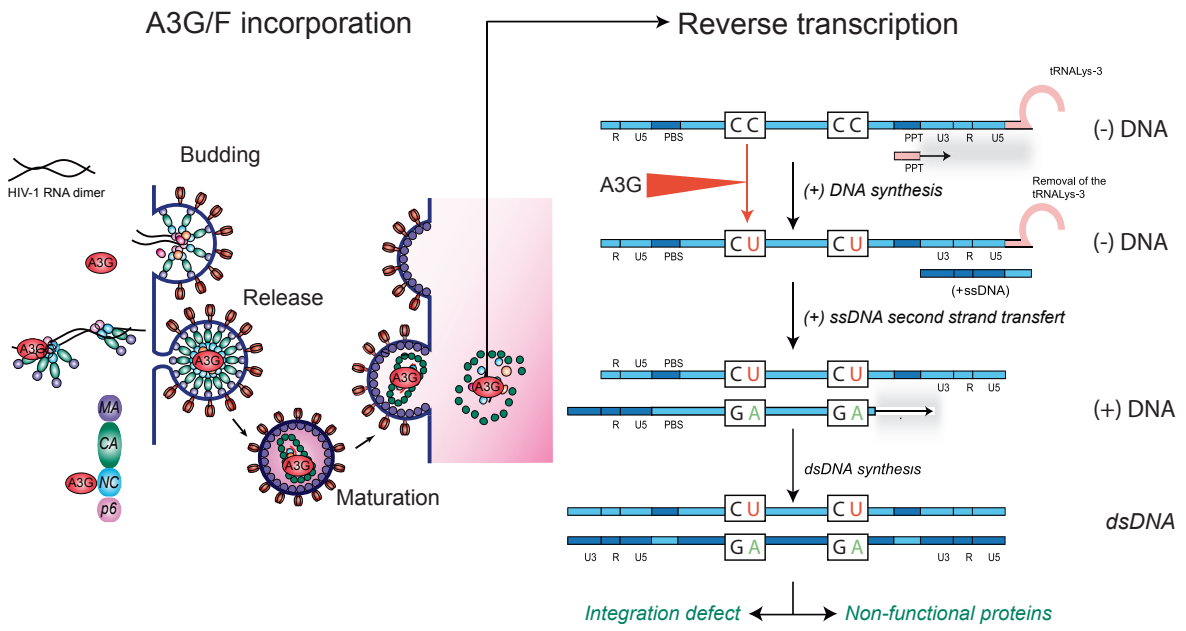

Figure 11. APOBEC3G/F impairs HIV-1ΔVif replication. A3G/F are incorporated into the viral particles and in the next viral cycle, A3G/F convert cytidines to uridines in the (-) DNA generating further integration defect or non-functional proteins production.

3.4.1.3 HIV-1 restriction by APOBEC3G/3F deamination-independent activity

Despite the fact that the antiviral activity of A3 family members is clearly associated to their cytidine deaminase activity (Harris and Liddament, 2004; Harris et al., 2003; Zheng et al., 2012), several studies showed that A3G/F also have an antiviral effect independently of their cytidine enzymatic activity. Shindo et al (2003) reported that the enzymatic activity of A3G is essential but not the only determinant of its antiviral activity. Indeed, the expression of the catalytically inactive domain alone (N-terminal domain) is sufficient to counteract HIV-1 replication (Li et al., 2004). Additionally, A3G mutants disrupted from their catalytically active domain are still capable of impairing HIV-1 infectivity and they can reduce the amount of HIV-1 cDNA generated in next viral cycle (Newman et al., 2005; Shindo et al., 2003). Similarly, it has been shown that A3G is also able to inhibit hepatitis B virus by a deamination-independent mechanism (Turelli et al., 2004).

Based on these observations, several studies have shown that A3G inhibits different steps of the reverse transcription process explaining how this deaminase-

independent activity decreases the level of viral cDNA (Bishop et al., 2006; Guo et al., 2006; Holmes et al., 2007; Li et al., 2004; Luo et al., 2007; Mangeat et al., 2003; Mbisa et al., 2007; Yang et al., 2007). Table 2 summarizes the effects of A3G/F *ex vivo* on the different reverse transcription steps of HIV-1ΔVif or HIV-1-derived clones (Henriet et al., 2009). Recently, Fehrholz et al (2012) have shown that A3G can also inhibit (–) RNA viruses such as measles (MV), mumps (MuV) and human respiratory syncytial virus (HRSV) independently of its deamination activity. Further studies showed that A3G can physically interact with the HIV-1 RT independently of the presence of other viral proteins or the genomic RNA. Additionally, residues 65 to 132 in the N-terminal domain of A3G are necessary for this interaction (Wang et al., 2012a).

Almost all of the previous studies cited in this section have been performed *ex vivo* using transfected cell lines, raising the possibility that A3G/F deamination-independent activity is an artifact of A3G/F overexpression and does not reflect the physiological microenvironment of HIV-1 target cells (Browne et al., 2009; Miyagi et al., 2007). However, Gillick et al (2013) have determined that both cytidine deamination and reverse transcription inhibition contribute to the antiviral effect of A3 proteins on HIV-1 virions from infected primary human $CD4^+$ T cell. Additionally, MacMillan et al (2013) showed that A3G/F deamination-independent activity occurs *in vivo* in mouse mammary tumor virus (MMTV)-infected mice. In this study, A3G is able to restrict MMTV reverse transcription independently to its deaminase activity.

Apart from the reverse transcription, Luo et al (2007) was the first to demonstrate that A3G/F also prevents viral DNA integration. Interestingly, wild-type A3G and A3F are able to interact with the PIC, especially with the integrase. This interaction negatively impairs the integration efficiency by 5- to 50-fold of HIV-1Δ*vif* (Luo et al., 2007; Mbisa et al., 2007, 2010). Indeed, A3G generates 6 base pairs (bp) extension at the viral U5 end of the 3' LTR causing the formation of aberrant 3'LTR.

Table 2. A3G/F effects on reverse transcription and integration *ex vivo* (Adapted from Henriet et al., 2009)

Fold change (reduction of products)					
Reverse transcription steps	A3G wt	A3G deaminase-minus	A3F wt	A3F deaminase-minus	Reference
tRNALys-3 annealing	2 (MT2, H9 or 293T)	1.5 (SupT1)			(Guo et al., 2006)
			2 (SupT1 and 293T)	1.4 (SupT1)	(Yang et al., 2007)
-ssDNA synthesis	>10 (SupT1)	2 (SupT1)	5 (SupT1)	5 (SupT1)	(Holmes et al., 2007)
	>20 (SupT1)		4 (SupT1)		(Bishop et al., 2006)
	2 (SupT1)				(Guo et al., 2006)
			2 (SupT1)		(Yang et al., 2007)
	2 (SupT1)				(Li et al., 2007)
	1.7 (HeLa)	1.7 (HeLa)	2 (HeLa)		(Luo et al., 2007)
First-strand transfer	3 (SupT1)	3 (SupT1)			(Li et al., 2007)
	1.15 (293T)				(Mbisa et al., 2007)
-ssDNA synthesis	20 (SupT1)	1.4 (SupT1)			(Guo et al., 2006)
			20 (SupT1)		(Yang et al., 2007)
	20 (SupT1)				(Li et al., 2007)
	3 (HeLa)	3 (HeLa)	5 (HeLa)		(Luo et al., 2007)
Second-strand transfer	10 (SupT1)	10 (SupT1)	>10 (SupT1)	10 (SupT1)	(Li et al., 2007)
	2-3 (293T)				(Mbisa et al., 2007)
Proviral DNA synthesis	5–10 (293T)				(Mbisa et al., 2007)
	3 (HeLa)				(Mangeat et al., 2003)
Integration	5 (293T)	No effect (293T)			(Mbisa et al., 2007
	3 (HeLa)	3 (HeLa)	>10 (HeLa)		(Luo et al., 2007)
	7 (HOS)				(Mariani et al., 2003)
	7.2		3.4		(Mbisa et al., 2010)

This aberrant structure causes ineffective +ssDNA transfer (Fig. 5E) and inefficient integration. In this mechanism, A3G deaminase activity is essential to generate the 6-bp extension. In contrast, A3F is not able to generate a 6-bp extension but impairs integration more efficiently than A3G by reducing the 3' processing of viral DNA at both the U5 and U3 ends (Mbisa et al., 2010).

Despite the fact that almost all studies cited above were carried out with wild-type A3G or A3F, there is evidence that A3G/F mutants can impair the integration of HIV-1Δ*vif* in a deamination-independent mechanism. In the same studied performed by Luo et al (2007), it was also reported that A3G C291S, an A3G mutant previously described as inactive for deamination activity (Newman et al., 2005), can also inhibit HIV-1Δ*vif* integration. This mutant is also capable of interacting with the integrase present in HIV-1Δ*vif* clones. This interaction may abrogate the structural conformation of the PIC preventing nuclear import and integration of viral DNA. Additionally, Mbisa et al (2010) also shown that the mechanism by which A3F impairs HIV-1Δ*vif* integration (described above) is partially dependent on A3F cytidine deaminase activity.

3.4.1.4. HIV-1 Vif: general characteristics and biological functions

Vif function in the infected cell

Vif is encoded for by all lentiviruses except for the Equine Infectious Anemia Virus. In HIV-1, the gene product is a 23 kDa basic protein that is produced in a Rev-dependent manner (Mandal et al., 2009) during the late phase of the replication cycle. This protein has been named Vif because its deletion has been associated with a reduction or a complete loss of viral infectivity (100 to 1,000 fold) (Strebel et al., 1987). Interestingly, this phenotype is cell-type specific since Vif was shown to be required in cells termed non-permissive such as lymphocytes, PBMC, or macrophages (Borman et al., 1995; Courcoul et al., 1995; Fan and Peden, 1992; Gabuzda et al., 1992; Sova and Volsky, 1993; von Schwedler et al., 1993). By contrast, production of infectious particles does not require a functional Vif in permissive cell lines such as non-hematopoietic cells (HeLa, 293T, Cos7) and some leukemic T-cells (Jurkat, SupT1, C8166) (Gabuzda et al., 1992; Sakai et al., 1993). The observation that some, but not all cell lines require Vif for the production of infectious virus, could be explained by the fact that either permissive cells express a positive factor that substitutes for the absence of Vif, or else non-permissive cells express a negative factor that is counteracted by Vif. The fusion of these two cell types, giving rise to heterokaryons, exhibited a non-permissive phenotype indicating the presence of an intrinsic antiviral factor in non-permissive cells (Madani and Kabat, 1998; Simon et al., 1998). By using subtractive cDNA cloning analyses (permissive versus non-permissive cells), Sheehy and collaborators identified the cellular factor APOBEC3G, or A3G (Sheehy et al., 2002). When expressed in permissive cells, this factor renders these cells non-permissive for the replication of HIV-1Δ*vif* viruses (by reducing their infectivity) and northern blot analysis showed that A3G mRNAs were exclusively expressed in non-permissive cells (Sheehy et al., 2002). Altogether, these results showed that A3G is necessary and sufficient to confer the non-permissive phenotype to cells targeted by HIV-1.

Vif-mediated neutralization of APOBEC3G

The different mechanisms used by Vif to prevent the antiviral activity of A3G/3F have been extensively studied (Conticello et al., 2003; Liu et al., 2005; Marin et al., 2003;

Mehle et al., 2004b; Sheehy et al., 2003; Stopak et al., 2003; Yu et al., 2003). The main mechanisms are briefly reviewed here (Fig. 12A), and readers can consult recent reviews for more detailed explanations (Albin and Harris, 2010; Henriet et al., 2009; Smith et al., 2009). Firstly, the inhibition of A3G packaging by Vif is associated with a strong reduction of its intracellular level, which has been attributed to the poly-ubiquitination and proteasomal degradation of A3G/3F by Vif (Conticello et al., 2003; Liu et al., 2005; Marin et al., 2003; Mehle et al., 2004b; Sheehy et al., 2003; Stopak et al., 2003; Yu et al., 2003). Indeed, Vif is able to bind A3G/3F through various domains (Fig. 13C), and to recruit an E3 ubiquitin ligase complex composed of Elongin B, C, Cullin 5, and Rbx2 leading to the poly-ubiquitination and degradation of A3G/3F (Luo et al., 2005; Mehle et al., 2004a; Mehle et al., 2006; Yu et al., 2003) (Fig. 12A, pathway 2). Very recently, the transcription cofactor CBF-β (Core Binding Factor) has been shown to be an integral component of this ubiquitin ligase complex and to be required for Vif-mediated degradation of A3G (Hultquist et al., 2012; Hultquist et al., 2011b; Jager et al., 2011; Zhang et al., 2011). Besides, Vif has also been shown to counteract A3G by inhibiting its translation (Fig. 12A, pathway 3) (Kao et al., 2003; Mariani et al., 2003; Stopak et al., 2003). Yet this process is not clearly understood, but our last study suggests that a steric hindrance mechanism may be considered as Vif was shown to specifically bind to the 5'-untranslated region (UTR) of A3G mRNA, that is required for the translational repression ((Mercenne et al., 2010) and S. Guerrero, J.-C. Paillart, unpublished results). Lastly, the simplest way to prevent A3G activity is probably to prevent its packaging into virions (Sheehy et al., 2003), and indeed reports showed that Vif was able to impede packaging and counteract the antiviral activity of a degradation-resistant A3G variant (Fig. 12A, pathway 1) (Mariani et al., 2003; Opi et al., 2007). Interestingly, during virus assembly, A3G interacts with the nucleocapsid (NC) domain of $Pr55^{Gag}$ and the genomic RNA, while the same partners are involved in the packaging of Vif (Burnett and Spearman, 2007; Khan et al., 2005; Luo et al., 2004; Schafer et al., 2004; Svarovskaia et al., 2004; Zennou et al., 2004), suggesting that Vif may prevent A3G packaging by means of a competition mechanism.

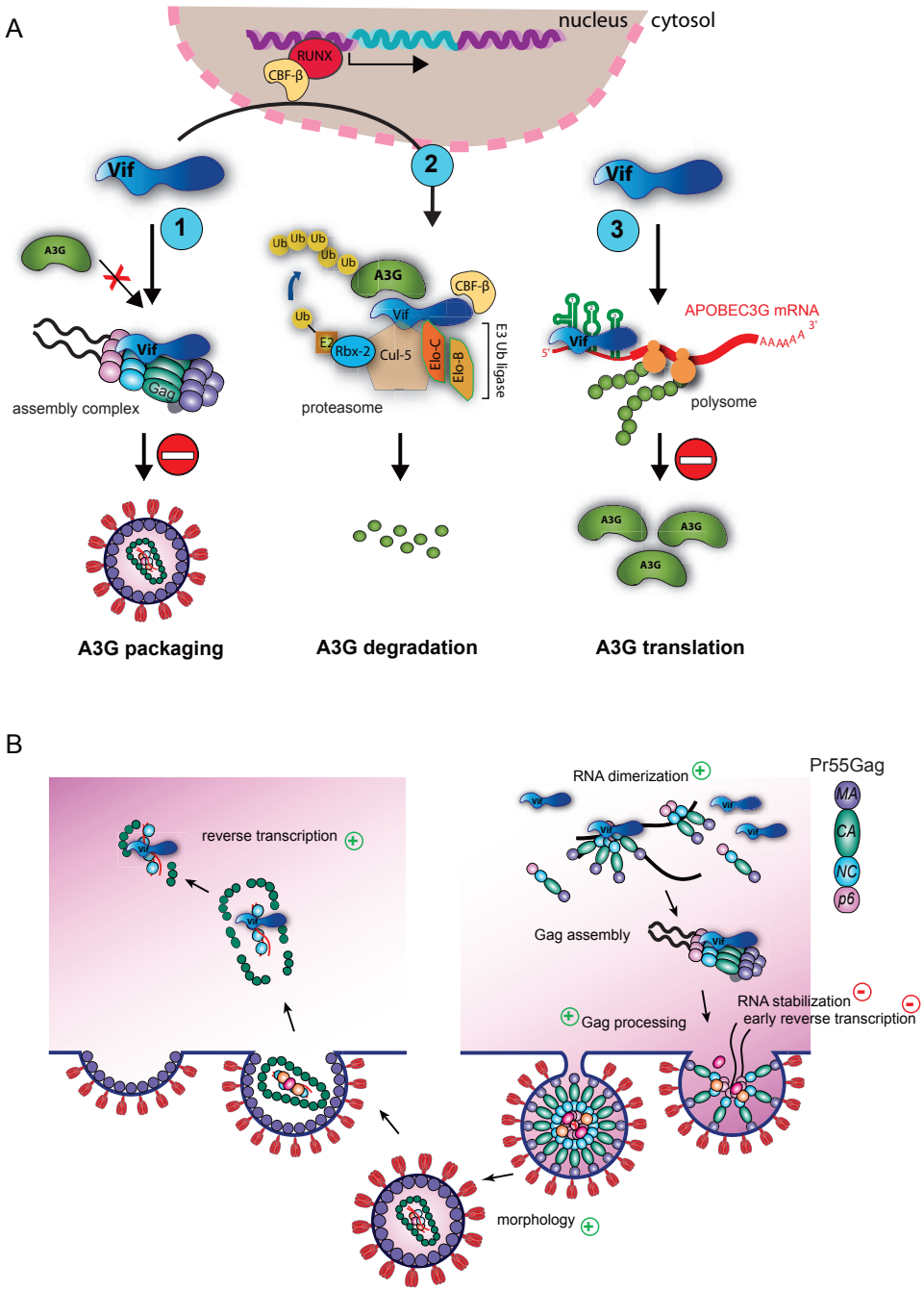

Figure 12: Schematic representation of the functions of Vif and cellular A3G in the course of HIV-1 replication. (A) During viral particle assembly, Vif is found in the cytoplasm of infected cells and is packaged at a low copy number into virions. Vif neutralizes A3G/A3F in virus-producing cells by different mechanisms. (1) Vif competes with A3G for binding to viral components like the nucleocapsid domain of Gag and/or the genomic RNA. (2) Vif binding to A3G recruits an E3 ubiquitin ligase that mediates the poly-ubiquitynation of A3G and its degradation. (3) Vif impairs the translation of A3G mRNA through an mRNA-binding mechanism. Taken together, these three different actions of Vif on translation, degradation and packaging not only deplete A3G from virus-producing cells but also prevent A3G from being incorporated in virions. (B) Intracellular Vif may also influence viral assembly by regulating in a timely fashion genomic RNA dimerization and protease (PR)-mediated cleavage of the Gag precursor molecules. Due to its chaperone activities, Vif could facilitate late events such as Gag precursor maturation, RNA dimer maturation and initiation of reverse transcription during and after viral budding. Finally, Vif might participate in virion morphology and in reverse transcription after viral entry. The green “plus” and red “minus” signs indicate the positive and negative effects of Vif, respectively.

Functions of Vif in virus assembly

Beside its action against the APOBEC3 restriction factors, Vif was found to be involved in the late steps of virus replication (Fig. 12B). Indeed Vif interacts with the $Pr55^{Gag}$ polyprotein precursor, that drives virus assembly, and the $Pr160^{Gag\text{-}Pol}$ precursor, possibly allowing its transient association with Gag assembly intermediates in the cytoplasm (Akari et al., 2004; Bardy et al., 2001; Bouyac et al., 1997; Lee et al., 1999). Accordingly Vif is able to counteract the effect of a betulinic acid derivative that inhibits HIV-1 Gag assembly (Dafonseca et al., 2008).

In addition, Vif, as an RNA-binding protein, can bind to the HIV-1 genomic RNA in vitro (Bernacchi et al., 2007; Henriet et al., 2005) and in infected cells (Dettenhofer et al., 2000; Zhang et al., 2000). This interaction seems to be required for Vif packaging, since inhibiting RNA packaging by mutating NC or the Psi packaging signal led to a complete absence of Vif in virions (Khan et al., 2001). This RNA-binding ability of Vif seems to be governed by its N-terminal domain (Fig. 13) (Khan et al., 2001; Zhang et al., 2000).

Vif was also reported to be required for normal virion morphology and optimal core stability (Borman et al., 1995; Ohagen and Gabuzda, 2000; Sakai et al., 1993). As this defect has been exclusively observed in ∆vif virions produced from non-permissive cells, it is likely a (direct or indirect) consequence of the expression of the antiretroviral factors A3G/3F in these cells, even though the involvement of another cellular factor cannot be totally excluded. In fact, it is known that APOBEC3G inhibits some of the reverse transcription steps that require the RNA chaperone activities of NC (Guo et al., 2007; Iwatani et al., 2007; Yang et al., 2007). These are precisely the steps that Vif is able to activate (Henriet et al., 2007). As NC is a more potent RNA chaperone activity than Vif (Henriet et al., 2007), Vif would not be required in the absence of A3G (i.e. in permissive cells), however, it would be required in restrictive cells, because NC chaperone activities are inhibited by APOBEC3G in these cells.

Moreover, NC and RT were less stably associated with the viral core in HIV-1∆*vif* particles (Hoglund et al., 1994), and $Pr55^{Gag}$ processing by the viral protease (PR) was altered at the MA-CA and CA-NC junctions (Akari et al., 2004; Bardy et al., 2001; Kotler et al., 1997). Even though Vif is dispensable for HIV-1 replication in permissive cells, it appears to be part of the HIV-1 replication machinery during early

reverse transcription and acts as an helper factor to promote reverse transcription and viral infectivity (Carr et al., 2008; Carr et al., 2006; Henriet et al., 2007; Kataropoulou et al., 2009). Indeed, HIV-1 Δvif replicated normally in permissive cells under optimal *in vitro* replication conditions; however, HIV-1 Δvif replication was impaired at the level of reverse transcription when cells were treated with a thymidylate synthase inhibitor that altered the cellular dNTP levels, suggesting that preventing the A3G anti-viral action is not the only biological function of Vif.

Vif functions in virus assembly could be viewed as controversial (Henriet et al., 2009) because Vif modulates PR activity but does not prevent maturation of newly made virions. Along this line little Vif is found in cell-free virions (between 10-100 molecules, with a Vif/Gag ratio of 1/47 to 1/89) while it is found in large quantity in cells (Vif/gag ratio 1:1.1 to 1:1.3) (Fouchier et al., 1996; Simon et al., 1999). One hypothesis could be that Vif acts as a temporal regulator of $Pr55^{Gag}$ assembly and processing and should thus be considered as a Janus factor with both protein and RNA chaperone activities (Henriet et al., 2007; Kovacs et al., 2009; Tompa and Kovacs, 2010) (see below section 5). In accordance with this notion, Vif might prevent premature Gag processing in the cytoplasm of infected cells, and/or modulate PR activity, thus inhibiting premature reverse transcription (Akari et al., 2000; Bardy et al., 2001; Kotler et al., 1997; Mougel et al., 2009). This could be achieved either by direct transient interactions with PR and $Pr55^{Gag}$ or by modulating $Pr55^{Gag}$-RNA interactions. Thus, a competition mechanism preventing the majority of Vif from being recruited into viral particles can be envisioned where Vif acts in a transient manner.

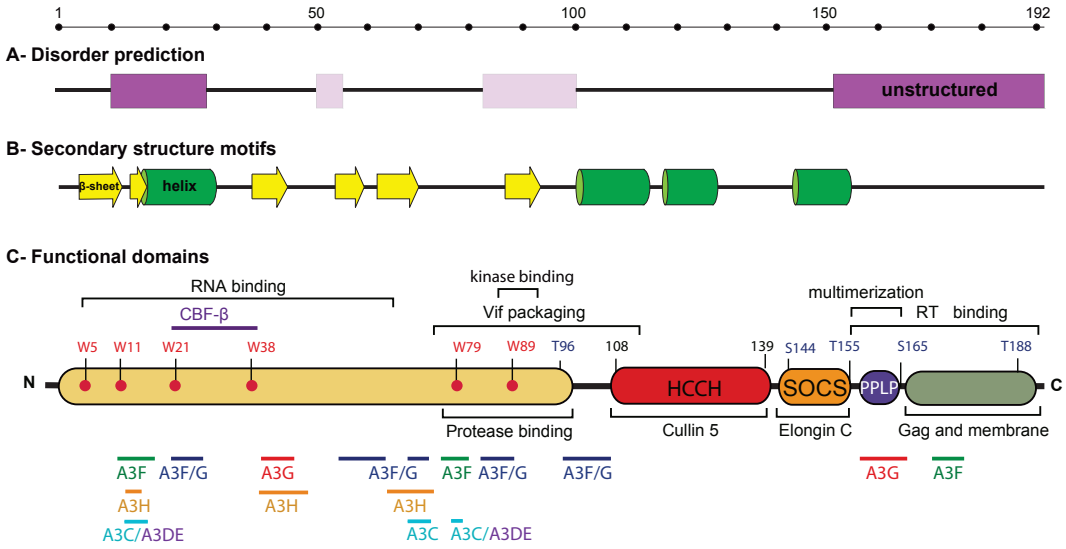

Vif model (Lv et al.) Vif model (Balaji et al.) Vif SOCS-Box (Stanley et al.)

Figure 13. Vif Sequence, structure and domains. (A) Vif disordered domain prediction according to *Predictor of Naturally Disordered Regions* (*PONDR*®): dark and light purple boxes correspond to highly disordered domains (PONDR score > 0.5), and slightly disordered domains (PONDR score between 0 and 0.2), respectively. (B) Vif secondary structure prediction showing strand in yellow arrows and helices in green was performed using PsiPred (McGuffin et al., 2000). (C) Schematic representation of Vif functional domains described in the text together with key residues and the interaction map with A3G, A3F, A3H, A3C, A3DE, and other Vif partners. (D) Vif multimerization domain, including the PPLP motif has been enlarged for a detailed description. (E) 3D structure of Vif. Left panel: structural model of Lv and collaborators (Lv et al., 2007), colored according to Vif functional domains in C; central panel: structural model (PDB: 1VZF) from Balaji and collaborators (Balaji et al., 2006); right panel: tridimensional structure of the Vif SOCS box (PDB: 3DCG - residues N_{140}-P_{156} - (Stanley et al., 2008)) with the same orientation as the left model.

3.4.1.5. Structural organization of Vif

Biochemical properties of Vif

The HIV-1 Vif protein is a small basic protein (pI=10.7) composed of 192 amino acids (23 kDa) where the N-terminus is enriched in tryptophan residues (Fig. 13C). The presence of a high number of conserved hydrophobic amino acids (38.5% of Vif, including 8 tryptophan and 16 leucine residues) might well explain why Vif has a strong tendency to form aggregates in solution (Fig. 13C). Interestingly, each of these tryptophan residues has been shown to be important for the binding of either A3G or A3F (see below and (Tian et al., 2006)). Several amino acids (T_{96}, S_{144}, T_{155}, S_{165}, T_{188}) are potential targets for cellular kinases (such as MAPK) and their phosphorylation seems to play important roles in HIV replication (Yang and Gabuzda, 1998; Yang et al., 1996). Indeed, mutating T_{96} or S_{144} leads to a marked decrease in virus infectivity. Finally, the L_{150} residue has been shown to be a processing site for HIV-1 PR (Khan et al., 2002) since mutating this residue affected viral infectivity, suggesting that Vif processing is important for function.

Alignment of HIV-1 Vif sequences highlights several conserved domains that correlate with the predicted secondary structure of Vif (Barraud et al., 2008). At the N-terminus, amino acids ^{63}RLVITTYW^{70} and ^{86}SIEW^{89} are important to form β-sheet structures that are involved in the regulation of Vif expression and in viral infectivity (Fujita et al., 2003). The last two amino acids, E_{88} and W_{89} of this β-sheet structure are also part of a hydrophilic region ^{88}EWRKKR^{93} and are critical for the replication of HIV-1 in target cells by enhancing the steady-state expression of Vif (Fig. 13B) (Fujita et al., 2003). In the central region, residues 108-139 constitute a non-consensus HCCH zinc finger motif that binds zinc and Cullin 5 (Mehle et al., 2006; Xiao et al., 2006). Next to this HCCH motif is the so-called SOCS box (^{144}SLQYLA^{149}) (Fig. 13C) due to high similarities with boxes present in SOCS (Suppressor Of Cytokine Signaling) proteins. The last highly conserved domain is the ^{161}PPLP^{164} motif also known as the Vif multimerization domain (Fig. 13C and 13D) (Yang et al., 2003; Yang et al., 2001). Interestingly, this motif belongs to the C-terminal region of Vif, predicted to be intrinsically disordered (Reingewertz et al., 2009), while being involved in many important interactions (see below).

Structured and disordered domains of Vif

Due to its intrinsic properties, characterization of the 3D-structure of Vif is still a challenging problem and a matter of intense research. In fact Vif has a high tendency to aggregate in solution, which hampers the production of large amounts of soluble Vif required for crystallization assays and NMR studies. The 3D-structure of Vif has been predicted on the basis of model proteins that share similar secondary structure elements (Fig. 13E) (Balaji et al., 2006; Lv et al., 2007). High secondary structure similarities were found between both the N- and C-terminal domains of Vif and NarI and the SOCS Box from the VHL protein, respectively (Iwai et al., 1999). These proteins can also bind to Elongin B and C. Moreover, this model correctly fits with the secondary structure prediction shown in the alignment (Fig. 13B), contrary to the model of Balaji and collaborators which predicts only one helix (Fig. 13E). If such models are helpful to understand Vif protein organization, they unfortunately lack important Vif sequence information such as the HCCH zinc finger motif, as well as the long C-terminal region predicted to be disordered (Reingewertz et al., 2010), which constitutes another limiting factor for the crystallization of the full length Vif protein.

Yet only a very short fragment of Vif corresponding to the SOCS Box (residues 139 to 179) has been crystallized in a complex with Elongin B and C (Stanley et al., 2008). The crystal structure of a shorter fragment (residues 140 to 156) has been solved at 2.4 Å resolution (PDB: 3DCG), showing a loop-helix structure that forms a highly hydrophobic interface allowing binding to Elongin C (Fig. 13E). Interestingly, the structure of this peptide could fit in the predicted model of Lv and collaborators (in place of another helix) and could also be included in place of an unstructured sequence in the model of Balaji and collaborators (Fig. 13E - SOCS box in orange). Despite the lack of full-length Vif 3D-structure, the function of Vif has been extensively investigated by mutational and functional domain analyses. As for other HIV-1 accessory proteins, Vif appears to be a multifunctional protein with several domains involved in specific and/or overlapping functions, notably the disordered C-terminus (Tompa and Kovacs, 2010).

The N-terminal tryptophan rich domain: A3G, genomic RNA and CBF-β

As mentioned above, the N-terminal region of Vif is enriched in hydrophobic amino acids, notably in tryptophan residues that are conserved. Mutagenesis studies have shown that these residues are important for binding to either A3F or A3G. Binding to A3F requires residues W_{11}, W_{79}, Q_{12} and the ^{14}DRMR^{17} motif (Fig. 13C) (Russell and Pathak, 2007; Schrofelbauer et al., 2006; Tian et al., 2006). Interestingly, binding to A3G involves other residues, namely W_5, W_{21}, W_{38}, W_{89}, I_9, K_{22}, E_{45}, N_{48} and the ^{40}YRHHY^{44} and ^{85}VSIEW^{89} motifs that are the key residues for A3G binding (Fig. 13C) (Mehle et al., 2007; Russell and Pathak, 2007; Santa-Marta et al., 2005; Simon et al., 2005; Wichroski et al., 2005). Other domains have been described to be important for A3G binding, especially the PPLP motif in the C-terminal domain (Fig. 13C). Such discontinuous interacting sites suggest that the correct folding of Vif is crucial to generate the binding platform allowing interaction with APOBEC3 proteins. More recently, Vif residues important for interaction with A3H, A3C and A3DE have also been identified in the N-terminal region (Binka et al., 2012; Pery et al., 2009; Zhang et al., 2008; Zhen et al., 2010)

The N-terminal region of Vif and more precisely the first 64 amino acids are also involved in genomic RNA binding both *in vitro* (Bernacchi et al., 2007; Henriet et al., 2005) and in infected cells (Dettenhofer et al., 2000; Zhang et al., 2000). Deletion analysis underlined the importance of amino acids 75-114 for the binding of Vif to RNA in infected cells (Khan et al., 2001). CBF-β (Core Binding Factor β), a partner of Vif involved in the E3 ubiquitin ligase recruitment, has recently been identified and the interaction domain mapped to the N-terminal domain of Vif, with an important role for W_{21} and W_{38} (Hultquist et al., 2011a; Jager et al., 2011; Zhang et al., 2011). Finally, Vif binds to the viral PR through residues 78-98 (Baraz et al., 2002) and to the cellular MDM2 E3-ligase involved in its degradation by the proteasome (Izumi et al., 2009).

The HCCH central zinc finger domain

One of the major functions of Vif is to recruit an E3 ubiquitin ligase in order to target A3G for proteasomal degradation. The E3 ligase recruited by Vif is composed of Elongin B, Elongin C, CBF-β, Cullin 5, and Rbx2 proteins (Yu et al., 2003). The

Cullin 5 binding domain (Yu et al., 2004b) involves residues C_{114} and C_{133} of the conserved HCCH zinc finger motif (Xiao et al., 2007) of the form H^{108}-$(X)_5$-C^{114}-$(X)_{18}$-C^{133}-$(X)_5$-H^{139} , that is different from a conventional zinc finger. In fact its primary structure is not found in other classes of zinc binding proteins and thus can be considered to be Vif specific. This motif represents a *bona fide* zinc finger (Mehle et al., 2006; Xiao et al., 2007), where each zinc-coordinating residue has been shown to be important for the binding of Cullin 5. Changing sequences and spacing between HCCH residues affected the binding to Cullin 5, viral infectivity, and A3G degradation (Mehle et al., 2006). Interestingly, the conformation of both the HCCH motif and the whole Vif protein is altered upon zinc binding (Paul et al., 2006). Moreover, the aggregation of Vif is favored by zinc, but in a reversible manner (Paul et al., 2006).

The SOCS box: Elongin C binding domain

This highly conserved sequence is composed of residues ^{144}SLQ-(Y/F)-LA^{149} and alanine substitution in the SLQ motif leads to important defects in virus infectivity (Schmitt et al., 2009). This region promotes the interaction with the heterodimer Elongin C/Elongin B (Yu et al., 2004b) and is therefore important for the recruitment of the E3 ubiquitin ligase that targets A3G for degradation. This interaction occurs *via* a hydrophobic platform on both proteins (Wolfe et al., 2010), requiring the SLQ residues and the last A_{149} of the motif (Yu et al., 2004b) together with α-helix 4 of Elongin C (Stanley et al., 2008). Very recently, it has been shown that interactions between Vif and Elongin C/B also involve downstream elements such as the Cullin 5 box and the ^{161}PPLP^{164} motif (see below and (Bergeron et al., 2010; Wolfe et al., 2010))

The intrinsically disordered C-terminal domain

The C-terminal region of Vif is intrinsically disordered (Fig 13A) and starts with a putative Cullin 5 box (residues 159-173), that is able to recruit Cullin 5 (Stanley et al., 2008) but with a lower efficiency compared to the HCCH zinc finger domain (Wolfe et al., 2010). This region encompasses the ^{161}PPLP^{164} motif involved in Vif multimerization (Fig. 13D) (Yang et al., 2003; Yang et al., 2001). This PPLP motif is also involved in the interaction with various partners such as A3G (Donahue et al.,

2008; Miller et al., 2007), Elongin B/Cullin 5 (Bergeron et al., 2010; Wolfe et al., 2010), HIV-1 RT (Kataropoulou et al., 2009) and the cellular kinase Hck (Douaisi et al., 2005; Hassaine et al., 2001). Finally, the last 25 residues are important for Vif interaction with $Pr55^{Gag}$ (Bouyac et al., 1997; Simon et al., 1999; Syed and McCrae, 2009), cytoplasmic membranes (Goncalves et al., 1995) and RT (Kataropoulou et al., 2009).

The disordered nature of the C-terminal region (see Fig. 13A) is in line with secondary structure prediction models (Reingewertz et al., 2010) and the 3D-structure analysis of Vif where only the first 15 amino acids of the analyzed peptide (40 residues) have been observed. No electron density was detected for the rest of the protein, reflecting the intrinsically disordered nature of the C-terminus (Stanley et al., 2008). Deuterium incorporation assays showed that this small part of Vif folds upon binding to Elongin C, which is also refolded upon Vif binding (Marcsisin and Engen, 2010). Such Vif-induced folding has also been observed in our laboratory upon Vif binding to specific RNA sites such as the Trans-acting Responsive element (TAR) (see below and (Bernacchi et al., 2011)).

3.4.1.6. Vif multimerization

Vif multimerization was initially detected *in vitro* by GST pull-down, co-immunoprecipitation and two hybrid assays (Yang et al., 2001). A deletion mutagenesis approach allowed to characterize residues 151-164, encompassing the conserved proline-rich region ^{161}PPLP^{164}, as the domain governing Vif multimerization. The importance of this ^{161}PPLP^{164} motif has been later highlighted using competitor peptides and deletion/substitution mutants (Bernacchi et al., 2011; Yang et al., 2003). Recently, this motif has been shown to be required for the assembly of an active E3 ubiquitin ligase complex, as a second binding motif for the Elongin C/B and Cullin5 (Bergeron et al., 2010; Wolfe et al., 2010).

Importance of the Vif PPLP motif in HIV-1 replication

This motif was found to be important for Vif function and virus infectivity since mutating this motif resulted in a 2.5-fold reduction of infectivity in non-permissive

cells (Donahue et al., 2008) and antagonist peptides containing the ^{161}PPLP^{164} motif drastically diminished virus replication (Miller et al., 2007; Yang et al., 2003). The reduced virus infectivity could be explained in both cases by the lost of Vif A3G-degradation function. Indeed, Miller and coworkers (Miller et al., 2007) showed that the antagonist peptides were associated with an augmented A3G packaging into viral particles. Donahue and collaborators showed that substituting AALP for PPLP impaired Vif-induced degradation of A3G, which was mainly due to the reduced binding of A3G, without affecting the interaction with Elongin C and Cullin 5 (Donahue et al., 2008). Similarly, this substitution favored A3G incorporation into virions but did not abrogate the translational regulation of A3G mRNA by Vif (Mercenne et al., 2010). However, the PPLP motif does not seem to be the only one to be involved in Vif multimerization as a recent study pointed out the involvement of domains such as the HCCH motif, the BC box and downstream residues (S165 and V166) in this property of Vif (Techtmann et al., 2012). It is also interesting to notice that while the PPLP motif is conserved in all HIV-1 isolates, this motif is absent in HIV-2 and SIV Vif (Barraud et al., 2008) and the C-terminal regions are the most divergent, beside the fact that both HIV-2/SIV Vif proteins are 25 amino acids longer than the HIV-1 Vif (Yamamoto et al., 1997). Whereas the HIV-1 Vif C-terminal region is highly hydrophilic (and seems important for the association with membranes), the same region of HIV-2 Vif is hydrophobic. Finally, while both Vif proteins have the same functions and are interchangeable in some cellular conditions (Reddy et al., 1995), differences in some structural domains (oligomerization domain for instance) may suggest that the mechanism of action of HIV-1 and HIV-2/SIV Vif proteins may not be completely identical. Up to now, oligomerization properties of HIV-2/SIV Vif proteins are unknown.

RNA binding and Vif folding

As mentioned above, the PPLP motif is located in a strategic binding platform for Vif partners. With respect to the involvement of the PPLP motif in Vif oligomerization, it is conceivable that the functions of those partners could be linked to the multimerization state of Vif. We recently report that alanine substitution of the PPLP motif (Vif-AALA) did not significantly affect the overall secondary structure of Vif, but affects its oligomerization state (Bernacchi et al., 2011). Nevertheless, Dynamic Light

Scattering experiments showed that the AALA Vif mutant was still able to form protein dimers, suggesting that other domains are involved in Vif-Vif interactions, as mentioned in another study using deuterium exchange assays (Marcsisin and Engen, 2010). Mutating the PPLP motif also led to a decrease of Vif binding affinity and specificity for nucleic acids (Bernacchi et al., 2011).

Interestingly, the high affinity binding of wild-type Vif to the TAR element led to the formation of high molecular mass complexes and was associated with Vif folding since the proportion of disorder, defined by circular dichroism experiments, decreased from 40% in absence of RNA to less than 20% in presence of TAR, and β-sheet structures increased from 40% to 70%. This folding process was not observed when AALA was substituted for the PPLP motif (Bernacchi et al., 2011). Altogether, these results showed that both the PPLP motif and RNA binding are important to induce, at least in part, Vif folding. As mentioned above, the Vif-Elongin C interacting domain has also been shown to undergo structural rearrangements upon binding (Marcsisin and Engen, 2010).

These observations strongly suggest that Vif (or at least its C-terminal domain) is disordered in its free form and can fold upon interactions, thus ensuring multiple functions (He et al., 2009). These properties are characteristic of proteins with RNA and/or protein chaperone activities (Tompa and Kovacs, 2010): as a general mechanism, such protein-protein and protein-RNA interactions induce the folding of both the chaperone and the target molecules upon binding, forming a functional complex (Semrad, 2011; Tompa and Csermely, 2004). This has already been described for several HIV-1 proteins such as the NC protein (Muriaux and Darlix, 2010; Rein, 2010) and more recently proposed for the Tat protein (Xue et al., 2011). This new potential role of Vif and its impact on HIV-1 replication are described below.

3.4.1.7. RNA chaperone activity of Vif

The three-dimensional structure of cellular and viral RNA molecules is crucial for function, but RNA molecules tend to adopt non-functional structures due to kinetic and thermodynamic folding traps (Herschlag, 1995). In order to prevent and resolve these non-functional conformations, proteins with RNA chaperone activity are essential during the RNA folding process (Cristofari and Darlix, 2002). An RNA

chaperone is defined as a partially disordered protein that binds transiently and non-specifically to RNA molecules, preventing their misfolding in an ATP independent-manner. Once the RNA has been correctly folded, the protein is no longer needed and the RNA conformation remains stable (Cristofari and Darlix, 2002).

Proteins with RNA chaperone activity are widespread and are implicated in essential cellular functions (Rajkowitsch et al., 2007). The list of RNA chaperones is constantly increasing and a database has been constructed (http://www.projects.mfpl.ac.at/rnachaperones/index.html) in which RNA chaperones are classified into families according to their primary function (Rajkowitsch et al., 2007). Here, we will focus on retrovirus-encoded RNA chaperones, specifically those encoded by HIV-1.

Nucleocapsid proteins (NCp) from Rous sarcoma virus (RSV) and murine leukaemia virus (MuLV) were the first retrovirus-encoded RNA chaperones to be described (Prats et al., 1988). Later, the RNA chaperone activity of HIV-1 NC was documented using different approaches. *In vitro*, HIV-1 NC increases hammerhead-ribozyme cleavage of an RNA substrate (Tsuchihashi et al., 1993), facilitates annealing of complementary DNA oligonucleotides and promotes strand exchange between complementary double-stranded and single-stranded DNA oligonucleotides (Tsuchihashi and Brown, 1994). In cell culture, NCp efficiently increases splicing of a thymidylate synthase mRNA mutant in a HIV-1 folding trap assay (Clodi et al., 1999). It has also been reported that in addition to NCp7, Vif and the transcription activator (Tat) possess RNA chaperone activity (Henriet et al., 2007; Kuciak et al., 2008a).

Next, we will briefly summarize the RNA chaperoning activity of Vif in parallel with that of NCp7 and Tat, and discuss how this could influence virus assembly and Gag processing, thus regulating the final stage of virion formation including reverse transcription by means of a molecular crowding phenomenon where Vif in excess has a negative impact on NC functions, which is relieved once virions are released from the cells and matured (Darlix et al., 2011a).

Dimerization of the genomic RNA

During virus assembly, the full-length viral genomic RNA is packaged in the form of a dimeric RNA (Chen et al., 2009; Housset et al., 1993) where the two copies are

physically linked through a site called the dimer linkage structure (DLS) located close to their 5' ends. Dimerization and subsequent packaging of the HIV-1 RNA dimer are mediated by interactions between the NC domain of $Pr55^{Gag}$ and the 5'-end of the viral genome (Reviewed in (Lu et al., 2011; Paillart et al., 1996; Paillart et al., 2004; Russell et al., 2004)). The HIV-1 genomic RNA can form two different kinds of dimers *in vitro*, termed loose and tight dimers, which are defined by their low or high thermostability, respectively (Paillart et al., 2004). This dimeric structure is important for viral infectivity (Shen et al., 2000). It has been shown that NCp promotes the formation of HIV-1 RNA loose and tight dimers and stabilizes the resulting dimeric structure (Muriaux et al., 1996). *In vitro*, Vif alone was also capable of stimulating the formation of the loose HIV-1 RNA dimer, but not formation of the tight dimer, at least when using long RNA fragments (600 nt long RNA). Interestingly, Vif also significantly inhibited NCp-induced tight RNA dimer formation. This inhibition might temporally prevent premature tight dimer formation in the cytoplasm of infected cells and thus assembly (Henriet et al., 2007) (Cimarelli and Darlix, 2002)

Initiation of reverse transcription

Reverse transcription is primed by the annealing of the cellular $tRNA^{Lys,3}$ onto the primer binding site (PBS) in the 5' region of the viral RNA genome. The $tRNA^{Lys,3}$ is selectively packaged into virions and used as a primer for reverse transcriptase (RT) to initiate minus-strand strong stop DNA synthesis ((−) ssDNA) (reviewed in (Isel et al., 2010)). HIV-1 NCp chaperones the annealing of the $tRNA^{Lys,3}$ primer onto the PBS by facilitating structural changes in the $tRNA^{Lys,3}$ as well as in the viral RNA (Barraud et al., 2007; Brule et al., 2002; Hargittai et al., 2004; Isel et al., 1995; Tisne, 2005; Tisne et al., 2004).

Henriet and collaborators showed that Vif can also promote the annealing of $tRNA^{Lys,3}$ to the PBS, which generates a functional $tRNA^{Lys,3}$/RNA complex, even though Vif was less efficient than the NC proteins used in this study (NCp15, NCp9 and NCp7) (Henriet et al., 2007). Interestingly, Vif also significantly inhibited NC-induced $tRNA^{Lys,3}$ annealing. This inhibition was observed using a Vif/NC ratio of 1/3, which is similar to the 1/2 Vif/$Pr55^{Gag}$ ratio in the assembly complexes in producing cells (Fouchier et al., 1996; Simon et al., 1999). However, in HIV-1 virions the Vif/NC ratio drops down to 1/20 - 1/40 and the inhibitory effect is then relieved. It has thus

been proposed that Vif might be a temporal regulator, preventing premature initiation of reverse transcription (Henriet et al., 2007). During virus assembly, the high concentration of Vif would inhibit NC-mediated $tRNA^{Lys,3}$ annealing through an interaction with the genomic RNA and the NC domain of $Pr55^{Gag}$ (Henriet et al., 2007). This hypothesis could explain that mutations in NC cause premature reverse transcription (Didierlaurent et al., 2008; Houzet et al., 2008) since such mutations could destabilize the interaction between Vif, the genomic RNA and the NC domain of $Pr55^{Gag}$.

In a manner similar to NCp7 and Vif (Beltz et al., 2003), Tat can anneal primer $tRNA^{Lys,3}$ onto the PBS of the HIV-1 RNA genome (Kameoka et al., 2002). Similarly to Vif, Tat might well regulate premature initiation of reverse transcription by inhibiting the RT activity (Kameoka et al., 2001). This inhibition is observed at high concentrations of Tat and during the late stages of viral replication (Kameoka et al., 2001). However, at a low concentration possibly found in viral particles (Chertova et al., 2006), Tat might be able to promote $tRNA^{Lys,3}$ annealing onto the PBS (Kameoka et al., 2002) and to stimulate reverse transcription through an interaction with RT (Apolloni et al., 2007).

Minus-strand DNA transfer

Once the (−) ssDNA has been synthesized by RT, it must be transferred onto the 3′-end of the viral genome to resume elongation of the (-)-strand DNA. This transfer is achieved by the annealing of the repeat regions (R) (containing the TAR element) at the 3’ ends of the (-) ssDNA and the (+) sense viral RNA (Basu et al., 2008). NCp7 chaperones minus-strand DNA transfer by promoting the annealing of the complementary (+) and (-) TAR sequences and preventing non-specific self-priming reactions (Driscoll and Hughes, 2000; Guo et al., 1997; Li et al., 1996). Vif is also able to stimulate (-) ssDNA transfer, although with a reduced efficiency compared to NC proteins (NCp15, NCp9 and NCp7) (Henriet et al., 2007). It was later demonstrated that Tat can also anneal complementary TAR DNA sequences and to promote DNA strand displacement (Kuciak et al., 2008a). A recent fluorescence study shed light on the mechanism of action (Boudier et al., 2010). In the presence of Tat, the complementary sequences anneal through their stem termini, forming an intermediate with 12 intermolecular base pairs that is finally converted to an

extended duplex. This mechanism is similar to that of NCp-induced annealing, except that Tat only marginally destabilizes the TAR structure and acts at much lower oligonucleotide fractional saturation (Boudier et al., 2010). In the same study Tat was also shown to cooperate with NCp in annealing the complementary TAR sequences. In addition, it was reported that the TAR DNA annealing activity of NCp7 was efficiently inhibited by small 2'O-methylated oligoribonucleotides (mODN). These mODNs are potent inhibitors of the HIV-1 reverse transcription complex (Grigorov et al., 2011).

Minus-strand DNA elongation

During (-) strand DNA elongation, RT has to resolve secondary structures in the RNA template causing pausing and eventually premature termination of DNA synthesis. The nucleic acid chaperone activity of NCp reduces RT pausing by transiently destabilizing these RNA secondary structures, thus promoting minus-strand DNA elongation (Ji et al., 1996; Wu et al., 1996). Vif is also capable of reducing RT pausing and enhancing minus-strand DNA elongation (Henriet et al., 2007). To support this observation, it was shown that Vif and NCp7 bind to several secondary structure motifs in the 5'-UTR of the genomic RNA (Bernacchi et al., 2007; Henriet et al., 2005). These results indicate that both NCp and Vif reduce RT pausing and promote RT processivity (Bampi et al., 2006).

Plus-strand DNA transfer

As (-) strand DNA synthesis proceeds, RT initiates (+) strand DNA synthesis using a polypurine tract (PPT) as a primer. The resulting short DNA product is known as the positive strong-stop DNA ((+) ssDNA). In order to complete (+) strand DNA synthesis, (+) ssDNA must be transferred to the 3' end of the (-) strand DNA. During this process, the PBS sequence at the 3' end of (+) ssDNA anneals to the (-) PBS sequence at the 3' end of the (-) strand DNA to form a circular intermediate (reviewed in (Basu et al., 2008)). These complementary PBS sequences cannot be annealed unless the primer tRNA is cleaved off from the 5'-end of the (-) strand DNA. Acting as a nucleic acid chaperone, NCp favors tRNA primer removal and chaperones PBS annealing (Isel et al., 2010).

In the next section, we present experimental evidences that extend our knowledge on the RNA chaperone properties of Vif by analyzing the annealing of DNA oligonucleotides TAR(-)/TAR(+), the dimerization of HIV-1 RNA fragments and the enhancement of ribozyme-directed RNA substrate cleavage by Vif, in parallel with HIV-1 NCp7.

3.4.1.8 HIV-1 Vif-mediated APOBEC3G translation inhibition

Mariani et al. (2003) were the first to observe that Vif inhibits A3G translation and suggested that this repression may contribute to the reduction of A3G encapsidation. The authors reported that Vif causes a 4.6 fold reduction in A3G synthesis by pulse-chase metabolic labeling experiments. To explain this reduction, they suggested that Vif may bind to the nascent A3G protein and interfere with the finalization of its synthesis. Thus, Vif-induced A3G degradation by the proteasome does not seem to be the only mechanism by which Vif reduces A3G encapsidation (Mariani et al., 2003). This suggests that Vif is able to counteract A3G by multiple pathways. Additionally, Kao et al (2003) showed that Vif causes the reduction of cell-associated A3G by 20–30% compared to an up to 50-fold reduction in virus-associated protein. This results supports the idea that Vif functions at different levels to reduce the intracellular levels of A3G preventing its packing.

A3G translational inhibition by Vif was also observed by Kao et al (2003). In this work, the authors observed that Vif-induced reduction of intracellular A3G is not due to an effect of Vif on the expression or stability of A3G mRNA, as previously reported by Sheehy et al. (2002). Instead, kinetic analyses suggested that Vif has an effect on the rate of A3G protein synthesis. A3G translational inhibition was finally confirmed by Stopak et al (2003). In this study, an *in vitro*-coupled transcription/translation assay was performed to study A3G translational inhibition by Vif. In order to discriminate between proteasome degradation and translational inhibition pathways, these experiments were carried out using a potent proteasome inhibitor (epoximicin). In these conditions only the translational inhibition is observed; thus, Vif was capable of impairing A3G translation by approximately 30–40%.

Based on these observations, our team showed that Vif binds to A3G mRNA and inhibits its translation *in vitro* (Mercenne et al., 2010). Indeed, filter binding assays and fluorescence titration curves revealed that Vif tightly binds to A3G mRNA (Kd =

120±10 nM). Vif binding affinity is higher for the 3'UTR than for the 5'UTR, although this region contained at least one high affinity Vif binding site (Kd = 27±6 nM). Similarly, Vif binds with high affinity to 5'-UTR of the genomic HIV-1 RNA (Kd = 45–55 nM) but very weakly or not to the central and the 3'UTR of this RNA. Vif does not interact either with *E. coli* tRNAs or 5S RNA and 3'-region of *Drosophila melanogaster* bicoid mRNA, showing that Vif is not a general RNA binding protein (Bernacchi et al., 2007; Henriet et al., 2005).

By chemical and enzymatic probing, Mercenne et al. (2010) determined the secondary structure of the UTRs present in the A3G mRNA and by enzymatic footprinting they characterized Vif binding sites. *In vitro* structure probing experiments showed that the 5'UTR and the 3'UTR folds into three structured domains separated by two single stranded junctions. Footprinting experiments revealed 3 to 4 Vif binding sites in the 5'UTR and 3 to 6 Vif binding sites in the 3'UTR (Fig. 14). Finally, they also demonstrated that Vif is able to inhibit A3G translation by performing a similar *in vitro*-coupled transcription/translation assay used by Stopak et al (2003). In these experiments, Vif caused a 2-fold reduction of A3G translation in a 5'UTR-dependent manner.

Despite the fact that A3G translational inhibition by Vif is clearly demonstrated, almost all of the studies cited in this section have been carried out *in vitro*. Therefore, it is important to study Vif-mediated A3G translational inhibition *ex vivo* using transfected cell lines or HIV-1 target cells, and/or *in vivo* using MMTV-infected mice. Moreover, the impact of this repression in HIV-1 virus infectivity remains undetermined. A3G translational inhibition by Vif is still a poorly understood pathway and further studies are needed to understand why the 5'UTR region of the A3G mRNA is required in this repression.

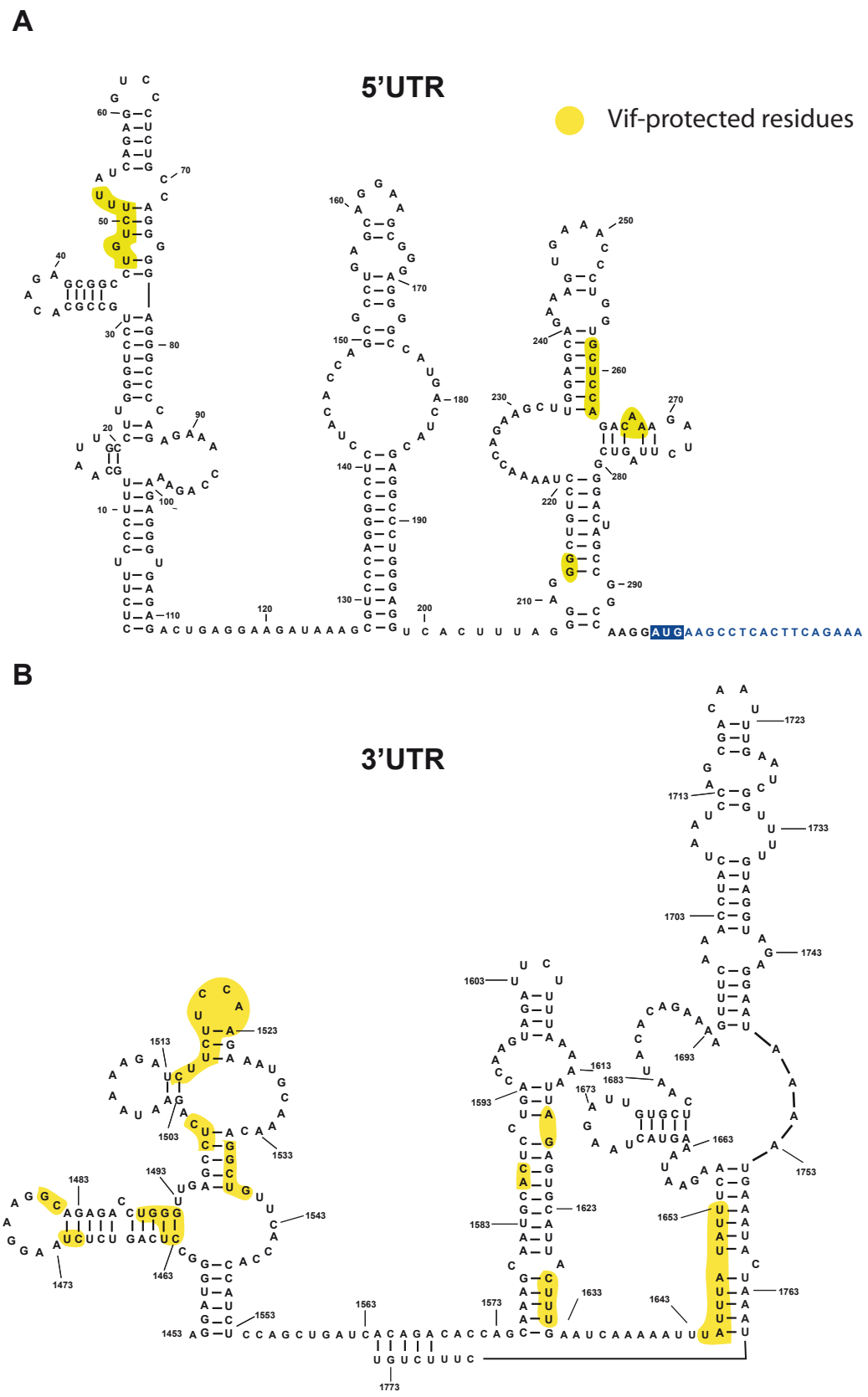

Figure 14. Structural model of the untranslated regions of A3G mRNA. Vif binding sites are colored in yellow and A3G start codon is boxed in blue. Adapted from Mercenne et al. (2010).

3.4.1.9 APOBEC3-Vif axis as a therapeutic strategy to block HIV-1 replication

Current antiretroviral strategies are focused on increasing the encapsidation of A3 proteins into the viral particles. If large quantities of A3 proteins are packaged into the virions, the genomic HIV-1 RNA would not be able to produce a competent double-stranded viral DNA. Albin and Harris (2010) propose several strategies to increase A3 encapsidation. For example, A3 proteins can be protected from degradation by shielding A3 proteins using chemical approaches. On the contrary, A3 encapsidation can be indirectly enhanced by blocking Vif interaction with either A3 proteins or with the proteasomal machinery. This can be achieved by using small molecules to target Vif itself. In this concern, Nathans et al. (2008) identified a small molecule (RN-18) that inhibits A3-Vif interaction. RN-18 decreases Vif levels and thus increases A3G/F/C levels when Vif and A3 proteins are present together. Additionally, Zuo et al. (2012) identified a potent small molecular compound (VEC-5) that targets Vif interaction with the proteasomal machinery, specifically with the ElonginC component. Recently, Huang et al. (2013) developed indolizine derivatives that also inhibit Vif from direct binding to the ElonginC protein. While the mechanisms by which these inhibitors perform their activity are still unclear, these compounds demonstrate that A3-Vif axis can be targeted by small molecules. However, there is still no compound in preclinical or clinical trials that acts on these interactions.

Despite the fact that the development of small molecules is the most promising field, progress in anti-HIV-1 gene therapy (Glazkova et al., 2012; Hoxie and June, 2012) suggest that A3-based strategies could be included in current anti-HIV-1 gene therapy approaches. In this concern, gene delivery strategies are focused on using A3 variants resistant to Vif-mediated degradation. Natural A3G D128K mutant (Xu et al., 2004) found in African green monkeys abrogates Vif binding to A3G and its subsequent proteasomal degradation. Thus, this variant could be the basis of new anti-HIV-1 gene therapy strategies.

3.4.2 TRIM5α

3.4.2.1 General characteristics and biological functions

TRIM5α belongs to the tripartite motif (TRIM) family of proteins. This family is defined by three domains: an N-terminal RING finger domain, one or two B-box domains, and a coiled-coil domain (CC). Some TRIM proteins also have a C-terminal PRYSPRY or a cyclophilin A domain (Fig. 15). These domains can be functionally divided into three activities: 1) an E3 ubiquitin ligase activity mediated by the N-terminal RING domain; 2) self-association activity (dimerization or high-order oligomerization) mediated by the BBox2 and CC domains and 3) a retrovirus-capsid recognition activity mediated by the C-terminal PRYSPRY or by the CypA domain (Grütter and Luban, 2012; Lukic and Campbell, 2012).

TRIM proteins are involved in many cellular processes, including cell signaling, cell proliferation, apoptosis and immune modulation. Among these proteins, only a few exhibit anti-retroviral properties such as TRIM11, TRIM15, and TRIM31 (Uchil et al., 2008), TRIM1 (Yap et al., 2004), TRIM28 (Allouch et al., 2011), and TRIM22 (Kajaste-Rudnitski et al., 2011). Among TRIM family members that blocks HIV-1 replication, TRIM5α is considered a model to study the anti-HIV-1 activity of TRIM proteins.

TRIM5α is an ISG (Sakuma et al., 2007) that interacts with HIV-1 capsid and blocks its replication soon after the virus enters into the cytoplasm of the target cell (Luban, 2012). Stremlau et al (2004) were the first to identified rhesus macaque TRIM5α (rhTRIM5α) by screening cDNA libraries from non-human primates cells (macaque and owl monkey). Non-human primates cells were used because early studies showed that HIV-1 infection is strongly impaired in these cells. Thus, rhTRIM5α was identified as the major element for this HIV-1 restriction phenotype present in these cells.

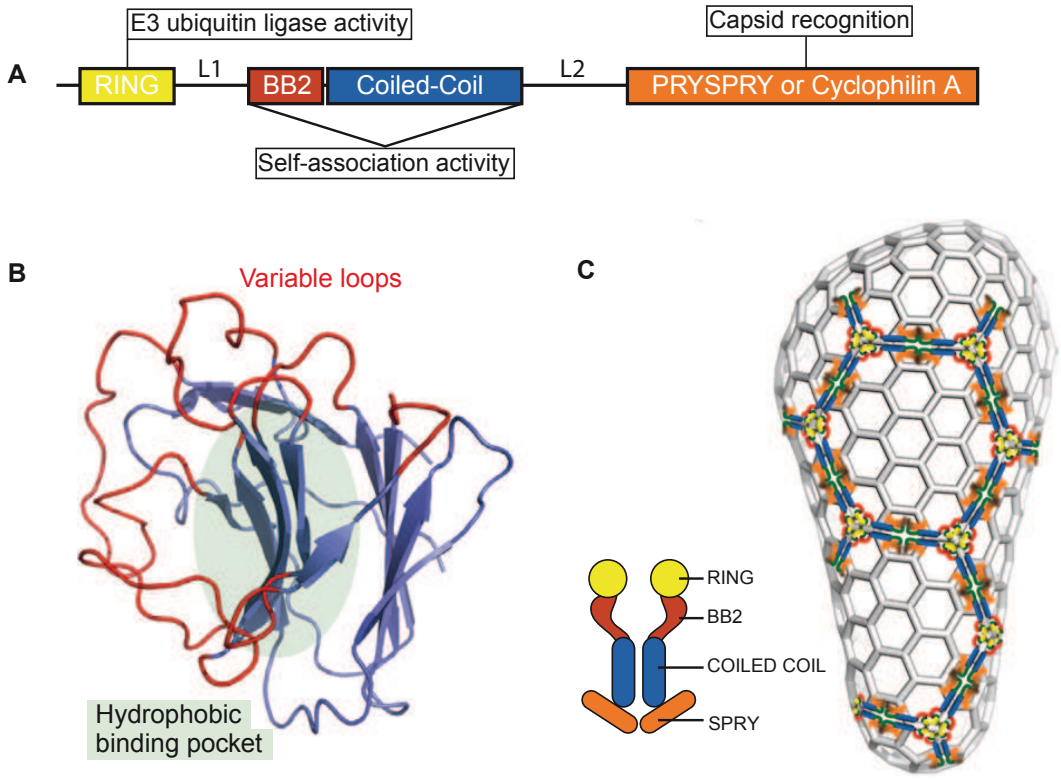

Figure 15. TRIM5α protein. A) Schematic representation of the TRIM5α protein domains. B) Ribbon representation of the TRIM5α PRYSPRY domain (PDB B30.2). The light green oval indicates the putative hydrophobic binding pocket and the variable loops are indicated in red. C) Schematic model of an HIV-1 capsid fullerene cone showing a putative recognition mode of capsid by TRIM5α. Adapted from Ganser-Pornillos et al. (2011) and Grütter and Luban (2012).

Stremlau et al (2004) also showed that rhTRIM5α potently inhibits HIV-1 infection, while the human TRIM5α (huTRIM5α) weakly inhibits HIV-1 replication but is able to restrict Equine Infectious Anemia Virus (EIAV) or N-tropic Murine leukemia viruses (MLV). These observations indicate that the anti-retroviral capacity occurs in a species-specific manner. The elements that governs substrate selection for a given TRIM5α are found mostly in the C-terminal PRYSPRY domain. In fact, the difference in the anti-retroviral specificity between huTRIM5α and rhTRIM5α is due to a small block of residues present in the PRYSPRY domain. In general, TRIM5α proteins poorly inhibit retroviruses that are found naturally in the same host species, but strongly restrict retroviruses that are found in other species.

Several lentivirus capsids bind to the a chaperone protein, named CypA and protects HIV-1 from TRIM5α activity (Ganser-Pornillos et al., 2011). However, in owl monkeys, and independently in some macaques, retrotransposition events have substituted the PRYSPRY domain by the CypA coding region (Brennan et al., 2008; Sayah et al., 2004). The resulting chimeric protein, called TRIMCyp presents strong antiviral activity against lentiviruses whose capsids bind CypA (Virgen et al., 2008).

3.4.2.1 Anti-retroviral activity of TRIM5α

The exact mechanism by which TRIM5α counteracts HIV-1 replication is unknown. Nevertheless, based on the study by Pertel et al (2011), it is clear that TRIM5α has a dual role in HIV-1 infection. TRIM5α counteracts HIV-1 not only by targeting the uncoating step (Fig 4, step 3), but also by activating the innate immune response.

TRIM5α and TRIMCyp are able to interact directly with the HIV-1 capsid protein through the C-terminal PRYSPRY or the CypA domain, respectively. This recognition should occur within the 15 min of viral entry, at least in the case of TRIMCyp. After recognition of the capsid, TRIM5α generates a hexameric lattice on the capsid structure (Fig. 15C). This event accelerates capsid uncoating before completion of reverse transcription resulting in the inhibition HIV-1 replication (Ganser-Pornillos et al., 2011; Perez-Caballero et al., 2005). Recently, (Valle-Casuso and Diaz-Griffero (2013) showed that TRIM5α proteins counteracts retroviral infection after the formation of late reverse transcripts (LRTs).

This inhibition requires TRIM5α E3 ubiquitin ligase activity, and probably recruitment of the proteasome machinery by the interaction with the interferon-inducible protein p62/sequestosome-1 (O'Connor et al., 2010) or with the proteasome subunit PSMC2 (also known as a RPT1) (Lukic et al., 2011) (Fig. 16). These observations may suggest that TRIM5α induced HIV-1 capsid ubiquitination promoting proteasome degradation. Nevertheless, TRIM5α-induced HIV-1 capsid degradation by the proteasome has been never demonstrated.

In addition to this inhibition mechanism, TRIM5α is able to activate the NF-κB pathway by a similar mechanism used by the TLR (Fig. 16). In this receptor-signaling route, activated TRIM5α cooperates with UBC13 and UEV1A E2 enzymes to trigger

the production of unanchored K63-linked ubiquitin chain. This results in the activation of TGF-activated kinase 1 (TAK1), and TAK1 in turn activates IκB kinase, leading to the activation of NF-κB (Pertel et al., 2011).

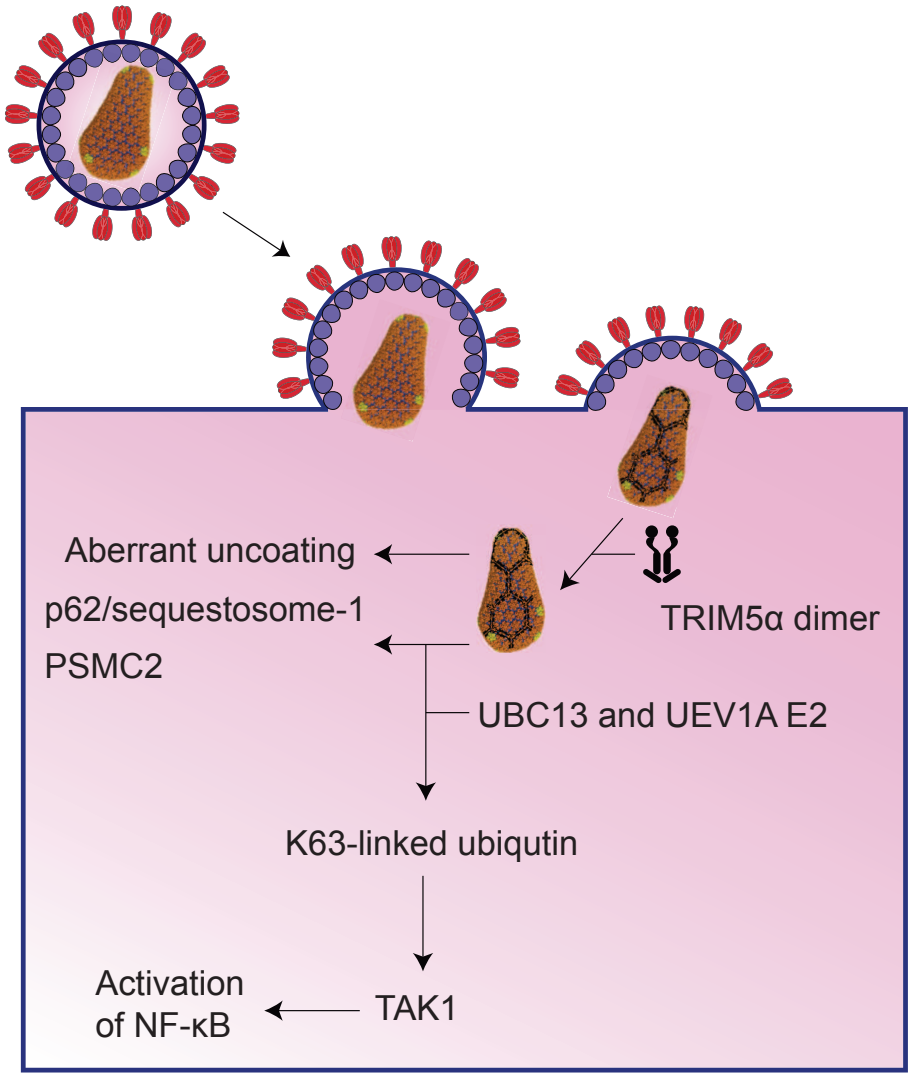

Figure 16. Schematic representation of HIV-1 inhibition by TRIM5α. Cytoplasmic TRIM5α probably exists as a dimer. After recognition of the capsid, TRIM5α generates a hexameric lattice on the capsid structure. This event causes prematurely viral uncoating and subsequent inhibition of the reverse transcription. TRIM5α recruits p62/sequestosome-1 and PSMC2 and probably stimulates capsid degradation by the proteasome. TRIM5α is also able to activate the NF-κB pathway. Adapted from Luban (2012).

3.4.3 Tetherin

Tetherin is an IFN-inducible type II membrane protein capable of blocking HIV-1 release (Fig 1, step 12). This protein is also named BST-2, CD317, HM1.24 (Van

Damme et al., 2008; Neil et al., 2008). Tetherin was identified based on the fact that Vpu accessory protein was necessary for efficient virion release in non-permissive cells. Indeed, initial reports showed that deletion of Vpu gene causes a 5-10-fold decrease in virus release from HIV-1 target cells (Strebel et al., 1988). This phenotype was later observed using electronic electron microscopy (Geraghty et al., 1994; Jolly, 2011) (Fig. 17). Subsequent studies characterized tetherin as a HIV-1 restriction factor and Vpu as its counter-restriction factor (Van Damme et al., 2008; Neil et al., 2008).

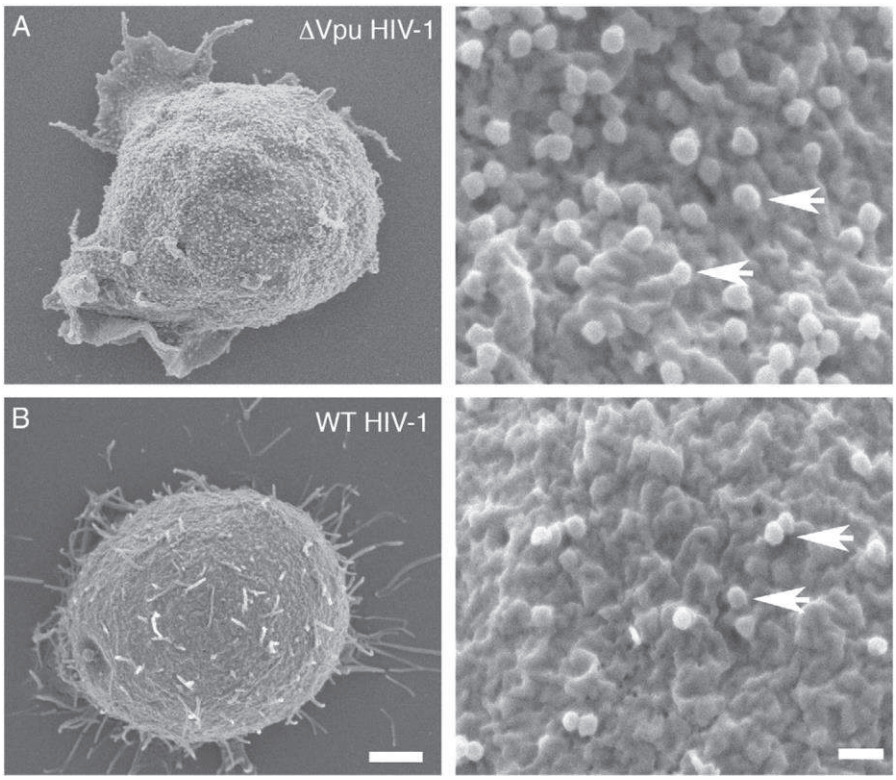

Figure 17. **Tetherin-releated phenotype**. Scanning electron micrographs (SEM) of Jurkat T cells infected with HIV-1Δ*Vpu* (A) and HIV-1 wild-type (B) after 7 days post-transfection. Left panel showed infected Jurkat T cells with a 500 nm magnification, while the right panel showed a higher magnification of 200 nm (Jolly, 2011).

3.4.3.1 Antiviral activity of tetherin

Tetherin is able to restrict several types of virus due to its ability to target the viral cell-derived lipid bilayer. Thus, tetherin has been shown to block the release of all retrovirus classes and several other viruses such as Ebola virus (Jouvenet et al., 2009), Nipah virus (Radoshitzky et al., 2010), vesicular stomatitis virus (Weidner et al., 2010) and Hepatitis C virus (hepaciviruses) (Pan et al., 2013). This broad

antiviral activity is accomplished due to the topology of tetherin that allows the simultaneous association of both the viral and the cellular membranes. Tetherin is composed of an N-terminal cytoplasmic (CT) domain, a α-helical trans-membrane (TM) domain, an extracellular (EC) coiled-coil domain and a C-terminal glycophosphatidylinositol (GPI) anchor (Fig. 18A).

Tetherin blocks the release of HIV-1Δ*Vpu* virions by tethering them to the plasma membrane of the infected cell (Neil et al., 2008). Two models are proposed to explain this mechanism. First, in the "EC self-interaction model", tetherin monomers interacting together by its EC domains are anchored at both ends (TM and GPI) to the viral and cellular membrane (Fig. 18B). Second, in the "membrane-spanning model" both ends (TM and GPI) of a tetherin dimer are anchored into the opposite side of the viral and the cellular membrane in a parallel or an anti-parallel configuration (Fig. 18B) (Zheng et al., 2012).

Both models are supported by the fact that specific cleavage of the GPI domain did not release nascent virions (Fitzpatrick et al., 2010). However, structural studies performed by Hinz et al., 2010 showed that the EC domain forms a parallel homodimer, suggesting that the membrane-spanning model in the parallel configuration better represents the tetherin restriction mechanism (Zheng et al., 2012).

3.4.3.2 HIV-1 Vpu counteracts tetherin

Vpu is type I trans-membrane protein of about 14 kDa encoded by HIV-1 and a few SIV strains. Vpu is composed of a single trans-membrane (TM) α-helix domain and a small cytoplasmic (CT) domain in which two α-helices are separated by a connector loop. In this connector two serine residues (positions 52 and 56) are phosphorylated (Fig. 18A). Other tetherin antagonists include Nef of SIV and ENV protein of HIV-2 and SIVtan (SIV from tantalus monkey) (Fig. 19).

Vpu removes tetherin from the cell surface by two main mechanisms. First, Vpu mediates tetherin relocalization from the plasma membrane to the trans-Golgi network (TGN) (Dubé et al., 2010). ENV protein of SIVtan and HIV-2 also promotes sequestration of the tetherin (Gupta et al., 2009; Hauser et al., 2010) (Fig. 19, step 1). The normal cellular trafficking of tetherin begins in the endoplasmic reticulum

(ER), continues to the Golgi apparatus, plasma membrane and finishes in recycled compartment (Fig. 19). Therefore, in this sequestration mechanism Vpu may divert the trafficking of the tetherin to an intracellular compartment.

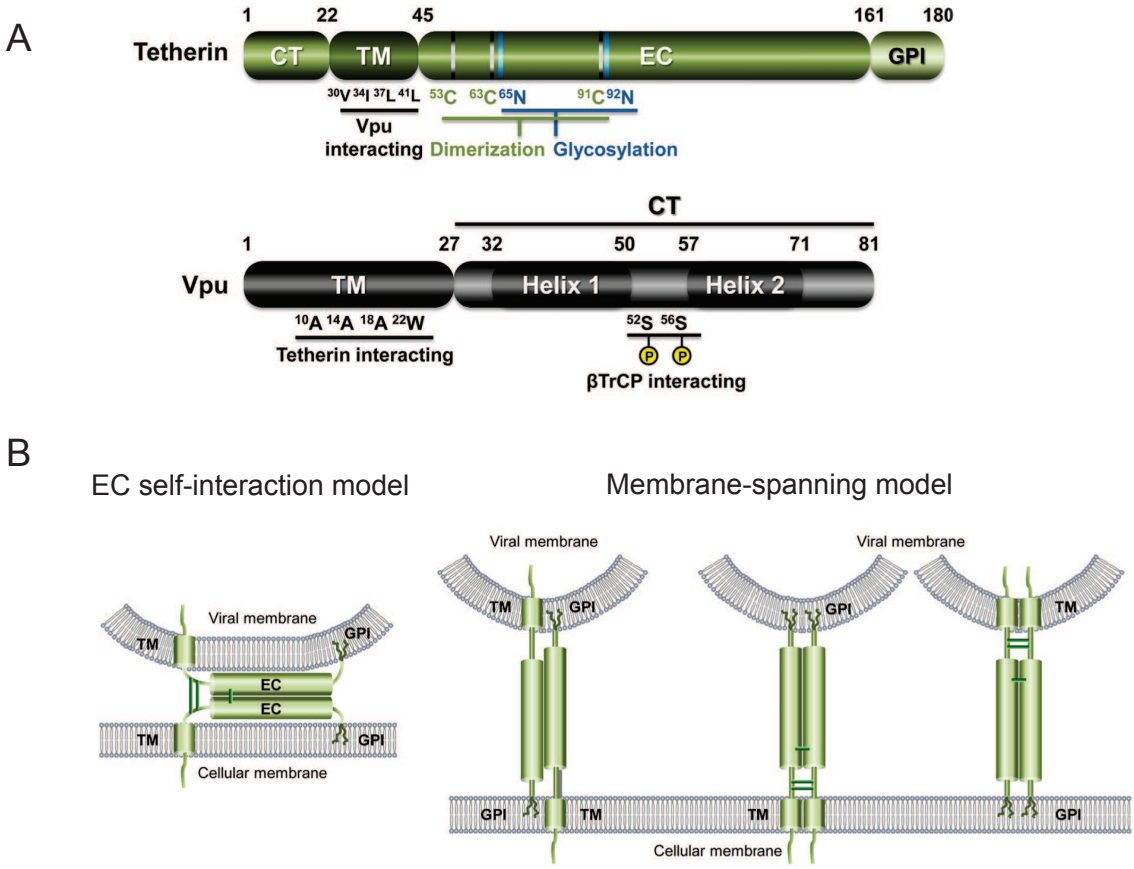

Figure 18. **Schematic representation of Tetherin and Vpu protein domains** (A) and mechanisms of tetherin activity showing two hypothetical models: the EC self-interaction model and the membrane-spanning model (B) (Zheng et al., 2012).

Second, Vpu mediates tetherin degradation by the proteasome (Fig. 19, step 2) by recruiting β-TrCP2 (β transducing repeat containing protein 2) a component of the E3 ubiquitin ligase complex. The phosphorylated serine residues (S52 and S56) of Vpu constitute the binding site for β-TrCP2. Additionally, ubiquitination of non-lysine residues in the CT domain triggers the ESCRT-dependent lysosomal degradation pathway (Fig. 19, step 3) (Janvier et al., 2011). It has also been shown that tetherin serves as a viral sensor to induce NFkB-dependent proinflammatory gene expression. This seems to be coupled to an aggregation of unreleased virions in the cell surface, resulting in the TAK1-mediated activation of NFkB and subsequent cytokine generation (Fig. 19, step 4) (Galão et al., 2012).

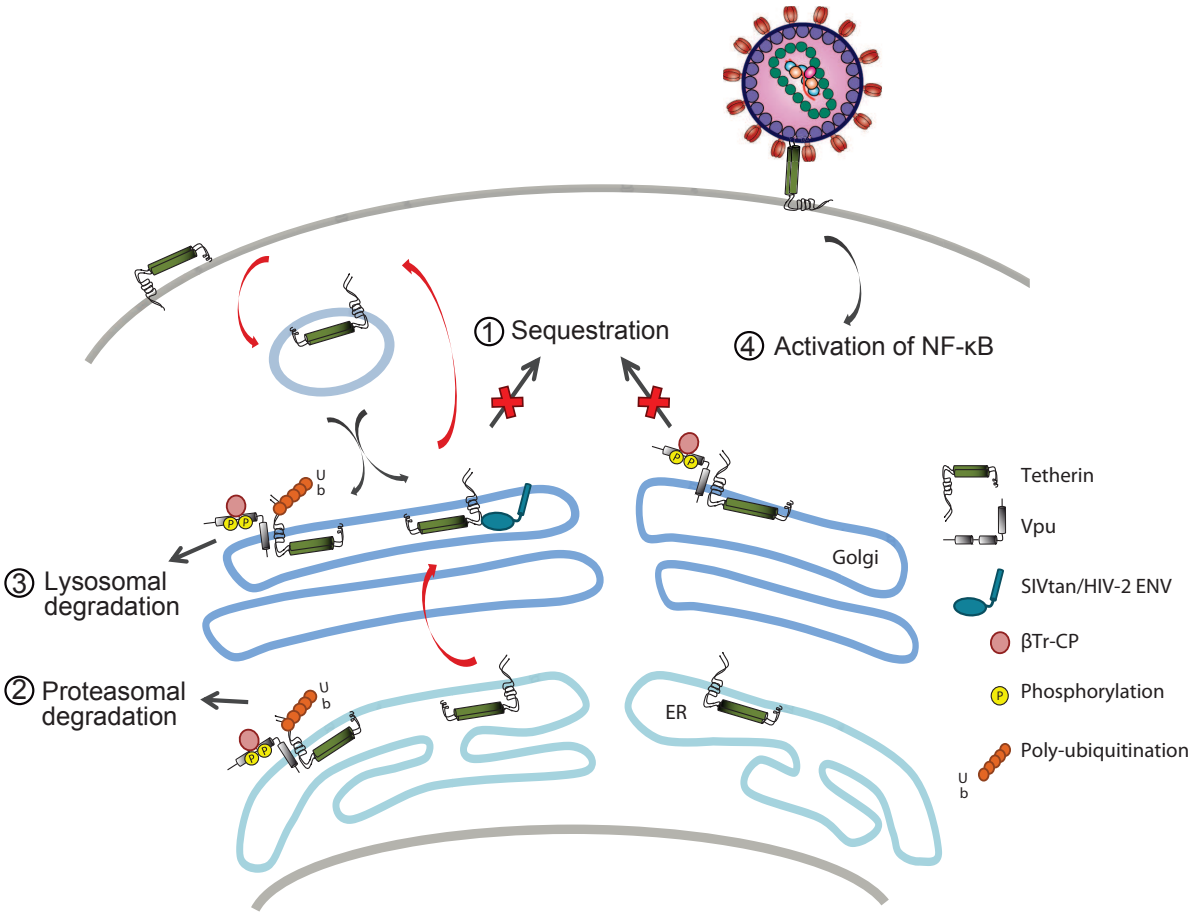

Figure 19. HIV-1 Vpu and SIVtan/HIV-2 ENV counter-restriction mechanisms. Red arrows represent the normal cellular trafficking of tetherin. First, Vpu mediates tetherin relocalization from the plasma membrane to the trans-Golgi network (TGN) (step 1). Second, Vpu mediates tetherin degradation by the proteasome (step 2). Third, Vpu induces tetherin degradation by the lysosomal (step 3). Finally, tetherin induce activation of the NFkB pathway (step 4) (Adapted from Kuhl et al., 2011).

3.4.4 SAMHD1 dNTP Hydrolase

3.4.4.1 General characteristics

Lafuse et al. (1995) were the first to identify SAMHD1 in mouse. In this study, they isolated two genes (Mg11, Mg21) after treatment of mouse peritoneal macrophages with IFN-γ. Mg21 encodes for a GTPase, while the Mg11 encodes for SAMHD1. Five years later, (Li et al., 2000b) identified human homologue of Mg21 from dendritic cells but its functions was still not clear, until it was reported that mutations in this gene are involved in the Aicardi–Goutières syndrome (AGS). AGS is characterized by elevated INF production that generates an immune-mediated neurodevelopmental disorder (Rice et al., 2009). This elevated INF production could

be stimulated by endogenous retroviruses that are not inhibited by SAMHD1 mutants in myeloid cells (Fig. 21A and B) (Goldstone et al., 2011).

The discovery of SAMHD1 antiretroviral activity dates back to early studies in which it was observed that myeloid cells (macrophages and dendritic cells) are more resistant to HIV-1 infection than $CD4^+$ T cells (Guyader et al., 1989; Yu et al., 1991). Further experiments to understand this phenotype showed that the Vpx (viral protein X) of HIV-2 or SIV, absent in HIV-1, disrupts this resistant phenotype in macrophages and dendritic cells (Kaushik et al., 2009; Yu et al., 1991). Affinity purification experiments identified SAMHD1 as a Vpx-interacting protein, and additionally studies showed that knockdown of SAMHD1 in myeloid cells caused the loss of the HIV-1 resistant phenotype (Hrecka et al., 2011; Laguette et al., 2011). Although SAMHD1 was identified in myeloid cells, it is also expressed in lymphoid cells including T and B cells (Baldauf et al., 2012; Descours et al., 2012). SAMHD1 is composed of an N-terminal nuclear localization domain, which has a NLS (nuclear localization sequence) (Brandariz-Nuñez et al., 2012), a sterile alpha motif domain (SAM) and a C-terminal dNTP phosphohydrolase domain (HD domain). The SAM and HD domains are also found in several other proteins (Fig. 20). SAM is found in transcription factors, RNA binding proteins and lipid kinases and serves as a protein-protein interaction domain (Qiao and Bowie, 2005). HD is found in helicases, nucleotidyltransferase and dGTPase, suggesting a possible role in nucleic acid metabolism (Aravind and Koonin, 1998).

3.4.4.2 SAMHD1 antiretroviral activity

SAMHD1 is a dGTP-stimulated deoxynucleoside triphosphates (dNTP) hydrolase (Berger et al., 2012; Goldstone et al., 2011; Yan et al., 2013). The crystal structure of SAMHD1 catalytic core, obtained by Goldstone et al. (2011) revealed that the protein is dimeric and biochemical experiments showed that SAMHD1 activity requires its dimeric configuration. Contrary to this result, Yan et al. (2013) recently demonstrated that, in the absence of dGTP, SAMHD1 is found in a non-catalytic monomeric or dimeric configuration. However, in the presence of dGTP, SAMHD1 forms tetramers and this configuration seems to be the catalytic active form (Fig. 21).

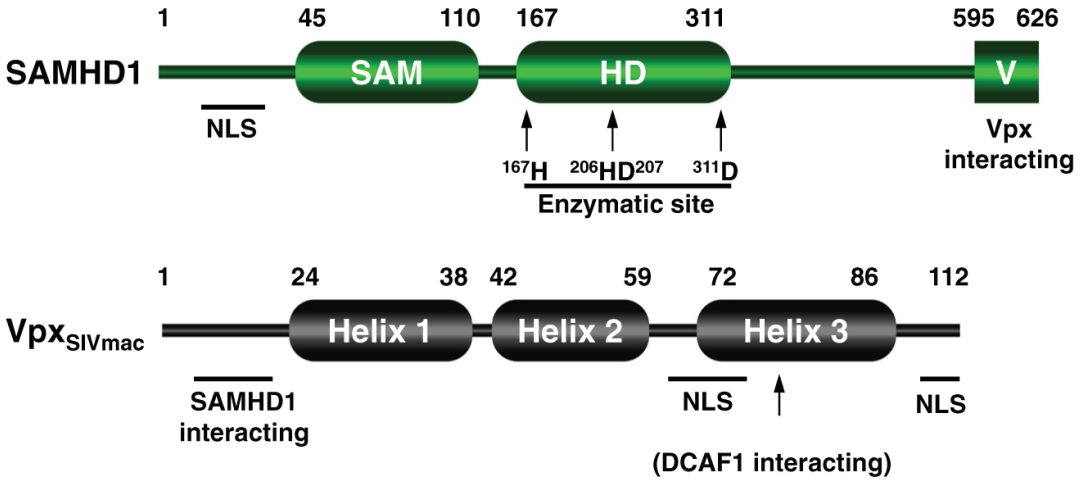

Figure 20. **Schematic representation of SAMHD1 and Vpx protein domains** (Zheng et al., 2012).

SAMHD1 counteracts HIV-1 replication in monocytes, macrophages, dendritic cells and resting $CD4^+$ T cells by decreasing the cellular dNTP levels (Fig 21C). This reduction leads to an efficient inhibition of viral cDNA synthesis during reverse transcription. The activation of SAMHD1 by the IFN due to a HIV-1 infection in human myeloid cells is still unclear. Berger et al. (2011a) reported that IFN-α induces SAMHD1 expression in monocytes. On the contrary, St Gelais et al., (2012) have shown that SAMHD1 expression is not regulated by IFN-α, β or γ in monocyte-derived dendritic cells or primary T lymphocytes. Dragin et al (2013) also showed that SAMHD1 expression is not upregulated by IFN-α in monocytes and in monocyte-derived macrophages. Recently, Riess et al (2013) showed that SAMHD1 expression is stimulated by type-1 and 2 IFN in a dose dependent manner in U937 cells (myeloid cells isolated from a histiocytic lymphoma).

3.4.4.3 Vpx protein counteracts SAMHD1

Vpx protein is also a nuclear protein like SAMHD1 and is composed by a C and N-terminal unstructured domains and three α-helices connected by two flexible loops. Vpx also possesses two NLS sequences and a SAMHD1-interacting domain (Fig. 20). The Vpx protein of HIV-2 or SIV is able to counteract SAMHD1 by promoting its degradation by the proteasome (Fig. 21D). Vpx stimulates the formation of an E3 ubiquitin ligase complex composed of DCAF1, DDB1, and CUL4. This complex

promotes polyubiquitination and subsequent degradation of SAMHD1 (Hrecka et al., 2011; Laguette et al., 2011). Vpx interacts with DCAF1 through the α-helix 3 region and recognizes the C-terminal domain of SAMHD1 through its N-terminal unstructured region (Khamsri et al., 2006).

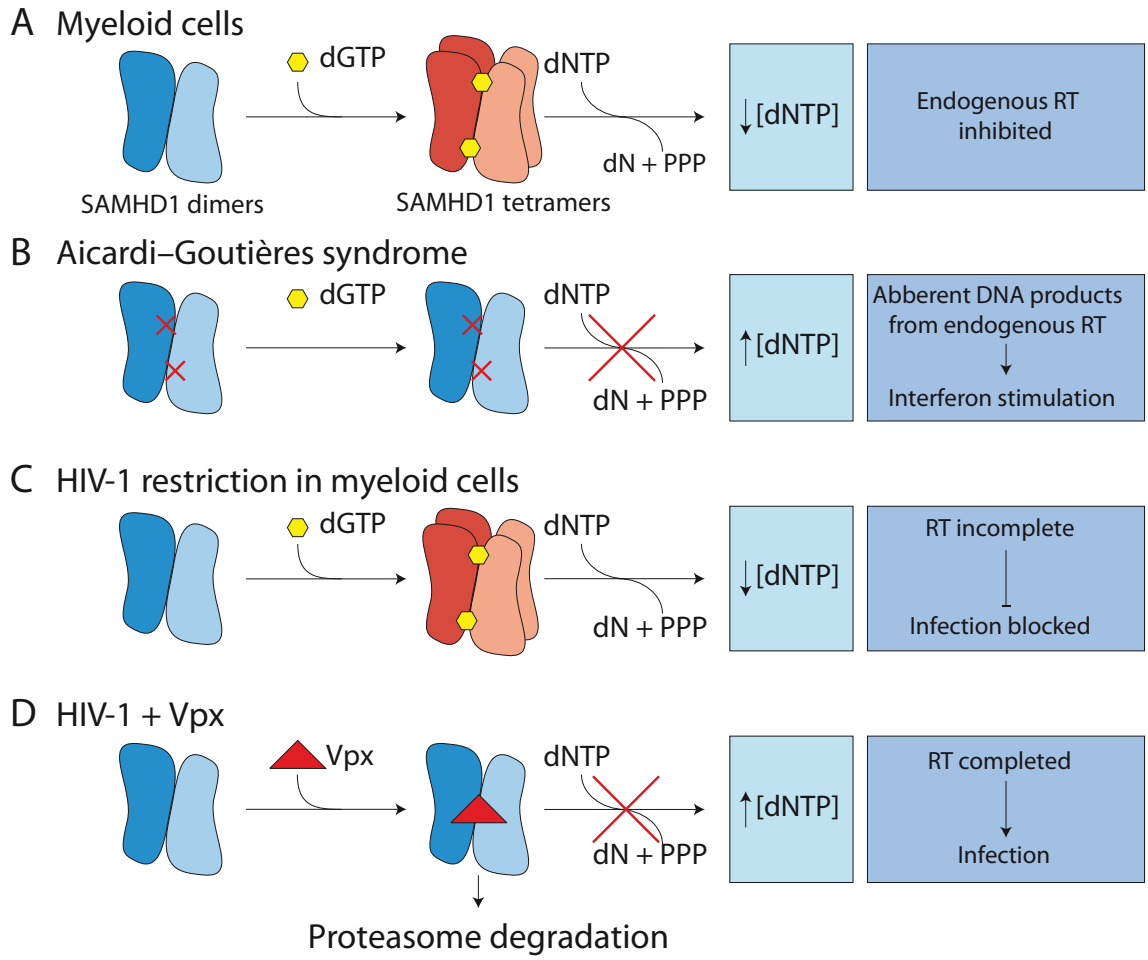

Figure 21. SAMHD1 activity in different contexts. A) Activation of SAMHD1 dimers by dGTP results in the formation of the catalytic active form. SAMHD1 tetramers are capable of catalyzing dNTPs into the composite deoxynucleoside and inorganic triphosphate inhibiting endogenous retrovirus. B) SAMHD1 mutations generate an inactive catalytic form incapable of inhibiting endogenous retrovirus causing AGS. C) SAMHD1 restricts HIV-1 infection in myeloid cells. D) Vpx of HIV-2 or SIV restricts HIV-1 infection. Adapted from Goldstone et al (2011) and updated from Yan et al (2013).

Vpx is closely related to Vpr, which is only encoded by HIV-1. Vpr also interacts with DCAF1 and DDB1 but is not able to target SAMHD1 degradation via the proteasome. Instead, this interaction triggers the host DNA-damage-response (DDR) pathway to initiate G2 cell cycle arrest (Planelles and Benichou, 2009). Despite the

fact that HIV-1 Vpr protein cannot degrade SAMHD1, an evolutionary study has shown that the ancestral Vpr protein had the capacity to neutralize SAMHD1 before it evolved to the Vpx protein in HIV-2 (Lim et al., 2012) whereas this capacity was lost in the current Vpr protein from HIV-1.

3.4.5 Other cellular proteins that limit HIV-1 replication

3.4.5.1 Schlafen 11

The Schlafen family

Schlafen 11 (SLF11) is an ISG and belongs to the Schlafen (SLFN) family, a group of proteins first reported in mouse. The family has been named Schlafen ("to sleep" in german) because SLFN1 causes a cell cycle arrest (Schwarz et al., 1998). To date, SLFN genes have been identified in every mammalian genome (except in *Ornithorhynchus anatinus*), in *Xenopus laevis* and in *Callorhinchus milii* (''elephant fish'') (Bustos et al., 2009). Initially, SLFN genes (mouse SLFN1, 2, 3, and 4) were classified as a family of genes implicated in thymocyte maturation (Schwarz et al., 1998). Further studies have shown that SLFN family is composed of different groups (Bell et al., 2006; Geserick et al., 2004; Schwarz et al., 1998). Mavrommatis et al. (2013) classified SLFN family based on the size of the encoded proteins in three groups: group I (37 to 42 kDa), group II (58-68 kDa) and group III (100-104 kDa).

All SLFN proteins present a putative AAA (ATPases Associated with diverse cellular Activities) domain in the N-terminal region, which is thought to be involved in GTP/ATP binding. SLFN members also have a SLFN box, a domain only found in this family and whose function is still not well understood (Geserick et al., 2004; Neumann et al., 2008). Groups I and II also present a SLFN-specific domain, termed SWADL domain (Ser-Trp-Ala-Asp-Leu) (Geserick et al., 2004; Neumann et al., 2008). Additionally, group III have a C-terminal DNA/RNA helicase-like domain, which can be involved DNA/RNA metabolism. Interestingly, these DNA/RNA helicase domains are also found in RIG-1 and MDA5, suggesting a possible role in pathogen recognition (Geserick et al., 2004; Schwarz et al., 1998).

In mice, ten murine SLFN genes have been reported (SLFN1L, 1-5, 8-10 and 14). Among these, SLFN 1, 2 and 3 have been extensively studied (Berger et al., 2010; Geserick et al., 2004; Sohn et al., 2007; Walsh et al., 2012). For example, SLFN2 has been shown to be implicated in cell differentiation and growth and in the immune response. Indeed, a SLFN mutant causes mice to be more susceptible to both viral and bacterial infections (Berger et al., 2010). Additionally, Sohn et al. (2007) have shown that the expression of SLFN2 is stimulated by bacterial lipopolysaccharide (LPS) and CpG-DNA (DNA containing immunostimulatory CpG motifs) by activating NF-κB and AP-1 pathways in macrophages. In humans, five SLFN genes have been identified (SLFN5, 11, 12, 13 and 14) (Bustos et al., 2009; Mavrommatis et al., 2013). Human SLFN proteins are members of the group III except for SLFN12 which lacks the C-terminal DNA/RNA helicase-like domain. Among these, only the functions of SLFN5 and 11 have been reported (Mavrommatis et al., 2013). SLFN5 has been shown to present negative regulatory effects on anchorage-independent cell growth of melanoma cells and invasion of malignant melanoma cells in collagen (Katsoulidis et al., 2010). In this study, SLFN5 knockdown in malignant melanoma cells increases anchorage-independent growth and invasion in three-dimensional collagen (Katsoulidis et al., 2010) . Recently, SLFN11 has been shown to present an anti-HIV-1 effect, as discussed below.

Schlafen 11 inhibits HIV-1 protein synthesis

Only one study published in *Nature* revealed that SLFN11 is able to block HIV-1 protein synthesis in a codon-usage-defined manner (Li et al., 2012a). In this study, Li et al. (2012a) first tested whether type-1 INFs are capable of inducing SLFN genes in human fibroblasts. The authors observed that the expression of SLFN5 and SLFN11 is induced by IFN-β in these cells. Second, they showed that HIV-1 virus production is increased in 293T cells depleted of SLFN11. In the same cell line, HIV-1 could activate an elevation of tRNA levels but not in 293T cells expressing SLFN11. These changes in cellular tRNA levels after HIV-1 infection were already reported by van Weringh et al. (2011). Together with the observation that SLFN11 directly bound tRNAs, Li et al. (2012a) concluded that SLFN11 affects the synthesis of viral proteins by limiting the availability of tRNAs.

Many viruses, including HIV-1, have a codon bias toward an adenosine at the third position of the codon. This preference leads to an inefficient codon usage compared to that of the host cells. To test the possibility that SLFN11 exploits this viral codon bias to specifically counteract HIV-1 protein synthesis, Li et al. (2012a) studied the effect of SLFN11 on natural green fluorescent protein (GFP) which have a similar codon preference. In these experiments, they observed that SLFN11 reduces GFP synthesis but this repression was not observed using a GFP optimized for mammalian expression. Thus, they finally showed that SLFN11 affects the synthesis of HIV-1 viral proteins in a codon-usage-based manner. SLFN11 seems to be a typical HIV-1 restriction factor with two main characteristics: immune induction and virus restriction (Fig. 8). However, an HIV-1 counter-restriction mechanism has not been reported yet and no evolutionary study has been performed to determine positive selection signatures in SLFN11 protein. In addition to its antiviral effect, SLFN11 sensitizes cancer cells to DNA-damaging agents, such as topoisomerase inhibitors or alkylating agents (Zoppoli et al., 2012).

3.4.5.2 MOV10

The Moloney Leukemia Virus 10 inactivated gene (MOV10) was first discovered in mouse and is part of the RNA interference machinery. MOV10 presents a potent anti-HIV-1 activity when it is ectopically expressed (Burdick et al., 2010; Wang et al., 2010). MOV10 also impairs SIV (Wang et al., 2010), hepatitis C virus (Schoggins et al., 2011), and vesicular stomatitis virus (Li et al., 2011). MOV10 decreases the production of HIV-1 infectious particles in viral producer cells by a mechanism that is not clearly understood. MOV10 performs its anti-HIV-1 activity, possibly by decreasing Gag expression and processing (Zheng et al., 2012). MOV10 is also capable to be packaged into viral particles by a specific interaction with $Pr55^{Gag}$. Thus, during the next viral cycle, MOV10 interferes with the reverse transcription process (Wang et al., 2010). In fact, MOV10 is packaged within the core, which facilitates MOV10 interaction with the viral genomic RNA and thereby blocking reverse transcription (Zheng et al., 2012). Up to now, no viral proteins have been shown to block MOV10 activity.

3.4.5.3 MX2

Myxovirus resistance 2 (MX2) is an IFN-induced dynamin-like large GTPase that has long been recognized as a protein implicated in several cellular functions, such as cell-cycle progression and nucleo-cytoplasmic transport (King et al., 2004; Melén et al., 1996). Recently, three independent studies reported that MX2 is an innate immunity protein that restricts HIV-1 infection (Goujon et al., 2013; Kane et al., 2013; Liu et al. 2013). MX2 presents two isoforms, a 78 kDa protein that contains a nuclear localization signal (NSL)-like sequence and a cytoplasmic 76 kDa protein (Melén et al., 1996). Liu et al. (2013) showed that MX2 impairs the replication of the HIV-1 strain NL4.3 in cell culture. Expression of MX2 blocked HIV-1 replication in CD4+T cell line while its depletion inhibited the antiviral effect of IFN-α in human astroglioma cell line. According to this report, MX2 does not block nuclear entry of the viral DNA but inhibits chromosomal integration. However, Goujon et al. (2013) report that MX2 blocks entry of HIV-1 replication complexes or disturbs their stability. Kane et al. (2013) also reported that MX2 impairs HIV-1 infection by inhibiting capsid-dependent nuclear import of sub-viral complexes.

4. HIV-1 tricks eukaryotic translation during infection

Eukaryotic translation is a complex process orchestrated by a wide range of elements, including several protein factors and three classes of RNA (rRNA, tRNA and mRNA). This process begins in the nucleus by the maturation and nuclear export of mRNAs, following by translation initiation, elongation and termination steps. Immediately after transcription, mRNAs are maturated to be exported through the nuclear pores to the cytoplasm. Once in the cytoplasm, translation initiates by the recruitment of the small ribosomal subunit (40S), which scans along the mRNA until it finds an initiation codon. At this point, the large ribosomal subunit (60S) is engaged to decode the mRNA and assembles amino acids to synthesize a protein. The elongation step is completed when the ribosome reaches a stop codon that triggers the termination step. Finally, the components of the translational machinery are recycled for further protein translation.

Eukaryotic translation, in particular at the initiation phase, is an important step for the regulation of gene expression. It allows the cell to respond to stimuli *ipso facto*, activating translation of accumulated mRNAs to produce specific proteins. This is the case of stress-related proteins or type I interferon proteins during viral infections. This step is often targeted by viruses to improve their viral fitness and pathogenicity. Thus, RNA or DNA eukaryotic viruses usurp the host translational machinery (ribosomes, tRNAs and several associated factors) to produce their own proteins. In order to assure optimal viral protein synthesis at the expense of cellular proteins, viruses inhibit host translation and hijack eukaryotic translation components to facilitate viral protein synthesis. To achieve this, as many other viruses, the human immunodeficiency viruses type I (HIV-1) has evolved several pathways that target different steps of the eukaryotic translation process. In this review, we will present all eukaryotic translation steps in which the HIV-1 proteins are involved in both host translation inhibition and host translation recruitment to improve viral replication.

4.1. Overview of eukaryotic translation

4.1.1 mRNA maturation and nuclear export

In the nucleus, the 5'-ends of nascent mRNAs are capped with a 7-methylguanosine (m^7G) and subsequently polyadenylated at their 3'-ends immediately after transcription. The m^7G cap is then recognize by the cap-binding complex (CBC), which is composed by the cap-binding proteins 80 and 20 (CBP80/20) (Izaurralde et al., 1994). mRNA export effectors (SR proteins; exon-exon junction complex - for review, see Müller-McNicoll and Neugebauer, 2013) are then loaded on mature mRNA molecules. These adapators molecules allow the recruitment of the heterodimer NXF1/NXT1 (nuclear RNA export factor 1 – NXF1 and its cofactor NTF2-related export protein-1 – NXT1) to export the mRNPs from the nucleus to the cytoplasm through the nuclear pore by interactions with the nucleoporins (Adams and Wente, 2013; Moore and Proudfoot, 2009) (Fig. 22, step 1 to 2).

4.1.2 Translation initiation

4.1.2.1 Pre-initiation complex assembly and mRNA activation

Once in the cytoplasm, mRNAs undergo a CBC-mediated pioneer round of translation, which is important for the quality control of the transcript (Maquat et al., 2010). CBC is then displaced of the m^7G and mRNAs are activated by the eIF4F complex (eIF4E, eIF4G and eIF4A) and eIF4B (Fig. 22, step 3). First, eIF4E interacts with the m^7G allowing the recruitment of eIF4A to the 5'-untranslated region (UTR) of the mRNA (LeFebvre et al., 2006). eIF4A, in conjunction with eIF4B, is then able to unwind the mRNA by its helicase activity enhanced by eIF4G to generate a single-stranded binding region for the 43S pre-initiation complex (43S PIC) (Hilbert et al., 2011; Özeş et al., 2011). Finally, mRNA acquires a "closed-loop" structure, necessary for an optimal mRNA recruitment into the 43S PIC (Fig. 22, step 6). This conformation is achieved by a simultaneous binding of PABP (Poly(A)-binding protein) and eIF4E to eIF4G (Uchida et al., 2002).

In parallel, ternary complex (TC) formation occurs through the assembly of the initiator methionyl-tRNA (Met-$tRNA_i^{Met}$), the eukaryotic initiation factor 2 (eIF2) and a GTP molecule (Fig. 22, step 4).

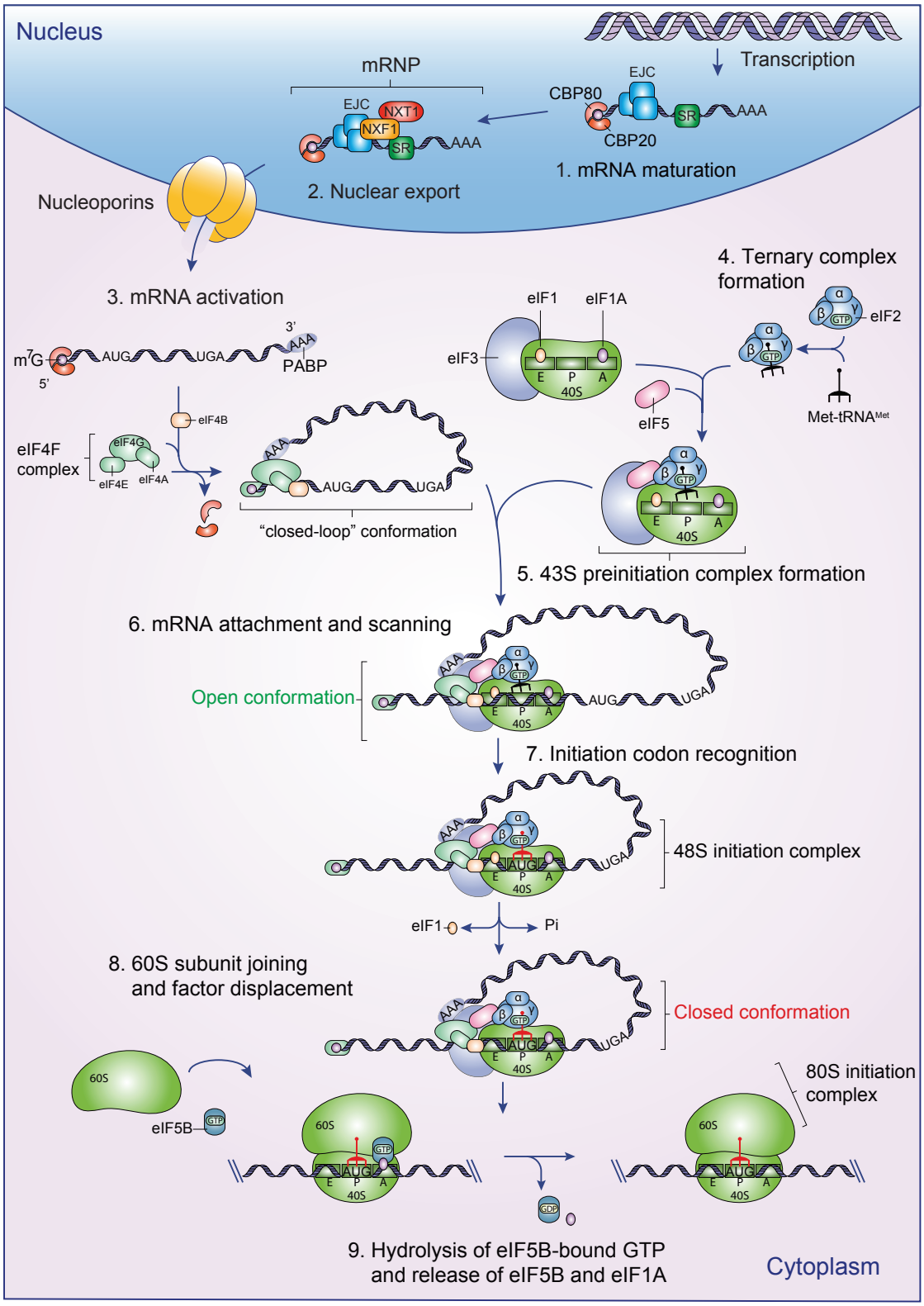

Figure 22. Eukaryotic translation initiation. mRNA maturation and nuclear export precede the translation initiation (steps 1 and 2). Once into the cytoplasm, mRNA is activated (step 3) and 43S pre-initiation complex formation occurs in parallel (step 4 to 5). mRNA recruits the 43S pre-initiation complex and the scanning begins until an initiation codon is detected (step 6). At this point, the 48S initiation complex is formed and the 60S subunit is recruited to finally accomplish the ribosome 80S initiation complex formation (step 7 to 9).

During the formation of this complex, the γ subunit of eIF2 binds to both Met-tRNA$_i^{Met}$ and the GTP molecule, while the α and β eIF2 subunits increase the affinity of the complex for the Met-tRNA$_i^{Met}$ (Naveau et al., 2010). The TC is then recruited to the ribosomal subunit 40S to assemble the 43S PIC (Fig. 22, step 5). In this process, other eIFs (eIF1, 1A, 3 and 5) are required to promote TC binding to the 40S subunit (Majumdar et al., 2003). eIF1 binds near the entry site (E), while the eIF1A binds near the A site. eIF3 presents a similar size as the 40S subunit and interacts with eIF2 to stabilize the binding of the TC within the PIC. eIF5 also interacts with eIF2 to promote the proper conformation of the 43S PIC (Yu et al., 2009).

4.1.2.2 Ribosomal scanning of the 5'UTR

Once the mRNA has been loaded, the 43S PIC scans the 5'UTR region until it recognizes a start codon (AUG) by complementarity with the anticodon Met-tRNA$_i$. The 43S PIC scanning is composed of two concomitant processes (Fig. 22, step 6). First, the unwinding process in which the secondary structures of the 5'UTR are unfolded to allow the mRNA to pass through the entry site (E) for a further base-by-base scanning in the P site. Second, the ribosomal movement process in which the 43S PIC moves along the 5'UTR until it reaches an AUG start codon in a suitable Kozak context (see below) (Hinnebusch and Lorsch, 2012).

Several factors have been implicated in the ribosomal movement process. Cryo-electron microscopy observations showed that eIF1 and eIF1A bind to 40S subunit and promote an "open", scanning-competent 43S PIC (Passmore et al., 2007). Omission of eIF1A and eIF1 potently reduces 43S PIC scanning in *in vitro* experiments, indicating that movement of 43S PIC requires this scanning-competent conformation (Pestova and Kolupaeva, 2002). Mutations in eIF4G affecting its mRNA binding capacity or its stability within the eIF4F complex also reduce scanning efficiency (Prévôt et al., 2003; Watanabe et al., 2010). Similarly, mutations of the eIF3 RNA recognition motif also affect 43S PIC scanning (Cuchalová et al., 2010). Additionally, Berthelot et al. (2004) proposed that the 43S PIC may move along the mRNA transcript by a bidirectional walking mode. Under this mechanism, the 43S PIC could move forwards but also backwards along the transcript.

In the unwinding process, eIF4A RNA helicase activity plays an important role along with other DEAD-box RNA helicases, including DExH box protein 29 (Dhx29), DEAD

box helicase 1 (Ded1) and DEAD box protein 3 (Ddx3) (Chuang et al., 1997; Pisareva et al., 2008; Rogers et al., 2001; Soto-Rifo and Ohlmann, 2013; Tarn and Chang, 2009). eIF4A promotes the 43S PIC attachment to the 5' end of mRNA and facilitates the scanning of this complex through structured domains present in the 5'UTR. To assist this process, eIF4G and eIF4B enhance eIF4A helicase activity (Rogers et al., 2001). Dhx29 directly binds the 40S subunit and enhances the scanning efficiency through highly structured 5′UTRs (Pisareva et al., 2008). Concerning Ded1 and Ddx3, it has been shown that these proteins particularly stimulate scanning of long and highly structured mRNAs (Chuang et al., 1997; Tarn and Chang, 2009).

4.1.2.3 Initiation codon recognition and 80S complex formation

In order to prevent incorrect base pairing of the Met-tRNA$_i$ to a non-AUG codon and to promote recognition of the correct start codon, 43S PIC employs a discriminatory sequence-based mechanism. This permissive sequence (GCC(A/G)CCAUGG) surrounding the start codon is termed Kozak consensus sequence and is principally composed of a purine at the -3 and a G at +4 positions (the A of the AUG codon is designated as +1). A "strong Kozak consensus" is established when either one or both -3 a +4 position match the Kozak sequence, otherwise is named ''weak Kozak consensus" (Kozak, 1984, 1986; Kozak and Chakraborti, 1996). Recently, Zur and Tuller (2013) showed that auxiliary signals before and after the mAUG are required for translation initiation in addition to the Kozak context. These signals include selection for less AUG codons both upstream and downstream of the mAUG, but also non-optimal nucleotide contexts near the alternative AUGs upstream and downstream of the mAUG.

eIF1 plays a key role in this initiation codon recognition mechanism (Fig. 22, step 7) in addition to its function in scanning. eIF1, as well as eIF1A and the β subunit of eIF2, allow the 43S PIC to discriminate between the correct start codon and non-AUG start codons or AUGs within a weak Kozak context (Pestova and Kolupaeva, 2002; Ivanov et al., 2010; Martin-Marcos et al., 2011; Pisarev et al., 2006). Pisarev et al. (2006) also reported that the α-subunit of eIF2 interacts with the purine at -3 position and this interaction allows the 43S PIC to recognize the -3 context of the Kozak sequence.

Once the AUG start codon has been recognized and the 48S complex formation is accomplished, eIF1 is ejected from the scanning complex (Fig. 22, step 7) (Maag et al., 2005). This in turn triggers the hydrolysis of eIF2-bound GTP and Pi release by the eIF5 GTPase activity. eIF5 binds to the β subunit of eIF2 and induces the hydrolysis of the GTP bound to the γ-subunit of eIF2 (Algire et al., 2005; Das et al., 2001). These events cause the transition from an “open” to a “closed” conformation of the scanning complex, which stabilizes the binding of the Met-tRNAi with the AUG start codon (Nanda et al., 2009). At this point, the remaining factors are dissociated to allow the joining of the 60S subunit and 80S initiation complex formation (Fig. 22, step 8). This process is mediated by eIF5B, a ribosome-dependent GTPase homologue to the prokaryotic initiation factor IF2 (Pestova et al., 2000). Thus, eIF5B is able to dissociate eIF3, eIF4B, eIF4F and eIF5, and by its GTPase activity eIF5B self-dissociates from the assembled 80S ribosome. This reaction also triggers the release of eIF1A to finally forms an elongation competent 80S ribosome (Fig. 22, step 9) (Jackson et al., 2010).

4.1.3 Translation elongation and termination

After the AUG start codon has been identified and the formation of the 80S ribosome has been achieved, translation elongation begins (Jackson et al., 2010). Thus, 80S ribosome decodes the mRNA sequence and mediates the addition of amino acids to elongate the growing polypeptide chain. Elongation is accomplished by the eukaryotic elongation factors eEF1A, eEF1B and eEF2 (Fig. 23) (Groppo and Richter, 2009; Kapp and Lorsch, 2004). eEF1A-GTP carries each aminoacylated tRNA to the 80S ribosome A site by codon-anticodon interactions (Fig. 23, step 1). When a correct interaction occurs, GTP hydrolysis on eEF1A is stimulated and eEF1A-GDP is released. The guanidine nucleotide exchange activity of the eEF1B converts then eEF1A-GDP to its active GTP form. After 80S ribosome-catalyzed peptide bond formation, eEF2 mediates 80S ribosome translocation through the hydrolysis of GTP (Fig. 23, step 3). In this process, the mRNA and tRNAs are moved through the ribosome by a dynamic progression.

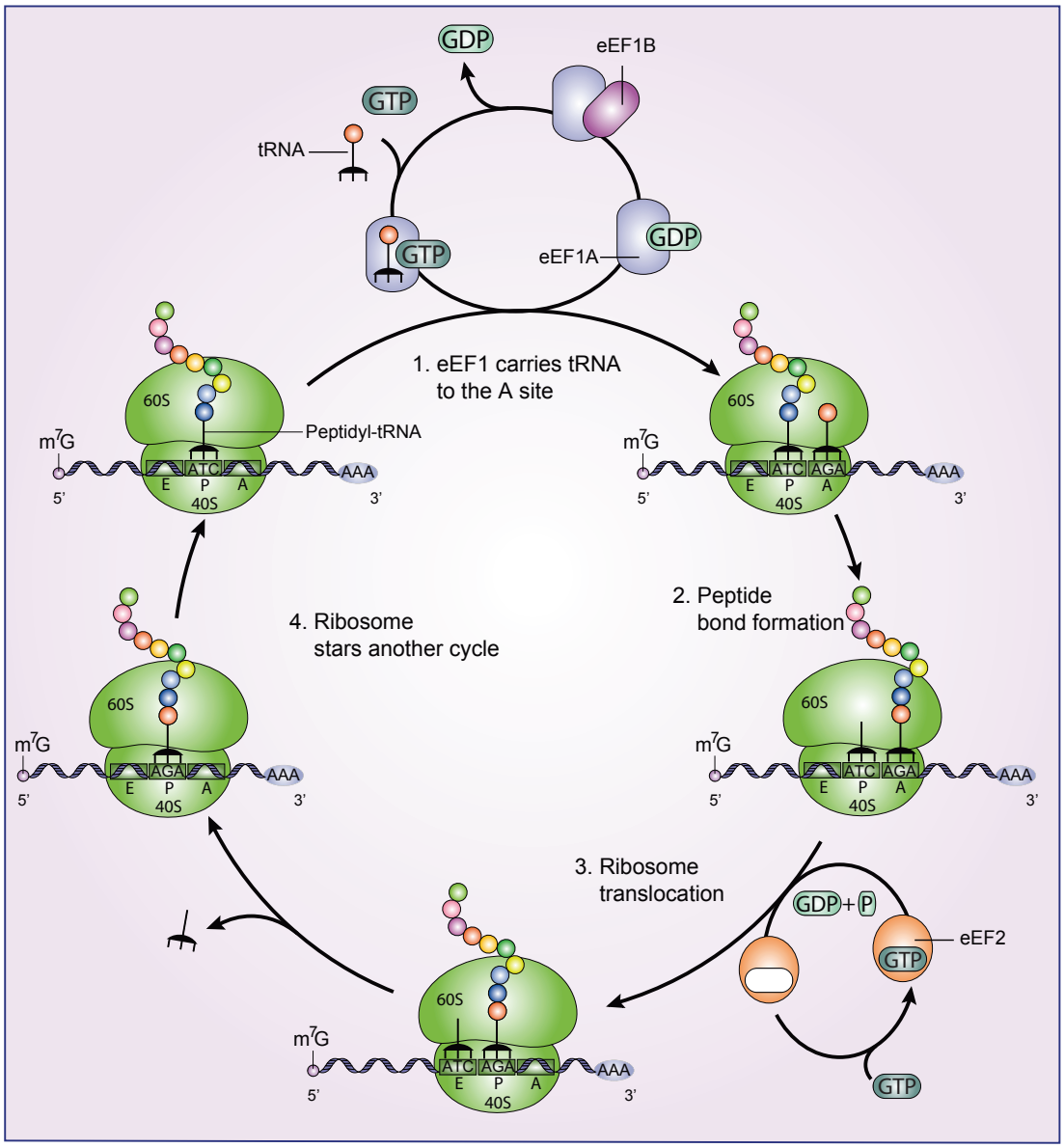

Figure 23. Eukaryotic translation elongation. eEF1A-GTP transports each aminoacylated tRNA to the A site of the 80S ribosome and eEF1A-GDP is re-activated by eEF1B (step 1). The 80S ribosome-mediated peptide bond formation (step 2) precedes ribosome translocation by eEF2 (step 3). Finally, the ribosome begins another cycle of peptide elongation (step 4).

Thus, the deacetylated tRNA is transferred to the 80S ribosome E site, re-positioning the peptidyl-tRNA in the P site and discharging the A site for the next round of amino acid incorporation (Fig. 23, step 4) (Aitken and Lorsch, 2012; Hinnebusch and Lorsch, 2012). Polypeptide elongation continues until a stop codon triggers translation termination step. This process is mediated by the eukaryotic translation termination factors eRF1 and eRF3 (Jackson et al., 2012). eRF1 mediates stop

codon recognition, while eRF3 potently stimulates peptide release. After protein release, eRF1 remains bound to the post-termination complex (post-TC), and in conjunction with the ATP-binding cassette protein ABCE1, dissociates the post-TC into the 60S subunit, and the tRNA- and mRNA- bound 40S subunit (Pisarev et al., 2010). Dissociation of tRNA is then stimulated by eIF3, eIF1 and eIF1A (Pisarev et al., 2010), Ligatin, or MCT-1/DENR (Skabkin et al., 2010). tRNA release by eIF3, eIF1 and eIF1A stimulates dissociation of the mRNA from the 40S subunit. Interestingly, at low concentration of Mg^{2+}, eIF3, eIF1 and eIF1A are able to mediate the entire termination process. In this alternative recycling mechanism, eIF3 is responsible for dissociating the post-TC (Pisarev et al., 2007).

4.1.4. Upstream open reading frames (uORF)

In silico and experimental data have demonstrate that about 50% of mammalian genes encode mRNAs that present at least one short uORF. uORF have a minimal length of 9 nucleotides including the stop codon and a median length of 48 nucleotides in human and mouse genes. Using luciferase reporter gene coupled with different uORF-containing 5'UTR, Calvo et al. (2009) observed that uORFs reduce protein expression by approximately 30-80%. In this study, a stronger inhibition was associated with different uORF properties regarding its position and context within the 5'UTR. These properties include evolutionary conservation, multiple uORFs, increased distance from the cap and a strong uAUG Kozak context. No association was found between the proximity of uORFs with the main AUG (mAUG) (Calvo et al., 2009).

Using the human single nucleotide polymorphisms (SNP) database (Smigielski et al., 2000), Calvo et al. (2009) also identified polymorphisms that produce or delete uORFs in 509 genes, named puORFs. Among these genes, 5 polymorphisms that create 1 uORF were tested for translational repression of luciferase reporter gene in comparison with their uORF-less SNP variants. The presence of the uORF in these genes reduces protein expression by 30–60%, showing that naturally occurring uORF-altering polymorphisms may regulate gene expression and alter human phenotype (Calvo et al., 2009).

Among these 509 genes, no genes implicated in HIV-1 infection were found except for the HIV-1 co-receptor CCR5 gene (Calvo et al., 2009). This CCR5 puORFs may

be implicated in HIV-1 susceptibility and AIDS progression, as previously published by Navratilova, 2006. Additionally, puORFs were also found in TRIM6, 45, 38 and 50, showing the possibility that puORFs may also exist in anti-HIV-1 restriction factors genes. Thus, these puORFs could be associated to the ability of long-term non-progressors (LTNP) to control HIV-1 infection.

4.1.5. Ribosomal translation after an uORF

In presence of an uORF in the 5'UTR, ribosomal scanning complex overcomes this sequence and translate the main ORF (mORF) by ribosomal re-initiation, leaky scanning or thanks to an IRES (Kozak, 2005). In these mechanisms, the AUG Kozak context could play an important role. A strong kozak context in uAUGs may promote ribosomal re-initiation, while a weak could favor leaky scanning. In humans, the mAUGs present a strong Kozak context in ~ 95% of cases, while the uAUGs have a lower value of 63% (Suzuki et al., 2000). This suggests that most uORF-containing mRNAs uses a leaky scanning mechanism to translate their mORF. Nevertheless, it was reported that mORF translation of an mRNA containing multiple uORFs is accomplished by both ribosomal re-initiation and leaky scanning (Wang and Rothnagel, 2004; Zhou and Song, 2006). For example, gene expression of the beta-site beta-amyloid precursor protein (APP)-cleaving enzyme 1 (BACE1) mRNA is regulated by six uAUGs in the 5'UTR. During BACE1 expression, ribosomes pass through some uAUGs by leaky scanning, translate an uORF initiated at the fourth uAUG and re-initiate BACE1 translation (Zhou and Song, 2006).

During the scanning of an uORF-containing mRNA, the 43S PIC may not recognize the uAUG if its Kozak context is weak. In this case, the 43S PIC continues to scan the 5'UTR until it reaches an AUG with an optimal Kozak sequence (Kozak, 2005). This mechanism has been named leaky scanning and can be suppressed by mRNA secondary structures (Fig. 24). Indeed, Kozak (1990) showed that downstream secondary structures promotes the recognition of an AUG in a weak Kozak context. These structures may slow down the scanning of the 43S PIC and increase AUG recognition.

Concerning the ribosomal re-initiation, this process could be defined as the capacity of the 40S subunit to regenerate a competent ribosomal complex, which is able to re-initiates translation at the mAUG after translating an uORF.

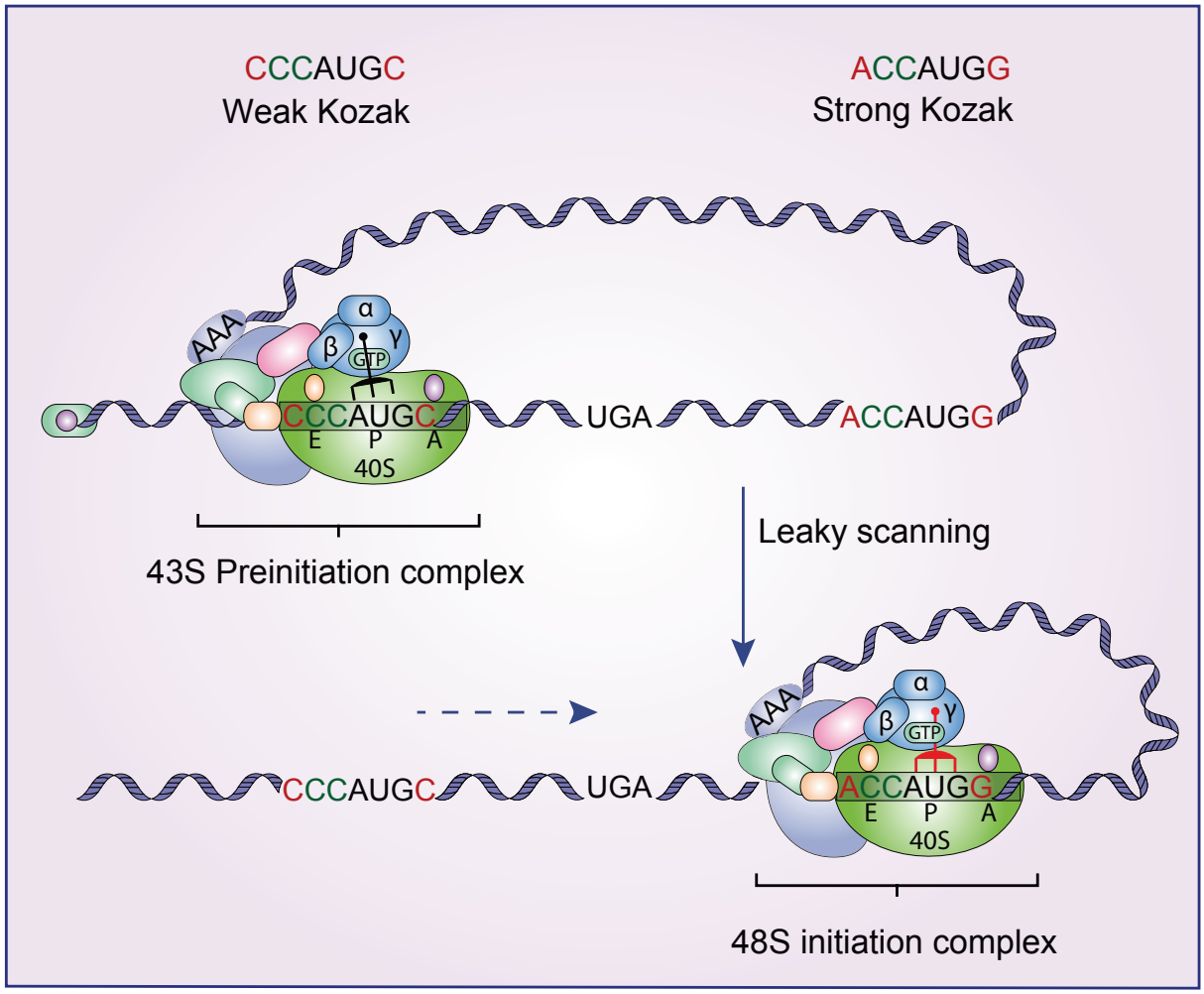

Figure 24. Leaky scanning mechanism. The 43S pre-initiation complex scans the 5'UTR and passes through the uAUG within a weak Kozak context. The 43S PIC then recognizes the mAUG in a strong Kozak context to initiate translation of the mORF.

This mechanism can regulate protein translation in response to environmental changes (Jackson et al., 2012). In this mechanism, uORF translation termination and post-termination events probably occurs conventionally with the activity of eRF1 and eRF3 release factors (Jackson et al., 2012). In this process, post-TC is not completely dissociated and 40S subunits remain on the mRNA and resume scanning even if they lack the ternary complex and other initiation factors. In the presence of eIF2, eIF3, eIF1, eIF1A and Met-tRNAi, Skabkin et al. (2013) showed that 40S subunits remain on the mRNA, scan bi-directionally, and re-initiate at upstream and

downstream AUGs if the regions surrounding the uORF stop codon are unstructured. At this point, new ternary complex and initiation factors are acquired *de novo* to form a competent 43S PIC capable of recognizing the mAUG (Fig. 25) (Kozak, 2005; Munzarová et al., 2011).

It is well established that re-initiation is more efficient when the uORFs sequences are small and the distance between the uORF stop codon and the mAUG is longer (Kozak, 2005). This distance increases the time available for reloading the initiation factors and therefore re-initiation is enhanced (Child et al., 1999; Lincoln et al., 1998). Re-initiation can also be enhanced by RNA motifs surrounding the uORF sequence, as it was reported in the GCN4 mRNA in yeast (Szamecz et al., 2008). eIF3 plays a critical role in this mechanism by interacting with these RNA motifs. Indeed, eIF3 interacts with a 5' enhancer region at the mRNA to promote 40S subunits stabilization on the uORF and subsequent downstream scanning (Munzarová et al., 2011; Szamecz et al., 2008). Concerning the peptide translated from an uORF, it was reported that only in rare cases, this small protein has regulatory effects (Fang et al., 2004; Kozak, 2005; Law et al., 2001). For example, the fungal arginine attenuator peptide (AAP) functions as nascent peptide within the ribosome tunnel to block translation in the presence of Arginine (Fang et al., 2004; Wei et al., 2012).

4.1.6. Translation through an IRES

Most mRNAs employ the scanning cap-dependent mechanism to initiate translation; although, a few mRNAs use internal ribosome entry sites (IRES). In this mechanism, the ribosome is attracted close to the mAUG principally by secondary and tertiary structures, but also by trans-acting factors and 18S rRNA sequence complementarity (Thompson, 2012; Xue and Barna, 2012).

IRES elements were first discovered in poliovirus RNA. These mRNAs are usually uncapped and IRESs are required for efficient translation. Later, IRESs were discovered in cellular mRNAs and it was reported that 10-15% of cellular mRNAs could be translated by this cap-independent mechanism (Spriggs et al., 2008).

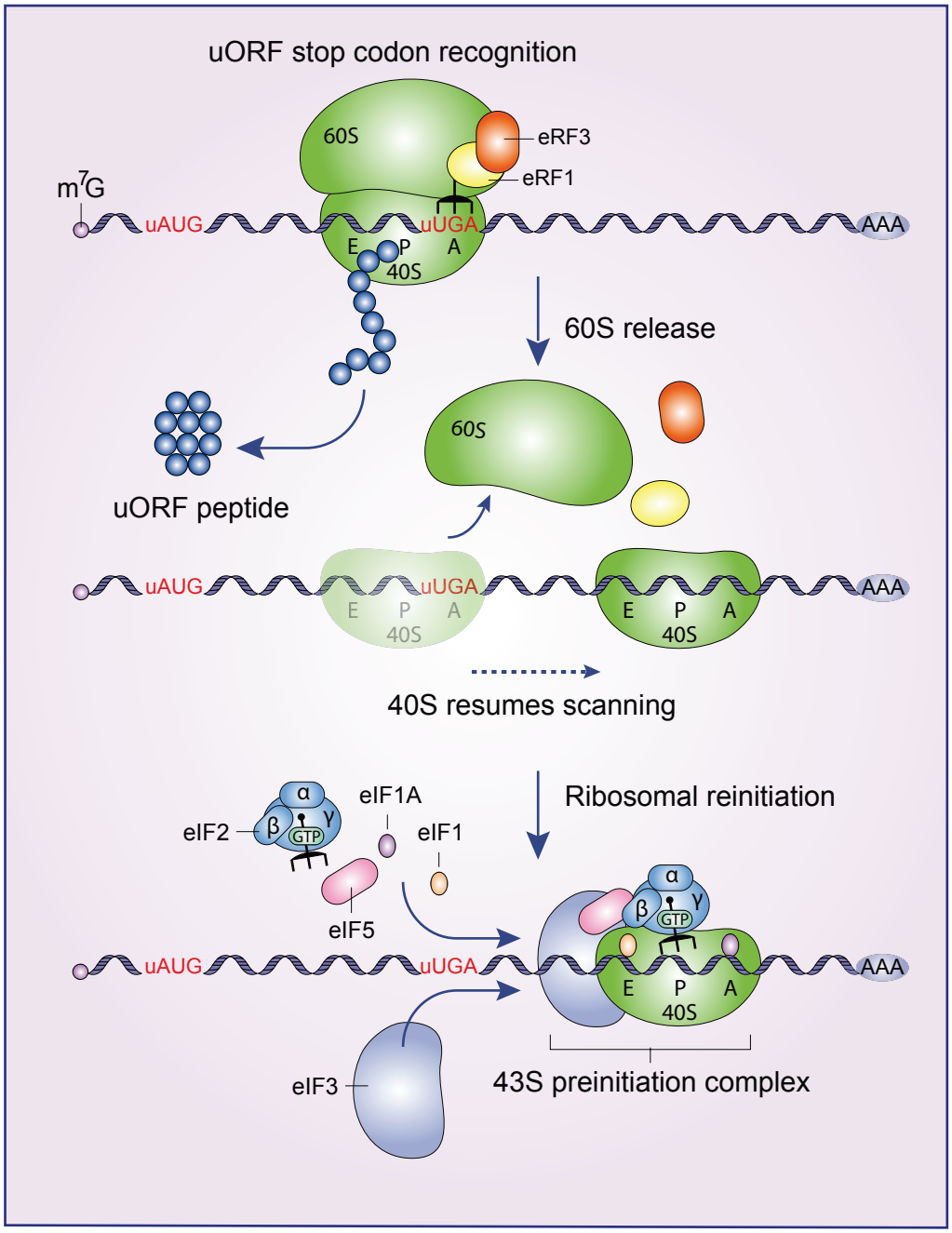

Figure 25.Translational re-initiation after an uORF. The termination events at the stop codon of the uORF occur conventionally and the 40S subunit continues scanning. The 40S subunit acquires new initiation factors to form a competent 43S pre-initiation complex capable of recognizing the mAUG.

These IRES-dependent mechanisms have been associated with stress-related genes, such as X-linked inhibitor of apoptosis (XIAP) factor or hypoxia-inducible factor 1A (HIF1A). IRES-mediated translation of these genes is activated when cap-dependent translation is reduced by stress conditions (Greijer and van der Wall,

2004; Holcik and Korneluk, 2000). IRESs are highly structured RNA regions that are able to directly recruit the 40S ribosomal subunit near or at the AUG start codon. This process requires a set of cellular proteins to support IRES-dependent translation, named IRES trans-acting factors (ITAFs), (Balvay et al., 2009; Thompson, 2012).

Recent evidence suggests that the ribosome *per se* enhances specific IRES recognition through its ribosomal proteins. For example, 40S ribosomal protein S25 (RPS25) is required for the IRES-mediated translation of two different IRES elements from the cricket paralysis virus (CrPV) and the hepatitis C virus (Landry et al., 2009). Similarly, RPS19 and RPS11 control IRES-dependent translation of two mRNAs implicated in murine and human erythroblasts differentiation, called cold shock domain containing protein E1 (CSDE1) and BCL-2 associated athanogene 1 (BAG1), respectively (Horos et al., 2012).

During viral infection, pathogen-associated molecular patterns (PAMPs) activate signaling cascades that inhibit global protein translation to generate an antiviral protective state. Moreover, Vpr also influences a global translation inhibition due to G2/M arrest (see below). In this regulatory mechanism, cap-dependent protein translation is targeted by post-translational modifications of the mRNA-ribonucleoprotein complexes that are required for translation initiation. In order to overcome this global translation down-regulation, many cellular and viral mRNAs uses IRESs to promote cap-independent translation.

4.2. HIV-1 tricks eukaryotic translation during infection

4.2.1. Hijacking the mRNA nuclear export machinery

Once the HIV-1 viral DNA is part of the host genome, viral mRNAs are produced as a variety of alternatively spliced species ensuring the synthesis of all HIV-1 structural and regulatory proteins. More than 40 different viral mRNAs are produced by alternative splicing from a single polycistronic pre-mRNA. These spliced mRNAs can be divided into two classes: multiply spliced (2 kb) and singly spliced (4 kb) RNAs (Leblanc et al., 2013). The multiply spliced viral mRNAs are exported from the nucleus to the cytoplasm by the endogenous NXF1/NXT1-mediated pathway (Fig. 26) (Adams and Wente, 2013; Moore and Proudfoot, 2009).

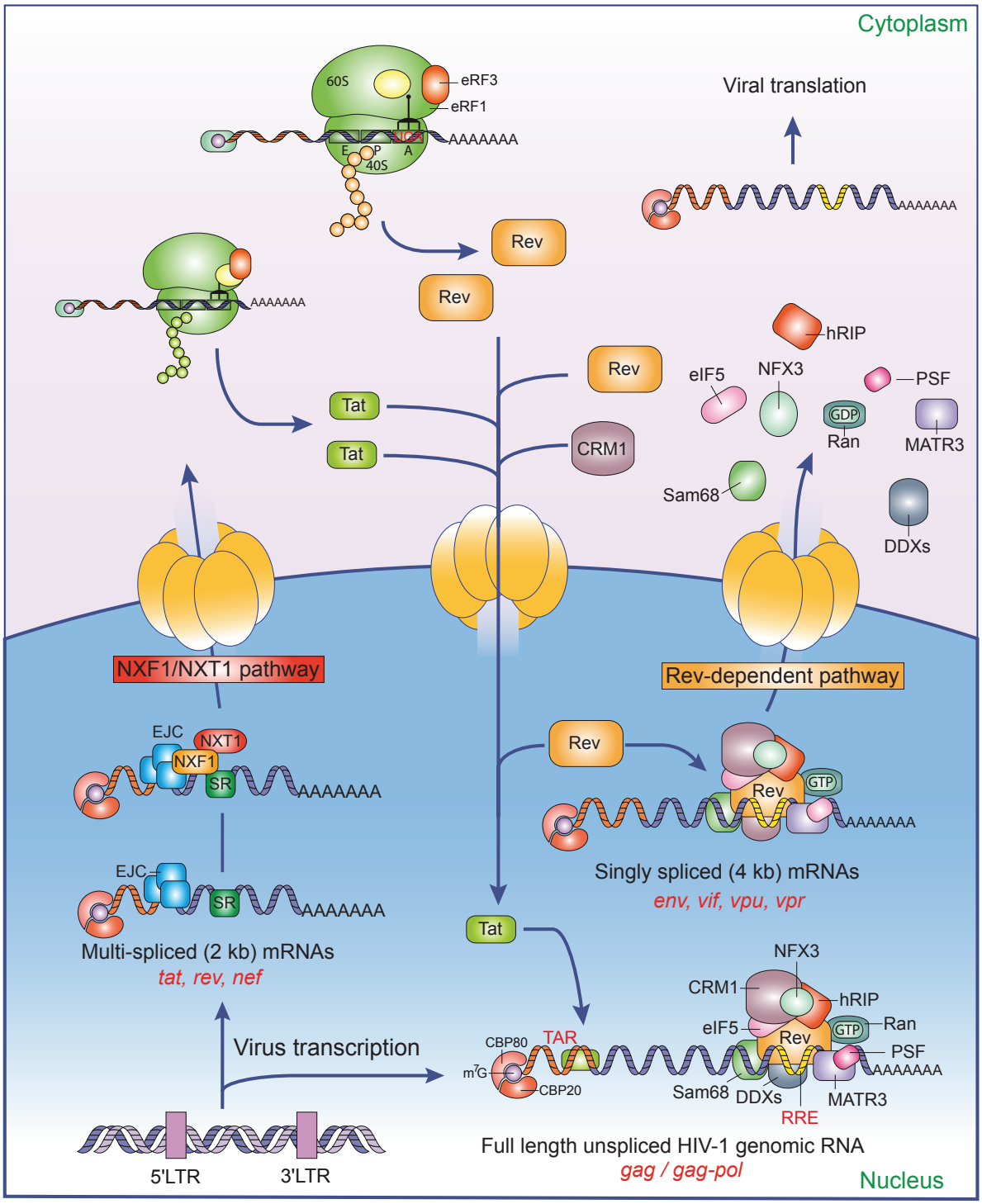

Figure 26. HIV-1 mRNA export. Multi-spliced (2 kb) mRNAs are exported by the endogenous NXF1/NXT1 pathway. Rev and Tat proteins are imported into the nucleus. Tat enhances viral transcription and Rev promotes nuclear export of full-length unspliced HIV-1 genomic mRNA and singly spliced (4 kb) mRNAs. The export of these mRNAs is mediated by several cellular factors.

One of these mRNAs encodes for the HIV-1 Rev protein which is transported back to the nucleus to facilitate nuclear export of singly spliced mRNAs and unspliced viral genomic RNA (Fernandes et al., 2012). HIV-1 Rev protein acts as a linker between the Rev response element (RRE), located within the *env* mRNA coding region (Fig. 26), and the host cellular proteins of the CRM1-dependent cargo pathway implicated in the mRNA nuclear export process (Fernandes et al., 2012). In this mechanism, Rev recruits the exportin CRM1 (Chromosome Region Maintenance 1) and the nuclear export factor Ran bound to guanosine triphosphatase (RanGTP). The Rev-CRM1-RanGTP complex interacts with the nuclear pore complex (NPC) to be transported through the nuclear pore to the cytoplasm. The hydrolysis of GTP to GDP allows the dissociation of the complex and the redirection of Rev back into the nucleus (Fernandes et al., 2012; Purcell and Martin, 1993; Tazi et al., 2010).

The reason why HIV-1 uses an adapter protein that recruit CRM1 to export their singly spliced and unspliced mRNAs is that eukaryotic cells established a nuclear mechanism to retain incompletely spliced mRNAs in the nucleus (Cullen, 2003a, 2003b). This process is mediated by a subset of splicing factors named commitment factors. These factors are then removed by the splicing machinery and mRNAs can be targeted for nuclear export (Takemura et al., 2011). Thus, HIV-1 had to develop a sequence-mediated nuclear export mechanism to overcome this endogenous retention mechanism.

Other cellular proteins have also been implicated in Rev-dependent HIV-1 RNA export. Among them are eIF5 (Ruhl et al., 1993), human Rev-interacting protein (hRIP) (Fritz et al., 1995), SRC-associated protein in mitosis of 68 kDa (Sam68) (Li et al., 2002) and several RNA helicases (Fig. 26) (Lorgeoux et al., 2012; Yasuda-Inoue et al., 2013). eIF5 interacts specifically to the HIV-1 Rev activation domain (Ruhl et al., 1993) and may serve as an adapter between Rev and CRM1 to promote HIV-1 nuclear export (Hofmann et al., 2001). hRIP interacts with the exportin CRM1 *via* the nuclear export factor 3 (NXF3) and with the HIV-1 Rev effector domain to promote HIV-1 RNA release from the perinuclear region to the cytoplasm (Sánchez-Velar et al., 2004). Sam68 interacts with the HIV-1 Rev protein to regulate the CRM1-mediated Rev nuclear export pathway. Down-regulation of Sam68 expression causes the retention of the Rev-CRM1 complex in the nucleus preventing nuclear export (Li et al., 2002). RNA helicases DDX1, DDX3, DDX5, DDX17, DDX21 and

DDX56 interact with HIV-1 Rev protein and synergistically improve HIV-1 RNA nuclear export (Fang et al., 2005; Yasuda-Inoue et al., 2013; Yedavalli et al., 2004). DDX3 has also been implicated in anti-viral immunity acting as a mediator in viral nucleic acids recognition. DDX3 binds the CARD-containing adapter mitochondrial antiviral signaling protein (MAVS) and promotes IFN-β production after the recognition of viral RNA by the retinoic acid-inducible gene I (RIG-I)-like receptors (RLRs) (Oshiumi et al., 2010). Since RLRs RIG-I and MDA5 detect HIV-1 RNA and generate an immune response through the MAVS adapter, it seems that HIV-1 hijacks DDX3 to improve HIV-1 Rev-dependent RNA export and thereby causing a reduction of IFN-β production (Fullam and Schröder, 2013). Additionally, Kula et al. (2011) showed that Matrin 3 (MATR3) acts as a cellular cofactor of Rev activity. MATR3 interacts with the HIV-1 viral RNA and promotes Rev-mediated nuclear export of unspliced HIV-1 RNAs. Recently, Kula et al. (2013) identified a novel cellular protein implicated in HIV-1 RNA export, the polypyrimidine tract-binding protein-associated splicing factor (PSF). PSF interacts with both the viral mRNA and MATR3 to promote viral mRNA export.

4.2.2. Targeting mRNA activation

In the G2/M phase of the cell cycle, cap-dependent translation is down-regulated by a series of consecutive events that lead to the disruption of the eIF4F complex, and thereby inhibition of the mRNA activation step (Fig. 22, step 3) (Kronja and Orr-Weaver, 2011). In this process, eIF4F complex formation is interrupted by targeting the eIF4E factor. eIF4E is regulated by a family of translational inhibitory proteins, named the eIF4E-binding proteins (4E-BPs). After hypophosphorylation, 4E-BPs compete with eIF4G for the same binding site on eIF4E, preventing eIF4F complex assembly (Kronja and Orr-Weaver, 2011; Richter and Sonenberg, 2005).

In HIV-1-infected cell, viral proteins alter cell function by affecting different cellular pathways. In this concern, HIV-1 viral protein R (Vpr) has been identified as a viral protein capable of arresting cells in the G2/M phase. Vpr mediates G2/M arrest *via* a complex signaling cascade involving activation of the ataxia telangiectasia mutated and Rad3-related kinase (ATR) (Planelles and Barker, 2010). In Vpr-induced G2/M arrest, host protein translation is also inhibited by a process involving the regulation of eIF4E activity. Despite the global reduction of host protein synthesis by Vpr-

induced G2/M arrest, translation of HIV-1 structural proteins is still maintained (Sharma et al., 2012). RNA-coimmunoprecipitation experiments showed that full-length unspliced HIV-1 genomic RNA and singly spliced mRNAs are associated with the CBC in contrast to multi-spliced viral and cellular mRNAs that are associated with eIF4E. Moreover, unspliced and singly spliced viral mRNAs retain their interaction with CBC during translation and packaging. Based on these observations, Sharma et al. (2012) hypothesized that unspliced and singly spliced viral mRNAs are translated by the ability of the CBC to activate mRNA during translation initiation. Thus, CBC retention could allow viral protein synthesis while the global protein translation is inhibited by eIF4E reduction.

4.2.3. Overcoming and inhibiting ribosome scanning

During the ribosomal scanning process, the unwinding step of all HIV-1 mRNAs is obstructed by their highly structured trans-activation response (TAR) RNA element present in the 5'UTR (de Breyne et al., 2013). In order to overcome this constraint, Soto-Rifo et al. (2012) have shown that RNA helicase DDX3 is required in this process. DDX3 directly binds to the HIV-1 5'UTR and interacts with eIF4G and PABP to promote translation initiation of the HIV-1 genomic mRNA (Soto-Rifo et al., 2012). DDX3 mediates pre-initiation complex assembly in an ATP-dependent manner. In this process, the HIV-1 genomic RNA is located in large cytoplasmic RNA granules alongside with DDX3, eIF4G and PABP but not with CBP20/80 and eIF4E (Soto-Rifo et al., 2013). *In vitro* experiments revealed that cytoplasmic DDX3 is able to bind the m^7G cap independently of eIF4E, showing that DDX3 could promote the formation of a pre-initiation complex in the absence of eIF4E. Thus, DDX3 substitutes eIF4E to stimulate compartmentalized translation initiation of HIV-1 genomic RNA (Soto-Rifo et al., 2013). As discussed above, DDX3 also interacts with Rev to enhance HIV-1 RNA nuclear export (Yasuda-Inoue et al., 2013). Interestingly, Groom et al. (2009), using an *in vitro* transcription/translation assay in rabbit reticulocyte lysates, have demonstrated that Rev also stimulates translation of HIV-1 mRNAs at low concentration. This stimulation is dependent on a Rev binding site, in addition to the RRE, present in the internal loop A of stem-loop 1 of HIV-1 RNA packaging signal (Greatorex et al., 2002). On the contrary, at high concentration, Rev inhibits mRNA translation in a non-specific manner. In this process, Rev may bind mRNAs and

block ribosomal scanning (Groom et al., 2009) by a mechanism that remains to be elucidated.

4.2.4. HIV-1 IRESs: thriving under cap-dependent translation inhibition

The HIV-1 genomic mRNA presents two IRESs: one in the viral 5'UTR, named HIV-1 IRES (Brasey et al., 2003) and a second within the gag coding region, known as HIV-1 Gag IRES (Buck et al., 2001) (Fig. 27). The HIV-1 IRES along with the 5' cap structure mediates translation of the structural proteins $Pr55^{Gag}$ and $Pr160^{Gag/Pol}$ (Berkhout et al., 2011; Brasey et al., 2003; Gendron et al., 2011). It was characterized in the proviral wild-type HIV-1 clone (pNL4.3) (Brasey et al., 2003) but also in the CXCR4 (X4)-tropic primary isolate HIV-LAI (Gendron et al., 2011) and in viral RNA isolated from clinical samples (Vallejos et al., 2012), showing the importance of these elements in HIV-1 replication. The minimal IRES activity of the HIV-1 IRES is harbored within the region spanning nucleotides 104 to 336 (Brasey et al., 2003). This region also contains several RNA motifs implicated in different functions of the HIV-1 life cycle (Fig. 27). The HIV-1 IRES has been shown to be implicated in different cellular states in which cap-dependent translation initiation is inhibited (de Breyne et al., 2013). Thus, HIV-1 IRES drives viral structural protein synthesis during the G2/M cell cycle transition (Brasey et al., 2003; Vallejos et al., 2011), during oxidative stress (Gendron et al., 2011) and HIV-1 protease-mediated cleavage of eIF4G and PABP. Although the molecular mechanism of the HIV-1 IRES-mediated translation remains largely unknown, several cellular proteins have been reported as cellular factors increasing the HIV-1 IRES activity (de Breyne et al., 2013). Among them are the heterogeneous nuclear ribonucleoprotein A1 (hnRNP A1) (Monette et al., 2009) and the Rev-cofactors DDX3, hRIP and eIF5 (Liu et al., 2011). On the contrary, the human embryonic lethal abnormal vision (ELAV)-like protein (HuR) has been identified as a negative regulator of the HIV-1 IRES activity (Rivas-Aravena et al., 2009). Additionally, *cis*-acting elements have also been shown to negatively modulate HIV-1 IRES activity. Brasey et al (2003) showed that the Gag ORF impacts the HIV-1 IRES-mediated translation initiation in the context of a bi-cistronic mRNA. Gendron et al (2011) identified another region located upstream of the PBS, the IRES negative element (IRENE) that also negatively regulates the HIV-1 IRES activity. Recently, Valiente-Echeverría et al. (2013) showed that the

instability element 1 (INS-1), a cis-acting regulatory element present within the gag ORF, also inhibits HIV-1 IRES activity.

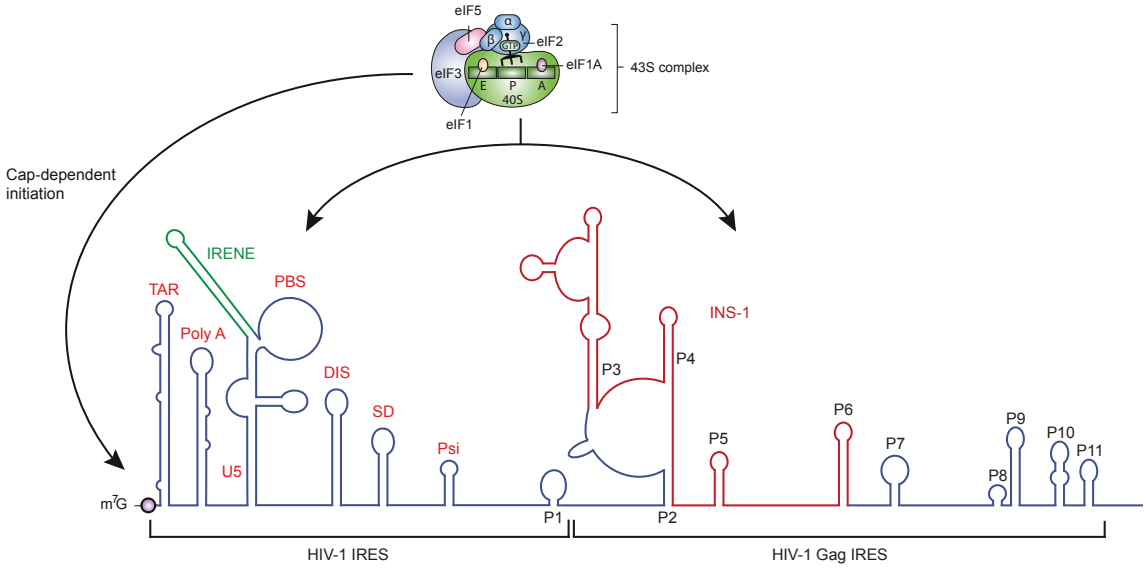

Figure 27. **HIV-1 IRESs.** HIV-1 IRES and HIV-1 Gag IRESs are represented. The 43S pre-initiation complex can mediate both cap-dependent and IRES-mediated translation initiation. Adapted from de Breyne et al. (2013).

Furthermore, several HIV-1 IRES ITAFs have been identified from G2/M-arrested cell extracts (Vallejos et al., 2011), including proteins that have already been identified to have a role in HIV-1 replication, such as the high mobility group protein HMG-I/HMG-Y (HMG-I(Y)) (Li et al., 2000a) or the activated RNA polymerase II transcriptional co-activator p15 (Holloway et al., 2000).

Concerning the HIV-1 Gag IRES, this element mediates translation of both full length Gag polyprotein and a N-truncated 40-kDa Gag (p40) isoform lacking the matrix domain (Buck et al., 2001; Weill et al., 2010). Despite the fact that p40 is much lower produced than $Pr55^{Gag}$, this protein seems to be important in wild-type replication of HIV-1 in cultured cells (Buck et al., 2001). Expression of p40 has also been observed in all HIV-1 clinical isolates from a large cohort of patients (n = 100) (de Breyne et al., 2013). By analyzing purified 48S complexes paused on the HIV-2 Gag IRES, Locker et al., (2011) identified the presence of all the canonical initiation factors, with the exception of eIF4E and eIF1. The authors also reported that HIV-2 Gag IRES directly recruits the 40S ribosomal subunit and eIF3, suggesting that the HIV-2 Gag IRES-mediated translation initiation could be mediated by a two-step mechanism. The initial event is the formation of a ternary eIF3/40S/IRES complex, followed by a

transfer of the ribosome onto the initiation codons mediated by a rearrangement of the complex stimulated by the canonical initiation factors (Locker et al., 2011). Additionally, Weill et al. (2010) showed that HIV-2 Gag IRES is capable of recruiting up to three initiation complexes on a single RNA molecule.

4.2.5. Targeting translation factors

In the course of the HIV-1 viral cycle, viral proteins target different cellular products, such as translation factors, to improve viral fitness and pathogenicity. By using a yeast two-hybrid screen assay, Cimarelli and Luban (1999) reported that the HIV-1 $Pr55^{Gag}$ binds to eEF1A through its matrix (MA) and nucleocapsid (NC) domains. The authors demonstrated that this interaction requires RNA and suggested that tRNA could probably mediate this interaction since both NC and eEF1A have been shown to bind tRNAs (Khan and Giedroc, 1992; Merrick, 2010). Thus, as cellular concentration of $Pr55^{Gag}$ increases in the cell, $Pr55^{Gag}$ association with eEF1A-tRNA complexes may induce translational inhibition. As a consequence of this inhibition, viral genomic RNA is released from the translation machinery. Subsequently, $Pr55^{Gag}$ interaction with the genomic RNA may lead to a further viral translation inhibition, thus stimulating RNA packaging into virions (Cimarelli and Luban, 1999). The authors also showed that both eEF1A and a truncated form of eEF1A of 34 to 36 kDa are incorporated into the virions. In addition, eEF1A can also interact with the cellular cytoskeleton, suggesting a possible role of eEF1A in virion assembly and budding (Ott et al., 2000). Despite these reports, direct evidence for a role of eEF1A in RNA packaging, virion assembly or budding remains to be demonstrated (Li et al., 2013). Similar to $Pr55^{Gag}$, HIV-1 Nef protein also interacts with eEF1A and forms a Nef/eEF1A/tRNA complex. Thus, Nef mediates a nucleocytoplasmic relocalization of eEF1A and tRNAs to prevent stress-induced apoptosis in primary human macrophages (Abbas et al., 2012). Moreover, Warren et al. (2012) have reported that the HIV-1 reverse transcription complex (RTC) recruits eEF1A and eEF1G to stimulate late steps of HIV-1 reverse transcription. eEF1A and eEF1G bind to the HIV-1 RTC through an interaction with the RTC components, reverse transcriptase (RT) and integrase (IN). This association enhances the stability of the RTC in the cytoplasm (Warren et al., 2012). Nevertheless, further studies will be needed to establish whether eEF1A and eEF1G function synergistically with the components of the RTC or independently during reverse transcription.

In addition to its principal function during HIV-1 virion maturation, the HIV-1 protease also impairs cap-dependent protein translation. Ventoso et al. (2001) were the first to report that HIV-1 protease is able to cleave the initiation factor eIF4G *ex vivo*, using the HIV-1 target C8166 cells. Further studies demonstrated that HIV-1 protease not only cleaves eIF4G but also PABP *in vitro* using rabbit reticulocyte lysates (Alvarez et al., 2006; Castelló et al., 2009; Ohlmann et al., 2002). Degradation of eIF4G and PABP leads to an inhibition of the cap- and PABP-dependent translation initiation (Alvarez et al., 2006; Castelló et al., 2009; Ohlmann et al., 2002; Ventoso et al., 2001). Jäger et al. (2012) reported that the HIV-1 protease also cleaves eIF3d, a subunit of eukaryotic translation initiation factor 3. This cleavage present a similar efficiency as the cleavage of the $Pr55^{Gag}$. This may also promote inhibition of cap-dependent protein synthesis. However, as discussed above, HIV-1 counteracts this inhibition by different pathways.

In the early phases of HIV-1 replication, the HIV-1 TAR RNA element activates the protein kinase RNA-activated (PKR), which mediates host translation inhibition to generate a protective antiviral state (Clerzius et al., 2011). PKR specifically interacts with the TAR element, inducing PKR dimerization, auto-phosphorylation and activation. Activated PKR phosphorylates eIF2 to block its recycling for ongoing translation, resulting in a potent translation inhibition (Sadler and Williams, 2007). HIV-1 indirectly prevents eIF2 phosphorylation by targeting PKR. Indeed, the HIV-1 Tat protein directly interacts with PKR, thus preventing eIF2 auto-phosphorylation which is essential for its function (Clerzius et al., 2011; McMillan et al., 1995). Moreover, during the late events of the HIV-1 replication, PKR activity is inhibited by a high concentration of the HIV-1 TAR element. Studies with TAR and other RNAs showed that high concentration of dsRNA inhibits PKR dimerization and therefore its activation (Lemaire et al., 2008).

II. OBJECTIVES

The HIV-1 Vif protein allows productive infection of non-permissive cells (including most natural HIV-1 targets cells) by counteracting cellular cytidine deaminases A3G and A3F and thus preventing their incorporation into viral particles. Vif targets A3G/F *via* two principal mechanisms: 1) Vif mediates A3G/F degradation through the proteasome and 2) Vif induces A3G/F translation inhibition (Henriet et al., 2009). The Vif-induced degradation of A3G through the proteasome pathway has been extensively studied, but little is known about the translational repression of A3G mRNA by Vif.

For many years, the Marquet-Paillart's research group "Retroviruses and RNA viruses", in which I conducted my PhD thesis, explored the molecular aspects of the Vif-mediated A3G translational inhibition. In this concern, they showed that Vif is able to inhibit A3G translation *in vitro* in a 5'UTR-dependent manner (Mercenne et al., 2010). *In vitro* A3G translational inhibition by Vif has been previously observed by other groups (Kao et al., 2003; Mariani et al., 2003; Stopak et al., 2003). However, the Vif-induced A3G translational inhibition has never been demonstrated *ex vivo* and the impact of this repression in HIV-1 virus infectivity remains undetermined. A3G translational inhibition by Vif is still a poorly understood pathway and further studies are needed to understand how the 5'UTR of A3G mRNA is required in this repression.

The general objective of this study is to understand how Vif is capable of inhibiting A3G translation. Does Vif-induced A3G translation inhibition also occur *ex vivo*? What are the A3G mRNA elements implicated in this mechanism? Does Vif-induced A3G translation repression has an impact in viral infectivity? By which molecular mechanism does Vif impair A3G translation?

In addition, this thesis analyzes another aspect of Vif protein, aiming to determine which domain(s) of Vif is (are) implicated in the RNA chaperone activity.

III. RESULTS & DISCUSSION

1. Article 1: Inhibition of APOBEC3G translation by Vif restores HIV-1 infectivity

Inhibition of APOBEC3G translation by Vif restores HIV-1 infectivity

Santiago X. Guerrero[1], Gaëlle Mercenne[3], Julien Batisse[1], Delphine Richer[1], Géraldine Laumond[2], Thomas Decoville[2], Christiane Moog[2], Roland Marquet[1] & Jean-Christophe Paillart[1#]

[1]Architecture et Réactivité de l'ARN, Université de Strasbourg, CNRS, IBMC, 15 rue René Descartes, 67084, Strasbourg cedex, France

[2]INSERM-UMR 1110, Interactions virus-hôte et maladies hépatiques, Université de Strasbourg, Institut de Virologie, rue Koeberlé, 67000 Strasbourg, France

[3] Present address: University of Utah - Department of Biochemistry, 15 N Medical Dr East, Salt Lake City, UT 84112-5650, USA

[#] To whom correspondence should be addressed:

E-mail: jc.paillart@ibmc-cnrs.unistra.fr

Dr. Jean-Christophe Paillart

UPR 9002 CNRS

Institut de Biologie Moléculaire et Cellulaire

15, Rue René Descartes,

67084 Strasbourg cedex, France

phone: (+33) (0)3 88 41 70 35; fax: (+33) (0)3 88 60 22 18

Classification: Biological Science, Biochemistry

Keywords: HIV-1, Vif, APOBEC3G, mRNA, translation

ABSTRACT

The HIV-1 viral infectivity factor (Vif) is a small basic protein essential for viral fitness and pathogenicity. Vif allows productive infection of non-permissive cells (including most natural HIV-1 targets) by counteracting cellular cytosine deaminases APOBEC3G (A3G) and A3F by different mechanisms and thus preventing its incorporation into viral particles. The Vif-induced degradation of A3G through the proteasome pathway has been extensively studied, but little is known about the translational repression of A3G mRNA by Vif. After cellular co-transfection of A3G mRNA constructs mutated in their untranslated regions (UTRs) in presence or absence of Vif, and in conditions where the proteasome-induced degradation of A3G was inhibited, we show that the 5'-UTR of A3G mRNA is crucial for the translational inhibition by Vif. The core binding factor, CBF-β, required to stabilize the Vif/A3G complex is dispensable for this specific repression. According to our previous secondary structural model of the 5'-UTR, the two distal stem-loop structures are sufficient for a complete translational inhibition of A3G. We show that residue K26 of Vif is critical for A3G neutralization, both for its proteasome-induced degradation and translation inhibition of its mRNA. Interestingly, we observe a strict correlation between the cellular reduction of A3G through translation inhibition and the quantity of A3G incorporated into viral particles. Both mechanisms account for about 50% decrease of A3G in cell. Thus, we showed for the first time that A3G mRNA translational inhibition by Vif is a 5'-UTR mRNA-dependent mechanism, and that any of these two mechanisms, degradation or translation, is sufficient to restore viral infectivity. Regulating the translation of A3G could thus be considered as a new target to restore a functional expression of A3G and viral restriction.

INTRODUCTION

Human immunodeficiency virus type 1 (HIV-1) and related lentiviruses require the viral accessory protein Vif to neutralize members of the APOBEC3 (Apolipoprotein B mRNA editing enzyme, catalytic polypeptide-like 3, here referred to as A3) family of restriction factors and render host cells permissive for productive viral replication (1,2). Among this family of cytidine deaminases, A3G and A3F have the most powerful antiretroviral activity and have been shown to block post-entry HIV-1 replication through more than one mechanism (3-7). In the absence of the HIV-1 viral infectivity factor (Vif), A3G is efficiently incorporated into progeny virions through interactions with the nucleocapsid domain of $Pr55^{Gag}$ and/or viral and non viral RNAs (8-12). This packaged A3G has been shown to be the most active on the viral genome rather than the pool of cytoplasmic A3G in newly infected cell (13). Once a new infection is initiated, the incorporated A3G will deaminate deoxycytidine to deoxyuridine in minus strand viral DNA during reverse transcription through its cytidine deaminase activity, resulting in hypermutation in the viral genome. As a result, the HIV-1 proviral DNA will be no longer functional or degrade rapidly (4,6,14,15). Beside, non-enzymatic antiretroviral activity of A3G/3F proteins has also been implicated in inhibiting the accumulation of HIV-1 reverse transcription products, and provirus integration (7,16-19). Cytidine deamination and inhibition of reverse transcription contribute to the antiviral activity of endogenous A3 proteins in CD4+ T cells (20).

To counteract the antiretroviral activity of A3G, HIV-1 expresses Vif, a small basic protein, which binds and targets newly synthesized A3G for degradation through different mechanisms, which leads at the end to reduced A3G incorporation into viral particles (21). First, it has now be well documented that Vif neutralizes A3 proteins by recruiting an E3 ubiquitin ligase complex that polyubiquitinates A3 proteins and targets them for proteasomal degradation ((22) reviewed in (2,21,23)). Vif is composed of several highly conserved motifs that form discontinuous surfaces, so that Vif can accommodate with all A3 proteins (N-terminus) and E3 ligase (C-terminus) (21). Recently, the cellular transcription factor CBF-β was identified as a critical cofactor and found to be associated with the ubiquitin-like Cul5/Rbx2/ElonginBC (CRL5) complex (24,25). CBF-β induces the stabilization of

Vif, thus allowing for efficient degradation of A3G and increased viral infectivity (26). Secondly, it has been proposed that Vif could reduce the intracellular level of A3G by affecting its translation (27-29) and recent *in vitro* data highlighted the importance of the untranslated regions (UTRs) of A3G mRNA in this process (30). Indeed, protein synthesis is principally regulated at the initiation stage of the translation and analyses of cellular mRNAs showed that both 5'- and 3-UTRs are of importance in translational initiation, either through the binding of RNA-binding proteins or miRNAs (31,32). Despite the fact that A3G translation inhibition by Vif seems to clearly occur, almost all studies have been carried out *in vitro* or by using unnatural A3G mRNA lacking UTRs.

In the present study, we examined the translational inhibition of A3G mRNA by Vif. By using A3G mRNA constructs mutated in their UTRs in conditions where the proteasome-induced degradation of A3G was inhibited, and thus, only translation can be observed, we showed that the 5'-UTR of A3G mRNA is crucial for the translational inhibition by Vif, and according to our previous secondary structural model of the 5'-UTR, the two distal stem-loop structures are sufficient for a complete translational inhibition. Interestingly, we observe a strict correlation between the cellular reduction of A3G through translation inhibition and the amount of A3G incorporated into viral particles, and showed for the first time that this inhibition, in complement to proteasomal-induced A3G degradation, is sufficient to restore viral infectivity. Thus, regulating the translation of A3G could thus be considered as a new target to restore a functional expression of A3G and viral restriction.

MATERIAL AND METHODS

Plasmids

Plasmids pCMV-hA3G, pCMV-hA3GΔUTR, pCMV-hA3GΔ5'UTR and pCMV-hA3GΔ3'UTR have been previously described (30). pCMV-hA3G SL1, SL2, SL3, SL1SL2 and SL2SL3 were generated by Quick-Change Site-directed Mutagenesis (Agilent Technology) based on the secondary structure model of the 5'-UTR of hA3G mRNA (30) and deletions were confirmed by DNA sequencing (GATC Biotech, Germany). For Vif expression, the pcDNA hVif encoding codon-optimized NL4.3 Vif was used (33). This plasmid and its nucleotide sequence are available through the NIH AIDS Research and Reference Reagent Program (catalog #10077). Mutations K26R and H42/H43-N were generated in the pcDNA hVif plasmid by Quick-Change Site-directed Mutagenesis (Agilent Technology) as recommended by the manufacturer. The infectious molecular clone pNL4-3 has been previously described and is also available through the NIH AIDS Research and Reference Reagent Program (catalog #114). The vif-defective pNL4-3 variant, pNL4-3Δvif, carrying a 178-bp out-of-frame deletion in the *vif* gene, has been previously reported (34). The dominant negative mutant of the Cul5, Cul5ΔRbx, was used to block A3G degradation by the proteasome (22). pNL4.3, pNL4.3Δvif, pNL4.3Δenv and pNL4.3ΔenvΔvif were generously provided by Dr. Klaus Strebel (National Institutes of Health, Bethesda, MD). The CBF-β expression plasmid and CBF-β-depleted HEK 293T cells (35) were kindly provided by Dr. Reuben S. Harris (Institute for Molecular Virology, University of Minnesota, Minneapolis, USA).

Cell Culture and transfection

HEK 293T and TZM-bl cells cells were maintained in Dulbecco's modified Eagle's medium (DMEM, Invitrogen) supplemented with 10% fetal bovine serum (FBS, EUROBIO) with antibiotics (PAA) and passaged upon confluence. HEK 293T cells expressing either a specific scrambled short hairpin (sh)RNA or a CBF-β specific shRNA were additionaly maintained with puromycin at a concentration of 0.75 µg/ml. Transfections of HEK 293T cells were carried out using the X-tremeGENE 9 DNA Transfection Reagent (Roche) as recommended by the manufacturer. Briefly, cells were seeded at 70% confluence in a 6-well plate and co-transfected with 50 ng of pCMV-hA3G constructs, 1 µg of pcDNA hVif or hVif mutants (K26R and H42/H43-N)

and 0.5 µg of Cul5ΔRbx in order to block A3G degradation by the proteasome. In parallel experiments, cells were exposed to chemical proteasome inhibitor such as ALLN (25 µM) for 18 h. For infectivity assays and study of A3G incorporation into HIV-1 particles, HEK 293T cells were co-transfected with 50 ng of pCMV-hA3G mutants, 0.5 µg of Cul5ΔRbx and 1 µg of HIV-1 pNL4.3 (pNL4.3 wt, pNL4.3Δvif). For infectivity assay, TZM-bl indicator cells were challenged with reverse transcriptase normalized virions and the resulted induction of luciferase was detected 48 h post-infection (36). To study the impact of CBF-β on Vif-mediated A3G translation inhibition, HEK 293T cells lines were co-transfected with 50 ng of pCMV-hA3G constructs, 1 µg of pcDNA hVif, 0.5 µg of Cul5ΔRbx and 100 ng of CBF-β expression plasmids.

Immuno-precipitation assays

HEK 293T cells were co-transfected with A3G-HA and different constructions of Vif (wild-type, H42/43N, and K26R), and 24 h post-transfection, cells were washed in PBS 1X and lysed in RIPA 1X supplemented with protease inhibitors. After centrifugation, an input fraction (50 µl) was kept to check protein expression level, and the remaining was incubated 2 h at 4°C with 1 µg of HA antibody (Santa Cruz, California, USA) on a rotating wheel. After equilibration, protein A Dynabeads (Life Technologies) were added and incubated for 1.5 h at 4°C. Beads were washed 5 times with cold RIPA 1X buffer, and eluted in glycine pH 2.8 + NuPAGE LDS sample buffer 1X (Life Technologies). After 10 min at 70°C, supernatant were loaded on NuPAGE gel (Life Technologies) and analyzed by western blot.

Immunoblotting

After 24 hours post-transfection, cells were harvested in 1× RIPA lysis buffer (PBS containing 1% NP40, 0.5% sodium deoxycholate, 0.05% SDS) supplemented with complete protease inhibitor cocktail (Roche). Virions from transfected 293T cells were concentrated by ultracentrifugation at 100,000 g, for 2 h at 4°C through a 20% sucrose cushion and harvested in 1× RIPA lysis buffer. Cell and virions lysates were adjusted to equivalent protein concentration by using Bradford reagent (BIO-RAD), fractionated by SDS/PAGE using NuPAGE® Novex® 4-12% Bis-Tris gels (Invitrogen) and transferred to a 22 µm PDFV membranes using the Trans-Blot®

Turbo™ Transfer System (BIO-RAD). Blots were probed with appropriate primary antibodies. Polyclonal anti-hA3G (#9968) and monoclonal anti-HIV-1 Vif (#319) antibodies were obtained through the NIH AIDS Research and Reference Reagent Program. Monoclonal anti-β-actin antibody was purchased from SIGMA (#A5316). An anti-CBFβ mouse monoclonal antibody was purchased from Santa Cruz (#sc-56751). An HIV-positive patient serum was used for the identification of HIV-1 p24 protein. The PDFV membranes were then incubated with horseradish peroxidase-conjugated secondary antibodies (BIO-RAD), and the proteins were visualized by enhanced chemiluminescence (ECL) using the ECL Plus Western blotting detection reagent (GE Healthcares). Bands were quantified using Image J (1.46r) by analyzing pixel density. Student's T-test was used to determine statistical significance.

RNA isolation, cDNA synthesis and real-time q-PCR

24 h post-transfection, total RNA was isolated from 293T cells using TRI Reagent (SIGMA) according to the manufacturer's instructions. After additional DNAse (Roche) digestion step, total RNA was isolated by phenol/chloroform extraction followed by ethanol precipitation. Total RNA (1 µg) was then reversed transcribed using the iScript™ Reverse Transcription Supermix (BIO-RAD) as recommended by the manufacturer. Subsequent real-time PCR analysis was performed using the KAPA SYBR® FAST qPCR Master Mix according to the manufacturer's specifications (KAPA BIOSYSTEMS) and was monitored on a CFX Real Time System (BIO-RAD). Gene-specific primers were: A3G forward primer, 5'-TCCACCCACATTCACTTTCA-3', and reverse primer 5'-TTCCAAAAGGGAATCACG TC-3'; β-actin forward primer, 5'-GGACTTCGAGCAAGAGATGG-3', and reverse primer 5'-AGCACTGTGTTGGCGTACAG-3'. The A3G mRNA levels were normalized to those of β-actin mRNA and relative quantification was determined using the standar curve based method.

RESULTS

Vif impairs translation of A3G mRNA

Three reports previously observed that Vif might interfere with A3G mRNA translation (27-29). Pulse-chase labeling (27-29) and *in vitro*-coupled transcription/translation (28) experiments were performed and showed that the steady-state level of A3G was decreased by 30-50% and that translational inhibition accounted for about 60-75%. Because of the unnaturally A3G mRNA expression vector used (expressing only the open reading frame – ORF), this system may not faithfully recapitulate events occurring with endogenous A3G mRNA. However, a recent study pointed out on potential role of untranslated regions (UTRs) of A3G mRNA on its translational regulation and they showed by using *in vitro*-couple transcription/translation that Vif caused a two-fold reduction of A3G translation in a 5'-UTR dependent manner (30). Despite the fact that A3G translation inhibition by Vif seems to clearly occur, almost all the studies cited above have been carried out *in vitro* or by using unnatural A3G mRNA. Therefore, we examined the level of A3G protein expressed in transfected HEK 293T cells from full-length UTR-containing A3G mRNA and from mutant RNAs deleted from their 5', 3' or both 5' and 3'-UTRs, in presence or in absence of HIV-1 Vif (Figure 1A). To directly analyze the effect of Vif on translational mRNA repression rather than on a cumulative effect with the proteasomal-induced degradation of A3G, we performed all our experiments in presence or absence of a dominant negative of Cul5 (Cul5ΔRbx), which has previously been shown to specifically inhibit A3G degradation through the proteasome pathway (22), or by using ALLN, a potent proteasome inhibitor (Figure 2). Moreover, to avoid saturating our system with overexpressed and non-physiological concentration of A3G, only 50 ng of A3G-expressing plasmids were transfected in HEK 293T cells.

Immunoblotting of normalized cell lysates with A3G-specific antibody revealed that the expression of wild-type A3G mRNA was reduced in presence of Vif (Figure 2). Quantitation of A3G signal (Figure 2B) revealed a 60% decreased of A3G protein in Vif-expressing cells. When we analyzed the UTR-truncated version of A3G mRNAs, we observed a similar decrease when the 3'-UTR was removed (50-60%);

surprisingly, this decrease was twice less pronounced (around 30%) when the 5'- or both UTRs were deleted (Figure 2B).

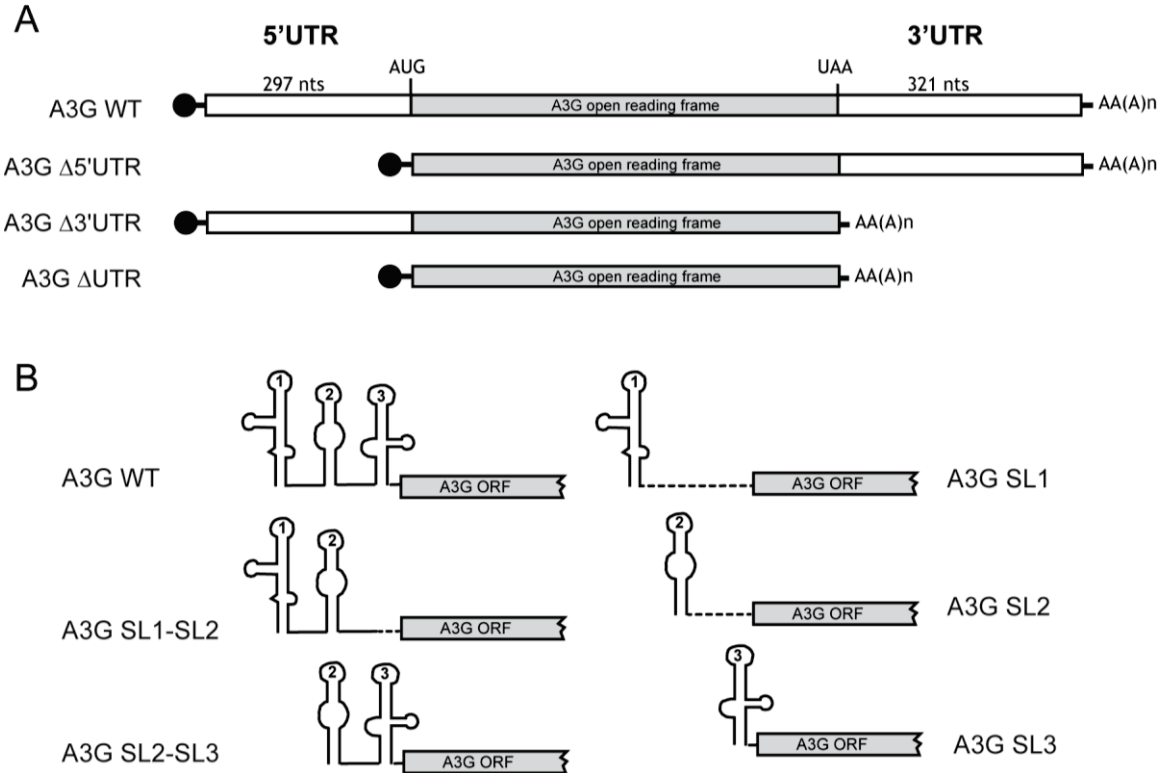

Figure 1: Schematic representation of A3G constructs used in this study. (A) Full-length UTR-containing A3G mRNA and mutants deleted from their 5', 3' or both 5' and 3'-UTRs are represented. (**B**) The secondary structure of the 5'UTR of wild-type and mutated A3G mRNAs is shown.

Interestingly, when the proteasomal pathway was blocked by using either a dominant negative of Cul5 (Cul5ΔRbx) or a chemical inhibitor (ALLN), we still observed a significant decrease of A3G (30-40%, i.e. 50% of total A3G inhibition without inhibitors) when expressed from the full-length or Δ3'UTR mRNAs (Figure 2A, lanes 4 & 5), whereas the two other deleted constructs, Δ5'-UTR and ΔUTR, were not dependent on the degradation process anymore, or not significantly affected (Figure 2A & 2B, middle and right histograms).

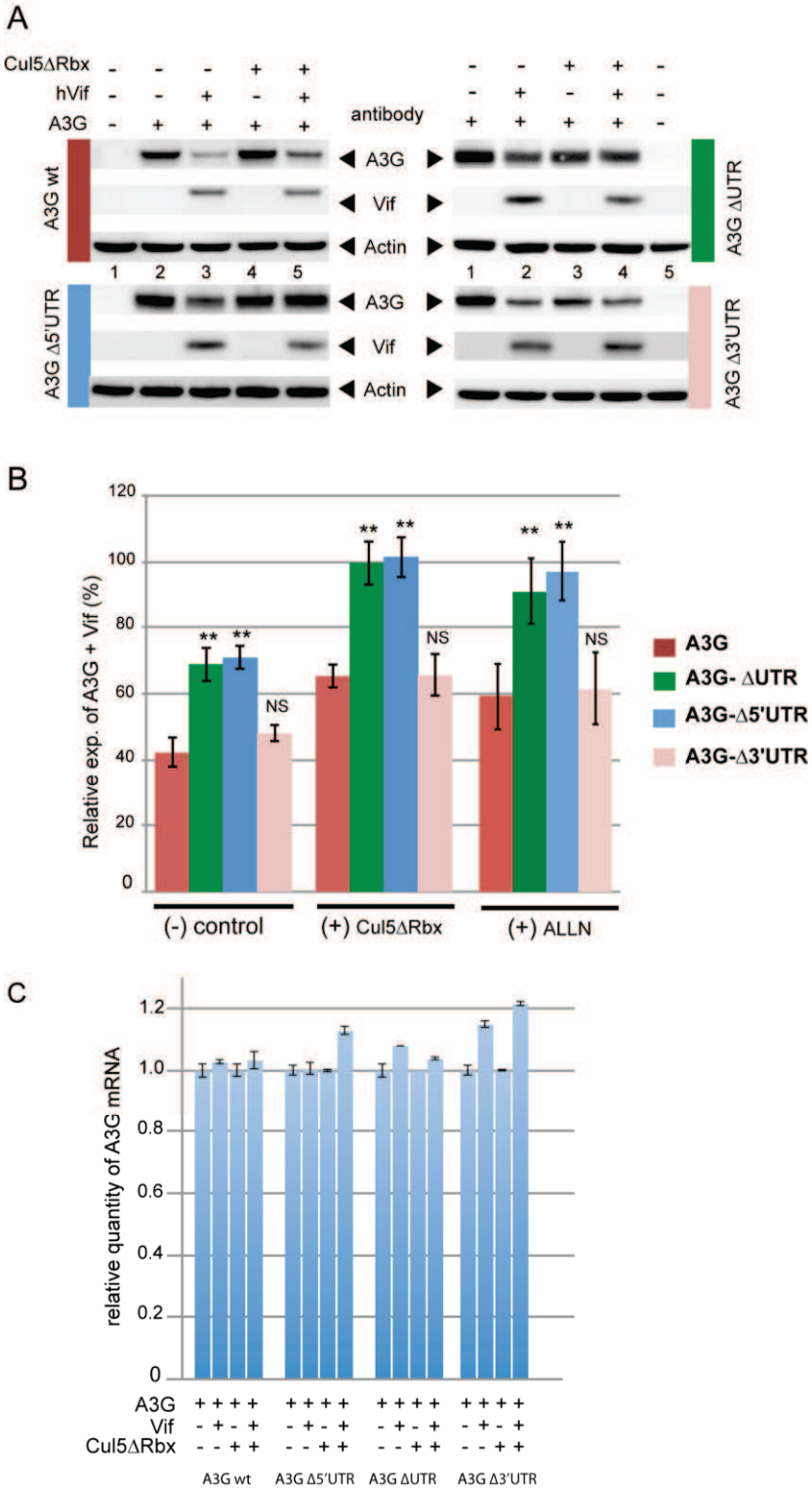

Figure 2: Vif inhibits A3G translation in a 5'UTR dependent manner. HEK 293T cells were transfected with different A3G constructs (wt, Δ5'UTR, Δ3'UTR and ΔUTR) and co-transfected with Vif +/- proteasome inhibitor Cul5ΔRbx. Proteasome inhibition was also carried out in presence or absence of ALLN. (**A**) Proteins were separated by SDS-PAGE and analyzed by immunoblotting. (**B**) Protein bands were quantified using Image J (1.46r) and relative expression of A3G in presence of Vif is represented in a histogram. (**C**) Total RNA was then extracted from transfected HEK 293T cells and A3G RT-qPCR was performed to study the relative expression of A3G constructs.

Consistent with previously published data (27,28,37), Vif did not affect A3G mRNA levels, which remained constant in all conditions and for all A3G mRNA constructs used (Figure 2C), suggesting the reduction in A3G protein is not due to differential expressions of the vectors or to mRNA degradation. Together, these results clearly demonstrate that Vif depletes A3G in a 5'-UTR mRNA dependent manner and that the translational inhibition imposed by Vif accounts for about 50% of the total A3G repression process.

Vif requires stem-loop 2 and 3 of A3G mRNA to reduce its translation

We previously determined by chemical/enzymatic probing and footprinting experiments that the secondary structure of the 5'-UTR of A3G mRNA is composed of three independent stem-loop (SL) motifs (Figure 1B), and that Vif binds to 3-4 high affinity binding sites in this region (30). In order to evaluate the specific sequences/motifs in the 5'-UTR that would be required to the A3G translational inhibition by Vif, we designed specific A3G mRNAs containing each of the individual SL motifs (A3G SL1, containing only SL1, A3G SL2 and A3G SL3) or two consecutive SL motifs (A3G SL1-SL2 and A3G SL2-SL2). All these constructs were further evaluated towards their Vif-induced translational inhibition after transfection of HEK 293T cells in presence or absence of proteasome inhibitors. First of all, in absence of proteasomal inhibition, expression of Vif more strongly affected the relative expression of full-length A3G mRNA as well as mRNA containing SL2 and SL3 motifs, whereas expression of all other mRNA constructs, while affected, was less severe (Figure 3A). Quantitation of immunoblots showed a 50-60% decrease for wild-type and SL2-SL3 mRNAs while reduction was twice less reduced for mutant RNAs containing only one SL or the one containing SL1 and SL2 (Figure 3B). More interestingly, when the proteasomal degradation of A3G was blocked, we still observed a significant reduction of A3G expression for wild-type and SL2-SL3 mRNAs (30-40%), while all other mRNAs were not affected by Vif anymore (Figure 3B). Again, the cellular level of wild-type and mutant A3G mRNAs were not affected by the presence of Vif or during proteasomal inhibition (Figure 3C), suggesting the reduction in A3G protein is at a posttranscriptional level.

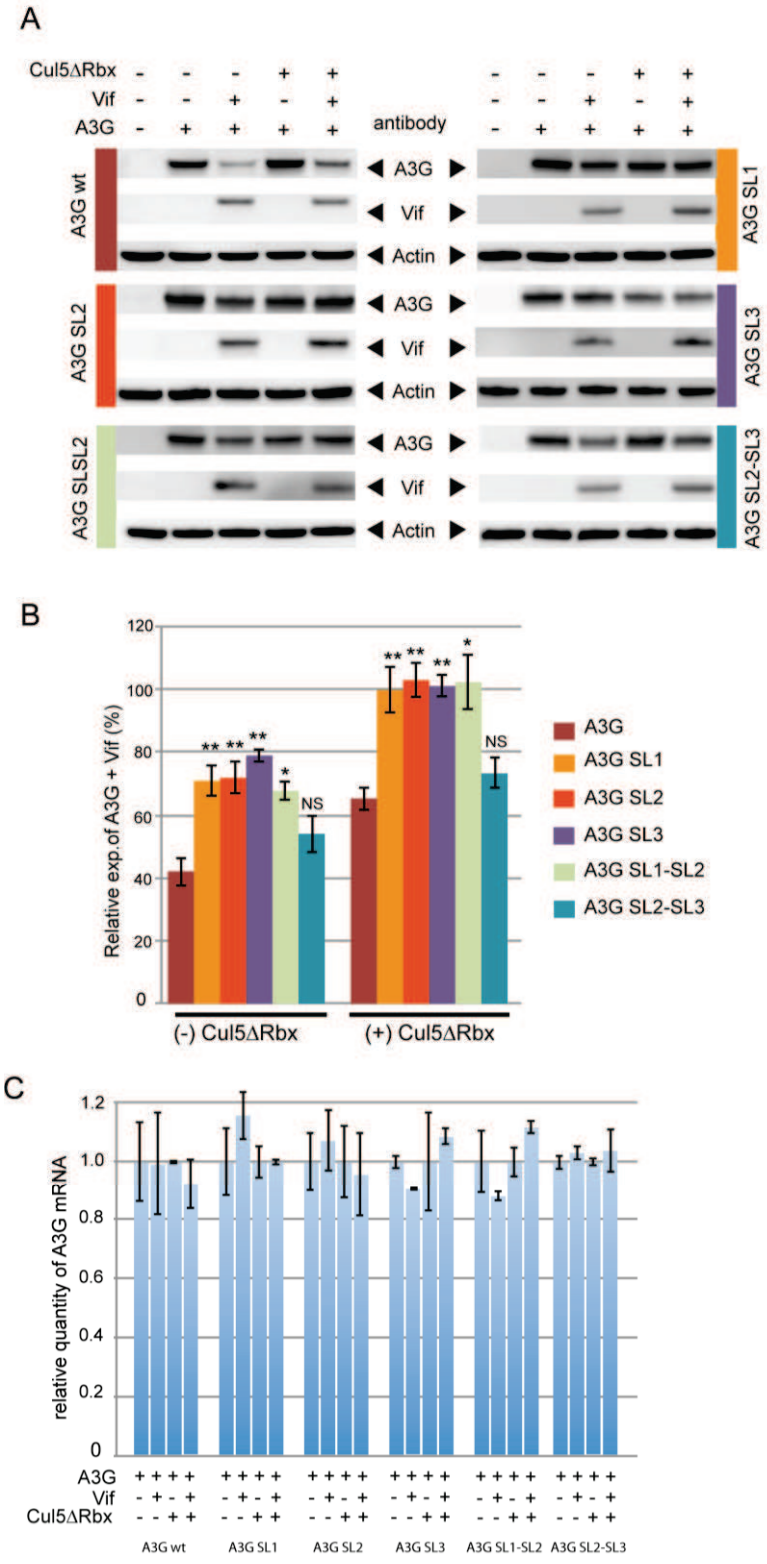

Figure 3: Vif requires SL2 and SL3 to impair A3G translation. HEK 293T cells were transfected with wild-type and mutated A3G constructs (A3G SL1, SL2, SL3, SL1-SL2 or SL2-SL3), and co-transfected with Vif +/- proteasome inhibitor Cul5ΔRbx. (**A**) Proteins were separated by SDS-PAGE and analyzed by immunoblotting. (**B**) Protein bands were quantified using Image J (1.46r) and relative expression of A3G in presence of Vif is represented in a histogram. (**C**) Total RNA was then extracted from transfected HEK 293T cells and A3G RT-qPCR was performed to study the relative expression of A3G constructs.

These data confirm the importance of the 5'-UTR of A3G mRNA and highlight SL2 and SL3 together as a minimal motif requires for the translational inhibition imposed by Vif.

The translational down-regulation of A3G is independent of CBF-β

It has recently been observed that Vif hijacks CBF-β to the ubiquitin-like Cul5/Rbx2/ElonginBC (CRL5) complex and that the CRL5/Vif/CBF-β complex is required for Vif-mediated A3G degradation and viral infectivity (24,25). To determine if CBF-β is required to the Vif-induced translational down-regulation of A3G mRNA, we transfected a constant amount of Vif and full-length A3G mRNA into HEK 293T cells expressing either a scrambled short hairpin (sh)RNA or a CBF-β-specific shRNA (kindly provided by R. Harris) (24). In parallel, and to discriminate the translational effect from the proteasomal degradation of A3G by Vif, we co-transfected the dominant negative mutant of Cul5. As previously observed, the levels of steady-state Vif were two to three-fold lower in CBF-β depleted cells than in the scrambled control cells (Figure 4, compare lanes 6 and 2, and 8 and 4), but this level was increased when CBF-β-depleted cells were complemented with a CBF-β expression plasmid (Figure 4, lanes 10 & 12). As expected from results presented above (Figure 2), we obtained similar down-regulation of wild-type A3G mRNA in presence of Vif in scrambled shRNA cells (Figure 4, lanes 1 to 4), with a translational inhibition corresponding to about 50% of the total A3G decrease. Interestingly, the depletion of CBF-β did not modify the behavior of Vif towards A3G, as we observed the same decrease in A3G level in presence (Figure 4, compare lanes 2 and 5) or in absence (Figure 4, compare lanes 4 and 8) of proteasome-induced A3G degradation. As proteasome blockage did not reverse this effect, our results suggest that CBF-β does not impact the translational inhibition of A3G imposed by Vif. Analogous data were obtained when CBF-β-depleted cells were complemented with a CBF-β expression plasmid (Figure 4, lanes 10-13).

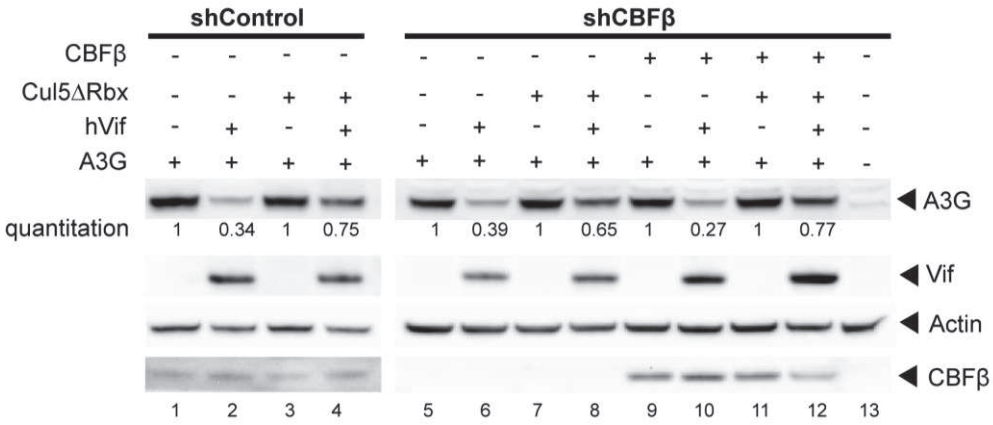

Figure 4: CBF-β is not required in Vif-mediated A3G translational inhibition. HEK 293T cells expressing a non-specific short-hairpin RNA (shControl) or a CBF-β specific short-hairpin RNA (shCBF-β) were transfected with wild-type A3G and co-transfected with Vif +/- proteasome inhibitor Cul5ΔRbx. Proteins were separated by SDS-PAGE and analyzed by immunoblotting. Bands were quantified using Image J (1.46r) and relative expression of A3G is showed under the A3G blot.

The Vif-induced translational inhibition reduces packaging of A3G

Vif and A3G are both packaged into virions and while the exact mechanism of their incorporation is still a matter of debate (10), they both required interactions with RNAs and/or proteins such as the nucleocapsid domain of HIV-1 precursor $Pr55^{Gag}$ (8,38-42). Thus, it has been suggested that Vif might directly interfere with A3G encapsidation through a binding competition mechanism that still need to be clarified (43,44). However, it is well known that the proteasomal-induced degradation of A3G reduces its incorporation into viral particles as a result of its lower concentration in cells. To investigate the possible correlation of A3G translational inhibition by Vif and its packaging into viral particles, we co-transfected wild-type (pNL4.3) or Vif deleted (pNL4.3Δvif) molecular clones of HIV-1 together with full-length, Δ5'UTR or SL2-SL3 A3G expression vectors (Figure 5). Note that amongst these constructs, only A3G Δ5'UTR is independent of the translational regulation by Vif. To distinguish the direct effect of Vif on A3G translation, these experiments were also performed in presence of the dominant negative mutant of Cul5 (Cul5ΔRbx). Cell lysates (Figure 5A) and concentrated virus fractions (Figure 5B) were analyzed by immunoblotting with specific Vif, A3G and CAp24 antibodies.

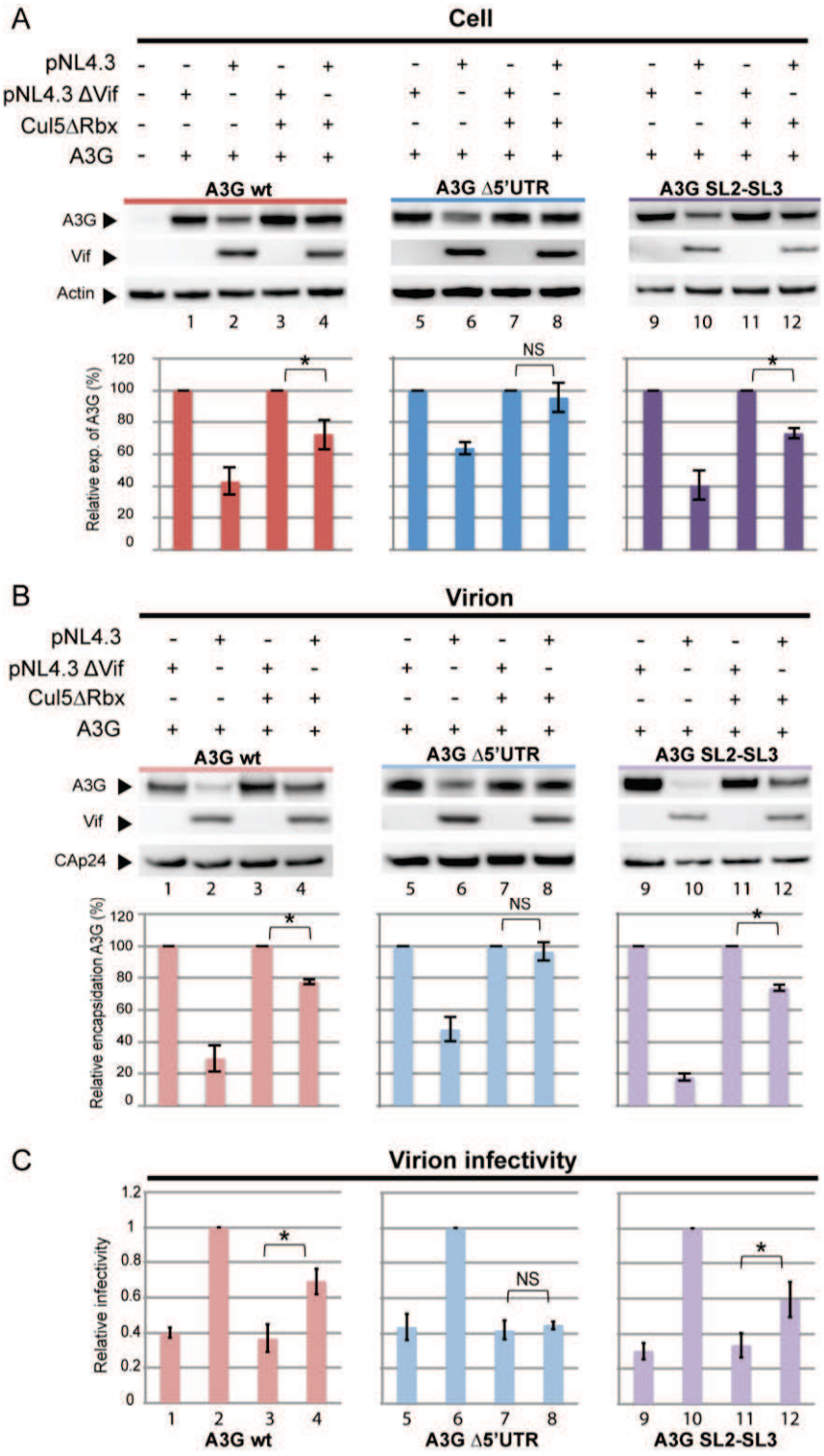

Figure 5: Effect of Vif-induced A3G translational inhibition in A3G packaging and viral infectivity. HEK 293T cells were co-transfected with HIV-1 pNL4.3 or pNL4.3Δvif constructs with wild-type A3G and Cul5ΔRbx. Proteins from cell lysates (**A**) and virions (**B**) were separated by SDS-PAGE and analyzed by immunoblotting. (**C**) Viral particles produced in HEK 293T cells were used in viral infectivity assay. Reverse transcriptase normalized virions were used to infect TZM-bl indicator cells and luciferase induction was detected 48 h post-infection.

Consistent with the results from Figure 2A and 3A, expression of Vif from a proviral molecular clones showed a strong 60-70% decrease of A3G when expressed from full-length or ΔSL2-SL3 constructs, whereas this reduction was less severe (30-40%) when the 5'UTR of A3G was removed (Figure 5A, lanes 2, 6 and 10). But still, amongst this reduction, about 50% could be attributed to a direct translational effect of Vif for wild-type and SL2-SL3 A3Gs (Figure 5A, lanes 4 and 12) while A3G Δ5'UTR is insensitive to any degradation when the proteasome was inhibited (Figure 5A, lane 8), suggesting the 5'-UTR is crucial for the translational inhibition.

Next, we analyzed the packaging of A3G proteins issues from these different transfections. Consistent with A3G expression level (Figure 5A), the presence of higher amount of A3G protein in cell resulted in increased packaging of A3G (Figure 5B, lanes 1, 3, 5, 7, 9 & 11 in absence of Vif). In contrast, the reduction of A3G in cell due to its degradation (Figure 5B, lanes 2, 6 & 10) or its direct translational inhibition (Figure 5B, lanes 4, 8 & 12) resulted in significant decreasing amount of virus-associated A3G. The relationship between Vif expression and A3G packaging in the different conditions studied (presence or absence of proteasomal degradation) was quantified (Figure 5B, histograms). It is interesting to note that a strict correlation is observed between the level of A3G present in cell and the amount of A3G incorporated into virions. Indeed, in conditions where only the translational inhibition of A3G by Vif was active (Figure 5B, righ columns of histograms), we observed a significant 20-30% decrease in packaged A3G expressed from wild-type and SL2-SL3 mRNAs. Importantly, the packaging of A3G expressed from the Δ5'-UTR construct was not affected at all (Figure 5B, middle histogram, righ column). Finally, the amount of Vif protein encapsidated into viral particles did not change, in all tested conditions, even when A3G was not down-regulated anymore (A3G Δ5'UTR), suggesting a competition mechanism for Vif and A3G packaging is unlikely. These results demonstrate that the translational inhibition of A3G by Vif is sufficient by itself to reduce the packaging of A3G.

The translational inhibition of A3G by Vif restores viral infectivity

To determine whether the translational repression of A3G by Vif impacts HIV-1 viral infectivity, wild-type (pNL4.3) or Vif-defective (pNL4.3Δvif) virus stocks were produced in HEK 293T cells after co-transfection with full-length, Δ5'UTR or SL2-SL3

A3G mRNAs in the presence or absence of proteasomal degradation (Figure 5). The infectivity of the resulting viruses was determined by infection of TZM-Bl indicator cells after normalization of virus preparation (45). As shown in Figure 5C, and as expected from the action of Vif on A3G expression and virion incorporation, viruses produced in the presence of Vif in normal conditions are fully infectious (bars 2, 6 and 10, the values were set to 1 for better comparison). On the contrary, in absence of Vif, A3G was efficiently encapsidated into viral particles, and viral infectivity was strongly decreased (Figure 5C, bars 1, 5 & 9 and 3, 6 & 11 in presence of Cul5ΔRbx). Interestingly, in absence of any proteasome-induced degradation of A3G (i.e. in presence of the dominant negative of Cul5) and in presence of Vif, we observed a partial restoration of viral infectivity when A3G was expressed from full-length and SL2-SL3 constructs (Figure 5C, bars 4 & 12). Relative infectivity rose from 0.3-0.4 to 0.6-0.7. However, in these conditions, Vif was not able to restore the infectivity of HIV-1 particles when A3G was synthesized from an mRNA deleted from its 5'-UTR (Figure 5C, compare bars 7 & 8). These results suggest that the translational regulation of A3G mRNA is an important regulatory mechanism that, together with the proteasome-induced degradation of A3G, account for the global infectivity imposed by the Vif.

Residues K26 of Vif is required for the translational inhibition of A3G.

The binding sites of A3G on Vif have been well characterized and are mainly localized in the N-terminus of the protein (46-52). Amongst these sites, K26 and H42/43 have been shown of importance for virus replication (53-55). Indeed, Vif K26R (conservative substitution), while still binding to A3G, completely lost its ability to neutralize A3G, and HIV-1 bearing this mutation replicated poorly in non-permissive cells lines (53,55). Similarly, Vif H42/43N severely impaired virus replication, consistent with the reduced capacity of this mutant to induce A3G degradation (54). However, contrary to Vif K26R, Vif H42/43N is defective for A3G binding, but still retained binding to EloB, EloC and Cul5. In order to test whether these residues could be important for the translational regulation of A3G, HEK 293T cells were transfected with Vif mutants together with full-length or Δ5'-UTR A3G constructions in presence or absence of proteasomal inhibition of A3G (Figure 6).

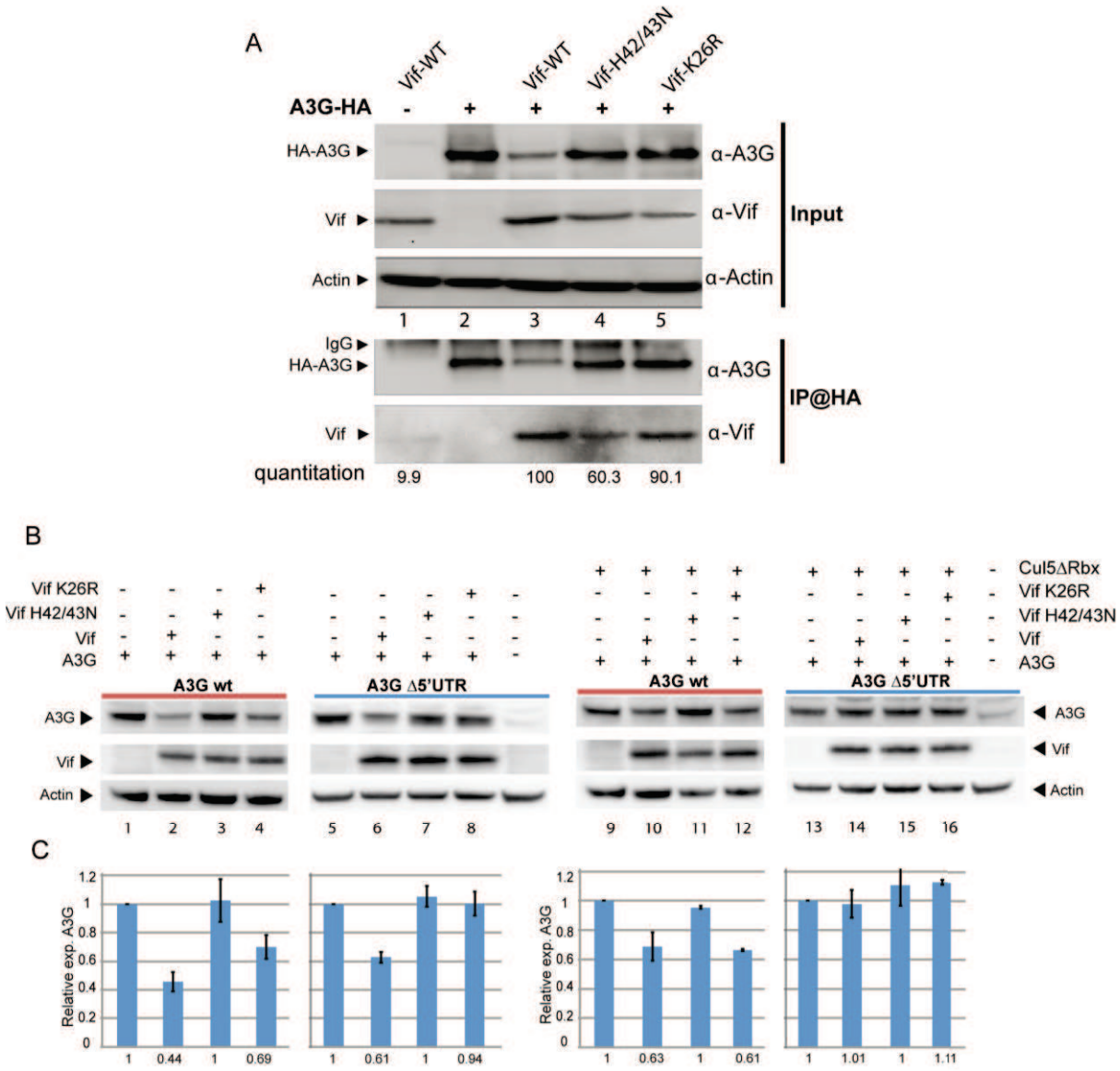

Figure 6. Vif K26 residue is required for the translational inhibition of A3G. (A) Wild-type A3G was co-immunoprecipitated with wild-type Vif, and mutants Vif K26R and Vif H42/43N. (**B**) HEK 293T cells were transfected with wild-type A3G and co-transfected with wild-type and mutated Vif (K26R or H42/43N). Proteins were separated by SDS-PAGE and analyzed by immunoblotting. (**C**) Bands were quantified using Image J (1.46r) and relative expression of A3G is represented in a histogram. (**D**) HEK 293T cells were co-transfected with HIV-1 pNL4.3, pNL4.3Δvif, pNL4.3 VifK26R or pNL4.3 H42/43N constructs with wild-type A3G +/- Cul5ΔRbx. Viral particles produced from HEK 293T cells were normalized (RT) and used to infect TZM-bl indicator cells and luciferase induction was detected 48 h post-infection.

First of all, we confirmed the behavior of these two mutants by co-immunoprecipitation and showed that Vif K26R retained its binding capacities with A3G while Vif H42/43N was twice less efficient (Figure 6A). Next, immunoblotting of normalized cell lysates revealed that the expression of wild-type A3G mRNA was partially reduced (30-40%) in presence of Vif K26R in comparison to wild-type Vif

(60% reduction) (Figure 6B,C, compare lanes 2 and 4), whereas Vif H42/43N was inefficient to counteract A3G (Figure 6B,C, lane 3), in agreement with previous studies (53-55). Again, as expected, in absence of the 5'-UTR on A3G mRNA, we did not observed any decrease of A3G protein with the two Vif mutant proteins (Figure 6B,C, lanes 5 to 8). More interestingly, when the proteasomal pathway was blocked, we observed that wild-type Vif and Vif K26R significantly and similarly decreased the translation of A3G (30-40%) when expressed from the full-length mRNAs (Figure 6B,C, lanes 9 & 12), whereas Vif H42/43N was still inefficient to reduce A3G (Figure 6B,C, lane 11). When the A3G Δ5'UTR construct was used in the same conditions, we did not observed any variation of A3G level anymore (Figure 6B,C, lanes 13 to 16), consistent with a role of the 5'-UTR of A3G mRNA in the translational regulation. Together, these results clearly demonstrate that Vif K26R, while defective in A3G degradation through the proteasome pathway, fully and only conserved its capacity to inhibit A3G expression through inhibition of A3G mRNA translation.

DISCUSSION

The HIV-1 Vif protein has been shown to be necessary for efficient viral infection in non-permissive cells by antagonizing the antiviral activity of A3G. Although the tethering of A3G by Vif to the E3 ubiquitin ligase complex (CBF-β, EloB/C, Cul5, Rbx) to induce its proteasomal degradation has been extensively studied since the discovery of A3G (37), little is known about the translational regulation of A3G by Vif regarding its molecular mechanism and/or its impact on viral replication. Indeed, HIV-1 is known to subvert almost all steps in the host translation process, first to stimulate and sustain viral mRNA translation and second, depending on cellular conditions, to modulate host mRNA translation in order to optimize its own replication (56,57).

In the present study, we extended our knowledge on the translational inhibition of A3G mRNA by the HIV-1 Vif protein. First, by using A3G mRNA constructs mutated in their 5'- and 3'-UTRs in conditions where the proteasome-induced degradation of A3G was inhibited, and thus only translation can be observed, we showed for the first time that the 5'-UTR of A3G mRNA is crucial for the translational inhibition by Vif in a cellular context (Fig. 2). Surprisingly, this translational inhibition is responsible for

about 50% of the total reduction of A3G protein expression (Fig. 2B). This reduction is not due to any effect of Vif at the transcriptional level or on mRNA degradation as qRT-PCR analyses showed that wild-type or mutated A3G mRNA levels were similar (Fig. 2C), as previously observed (27,28,37). According to our previous secondary structural model of the 5'-UTR of A3G mRNA (30), the two distal stem-loop structures, SL2 and SL3, seem to represent the minimal platform necessary and sufficient for Vif to impose its effect on A3G translation (Fig. 3). Of note, based on *in vitro* foot-printing experiments (30), three Vif-binding sites were identified in these two motifs, suggesting that Vif may slow-down the ribosome scanning process on the 5'-UTR of A3G mRNA, thus reducing A3G translation. This inhibition is not total, as a certain amount of A3G protein is still observed in the different conditions used (Fig. 2 and 3), confirming that A3G can escape this dual inhibition by Vif and exert its deaminase activity during reverse transcription after its incorporation into viral particles. Indeed, when we analyzed the content of those particles, we observed a strict correlation between the cellular reduction of A3G through translation inhibition (Fig. 5A) and the quantity of A3G incorporated into viral particles (Fig. 5B). Consequently, the virions produced in those conditions are twice more infectious with the exception of viruses containing A3G produced from mRNAs that are not dependent from the Vif-regulated translation (A3G Δ5'UTR, Fig. 5C). These results are without any precedent and show that the translational inhibition of A3G by Vif is not negligible and accounts for about 50% of virion infectivity.

How Vif interferes with the translation of A3G in the cell remains subject to further investigations. Recently, the transcription factor CBF-β has been shown to stabilize the Vif/A3G complex and induce the degradation of A3G (24,25). Interestingly, this CBF-β/Vif interaction does not seem to be required to induce the translational repression of A3G as similar inhibition has been observed in conditions where CBF-β was repressed in the cell (Fig. 4). Although specific amino acids in Vif have been shown to necessary for A3G binding and proteasomal degradation, none has been identify to be required in the A3G translational inhibition yet. Interestingly, we identified amino acid K26 in the N-terminus of Vif as an important residue for the cellular repression of A3G (Fig. 6). Indeed, although the wild-type Vif is efficient in the degradation and the translational inhibition of A3G, the replacement of a lysine to an arginine at position 26 allowed this new Vif protein to exclusively conserve its

action on A3G translation (40% reduction), whether proteasome pathway was inhibited or not. In addition, this reduction by Vif K26R is still dependent on the 5'UTR of A3G mRNA. These results are of importance in further studies aiming at deciphering the mechanisms of A3G translational inhibition by Vif (no need to use proteasome inhibitors) and suggest that proteasomal inhibition and translational repression are likely distinct properties of Vif. Moreover, the fact that a conservative change (K26R) did not perturb the translational inhibition of A3G suggest that this residue is involved in mRNA binding. Indeed, the region encompassing amino acids 1 to 64 has previously been shown to be involved in the RNA binding capacities of Vif (58). From these results, the most obvious model of translational inhibition of A3G by Vif is a stalling mechanism where the binding of Vif, through its N-terminus, to the SL2-SL3 domain of the 5'-UTR of A3G mRNA prevents the ribosome scanning process and reduces A3G translation (Fig. 7). As the degradation of A3G involves the binding of the E3-ubiquitin ligase complex to the C-terminus of Vif, this could explain why the two mechanisms are mutually exclusive. In addition, the fact that the N-terminus of Vif is involved in both RNAs and A3G/F binding suggest that one type of A3G regulation may prevent the other one depending on cellular conditions, and/or mRNA and Vif/A3G protein concentrations.

Taken together, our findings shed new light on the mechanism by which HIV-1 Vif interferes with the expression of A3G. We showed for the first time that A3G mRNA translational inhibition by Vif is a 5'-UTR mRNA-dependent mechanism that accounts for about 50% decrease of A3G in cell. Any of the two mechanisms described so far, degradation and translation, are sufficient to restore viral infectivity. Thus, regulating the translation of A3G could thus be considered as a new target to restore a functional expression of A3G and viral restriction.

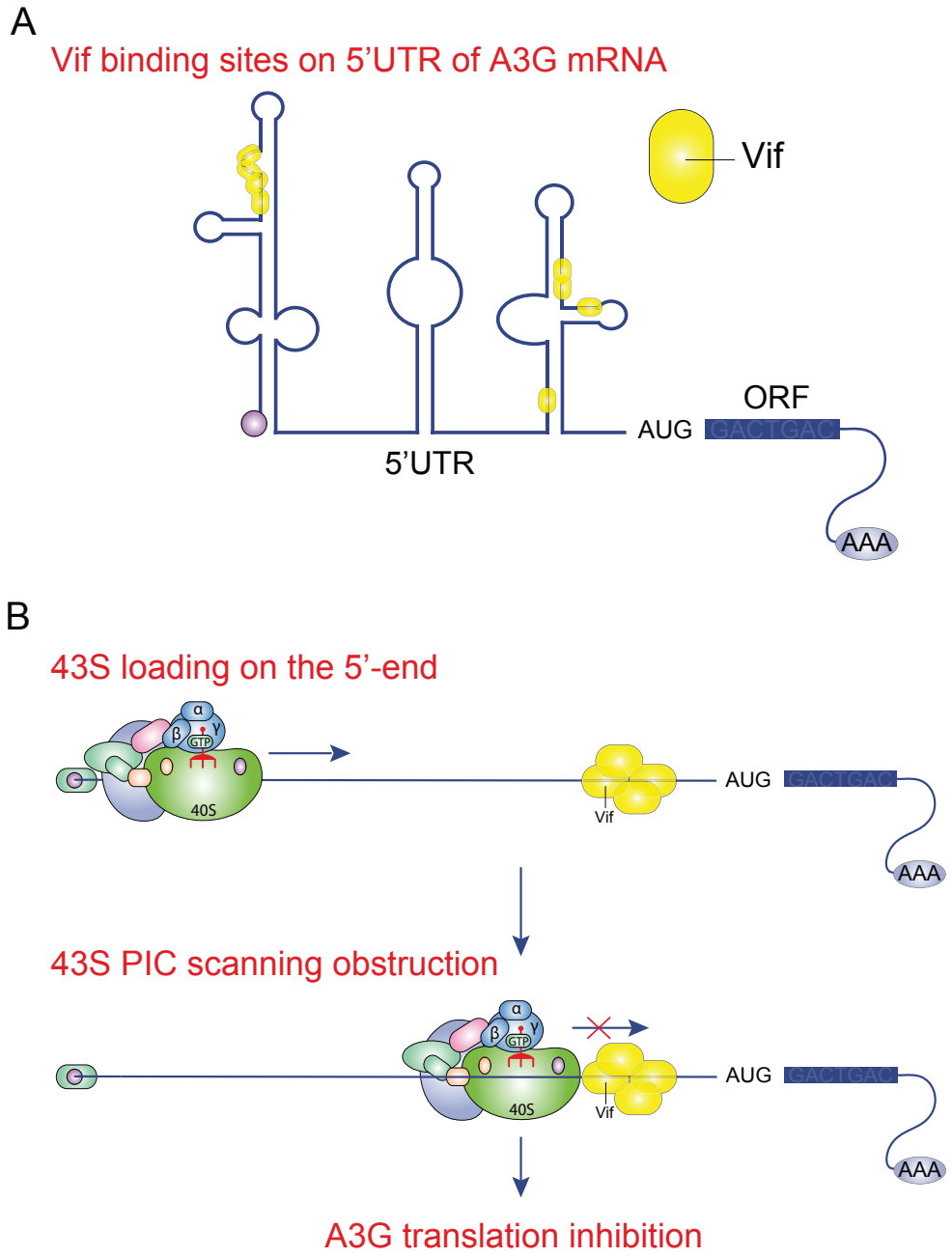

Figure 7. Model depicting how Vif impairs the translation of A3G mRNA in cell. (A) Schematic representation of Vif binding sites on the 5'-UTR of A3G mRNA (adapted from (30)). **(B)** Model of A3G translational inhibition. Vif binds the domain SL2-SL3 in the 5'UTR of A3G mRNA and may potentially obstruct the scanning of the 43S pre-initiation complex thus reducing A3G translation.

ACKNOWLEDGEMENTS

We are grateful to Dr. Redmond Smyth for critical reading of the manuscript. The following reagents were obtained through the AIDS Research and Reference Reagent Program, Division of AIDS, NIAID, NIH: A3G polyclonal antibody (#9968) from Dr. Warner Greene and Vif monoclonal antibody (#319) from Dr. Michael H. Malim.

The authors declare no conflict of interest.

Author contributions: J.-C.P. designed research; S.X.G., G.M., J.B., T.D, G.L & D.R. performed research; J.-C.P., R.M., S.X.G. & C.M analyzed data; J.-C.P. wrote the paper**.**

REFERENCES

1. Harris, R.S., Hultquist, J.F. and Evans, D.T. (2012) The restriction factors of human immunodeficiency virus. *J Biol Chem*, **287**, 40875-40883.

2. Henriet, S., Mercenne, G., Bernacchi, S., Paillart, J.C. and Marquet, R. (2009) Tumultuous relationship between the human immunodeficiency virus type 1 viral infectivity factor (Vif) and the human APOBEC-3G and APOBEC-3F restriction factors. *Microbiol. Mol. Biol. Rev.*, **73**, 211-232.

3. Esnault, C., Heidmann, O., Delebecque, F., Dewannieux, M., Ribet, D., Hance, A.J., Heidmann, T. and Schwartz, O. (2005) APOBEC3G cytidine deaminase inhibits retrotransposition of endogenous retroviruses. *Nature*, **433**, 430-433.

4. Lecossier, D., Bouchonnet, F., Clavel, F. and Hance, A.J. (2003) Hypermutation of HIV-1 DNA in the absence of the Vif protein. *Science*, **300**, 1112.

5. Malim, M.H. (2009) APOBEC proteins and intrinsic resistance to HIV-1 infection. *Philos Trans R Soc Lond B Biol Sci*, **364**, 675-687.

6. Mangeat, B., Turelli, P., Caron, G., Friedli, M., Perrin, L. and Trono, D. (2003) Broad antiretroviral defence by human APOBEC3G through lethal editing of nascent reverse transcripts. *Nature*, **424**, 99-103.

7. Mbisa, J.L., Barr, R., Thomas, J.A., Vandegraaff, N., Dorweiler, I.J., Svarovskaia, E.S., Brown, W.L., Mansky, L.M., Gorelick, R.J., Harris, R.S. *et al.* (2007) Human immunodeficiency virus type 1 cDNAs produced in the presence of APOBEC3G exhibit defects in plus-strand DNA transfer and integration. *J Virol*, **81**, 7099-7110.

8. Alce, T.M. and Popik, W. (2004) APOBEC3G is incorporated into virus-like particles by a direct interaction with HIV-1 Gag nucleocapsid protein. *J Biol Chem*, **279**, 34083-34086.

9. Douaisi, M., Dussart, S., Courcoul, M., Bessou, G., Vigne, R. and Decroly, E. (2004) HIV-1 and MLV Gag proteins are sufficient to recruit APOBEC3G into virus-like particles. *Biochem. Biophys. Res. Commun.*, **321**, 566-573.

10. Strebel, K. and Khan, M.A. (2008) APOBEC3G encapsidation into HIV-1 virions: which RNA is it? *Retrovirology*, **5**, 55.

11. Svarovskaia, E.S., Xu, H., Mbisa, J.L., Barr, R., Gorelick, R.J., Ono, A., Freed, E.O., Hu, W.S. and Pathak, V.K. (2004) Human apolipoprotein B mRNA-editing enzyme-catalytic polypeptide-like 3G (APOBEC3G) is incorporated into HIV-1 virions through interactions with viral and nonviral RNAs. *J Biol Chem*, **279**, 35822-35828.

12. Zennou, V., Perez-Caballero, D., Gottlinger, H. and Bieniasz, P.D. (2004) APOBEC3G incorporation into human immunodeficiency virus type 1 particles. *J Virol*, **78**, 12058-12061.

13. Wissing, S., Galloway, N.L. and Greene, W.C. (2010) HIV-1 Vif versus the APOBEC3 cytidine deaminases: an intracellular duel between pathogen and host restriction factors. *Molecular aspects of medicine*, **31**, 383-397.

14. Harris, R.S., Bishop, K.N., Sheehy, A.M., Craig, H.M., Petersen-Mahrt, S.K., Watt, I.N., Neuberger, M.S. and Malim, M.H. (2003) DNA deamination mediates innate immunity to retroviral infection. *Cell*, **113**, 803-809.

15. Zhang, H., Yang, B., Pomerantz, R.J., Zhang, C., Arunachalam, S.C. and Gao, L. (2003) The cytidine deaminase CEM15 induces hypermutation in newly synthesized HIV-1 DNA. *Nature*, **424**, 94-98.

16. Li, X.Y., Guo, F., Zhang, L., Kleiman, L. and Cen, S. (2007) APOBEC3G inhibits DNA strand transfer during HIV-1 reverse transcription. *J Biol Chem*, **282**, 32065-32074.

17. Mbisa, J.L., Bu, W. and Pathak, V.K. (2010) APOBEC3F and APOBEC3G inhibit HIV-1 DNA integration by different mechanisms. *J Virol*, **84**, 5250-5259.

18. Newman, E.N., Holmes, R.K., Craig, H.M., Klein, K.C., Lingappa, J.R., Malim, M.H. and Sheehy, A.M. (2005) Antiviral function of APOBEC3G can be dissociated from cytidine deaminase activity. *Curr Biol*, **15**, 166-170.

19. Wang, X., Ao, Z., Chen, L., Kobinger, G., Peng, J. and Yao, X. (2012) The cellular antiviral protein APOBEC3G interacts with HIV-1 reverse transcriptase and inhibits its function during viral replication. *J Virol*, **86**, 3777-3786.

20. Gillick, K., Pollpeter, D., Phalora, P., Kim, E.Y., Wolinsky, S.M. and Malim, M.H. (2013) Suppression of HIV-1 infection by APOBEC3 proteins in primary human CD4(+) T cells is associated with inhibition of processive reverse transcription as well as excessive cytidine deamination. *J Virol*, **87**, 1508-1517.

21. Zheng, Y.H., Jeang, K.T. and Tokunaga, K. (2012) Host restriction factors in retroviral infection: promises in virus-host interaction. *Retrovirology*, **9**, 112.

22. Yu, X., Yu, Y., Liu, B., Luo, K., Kong, W., Mao, P. and Yu, X.F. (2003) Induction of APOBEC3G ubiquitination and degradation by an HIV-1 Vif-Cul5-SCF complex. *Science*, **302**, 1056-1060.

23. Albin, J.S. and Harris, R.S. (2010) Interactions of host APOBEC3 restriction factors with HIV-1 in vivo: implications for therapeutics. *Expert reviews in molecular medicine*, **12**, e4.

24. Jager, S., Kim, D.Y., Hultquist, J.F., Shindo, K., Larue, R.S., Kwon, E., Li, M., Anderson, B.D., Yen, L., Stanley, D. *et al.* (2011) Vif hijacks CBF-beta to degrade APOBEC3G and promote HIV-1 infection. *Nature*.

25. Zhang, W., Du, J., Evans, S.L., Yu, Y. and Yu, X.F. (2011) T-cell differentiation factor CBF-beta regulates HIV-1 Vif-mediated evasion of host restriction. *Nature*.

26. Kim, D.Y., Kwon, E., Hartley, P.D., Crosby, D.C., Mann, S., Krogan, N.J. and Gross, J.D. (2013) CBFbeta stabilizes HIV Vif to counteract APOBEC3 at the expense of RUNX1 target gene expression. *Mol Cell*, **49**, 632-644.

27. Kao, S., Khan, M.A., Miyagi, E., Plishka, R., Buckler-White, A. and Strebel, K. (2003) The human immunodeficiency virus type 1 Vif protein reduces intracellular expression and inhibits packaging of APOBEC3G (CEM15), a cellular inhibitor of virus infectivity. *J Virol*, **77**, 11398-11407.

28. Stopak, K., de Noronha, C., Yonemoto, W. and Greene, W.C. (2003) HIV-1 Vif blocks the antiviral activity of APOBEC3G by impairing both its translation and intracellular stability. *Mol Cell*, **12**, 591-601.

29. Mariani, R., Chen, D., Schrofelbauer, B., Navarro, F., Konig, R., Bollman, B., Munk, C., Nymark-McMahon, H. and Landau, N.R. (2003) Species-specific exclusion of APOBEC3G from HIV-1 virions by Vif. *Cell*, **114**, 21-31.

30. Mercenne, G., Bernacchi, S., Richer, D., Bec, G., Henriet, S., Paillart, J.C. and Marquet, R. (2010) HIV-1 Vif binds to APOBEC3G mRNA and inhibits its translation. *Nucleic Acids Res*, **38**, 633-646.

31. Jackson, R.J., Hellen, C.U. and Pestova, T.V. (2010) The mechanism of eukaryotic translation initiation and principles of its regulation. *Nature reviews. Molecular cell biology*, **11**, 113-127.

32. Wilkie, G.S., Dickson, K.S. and Gray, N.K. (2003) Regulation of mRNA translation by 5'- and 3'-UTR-binding factors. *Trends in biochemical sciences*, **28**, 182-188.

33. Nguyen, K.L., llano, M., Akari, H., Miyagi, E., Poeschla, E.M., Strebel, K. and Bour, S. (2004) Codon optimization of the HIV-1 vpu and vif genes stabilizes their mRNA and allows for highly efficient Rev-independent expression. *Virology*, **319**, 163-175.

34. Karczewski, M.K. and Strebel, K. (1996) Cytoskeleton association and virion incorporation of the human immunodeficiency virus type 1 Vif protein. *J Virol*, **70**, 494-507.

35. Jager, S., Cimermancic, P., Gulbahce, N., Johnson, J.R., McGovern, K.E., Clarke, S.C., Shales, M., Mercenne, G., Pache, L., Li, K. *et al.* (2012) Global landscape of HIV-human protein complexes. *Nature*, **481**, 365-370.

36. Tudor, D., Derrien, M., Diomede, L., Drillet, A.S., Houimel, M., Moog, C., Reynes, J.M., Lopalco, L. and Bomsel, M. (2009) HIV-1 gp41-specific monoclonal mucosal IgAs derived from highly exposed but IgG-seronegative individuals block HIV-1 epithelial transcytosis and neutralize CD4(+) cell infection: an IgA gene and functional analysis. *Mucosal immunology*, **2**, 412-426.

37. Sheehy, A.M., Gaddis, N.C., Choi, J.D. and Malim, M.H. (2002) Isolation of a human gene that inhibits HIV-1 infection and is suppressed by the viral Vif protein. *Nature*, **418**, 646-650.

38. Cen, S., Guo, F., Niu, M., Saadatmand, J., Deflassieux, J. and Kleiman, L. (2004) The interaction between HIV-1 Gag and APOBEC3G. *J Biol Chem*, **279**, 33177-33184.

39. Schafer, A., Bogerd, H.P. and Cullen, B.R. (2004) Specific packaging of APOBEC3G into HIV-1 virions is mediated by the nucleocapsid domain of the gag polyprotein precursor. *Virology*, **328**, 163-168.

40. Kao, S., Akari, H., Khan, M.A., Dettenhofer, M., Yu, X.F. and Strebel, K. (2003) Human immunodeficiency virus type 1 Vif is efficiently packaged into virions during productive but not chronic infection. *J Virol*, **77**, 1131-1140.

41. Khan, M.A., Aberham, C., Kao, S., Akari, H., Gorelick, R., Bour, S. and Strebel, K. (2001) Human immunodeficiency virus type 1 Vif protein is packaged into the nucleoprotein complex through an interaction with viral genomic RNA. *J Virol*, **75**, 7252-7265.

42. Khan, M.A., Kao, S., Miyagi, E., Takeuchi, H., Goila-Gaur, R., Opi, S., Gipson, C.L., Parslow, T.G., Ly, H. and Strebel, K. (2005) Viral RNA is required for the association of APOBEC3G with human immunodeficiency virus type 1 nucleoprotein complexes. *J Virol*, **79**, 5870-5874.

43. Opi, S., Kao, S., Goila-Gaur, R., Khan, M.A., Miyagi, E., Takeuchi, H. and Strebel, K. (2007) Human immunodeficiency virus type 1 Vif inhibits packaging and antiviral activity of a degradation-resistant APOBEC3G variant. *J Virol*, **81**, 8236-8246.

44. Kao, S., Goila-Gaur, R., Miyagi, E., Khan, M.A., Opi, S., Takeuchi, H. and Strebel, K. (2007) Production of infectious virus and degradation of APOBEC3G are separable functional properties of human immunodeficiency virus type 1 Vif. *Virology*, **369**, 329-339.

45. Platt, E.J., Bilska, M., Kozak, S.L., Kabat, D. and Montefiori, D.C. (2009) Evidence that ecotropic murine leukemia virus contamination in TZM-bl cells does not affect the outcome of neutralizing antibody assays with human immunodeficiency virus type 1. *J Virol*, **83**, 8289-8292.

46. Tian, C., Yu, X., Zhang, W., Wang, T., Xu, R. and Yu, X.F. (2006) Differential requirement for conserved tryptophans in human immunodeficiency virus type 1 Vif for the selective suppression of APOBEC3G and APOBEC3F. *J Virol*, **80**, 3112-3115.

47. Schrofelbauer, B., Senger, T., Manning, G. and Landau, N.R. (2006) Mutational alteration of human immunodeficiency virus type 1 Vif allows for functional interaction with nonhuman primate APOBEC3G. *J Virol*, **80**, 5984-5991.

48. Dang, Y., Davis, R.W., York, I.A. and Zheng, Y.H. (2010) Identification of 81LGxGxxIxW89 and 171EDRW174 domains from human immunodeficiency virus type 1 Vif that regulate APOBEC3G and APOBEC3F neutralizing activity. *J Virol*, **84**, 5741-5750.

49. Dang, Y., Wang, X., York, I.A. and Zheng, Y.H. (2010) Identification of a critical T(Q/D/E)x5ADx2(I/L) motif from primate lentivirus Vif proteins that regulate APOBEC3G and APOBEC3F neutralizing activity. *J Virol*, **84**, 8561-8570.

50. Russell, R.A. and Pathak, V.K. (2007) Identification of two distinct human immunodeficiency virus type 1 Vif determinants critical for interactions with human APOBEC3G and APOBEC3F. *J Virol*, **81**, 8201-8210.

51. Santa-Marta, M., Aires da Silva, F., Fonseca, A. and Goncalves, J. (2005) HIV-1 Vif can directly inhibit APOBEC3G-mediated cytidine deamination by using a single amino acid interaction and without protein degradation. *J Biol Chem*, **280**, 8765-8775.

52. Yamashita, T., Kamada, K., Hatcho, K., Adachi, A. and Nomaguchi, M. (2008) Identification of amino acid residues in HIV-1 Vif critical for binding and exclusion of APOBEC3G/F. *Microbes Infect*, **10**, 1142-1149.

53. Khamsri, B., Fujita, M., Kamada, K., Piroozmand, A., Yamashita, T., Uchiyama, T. and Adachi, A. (2006) Effects of lysine to arginine mutations in HIV-1 Vif on its expression and viral infectivity. *Int J Mol Med*, **18**, 679-683.

54. Mehle, A., Wilson, H., Zhang, C., Brazier, A.J., McPike, M., Pery, E. and Gabuzda, D. (2007) Identification of an APOBEC3G binding site in human immunodeficiency virus type 1 Vif and inhibitors of Vif-APOBEC3G binding. *J Virol*, **81**, 13235-13241.

55. Dang, Y., Wang, X., Zhou, T., York, I.A. and Zheng, Y.H. (2009) Identification of a novel WxSLVK motif in the N terminus of human immunodeficiency virus and simian immunodeficiency virus Vif that is critical for APOBEC3G and APOBEC3F neutralization. *J Virol*, **83**, 8544-8552.

56. Walsh, D. and Mohr, I. (2011) Viral subversion of the host protein synthesis machinery. *Nature reviews. Microbiology*, **9**, 860-875.

57. de Breyne, S., Soto-Rifo, R., Lopez-Lastra, M. and Ohlmann, T. (2013) Translation initiation is driven by different mechanisms on the HIV-1 and HIV-2 genomic RNAs. *Virus research*, **171**, 366-381.

58. Zhang, H., Pomerantz, R.J., Dornadula, G. and Sun, Y. (2000) Human immunodeficiency virus type 1 Vif protein is an integral component of an mRNP complex of viral RNA and could be involved in the viral RNA folding and packaging process. *J Virol*, **74**, 8252-8261.

2. Insights into the Vif-meditated A3G translation inhibition

2.1 *In silico* analysis of the 5'UTR of the A3G mRNA

To further understand the mechanism by which Vif inhibits A3G mRNA in a 5'UTR-dependent manner we searched for *cis*-acting elements in the 5'UTR that could contribute to this repression. Herein, using a computational platform capable of identifying RNA regulatory elements (RegRNA 2.0, Chang et al., 2013), we identified a terminal oligopyrimidine tract (TOP) and an uORF within the 5'UTR of the A3G mRNA sequence determined by Mercenne et al. (2010) (Fig. 28A). TOP elements are thought to serve as *cis*-regulatory sequences that inhibit the binding of proteins implicated in the translational regulation (Yamashita et al., 2008). uORFs are also *cis*-regulatory elements that negatively regulate translation of downstream ORF (Calvo et al., 2009).

Since ~50% of eukaryotic genes with annotated uORFs expressed unique transcript isoforms (TIFs) both with and without the uORF (Ingolia et al., 2009; Pelechano et al., 2013), we determined the transcript variation among other A3G mRNA sequences available in the NCBI nucleotide database. As we expected, we observed different TIFs of A3G mRNA both with and without the uORF (Fig. 28B). This uORF is present in three A3G mRNA sequences and absent in two, suggesting that A3G translation could be repressed in the uORF-containing TIFs and enhanced in ΔuORF-TIFs. On the contrary, the TOP element was found in only one A3G mRNA variant (hA3G v2) 60 nucleotides after the cap. This element may not be functional because TOP elements reported so far exert their function only if they are positioned immediately after the cap (Meyuhas, 2000).

Detailed analysis of these elements revealed that the TOP sequence is composed of a 5' cytidine followed by an uninterrupted stretch of 11 pyrimidines immediately after the cap with a C/U ratio = 5/7 (Fig. 29A). This sequence corresponds exactly to the current definition of this type of RNA elements (Meyuhas, 2000). Using NCBI BLAST tool, we found that two human A3F mRNAs (hA3F v1 and v2) present a similar sequence of 8 pyrimidines, starting with a thymine instead of a cytidine. However, all TOP elements reported so far start with a cytidine (Labban and Sossin, 2011;

Markou et al., 2010; Meyuhas, 2000), suggesting that these A3F mRNA sequences may not function as TOP elements.

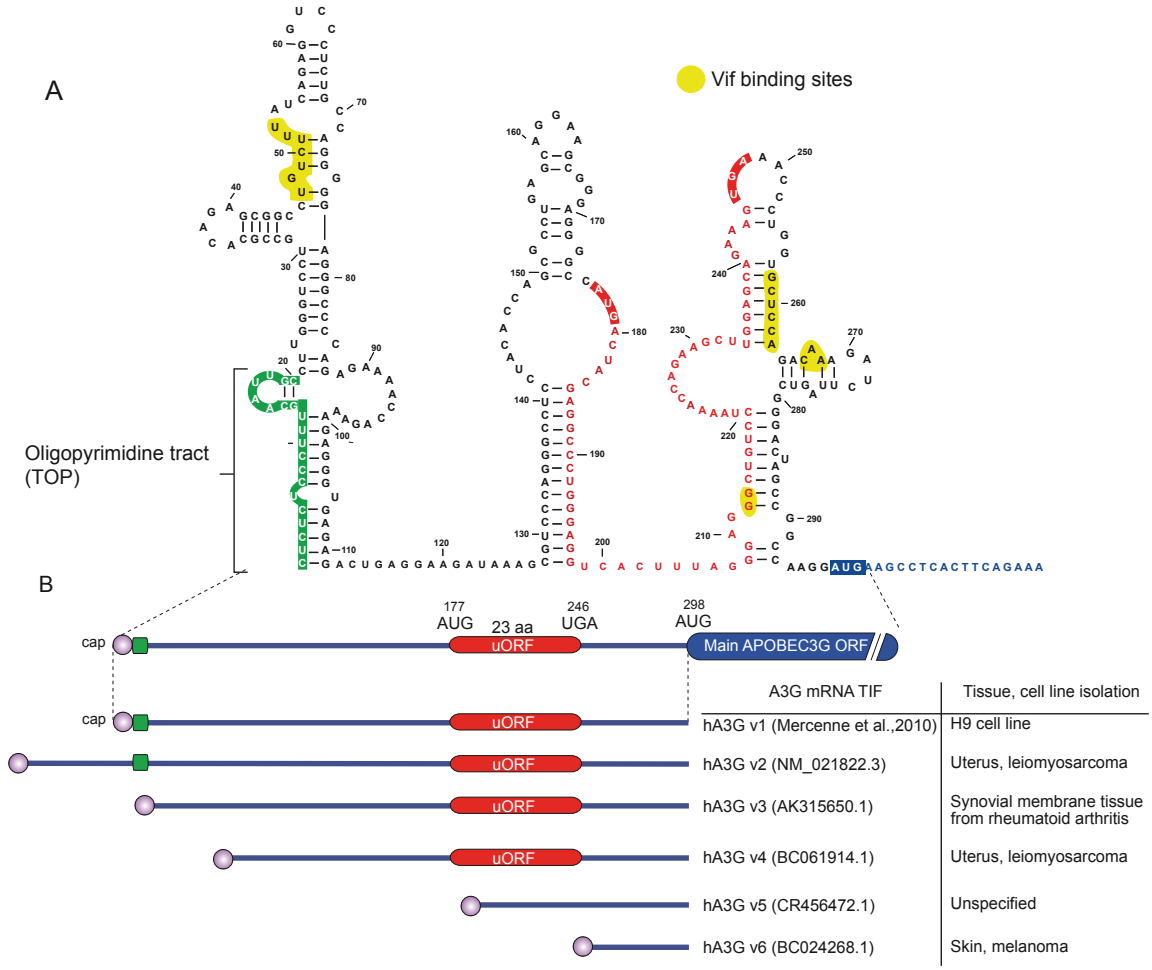

Figure 28. ***In silico*** **analysis of the 5'UTR of the A3G mRNA.** A) Previously reported A3G mRNA 5'UTR structure (Mercenne et al., 2010) showing the Vif-binding sites (yellow), the TOP element (green) and the uORF (red). B) A comparison of the A3G 5'UTR with other experimentally determined A3G transcripts according to a computational alignment of the 5'UTR sequences. NM_021822.3, BC061914.1 and BC024268.1 (Strausberg et al., 2002), AK315650.1 (Isogai and Yamamoto, 2008), CR456472.1 (Collins et al., 2004)

Moreover, this A3G TOP element is also present in computationally predicted A3G/F primate mRNA sequences but 37-60 nucleotides after the cap; although, TOP elements present within the 5'UTR are incapable of exerting their function (Meyuhas, 2000). Therefore, the A3G mRNA variant, experimentally determined by Muckenfuss et al. (2007) and used by Mercenne et al. (2010) to determine the structure of the A3G mRNA 5'UTR, is the first report of a TOP-containing A3G mRNA. This variant was isolated from HIV-1 target cells (H9 cells) and may better represent A3G

transcription during HIV-1 infection. In contrast, the other A3G mRNA sequences studied here were obtained from different tissue and cell lines (Collins et al., 2004; Isogai and Yamamoto, 2008; Strausberg et al., 2002) that are not implicated in HIV-1 infection (Fig. 28B and Fig. 29A).

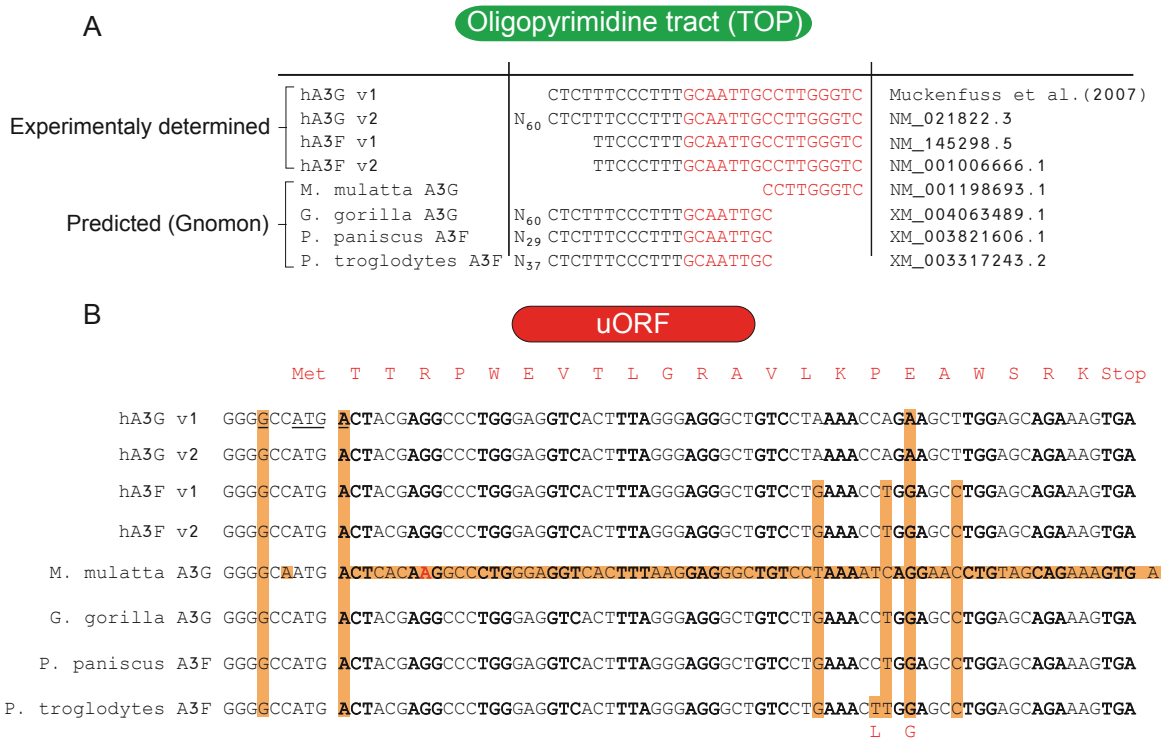

Figure 29. Detailed analysis of the TOP and the uORF elements. A) A sequence alignment of the A3G TOP element with different human and primate A3G/F sequences. B) A sequence alignment of the A3G uORF with different human and primate A3G/F uORF sequences.

Indirectly, we showed that the TOP element is not required in either A3G translation or Vif-mediated A3G translation inhibition (Fig 3A-B. from the article "***Inhibition of APOBEC3G translation by Vif restores HIV-1 infectivity***"). This is demonstrated by comparing the expression profile between A3G wt and A3G SL2-SL3 mutant (Fig 3A-B). A3G wt holds the TOP element in SL1, while SL2-SL3 mutant does not present this element. Despite this, A3G wt and A3G SL2-SL3 show similar expression profiles when they are transfected alone or co-transfected with Cul5ΔRbx and Vif plasmids (Fig 3A-B).

Concerning the uORF of the hA3G mRNA v1, our analysis showed that this element is encoded between the SL2 and SL3 domains of the 5'UTR (Fig. 28A). Of note, these two domains are required for Vif-mediated A3G translation inhibition (Fig 3.

from the article "***Inhibition of APOBEC3G translation by Vif restores HIV-1 infectivity***"). The uORF is positioned 177 nt after the cap and the distance between the uORF stop codon and the mAUG is 49 nt. The length of the uORF is 72 nucleotides which is 24 nucleotides more than the median length of the human and mouse uORFs (48 nt) (Calvo et al., 2009). The uORF potentially codes for a 23 amino acid protein without any particular motif according to the PROSITE database (Sigrist et al., 2002). This uORF is also present in two human A3F mRNA variants with high similarities at nucleotide (94%) and amino acid (96%) levels (Fig. 29B). Moreover, this sequence is also conserved in A3G/F primate mRNA sequences. Interestingly, a single-nucleotide insertion in *Macaca mulatta* 5'UTR inactivates the uORF due to a frameshift in its sequence that place the uORF stop codon out of frame with the uAUG (Fig. 29B).

According to the definition of the Kozak context, a "strong Kozak consensus" is established when either one or both -3 a +4 position match the Kozak sequence (GCC(A/G)CC**AUG**G) (Kozak, 1984, 1986; Kozak and Chakraborti, 1996). Taking this definition into account, we conclude that both the uAUG (GGGGCC**AUG**A) and the mAUG (CCAAGG**AUG**A) possess a strong Kozak context with a purine at -3 position. The strong Kozak context of the uAUG suggests that the mORF (main ORF) could be translated more preferentially by a re-initiation or an IRES-mediated mechanism than by leaky scanning; however, our experimental data favor this last mechanism (see below)

2.2 The uORF negatively regulates A3G translation

Since uORFs reduce protein expression by approximately 30-80% (Calvo et al., 2009), we determined the effect of the uORF on A3G expression. We performed site-directed mutagenesis on the uAUG (uAUG/uAAG) and the uUGA (A3G UGA/ΔU-AG) to inactivate the uORF (Fig. 30A). The expression of these mutants was then studied *in vitro* using rabbit reticulocyte lysate (collaboration with B. Sargueil, University of Paris Descartes, Paris) and *ex vivo* using HEK293T cells. As expected, the uORF negatively regulates A3G expression by 50% *in vitro* (Fig. 30B, lane 2) and 40% *ex vivo* (Fig. 30B, lane 5). The deletion of the A3G UGA/ΔU-AG placed the uAUG in frame with the mORF, allowing us to study also the uAUG

recognition by the 43SPIC. If the uAUG is recognized a “long A3G protein” should be detected and revealed with the A3G antibody. Indeed, this “long A3G protein” is detected *in vitro* and *ex vivo* (Fig. 30B, lane 3 and 6), suggesting that translation could also start at the uAUG, which is consistent with the Kozak context of the uAUG. These observations suggest that the translation of the mORF, in a wild type context, could be accomplished by a re-initiation mechanism after translating the uORF. However, in the A3G UGA/ΔU-AG mutant, where re-initiation is impossible, the wild type A3G protein is still detected (Fig. 30B, lane 3 and 6), suggesting that translation of the mORF can also be achieved by leaky scanning or through an IRES.

2.3 A3G translation initiation mechanism

In order to characterize the mechanism of Vif-mediated A3G translation inhibition, it is important to determine first the mechanism of A3G translation initiation. We therefore performed several mutations in the A3G 5’UTR to study different aspects of the mORF translation initiation mechanism (Fig. 31A). These mutants were then transfected into 293T cells to determine their relative expression (Fig. 31B). First, we confirmed our previous observations (see section 2.2) concerning the regulation of A3G expression by the uORF (Fig. 31B, lines 2 and 3). We next define the importance of the uORF peptide as a *trans*-acting element capable of regulating the mORF translation. To achieve this, we changed the uORF amino acid sequence and we studied its effect on A3G expression. We observed no effect of the putative peptide in A3G expression (Fig. 31B, lane 4). This result is consistent with the fact that only in rare cases peptide expressed from an uORF has regulatory effects (Fang et al., 2004; Kozak, 2005; Law et al., 2001). However, when we deleted the whole uORF sequence, we detected a three-fold increase in A3G expression (Fig. 31B, lane 5), suggesting that the uORF element (the nucleotide sequence) negatively regulates A3G expression.

To test the possibility that the mAUG could be recognized by leaky scanning, re-initiation or by an IRES-mediated mechanism, we performed different mutants based on previous reports. For example, it is well established that re-initiation is more efficient when the uORF sequences are small or the distance between the uORF

stop codon and the mAUG is longer (Kozak, 2005). Thus, reducing the uORF length and indirectly increasing the distance between the uUGA and the mAUG should enhance A3G expression. Therefore, if A3G translation initiation is mediated by a re-initiation mechanism, A3G 2XUGA 2aa, 5aa and 15aa mutants should present an A3G expression profile as followed: A3G 2XUGA 2aa > 5aa > 15aa > wt. However, A3G 2XUGA 2aa and 15aa mutants present an A3G expression similar to the wild-type construct (Fig. 31B, lane 6 and 8).

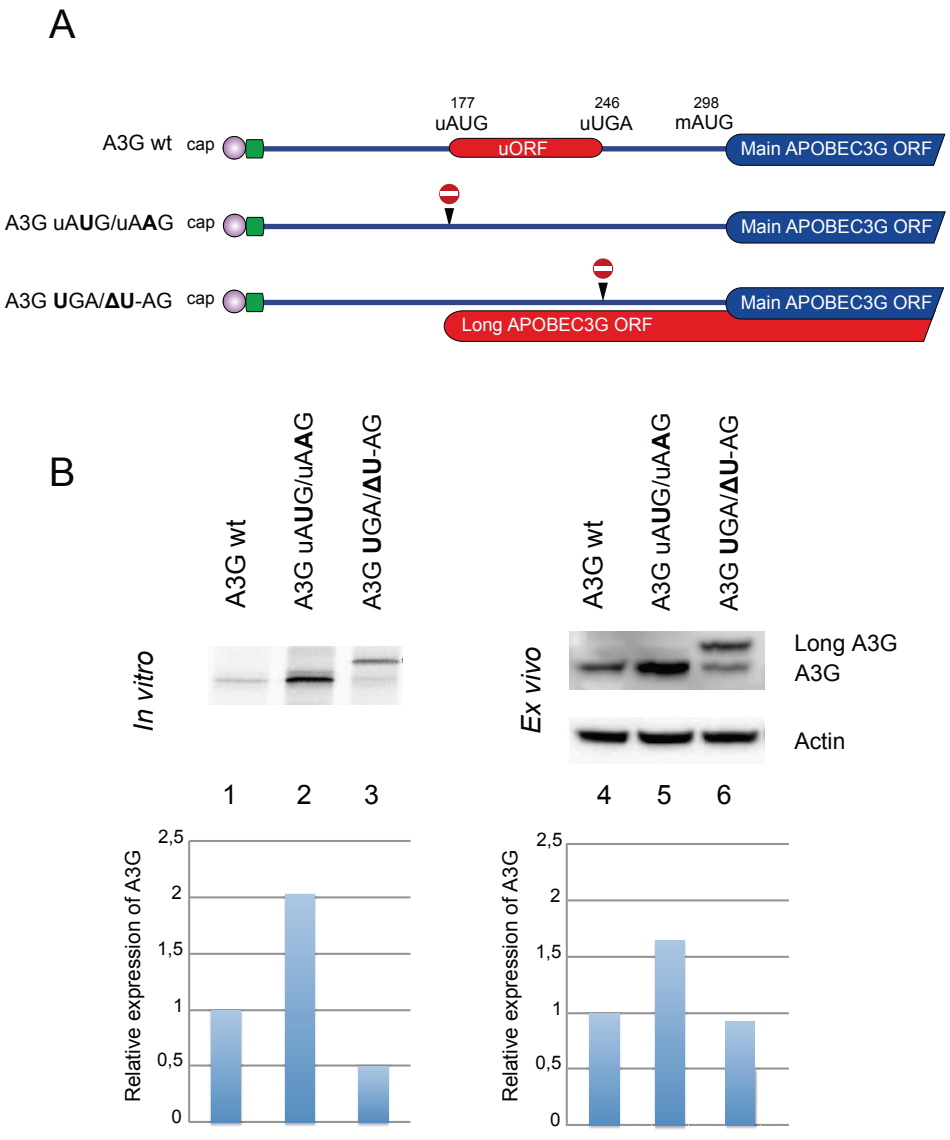

Figure 30. The uORF negatively regulates A3G translation. A) Schematic representation of the A3G wt, A3G uAUG/uAAG and A3G UGA/ΔU-AG mutants. B) In vitro transcription/translation assay in rabbit reticulocyte lysates and ex vivo A3G translation assay using HEK293T cells. Proteins were separated by SDS-PAGE and analyzed by autoradiography (in vitro assay) and by immunoblotting (ex vivo assay). Bands were quantified using Image J (1.46r) and relative expression of A3G is represented in a histogram.

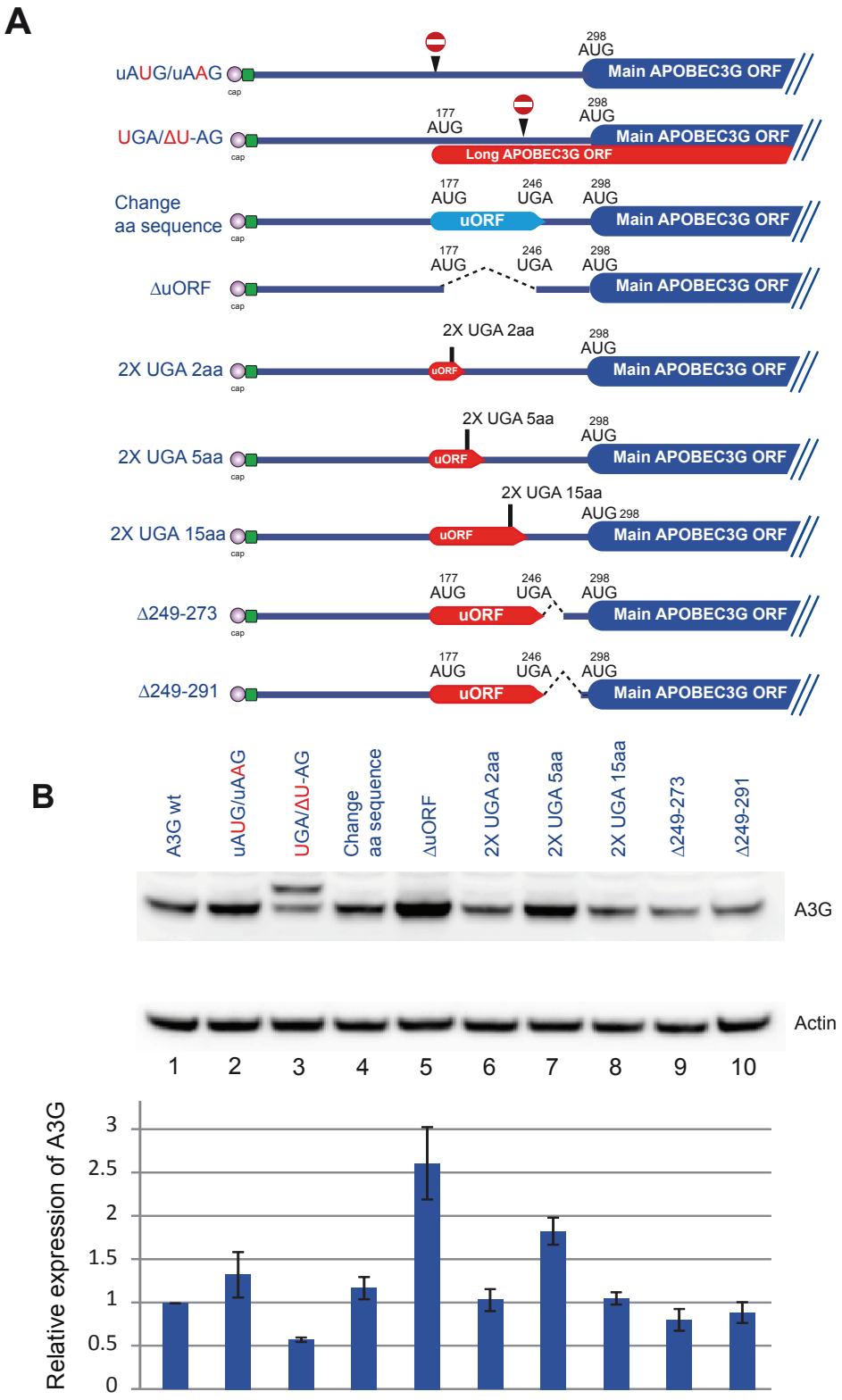

Figure 31. Mechanism of A3G translation initiation. A) A schematic representation of different A3G 5'UTR mutants. **B)** Ex vivo A3G translation assay using HEK293T cells. Proteins were separated by SDS-PAGE and analyzed by immunoblotting. Bands were quantified using Image J (1.46r) and relative expression of A3G is represented in a histogram.

On the contrary, only the 2XUGA 5aa mutant shows an increase in A3G expression (Fig. 31B, lane 7). No explanation for this increase has been found yet. The fact that A3G 2XUGA 2aa and 15aa mutants present a similar A3G expression as the wt suggest that A3G translation initiation is probably not mediated by a re-initiation mechanism. To validate this hypothesis, we reduce the distance between the uUGA and the mAUG (∆249-273 and ∆249-291 mutants). If A3G translation initiation is accomplished by a re-initiation mechanism, reducing this distance should decrease A3G expression. However, none of these mutants present a reduction in A3G expression compared to the wt A3G (Fig. 31B, lane 9 and 10). These results (Fig. 31B, lane 6, 8, 9 and 10) allow us to conclude that translation of the mORF is not initiated by a re-initiation mechanism.

The ∆249-273 and ∆249-291 mutants also allow us to validate the possibility that A3G translation could be mediated by an IRES. In an IRES-dependent translation mechanism, the ribosome is attracted close to the mAUG by secondary and tertiary structures present close to the translation initiation site (Thompson, 2012; Xue and Barna, 2012). Therefore, deleting the sequence between the uUGA and the mAUG could inactivate secondary and tertiary structures required for the IRES. Thus, A3G expression of ∆249-273 and ∆249-291 mutants could be potentially decreased in a hypothetical IRES-dependent A3G translation mechanism. Nevertheless, these two mutants present a similar expression profile as wt A3G (Fig. 31B, lane 9 and 10). In addition, other A3G mutants that destabilize the secondary and tertiary structures of the 5'UTR could be used to study a possible IRES-mediated translation initiation. For example, the A3G SL2-SL3 mutant is disrupted from its SL1 and nevertheless presents a similar expression profile as wt A3G (Fig 3A-B from the article "***Inhibition of APOBEC3G translation by Vif restores HIV-1 infectivity***"). These results show that A3G translation is probably not mediated by an IRES. However, further experiments are required to validate this hypothesis.

Taking all these results into account, we propose a model of A3G translation initiation (Fig 33A) based on the facts that (1) the uORF negatively regulates A3G expression by 40% (Fig. 30B, line 5 and Fig. 31B line 2), (2) wt A3G expression is still observed in the A3G UGA/ΔU-AG mutant, (3) the uAUG is recognized by the 43S complex (Fig. 30B, line 6), (4) A3G translation is not mediated by a re-initiation

mechanism (Fig. 31B, lane 6, 8, 9 and 10) and (5) an IRES is probably absent in the 5'UTR (Fig. 31B, lane 9 and 10). In this model, 60% of the 43S PICs pass through the uAUG by a leaky scanning and initiate translation at the mAUG. However, 40% of the 43S PICs are "trapped" to translate the uORF and thereby reduce A3G translation (Fig 33A).

2.4 The uORF is required in Vif-mediated A3G translation inhibition

To further characterize the molecular mechanism of Vif-mediated A3G translation inhibition, we determined the uORF effect on this translational repression. We performed the aforementioned translation inhibition assay (see article "***Inhibition of APOBEC3G translation by Vif restores HIV-1 infectivity"***) with the uORF-inactivated A3G mutants (A3G uAUG/uAAG and UGA/ΔU-AG) (Fig. 32A). When we co-transfected the wild-type A3G construct with Vif and the Cul5ΔRbx1 mutant, we observed a typical 30-40% reduction in A3G synthesis due to A3G translational repression by Vif (Fig 32B, lane 4). However, this translational inhibition is neither observed in the A3G uAUG/uAAG mutant nor in both forms of A3G UGA/ΔU-AG mutant (Fig 32B, lane 8 and 12). These results clearly show that the uORF is required in the Vif-mediated A3G translation inhibition.

2.5 A model of the mechanism of Vif-mediated A3G translation inhibition

According to these results and using our A3G translation initiation model (Fig 33A), we propose a possible mechanism by which Vif inhibits A3G translation (Fig 33B).

- First, we demonstrated that Vif cannot inhibit A3G translation of the A3G uAUG/uAAG and UGA/ΔU-AG mutants (Fig 32B, lane 8 and 12). In the A3G uAUG/uAAG mutant, the mAUG recognition is mediated by a classical scanning mechanism because the uAUG is not functional. On the contrary, in the A3G UGA/ΔU-AG mutant, the 43S PIC passes through the functional uAUG to recognize the mAUG. Both mutants translate their mORF by an uninterrupted scanning process and since Vif cannot inhibit A3G translation in these mutants, we conclude that Vif is incapable of blocking 43S PIC scanning of A3G transcript in a wild type context.

- Second, we showed that 60% of the ribosomes pass through the uAUG by a leaky scanning mechanism and translate the mORF as observed in the A3G UGA/ΔU-AG mutant. Taking these results into account, we conclude that Vif is unable to block A3G translation that has been initiated by these ribosomes. Therefore, Vif must inhibit A3G translation by acting on the uORF translation step.

- Third, we demonstrated that an uORF negatively regulates A3G expression by a mechanism in which 40% of ribosomes are forced to translate the uORF. After translating this uORF, termination and post-termination events probably occur conventionally, with stop codon recognition by eRF1 and eRF3 and 60S subunit release (Kozak, 2005; Munzarová et al., 2011). Since a Vif-binding site was previously determined 9 nt after the uORF stop codon (Mercenne et al., 2010) and since a ribosome covers about 30 nucleotides on mRNAs (Sharma and Chowdhury, 2011), we propose that Vif could inhibit uORF translation termination and promote ribosomal stalling. Vif-mediated ribosomal stalling cannot occur in uORF translation initiation or elongation because A3G translation inhibition by Vif is not observed in the long A3G form (Fig. 32A, lane 12). Ribosomal stalling at uORF translation termination could obstruct the scanning of newly 43S PICs that have passed through the uAUG and, therefore, inhibiting A3G translation. A similar translation repression mechanism has been previously reported in the human cytomegalovirus gpUL4 (gp48) transcript. In this model, ribosome arrests at termination of the uORF2 translation by a mechanism dependent of the nascent uORF2 peptide. These stalled ribosomes consequently block other ribosomes from reaching the mORF (Cao and Geballe, 1996).

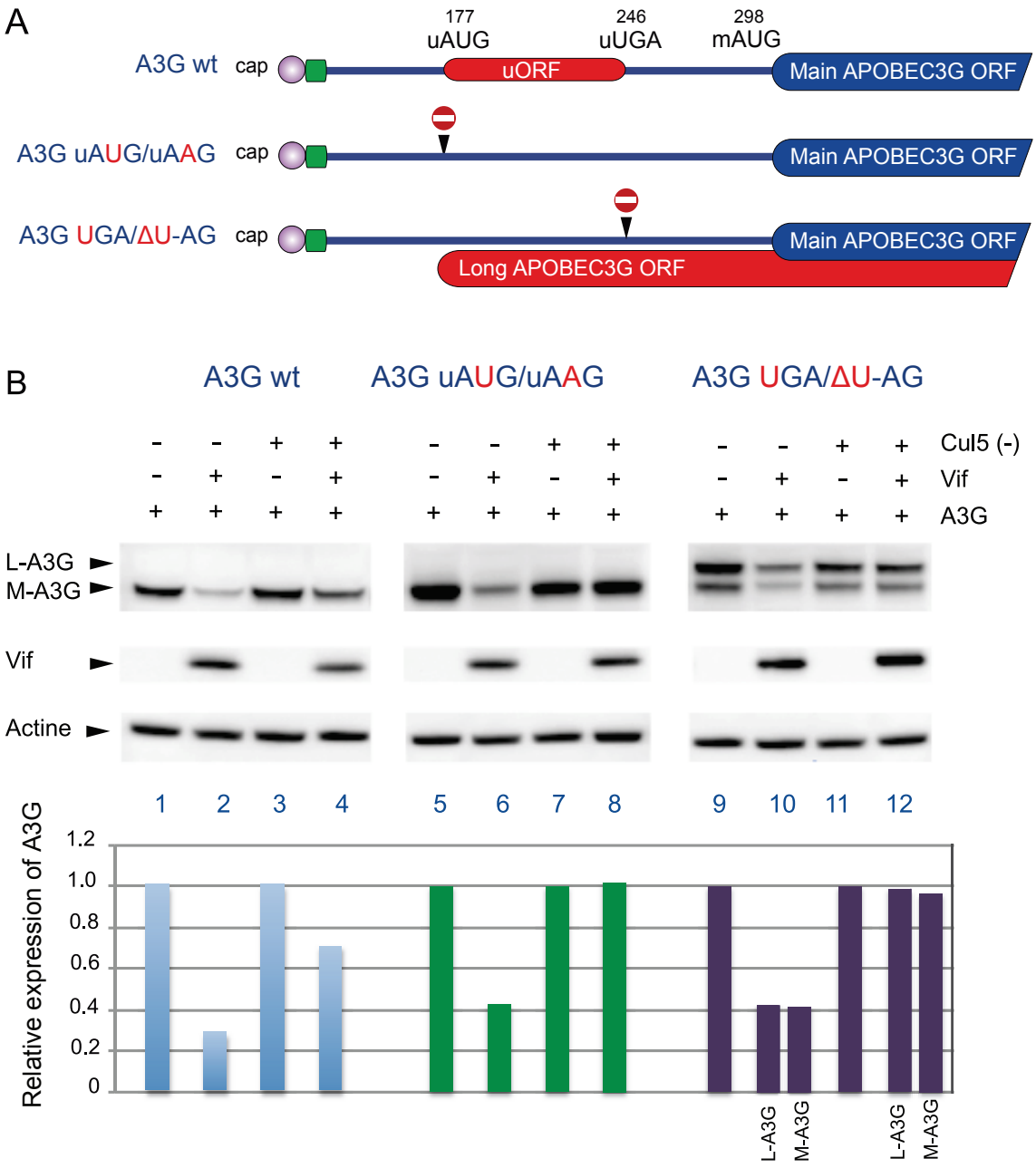

Figure 32. Effect of the uORF on Vif-mediated A3G translation inhibition. A) Schematic representation of the A3G wt, A3G uAUG/uAAG and A3G UGA/ΔU-AG mutants. **B)**. *Ex vivo* translation inhibition assay using HEK293T cells. Proteins were separated by SDS-PAGE and analyzed by immunoblotting. Bands were quantified using Image J (1.46r) and relative expression of A3G is represented in a histogram. A3G (lanes 1, 5 and 9) and A3G transfected with Cul5 (-) (lanes 3, 7 and 11) are set up to 1.

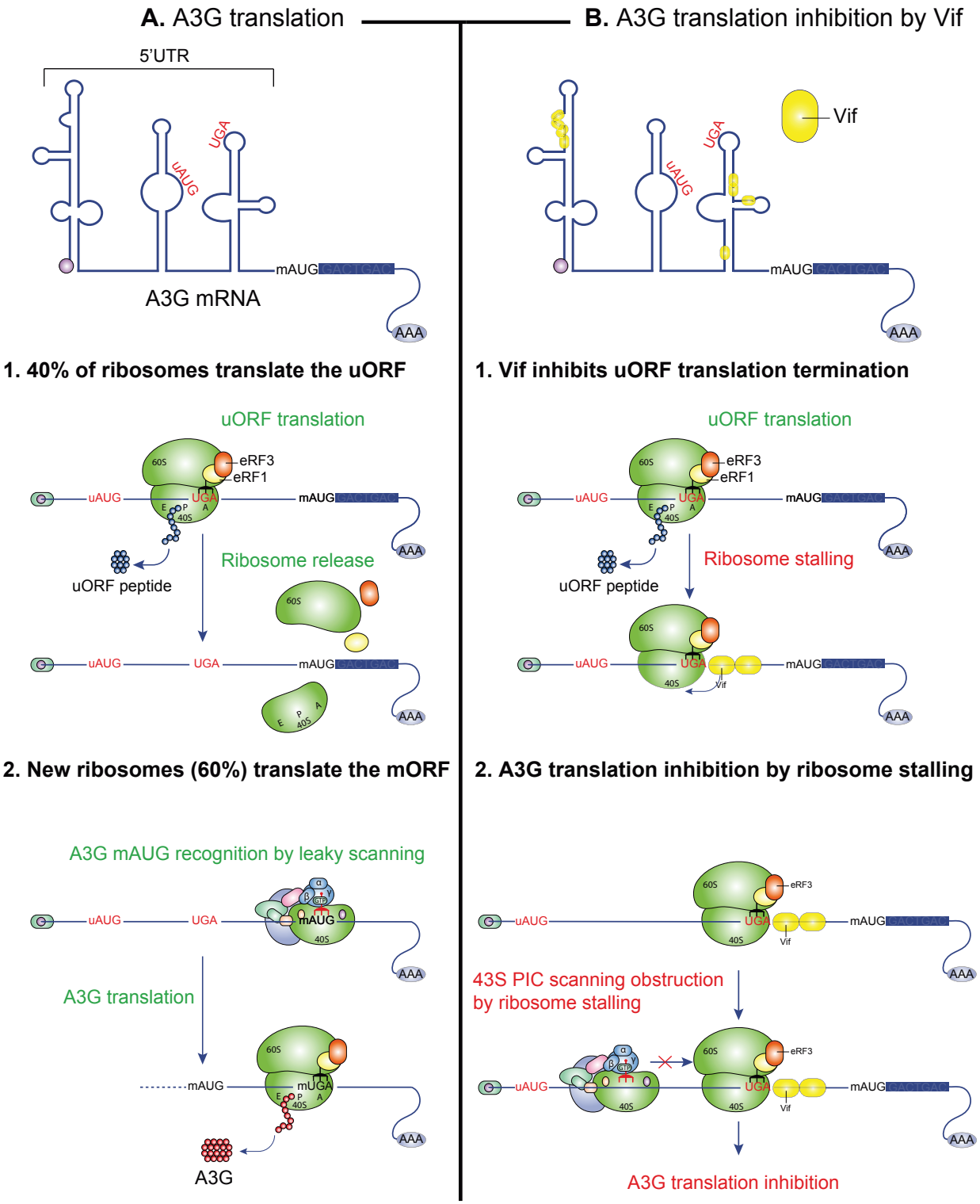

Figure 33. A3G translation and its inhibition by Vif. A) Schematic representation of the A3G translational model. In this model, an uORF negatively regulates A3G expression. 60% of ribosomes initiate at the mAUG, while 40% are committed to translate the uORF and thereby reduce A3G translation. **B)** Schematic representation of Vif-mediated A3G translation. In this model, Vif inhibits uORF translation termination and causes 43S PIC scanning obstruction by ribosome stalling.

3. The RNA chaperone activity of HIV-1 Vif

3.1. Article 2: The C-terminal domain of the HIV-1 Vif protein is responsible for its RNA chaperone activity

This article describes the RNA binding properties and chaperoning activities of the full-length HIV-1 Vif protein and of its functional domains. This work was carried out in collaboration with Dr. Carine Tisné of the “Laboratoire de Cristallographie et RMN Biologiques, CNRS, Université Paris Descartes”. My contribution in this study was to identify which functional domain carries the RNA chaperone activity. This activity was studied by the capacity of Vif and its domains to induce *in vitro* the dimerization of HIV-1 RNA fragments and to promote the annealing of DNA/RNA molecules (TAR assays). Both assays showed that the C-terminal domain of the HIV-1 Vif protein is responsible for its RNA chaperone activity.

The C-terminal domain of the HIV-1 Vif protein is responsible for its RNA chaperone activity

Dona Sleiman[1,§], Serena Bernacchi[2,§], Santiago Guerrero[2], Franck Brachet[1], Valéry Larue[1], Jean-Christophe Paillart[2,*] & Carine Tisné[1,*]

[1]Laboratoire de Cristallographie et RMN Biologiques, CNRS, Université Paris Descartes, Paris Sorbonne Cité, 4 avenue de l'Observatoire, 75006 Paris.

[2]Architecture et Réactivité de l'ARN, CNRS, Université de Strasbourg, Institut de Biologie Moléculaire et Cellulaire, 15 rue René Descartes, 67084 Strasbourg, France.

§ The two first authors contributed equally to this work

* To whom correspondence should be addressed:

Carine Tisné, carine.tisne@parisdescartes.fr

Phone: + 33 1 53 73 15 72 ; Fax: + 33 1 53 73 99 25

Jean-Christophe Paillart, jc.paillart@ibmc-cnrs.unistra.fr

Phone: + 33 3 88 41 70 35 ; Fax: + 33 3 88 60 22 18

ABSTRACT

The viral infectivity factor (Vif) is essential for the productive infection and dissemination of HIV-1 in non-permissive cells. In those cells, Vif neutralizes the cellular anti-HIV defense by interacting with the cellular cytosine deaminases APOBEC3G (A3G) and A3F and inhibiting their antiviral activities by diverse mechanisms including their degradation through the ubiquitin/proteasome pathway and their translational inhibition. In addition, Vif appears to be an active partner of the late steps of viral replication by interacting with Pr55Gag, reverse transcriptase and genomic RNA. While several biophysical properties of Vif have already been characterized, its tridimensional structure is still unknown. Here, we expressed and purified wild-type and functional domains of Vif, and analyzed their RNA binding properties and chaperoning activities. First, we showed by CD and NMR spectroscopies that the N-terminal domain of Vif is highly structured in solution, whereas its C-terminal domain remains mainly unfolded, either alone or within the full-length Vif. More strikingly, both domains exhibited substantial RNA binding capacities with dissociation constants in the nanomolar range. Moreover, we showed by NMR chemical shift mapping that Vif and NCp7 share the same binding sites on $tRNA^{Lys}_3$, and could thus compete for $tRNA^{Lys}_3$ binding. Finally, we showed that the basic unfolded domains of Vif and NCp7 are mainly responsible for their RNA annealing chaperone activities. Altogether, our results highlight the importance of the basic and intrinsically disordered nature of the C-terminal domain of Vif in its ability to interact with several partners including nucleic acids.

INTRODUCTION

In addition to structural and enzymatic proteins essential for virus replication, the HIV-1 genome encodes six regulatory proteins (Tat, Rev, Nef, Vif, Vpr and Vpu) that modulate virus fitness and infectivity *in vivo*. Amongst these proteins, Vif (Viral Infectivity Factor), a 23 kDa highly basic protein, has been shown to be essential for viral pathogenesis by allowing HIV-1 replication in non-permissive cells, such as $CD4^+$ T lymphocytes and macrophages, the natural cell targets of the virus (1). In those cells, Vif neutralizes the cellular anti-HIV defense by interacting with the cellular cytosine deaminases APOBEC3G (APOlipoprotein B mRNA-Editing enzyme-Catalytic, polypeptide-like 3G or A3G) and A3F and inhibiting their antiviral activities (2). In the absence of a functional Vif, A3G/3F proteins deaminate cytidines into uridines in the minus strand DNA (3-5) and inhibit reverse transcription and integration through deaminase-independent mechanisms (6). Vif counteracts A3G/3F and allows HIV-1 replication by hijacking several cellular processes. Firstly, Vif targets A3G/3F for degradation *via* the proteasome by recruiting an E3 ubiquitin ligase cellular complex composed of Elongin B (EloB), Elongin C (EloC), Cullin 5 (Cul5) and RING-box protein 2 (Rbx2) (7-9). CBF-β the transcriptional Core Binding Factor-β, has recently been shown to be an integral component of this complex, directly interacting with Vif and favoring the specific poly-ubiquitination and degradation of A3G (10-12). Secondly, Vif has been proposed to downregulate A3G translation by binding to the 5'-UTR (untranslated region) of its mRNA, thus likely preventing its scanning by the ribosome (13). These two mechanisms seem to be independent pathways utilized by Vif to reduce the expression of A3G (14,15), and to indirectly interfere with its packaging (16). In addition, Vif has been proposed to promote the assembly of A3G into presumably packaging-incompetent high molecular mass complexes (17).

Vif consists of several functional and conserved domains (Figure 1) (for reviews see (Barraud, 2008 #27;Batisse, 2012 #28;(18)). The N-terminal domain (NTD) of Vif (residues 1-100) is enriched in hydrophobic amino acids, notably in conserved tryptophan residues. Mutagenesis studies have shown that these residues and other motifs/sequences are important for binding to A3G/3F {Tian, 2006 #33;Schrofelbauer, 2006 #30;Dang, 2010 #31;Dang, 2010 #32;Russell, 2007

#34;Santa-Marta, 2005 #35;Yamashita, 2008 #37}, but also to A3H, A3C and A3DE (19-22).

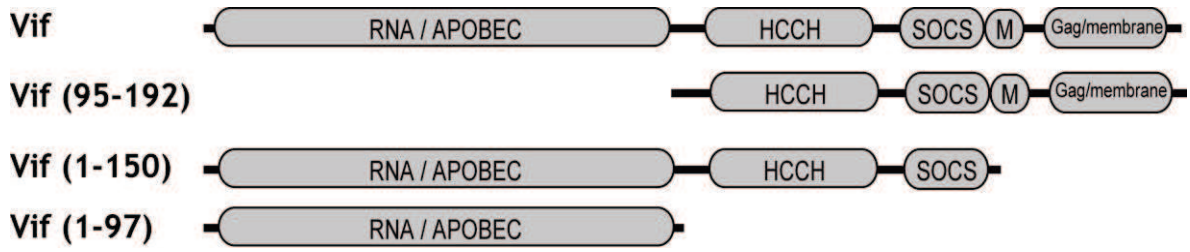

Figure 1. Schematic representation of the HIV-1 Vif functional domains and of the Vif constructions studied in this paper. HIV-1 Vif contains several functional domains, including an RNA/APOBEC binding domain, a conserved zinc-binding hydrophobic HCCH motif and a downstream SOCS-box, a multimerization domain (M) and a Gag/membrane binding domain. The number in parenthesis corresponds to the number of Vif amino acids encompassed in each construction.

In particular, the NTD residues W11, Y30 and Y40 are important for its binding to RNA *in vitro* (23) and in infected cells (24). Moreover, residues W21 and W38 are involved in binding to CBF-□ (10,11,25). The central domain (residues 108-139) constitutes a non-consensus HCCH zinc-binding motif that binds Cul5 (26,27). Finally, the C-terminal domain (CTD) consists of (i) a SOCS-box motif (^{144}SLQ(Y/F)LAL^{150}) that promotes the interaction with EloC/EloB (28), and is therefore important for the recruitment of the E3 ubiquitin ligase that targets A3G for degradation (29); (ii) an oligomerization domain (residues 151-164) containing a ^{161}PPLP^{164} motif critical for Vif oligomerization (30-32) and that allows the interaction with the cellular kinase Hck (33,34); and (iii) a domain (residues 172-192) important for binding with Pr55^{Gag} (35-37), membranes (38), and RT (39).

While characterization of the 3D-structure of Vif in its unbound state remains a challenging problem and a matter of intense research, several biophysical properties of the protein have already been characterized. For instance, Vif has been shown to be structurally unfolded (40-42), and the disordered nature of the C-terminal region is in line with secondary structure prediction models (43)(see supplementary Figure 1). Moreover, conformational refolding of Vif has been observed upon self-oligomerization (40), binding to Elongin C (44) and to specific RNA motifs such as

the Trans-acting Responsive (TAR) element (45), confirming the importance of unstructured regions in the multi-functional properties of Vif.

Vif has previously been shown to be an RNA binding protein with preferential binding to short RNA motifs present in the 5' region of HIV-1 genomic RNA as well as to APOBEC3G mRNA (13,45-49). Moreover, Vif seems to participate to several important steps of the viral replication cycle such as the reverse transcription (47,50), and HIV-1 genomic RNA dimerization (30,47) thanks to its RNA chaperone activity (30,47). The basic and intrinsically disordered nature of the HIV-1 Vif protein may account for its ability to interact with several other proteins and nucleic acids in a manner similar to RNA chaperones such as the HIV-1 NCp7 (51,52) and Tat (53) proteins or the cellular fragile X mental retardation protein FMRP (54). In this respect, the N-terminal region of Vif was previously described to be responsible for its specific RNA binding affinity whereas the C-terminal region (156-192), which contains many positively charged residues, seemed to contribute to non-specific RNA binding (23). To examine this possibility, we purified full-length HIV-1 Vif and individual domains of this protein and analyzed their nucleic acid binding activities for a panel of different RNAs. For each Vif domain, we also analyzed its oligomerization state and its secondary structures elements *in vitro*. Moreover, we showed by NMR chemical shift mapping that Vif and NCp7 share the same binding sites on $tRNA^{Lys}_3$, with a joined participation of the NTD (1-97) and CTD (95-192) of Vif. Finally, we showed that Vif has potent RNA chaperone activities and provided direct evidence for an important role of the unstructured CTD of Vif in this capacity.

MATERIALS AND METHODS

Expression and purification of Vif and its domains

Vif expression vectors were constructed by PCR and cloning into the pET-52b(+) (Novagen) vector. First, pD10Vif expression vector (Vif HXB2) was PCR-amplified with the corresponding forward (F) and reverse (R) primers: (F Vif) 5'GGTCCATGG AAAACAGATGGCAG3' and (R Vif) 5'GGTGAGCTCGTGTCCATTCATTGTG3'; (R Vif 1-97) 5'GGTGAGCTCTTGTGTGCTATATCTCTT3'; (R Vif1-150) 5'GGTGAGCTC TAGTGCCAAGTATTG TAG3' giving rise to vectors expressing full-length Vif, domains 1-97 and 1-150 of Vif, respectively. Primers (F Vif95-192) 5'GGTCCATGG

TAGACCCTGAACTAGCAGAC3' and (R Vif 95-192) 5'CACAATGAATGGACAC GAGCTC3' gave a plasmid expressing domain 95-192 of Vif. Forward primers contain a NcoI restriction site (underlined) while reverse primers contain a SacI restriction site (underlined). After purification of the PCR products (Nucleospin PCR clean-up, Macherey Nagel), DNA fragments were digested with NcoI and SacI, and cloned into pET-52b(+) vector previously digested with the same restriction enzymes. The sequence of all constructs, pET52b(+) Vif, Vif (1-97), Vif (1-150) and Vif (95-192), was confirmed by DNA sequencing (GATC Biotech, Germany).

Escherichia coli BL21(DE3) competent cells were transformed with plasmids coding for Vif, Vif (1-97), Vif (1-150), and Vif (95-192). Expression of Vif and its domains were induced by addition of 1 mM IPTG in exponential phase of cultures (absorbance at 600 nm around 0.6). After 3 h of induction at 37°C, bacteria were harvested by centrifugation at 6,000 g during 15 min, lysed in denaturating lysis buffer (6 M guanidine hydrochloride, 100 mM sodium phosphate, 10 mM Tris-HCl pH 8) at room temperature and stirred overnight. Cellular debris was separated by centrifugation at 27,000 g during 30 min at 4°C and the cleared lysate was loaded onto a Ni-NTA agarose column. The column was washed with lysis buffer and elution was performed by decreasing the pH from 6.5 to 4.5. Fractions containing Vif proteins were analyzed on 14% SDS–PAGE and pooled. Proteins were then renatured by slow dialysis against buffers with decreasing guadinium chloride concentration, and finally against the following buffers: Vif (50 mM MOPS, 1 mM DTT, 50 mM NaCl, pH 6.5), Vif (1-97) (50 mM MOPS, 50 mM NaCl pH 6.5), Vif (95-192) (50 mM MES, 9.6 mM NaCl, 0.4 mM KCl, 2 mM $MgCl_2$, 2 mM $CaCl_2$, 1 mM DTT, pH 6.5) and Vif (1-150) (50 mM MOPS, 1 mM DTT, 50 mM NaCl, pH 6.5). The same protocol was followed to produce ^{15}N-labeled Vif (95-192) except that the LB media was changed for spectra 9 (15N) media (Cambridge isotope laboratories or Cortecnet). The proteins were concentrated using Centriprep YM 3 (Millipore) up to 0.4 mg/mL and centrifuged at 100,000 g for 30 min at 4°C before adding 10% glycerol. Since Vif tends to aggregate, protein stock solutions were centrifuged at 100,000 g for 30 min at 4°C immediately prior to use. For NMR samples, no glycerol was added.

Nucleic acids preparation

Plasmids pHXB2 corresponding to parts of *gag* were obtained as previously described (46). To express RNA fragments corresponding to nucleotides 499-996 (RNA B) and 499-799 (Short RNA B) of HIV-1 genome, plasmids were linearized with PvuII and SalI, respectively, and then used as template for *in vitro* run off transcription with bacteriophage T7 RNA polymerase under conditions previously described (55). After 3 h at 37°C, the reaction mixture was incubated for 1 h at 37°C with RNase-free DNase I (Roche), and then extracted with phenol-chloroform. RNAs were then purified with FPLC (Pharmacia) using a Bio-Sil TSK250/GSW2000W column (TOSOH Bioscience) in a buffer containing 200 mM sodium acetate (pH 6.5) and 1% (v/v) methanol as previously described (56), precipitated in ethanol and dissolved in Milli-Q water (Millipore) prior to use.

^{15}N-labelled $tRNA^{Lys}_3$ was expressed in *E. coli* (JM101TR strain) from a recombinant plasmid and purified as previously described (57). The RNA oligonucleotide corresponding to the apical part of the TAR hairpin ($^{5'}$CGAGCCUGGGAGCUCG$^{3'}$) was purchased from Microsynth or Dharmacon and purified using HPLC (ÄKTA design-Unicorn) system with a (PA-100) anion exchange column (Dionex), and concentrated with Centricon ® (Millipore).

Diffusion light scattering (DLS)

Samples were prepared in their buffers, and final protein sample concentrations were determined after ultracentrifugation. Intensities of scattered light and correlation times were measured with a Zetasizer Nano S (Malvern, UK). Measurements were performed in a single 50 µl trUView cuvette (Biorad Laboratories, CA, USA), maintained at 20°C. DLS fluctuations of the scattering intensity due to Brownian motion were recorded at microsecond time intervals. An autocorrelation function was then derived, allowing determination of diffusion coefficients, D. Assimilating proteins in solution to spheres, diffusion coefficients were related to the hydrodynamic radius of the particles, R_h via the Stokes-Einstein equation:

$$D = kT / Rh\, 6\pi\, \mu$$

in which k is the Boltzmann constant, T the temperature (K), and µ the solvent viscosity. All experimental data were corrected for solvent viscosity (measured with a

3.5 ml micro-Ubbelohde capillary viscosimeter tube from Schott, Germany), and refractive index (measured with an Abbe´s refractometer). To analyze the oligomerization of Vif and its domains, scattering data of Vif and its domains were then analyzed using DLS analysis software (Malvern, UK).

Circular dichroism (CD)

Vif protein samples were prepared anaerobically in 50 mM MOPS, 150 mM NaCl, pH 6.5. Far-UV CD spectra (190–250 nm) were measured with a Jasco J-810 spectropolarimeter (Jasco Inc., Easton, MD, USA). Samples were placed in rectangular quartz cuvettes of 2 mm path length maintained at 20°C. Spectra were acquired at 50 nm/min with a time constant of 1 s and bandwidth equal to 1 nm. Each spectrum represents the average of at least 15 successive baseline-corrected scans. The mean residue molar ellipticity was determined according to equation:

$[\theta] = (\theta \bullet M_R)/(10 \bullet \lambda \bullet c)$

where θ is the measured ellipticity in millidegrees, M_R is the mean residue mass, λ the optical path length and c, the protein concentration. Deconvolution of far-UV CD spectra and consequent secondary structure of protein content was estimated by Dichroweb (http://dichroweb.cryst.bbk.ac.uk/html/home.shtml).

Steady state fluorescence measurements

Fluorescence measurements were recorded in quartz cells at 20 ± 0.2°C on a Fluoromax-4 fluorometer (HORIBA Jobin-Yvon Inc., NJ, USA). The excitation wavelength was set at 295 nm for selective excitation of Trp residues. The emission wavelength was scanned from 310 to 500 nm. The integration time was 0.1 s, and the excitation and emission bandwidths were 5 nm. Fluorescence titrations were performed by adding increasing amounts of nucleic acid to 100 nM of protein in 30 mM Tris–HCl (pH 7.5), 200 mM NaCl and 10 mM $MgCl_2$. Fluorescence intensities were then corrected for buffer fluorescence and dilution effect. To determine the binding parameters of Vif proteins to RNA fragments, we measured the decrease of the fluorescence intensity, I, at a fixed concentration of protein in presence of increasing RNA concentrations. Fluorescence intensities were corrected for dilution and were fitted using the following equation:

$$I = I_0 - \frac{I_0 - I_\infty}{2nN_t}\left(K_d + L_t + nN_t - \sqrt{\left(K_d + L_t + nN_t\right)^2 - 4L_t nN_t} \right)$$

where I_0: Fluorescence intensity without RNA, I: fluorescence intensity at a given concentration of RNA, I_∞: fluorescence intensity at the plateau, n: number of RNA binding sites on the protein, L_t: total concentration of RNA, N_t: total concentration of protein. Confidence limits on the Kd were estimated by Monte-Carlo sampling using the MC-Fit program (58).

NMR chemical shift mapping

NMR data were recorded at 20°C on a Bruker Avance DRX600 spectrometer equipped with a TCI cryoprobe. 1D ^{1}H NMR spectra were recorded using a watergate sequence for solvent suppression (59). 512 scans were usually acquired. ^{1}H-^{15}N TROSY experiments (60,61) were carried out with 128 t1 increments and 2048 t2 data points per increment. The t1 dimension was acquired with the echo-antiecho method. For Vif (1-97) at 40 μM and Vif (95-192) at 36 μM, 1 equivalent of $tRNA^{Lys}_3$ stock at 0.9 mM was directly added to the protein sample. For full-length Vif, the previous operating mix led to precipitation of the protein. So, the complex components were mixed diluted at a 1:1 ratio and were then concentrated in a Centriprep YM 3 (Millipore) to a final concentration of each species around 20 μM. Chemical shift variations Δ(H,N) were derived from ^{1}H and ^{15}N shift differences : $\Delta(H,N) = [(\Delta^{15}N\ W_N)^2 + (\Delta^1H\ W_H)^2]^{1/2}$, where $\Delta = n_{complex} - n_{free}$ and W_H=1 and W_N=1/6.

RNA chaperon activity

DNA and RNA substrates: Oligodeoxynucleotides (ODNs) used for the TAR(+)/TAR(-) DNA annealing assay corresponded to nucleotides 1-56 of the HIV-1 RNA sequence (MAL isolate, Accession Number X04415.1) in the sense and antisense orientations, as previously described (62). RNA fragments used in the RNA dimerization assay corresponded to nts 1-615 of the HIV-1 MAL genomic RNA.

Proteins: HIV-1 NCp7 and NC (12-53) proteins were synthesized and purified as described (63). The HIV-1 Tat protein was synthesized as reported in (53,63).

RNA dimerization assay: RNA dimerization was performed as described previously (47). Briefly, 100 nM of unlabeled HIV-1 1–615 RNA fragment were diluted in 10 µl of water together with the corresponding labeled RNA (5,000 cpm, 3–5 nM). Samples were denatured for 2 min at 90°C, and snap-cooled on ice for 2 min. Dimerization was initiated by addition of Vif proteins under conditions disfavoring salt-induced RNA dimerization (50 mM sodium cacodylate pH 7.5, 50 mM NaCl, 0.1 mM $MgCl_2$). RNA samples were incubated 30 min at 37°C, deproteinized, and resuspended in glycerol-containing loading buffer, split in two equal volumes and analyzed on a 0.8% agarose gel in native (Tris–Borate 0.5X, $MgCl_2$ 0.1 mM, run at 4°C) or semi-denaturating (TBE 1X, run at 20°C) electrophoresis conditions. Gels were fixed in 10% trichloroacetic acid for 10 min and dried for 1 h under vacuum at room temperature. Radioactive bands corresponding to monomeric and dimeric species were visualized and quantified using a FLA 5000 (Fuji).

TAR(-)/TAR(+) DNA annealing assay: The DNA annealing assay was performed as described in (62,64). Briefly, 0.03 pmol of the TAR(+) and ^{32}P-TAR(-) ODNs were incubated in 10 µl of buffer A with increasing concentrations of Vif, NCp7 or Tat proteins, as indicated in legend to Figure 7. Reactions were performed at 37°C for 5 min except for the positive control that was incubated at 65°C. To stop the reaction and remove the protein from the ^{32}P-ODN, 5 µl of a solution containing 20% glycerol, 20 mM EDTA pH 8.0, 2% SDS, 0.25% bromophenol blue and 0.4 mg/ml calf liver tRNA were added. Samples were resolved by 8% native PAGE in 50 mM Tris–borate pH 8.3, 1 mM EDTA at 4°C. Subsequently, gels were fixed, autoradiographed, and the amounts of labeled single-stranded and double-stranded DNA were visualized and quantified using a FLA 5000 (Fuji).

RESULTS

Rationale for the design of HIV-1 Vif domains

We first predicted disorder of the HIV-1 Vif protein (HXB2 isolate) using various software tools (Supplementary Table 1). Most tools predicted a disordered protein

from residue L150. It is interesting to note that Vif has a cleavage site for the HIV-1 protease after this residue, releasing a 151-192 segment (65,66). The C-terminal domain is predicted to be unfolded and this has been actually demonstrated in solution by NMR (42). We thus decided to study a truncated protein containing the first 150 residues of Vif, namely Vif (1-150). This part of the protein contains, in addition to the tryptophan-rich domain, the HCCH motif and the SOCS-box (Figure 1). We then attempted to define the NTD of Vif that contains its RNA binding activity. The 97 residues at the N-terminus of Vif containing the tryptophan-rich region seemed to be appropriate (Vif (1-97)). This part of Vif is rich in hydrophobic amino acids and is predicted to be ordered by all structure prediction programs. We also chose to analyze the CTD of Vif, Vif (95-192), which contains the C-terminal part of Vif from residue 95. Therefore, this domain includes the HCCH motif, the SOCS-box, and the multimerization PPLP domain and is predicted unstructured by all disorder prediction programs. The whole Vif protein has been studied in parallel to these domains.

Overexpression of Vif and its domains in the soluble fraction of *E. coli* lysate was possible in ArcticExpress(DE3)RIL and BL21(DE3)pLysS strains of *E. coli*. However, purification of Vif and its domains from the soluble fraction remained difficult. Indeed, Vif and its domains were highly bound to nucleic acids and the disruption of these interactions by a polyethyleneimine (PEI) treatment, for instance, led to precipitation of Vif proteins. Therefore, Vif and its domains were overproduced in *E. coli* and purified in denaturating conditions as previously described (13,47). The renaturating conditions for each domain were adjusted so that each domain could solubilized and concentrated to a final concentration around 40 µmol/L.

It is now well established that Vif self-associates both *in vitro* (31,40) and *in vivo* (30) through the proline-rich ^{161}PPLP^{164} domain. However, the mutation of the ^{161}PPLP^{164} motif to ^{161}AALA^{164} did not completely abolish the oligomerization of Vif, but reduced the size of Vif multimers (48). This strong tendency of Vif to self-associate and to aggregate has so far hampered Vif to be amenable to X-ray or NMR studies. We thought that working with various domains of Vif could facilitate such a study. Thus, we first focused on Vif domains characterization regarding their self-association, their proper folding, and then on their RNA binding and chaperoning activities.

The overproduced HIV-1 Vif domains are folded as predicted by secondary structure programs

According to our experimental strategy, Vif and its domains were ultracentrifuged and soluble fractions were used to analyze (i) their oligomerization status by DLS (Figure 2), (ii) their secondary structure by CD (Supplementary Table 2 and Supplementary Figure 1), and (iii) their amenability to structural studies by NMR (Figure 3, Supplementary Figures 2 and 3).

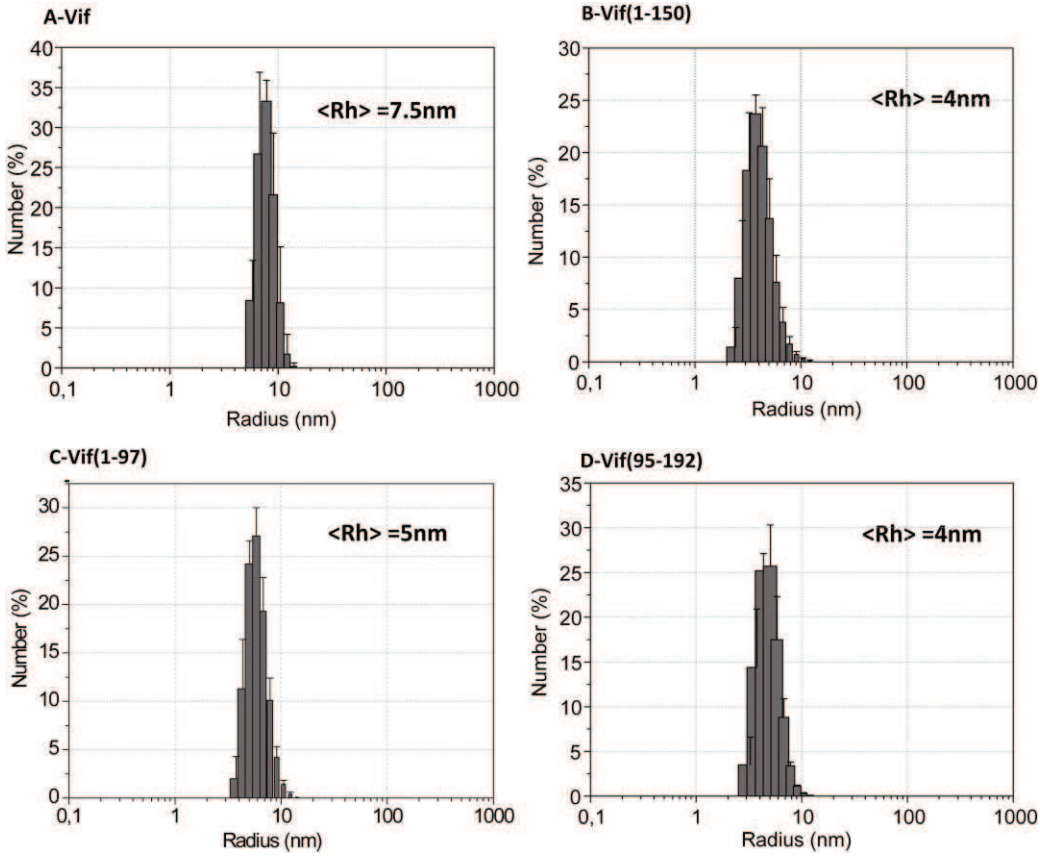

Figure 2. Dynamic light scattering by the HIV-1 Vif protein and its domains. (**A**) HIV-1 Vif, (**B**) Vif (1-150), (**C**) Vif (1-97), (**D**) Vif (95-192). The average hydrodynamic radius is indicated for each Vif protein domain.

DLS allowed us to investigate the homogeneity of the samples and to determine the self-association of Vif domains in solution. DLS was essential to assess the quality of the protein samples before further experiments. Heterogeneous samples presenting two or more protein size populations in solution were discarded from all our analyses. We found that Vif proteins were mainly mono-dispersed, with a poly-dispersity index of about 0.3-0.4 for all tested proteins (Figure 2). Moreover, we observed that addition of 10% glycerol prevented massive aggregation. A mean

hydrodynamic radius of 7.5 nm was measured for Vif, which corresponds to a multimer containing 15 to 19 proteins, in agreement with previously published data (45,48,49). For Vif domains, the hydrodynamic radius varied from 4 to 5 nm. Assuming spherical organization of the multimers, this could correspond to multimers of 4-5 proteins for Vif (1-150) and 7-9 proteins in the case of Vif (1-97) and Vif (95-192). Therefore, Vif (1-150) and Vif (1-97) form multimers despite the absence of the ^{161}PPLP^{164} oligomerization site. On the contrary, Vif (95-192), despite the presence of the ^{161}PPLP^{164} motif, formed multimers of no more than 10 proteins. Taken together, these results suggest that domains outside the C-terminus of Vif also contribute to multimerization, in agreement with previous studies performed on full-length Vif protein {Batisse, 2012 #28;Bernacchi, 2011 #64;(67). Moreover, the ^{161}PPLP^{164} domain is not conserved amongst HIV-2 and SIV {Barraud, 2008 #27}, confirming that other unknown domains can be used to form oligomers.

The conformation of Vif and its domains were further investigated using far-UV CD (Supplementary Figure 1 and Supplementary Table 1). CD spectra in the far-UV domain (180-260 nm) gives information on the secondary structure of proteins, namely their contents in α-helix, β-strands, and random secondary structures. Analysis of Vif CD spectrum yields 15% of α-helix, 33% of β-strands and 52% of disordered regions, in good agreement with previous studies (45,48,49) and with secondary structure prediction (Supplementary Table 1). As expected from secondary structure prediction (30,68-70), wild-type Vif protein, Vif (1-150) and Vif (1-97) show an overall organization enriched in β-strands, while Vif (95-192) is essentially unstructured. The sum of secondary structures predicted and observed by CD are very similar (Supplementary Table 2), even if limited differences exist in the type of secondary structures. These results show that the overproduced Vif domains were folded as predicted after the denaturation-renaturation process.

The significant percentage of disordered regions in Vif most likely arises from its C-terminal domain. Indeed, the percentage of random structures was smaller in Vif (1-150) and Vif (1-97), where the C-terminal region is missing. Vif (1-97) presented the highest percentage of secondary structures (68%) and the lowest of random domains (32%). This domain could have been amenable to structural study by NMR or X-ray crystallography. Unfortunately, its poor solubility and oligomerization tendency prevented us from solving its 3D structure by NMR or X-ray

crystallography. We thus confirmed that the CTD of Vif is disordered in solution, while the NTD corresponds to the most structured domain.

We then studied the 1D ^{1}H NMR spectrum of Vif and its domains (Supplementary Figure 2). Taking into account that these proteins forms multimers in solution, the poor dispersion of NMR signals in the amide region (7.5-10 ppm) indicated that the observable protons are not involved in the hydrophobic core of the proteins, but belong to their unfolded domains. This feature is confirmed by the observation that the 1D ^{1}H NMR spectrum of Vif and Vif (95-192) are identical. Therefore, the only observable part of the Vif protein by NMR is its C-terminal domain. We subsequently labeled Vif (95-192) by ^{15}N-nitrogen to precisely analyze this domain by 2D NMR spectroscopy (Figure 3).

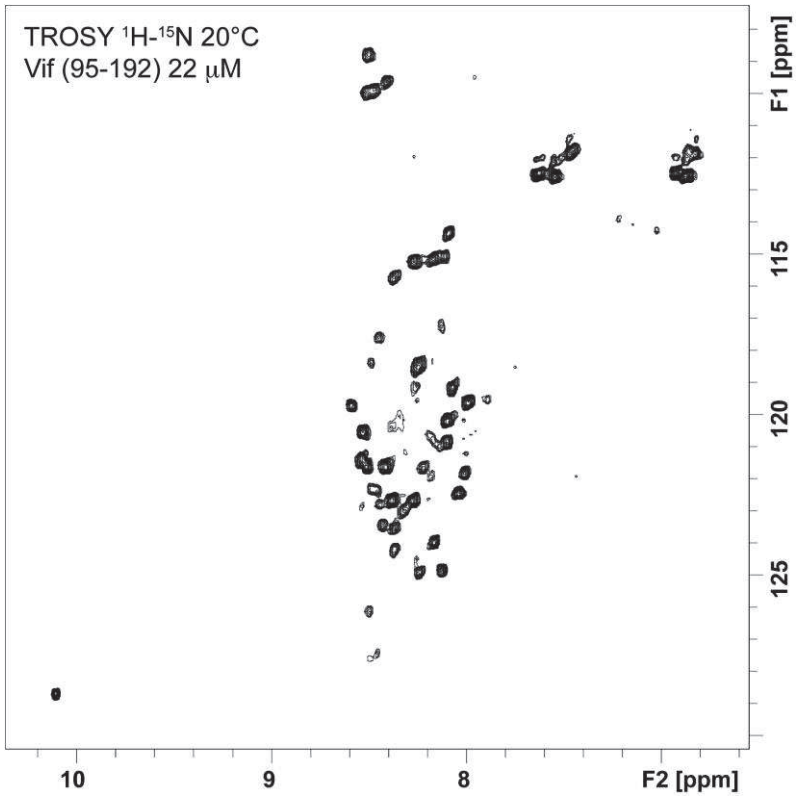

Figure 3. ^{1}H-^{15}N TROSY spectrum of Vif (95-192). The spectrum was recorded at 20°C in the protein buffer. The sample (22 µM, glycerol free) was centrifuged for 30 min at 100,000 g before use.

Amide group signals were poorly dispersed in the proton dimension (0.5 ppm) and covered 10 ppm in the nitrogen dimension. The signal at 10.07 ppm corresponds to the indol NH of the unique tryptophan (W174) present in Vif (95-192). This proton signal is also observable in the wild-type Vif spectrum while the 6 other tryptophan

(W5, W11, W21, W38, W70, W79) indol protons remained unobservable. The poor dispersion of the amide groups and the linewidth of the NMR signals of Vif (95-192) confirmed that this protein is not structured and forms multimers. The addition of zinc ions did not allow further structuration, but an additional broadening of signals was observed (Supplementary Figure 3). For Vif (1-97), very few large signals are observed, confirming that this protein formed a high molecular weight complex with a low percentage of unstructured regions (Supplementary Figure 2).

Altogether, these biophysical analyses suggested that Vif and its domains can be produced under soluble and homogenous samples, and fold as expected, with a highly structured NTD and an unstructured CTD.

The N and C-terminal domains of HIV-1 Vif both bind nucleic acids

The HIV-1 genomic RNA and the APOBEC3G mRNA were previously described as containing specific Vif binding sites (45,46,48,49). In the HIV-1 RNA, several regions can be bound by Vif, namely the TAR, poly(A), and DIS (Dimerization initiation Site) stem-loops located in the 5'-untranslated region, and a short sequence within nucleotides 499-996 (RNA B), in the Gag coding region (46). In line with these studies, we focused our attention on RNA B and on a shorter version corresponding to the first 300 nucleotides of RNA B (Short RNA B). Interestingly, it was previously observed that this short domain contains a very high affinity binding site for Vif (48). We also investigated the binding of Vif domains to the apical part of the TAR stem-loop (16 nts) and to $tRNA^{Lys}_3$ (76 nts), since Vif inhibits some functions of the HIV-1 nucleocapsid protein (NCp7) such as the annealing of $tRNA^{Lys}_3$ to the PBS (Primer Binding Site) of the HIV-1 RNA (47). Moreover, ^{15}N-labeled $tRNA^{Lys}_3$ and the NMR assignment of its imino groups were already available in one of our groups (71,72), thereby opening the use of NMR to study these Vif binding to $tRNA^{Lys}_3$.

Considering the biochemical characteristics of Vif protein and its different domains, fluorescence spectroscopy and NMR chemical shift mapping were our preferred methods to investigate the interaction between Vif domains and RNAs. Indeed, Vif contains 8 tryptophans that confer an intrinsic fluorescence signal to the protein. Similarly, Vif (1-97) and Vif (1-150) have 7 tryptophan residues, while Vif (95-192) possesses only one. However, this single tryptophan residue was sufficient to analyze the RNA binding capacity of Vif (95-192). Upon RNA binding, the

fluorescence of Vif and its domains was attenuated (Figure 4 and Supplementary Figure 4), and fluorescence quenching was used to obtain titration curves and to determine dissociation constants.

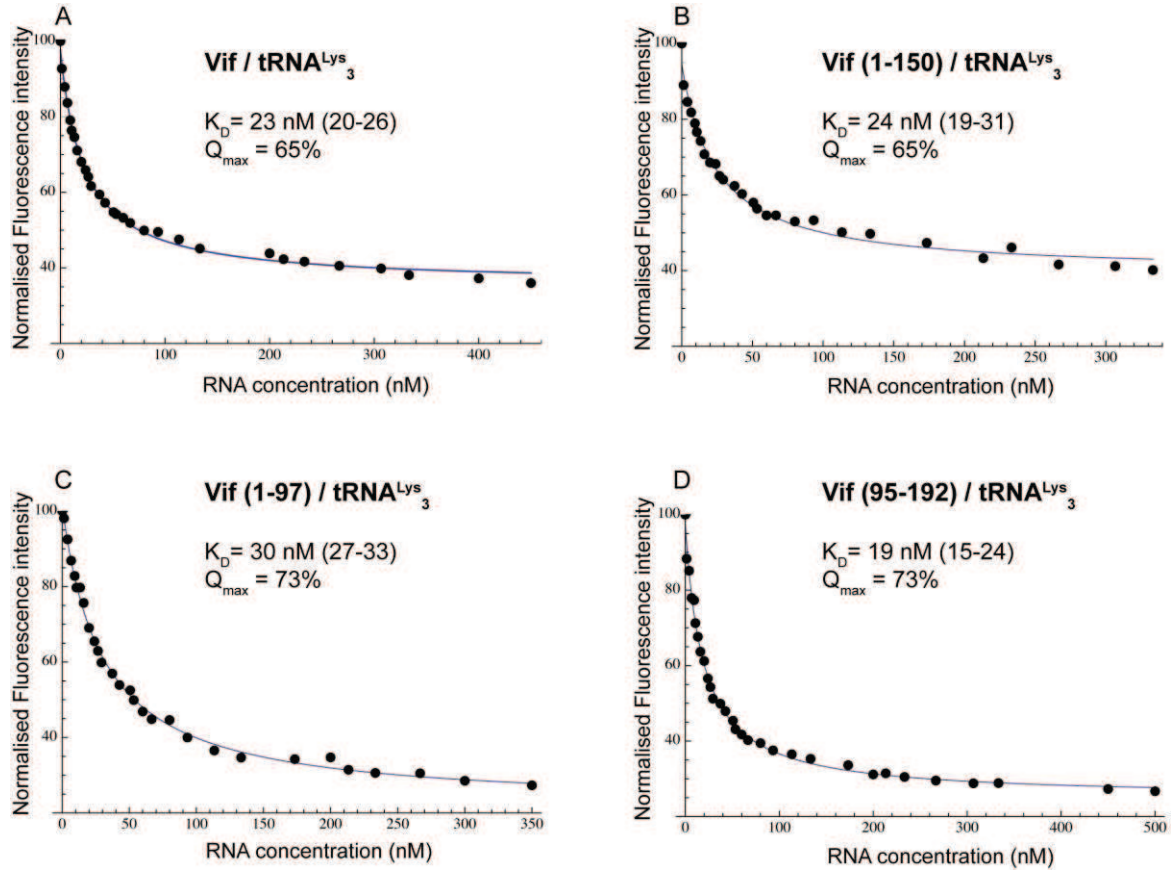

Figure 4. Fluorescence titrations of Vif and its domains with tRNA$^{Lys}_3$ at 25°C. (**A**) Vif, (**B**) Vif (1-150), (**C**) Vif (1-97) and (**D**) Vif (95-192). The dissociation constants (K_D) are indicated in nM with the 95% confidence interval between parenthesis. The maximal fluorescence quenching (Q_{max}) obtained for each titration is indicated as a percentage (%). The measurements were performed in a Tris-Cl (30 mM, pH 7.5) buffer containing 200 mM NaCl and 10 mM $MgCl_2$.

Titration curves of Vif and its domains with tRNA$^{Lys}_3$ are presented in Figure 4 as examples, while Table 1 summarizes the K_d values derived from fitting of the relative binding curves (see Materials and Methods). Dissociation constant analysis (Table 1) allowed us to observe that the NTD, Vif (1-97), which corresponds to the previously described Vif RNA binding domain binds to the different tested RNAs similarly to full-length Vif (23,24). Globally, the K_d magnitudes range from 10 to 34 nM, which correspond to high affinity binding. More surprisingly, the C-terminal domain of Vif, Vif (95-192), also highly bound to RNAs (Table 1), with relative dissociation

constants ranging from 16 to 26 nM (Table 1 and Supplementary Figure 4). Beside, we also showed that Vif (1-150) seems to be the least efficient for RNA binding (Table 1). In this case, K_d values ranged from 30 to 51 nM. This result indicates that the HCCH and SOX-box domains do not participate in RNA binding. This is in agreement with previous results showing that no interaction could be observed between a peptide containing the HCCH motif and nucleic acids (JCP, unpublished data).

Table 1. Dissociation constants (K_D) derived from fluorescence titrations.Each K_D value is the average of five titrations, the mean standard deviation is indicated in parenthesis. The maximal attenuation Q_{max} is also indicated.

	ARN B	**ARN B short**	**ARNt$^{Lys}_3$**	**TAR**
Vif FL				
K_D (nM)	30 ± 3	13 ±2	27 ±5	31 ±4
Q_{max}	50%	70%	65%	56%
Vif Q97				
K_D (nM)	31 ±5	10 ±2	34 ±4	32 ±4
Q_{max}	76%	65%	73%	62%
Vif S95				
K_D (nM)	26 ±4	16 (±2	16 ±3	20 ±2
Q_{max}	62%	60%	73%	66%
Vif L150				
K_D (nM)	47 ±2	27 (±2	51 ±7	31 ±4
Q_{max}	60%	56%	65%	54%

The dissociation constants of Vif domains for small RNA (TAR and $tRNA^{Lys}_3$) were very similar. Interestingly, the comparison of K_d values obtained for RNA B and its shorter version lead to the observation that highly specific binding sites for Vif are present in the short RNA B (Table 1). These results are in good agreement with previous results (45) confirming the presence of preferential binding sites in this region of the HIV-1 genomic RNA. It is thus possible that these high affinity binding sites are somehow buried in the complete RNA B, while exposed in its truncated form and available to interact with Vif.

The different domains of Vif also showed rather good affinity for small and highly structured RNAs such as TAR and $tRNA^{Lys\ 3}$ (Table 1). Since those regions are absolutely required for essential steps in reverse transcription, these interactions could be related to different functions played by Vif protein during the HIV-1 life cycle.

Vif and NCp7 proteins share the same binding sites on $tRNA^{Lys}_3$

Our fluorescence spectroscopy results showed that Vif and its domains bind TAR and $tRNA^{Lys}_3$, two RNAs suitable for NMR studies. All our attempts to obtain TAR/Vif or Vif domains complexes at concentrations required for recording NMR spectra (around 10-40 µmol/l) were unfruitful due to massive precipitation of the proteins, thus preventing any further NMR studies. Fortunately, the situation was more favorable for the study of the $tRNA^{Lys}_3$/Vif interaction. Therefore, $tRNA^{Lys}_3$ was used to investigate the binding of Vif and its domains by NMR chemical shift mapping. This method consists of labeling one of the partners of a complex with nitrogen 15 ($tRNA^{Lys}_3$ in our case) and in monitoring the variation of chemical shifts upon binding with the non-labeled partner (Vif and its domains). Indeed, ^{15}N-labeled $tRNA^{Lys}_3$ was produced as previously described (57) and the chemical shifts of its imino groups were used to monitor its interaction with Vif (Figure 5A, Supplementary Figure 5 and 6). The imino groups involved in the protein-binding site experience the largest variations of chemical shifts (Supplementary Figure 5, 6 and 7). For instance, the imino groups of U12, G15, T54 and G70 undergo the largest variation of chemical shift, between 0.05 and 0.08 ppm upon binding to Vif. Our NMR data indicate that Vif is most strongly bound to the T-arm, the acceptor arm, the variable loop, and the D-arm of $tRNA^{Lys}_3$ (Figure 5B).

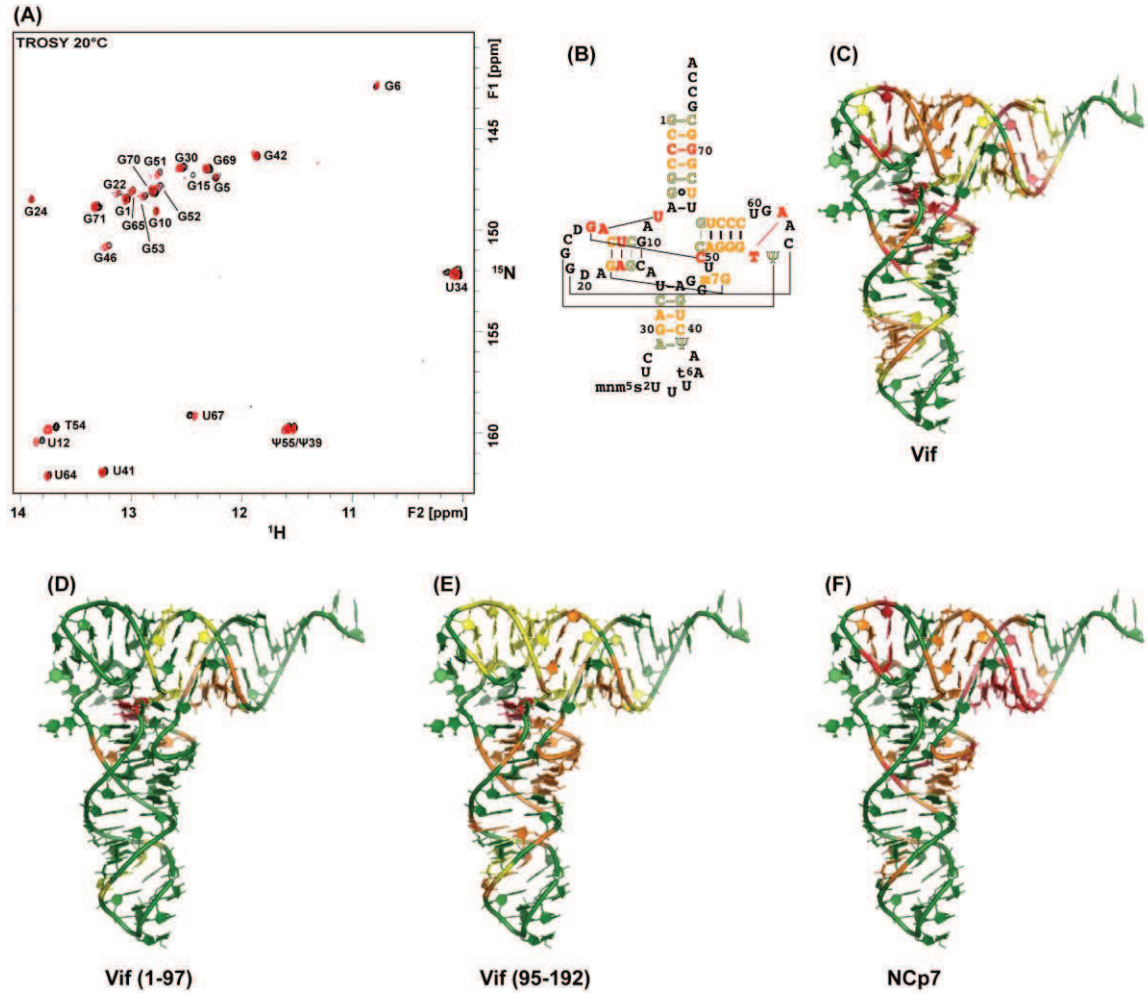

Figure 5. NMR chemical shift mapping of the binding sites of Vif proteins on $tRNA^{Lys}_3$. (**A**) two NMR spectra (2D ^{1}H-^{15}N TROSY) acquired at 20°C are superimposed: in black for the $tRNA^{Lys}_3$ alone (reference spectrum) and in red for the $tRNA^{Lys}_3$/Vif complex. (**B**) The NMR chemical shift mapping is reported on the secondary structure of $tRNA^{Lys}_3$ with the following color code: the base pairs for which the chemical shift variation of the imino group upon addition of the protein is ≥ 0.05 ppm are in red, between 0.03 and 0.05 ppm in orange and equal to 0.02 ppm in yellow. Mapping on the $tRNA^{Lys}_3$ 3D structure (PDB code 1FIR) of the binding sites of the Vif protein and its domains: (**C**) Vif, (**D**) Vif (1-97), (**E**) Vif (95-192) at 2 equivalents and (**F**) NCp7 at 3 equivalents {Tisne, 2001 #664}. The color code is the same as in B.

The NMR footprint more clearly appears when reported on the 3D structure of $tRNA^{Lys}_3$ (Figure 5C). Vif thus presented a strong binding site located in the core of $tRNA^{Lys}_3$. Interestingly, Vif (1-97) did not bind the T-arm of $tRNA^{Lys}_3$ (Figure 5D), but still bound to the variable loop/D-arm and to the acceptor arm. Vif (95-192) showed a more dispersed interaction but was still capable of binding to the $tRNA^{Lys}_3$ T- and D-arms. Unfortunately, we were not able to examine Vif (1-150) binding to $tRNA^{Lys}_3$ due

to the poor solubility of this protein. NMR chemical shift mapping of the interaction between NCp7 and $tRNA^{Lys}_3$ was previously published (73) (figure 5F). Interestingly, these interactions were almost identical with that of Vif, suggesting that these two proteins share the same binding sites on $tRNA^{Lys}_3$. Taken together, these results suggest that the interaction with the T-arm of $tRNA^{Lys}_3$ is dependent on the C-terminal domain while the interaction with the D arm/variable loop occurs through its N-terminal part.

The RNA chaperone activity of Vif is driven by its C-terminal domain (95-192)

In order to identify the domain of Vif involved in RNA chaperoning, we compared the capacity of full-length Vif and Vif domains (i) to modulate HIV-1 RNA dimerization (Figure 6) and (ii) to activate the annealing of two complementary oligodeoxynucleotides (TAR(+)/TAR(-) assay) *in vitro* (Figure 7).

- *HIV-1 RNA dimerization assay*. HIV-1 RNA can form two different types of dimers *in vitro*, termed loose and tight dimers depending on their thermal stability that are correlated to the process of viral maturation after particle budding (for a review see (74)). Using an RNA fragment encompassing the first 615 nucleotides of HIV-1 genomic RNA, RNA dimerization was analyzed under two different electrophoresis conditions: (i) native conditions under which both loose and tight dimers are stable (Figure 6A) and (ii) semi-denaturing conditions in which only tight dimers are stable (Figure 6B) (47). Vif and Vif (95-192), both stimulated RNA dimerization in a concentration dependent manner (Figure 6A), with a dimerization yield of 64% and 79% at 1 µM for Vif and Vif (95-192), respectively (Figure 6C). This Vif-induced RNA dimer is a tight dimer, as it is still observed during electrophoresis under semi-denaturing conditions (Figure 6B). Interestingly, these two Vif proteins were also able to induce the formation of multimers of RNAs (Figure 6B). However, while increasing concentration of Vif (1-150) and Vif (1-97) progressively increased the dimerization yield from 10 to 45%, respectively, in native conditions (Figure 6A and 6C, left histogram), only RNA dimers obtained with Vif (1-97) marginally increased under semi-denaturing conditions (Figure 6B and 6C, right histogram). These results suggest that Vif (1-97) was mainly able to induce the formation of loose dimers, whereas Vif (1-150) presented an intermediate behavior (compare Figure 6A and 6B). Thus, as Vif and Vif (95-192) mimic the RNA chaperon activity of the HIV-1

NCp7 protein, our results suggest that the RNA chaperon activity of Vif mediated its C-terminal domain encompassing the Cullin 5 and Elongin C binding motifs as well as the PPLP oligomerization sequence.

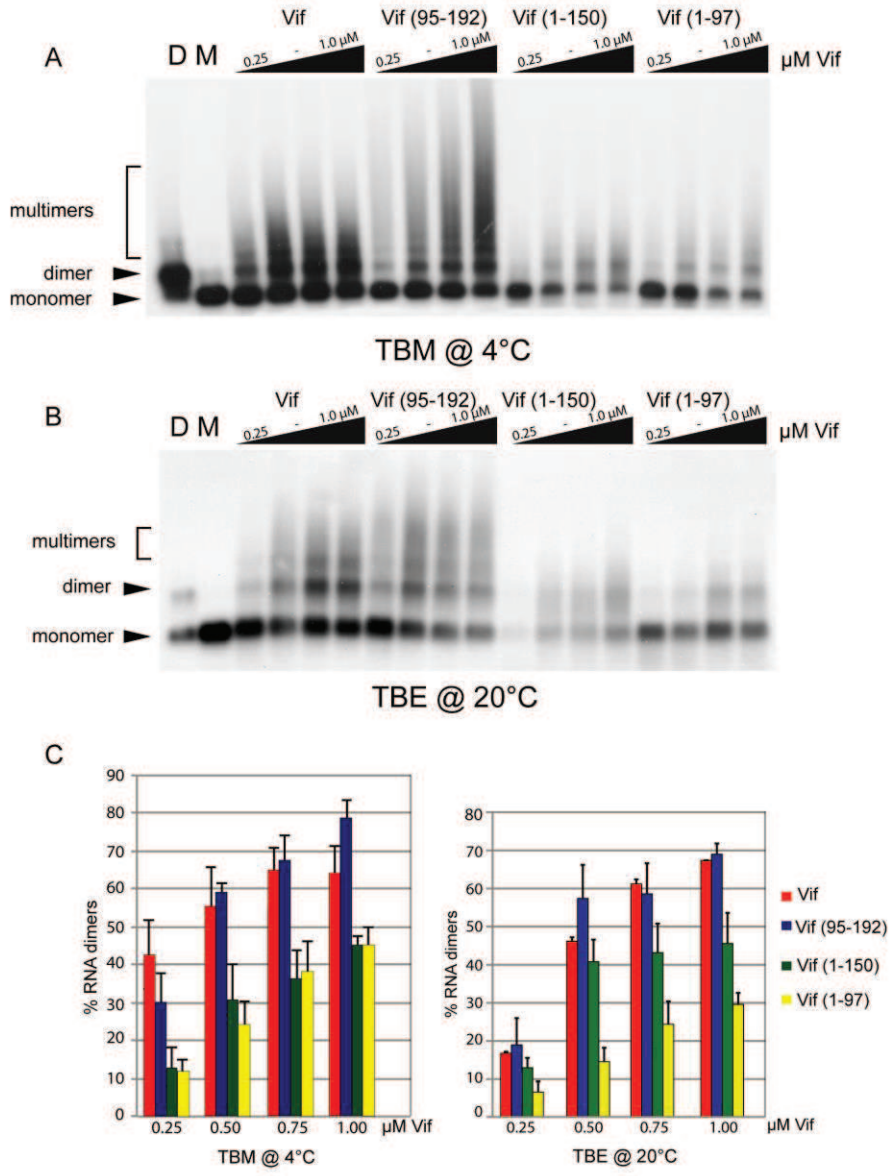

Figure 6. HIV-1 RNA dimerization induced by Vif and its domains. HIV RNA 1-615 was allowed to dimerize in the presence of increasing concentration of Vif , Vif (95-192), Vif (1-150), and Vif (1-97) (0.25, 0.5, 0.75 and 1 µM), and run on a 0.8% agarose gel in native (**A**), or semi-denaturing (**B**) conditions after protein removal. Lanes D and M correspond to control incubation of RNA in dimeric (D) or monomeric (M) buffers (see Material and Methods for composition) (**C)** Percentage of RNA dimer as a function of the concentration of Vif protein and its domain.

- *TAR(+)/TAR(-) annealing assay:* The annealing of the complementary TAR sequences is essential to achieve (-) strand strong stop DNA transfer, and amongst the various standard RNA chaperoning assays, the annealing of a TAR oligodeoxynucleotide (TAR+) to its complementary sequence (TAR-) has been used in many occasions (53,54). To identify the potential domain(s) of Vif involved in RNA chaperon activity, we compared the ability of Vif and its domains to promote the annealing of two complementary TAR sequences with that of NCp7, NC (12-53) (peptide 12-53 of NCp7) and Tat, two other RNA chaperon proteins. In the absence of protein, TAR(+)/TAR(-) annealing occurred at 65°C in high salt conditions in the positive control (Figure 7A, lanes 1). No TAR(+)/TAR(-) annealing was observed at 37°C in the negative control (Figure 7A, lane 2). Incubation with NCp7 or Tat at 37°C for 5 min favored TAR(+)/TAR(-) annealing at a protein concentration starting at 2.75 nM and 11 nM for NCp7 and Tat, corresponding to a protein to nucleotide molar ratio of 1/40 and 1/10, respectively (Figure 7A, lanes 3 to 10). Interestingly, in the presence of Vif, TAR(+)/TAR(-) annealing was also observed, but started at a lower protein to nucleotide molar ratio of 1/40 (Figure 7A, lanes 11-14), indicating that Vif annealing activity was slightly more efficient than that observed for NCp7 and Tat. Indeed, 22% of TAR-annealed complex were obtained at a 2.75 nM Vif concentration, while two-times less complex was obtained with the same concentration of NCp7 or Tat (Figure 7B). At a higher protein concentration (22 nM), this difference is lost between Vif and NCp7 (Figure 7B). As expected from previous studies (53,54,75), the NC12-53 peptide was found to be poorly active in TAR-annealing activity and other RNA chaperoning assays. Indeed, 70% of TAR annealed complex was obtained at 200 nM, whereas ten times less Vif protein is necessary to obtain this percentage (Figure 7B). Surprisingly, when we analyzed the truncated domains of Vif, we showed that all of them were able to stimulate TAR(-)/TAR(+) annealing at a level comparable to what was observed with Vif (Figure 7A). However, the Vif (95-192) domain seems to possess the highest annealing activity as 30% and 80% of TAR(-)/TAR(+) complex are formed at the lowest (2.75 µM) and highest (22 µM) concentration of Vif (95-192), respectively (Figure 7A & B, compare with Vif lanes 11 and 14). Taken together, these results indicate that Vif possesses a strong RNA chaperone activity that is mainly driven by its C-terminal domain.

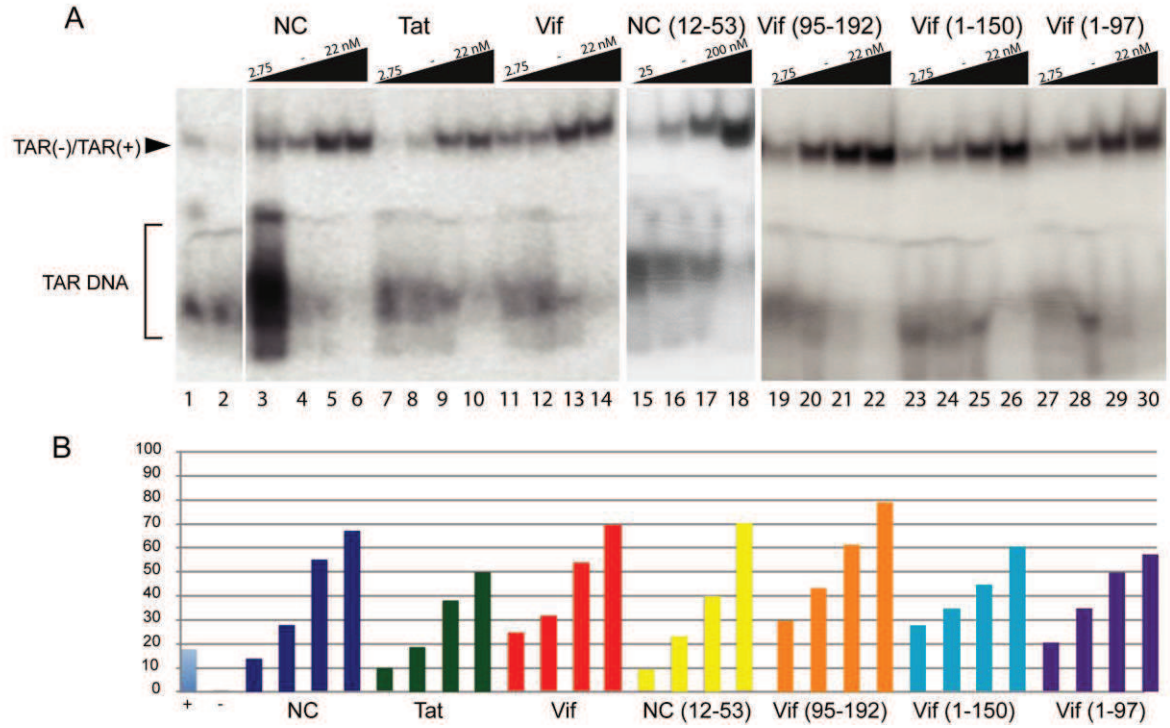

Figure 7. Stimulation of HIV-1 TAR(+)/TAR(-) DNA annealing by Vif and its domains. A) TAR(+) and ^{32}P-labeled TAR(-) DNA oligonucleotides were co-incubated in the presence of increasing concentrations of NCp7 (wild-type and fragment 12-53), Tat, and Vif (full-length and domains). The protein concentrations were 2.75, 5.50, 11 and 22 nM except for NC (12-53) for which the concentrations were 25, 50, 100 and 200 nM. In the absence of protein, double-stranded TAR DNA was formed upon incubation at 65°C for 30 min (Ct+, lanes 1) but not at 37°C (Ct-, lanes 2). TAR(+)/TAR(-) was annealed at 37°C for 5 min with HIV-1 NCp7 (protein/nt molar ratios of 1/40, 1/20, 1/10 and 1/5) (lanes 3-6), Tat (lanes 7-10), Vif (lanes 11-14), NC (12-53) (lanes 15-18), Vif (95-192) (lanes 19-22), Vif (1-150) (lanes 23-26), and Vif (1-97) (lanes 27-30). B) Percentage of TAR(+)/TAR(-) DNA complex as a function of the protein concentration.

DISCUSSION

In this paper, we investigated the RNA binding properties and chaperoning activities of HIV-1 Vif functional domains. First, using CD and NMR spectroscopies, we showed that the NTD of Vif, encompassing residues 1-97, is the most structured in solution, whereas the CTD (95-192) domain remains mainly unfolded either alone or within the full-length Vif. More strikingly, we showed that Vif (1-97), (1-150) and (95-192) conserved substantial RNA binding capacities. Actually, both the N- and CTD of Vif are able to bind with high affinity RNAs that were previously described as Vif preferential binding sites (45), as well as to $tRNA^{Lys}_3$. More precisely, the NTD has a

definite and specific binding site to the inside of the L-shape of $tRNA^{Lys}_{3,}$ whereas the fingerprint with the CTD is more diffused, most likely indicating a less specific binding. Interestingly, the CTD is responsible for the interaction with the T-arm of $tRNA^{Lys}_{3,}$ whereas the NTD of Vif is not able to bind this arm that needs to be annealed to the PBS region to promote efficient initiation of reverse transcription. Interestingly, NMR chemical shift mapping demonstrates that Vif and NCp7 share the same binding sites on $tRNA^{Lys}_{3}$ and could thus compete for $tRNA^{Lys}_{3}$ binding. Finally, we showed that RNA chaperone activities of Vif and NCp7 are mostly driven by their basic unfolded domains. In any case, Vif presented an annealing activity slightly more efficient than was observed for NCp7 and Tat proteins.

Using *in vitro* binding with poly(G)-conjugated beads, Zhang *et al*. (23) previously showed that a peptide from amino acids 1 to 64 of HIV-1 Vif possesses a strong RNA binding activity. Moreover, highly conserved amino acids are present in the N-terminus of Vif proteins from several primate lentivirus strains. Mutation of hydrophobic residues such as W11, Y30, and Y40 significantly decreased Vif RNA binding activity. In addition, it was showed that the C-terminus of Vif (156-192), which harbors many positive charged amino acids, has an RNA binding activity as well (23). Here, our analysis clearly demonstrates that the CTD of Vif (domain 95-192) is also able to bind RNAs with high affinity, and that the RNA chaperone activity is mainly driven by this domain. Vif (1-97) contains 11 arginines and 5 lysines compared to 4 arginines and 9 lysines for Vif (95-192). Therefore, in our design, the NTD of Vif harbors a positive global charge of +8 compared to +6 for the CTD of Vif. However, the main difference between these two domains lies in the feature that the CTD of Vif is unfolded and thus all the positive charges are accessible. The interactions between Vif (95-192) and nucleic acids are then mainly driven by electrostatic interactions and are most likely non-specific. Moreover, it has been demonstrated that Vif proteins from several strains of HIV-1, HIV-2, and SIV are composed of heterogeneous sequences, yet they can functionally complement each other (76). Actually, the unfolded characteristic of the CTD is conserved for Vif from HIV-2 and SIV (C. Tisné, unpublished results). Moreover, while the sequences of Vif from HIV-1, HIV-2 and SIV strains are highly divergent in the CTD, we still observe a high number of arginines and lysines in the CTD of Vif (10-17 according to the strain), and thus a conservation of a significant net positive charge.

Altogether, it seems that the NTD of Vif binds specifically some RNAs whereas the CTD, outside the HCCH and SOCS-box domains, possesses the ability to bind RNAs in a non-specific manner allowing it to display a strong RNA chaperone activity. Therefore, the basicity and unfolded characteristics of the CTD of Vif in primate lentiviruses are probably of importance to conserve RNA binding and RNA chaperone activities. Several RNA chaperone proteins share the same structural properties. Indeed, it was found that the prevalence of functional regions in RNA chaperones without a well-defined 3D structure is very high, and such intrinsically disordered domains were proposed to support chaperone activity (77,78).

At this point, comparing NCp7 and Vif seems very interesting. Indeed, NCp7 is the most efficient RNA chaperone protein encountered in HIV (52). It has 15 basic residues, lysine or arginine, positively charged at physiological pH. These charges are responsible for an electrostatic, usually unspecific, interaction with nucleic acids, allowing the protein to completely cover the genome in virions (79-83). However, eleven NCp7-binding sites were identified on genomic RNA inside native virions (84), and all sites feature a general consensus characterized by a G-rich single-stranded sequence flanked by stable helices, in agreement with previous NMR studies. Indeed, structural studies (85-88) showed that the CCHC-like zinc knuckles of NCp7 contain hydrophobic residues forming an ideal surface for specific recognition of guanine residues located in RNA loops. Regarding the RNA chaperone activity, the N-terminal basic residues of NCp7 are responsible for some of the activity, like annealing and aggregation of nucleic acids, whereas the zinc-fingers are responsible for the destabilization of nucleic acids (89-97). Indeed, the efficiency of the NCp7 NTD to promote annealing of complementary RNA is exemplified in our experiments by comparing the annealing activity of NCp7 and NC (12-53) lacking the N-terminal part (Figure 7). Actually, we observed that NC (12-53) lost its annealing activity. The nature of this effect is essentially electrostatic, due to the charge complementarities between nucleic acids backbone and the positively charged residues. Interestingly, the basic and unfolded CTD of Vif clearly drives nucleic acids annealing activity of the protein. More generally, many proteins do not have well-ordered structures in their functional parts, representing hybrids that possess both ordered and disordered regions. Coherently, the highly structured Vif NTD is responsible for a specific

interaction with nucleic acids, and similarly NCp7 can specifically bind to RNA *via* its zinc-knuckles (Vuilleumier, 1999 #94).

Vif is known to promote the hybridization between viral RNA and $tRNA^{Lys}_3$ generating a functional complex, even though Vif seems to be less efficient than NCp7 (47). When both Vif and NCp7 are present, Vif inhibits NCp7-assisted hybridization of $tRNA^{Lys}_3$ to the viral RNA. Here, we showed that Vif and NCp7 share the same binding site on $tRNA^{Lys}_3$ (Figure 5). This result leads to the conclusion that Vif and NCp7 are probably in competition for the same binding sites. It might be that the inhibiting effect of Vif would be probably reduced during the last steps of virions assembly since only a small amount of Vif is packaged into viral particles (14,98), suggesting that Vif could act as a temporal regulator of NCp7 activities (47).

Disorder is unevenly distributed within partially unfolded proteins and is typically more common at protein termini. Disordered tails are usually engaged in a wide range of functions, some of which are unique for termini, and cannot be found in other disordered parts of a protein (for a recent review (99)). Vif and NCp7 present disordered C- and N-terminal tails, respectively, and in both cases, these tails are responsible for non-specific RNA annealing activity. Moreover, in the case of Vif, its CTD (95-192) is involved in interaction with several partners to recruit an E3 ubiquitin ligase namely, EloC through its SOCS-box domain and Cul5 *via* the HCCH domain. Recently, it was shown that human E3 ubiquitin ligases also contain disordered regions that undergo induced folding (or mutual induced folding) in the presence of the partner (100). In this view, those structural disordered domains in E3 ligases behave as substrate/adaptor binding domains allowing the mechanism of ubiquitin transfer by long-range conformational transitions. The conserved disorder of the CTD of Vif in primate lentiviruses could thus have a crucial role not only to recruit the E3 ubiquitin ligase complex but also to induce mutual folding of binding partners according to Vif different roles during the viral life cycle.

ACKNOWLEDGEMENTS

We are grateful to Drs. Roland Marquet and Redmond Smyth for critical reading of the manuscript. We thank Dr. Jean-Luc Darlix (UMR 7213 CNRS, Université de Strasbourg, France) for the gift of TAR(+)/TAR(-) system. This work was supported

by grants from the French National Agency for Research on AIDS and Viral Hepatitis (ANRS) to CT, JCP and SB, and by doctoral fellowships from ANRS to SG.

REFERENCES

1. Malim, M.H. and Bieniasz, P.D. (2012) HIV Restriction Factors and Mechanisms of Evasion. *Cold Spring Harb Perspect Med*, **2**, a006940.

2. Harris, R.S., Hultquist, J.F. and Evans, D.T. (2012) The restriction factors of human immunodeficiency virus. *J Biol Chem*, **287**, 40875-40883.

3. Sheehy, A.M., Gaddis, N.C., Choi, J.D. and Malim, M.H. (2002) Isolation of a human gene that inhibits HIV-1 infection and is suppressed by the viral Vif protein. *Nature*, **418**, 646-650.

4. Mangeat, B., Turelli, P., Caron, G., Friedli, M., Perrin, L. and Trono, D. (2003) Broad antiretroviral defence by human APOBEC3G through lethal editing of nascent reverse transcripts. *Nature*, **424**, 99-103.

5. Mariani, R., Chen, D., Schrofelbauer, B., Navarro, F., Konig, R., Bollman, B., Munk, C., Nymark-McMahon, H. and Landau, N.R. (2003) Species-specific exclusion of APOBEC3G from HIV-1 virions by Vif. *Cell*, **114**, 21-31.

6. Bishop, K.N., Holmes, R.K. and Malim, M.H. (2006) Antiviral potency of APOBEC proteins does not correlate with cytidine deamination. *J Virol*, **80**, 8450-8458.

7. Marin, M., Rose, K.M., Kozak, S.L. and Kabat, D. (2003) HIV-1 Vif protein binds the editing enzyme APOBEC3G and induces its degradation. *Nat Med*, **9**, 1398-1403.

8. Mehle, A., Goncalves, J., Santa-Marta, M., McPike, M. and Gabuzda, D. (2004) Phosphorylation of a novel SOCS-box regulates assembly of the HIV-1 Vif-Cul5 complex that promotes APOBEC3G degradation. *Genes Dev*, **18**, 2861-2866.

9. Yu, X., Yu, Y., Liu, B., Luo, K., Kong, W., Mao, P. and Yu, X.F. (2003) Induction of APOBEC3G ubiquitination and degradation by an HIV-1 Vif-Cul5-SCF complex. *Science*, **302**, 1056-1060.

10. Jager, S., Kim, D.Y., Hultquist, J.F., Shindo, K., Larue, R.S., Kwon, E., Li, M., Anderson, B.D., Yen, L., Stanley, D. *et al.* (2011) Vif hijacks CBF-beta to degrade APOBEC3G and promote HIV-1 infection. *Nature*.

11. Zhang, W., Du, J., Evans, S.L., Yu, Y. and Yu, X.F. (2011) T-cell differentiation factor CBF-beta regulates HIV-1 Vif-mediated evasion of host restriction. *Nature*.

12. Hultquist, J.F., Binka, M., LaRue, R.S., Simon, V. and Harris, R.S. (2012) Vif proteins of human and simian immunodeficiency viruses require cellular CBFbeta to degrade APOBEC3 restriction factors. *J Virol*, **86**, 2874-2877.

13. Mercenne, G., Bernacchi, S., Richer, D., Bec, G., Henriet, S., Paillart, J.C. and Marquet, R. (2010) HIV-1 Vif binds to APOBEC3G mRNA and inhibits its translation. *Nucleic Acids Res*, **38**, 633-646.

14. Kao, S., Khan, M.A., Miyagi, E., Plishka, R., Buckler-White, A. and Strebel, K. (2003) The human immunodeficiency virus type 1 Vif protein reduces intracellular expression and inhibits packaging of APOBEC3G (CEM15), a cellular inhibitor of virus infectivity. *J Virol*, **77**, 11398-11407.

15. Stopak, K., de Noronha, C., Yonemoto, W. and Greene, W.C. (2003) HIV-1 Vif blocks the antiviral activity of APOBEC3G by impairing both its translation and intracellular stability. *Mol Cell*, **12**, 591-601.

16. Opi, S., Kao, S., Goila-Gaur, R., Khan, M.A., Miyagi, E., Takeuchi, H. and Strebel, K. (2007) Human immunodeficiency virus type 1 Vif inhibits packaging and antiviral activity of a degradation-resistant APOBEC3G variant. *J Virol*, **81**, 8236-8246.

17. Goila-Gaur, R. and Strebel, K. (2008) HIV-1 Vif, APOBEC, and intrinsic immunity. *Retrovirology*, **5**, 51.

18. Henriet, S., Mercenne, G., Bernacchi, S., Paillart, J.C. and Marquet, R. (2009) Tumultuous relationship between the human immunodeficiency virus type 1 viral infectivity factor (Vif) and the human APOBEC-3G and APOBEC-3F restriction factors. *Microbiol Mol Biol Rev*, **73**, 211-232.

19. Zhang, W., Chen, G., Niewiadomska, A.M., Xu, R. and Yu, X.F. (2008) Distinct Determinants in HIV-1 Vif and Human APOBEC3 Proteins Are Required for the Suppression of Diverse Host Anti-Viral Proteins. *PLoS ONE*, **3**, e3963.

20. Pery, E., Rajendran, K.S., Brazier, A.J. and Gabuzda, D. (2009) Regulation of APOBEC3 proteins by a novel YXXL motif in human immunodeficiency virus type 1 Vif and simian immunodeficiency virus SIVagm Vif. *J Virol*, **83**, 2374-2381.

21. Binka, M., Ooms, M., Steward, M. and Simon, V. (2012) The Activity Spectrum of Vif from Multiple HIV-1 Subtypes against APOBEC3G, APOBEC3F, and APOBEC3H. *J Virol*, **86**, 49-59.

22. Zhen, A., Wang, T., Zhao, K., Xiong, Y. and Yu, X.F. (2010) A single amino acid difference in human APOBEC3H variants determines HIV-1 Vif sensitivity. *J Virol*, **84**, 1902-1911.

23. Zhang, H., Pomerantz, R.J., Dornadula, G. and Sun, Y. (2000) Human immunodeficiency virus type 1 Vif protein is an integral component of an mRNP complex of viral RNA and could be involved in the viral RNA folding and packaging process. *J Virol*, **74**, 8252-8261.

24. Khan, M.A., Aberham, C., Kao, S., Akari, H., Gorelick, R., Bour, S. and Strebel, K. (2001) Human immunodeficiency virus type 1 Vif protein is packaged into the nucleoprotein complex through an interaction with viral genomic RNA. *J Virol*, **75**, 7252-7265.

25. Hultquist, J.F., Binka, M., Larue, R.S., Simon, V. and Harris, R.S. (2011) Vif Proteins of Human and Simian Immunodeficiency Viruses Require Cellular CBFbeta to Degrade APOBEC3 Restriction Factors. *J Virol*.

26. Mehle, A., Thomas, E.R., Rajendran, K.S. and Gabuzda, D. (2006) A zinc-binding region in Vif binds Cul5 and determines cullin selection. *J Biol Chem*, **281**, 17259-17265.

27. Xiao, Z., Ehrlich, E., Luo, K., Xiong, Y. and Yu, X.F. (2007) Zinc chelation inhibits HIV Vif activity and liberates antiviral function of the cytidine deaminase APOBEC3G. *Faseb J*, **21**, 217-222.

28. Yu, Y., Xiao, Z., Ehrlich, E.S., Yu, X. and Yu, X.F. (2004) Selective assembly of HIV-1 Vif-Cul5-ElonginB-ElonginC E3 ubiquitin ligase complex through a novel SOCS box and upstream cysteines. *Genes & development*, **18**, 2867-2872.

29. Stanley, B.J., Ehrlich, E.S., Short, L., Yu, Y., Xiao, Z., Yu, X.F. and Xiong, Y. (2008) Structural insight into the human immunodeficiency virus Vif SOCS box and its role in human E3 ubiquitin ligase assembly. *J Virol*, **82**, 8656-8663.

30. Batisse, J., Guerrero, S., Bernacchi, S., Sleiman, D., Gabus, C., Darlix, J.L., Marquet, R., Tisne, C. and Paillart, J.C. (2012) The role of Vif oligomerization and RNA chaperone activity in HIV-1 replication. *Virus Res*, **169**, 361-376.

31. Yang, S., Sun, Y. and Zhang, H. (2001) The multimerization of human immunodeficiency virus type I Vif protein: a requirement for Vif function in the viral life cycle. *J Biol Chem*, **276**, 4889-4893.

32. Yang, B., Gao, L., Li, L., Lu, Z., Fan, X., Patel, C.A., Pomerantz, R.J., DuBois, G.C. and Zhang, H. (2003) Potent Suppression of Viral Infectivity by the Peptides That Inhibit Multimerization of Human Immunodeficiency Virus Type 1 (HIV-1) Vif Proteins. *J Biol Chem*, **278**, 6596-6602.

33. Hassaine, G., Courcoul, M., Bessou, G., Barthalay, Y., Picard, C., Olive, D., Collette, Y., Vigne, R. and Decroly, E. (2001) The tyrosine kinase Hck is an inhibitor of HIV-1 replication counteracted by the viral vif protein. *J Biol Chem*, **276**, 16885-16893.

34. Douaisi, M., Dussart, S., Courcoul, M., Bessou, G., Lerner, E.C., Decroly, E. and Vigne, R. (2005) The tyrosine kinases Fyn and Hck favor the recruitment of tyrosine-phosphorylated APOBEC3G into vif-defective HIV-1 particles. *Biochemical and biophysical research communications*, **329**, 917-924.

35. Bouyac, M., Courcoul, M., Bertoia, G., Baudat, Y., Gabuzda, D., Blanc, D., Chazal, N., Boulanger, P., Sire, J., Vigne, R. *et al.* (1997) Human immunodeficiency virus type 1 Vif protein binds to the Pr55Gag precursor. *J Virol*, **71**, 9358-9365.

36. Simon, J.H., Carpenter, E.A., Fouchier, R.A. and Malim, M.H. (1999) Vif and the p55(Gag) polyprotein of human immunodeficiency virus type 1 are present in colocalizing membrane-free cytoplasmic complexes. *J Virol*, **73**, 2667-2674.

37. Syed, F. and McCrae, M.A. (2009) Interactions in vivo between the Vif protein of HIV-1 and the precursor (Pr55(GAG)) of the virion nucleocapsid proteins. *Arch Virol*, **154**, 1797-1805.

38. Goncalves, J., Shi, B., Yang, X. and Gabuzda, D. (1995) Biological activity of human immunodeficiency virus type 1 Vif requires membrane targeting by C-terminal basic domains. *J Virol*, **69**, 7196-7204.

39. Kataropoulou, A., Bovolenta, C., Belfiore, A., Trabatti, S., Garbelli, A., Porcellini, S., Lupo, R. and Maga, G. (2009) Mutational analysis of the HIV-1 auxiliary protein Vif identifies independent domains important for the physical and functional interaction with HIV-1 reverse transcriptase. *Nucleic Acids Res*, **37**, 3660-3669.

40. Auclair, J.R., Green, K.M., Shandilya, S., Evans, J.E., Somasundaran, M. and Schiffer, C.A. (2007) Mass spectrometry analysis of HIV-1 Vif reveals an increase in ordered structure upon oligomerization in regions necessary for viral infectivity. *Proteins*, **69**, 270-284.

41. Marcsisin, S.R., Narute, P.S., Emert-Sedlak, L.A., Kloczewiak, M., Smithgall, T.E. and Engen, J.R. (2011) On the solution conformation and dynamics of the HIV-1 viral infectivity factor. *Journal of molecular biology*, **410**, 1008-1022.

42. Reingewertz, T.H., Benyamini, H., Lebendiker, M., Shalev, D.E. and Friedler, A. (2009) The C-terminal domain of the HIV-1 Vif protein is natively unfolded in its unbound state. *Protein Eng Des Sel*, **22**, 281-287.

43. Reingewertz, T.H., Shalev, D.E. and Friedler, A. (2010) Structural disorder in the HIV-1 Vif protein and interaction-dependent gain of structure. *Protein and peptide letters*, **17**, 988-998.

44. Marcsisin, S.R. and Engen, J.R. (2010) Molecular insight into the conformational dynamics of the Elongin BC complex and its interaction with HIV-1 Vif. *Journal of molecular biology*, **402**, 892-904.

45. Bernacchi, S., Henriet, S., Dumas, P., Paillart, J.C. and Marquet, R. (2007) RNA and DNA binding properties of HIV-1 Vif protein: a fluorescence study. *J Biol Chem*, **282**, 26361-26368.

46. Henriet, S., Richer, D., Bernacchi, S., Decroly, E., Vigne, R., Ehresmann, B., Ehresmann, C., Paillart, J.C. and Marquet, R. (2005) Cooperative and specific binding of Vif to the 5' region of HIV-1 genomic RNA. *Journal of molecular biology*, **354**, 55-72.

47. Henriet, S., Sinck, L., Bec, G., Gorelick, R.J., Marquet, R. and Paillart, J.C. (2007) Vif is a RNA chaperone that could temporally regulate RNA dimerization and the early steps of HIV-1 reverse transcription. *Nucleic Acids Res*, **35**, 5141-5153.

48. Bernacchi, S., Mercenne, G., Tournaire, C., Marquet, R. and Paillart, J.C. (2011) Importance of the proline-rich multimerization domain on the oligomerization and nucleic acid binding properties of HIV-1 Vif. *Nucleic Acids Res*, **39**, 2404-2415.

49. Freisz, S., Mezher, J., Hafirassou, L., Wolff, P., Nomine, Y., Romier, C., Dumas, P. and Ennifar, E. (2012) Sequence and structure requirements for specific recognition of HIV-1 TAR and DIS RNA by the HIV-1 Vif protein. *RNA Biol*, **9**, 966-977.

50. Dettenhofer, M., Cen, S., Carlson, B.A., Kleiman, L. and Yu, X.F. (2000) Association of human immunodeficiency virus type 1 Vif with RNA and its role in reverse transcription. *J Virol*, **74**, 8938-8945.

51. Ivanyi-Nagy, R., Davidovic, L., Khandjian, E.W. and Darlix, J.L. (2005) Disordered RNA chaperone proteins: from functions to disease. *Cell Mol Life Sci*, **62**, 1409-1417.

52. Darlix, J.L., Godet, J., Ivanyi-Nagy, R., Fosse, P., Mauffret, O. and Mely, Y. (2011) Flexible nature and specific functions of the HIV-1 nucleocapsid protein. *Journal of molecular biology*, **410**, 565-581.

53. Kuciak, M., Gabus, C., Ivanyi-Nagy, R., Semrad, K., Storchak, R., Chaloin, O., Muller, S., Mely, Y. and Darlix, J.L. (2008) The HIV-1 transcriptional activator Tat has potent nucleic acid chaperoning activities in vitro. *Nucleic acids research*, **36**, 3389-3400.

54. Gabus, C., Mazroui, R., Tremblay, S., Khandjian, E.W. and Darlix, J.L. (2004) The fragile X mental retardation protein has nucleic acid chaperone properties. *Nucleic acids research*, **32**, 2129-2137.

55. Paillart, J.C., Skripkin, E., Ehresmann, B., Ehresmann, C. and Marquet, R. (2002) In vitro evidence for a long range pseudoknot in the 5'-untranslated and matrix coding regions of HIV-1 genomic RNA. *The Journal of biological chemistry*, **277**, 5995-6004.

56. Marquet, R., Baudin, F., Gabus, C., Darlix, J.L., Mougel, M., Ehresmann, C. and Ehresmann, B. (1991) Dimerization of human immunodeficiency virus (type 1) RNA: stimulation by cations and possible mechanism. *Nucleic Acids Res.*, **19**, 2349-2357.

57. Tisne, C., Rigourd, M., Marquet, R., Ehresmann, C. and Dardel, F. (2000) NMR and biochemical characterization of recombinant human tRNA(Lys)3 expressed in Escherichia coli: identification of posttranscriptional nucleotide modifications required for efficient initiation of HIV-1 reverse transcription. *Rna*, **6**, 1403-1412.

58. Dardel, F. (1994) MC-Fit: using Monte-Carlo methods to get accurate confidence limits on enzyme parameters. *Comput Appl Biosci*, **10**, 273-275.

59. Piotto, M., Saudek, V. and Sklenar, V. (1992) Gradient-tailored excitation for single-quantum NMR spectroscopy of aqueous solutions. *Journal of biomolecular NMR*, **2**, 661-665.

60. Pervushin, K., Riek, R., Wider, G. and Wuthrich, K. (1997) Attenuated T2 relaxation by mutual cancellation of dipole-dipole coupling and chemical shift anisotropy indicates an avenue to NMR structures of very large biological macromolecules in solution. *Proceedings of the National Academy of Sciences of the United States of America*, **94**, 12366-12371.

61. Weigelt, J. (1998) Single scan, sensitivity- and gradient-enhanced TROSY for multidimensional NMR experiments. *J. Am. Chem. Soc.*, **120**, 10778-10779.

62. Kuciak, M., Gabus, C., Ivanyi-Nagy, R., Semrad, K., Storchak, R., Chaloin, O., Muller, S., Mely, Y. and Darlix, J.L. (2008) The HIV-1 transcriptional activator Tat has potent nucleic acid chaperoning activities in vitro. *Nucleic Acids Res*, **36**, 3389-3400.

63. Ivanyi-Nagy, R., Lavergne, J.P., Gabus, C., Ficheux, D. and Darlix, J.L. (2008) RNA chaperoning and intrinsic disorder in the core proteins of Flaviviridae. *Nucleic acids research*, **36**, 712-725.

64. Batisse, J., Guerrero, S., Bernacchi, S., Sleiman, D., Gabus, C., Darlix, J.L., Marquet, R., Tisne, C. and Paillart, J.C. (2012) The role of Vif oligomerization and RNA chaperone activity in HIV-1 replication. *Virus Res.*, **169**, 361-376.

65. Huvent, I., Hong, S.S., Fournier, C., Gay, B., Tournier, J., Carriere, C., Courcoul, M., Vigne, R., Spire, B. and Boulanger, P. (1998) Interaction and co-encapsidation of human immunodeficiency virus type 1 Gag and Vif recombinant proteins. *J Gen Virol*, **79 (Pt 5)**, 1069-1081.

66. Khan, M.A., Akari, H., Kao, S., Aberham, C., Davis, D., Buckler-White, A. and Strebel, K. (2002) Intravirion processing of the human immunodeficiency virus type 1 Vif protein by the viral protease may be correlated with Vif function. *J Virol*, **76**, 9112-9123.

67. Techtmann, S.M., Ghirlando, R., Kao, S., Strebel, K. and Maynard, E.L. (2012) Hydrodynamic and functional analysis of HIV-1 Vif oligomerization. *Biochemistry*, **51**, 2078-2086.

68. Balaji, S., Kalpana, R. and Shapshak, P. (2006) Paradigm development: comparative and predictive 3D modeling of HIV-1 Virion Infectivity Factor (Vif). *Bioinformation*, **1**, 290-309.

69. Barraud, P., Paillart, J.C., Marquet, R. and Tisne, C. (2008) Advances in the structural understanding of Vif proteins. *Curr HIV Res*, **6**, 91-99.

70. Lv, W., Liu, Z., Jin, H., Yu, X. and Zhang, L. (2007) Three-dimensional structure of HIV-1 VIF constructed by comparative modeling and the function characterization analyzed by molecular dynamics simulation. *Org Biomol Chem*, **5**, 617-626.

71. Sleiman, D., Goldschmidt, V., Barraud, P., Marquet, R., Paillart, J.C. and Tisne, C. (2012) Initiation of HIV-1 reverse transcription and functional role of nucleocapsid-mediated tRNA/viral genome interactions. *Virus Res*, **169**, 324-339.

72. Tisne, C., Roques, B.P. and Dardel, F. (2004) The annealing mechanism of HIV-1 reverse transcription primer onto the viral genome. *The Journal of biological chemistry*, **279**, 3588-3595.

73. Tisne, C., Roques, B.P. and Dardel, F. (2001) Heteronuclear NMR studies of the interaction of tRNA(Lys)3 with HIV-1 nucleocapsid protein. *Journal of molecular biology*, **306**, 443-454.

74. Paillart, J.C., Dettenhofer, M., Yu, X.F., Ehresmann, C., Ehresmann, B. and Marquet, R. (2004) First snapshots of the HIV-1 RNA structure in infected cells and in virions. *J Biol Chem*, **279**, 48397-48403.

75. Bampi, C., Bibillo, A., Wendeler, M., Divita, G., Gorelick, R.J., Le Grice, S.F. and Darlix, J.L. (2006) Nucleotide excision repair and template-independent addition by HIV-1 reverse transcriptase in the presence of nucleocapsid protein. *The Journal of biological chemistry*, **281**, 11736-11743.

76. Simon, J.H., Southerling, T.E., Peterson, J.C., Meyer, B.E. and Malim, M.H. (1995) Complementation of vif-defective human immunodeficiency virus type 1 by primate, but not nonprimate, lentivirus vif genes. *J Virol*, **69**, 4166-4172.

77. Tompa, P. (2012) Intrinsically disordered proteins: a 10-year recap. *Trends Biochem Sci*, **37**, 509-516.

78. Kovacs, D. and Tompa, P. (2012) Diverse functional manifestations of intrinsic structural disorder in molecular chaperones. *Biochem Soc Trans*, **40**, 963-968.

79. Fisher, R.J., Rein, A., Fivash, M., Urbaneja, M.A., Casas-Finet, J.R., Medaglia, M. and Henderson, L.E. (1998) Sequence-specific binding of human immunodeficiency virus type 1 nucleocapsid protein to short oligonucleotides. *J Virol*, **72**, 1902-1909.

80. Henderson, L.E., Bowers, M.A., Sowder, R.C., 2nd, Serabyn, S.A., Johnson, D.G., Bess, J.W., Jr., Arthur, L.O., Bryant, D.K. and Fenselau, C. (1992) Gag proteins of the highly replicative MN strain of human immunodeficiency virus type 1: posttranslational modifications, proteolytic processings, and complete amino acid sequences. *J Virol*, **66**, 1856-1865.

81. Karpel, R.L., Henderson, L.E. and Oroszlan, S. (1987) Interactions of retroviral structural proteins with single-stranded nucleic acids. *J Biol Chem*, **262**, 4961-4967.

82. Khan, R. and Giedroc, D.P. (1994) Nucleic acid binding properties of recombinant Zn2 HIV-1 nucleocapsid protein are modulated by COOH-terminal processing. *J Biol Chem*, **269**, 22538-22546.

83. You, J.C. and McHenry, C.S. (1993) HIV nucleocapsid protein. Expression in Escherichia coli, purification, and characterization. *J Biol Chem*, **268**, 16519-16527.

84. Wilkinson, K.A., Gorelick, R.J., Vasa, S.M., Guex, N., Rein, A., Mathews, D.H., Giddings, M.C. and Weeks, K.M. (2008) High-throughput SHAPE analysis reveals

structures in HIV-1 genomic RNA strongly conserved across distinct biological states. *PLoS biology*, **6**, e96.

85. Amarasinghe, G.K., De Guzman, R.N., Turner, R.B., Chancellor, K.J., Wu, Z.R. and Summers, M.F. (2000) NMR structure of the HIV-1 nucleocapsid protein bound to stem-loop SL2 of the psi-RNA packaging signal. Implications for genome recognition. *Journal of molecular biology*, **301**, 491-511.

86. Bazzi, A., Zargarian, L., Chaminade, F., Boudier, C., De Rocquigny, H., Rene, B., Mely, Y., Fosse, P. and Mauffret, O. (2011) Structural insights into the cTAR DNA recognition by the HIV-1 nucleocapsid protein: role of sugar deoxyriboses in the binding polarity of NC. *Nucleic Acids Res*, **39**, 3903-3916.

87. Bourbigot, S., Ramalanjaona, N., Boudier, C., Salgado, G.F., Roques, B.P., Mely, Y., Bouaziz, S. and Morellet, N. (2008) How the HIV-1 nucleocapsid protein binds and destabilises the (-)primer binding site during reverse transcription. *Journal of molecular biology*, **383**, 1112-1128.

88. De Guzman, R.N., Wu, Z.R., Stalling, C.C., Pappalardo, L., Borer, P.N. and Summers, M.F. (1998) Structure of the HIV-1 nucleocapsid protein bound to the SL3 psi-RNA recognition element. *Science*, **279**, 384-388.

89. Williams, M.C., Gorelick, R.J. and Musier-Forsyth, K. (2002) Specific zinc-finger architecture required for HIV-1 nucleocapsid protein's nucleic acid chaperone function. *Proceedings of the National Academy of Sciences of the United States of America*, **99**, 8614-8619.

90. Williams, M.C., Rouzina, I., Wenner, J.R., Gorelick, R.J., Musier-Forsyth, K. and Bloomfield, V.A. (2001) Mechanism for nucleic acid chaperone activity of HIV-1 nucleocapsid protein revealed by single molecule stretching. *Proceedings of the National Academy of Sciences of the United States of America*, **98**, 6121-6126.

91. Narayanan, N., Gorelick, R.J. and DeStefano, J.J. (2006) Structure/function mapping of amino acids in the N-terminal zinc finger of the human immunodeficiency virus type 1 nucleocapsid protein: residues responsible for nucleic acid helix destabilizing activity. *Biochemistry*, **45**, 12617-12628.

92. Cruceanu, M., Gorelick, R.J., Musier-Forsyth, K., Rouzina, I. and Williams, M.C. (2006) Rapid kinetics of protein-nucleic acid interaction is a major component of HIV-1 nucleocapsid protein's nucleic acid chaperone function. *Journal of molecular biology*, **363**, 867-877.

93. Urbaneja, M.A., Wu, M., Casas-Finet, J.R. and Karpel, R.L. (2002) HIV-1 nucleocapsid protein as a nucleic acid chaperone: spectroscopic study of its helix-destabilizing properties, structural binding specificity, and annealing activity. *Journal of molecular biology*, **318**, 749-764.

94. Le Cam, E., Coulaud, D., Delain, E., Petitjean, P., Roques, B.P., Gerard, D., Stoylova, E., Vuilleumier, C., Stoylov, S.P. and Mely, Y. (1998) Properties and growth mechanism of the ordered aggregation of a model RNA by the HIV-1 nucleocapsid protein: an electron microscopy investigation. *Biopolymers*, **45**, 217-229.

95. Stoylov, S.P., Vuilleumier, C., Stoylova, E., De Rocquigny, H., Roques, B.P., Gerard, D. and Mely, Y. (1997) Ordered aggregation of ribonucleic acids by the human immunodeficiency virus type 1 nucleocapsid protein. *Biopolymers*, **41**, 301-312.

96. Bernacchi, S., Stoylov, S., Piemont, E., Ficheux, D., Roques, B.P., Darlix, J.L. and Mely, Y. (2002) HIV-1 nucleocapsid protein activates transient melting of least stable parts of the secondary structure of TAR and its complementary sequence. *Journal of molecular biology*, **317**, 385-399.

97. Guo, J., Wu, T., Anderson, J., Kane, B.F., Johnson, D.G., Gorelick, R.J., Henderson, L.E. and Levin, J.G. (2000) Zinc finger structures in the human immunodeficiency virus type 1 nucleocapsid protein facilitate efficient minus- and plus-strand transfer. *J Virol*, **74**, 8980-8988.

98. Camaur, D. and Trono, D. (1996) Characterization of human immunodeficiency virus type 1 Vif particle incorporation. *J Virol*, **70**, 6106-6111.

99. Uversky, V.N. (2013) The most important thing is the tail: Multitudinous functionalities of intrinsically disordered protein termini. *FEBS Lett*, **587**, 1891-1901.

100. Bhowmick, P., Pancsa, R., Guharoy, M. and Tompa, P. (2013) Functional diversity and structural disorder in the human ubiquitination pathway. *PloS one*, **8**, e65443.

Supplementary Tables

Supplementary Table 1. Prediction of Vif disordered domain (HIV-1 HXB2 isolate) according to (1) www.**disprot**.org , (2) www.bioinf.cs.ucl.ac.uk/**disopred** , (3) www.**iupred**.enzim.hu , (4) www.**globplot**.embl.de , (5) www.**protein**.cribi.unipd.it/**spritz** , (6) www.genomics.eu.org/spip/PreLink, (7) www.sbc.su.se/~maccallr/disorder, (8) www.bip.weizmann.ac.il/fldbin/findex, (9) www.strubi.ox.ac.uk/**RONN**/. Predicted disordered residus are indicated in red.

Residue number / programme	0 20 40 60 80 100 120 140 160 180 192
Disprot[1]	
Disopred[2]	
Iupred[3]	
Globplot[4]	
Spritz[5]	
Prelink[6]	
Drippred[7]	
Foldindex[8]	
RONN[9]	

Supplementary Table 2. Analysis of the CD spectra of Vif and its domain. The data were fit using the K2D software http://www.embl.de/~andrade/k2d.html {Andrade, 1993 #773}. The percentage of the secondary structure elements calculated from the Vif secondary structure predicted by PSIPRED http://bioinf.cs.ucl.ac.uk/psipred/ is given between parenthesis.

Secondary structure / Proteins	**α-helix**	**β-strands**	**Random**
Vif	15% (22%)	33% (26%)	52% (52%)
Vif (1-150)	2% (26%)	51% (31%)	47% (43%)
Vif (1-97)	25% (14%)	43% (45%)	32% (41%)
Vif (95-192)	20% (31%)	15% (5%)	65% (63%)

Supplementary Figures

Supplementary Figure 1. Circular dichroism spectra of Vif and its domains.

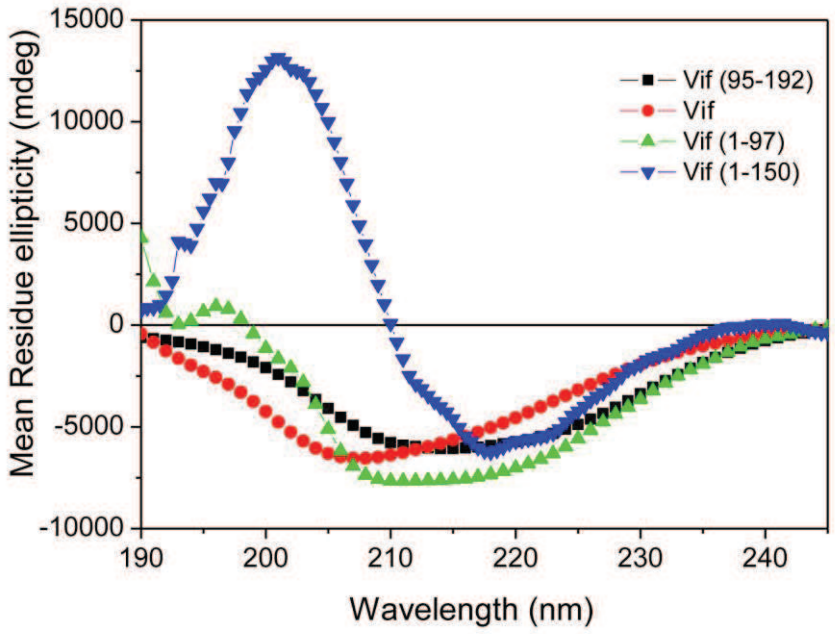

Supplementary Figure 2. 1D ^{1}H NMR spectra of Vif and its domains. (**A**) Vif (1-97), (**B**) Vif, (**C**) Vif (95-192). Spectra were recorded at 20°C in the protein buffer. Proteins were centrifuged for 30 min at 100,000 g before use and the spectra were recorded on the supernatant.

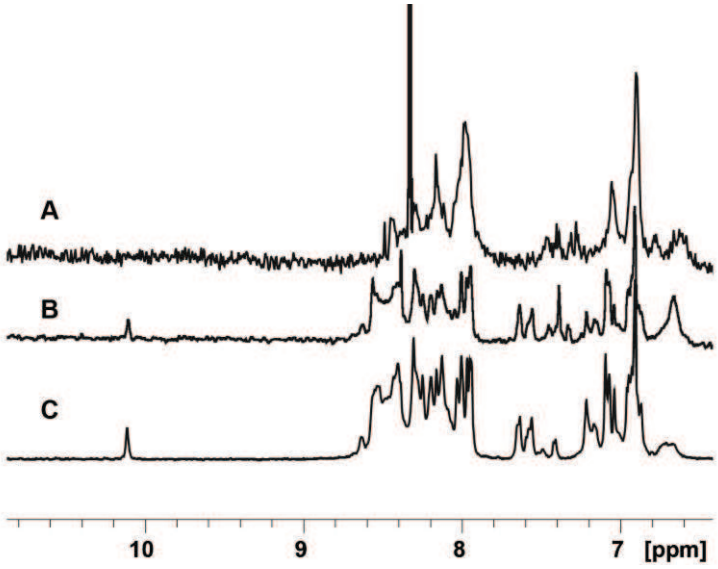

Supplementary Figure 3. 1D ^{1}H NMR spectra of Vif (95-192). Spectra were recorded at 20°C with (**A**) or without (**B**) 1 equivalent of $ZnCl_2$. Sample concentration was 22 µM.

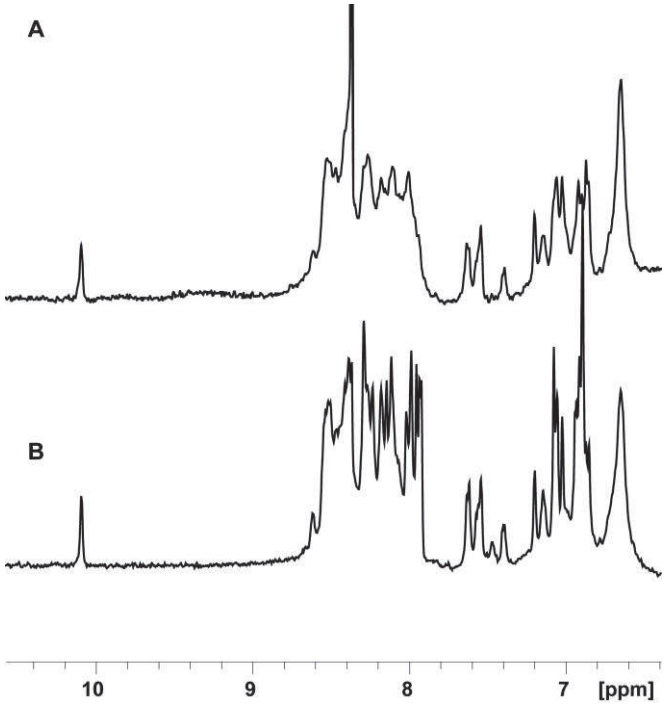

Supplementary Figure 4. Fluorescence titrations of Vif (95-192) with HIV-1 RNAs at 25°C. (**A**) Short RNA B and (**B**) TAR RNA. The dissociation constants (K_D) are indicated in nM with the confidence interval at 95% in parenthesis. The maximal fluorescence attenuation Q_{max} obtained for each titration is indicated as a percentage (%). Measurements were performed in a Tris-HCl (30 mM, pH 7.5) buffer containing 200 mM NaCl and 10 mM $MgCl_2$.

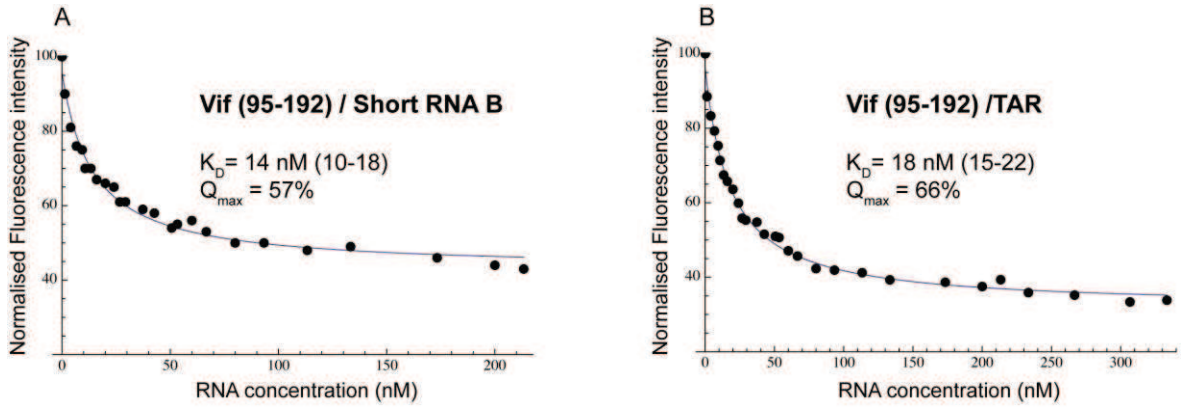

Supplementary Figure 5. NMR chemical shift mapping of the binding sites of Vif proteins on $tRNA^{Lys}_3$. The NMR chemical shift mapping of Vif (**A**) and Vif (1-97) (**B**) is reported on the secondary structure of $tRNA^{Lys}_3$ (left) with the following color code: the base pairs for which the chemical shift variation of its imino group upon addition of the protein is ≥ 0.05 ppm are in red, between 0.03 and 0.05 ppm in orange and equal to 0.02 ppm in yellow. On the right side, two NMR spectra (2D ^{1}H-^{15}N TROSY) acquired at 20°C are superimposed: in black for the $tRNA^{Lys}_3$ alone (reference spectrum) and in red for the $tRNA^{Lys}_3$/protein complex.

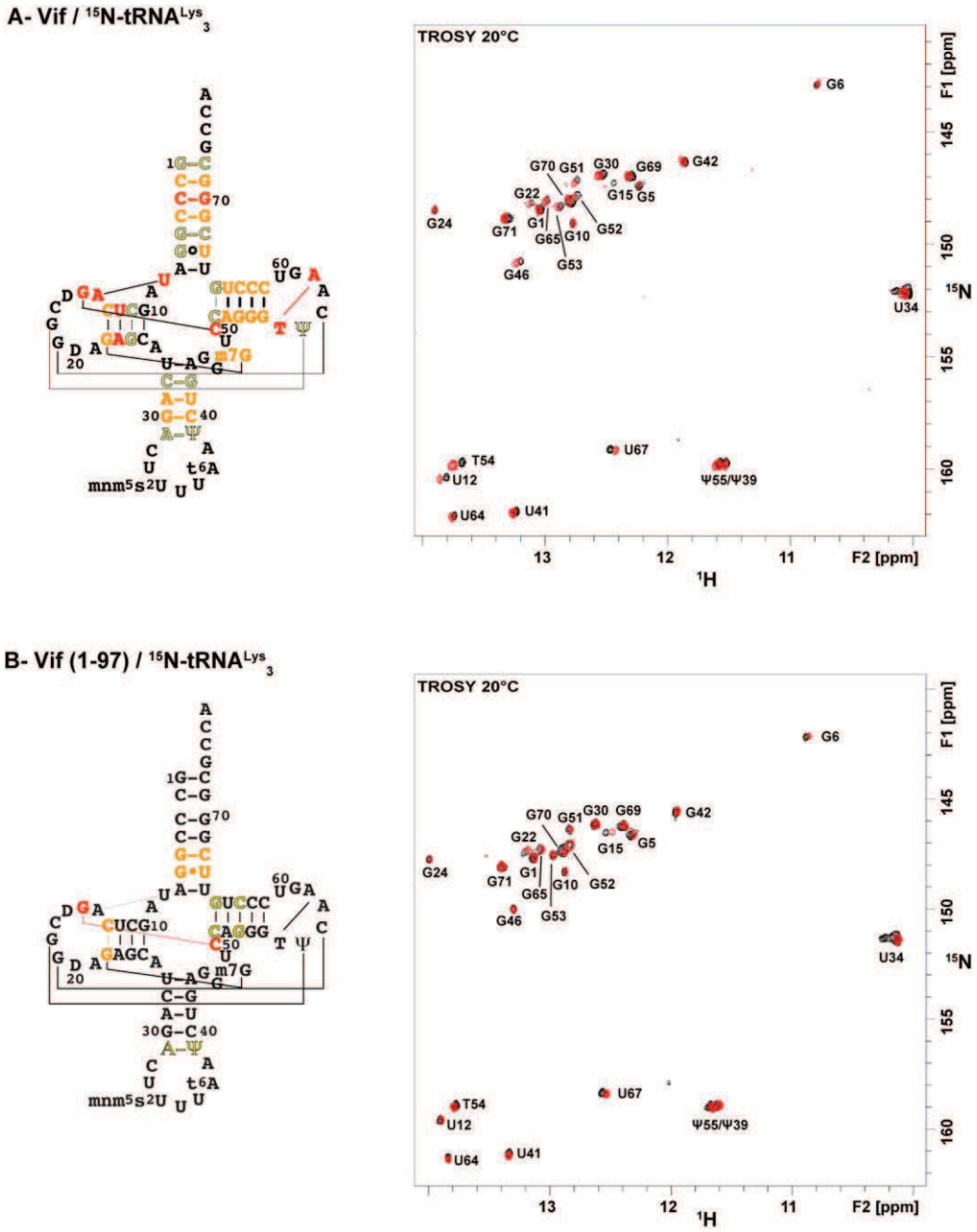

Supplementary Figure 6. NMR chemical shift mapping of the binding sites of Vif (95-192) on $tRNA^{Lys}_3$. Interaction of Vif (95-192) at 1 (**A**) or 2 (**B**) equivalent(s) of the protein. In each panel, the NMR chemical shift mapping is reported on the secondary structure of $tRNA^{Lys}_3$ (left). The color code is the same as in supplementary Figure 5. On the right side, two NMR spectra (2D ^{1}H-^{15}N TROSY) acquired at 20°C are superimposed: in black for the $tRNA^{Lys}_3$ alone (reference spectrum) and in red for the $tRNA^{Lys}_3$/protein complex.

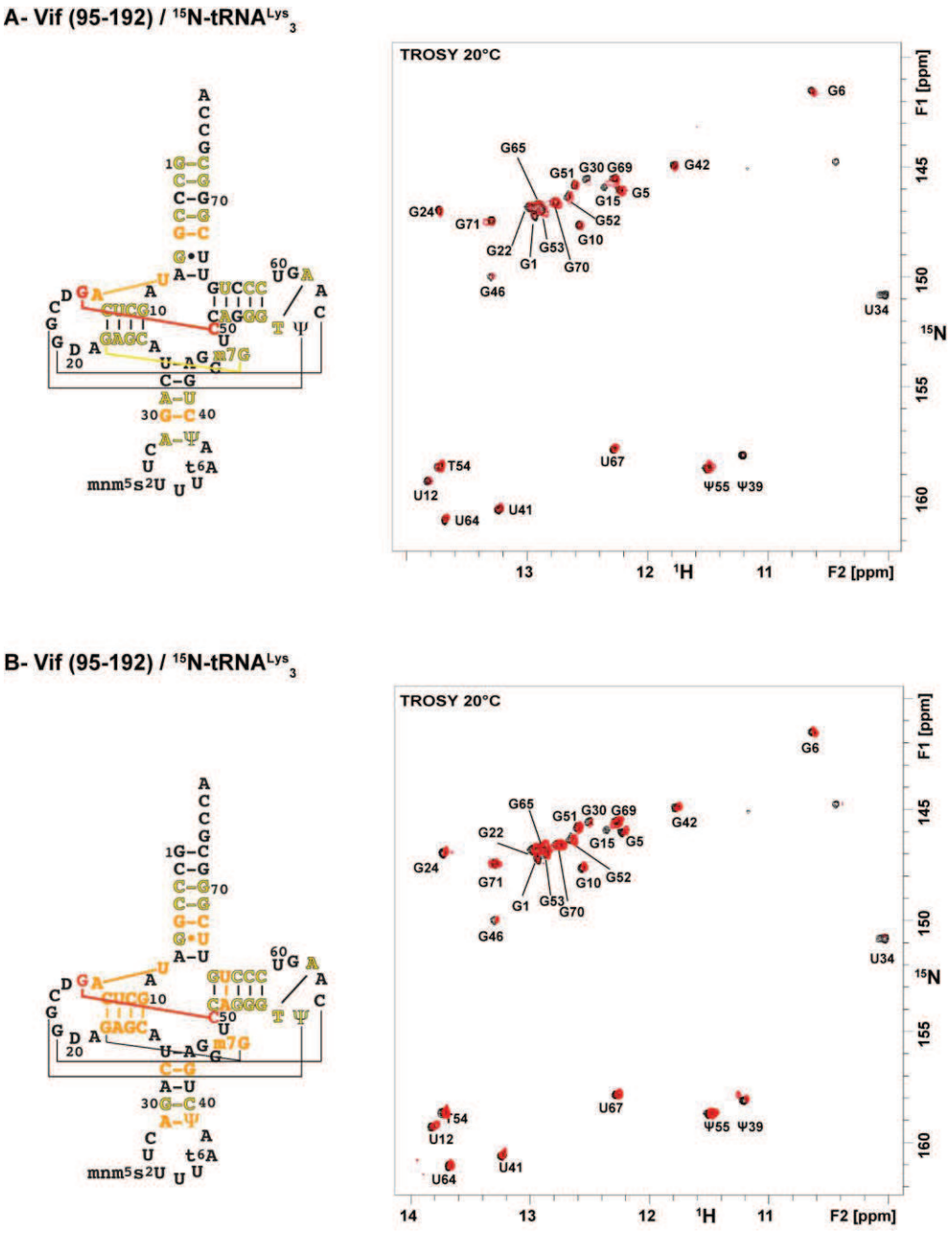

Supplementary Figure 7. Mapping on $tRNA^{Lys}_3$ structure (PDB code 1FIR) of the binding sites of Vif and its domains: (**A**) Vif, (**B**) Vif (1-97), (**C**) Vif (95-192), (**D**) Vif (95-192) at 2 equivalents and (**E**) NCp7 at 3 equivalents. The base pairs for which the chemical shift variation of its imino group upon addition of the protein is equal or superior to 0.05 are in red, between 0.03 and 0.05 ppm are in orange and equal to 0.02 ppm are in yellow.

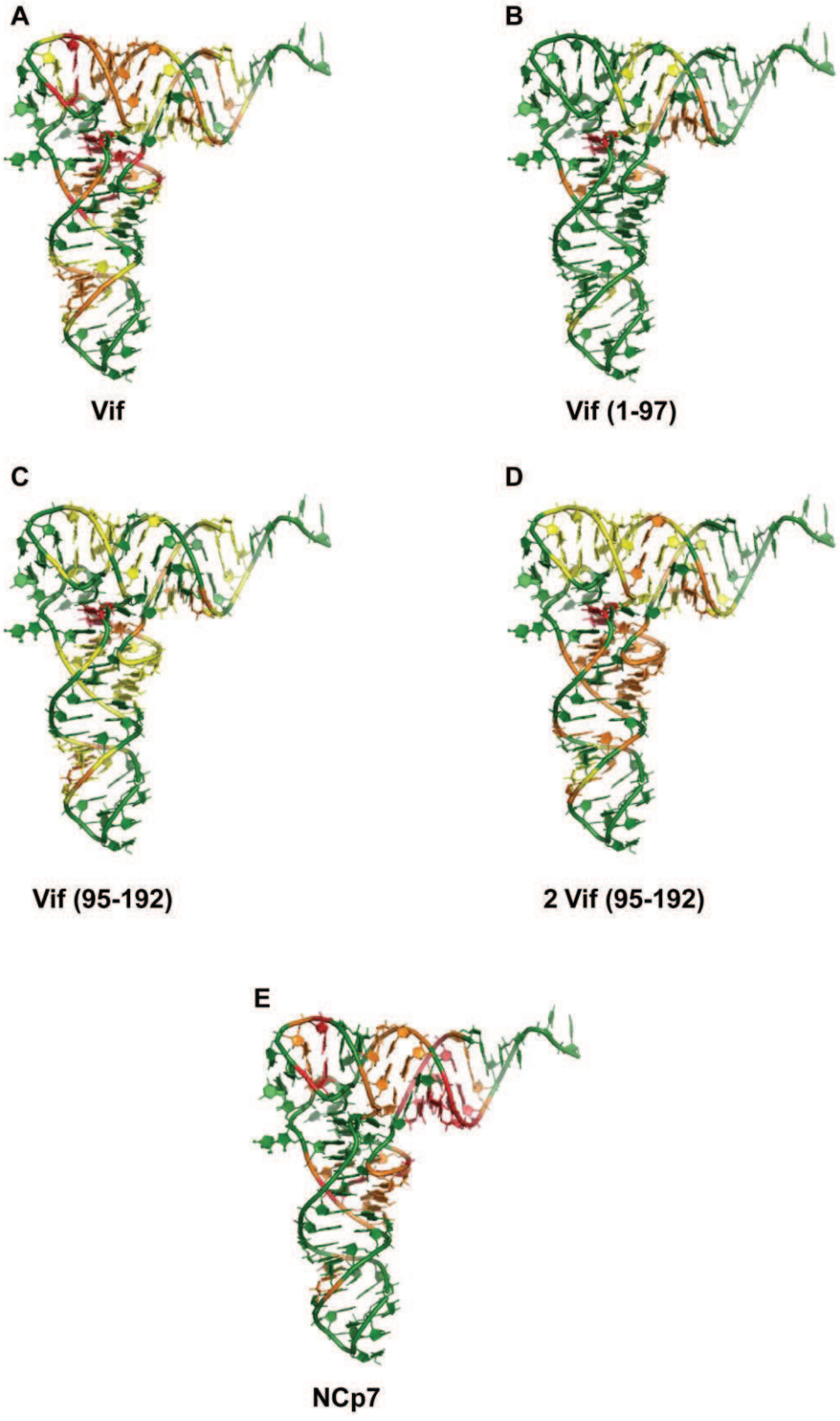

3.2. Sumplementary experiments (from the article: The role of Vif oligomerization and RNA chaperone activity in HIV-1 replication)

3.2.1 HIV-1 Vif activates TAR(+)/TAR(-) annealing

The annealing of the complementary TAR sequences is essential to achieve (-) strand DNA transfer. To better understand Vif-induced (-) strand DNA transfer, we compared the ability of Vif to promote the annealing of two complementary TAR sequences with that of NCp7 and Tat. In the absence of protein, TAR(+)/TAR(-) annealing occurred at 65°C in high salt conditions in the positive control (Fig. 34A, Ct+). No TAR(+)/TAR(-) annealing was observed at 37°C in the negative control (Fig. 34A, Ct-). Incubation with NCp7 or Tat at 37°C for 5 min favored TAR(+)/TAR(-) annealing at protein to nucleotide molar ratios of 1/20, 1/10 and 1/5 (Fig. 34A, lanes 3-8). In the presence of Vif, TAR(+)/TAR(-) annealing was also observed, but at higher protein to nucleotide molar ratios of 1/30, 1/15 and 1/10 (Fig. 34A, lanes 11-13), indicating that Vif annealing activity was slightly less efficient than that observed for NCp7 or Tat.

3.2.2 Inhibition of Vif-mediated TAR(+)/TAR(-) annealing by 2'O-methylated ODNs

In an attempt to characterize molecules capable of inhibiting the chaperoning activity of Vif, we used methylated oligonucleotides (mODN) found to bind to NCp7 and extensively impair its chaperoning activity *in vitro* and virus replication in T-cells and macrophages (Grigorov et al., 2011). To this end, we monitored the effect of mODNs on Vif-mediated *TAR(+)/TAR(-) annealing* as previously reported for NCp7 (Fig. 34B) (Grigorov et al., 2011). In the positive control of Vif-mediated TAR(+)/TAR(-) annealing, Vif was used at a protein to nucleotide molar ratio of 1/30 (Fig. 34B, line 3). We observed no effect on the TAR(+)/TAR(-) annealing by Vif after addition of increasing concentrations (100-400 μM) of mODN-11 and mODN-9UU (Fig. 34B, lanes 4-6 and 10-12, respectively). However, addition of mODN-9 GU drastically reduced TAR(+)/TAR(-) annealing by Vif (Fig. 34B, lanes 7-9). This result suggests that mODNs could be used to inhibit not only the nucleic RNA chaperone activity of NCp7 (Grigorov et al., 2011) but also that of Vif.

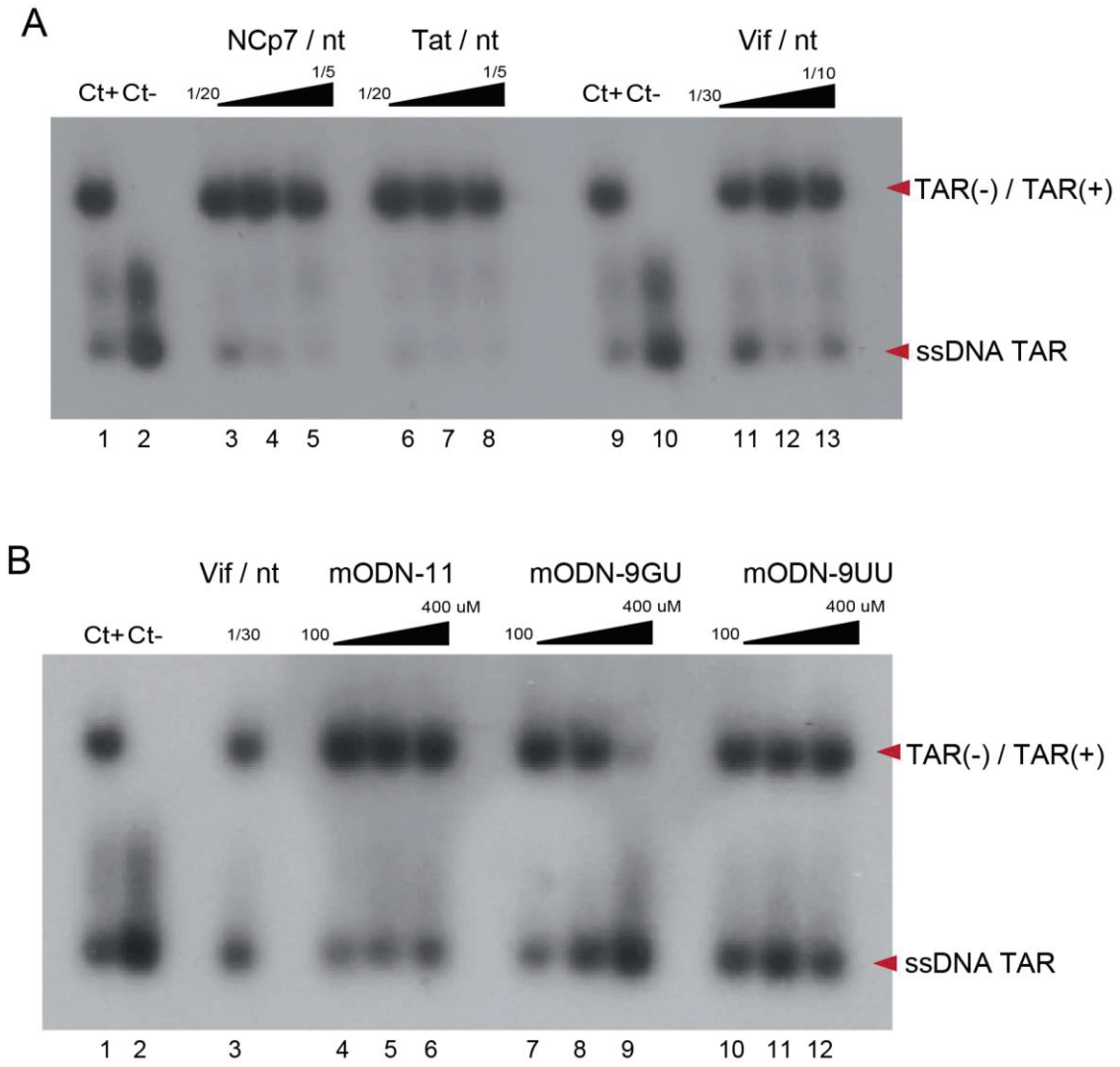

Figure 34. Stimulation of HIV-1 TAR(+)/TAR(-) DNA annealing by Vif. A) TAR(+) and ^{32}P-labeled TAR(-) DNA oligonucleotides were co-incubated in the presence of increasing concentrations of NCp7, Tat and Vif. In the absence of protein, double-stranded TAR DNA was formed by annealing upon incubation at 65°C for 30 min (Ct+, lanes 1 and 9) but not at 37°C (Ct-, lanes 2 and 10). Lanes 3-5: TAR(+)/TAR(-) annealing at 37°C for 5 min with HIV-1 NCp7 at protein/nt molar ratios of 1/20, 1/10 and 1/5. Lanes 6-8: TAR(+)/TAR(-) annealing at 37°C for 5 min with HIV-1 Tat at protein/nt molar ratios of 1/20, 1/10 and 1/5. Lanes 11-13: TAR(+)/TAR(-) annealing at 37°C for 5 min with HIV-1 Vif at protein/nt molar ratios of 1/30, 1/15 and 1/10. B) Inhibition of Vif-mediated TAR DNA annealing by methylated ODNs (mODN). TAR(+) and ^{32}P-labeled TAR(-) DNA were co-incubated in the presence of HIV-1 Vif and increasing concentrations of either one of the mODNs. Upon annealing in the absence of protein at 65°C for 30 min a double-stranded TAR DNA was formed (Ct+, lane 1) but not at 37°C (Ct-, lane 2). Lane 3-12 : TAR(+)/TAR(-) annealing at 37°C for 5 min with HIV-1 Vif at protein/nt molar ratio of 1/30 in the absence of mODN (lane 3) or with increasing concentrations (100-400 µM) of mODN-11 (lanes 4-6), mODN-9GU (lanes 7-9), and mODN-9UU (lanes 10-12), respectively.

3.2.3 Vif activates hammerhead ribozyme-directed RNA cleavage

The hammerhead ribozyme cleavage assay was used to monitor two RNA chaperone properties: the annealing of the RNA substrate to the ribozyme, and the subsequent dissociation of the RNA products (Fig. 35A) (Cristofari and Darlix, 2002). We observed enhanced ribozyme-directed cleavage of RNA S14 after addition of increasing concentrations of Vif at protein to nucleotide molar ratios between 1/50 and 1/3 (Fig. 35B, lanes 3-7). As expected, we observed the same effect with NCp7 (Fig. 35B, lanes 8-10). No hammerhead ribozyme-directed RNA cleavage was detected using NC(12-53) which has only little nucleic acid chaperone activity (Fig. 35B, lanes 11-13) (Cristofari and Darlix, 2002; Darlix et al., 2011b; Kuciak et al., 2008b).

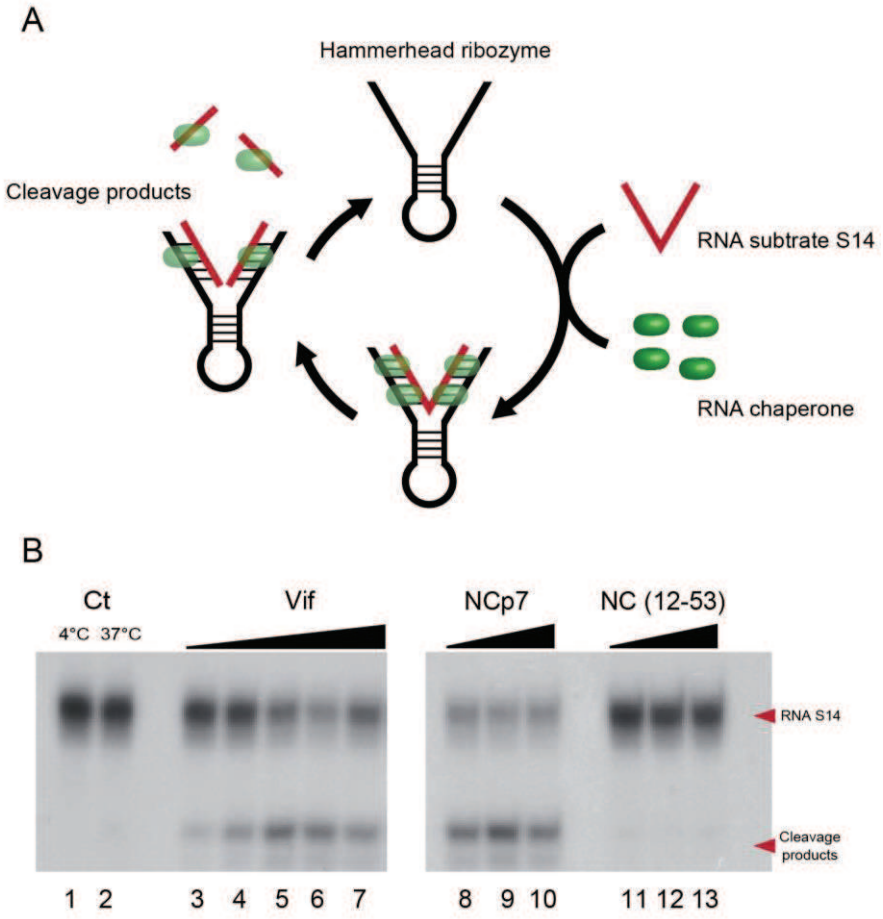

Figure 35. **Enhancement of hammerhead ribozyme-induced cleavage by HIV- 1 Vif protein**. A) Schematic representation of hammerhead ribozyme cleavage of RNA. B) R3 ribozyme and an excess of the S14 substrate RNA were co-incubated with increasing concentrations of Vif, NCp7 and NCp(12-53). RNA S14 is 61 nts in length, while the cleavage product is 49 nts long. Lanes 1-2: control cleavage of the RNA S14 substrate by the hammerhead ribozyme for 30 min at 4°C or 37°C. Lanes 3-13: incubation for 10 min with Vif at protein/nt molar ratios of 1/50, 1/40, 1/30, 1/20 and 1/15 (lanes 3-7), with NCp7 at protein/nt molar ratios of 1/20, 1/10, 1/5 (lanes 8-10) and with NCp(12-53) at protein/nt molar ratios of 1/10, 1/5, 1/2 (lanes 11-13).

3.2.4 Vif induces the formation of HIV-1 RNA loose and tight dimers

Previously, we reported that Vif is able to induce the formation of loose RNA dimers in a RNA dimerization assay using RNA fragments containing the first 615 nts of the HIV-1 genomic RNA (Henriet et al., 2007). Moreover, in the presence of NCp7, Vif was able to inhibit NC-induced tight RNA dimer formation (Henriet et al., 2007). We now report that Vif is able to form both loose and tight RNA dimers when dimerization assays were carried out with an RNA corresponding to the first 311 nts of the HIV-1 genome (Fig. 36A). The dimerization experiment was carried out with increasing concentrations of Vif (0-5 µM) and in the absence or presence of NCp7 (NCp7/nucleotide ratio of 1/7). We analyzed RNA dimerization using two different electrophoresis conditions: 1) native conditions in which both loose and tight dimers are stable (Fig. 36A, upper panel) and 2) semi-denaturing conditions in which only tight dimers are preserved (Fig. 36A, lower panel). In the absence of NCp7, Vif stimulated both loose and tight RNA dimers formation, as observed by the presence of RNA dimers under both electrophoresis conditions, with a dimerization yield of ~ 40% at 5 µM Vif (Fig. 36A). In the absence of Vif (Fig. 36A, lane 5), NCp7 induced >90% RNA dimer under both electrophoresis conditions. When increasing concentrations of Vif were added, we observed a reduction of the NCp7-induced tight RNA dimer formation (Fig. 36A, lanes 5-8), indicating a competition between Vif and NCp7, as previously observed (Henriet et al., 2007). These observations suggest that Vif favors the formation of tight RNA 1-311 dimers (Fig. 36B), contrary to what was observed for RNA 1-615 (Henriet et al., 2007). Indeed, in the RNA 1-311 context, the dimerization initiation site (DIS), responsible for RNA dimerization, is located directly at the 3'-end of the molecule, which probably induced a reduction of topological constraints and could thus allow the formation of an extended duplex (Fig. 36B). Conversely, the DIS of RNA 1-615 is located in the middle of the sequence, and in this context, Vif and/or NCp7 may stabilize the RNA dimer *via* different loop-loop interactions. It is thus likely that the tight dimers formed by RNA 1-311 differ from those formed by RNA 1-615, and presumably by full length genomic RNA.

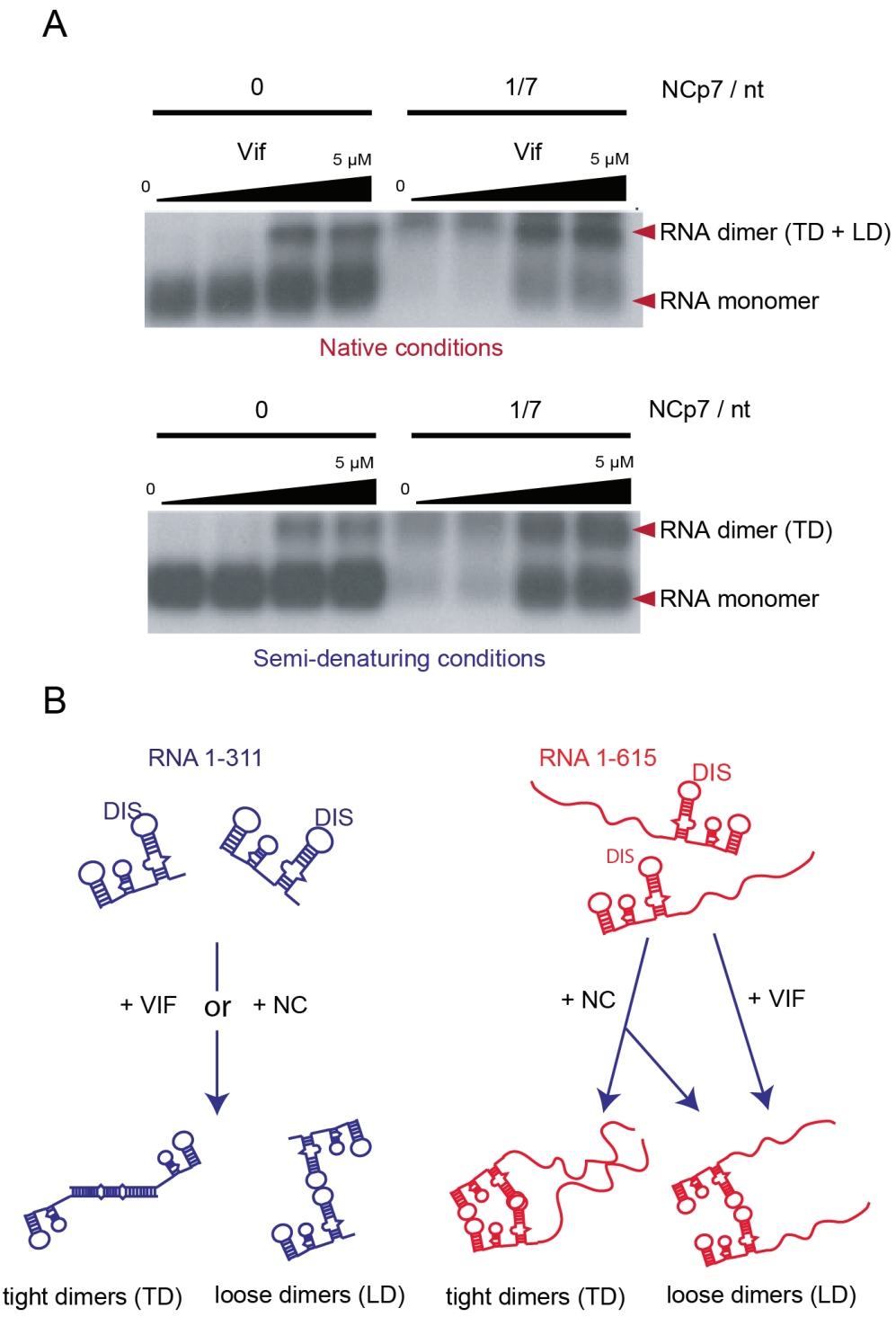

Figure 36. RNA dimerization induced by Vif and NCp7. **A**) HIV RNA 1-311 was allowed to dimerize in the presence of increasing concentration of Vif (0, 0.2, 2.0 and 5.0 uM), in the absence or in presence of NCp7 at a protein/nt molar ratio of 1/7. After protein removal, RNA was visualized under native and semi-denaturing electrophoresis conditions. **B)** Schematic representation of Vif and NCp-induced RNA dimerization under native and semi-denaturing conditions.

IV. CONCLUSIONS AND PERSPECTIVES

1. Scientific repercussions of the Vif-mediated A3G translation inhibition

In this study, we first demonstrated *ex vivo*, using HEK 293T cells, that the HIV-1 Vif protein inhibits A3G translation by a 5'UTR-dependent mechanism. In addition to all reports showing an A3G translation inhibition by Vif *in vitro*, this thesis demonstrates that A3G translation inhibition also occurs in cell. Moreover, we reported that 50% of A3G reduction by Vif is due to a translation inhibition, showing that this mechanism is equally important to the proteasome-mediated A3G degradation pathway. Additionally, translational inhibition of A3G reduces A3G incorporation into viral particles resulting in a 50% increase of HIV-1 infectivity. Therefore, Vif-mediated A3G translational repression significantly impacts HIV-1 viral restriction induced by A3G. These results have thus to be considered for further A3G-Vif researches.

First and most importantly, antiretroviral compound development targeting the A3G-Vif axis must take into account this substantial Vif-mediated A3G translational repression to achieve a significant A3G incorporation into viral particles. Thus, a common Vif domain implicated in both A3G reduction mechanisms has to be targeted. For instance, the Vif N-terminal domain that holds the RNA binding activity, the CBF-β interacting domain and several motifs that have been implicated in A3G/F interaction could be an interesting candidate. In fact, CBF-β is a key component of the proteasome-mediated A3G degradation pathway and the RNA binding domain could be implicated in the translation inhibition mechanism, according to our Vif-mediated A3G translation inhibition hypothesis.

Second, most A3G-Vif studies use A3G constructs lacking the UTRs to perform different experiments. This type of studies cannot take into account the reduction of A3G due to its translational inhibition by Vif because Vif requires the 5'UTR to perform its translational repression activity. Thus, the results of such studies may not correctly represent the activity of Vif on A3G reduction. Importantly, since HIV-1 replication is targeted by other members of the A3 sub-family, Vif could also mediate translational inhibition of these members. Thus, this study can be extended to other

A3 proteins, such as A3F. This translational repression of A3F by Vif is ongoing in the lab (Thesis study of C. Libre) and preliminary experiments showed that A3F, as A3G, is dependent on its 5'UTR to be regulated at the translational level by Vif.

2. Understanding the molecular basis of the Vif-induced A3G translational inhibition

In this work, we showed that Vif impairs A3G translation by a 5'UTR-dependent mechanism. Based on the 5'UTR secondary structure, we demonstrated that stem-loop SL2 and SL3 are required in this mechanism. Moreover, we reported that an uORF present within these structures is required for Vif to repress A3G translation. To understand how Vif inhibits A3G translation, we first determined the importance of the uORF in A3G translation. Thus, we showed that this element negatively influences A3G translation. Interestingly, uORF-altering mutations in human genes have been shown to be implicated in human diseases (Calvo et al., 2009). Therefore, it is possible that single nucleotide polymorphisms (SNP) in A3G uORF could generate certain phenotypes in human populations. Specifically, uORF SNPs that inactivate the A3G uORF (single nucleotide substitutions or deletions in the uORF start and stop codons) could prevent A3G translation inhibition by Vif and enhance A3G incorporation into virions. This could explain in part the ability of long-term non-progressors (LTNP) to control HIV-1 infection. However, no study has addressed this possibility to date.

We also proposed a model of A3G translation in which about 50% of the 43S PICs pass through the uAUG by a leaky scanning mechanism and initiate translation of the mORF. The remaining of the 43S PICs complexes is trapped to translate the uORF and thereby reduces A3G translation. Concerning the short peptide expressed from the uORF, we showed that this peptide does not have any activity on A3G translation. However, the function of this peptide, if there is any, remains to be elucidated in more details. Based on this model, we hypothesize that Vif inhibits uORF translation termination and/or promote ribosomal stalling. This event, in turn, could obstruct the scanning of new 43S PICs that have passed through the uAUG and thereby inhibit A3G translation. To validate this hypothesis, it would be important to first identify and mutate the Vif binding sites that cover the 259-267 nucleotide

region of the A3G 5'UTR. These Vif-binding sites could be implicated in Vif-mediated ribosomal stalling according to our hypothesis. Second, the interaction of Vif with eukaryotic translation termination factors, such as eRF1 or eRF3, could also promote the inhibition of uORF translation termination. Despite this concern, the study of Vif interaction with all components of the eukaryotic translation machinery seems to be important to understand the Vif-mediated A3G translational inhibition.

3. HIV-1 Vif RNA chaperone activity

An RNA chaperone is a partially disordered protein that binds transiently and non-specifically to RNAs, promoting a correct RNA folding state. We previously reported that Vif possesses an RNA chaperone activity that facilitates different steps of the HIV-1 life cycle, such as RNA dimer maturation and initiation of reverse transcription (Batisse et al., 2012; Henriet et al., 2007). In this thesis, we extend this knowledge by studying the RNA binding and chaperoning properties of HIV-1 Vif functional domains. We showed that the N-terminal domain (NTD) is highly structured in solution, whereas its C-terminal domain (CTD) remains mainly unfolded. We observed that the CTD, as well as the NTD of Vif, are able to bind RNAs with high affinity, and that the RNA chaperone activity is mainly driven by the CTD. It seems however that the NTD of Vif binds RNAs with high specificity whereas the CTD binds RNAs in a non-specific manner allowing it to display a stronger RNA chaperone activity. We also demonstrated that Vif and NCp7 share the same binding sites on $tRNA^{Lys3}$, and could thus compete for $tRNA^{Lys3}$ binding. This result may explain previous observations by which Vif inhibits NCp7-assisted hybridization of $tRNA^{Lys3}$ to viral RNA (Henriet et al., 2007). Finally, we showed that the RNA chaperone activities of Vif and NCp7 are mostly driven by their basic disordered domains. Giving that the CTD is the binding domain of several partners of the E3 ubiquitin ligase complex (to induce A3G degradation through the proteasome), it is likely that the conserved disorder of the CTD in primate lentiviruses has a crucial role in different steps of the HIV-1 life cycle. To further study Vif RNA chaperone activity during the HIV-1 life cycle, *ex vivo* experiments could provide solid evidence of the importance of Vif chaperoning activities. In this concern, only limited approaches to study RNA chaperone activity *ex vivo* have been described so far.

In section III-2-2.5 we presented a model of Vif-mediated A3G translation inhibition in which a Vif binding site within the 5'UTR of A3G mRNA could be implicated in this repression. Vif binds strongly to A3G mRNA (Mercenne et al., 2010) and to the 5'-region of HIV-1 genomic RNA (Bernacchi et al., 2007), while it binds very weakly or does not bind at all to the central and 3'-regions of this RNA, or to heterologous RNAs (Bernacchi et al., 2007; Henriet et al., 2005). This indicates that Vif is not an unspecific RNA binding protein. Based on these observations, it is possible that Vif may specifically bind the A3G mRNA through its NTD and inhibits A3G translation. However, since its CTD holds a RNA chaperone activity that could change the RNA folding state, it is possible that this domain can be implicated in A3G translation inhibition, changing the A3G mRNA folding. Further experiments will be required to determine if both domains are implicated in A3G translational inhibition.

V. RÉSUMÉ FRANÇAIS

Rôle de la protéine Vif dans la réplication du VIH-1 : régulation traductionnelle du facteur de restriction APOBEC3G et activité chaperon d'ARN

INTRODUCTION ET OBJECTIFS

Le génome du VIH-1 code, en plus des protéines structurales et enzymatiques (Gag, Pol et Env) nécessaires à la réplication virale, plusieurs protéines régulatrices (Tat, Rev) et auxiliaires (Nef, Vif, Vpu, Vpr). Ces protéines ne se retrouvent habituellement que chez les lentivirus et leur rôle est d'augmenter le «fitness» viral dans l'hôte infecté par divers mécanismes (internalisation et dégradation des CD4, apoptose, trafic cellulaire, etc). Parmi elles, Vif (Viral Infectivity Factor), une petite protéine très basique de 23 kDa, est essentielle à la formation de particules virales infectieuses dans les cellules dites «non-permissives» (lymphocytes T CD4+, monocytes, macrophages), alors que des virus ΔVif se répliquent efficacement dans des lignées cellulaires T dites « permissives » (Jurkat, CEMSS...).

Les cellules non-permissives expriment de façon spécifique les facteurs de restriction APOBEC3G (APOlipoprotein B mRNA-Editing enzyme Catalytic polypeptide 3G ou A3G) et A3F, deux cytidine désaminases dont l'action hypermutatrice lors de la synthèse du brin (-) de l'ADN proviral est létale pour le virus. En réponse à ce mécanisme de défense, sans doute à l'origine dirigé contre les rétrovirus endogènes, les rétrovirus ont co-évolué en exprimant la protéine Vif.

Vif réduit de façon considérable le taux d'expression des protéines A3G/3F par trois mécanismes principaux (Fig 1.): (1) en recrutant une E3 ubiquitine ligase, Vif induit la degradation d'A3G par le protéasome ; ce mécanisme est le mieux documenté. (2) Par compétition directe avec les sites d'encapsidation des protéines A3G au niveau de l'ARN génomique et du domaine NC du précurseur Pr55Gag. (3) En régulant négativement la traduction de l'ARNm d'A3G. Les mécanismes expliquant cette inhibition sont totalement inconnus à l'heure actuelle, mais il est vraisemblable qu'ils impliquent les propriétés de fixation aux ARN de Vif.

La compréhension de ces différents processus est importante d'un point de vue thérapeutique car leur inhibition permettrait une encapsidation accrue des protéines A3G/3F et une baisse importante de l'infectivité virale.

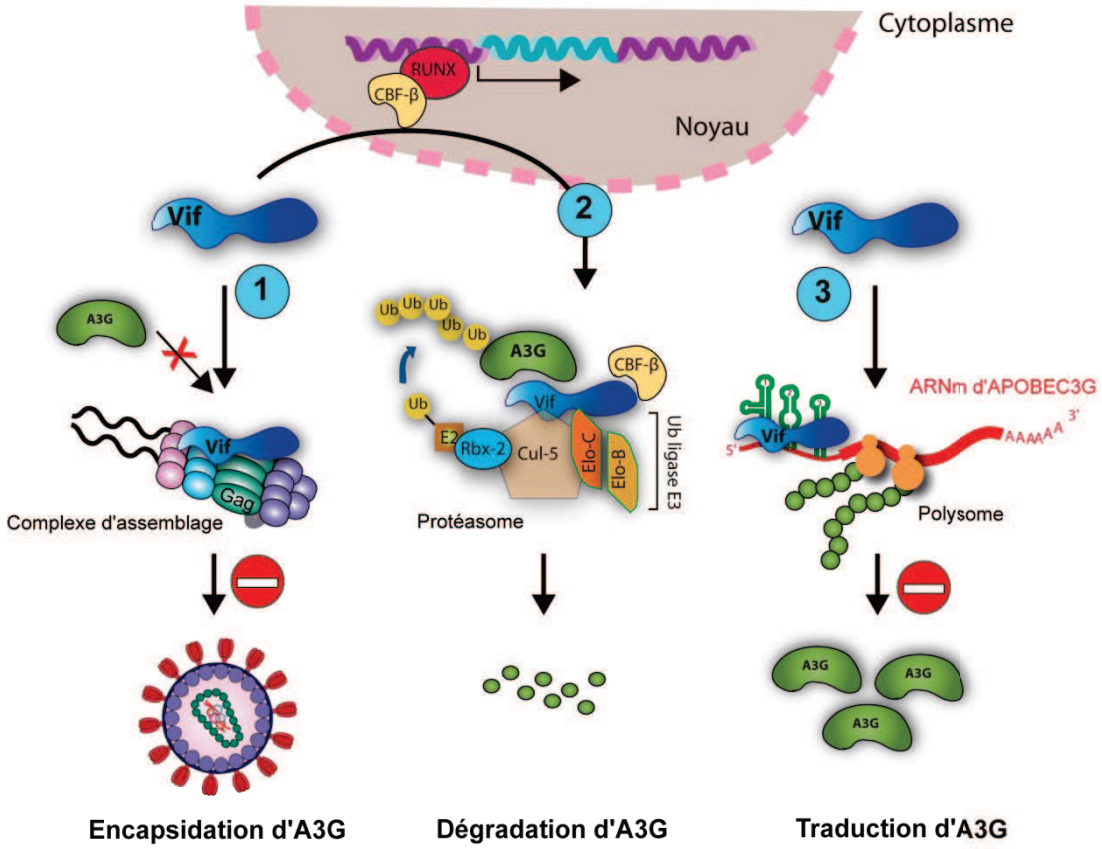

Figure 1. Représentation schématique du mode d'action des protéines Vif sur A3G et sur l'assemblage des particules virales du VIH-1. (1) Par compétition sur les sites ARN et protéique (NC), Vif pourrait empêcher l'encapsidation des protéines A3G. (2) Vif recrute les facteurs de poly-ubiquitination pour la dégradation d'A3G. (3) En se fixant à l'ARNm d'A3G, Vif pourrait inhiber sa traduction.

Pour aborder le rôle de Vif dans la régulation traductionnelle d'A3G, Mercenne *et al.* (2010) a déjà caractérisé les sites de liaison de Vif sur l'ARNm d'A3G au niveau des fragments correspondant aux regions non traduites (UTR, UnTranslated Regions). Vif possède une forte affinité pour la 3'- ainsi que la 5'-UTR, et plusieurs sites de fixation ont été déterminés par des expériences d'empreintes enzymatiques.

Ensuite, Mercenne *et al.* (2010) a déterminé la structure des UTRs par des expériences de « probing » chimique et enzymatique. Il a été montré alors que ces régions sont hautement structurées avec 3 tiges-boucles présentes dans la partie 5'UTR mais aussi dans la partie 3'UTR.

Finalement, il a été analysé l'effet de Vif sur la traduction d'A3G dans des systèmes reconstitués *in vitro* en présence/absence d'inhibiteurs du protéasome. Ces expériences ont confirmé que Vif inhibe la traduction de l'ARNm d'A3G et que la 5'-UTR est un élément majeur de cette répression *in vitro*. A partir de ces résultats, l'objectif de ce travail de thèse a été de déterminer le rôle et le mécanisme de la régulation traductionnelle du facteur de restriction A3G par la protéine Vif du VIH-1 *ex vivo*. En parallèle, nous nous sommes intéressés à déterminer les domaines de la protéine Vif impliqués dans l'activité chaperon d'ARN.

RESULTATS

Identification des domaines de l'ARNm d'A3G impliqués dans la régulation traductionnelle

D'abord, nous avons démontré *ex vivo* l'importance de la région 5'-UTR de l'ARNm d'A3G dans la régulation traductionnelle d'A3G par Vif. Ce résultat a été obtenu par l'analyse des « westerns blots » issus de co-transfections de différents vecteurs d'expression d'A3G (Fig. 2A) en présence ou absence de Vif dans des cellules HEK293T. Afin d'étudier seulement l'inhibition traductionnel, nous avons utilisé un dominant négatif de la Cullin 5 (Cul5Δ - protéine impliquée dans la dégradation *via* le protéasome). Ce dominant négatif agit comme un inhibiteur de la dégradation d'A3G par le protéasome et permet d'étudier uniquement l'inhibition traductionnelle d'A3G par Vif.

Ainsi, en présence du dominant négatif de la Cul5 et Vif, on observe une réduction d'A3G (Fig. 3A, ligne 5). Cette réduction est aussi observée quand on transfecte le mutant A3G Δ3'UTR mais pas quand on utilise les mutants A3G Δ5'UTR et A3G Δ'UTR (Fig. 3A et B). Ces résultats démontrent que l'inhibition traductionnelle d'A3G par Vif est dépendante de la région 5'UTR.

Des expériences de RT-qPCR ont permis de démontrer que les niveaux d'ARNm d'A3G est le même dans tous nos conditions. Cela montre que les différences observées dans l'expression d'A3G ne sont pas dû à une expression différentielle de nos plasmides (Fig. 3C)

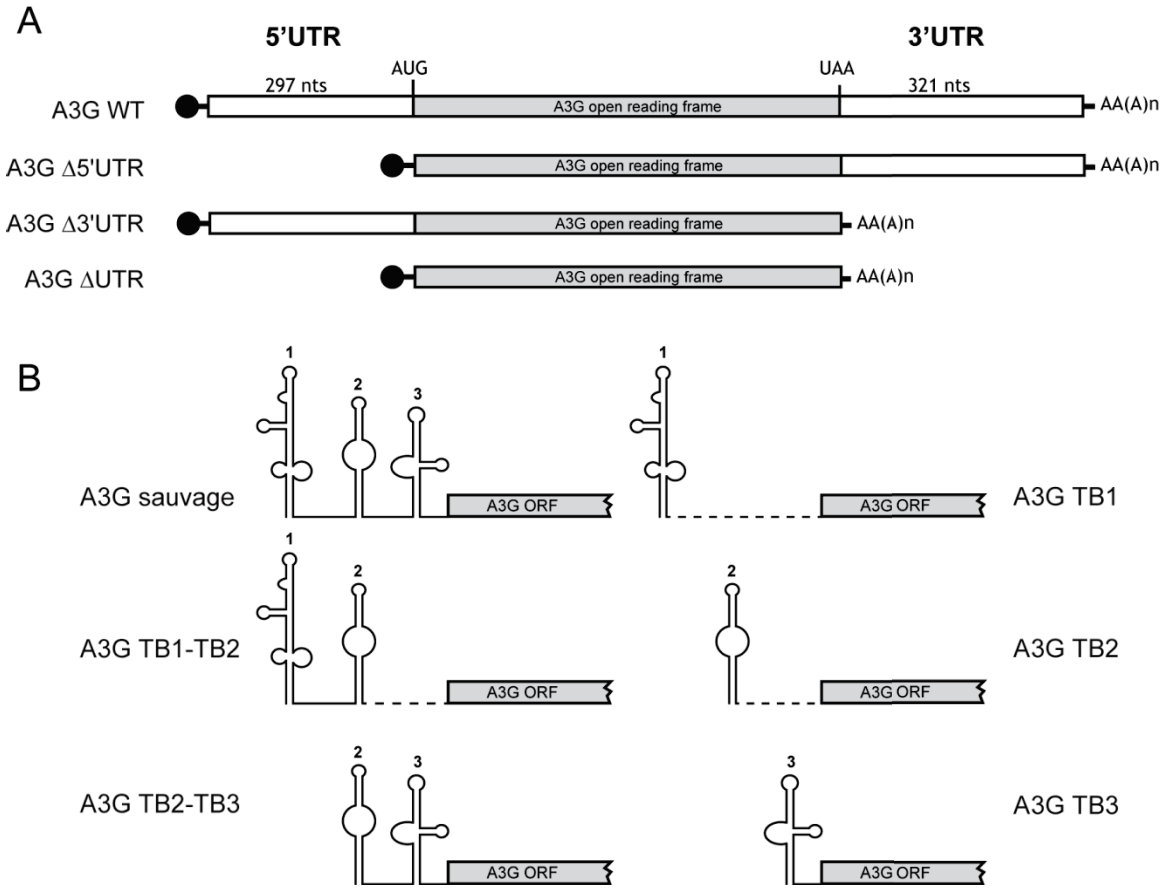

Figure 2. Mutants d'A3G étudiés. (A) Délétions des parties non traduits de l'ARNm d'A3G. (B) Mutants de la partie 5'UTR**.**

Nous avons ensuite identifié les domaines de la partie 5'UTR de l'ARNm d'A3G impliqués dans la régulation traductionnelle. Pour identifier ces domaines, des mutants d'A3G (Fig 2B) permettant d'étudier chacun des motifs en tige-boucle de la région 5'UTR de l'ARNm d'A3G ont été co-transfectés dans des cellules HEK293T en présence ou en absence de Vif et du dominant négatif de la Cullin 5. Nous avons ainsi observé que les domaines d2 et d3 (de façon simultanée) sont nécessaires à l'inhibition traductionnelle d'A3G (Fig 4).

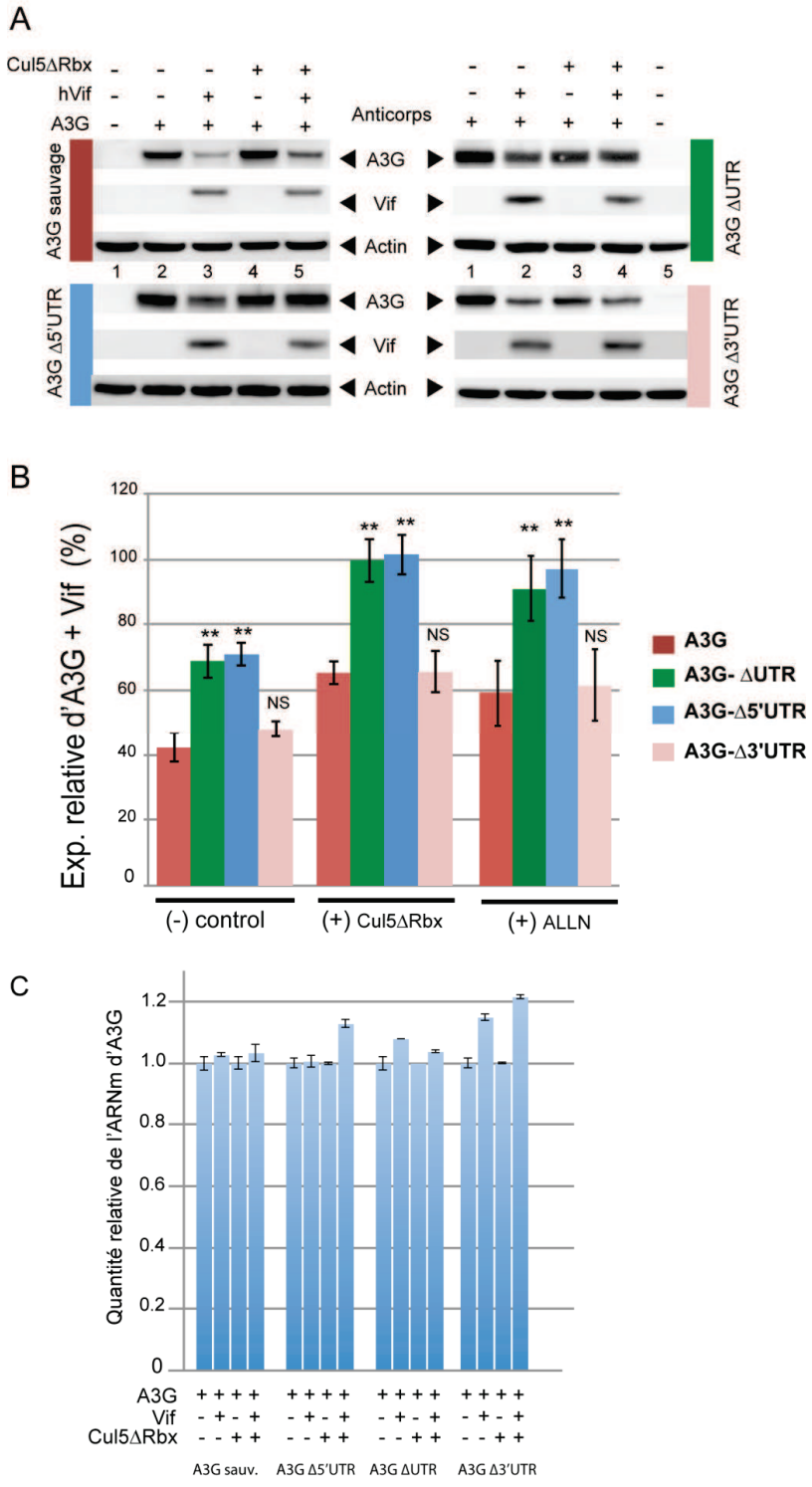

Figure 3. Identification des régions non traduites de l'ARNm d'A3G impliquées dans la régulation traductionnelle. Les différents mutants des régions non traduites d'A3G ont été transfectés en présence ou en absence de Vif (+/- dominant négatif de la Cullin 5). Les protéines A3G et Vif ont été détectées par western blot (A), puis les signaux ont été quantifiées et normalisées par rapport au contrôle interne (actine) et les valeurs reportées sur les histogrammes (B).

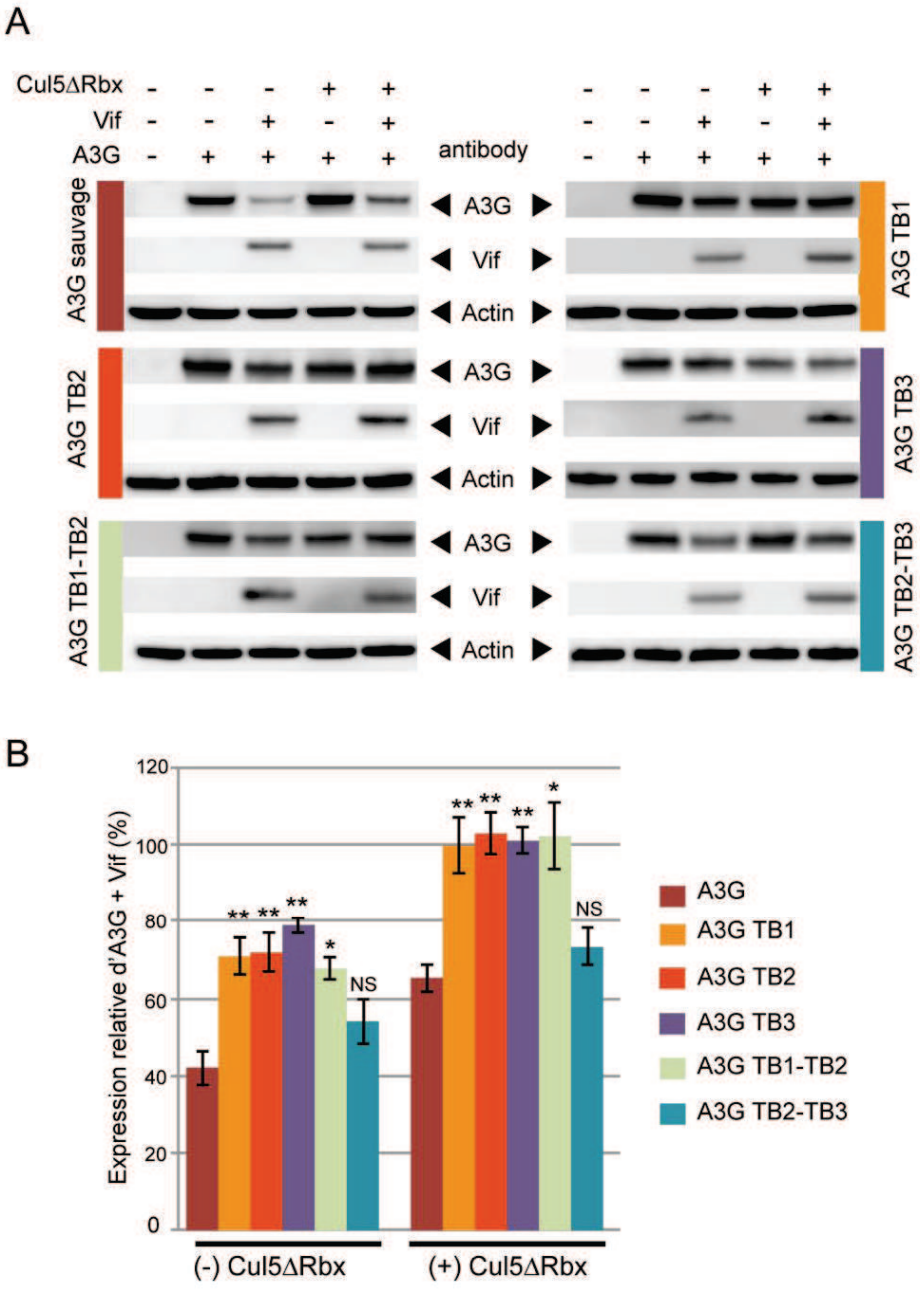

Figure 4. Identification des domaines de l'ARNm d'A3G impliqués dans la régulation traductionnelle. Les différents mutants de la 5'-UTR d'A3G ont été transfectés en présence ou en absence de Vif (+/- dominant négatif de la Cullin 5). Les protéines A3G et Vif ont été détectées par western blot (A), puis les signaux ont été quantifiées et normalisées par rapport au contrôle interne (actine) et les valeurs reportées sur les histogrammes (B).

Compréhension fine du mécanisme de régulation traductionnelle

Apres avoir déterminé l'importance des domaines d2 et d3 dans l'inhibition traductionnelle, nous avons constaté la présence d'un élément TOP est une petite uORF (Upstream Open Reading Frame) (Fig 5A). Cette séquence se trouve chez d'autre isoformes de l'ARNm d'A3G (Fig. 5B) et code pour un peptide putatif de 23 acides aminés. Cette séquence n'est pas retrouvée dans les 5'-UTR des autres désaminases. Seule A3D (NM_152426.3) contient une séquence codante putative exprimant 9 acides aminés (Met-LVRLVSNS).

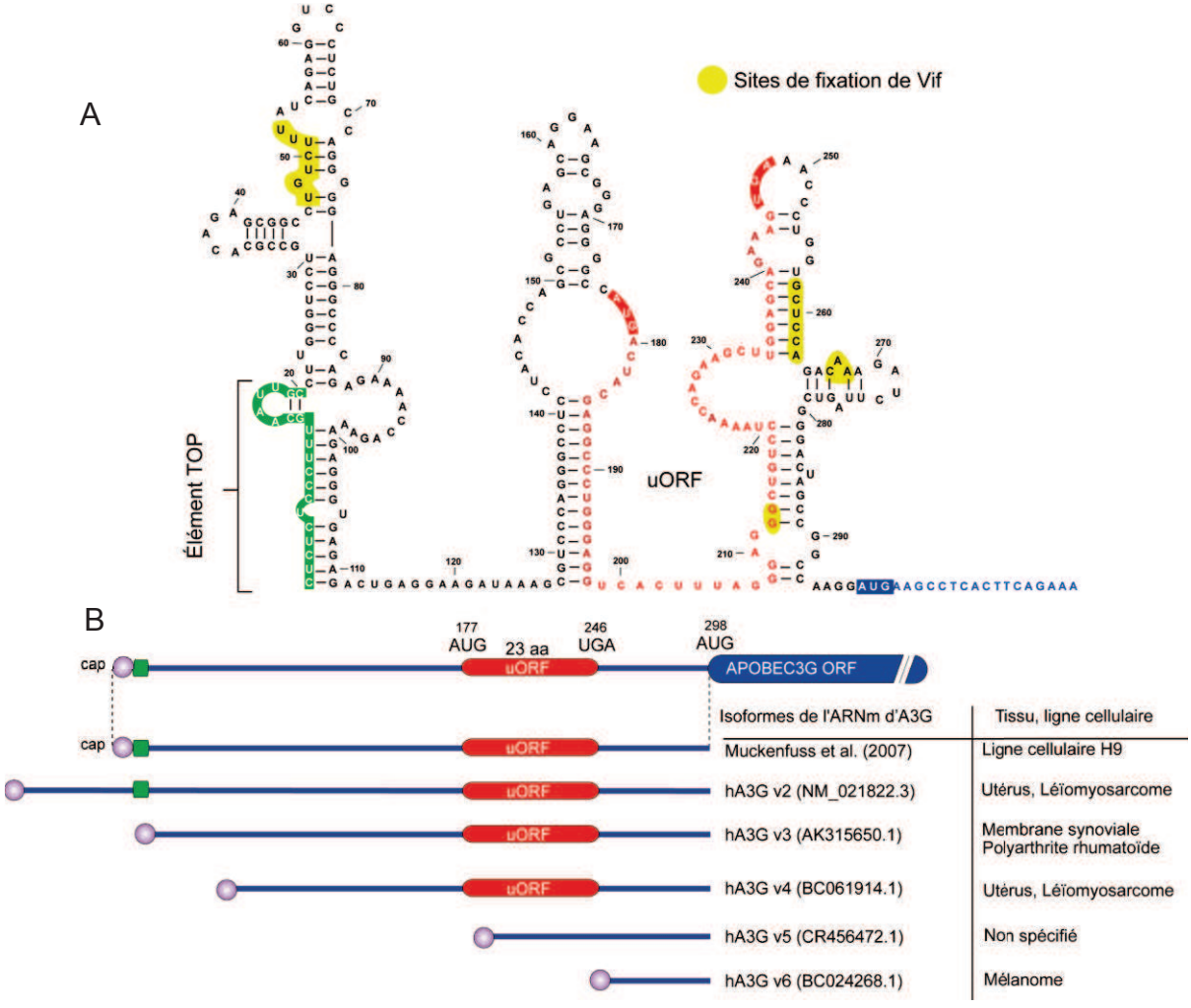

Figure 5. Analyse *in sillico* de la région 5'UTR de l'ARNm d'A3G. (A) Structure secondaire de la région 5'UTR montrant les sites de fixation de Vif (jaunes), l'élément TOP (vert) et l'uORF (rouge). (B) Alignement de la partie 5'UTR avec d'autres isoformes de l'ARNm d'A3G.

Concernant l'élément TOP, nous avons observé indirectement qu'il n'est pas impliqué dans l'inhibition traductionnelle d'A3G par Vif car le mutant A3G TB2-TB3, qui ne possède pas l'élément TOP se comporte comme le sauvage (Fig. 4).

Les uORF, présents dans 50 % des gènes eucaryotes, interviennent principalement dans des mécanismes de régulation traductionnelle. Dans la plupart des cas, la présence d'une uORF régule négativement l'expression de l'ORF majeure. Afin de comprendre sa fonction et son implication dans l'inhibition traductionnelle d'A3G par Vif, nous avons tout d'abord determiné *in vitro* et *ex vivo* l'expression des mutants du codon initiateur AUG (AUG/AAG) et du codon stop UGA (UGA-ΔU/GA) de cette petite uORF (Fig 6A). Nous avons ainsi constaté que l'expression de l'uORF régule négativement la traduction de l'ORF majeure d'A3G. En effet, A3G est en moyenne deux fois plus exprimée lorsque le codon d'initiation de l'uORF est substitué (uAAG) (Fig 6B).

En ce qui concerne le mutant A3G ΔuUGA, nous avons constaté l'expression des 2 formes d'A3G (Fig. 6B, ligne 6): une forme longue exprimée à partir de l'uAUG et la forme principale exprimée à partir de l'AUG original. Ces résultats suggèrent que les deux codons d'initiation sont utilisés par le ribosome dans la cellule. Plusieurs mécanismes peuvent être mis en jeu pour expliquer ce phénomène comme le leaky-scanning (ignorance du 1er AUG pour former la forme d'A3G mature), la ré-initiation (reprise du scanning de la sous-unité 40S du ribosome après synthèse à l'uORF) ou l'entrée interne du ribosome (entrée directe du 43S au niveau de l'AUG de l'ORF principale d'A3G).

Dans un deuxième temps, les mutants d'A3G uAAG et ΔuUGA ont été co-transfectés dans des cellules HEK293T en présence ou en absence de Vif et du dominant négatif de la Cullin 5 (Fig. 7). Comme préalablement observé, la forme sauvage d'A3G est régulée négativement par Vif en présence du mutant de la Cullin 5 (Fig. 7, ligne 1). En revanche, cette inhibition traductionnelle est levée lorsque le codon initiateur (uAUG) ou terminateur (uUGA) sont mutés (Fig. 7, ligne 8 et 12). Ainsi, il semble que l'expression de l'uORF en amont de l'ORF principale d'A3G soit requise pour que Vif exerce son activité inhibitrice au niveau traductionnel.

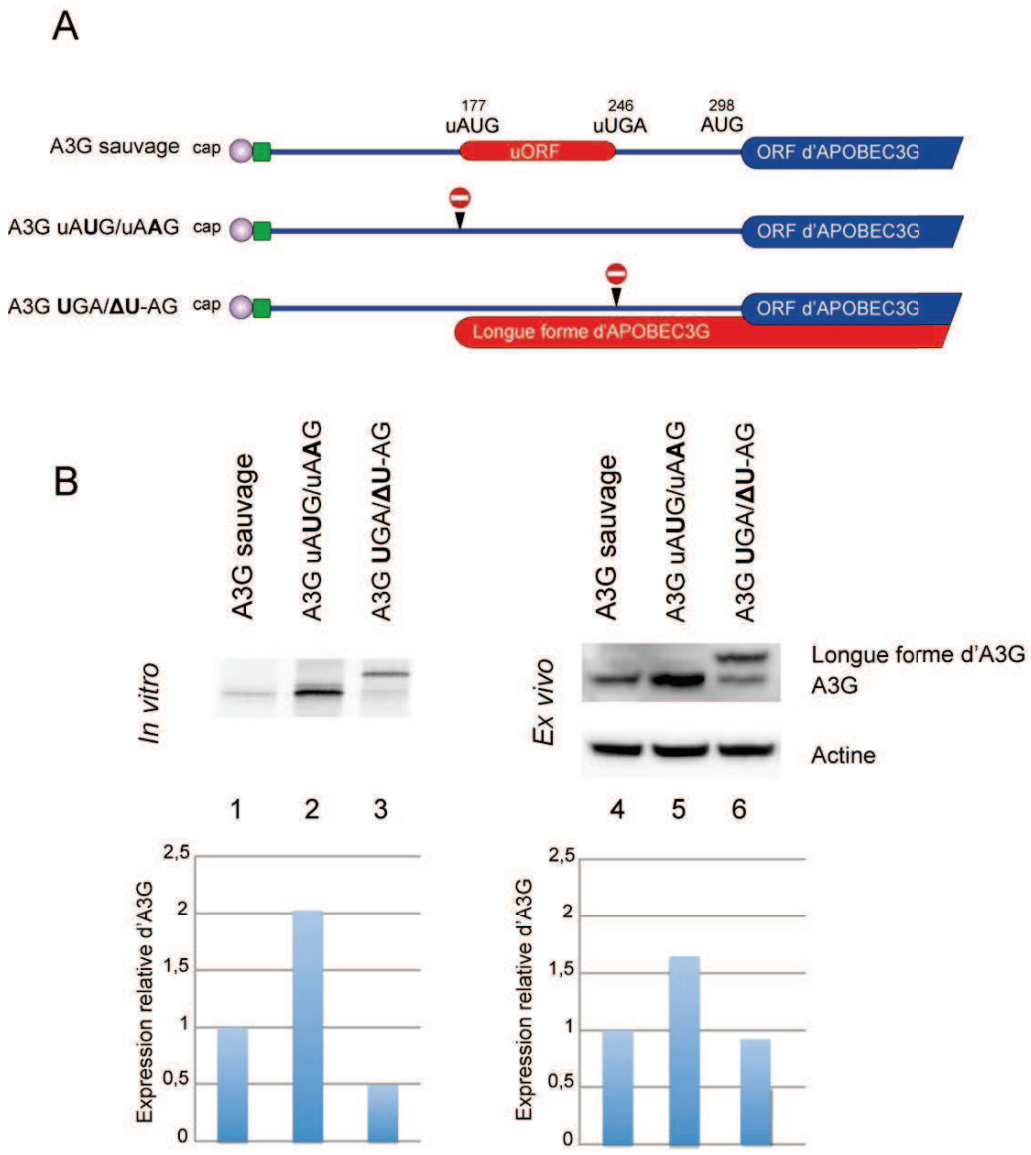

Figure 6. L'uORF régule négativement la traduction de l'ORF majeure d'A3G. Représentation des mutants des codons AUG et UGA de l'uORF (A) ainsi que son expression *in vitro* en utilisant des réticulocytes de lapins et *ex vivo* après transfection des cellules HEK293T (B).

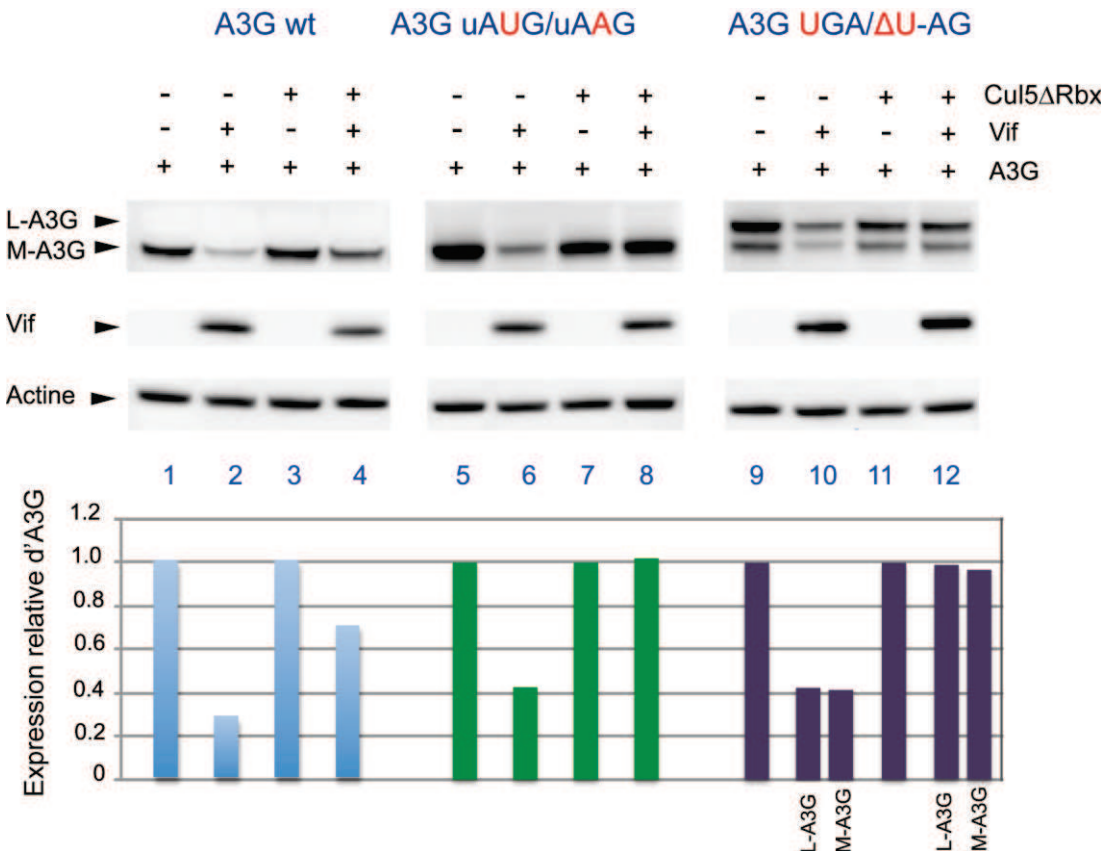

Figure 7. L'uORF est requise dans l'inhibition traductionnelle d'A3G par Vif. Le différents mutants de l'uORF ont été transfectés en présence ou en absence de Vif (+/- dominant négatif de la Cullin 5). Les protéines A3G et Vif ont été détectées par western blot, puis les signaux ont été quantifiées et normalisées par rapport au contrôle interne (actine) et les valeurs reportées sur les histogrammes.

Impact de la régulation traductionnelle d'A3G sur l'infectivité virale

Ensuite, nous avons déterminé l'impact de la régulation traductionnelle d'A3G sur l'encapsidation d'A3G dans les particules virales et sur l'infectivité virale de ces particules (Fig. 8). Nous avons ainsi déterminé le taux des protéines A3G encapsidées dans les particules virales. Ces essais ont été réalisés avec deux clones moléculaires du VIH-1 (pNL4.3 et pNL4.3ΔVif), en présence de la forme sauvage d'A3G (pCMV-A3G WT), de la forme dépourvue de la région 5'-UTR (pCMV-A3G Δ5'UTR) et de la forme contenant les tiges boucles 2 et 3 (pCMV-A3G d2d3) qui se comporte comme la forme sauvage.

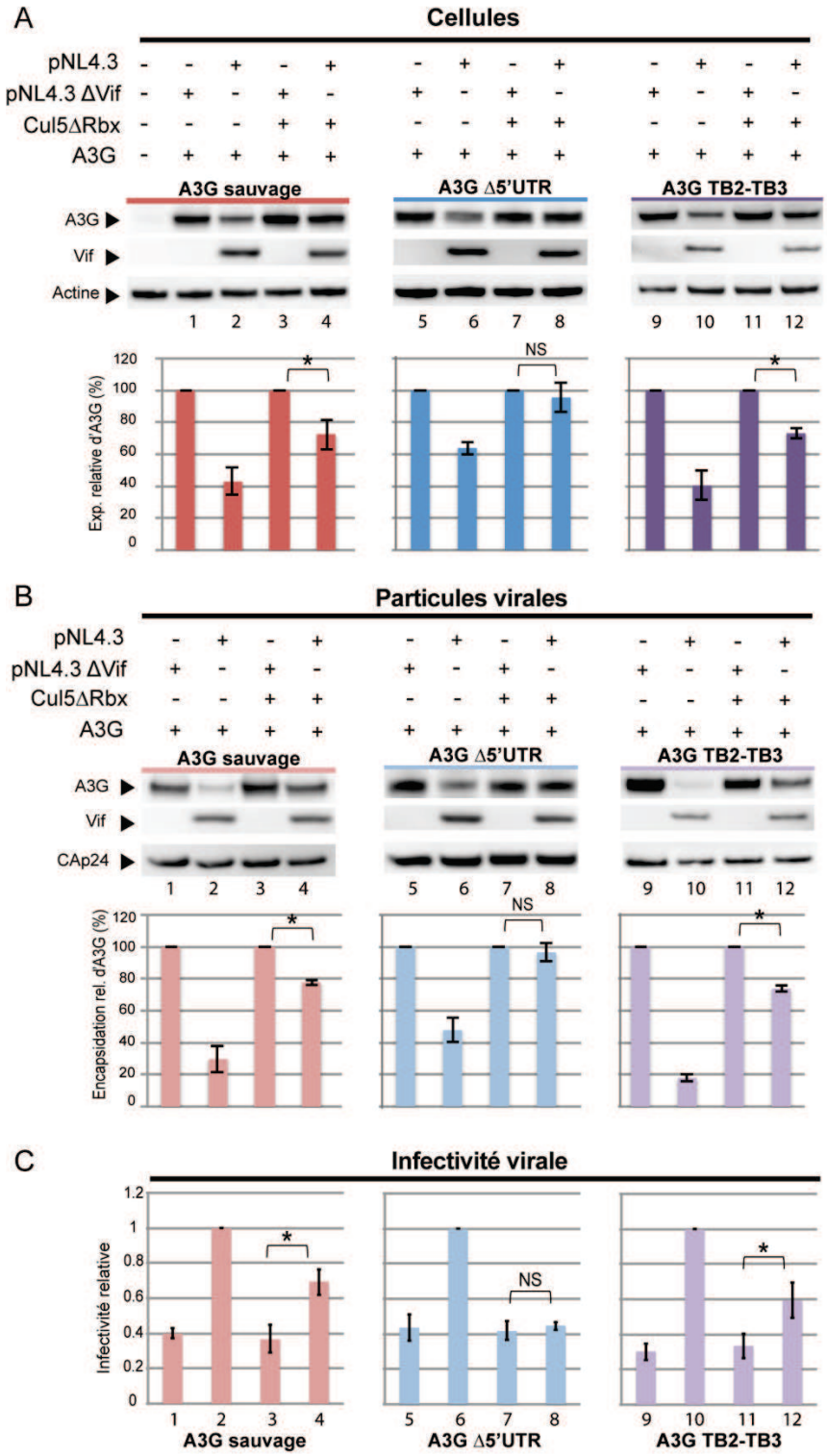

Figure 8. L'inhibition traductionnelle d'A3G par Vif augmente l'infectivite virale. Impact de la régulation traductionnelle d'A3G par Vif sur l'incorporation d'A3G (A et B) et sur l'infectivité virale (C).

De même, afin de séparer l'effet traductionnel de la dégradation d'A3G par Vif, ces expériences ont été réalisées en présence du dominant négatif de la Cullin 5. Nous avons alors observé que l'inhibition traductionnelle d'A3G par Vif réduit l'incorporation d'A3G dans les particules virales avec un profil de diminution d'A3G similaire à celui observé dans les cellules (Fig. 8A et 8B).

Dans un deuxième temps, nous avons mesuré l'infectivité des virions produits lors des tests précédents en utilisant des cellules indicatrices TZM-bl (mais cette fois-ci avec un clone moléculaire infectieux du VIH-1 - collaboration avec C. Moog de l'Institut de Virologie de Strasbourg). Ces expériences ont montré que l'inhibition traductionnelle d'A3G par Vif augmente l'infectivité virale de 50% (Fig. 8C, lignes 4 et 12).

Activité chaperon d'ARN de Vif

Finalement, en collaboration avec le Dr C. Tisné (Faculté de Pharmacie, Université Paris-Descartes), nous avons déterminé les domaines de la protéine Vif impliqués dans l'activité chaperon d'ARN. En utilisant des essais de dimérisation des fragments d'ARN du VIH-1, nous avons pu mettre en évidence que le domaine C-terminal de la protéine Vif était impliqué dans cette activité (Fig. 9). Ce résultat a été confirmé par des expériences d'hybridation des oligonucléotides d'ADN TAR du VIH-1 (Fig. 10).

CONCLUSIONS

En conclusion, Vif inhibe la traduction d'A3G *ex vivo* par un mécanisme dépendant de la partie 5'UTR et spécifiquement de la présence d'un uORF identifié dans les domaines D2 et D3 de cette région. Nous avons également montré que 50 % de la réduction d'A3G issu de l'activité de Vif est due à l'inhibition traductionnelle. L'inhibition traductionnelle d'A3G par Vif est capable de réduire l'incorporation d'A3G dans les particules virales ce qui donne lieu à une augmentation de 50% de l'infectivité virale. De plus, le domaine C-terminal de la protéine Vif est impliqué dans son activité chaperon d'ARN. Ces résultats nous ont permis de mieux comprendre ce phénomène de restriction cellulaire et pourraient être importants dans le développement de nouvelles stratégies d'inhibition de la réplication virale qui ciblerait spécifiquement l'interaction de Vif avec l'ARNm d'A3G.

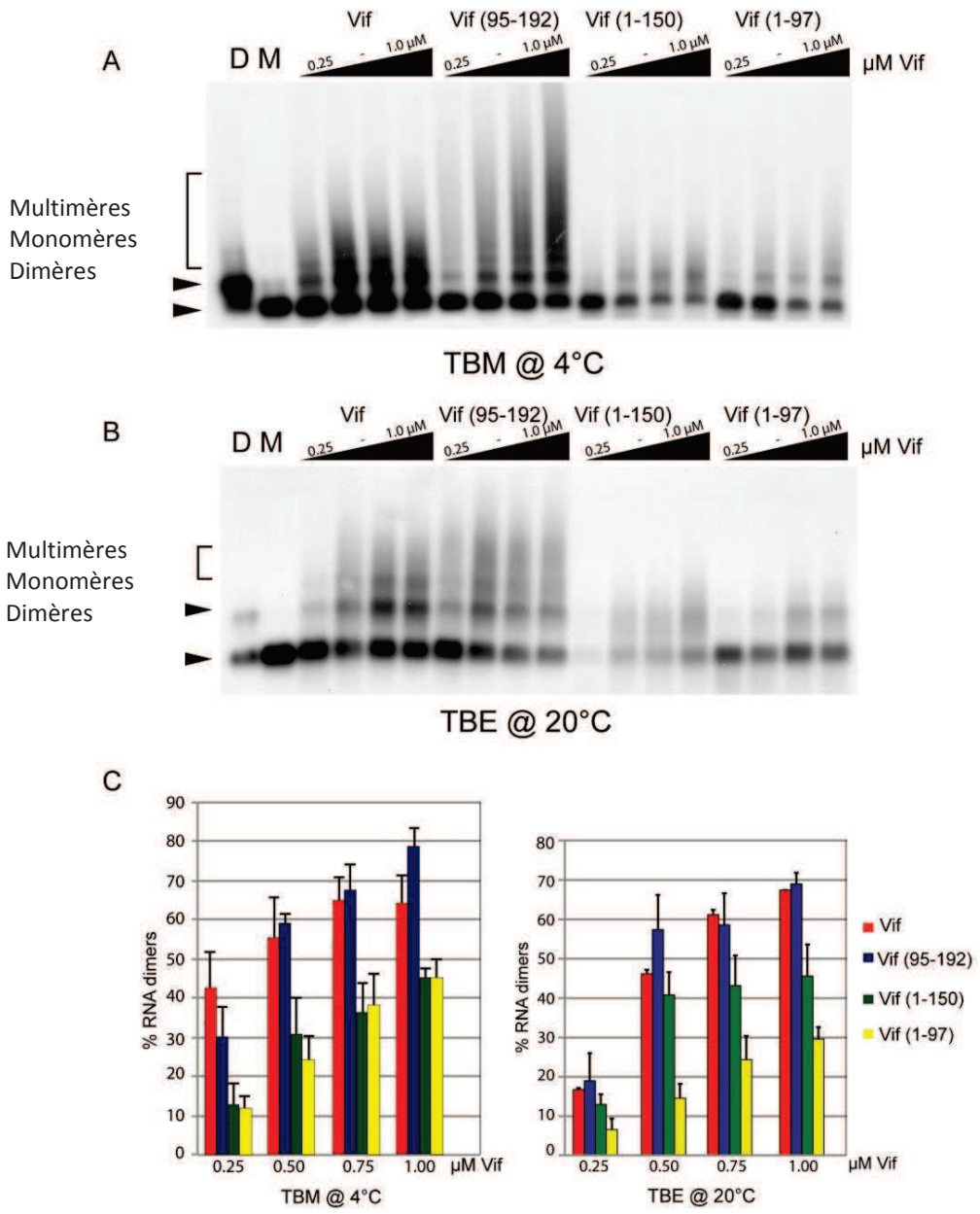

Figure 9. La dimérisation de l'ARN du VIH-1 est induite par Vif. L'ARN du VIH-1 1-615 a été utilisé dans une expérience de dimérisation en présence des concentration croissantes de Vif sauvage, Vif (95-192), Vif (1-150) et Vif (1-97) (0,25, 0,5, 0,75 et 1 µM) et migré dans un gel d'agarose native (0,8%) **(A)** ou semi-dénaturant **(B)**. Le pourcentage de dimères a été quantifié et représenté dans des histogrammes **(C).**

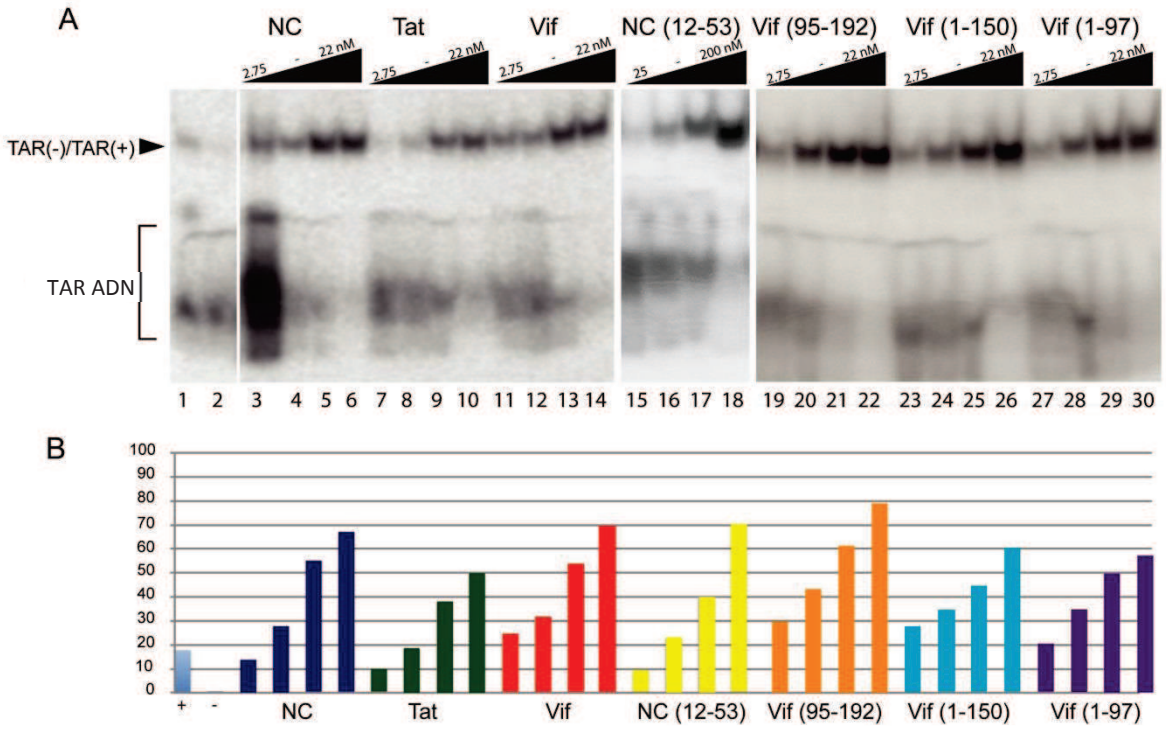

Figure 10. Stimulation de l'hybridation d'oligonucléotides TAR(+)/TAR(-) du VIH-1 par Vif et ses domaines. (A) Les oligonucléotides TAR(+) et TAR(-) ^{32}P ont été incubé en presence des concentrations croissantes du NCp7 (sauvage and fragment 12-53 comme control negative), Tat and Vif (sauvage et ses domaines). Les concentration des proteines ont été de 2,75, 5,50, 11 and 22 nM a l'exceptionse de NC (12-53) qui a été de 25, 50, 100 et 200 nM. Sans protéines, des dimères TAR(+)/TAR(-) ont été observés après 30 min. d'incubation à 65°C (Ct +, ligne 1). Les dimères TAR(+)/TAR(-) n'ont pas été formés à 37°C (Ct -, ligne 2). Les oligonucléotides TAR(+) et TAR(-) ^{32}P ont été hybridés pendant 5 min. à 37°C avec VIH-1 NCp7 (lignes 3-6), Tat (lignes 7-10), Vif (lignes 11-14), NC (12-53) (lignes 15-18), Vif (95-192) (lignes 19-22), Vif (1-150) (lignes 23-26), and Vif (1-97) (lignes 27-30). **(B)** Quantification des complexes TAR(+)/TAR(-).

VI. APPENDIX

Article 3: The role of Vif oligomerization and RNA chaperone activity in HIV-1 replication

In this review, we describe different aspects of Vif in HIV-1 replication. First, we present an overview on general characteristics and biological functions of Vif. We describe all different Vif-mediated pathways that lead to the reduction of A3G/F cellular levels. Vif targets A3G/F *via* two principal mechanisms: 1) Vif mediates A3G/F degradation through the proteasome (discussed in this review) and 2) Vif induces A3G/F translation inhibition (discussed below). Second, we present the structural organization of Vif and how its intrinsically disordered domains could play an important role in Vif multimerization and RNA chaperone activity. Finally, we show new experimental evidences that confirm Vif RNA chaperone activity.

Virus Research 169 (2012) 361–376

Contents lists available at SciVerse ScienceDirect

Virus Research

journal homepage: www.elsevier.com/locate/virusres

The role of Vif oligomerization and RNA chaperone activity in HIV-1 replication

Julien Batisse[a,1], Santiago Guerrero[a,1], Serena Bernacchi[a], Dona Sleiman[b], Caroline Gabus[c], Jean-Luc Darlix[c,2], Roland Marquet[a], Carine Tisné[b], Jean-Christophe Paillart[a,*]

[a] Architecture et Réactivité de l'ARN, Université de Strasbourg, CNRS, Institut de Biologie Moléculaire et Cellulaire, 15 rue René Descartes, 67084 Strasbourg, France
[b] Laboratoire de Cristallographie et RMN biologiques, Université Paris-Descartes, CNRS UMR 8015, 4 avenue de l'Observatoire, 75006 Paris, France
[c] Département de virologie Humaine, ENS-L, Université de Lyon I, INSERM-U758, 46 Allée d'Italie, Lyon, France

ARTICLE INFO

Article history:
Available online 21 June 2012

Keywords:
HIV-1
Vif
Protein oligomerization
RNA chaperone

ABSTRACT

The viral infectivity factor (Vif) is essential for the productive infection and dissemination of HIV-1 in non-permissive cells that involve most natural HIV-1 target cells. Vif counteracts the packaging of two cellular cytidine deaminases named APOBEC3G (A3G) and A3F by diverse mechanisms including the recruitment of an E3 ubiquitin ligase complex and the proteasomal degradation of A3G/A3F, the inhibition of A3G mRNA translation or by a direct competition mechanism. In addition, Vif appears to be an active partner of the late steps of viral replication by participating in virus assembly and Gag processing, thus regulating the final stage of virion formation notably genomic RNA dimerization and by inhibiting the initiation of reverse transcription. Vif is a small pleiotropic protein with multiple domains, and recent studies highlighted the importance of Vif conformation and flexibility in counteracting A3G and in binding RNA. In this review, we will focus on the oligomerization and RNA chaperone properties of Vif and show that the intrinsic disordered nature of some Vif domains could play an important role in virus assembly and replication. Experimental evidence demonstrating the RNA chaperone activity of Vif will be presented.

1. Introduction

Lentiviruses differ from simple retroviruses such as alpha and gamma retroviruses by the presence of regulatory genes in their genome. In addition to the structural and enzymatic proteins required for viral replication, HIV-1 encodes for several additional proteins. These proteins can be subdivided into two groups: the so-called essential proteins Tat and Rev and the auxiliary proteins, namely Nef, Vpr, Vpu and Vif. Although the latter proteins are not required for viral replication in certain tissue cultures, they are key factors for virus dissemination *in vivo* and pathogenesis.

The viral infectivity factor (Vif) is a highly basic 23 kDa protein that is essential for HIV-1 replication in non-permissive cells including lymphocytes, macrophages and a few T-cell lines (Fisher et al., 1987; Gabuzda et al., 1992; Madani and Kabat, 1998; Simon et al., 1998; Strebel et al., 1987; Zou and Luciw, 1996). Ten years ago, the group of M. Malim demonstrated that Vif neutralizes a potent intracellular innate defense that protects mammals from retrovirus infection and retro-elements that tend to persistently invade their genome (Malim and Emerman, 2008; Sheehy et al., 2002). This component of innate immunity, called APOBEC3G (apolipoprotein B mRNA-editing enzyme-catalytic, polypeptide-like 3G or A3G) is closely related to APOBEC1, a cytidine deaminase that causes a specific cytosine to uracil change in the apolipoprotein B mRNA (Teng et al., 1993). Other members of this family include APOBEC2, A3A to A3H, and the AID enzyme that causes hypermutation of immunoglobulin genes (Harris et al., 2002). Since then, A3G was found to be a potent cytidine deaminase that causes lethal hypermutations of HIV-1 and other retroviruses during cDNA synthesis by reverse transcriptase (RT) (Henriet et al., 2009; Lecossier et al., 2003; Mangeat et al., 2003; Mariani et al., 2003; Zhang et al., 2003). Beside its crucial counteracting activity against cellular antiviral factors, early studies revealed that Vif was also playing a role in virion assembly, favoring conformational rearrangements of the viral core (Borman et al., 1995; Hoglund et al., 1994; von Schwedler et al., 1993). It was proposed that Vif acts as a temporal regulator of viral assembly (Henriet et al., 2007). Although a large amount of data clearly showed the important role of Vif in viral pathogenesis, antiviral strategies aimed at inhibiting Vif in infected cells are slowed down due to the lack of structural information on Vif

Abbreviations: HIV-1, human immunodeficiency virus type 1; SIV, Simian immunodeficiency virus; RSV, Rous sarcoma virus; MuLV, murine leukemia virus; Vif, virion infectivity factor; APOBEC3G, apolipoprotein B mRNA-editing enzyme-catalytic, polypeptide-like 3G; SOCS, suppressor of cytokine signaling; NC, nucleocapsid protein; Tat, transcription activator protein; DLS, dimer linkage structure; PBS, primer binding site; PPT, polypurine tract.

* Corresponding author. Tel.: +33 3 88 41 70 35; fax: +33 3 88 60 22 18.
E-mail address: jc.paillart@ibmc-cnrs.unistra.fr (J.-C. Paillart).
[1] These authors equally contributed to this work.
[2] Present address: Laboratoire de Biophotonique et Pharmacologie, Faculté de Pharmacie, UMR 7213 CNRS, Université de Strasbourg, 67401 Illkirch, France.

0168-1702/$ – see front matter © 2012 Elsevier B.V. All rights reserved.
http://dx.doi.org/10.1016/j.virusres.2012.06.018

(Barraud et al., 2008). However recent biochemical studies revealed the importance of Vif oligomerization, conformation and flexibility in counteracting A3G and in binding RNA (Bergeron et al., 2010; Bernacchi et al., 2011; Marcsisin et al., 2011; Reingewertz et al., 2010; Wolfe et al., 2010). This prompted us to review the oligomerization and RNA chaperone activities of Vif involved in HIV-1 viral assembly and replication. Firstly we present an overview of the general characteristics and structural organization of Vif, and secondly we show that the intrinsically disordered domains of Vif could play an important role in Vif multimerization and RNA chaperone activity. Results demonstrating this latter activity are presented suggesting that this property may help Vif to achieve its pleiotropic functions during virus infection.

2. HIV-1 Vif: general characteristics and biological functions

2.1. Vif function in the infected cell

Vif is encoded for by all lentiviruses except for the Equine Infectious Anemia Virus. In HIV-1, the gene product is a 23 kDa basic protein that is produced in a Rev-dependent manner (Mandal et al., 2009) during the late phase of the replication cycle. This protein has been named Vif because its deletion has been associated with a reduction or a complete loss of viral infectivity (100–1000-fold) (Strebel et al., 1987). Interestingly, this phenotype is cell-type specific since Vif was shown to be required in cells termed non-permissive such as lymphocytes, PBMC, or macrophages (Borman et al., 1995; Courcoul et al., 1995; Fan and Peden, 1992; Gabuzda et al., 1992; Sova and Volsky, 1993; von Schwedler et al., 1993). By contrast, production of infectious particles does not require a functional Vif in permissive cell lines such as non-hematopoietic cells (HeLa, 293T, Cos7) and some leukemic T-cells (Jurkat, SupT1, C8166) (Gabuzda et al., 1992; Sakai et al., 1993). The observation that some, but not all cell lines require Vif for the production of infectious virus, could be explained by the fact that either permissive cells express a positive factor that substitutes for the absence of Vif, or else non-permissive cells express a negative factor that is counteracted by Vif. The fusion of these two cell types, giving rise to heterokaryons, exhibited a non-permissive phenotype indicating the presence of an intrinsic antiviral factor in non-permissive cells (Madani and Kabat, 1998; Simon et al., 1998). By using subtractive cDNA cloning analyses (permissive cells *versus* non-permissive cells), Sheehy and collaborators identified the cellular factor APOBEC3G, or A3G (Sheehy et al., 2002). When expressed in permissive cells, this factor renders these cells non-permissive for the replication of HIV-1Δ*vif* viruses (by reducing their infectivity) and northern blot analysis showed that A3G mRNAs were exclusively expressed in non-permissive cells (Sheehy et al., 2002). Altogether, these results showed that A3G is necessary and sufficient to confer the non-permissive phenotype to cells targeted by HIV-1.

2.2. The APOBEC3 family and its innate antiviral function

A3G is an enzyme member of the APOBEC family of cytidine deaminases, which includes (i) APOBEC1 and activation induced deaminase (AID) encoded for by genes arranged in tandem on chromosome 12, (ii) APOBEC2 located on chromosome 6 and (iii) A3A to A3H arranged in tandem on chromosome 22 (Jarmuz et al., 2002; Kitamura et al., 2011). A3G and A3F, the most closely related A3 family members, are expressed primarily in lymphoid and myeloid cell lineages (Jarmuz et al., 2002; Liddament et al., 2004; Wiegand et al., 2004). A3F constitutes the second highly potent anti-HIV host factor that specifically inhibits HIV-1Δvif infectivity and is sensitive to Vif (Liddament et al., 2004; Wiegand et al., 2004; Zheng et al., 2004). Although a consensus concerning anti-HIV activities of other A3 proteins has not currently been reached, it is now generally admitted that A3G, A3F, A3DE and A3H (under certain conditions) are sensitive to Vif, while A3A, A3B and A3C are probably not the most relevant factors for HIV-1 restriction *in vivo* (for a recent review, see Albin and Harris, 2010), except for A3A in monocytic cells (Berger et al., 2011).

A3 proteins contain one (A3A, A3C and A3H) or a duplication (A3B, A3DE, A3F, and A3G) of the catalytic site, which contains a Cys-His Zn^{2+} coordination motif characteristic of cytidine deaminases (Jarmuz et al., 2002). Concerning A3G, the second active site was shown to be the effective one (Shindo et al., 2003). In non-permissive cells, A3G and A3F are recruited into viral particles, leading to a ~1000-fold reduction in infectivity of HIV-1Δ*vif* (Liddament et al., 2004; Mariani et al., 2003; Marin et al., 2003; Sheehy et al., 2003; Stopak et al., 2003; Wiegand et al., 2004). This restriction results from an intense cytidine deamination of the newly made (−) strand viral DNA during reverse transcription (Harris et al., 2003; Mangeat et al., 2003; Zhang et al., 2003), causing G to A transitions within the (+) strand DNA (Lecossier et al., 2003). These transitions were found all over the genome, but with a graded frequency in the 5′ to 3′ direction suggesting that modifications occur preferentially in regions ((−) strand) that become and stay transiently single-stranded during the reverse transcription (regions 3′ to the PPTs and to the PBS) (Suspene et al., 2006; Yu et al., 2004a). The target sequence preference for A3 proteins has been extensively studied (Harris et al., 2003; Yu et al., 2004a; Zhang et al., 2003). A3G, for instance, preferentially mutates cytidine residues that are preceded by two cytidines (5′-CCC̲A-3′ in (−) strand DNA, the underlined nucleotide being targeted) (for review see Henriet et al., 2009). While G to A hypermutations resulting in lethal mutagenesis was initially believed to be the only mechanism of viral inhibition, it later appeared that these restriction factors can also inhibit viral replication independently of their enzymatic activity and interfere with primer $tRNA^{lys,3}$ annealing, (−) and (+) strand DNA transfer, viral DNA synthesis and integration (Anderson and Hope, 2008; Bishop et al., 2006, 2008; Guo et al., 2007; Holmes et al., 2007; Iwatani et al., 2007; Li et al., 2007; Luo et al., 2007; Mbisa et al., 2007; Miyagi et al., 2007; Newman et al., 2005; Yang et al., 2007).

2.3. Vif-mediated neutralization of APOBEC3G

The different mechanisms used by Vif to prevent the antiviral activity of A3G/3F have been extensively studied (Conticello et al., 2003; Liu et al., 2005; Marin et al., 2003; Mehle et al., 2004b; Sheehy et al., 2003; Stopak et al., 2003; Yu et al., 2003). The main mechanisms are briefly reviewed here (Fig. 1A), and readers can consult recent reviews for more detailed explanations (Albin and Harris, 2010; Henriet et al., 2009; Smith et al., 2009). Firstly, the inhibition of A3G packaging by Vif is associated with a strong reduction of its intracellular level, which has been attributed to the poly-ubiquitination and proteasomal degradation of A3G/3F by Vif (Conticello et al., 2003; Liu et al., 2005; Marin et al., 2003; Mehle et al., 2004b; Sheehy et al., 2003; Stopak et al., 2003; Yu et al., 2003). Indeed, Vif is able to bind A3G/3F through various domains (Fig. 2C), and to recruit an E3 ubiquitin ligase complex composed of Elongin B, C, Cullin 5, and Rbx2 leading to the poly-ubiquitination and degradation of A3G/3F (Luo et al., 2005; Mehle et al., 2004a, 2006; Yu et al., 2003) (Fig. 1A, pathway 2). Very recently, the transcription cofactor CBF-β (core binding factor β) has been shown to be an integral component of this ubiquitin ligase complex and to be required for Vif-mediated degradation of A3G (Hultquist et al., 2011b, 2012; Jager et al., 2011; Zhang et al., 2011). Besides, Vif has also been shown to counteract A3G by inhibiting its translation

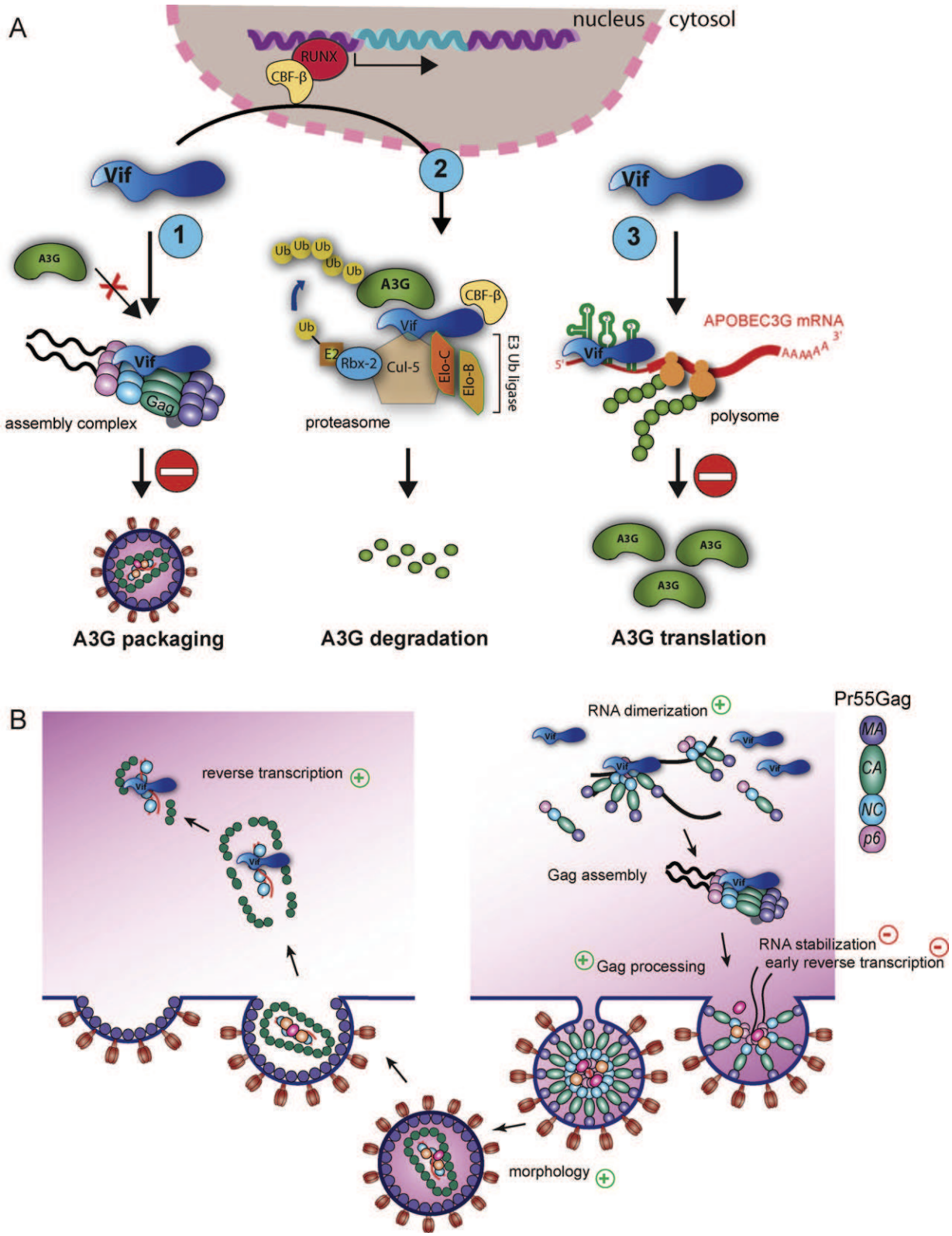

Fig. 1. Schematic representation of the functions of Vif and cellular A3G in the course of HIV-1 replication. (A) During viral particle assembly, Vif is found in the cytoplasm of infected cells and is packaged at a low copy number into virions. Vif neutralizes A3G/A3F in virus-producing cells by different mechanisms. (1) Vif competes with A3G for binding to viral components like the nucleocapsid domain of Gag and/or the genomic RNA. (2) Vif binding to A3G recruits an E3 ubiquitin ligase that mediates the poly-ubiquitynation of A3G and its degradation. (3) Vif impairs the translation of A3G mRNA through an mRNA-binding mechanism. Taken together, these three different actions of Vif on translation, degradation and packaging not only deplete A3G from virus-producing cells but also prevent A3G from being incorporated in virions. (B) Intracellular Vif may also influence viral assembly by regulating in a timely fashion genomic RNA dimerization and protease (PR)-mediated cleavage of the Gag precursor molecules. Due to its chaperone activities, Vif could facilitate late events such as Gag precursor maturation, RNA dimer maturation and initiation of reverse transcription during and after viral budding. Finally, Vif might participate in virion morphology and in reverse transcription after viral entry. The green "plus" and red "minus" signs indicate the positive and negative effects of Vif, respectively.

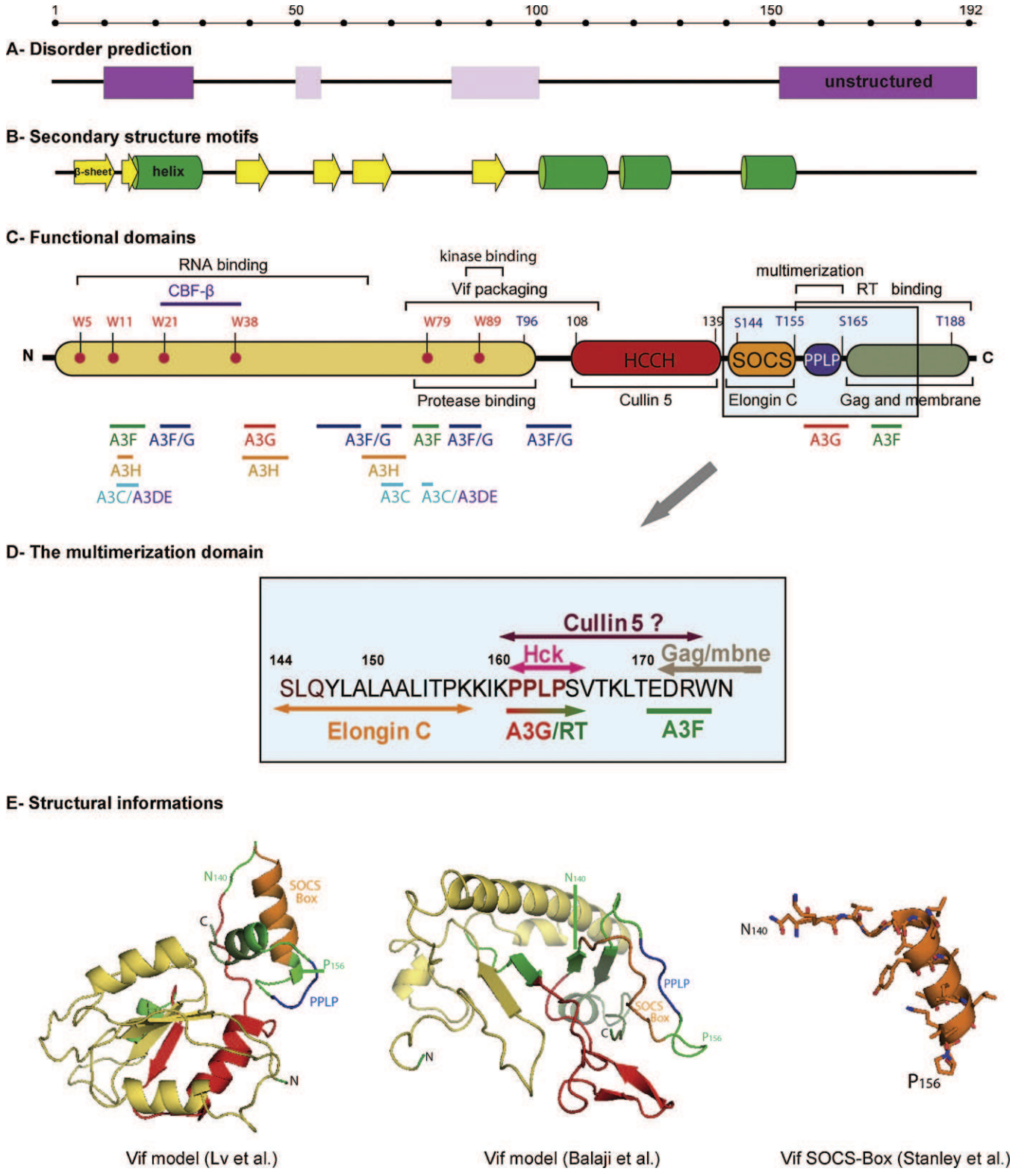

Fig. 2. Vif Sequence, structure and domains. (A) Vif disordered domain prediction according to Predictor of Naturally Disordered Regions (PONDR®): dark and light purple boxes correspond to highly disordered domains (PONDR score > 0.5), and slightly disordered domains (PONDR score between 0 and 0.2), respectively. (B) Vif secondary structure prediction showing strand in yellow arrows and helices in green was performed using PsiPred (McGuffin et al., 2000). (C) Schematic representation of Vif functional domains described in the text together with key residues and the interaction map with A3G, A3F, A3H, A3C, A3DE, and other Vif partners. (D) Vif multimerization domain, including the PPLP motif has been enlarged for a detailed description. (E) 3D structure of Vif. Left panel: structural model of Lv and collaborators (Lv et al., 2007), colored according to Vif functional domains in C; central panel: structural model (PDB: 1VZF) from Balaji and collaborators (Balaji et al., 2006); right panel: tridimensional structure of the Vif SOCS box (PDB: 3DCG – residues N_{140}–P_{156} – Stanley et al., 2008) with the same orientation as the left model.

(Fig. 1A, pathway 3) (Kao et al., 2003; Mariani et al., 2003; Stopak et al., 2003). Yet this process is not clearly understood, but our last study suggests that a steric hindrance mechanism may be considered as Vif was shown to specifically bind to the 5′-untranslated region (UTR) of A3G mRNA, that is required for the translational repression (Mercenne et al., 2010; Guerrero and Paillart, unpublished results). Lastly, the simplest way to prevent A3G activity is probably to prevent its packaging into virions (Sheehy et al., 2003), and indeed reports showed that Vif was able to impede packaging and counteract the antiviral activity of a degradation-resistant A3G variant (Fig. 1A, pathway 1) (Mariani et al., 2003; Opi et al., 2007). Interestingly, during virus assembly, A3G interacts with the nucleocapsid (NC) domain of $Pr55^{Gag}$ and the genomic RNA, while the same partners are involved in the packaging of Vif (Burnett and Spearman, 2007; Khan et al., 2005; Luo et al., 2004; Schafer et al., 2004; Svarovskaia et al., 2004; Zennou et al., 2004), suggesting that Vif may prevent A3G packaging by means of a competition mechanism.

2.4. Functions of Vif in virus assembly

Beside its action against the APOBEC3 restriction factors, Vif was found to be involved in the late steps of virus replication (Fig. 1B). Indeed Vif interacts with the $Pr55^{Gag}$ polyprotein precursor, that drives virus assembly, and the $Pr160^{Gag\text{-}Pol}$ precursor, possibly allowing its transient association with Gag assembly intermediates in the cytoplasm (Akari et al., 2004; Bardy et al., 2001; Bouyac et al., 1997; Lee et al., 1999). Accordingly Vif is able to counteract the effect of a betulinic acid derivative that inhibits HIV-1 Gag assembly (Dafonseca et al., 2008).

In addition, Vif, as an RNA-binding protein, can bind to the HIV-1 genomic RNA *in vitro* (Bernacchi et al., 2007; Henriet et al., 2005) and in infected cells (Dettenhofer et al., 2000; Zhang et al., 2000). This interaction seems to be required for Vif packaging, since inhibiting RNA packaging by mutating NC or the Psi packaging signal led to a complete absence of Vif in virions (Khan et al., 2001). This RNA-binding ability of Vif seems to be governed by its N-terminal domain (Fig. 2C) (Khan et al., 2001; Zhang et al., 2000).

Vif was also reported to be required for normal virion morphology and optimal core stability (Borman et al., 1995; Ohagen and Gabuzda, 2000; Sakai et al., 1993). As this defect has been exclusively observed in Δ*vif* virions produced from non-permissive cells, it is likely a (direct or indirect) consequence of the expression of the antiretroviral factors A3G/3F in these cells, even though the involvement of another cellular factor cannot be totally excluded. In fact, it is known that APOBEC3G inhibits some of the reverse transcription steps that require the RNA chaperone activities of NC (Guo et al., 2007; Iwatani et al., 2007; Yang et al., 2007). These are precisely the steps that Vif is able to activate (Henriet et al., 2007). As NC is a more potent RNA chaperone activity than Vif (Henriet et al., 2007), Vif would not be required in the absence of A3G (*i.e.* in permissive cells), however, it would be required in restrictive cells, because NC chaperone activities are inhibited by APOBEC3G in these cells.

Moreover, NC and RT were less stably associated with the viral core in HIV-1Δ*vif* particles (Hoglund et al., 1994), and $Pr55^{Gag}$ processing by the viral protease (PR) was altered at the MA-CA and CA-NC junctions (Akari et al., 2004; Bardy et al., 2001; Kotler et al., 1997). Even though Vif is dispensable for HIV-1 replication in permissive cells, it appears to be part of the HIV-1 replication machinery during early reverse transcription and acts as an helper factor to promote reverse transcription and viral infectivity (Carr et al., 2006, 2008; Henriet et al., 2007; Kataropoulou et al., 2009). Indeed, HIV-1Δ*vif* replicated normally in permissive cells under optimal *in vitro* replication conditions; however, HIV-1Δ*vif* replication was impaired at the level of reverse transcription when cells were treated with a thymidylate synthase inhibitor that altered the cellular dNTP levels, suggesting that preventing the A3G anti-viral action is not the only biological function of Vif.

Vif functions in virus assembly could be viewed as controversial (Henriet et al., 2009) because Vif modulates PR activity but does not prevent maturation of newly made virions. Along this line little Vif is found in cell-free virions (between 10 and 100 molecules, with a Vif/Gag ratio of 1/47 to 1/89) while it is found in large quantity in cells (Vif/gag ratio 1:1.1 to 1:1.3) (Fouchier et al., 1996; Simon et al., 1999). One hypothesis could be that Vif acts as a temporal regulator of $Pr55^{Gag}$ assembly and processing and should thus be considered as a Janus factor with both protein and RNA chaperone activities (Henriet et al., 2007; Kovacs et al., 2009; Tompa and Kovacs, 2010) (see Section 5). In accordance with this notion, Vif might prevent premature Gag processing in the cytoplasm of infected cells, and/or modulate PR activity, thus inhibiting premature reverse transcription (Akari et al., 2000; Bardy et al., 2001; Kotler et al., 1997; Mougel et al., 2009). This could be achieved either by direct transient interactions with PR and $Pr55^{Gag}$ or by modulating $Pr55^{Gag}$–RNA interactions. Thus, a competition mechanism preventing the majority of Vif from being recruited into viral particles can be envisioned where Vif acts in a transient manner.

3. Structural organization of Vif

3.1. Biochemical properties of Vif

The HIV-1 Vif protein is a small basic protein (pI = 10.7) composed of 192 amino acids (23 kDa) where the N-terminus is enriched in tryptophan residues (Fig. 2C). The presence of a high number of conserved hydrophobic amino acids (38.5% of Vif, including 8 tryptophan and 16 leucine residues) might well explain why Vif has a strong tendency to form aggregates in solution (Fig. 2C). Interestingly, each of these tryptophan residues has been shown to be important for the binding of either A3G or A3F (see below and Tian et al., 2006). Several amino acids (T_{96}, S_{144}, T_{155}, S_{165}, T_{188}) are potential targets for cellular kinases (such as MAPK) and their phosphorylation seems to play important roles in HIV replication (Yang and Gabuzda, 1998; Yang et al., 1996). Indeed, mutating T_{96} or S_{144} leads to a marked decrease in virus infectivity. Finally, the L_{150} residue has been shown to be a processing site for HIV-1 PR (Khan et al., 2002) since mutating this residue affected viral infectivity, suggesting that Vif processing is important for function.

Alignment of HIV-1 Vif sequences highlights several conserved domains that correlate with the predicted secondary structure of Vif (Barraud et al., 2008). At the N-terminus, amino acids ^{63}RLVITTYW^{70} and ^{86}SIEW^{89} are important to form β-sheet structures that are involved in the regulation of Vif expression and in viral infectivity (Fujita et al., 2003). The last two amino acids, E_{88} and W_{89} of this β-sheet structure are also part of a hydrophilic region ^{88}EWRKKR^{93} and are critical for the replication of HIV-1 in target cells by enhancing the steady-state expression of Vif (Fig. 2B) (Fujita et al., 2003). In the central region, residues 108–139 constitute a non-consensus HCCH zinc finger motif that binds zinc and Cullin 5 (Mehle et al., 2006; Xiao et al., 2006). Next to this HCCH motif is the so-called SOCS box (^{144}SLQYLA^{149}) (Fig. 2C) due to high similarities with boxes present in SOCS (suppressor of cytokine signaling) proteins. The last highly conserved domain is the ^{161}PPLP^{164} motif also known as the Vif multimerization domain (Fig. 2C and D) (Yang et al., 2001, 2003). Interestingly, this motif belongs to the C-terminal region of Vif, predicted to be intrinsically disordered (Reingewertz et al., 2009), while being involved in many important interactions (see below).

3.2. Structured and disordered domains of Vif

Due to its intrinsic properties, characterization of the 3D-structure of Vif is still a challenging problem and a matter of intense research. In fact Vif has a high tendency to aggregate in solution, which hampers the production of large amounts of soluble Vif required for crystallization assays and NMR studies. The 3D-structure of Vif has been predicted on the basis of model proteins that share similar secondary structure elements (Fig. 2E) (Balaji et al., 2006; Lv et al., 2007). High secondary structure similarities were found between both the N- and C-terminal domains of Vif and NarI and the SOCS Box from the VHL protein, respectively (Iwai et al., 1999). These proteins can also bind to Elongin B and C. Moreover, this model correctly fits with the secondary structure prediction shown in the alignment (Fig. 2B), contrary to the model of Balaji and collaborators which predicts only one helix (Fig. 2E). If such models are helpful to understand Vif protein organization, they unfortunately lack important Vif sequence information such as the HCCH zinc finger motif, as well as the long C-terminal region predicted to be disordered (Reingewertz et al., 2010), which constitutes another limiting factor for the crystallization of the full length Vif protein.

Yet only a very short fragment of Vif corresponding to the SOCS Box (residues 139–179) has been crystallized in a complex with Elongin B and C (Stanley et al., 2008). The crystal structure of a shorter fragment (residues 140–156) has been solved at 2.4 Å resolution (PDB: 3DCG), showing a loop-helix structure that forms a highly hydrophobic interface allowing binding to Elongin C (Fig. 2E). Interestingly, the structure of this peptide could fit in the predicted model of Lv and collaborators (in place of another helix) and could also be included in place of an unstructured sequence in the model of Balaji and collaborators (Fig. 2E – SOCS box in orange). Despite the lack of full-length Vif 3D-structure, the function of Vif has been extensively investigated by mutational and functional domain analyses. As for other HIV-1 accessory proteins, Vif appears to be a multifunctional protein with several domains involved in specific and/or overlapping functions, notably the disordered C-terminus (Tompa and Kovacs, 2010).

3.3. Functional domains of Vif

3.3.1. The N-terminal tryptophan rich domain: A3G, genomic RNA and CBF-β binding

As mentioned above, the N-terminal region of Vif is enriched in hydrophobic amino acids, notably in tryptophan residues that are conserved. Mutagenesis studies have shown that these residues are important for binding to either A3F or A3G. Binding to A3F requires residues W_{11}, W_{79}, Q_{12} and the ^{14}DRMR^{17} motif (Fig. 2C) (Russell and Pathak, 2007; Schrofelbauer et al., 2006; Tian et al., 2006). Interestingly, binding to A3G involves other residues, namely W_5, W_{21}, W_{38}, W_{89}, I_9, K_{22}, E_{45}, N_{48} and the ^{40}YRHHY^{44} and ^{85}VSIEW^{89} motifs that are the key residues for A3G binding (Fig. 2C) (Mehle et al., 2007; Russell and Pathak, 2007; Santa-Marta et al., 2005; Simon et al., 2005; Wichroski et al., 2005). Other domains have been described to be important for A3G binding, especially the PPLP motif in the C-terminal domain (Fig. 2C). Such discontinuous interacting sites suggest that the correct folding of Vif is crucial to generate the binding platform allowing interaction with APOBEC3 proteins. More recently, Vif residues important for interaction with A3H, A3C and A3DE have also been identified in the N-terminal region (Binka et al., 2012; Pery et al., 2009; Zhang et al., 2008; Zhen et al., 2010).

The N-terminal region of Vif and more precisely the first 64 amino acids are also involved in genomic RNA binding both *in vitro* (Bernacchi et al., 2007; Henriet et al., 2005) and in infected cells (Dettenhofer et al., 2000; Zhang et al., 2000). Deletion analysis underlined the importance of amino acids 75–114 for the binding of Vif to RNA in infected cells (Khan et al., 2001). CBF-β (core binding factor β), a partner of Vif involved in the E3 ubiquitin ligase recruitment, has recently been identified and the interaction domain mapped to the N-terminal domain of Vif, with an important role for W_{21} and W_{38} (Hultquist et al., 2011a; Jager et al., 2011; Zhang et al., 2011). Finally, Vif binds to the viral PR through residues 78–98 (Baraz et al., 2002) and to the cellular MDM2 E3-ligase involved in its degradation by the proteasome (Izumi et al., 2009).

3.3.2. The HCCH central zinc finger domain

One of the major functions of Vif is to recruit an E3 ubiquitin ligase in order to target A3G for proteasomal degradation. The E3 ligase recruited by Vif is composed of Elongin B, Elongin C, CBF-β, Cullin 5, and Rbx2 proteins (Yu et al., 2003). The Cullin 5 binding domain (Yu et al., 2004b) involves residues C_{114} and C_{133} of the conserved HCCH zinc finger motif (Xiao et al., 2007) of the form H^{108}-$(X)_5$-C^{114}-$(X)_{18}$-C^{133}-$(X)_5$-H^{139}, that is different from a conventional zinc finger. In fact its primary structure is not found in other classes of zinc binding proteins and thus can be considered to be Vif specific. This motif represents a *bona fide* zinc finger (Mehle et al., 2006; Xiao et al., 2007), where each zinc-coordinating residue has been shown to be important for the binding of Cullin 5. Changing sequences and spacing between HCCH residues affected the binding to Cullin 5, viral infectivity, and A3G degradation (Mehle et al., 2006). Interestingly, the conformation of both the HCCH motif and the whole Vif protein is altered upon zinc binding (Paul et al., 2006). Moreover, the aggregation of Vif is favored by zinc, but in a reversible manner (Paul et al., 2006).

3.3.3. The SOCS box: Elongin C binding domain

This highly conserved sequence is composed of residues ^{144}SLQ-(Y/F)-LA^{149} and alanine substitution in the SLQ motif leads to important defects in virus infectivity (Schmitt et al., 2009). This region promotes the interaction with the heterodimer Elongin C/Elongin B (Yu et al., 2004b) and is therefore important for the recruitment of the E3 ubiquitin ligase that targets A3G for degradation. This interaction occurs *via* a hydrophobic platform on both proteins (Wolfe et al., 2010), requiring the SLQ residues and the last A_{149} of the motif (Yu et al., 2004b) together with α-helix 4 of Elongin C (Stanley et al., 2008). Very recently, it has been shown that interactions between Vif and Elongin C/B also involve downstream elements such as the Cullin 5 box and the ^{161}PPLP^{164} motif (see below and (Bergeron et al., 2010; Wolfe et al., 2010))

3.3.4. The intrinsically disordered C-terminal domain

The C-terminal region of Vif is intrinsically disordered (Fig. 2A) and starts with a putative Cullin 5 box (residues 159–173), that is able to recruit Cullin 5 (Stanley et al., 2008) but with a lower efficiency compared to the HCCH zinc finger domain (Wolfe et al., 2010). This region encompasses the ^{161}PPLP^{164} motif involved in Vif multimerization (Fig. 2D) (Yang et al., 2001, 2003). This PPLP motif is also involved in the interaction with various partners such as A3G (Donahue et al., 2008; Miller et al., 2007), Elongin B/Cullin 5 (Bergeron et al., 2010; Wolfe et al., 2010), HIV-1 RT (Kataropoulou et al., 2009) and the cellular kinase Hck (Douaisi et al., 2005; Hassaine et al., 2001). Finally, the last 25 residues are important for Vif interaction with $Pr55^{Gag}$ (Bouyac et al., 1997; Simon et al., 1999; Syed and McCrae, 2009), cytoplasmic membranes (Goncalves et al., 1995) and RT (Kataropoulou et al., 2009).

The disordered nature of the C-terminal region (see Fig. 2A) is in line with secondary structure prediction models (Reingewertz et al., 2010) and the 3D-structure analysis of Vif where only the first 15 amino acids of the analyzed peptide (40 residues) have been observed. No electron density was detected for the rest of the

protein, reflecting the intrinsically disordered nature of the C-terminus (Stanley et al., 2008). Deuterium incorporation assays showed that this small part of Vif folds upon binding to Elongin C, which is also refolded upon Vif binding (Marcsisin and Engen, 2010). Such Vif-induced folding has also been observed in our laboratory upon Vif binding to specific RNA sites such as the Trans-acting Responsive element (TAR) (see below and Bernacchi et al., 2011).

4. Vif multimerization

Vif multimerization was initially detected *in vitro* by GST pull-down, co-immunoprecipitation and two hybrid assays (Yang et al., 2001). A deletion mutagenesis approach allowed to characterize residues 151–164, encompassing the conserved proline-rich region ^{161}PPLP^{164}, as the domain governing Vif multimerization. The importance of this ^{161}PPLP^{164} motif has been later highlighted using competitor peptides and deletion/substitution mutants (Bernacchi et al., 2011; Yang et al., 2003). Recently, this motif has been shown to be required for the assembly of an active E3 ubiquitin ligase complex, as a second binding motif for the Elongin C/B and Cullin5 (Bergeron et al., 2010; Wolfe et al., 2010).

4.1. Importance of the Vif PPLP motif in HIV-1 replication

This motif was found to be important for Vif function and virus infectivity since mutating this motif resulted in a 2.5-fold reduction of infectivity in non-permissive cells (Donahue et al., 2008) and antagonist peptides containing the ^{161}PPLP^{164} motif drastically diminished virus replication (Miller et al., 2007; Yang et al., 2003). The reduced virus infectivity could be explained in both cases by the lost of Vif A3G-degradation function. Indeed, Miller and coworkers (Miller et al., 2007) showed that the antagonist peptides were associated with an augmented A3G packaging into viral particles. Donahue and collaborators showed that substituting AALP for PPLP impaired Vif-induced degradation of A3G, which was mainly due to the reduced binding of A3G, without affecting the interaction with Elongin C and Cullin 5 (Donahue et al., 2008). Similarly, this substitution favored A3G incorporation into virions but did not abrogate the translational regulation of A3G mRNA by Vif (Mercenne et al., 2010). However, the PPLP motif does not seem to be the only one to be involved in Vif multimerization as a recent study pointed out the involvement of domains such as the HCCH motif, the BC box and downstream residues (S165 and V166) in this property of Vif (Techtmann et al., 2012). It is also interesting to notice that while the PPLP motif is conserved in all HIV-1 isolates, this motif is absent in HIV-2 and SIV Vif (Barraud et al., 2008) and the C-terminal regions are the most divergent, beside the fact that both HIV-2/SIV Vif proteins are 25 amino acids longer than the HIV-1 Vif (Yamamoto et al., 1997). Whereas the HIV-1 Vif C-terminal region is highly hydrophilic (and seems important for the association with membranes), the same region of HIV-2 Vif is hydrophobic. Finally, while both Vif proteins have the same functions and are interchangeable in some cellular conditions (Reddy et al., 1995), differences in some structural domains (oligomerization domain for instance) may suggest that the mechanism of action of HIV-1 and HIV-2/SIV Vif proteins may not be completely identical. Up to now, oligomerization properties of HIV-2/SIV Vif proteins are unknown.

4.2. RNA binding and Vif folding

As mentioned above, the PPLP motif is located in a strategic binding platform for Vif partners. With respect to the involvement of the PPLP motif in Vif oligomerization, it is conceivable that the functions of those partners could be linked to the multimerization state of Vif. We recently report that alanine substitution of the PPLP motif (Vif-AALA) did not significantly affect the overall secondary structure of Vif, but affects its oligomerization state (Bernacchi et al., 2011). Nevertheless, Dynamic Light Scattering experiments showed that the AALA Vif mutant was still able to form protein dimers, suggesting that other domains are involved in Vif-Vif interactions, as mentioned in another study using deuterium exchange assays (Marcsisin and Engen, 2010). Mutating the PPLP motif also led to a decrease of Vif binding affinity and specificity for nucleic acids (Bernacchi et al., 2011).

Interestingly, the high affinity binding of wild-type Vif to the TAR element led to the formation of high molecular mass complexes and was associated with Vif folding since the proportion of disorder, defined by circular dichroism experiments, decreased from 40% in absence of RNA to less than 20% in presence of TAR, and β-sheet structures increased from 40% to 70%. This folding process was not observed when AALA was substituted for the PPLP motif (Bernacchi et al., 2011). Altogether, these results showed that both the PPLP motif and RNA binding are important to induce, at least in part, Vif folding. As mentioned above, the Vif-Elongin C interacting domain has also been shown to undergo structural rearrangements upon binding (Marcsisin and Engen, 2010).

These observations strongly suggest that Vif (or at least its C-terminal domain) is disordered in its free form and can fold upon interactions, thus ensuring multiple functions (He et al., 2009). These properties are characteristic of proteins with RNA and/or protein chaperone activities (Tompa and Kovacs, 2010): as a general mechanism, such protein–protein and protein–RNA interactions induce the folding of both the chaperone and the target molecules upon binding, forming a functional complex (Semrad, 2011; Tompa and Csermely, 2004). This has already been described for several HIV-1 proteins such as the NC protein (Muriaux and Darlix, 2010; Rein, 2010) and more recently proposed for the Tat protein (Xue et al., 2011). This new potential role of Vif and its impact on HIV-1 replication are described below.

5. RNA chaperone activity of Vif

The three-dimensional structure of cellular and viral RNA molecules is crucial for function, but RNA molecules tend to adopt non-functional structures due to kinetic and thermodynamic folding traps (Herschlag, 1995). In order to prevent and resolve these non-functional conformations, proteins with RNA chaperone activity are essential during the RNA folding process (Cristofari and Darlix, 2002). An RNA chaperone is defined as a partially disordered protein that binds transiently and non-specifically to RNA molecules, preventing their misfolding in an ATP independent-manner. Once the RNA has been correctly folded, the protein is no longer needed and the RNA conformation remains stable (Cristofari and Darlix, 2002).

Proteins with RNA chaperone activity are widespread and are implicated in essential cellular functions (Rajkowitsch et al., 2007). The list of RNA chaperones is constantly increasing and a database has been constructed (http://www.projects.mfpl.ac.at/rnachaperones/index.html) in which RNA chaperones are classified into families according to their primary function (Rajkowitsch et al., 2007). Here, we will focus on retrovirus-encoded RNA chaperones, specifically those encoded by HIV-1.

Nucleocapsid proteins (NCp) from Rous sarcoma virus (RSV) and murine leukemia virus (MuLV) were the first retrovirus-encoded RNA chaperones to be described (Prats et al., 1988). Later, the RNA chaperone activity of HIV-1 NC was documented using different approaches. *In vitro*, HIV-1 NC increases hammerhead-ribozyme

cleavage of an RNA substrate (Tsuchihashi et al., 1993), facilitates annealing of complementary DNA oligonucleotides and promotes strand exchange between complementary double-stranded and single-stranded DNA oligonucleotides (Tsuchihashi and Brown, 1994). In cell culture, NCp efficiently increases splicing of a thymidylate synthase mRNA mutant in a HIV-1 folding trap assay (Clodi et al., 1999). It has also been reported that in addition to NCp7, Vif and the transcription activator (Tat) possess RNA chaperone activity (Henriet et al., 2007; Kuciak et al., 2008).

Next, we will briefly summarize the RNA chaperoning activity of Vif in parallel with that of NCp7 and Tat, and discuss how this could influence virus assembly and Gag processing, thus regulating the final stage of virion formation including reverse transcription by means of a molecular crowding phenomenon where Vif in excess has a negative impact on NC functions, which is relieved once virions are released from the cells and matured (Darlix et al., 2011).

5.1. Dimerization of the genomic RNA

During virus assembly, the full-length viral genomic RNA is packaged in the form of a dimeric RNA (Chen et al., 2009; Housset et al., 1993) where the two copies are physically linked through a site called the dimer linkage structure (DLS) located close to their 5′ ends. Dimerization and subsequent packaging of the HIV-1 RNA dimer are mediated by interactions between the NC domain of $Pr55^{Gag}$ and the 5′-end of the viral genome (reviewed in Lu et al., 2011; Paillart et al., 1996, 2004; Russell et al., 2004). The HIV-1 genomic RNA can form two different kinds of dimers *in vitro*, termed loose and tight dimers, which are defined by their low or high thermostability, respectively (Paillart et al., 2004). This dimeric structure is important for viral infectivity (Shen et al., 2000). It has been shown that NCp promotes the formation of HIV-1 RNA loose and tight dimers and stabilizes the resulting dimeric structure (Muriaux et al., 1996). *In vitro*, Vif alone was also capable of stimulating the formation of the loose HIV-1 RNA dimer, but not formation of the tight dimer, at least when using long RNA fragments (600-nt long RNA). Interestingly, Vif also significantly inhibited NCp-induced tight RNA dimer formation. This inhibition might temporally prevent premature tight dimer formation in the cytoplasm of infected cells and thus assembly (Henriet et al., 2007; Cimarelli and Darlix, 2002).

5.2. Initiation of reverse transcription

Reverse transcription is primed by the annealing of the cellular $tRNA^{Lys,3}$ onto the primer binding site (PBS) in the 5′ region of the viral RNA genome. The $tRNA^{Lys,3}$ is selectively packaged into virions and used as a primer for reverse transcriptase (RT) to initiate minus-strand strong stop DNA synthesis ((−) ssDNA) (reviewed in Isel et al., 2010). HIV-1 NCp chaperones the annealing of the $tRNA^{Lys,3}$ primer onto the PBS by facilitating structural changes in the $tRNA^{Lys,3}$ as well as in the viral RNA (Barraud et al., 2007; Brule et al., 2002; Hargittai et al., 2004; Isel et al., 1995; Tisné, 2005; Tisné et al., 2004).

Henriet and collaborators showed that Vif can also promote the annealing of $tRNA^{Lys,3}$ to the PBS, which generates a functional $tRNA^{Lys,3}$/RNA complex, even though Vif was less efficient than the NC proteins used in this study (NCp15, NCp9 and NCp7) (Henriet et al., 2007). Interestingly, Vif also significantly inhibited NC-induced $tRNA^{Lys,3}$ annealing. This inhibition was observed using a Vif/NC ratio of 1/3, which is similar to the 1/2 Vif/$Pr55^{Gag}$ ratio in the assembly complexes in producing cells (Fouchier et al., 1996; Simon et al., 1999). However, in HIV-1 virions the Vif/NC ratio drops down to 1/20 to 1/40 and the inhibitory effect is then relieved. It has thus been proposed that Vif might be a temporal regulator, preventing premature initiation of reverse transcription (Henriet et al., 2007). During virus assembly, the high concentration of Vif would inhibit NC-mediated $tRNA^{Lys,3}$ annealing through an interaction with the genomic RNA and the NC domain of $Pr55^{Gag}$ (Henriet et al., 2007). This hypothesis could explain that mutations in NC cause premature reverse transcription (Didierlaurent et al., 2008; Houzet et al., 2008) since such mutations could destabilize the interaction between Vif, the genomic RNA and the NC domain of $Pr55^{Gag}$.

In a manner similar to NCp7 and Vif (Beltz et al., 2003), Tat can anneal primer $tRNA^{Lys,3}$ onto the PBS of the HIV-1 RNA genome (Kameoka et al., 2002). Similarly to Vif, Tat might well regulate premature initiation of reverse transcription by inhibiting the RT activity (Kameoka et al., 2001). This inhibition is observed at high concentrations of Tat and during the late stages of viral replication (Kameoka et al., 2001). However, at a low concentration possibly found in viral particles (Chertova et al., 2006), Tat might be able to promote $tRNA^{Lys,3}$ annealing onto the PBS (Kameoka et al., 2002) and to stimulate reverse transcription through an interaction with RT (Apolloni et al., 2007).

5.3. Minus-strand DNA transfer

Once the (−) ssDNA has been synthesized by RT, it must be transferred onto the 3′-end of the viral genome to resume elongation of the (−)-strand DNA. This transfer is achieved by the annealing of the repeat regions (R) (containing the TAR element) at the 3′ ends of the (−) ssDNA and the (+) sense viral RNA (Basu et al., 2008). NCp7 chaperones minus-strand DNA transfer by promoting the annealing of the complementary (+) and (−) TAR sequences and preventing non-specific self-priming reactions (Driscoll and Hughes, 2000; Guo et al., 1997; Li et al., 1996). Vif is also able to stimulate (−) ssDNA transfer, although with a reduced efficiency compared to NC proteins (NCp15, NCp9 and NCp7) (Henriet et al., 2007). It was later demonstrated that Tat can also anneal complementary TAR DNA sequences and to promote DNA strand displacement (Kuciak et al., 2008). A recent fluorescence study shed light on the mechanism of action (Boudier et al., 2010). In the presence of Tat, the complementary sequences anneal through their stem termini, forming an intermediate with 12 intermolecular base pairs that is finally converted to an extended duplex. This mechanism is similar to that of NCp-induced annealing, except that Tat only marginally destabilizes the TAR structure and acts at much lower oligonucleotide fractional saturation (Boudier et al., 2010). In the same study Tat was also shown to cooperate with NCp in annealing the complementary TAR sequences. In addition, it was reported that the TAR DNA annealing activity of NCp7 was efficiently inhibited by small 2′O-methylated oligoribonucleotides (mODN). These mODNs are potent inhibitors of the HIV-1 reverse transcription complex (Grigorov et al., 2011).

5.4. Minus-strand DNA elongation

During (−) strand DNA elongation, RT has to resolve secondary structures in the RNA template causing pausing and eventually premature termination of DNA synthesis. The nucleic acid chaperone activity of NCp reduces RT pausing by transiently destabilizing these RNA secondary structures, thus promoting minus-strand DNA elongation (Ji et al., 1996; Wu et al., 1996). Vif is also capable of reducing RT pausing and enhancing minus-strand DNA elongation (Henriet et al., 2007). To support this observation, it was shown that Vif and NCp7 bind to several secondary structure motifs in the 5′-UTR of the genomic RNA (Bernacchi et al., 2007; Henriet et al., 2005). These results indicate that both NCp and Vif reduce RT pausing and promote RT processivity (Bampi et al., 2006).

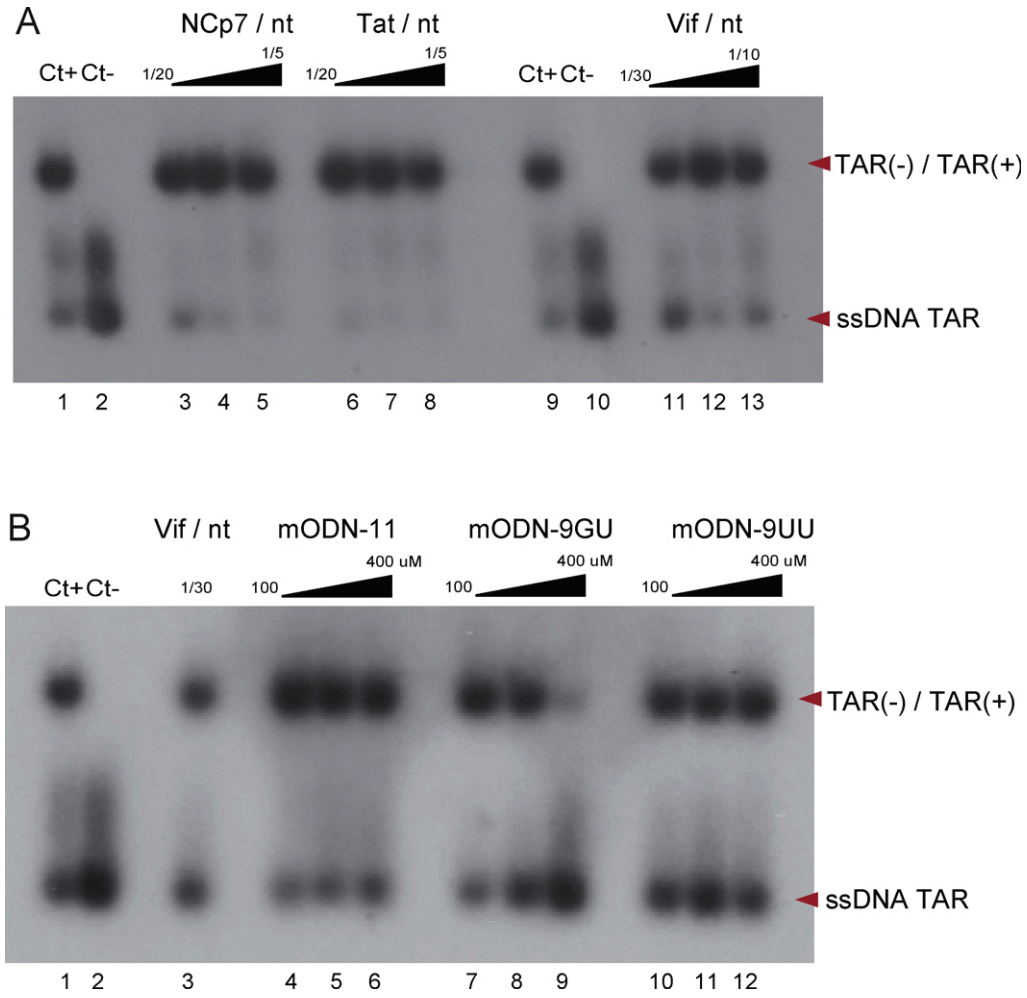

Fig. 3. Stimulation of HIV-1 TAR(+)/TAR(−) DNA annealing by Vif. (A) TAR(+) and ^{32}P-labeled TAR(−) DNA oligonucleotides were co-incubated in the presence of increasing concentrations of NCp7, Tat and Vif. In the absence of protein, double-stranded TAR DNA was formed by annealing upon incubation at 65 °C for 30 min (Ct+, lanes 1 and 9) but not at 37 °C (Ct−, lanes 2 and 10). Lanes 3–5: TAR(+)/TAR(−) annealing at 37 °C for 5 min with HIV-1 NCp7 at protein/nt molar ratios of 1/20, 1/10 and 1/5. Lanes 6–8: TAR(+)/TAR(−) annealing at 37 °C for 5 min with HIV-1 Tat at protein/nt molar ratios of 1/20, 1/10 and 1/5. Lanes 11–13: TAR(+)/TAR(−) annealing at 37 °C for 5 min with HIV-1 Vif at protein/nt molar ratios of 1/30, 1/15 and 1/10. (B) Inhibition of Vif-mediated TAR DNA annealing by methylated ODNs (mODN). TAR(+) and ^{32}P-labeled TAR(−) DNA were co-incubated in the presence of HIV-1 Vif and increasing concentrations of either one of the mODNs. Upon annealing in the absence of protein at 65 °C for 30 min a double-stranded TAR DNA was formed (Ct+, lane 1) but not at 37 °C (Ct−, lane 2). Lane 3–12: TAR(+)/TAR(−) annealing at 37 °C for 5 min with HIV-1 Vif at protein/nt molar ratio of 1/30 in the absence of mODN (lane 3) or with increasing concentrations (100–400 μM) of mODN-11 (lanes 4–6), mODN-9GU (lanes 7–9), and mODN-9UU (lanes 10–12), respectively.

5.5. Plus-strand DNA transfer

As (−) strand DNA synthesis proceeds, RT initiates (+) strand DNA synthesis using a polypurine tract (PPT) as a primer. The resulting short DNA product is known as the positive strong-stop DNA ((+) ssDNA). In order to complete (+) strand DNA synthesis, (+) ssDNA must be transferred to the 3′ end of the (−) strand DNA. During this process, the PBS sequence at the 3′ end of (+) ssDNA anneals to the (−) PBS sequence at the 3′ end of the (−) strand DNA to form a circular intermediate (reviewed in Basu et al., 2008). These complementary PBS sequences cannot be annealed unless the primer tRNA is cleaved off from the 5′-end of the (−) strand DNA. Acting as a nucleic acid chaperone, NCp favors tRNA primer removal and chaperones PBS annealing (Isel et al., 2010).

In the next section, we present experimental evidences that extend our knowledge on the RNA chaperone properties of Vif by analyzing the annealing of DNA oligonucleotides TAR(−)/TAR(+), the dimerization of HIV-1 RNA fragments and the enhancement of ribozyme-directed RNA substrate cleavage by Vif, in parallel with HIV-1 NCp7.

6. The RNA chaperone activity of HIV-1 Vif: experimental evidence

6.1. Materials and methods

6.1.1. DNA and RNA substrates

Oligodeoxynucleotides (ODNs) used for the TAR(−)/TAR(+) DNA annealing assay corresponded to nucleotides 1–56 of the HIV-1 RNA sequence (MAL isolate) in the sense and antisense orientations, as previously described in Kuciak et al. (2008). RNA fragments used in the RNA dimerization assay corresponded to nts 1–311 of the HIV-1 MAL isolate. The R3 ribozyme and the S14 substrate RNAs were used for the hammerhead ribozyme cleavage assay. Methylated oligoribonucleotides mODN-11, mODN-9GU, mODN-9UU and non-methylated ODN-12 are described in Grigorov et al. (2011).

6.1.2. In vitro transcribed RNAs

RNAs used for the ribozyme assay were synthesized by *in vitro* transcription with T7 RNA polymerase as previously published (Kuciak et al., 2008). For dimerization assay, RNA 1–311 was obtained from run-off transcription of plasmid pJCB that was

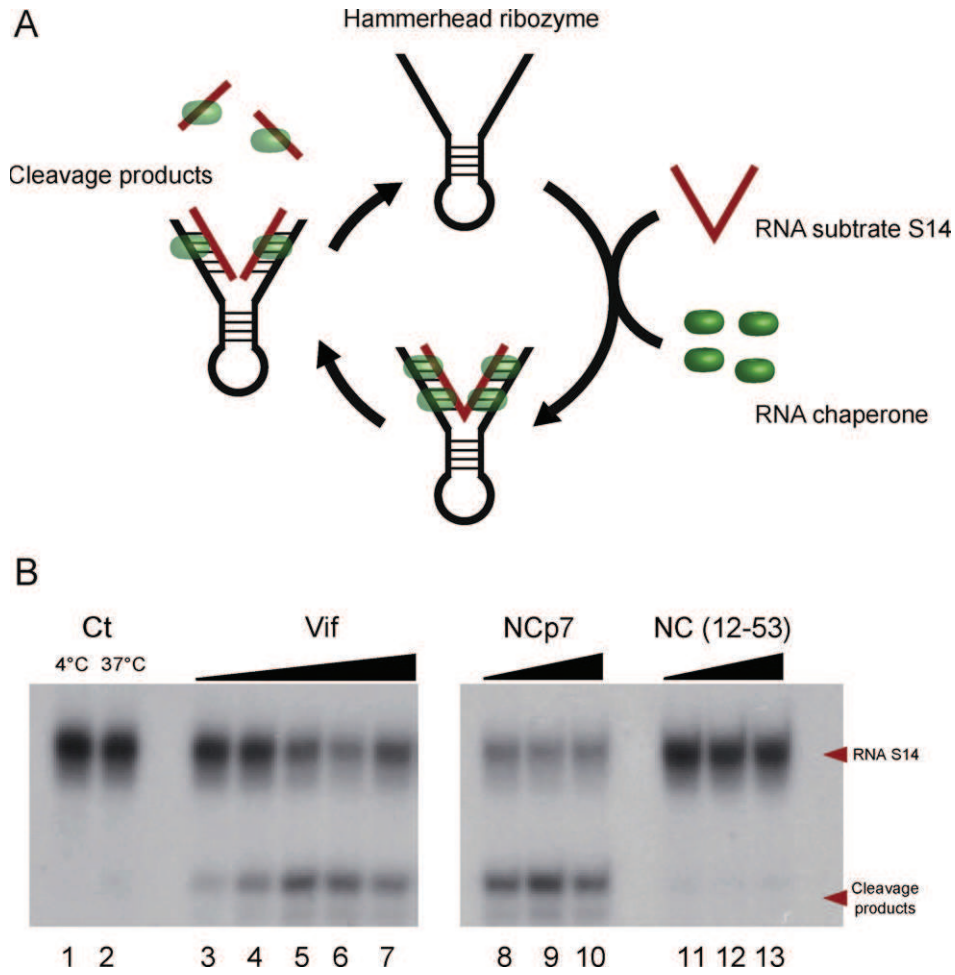

Fig. 4. Enhancement of hammerhead ribozyme-induced cleavage by HIV-1 Vif protein. (A) Schematic representation of hammerhead ribozyme cleavage of RNA. (B) R3 ribozyme and an excess of the S14 substrate RNA were co-incubated with increasing concentrations of Vif, NCp7 and NCp(12–53). RNA S14 is 61 nts in length, while the cleavage product is 49 nts long. Lanes 1 and 2: control cleavage of the RNA S14 substrate by the hammerhead ribozyme for 30 min at 4 °C or 37 °C. Lanes 3–13: incubation for 10 min with Vif at protein/nt molar ratios of 1/50, 1/40, 1/30, 1/20 and 1/15 (lanes 3–7), with NCp7 at protein/nt molar ratios of 1/20, 1/10, 1/5 (lanes 8–10) and with NCp(12–53) at protein/nt molar ratios of 1/10, 1/5, 1/2 (lanes 11–13).

linearized using Rsa I restriction endonuclease (Henriet et al., 2005). Reverse transcription of a viral RNA fragment corresponding to the very 3′ 620 nts of the HIV-1 genomic RNA was as described in Kuciak et al. (2008).

6.1.3. Proteins

Wild-type HIV-1 Vif protein was expressed in *Escherichia coli* with an N-terminal 6-His tag and purified as previously described (Bernacchi et al., 2011). HIV-1 NCp7 and NC(12–53) were synthesized and purified as described in Ivanyi-Nagy et al. (2008). HIV-1 Tat protein was synthesized as reported in Ivanyi-Nagy et al. (2008) and Kuciak et al. (2008).

6.1.4. TAR(−)/TAR(+) DNA annealing assay

The DNA annealing assay was performed as described in Grigorov et al. (2011). Briefly, 0.03 pmol of the TAR(+) and ^{32}P-TAR(−) ODNs were incubated in 10 μl of buffer A (25 mM Tris-HCl, 0.2 mM $MgCl_2$ and 30 mM NaCl) with increasing concentrations of Vif, NCp7 or Tat proteins, as indicated in the figure legends (Fig. 3). In an attempt to inhibit the nucleic acid chaperoning activity of Vif, we used 2′O-methylated oligoribonucleotides (mODN) at increasing concentrations (100–300 nM) since such mODNs were found to strongly inhibit NCp7 *in vitro* and HIV-1 replication in T cells and macrophages (Grigorov et al., 2011). First viral proteins of interest were pre-incubated with the mODNs and subsequently used in the annealing assay (see below). Annealing reactions were performed at 37 °C for 5 min except for the positive control that was incubated at 65 °C for 30 min and put at 4 °C. To stop the reaction and remove the protein from the ^{32}P-ODN, 5 μl of a solution containing 20% glycerol, 20 mM EDTA pH 8.0, 2% SDS, 0.25% bromophenol blue and 0.4 mg/ml calf liver tRNA were added. Samples were resolved by 8% native PAGE in 50 mM Tris–borate pH 8.3, 1 mM EDTA at 4 °C. Subsequently, gels were autoradiographed and the amounts of labeled single-stranded and double-stranded DNA were assessed by phosphorimaging.

6.1.5. Hammerhead ribozyme cleavage assay

Hammerhead ribozyme cleavage assay was carried out as previously described (Kuciak et al., 2008). Briefly, ribozyme and substrate RNAs were independently heated for 1 min at 90 °C in water. The reaction buffer was added to final concentrations of 5 mM $MgCl_2$, 100 mM NaCl, 20 mM Tris–HCl, pH 7.5. After slow cooling to 37 °C, RNAs were incubated for 5 min at 20 °C. Ribozyme (0.02 pmol) and RNA substrate (0.08 pmol) were then combined in a final volume of 10 μl. NCp7, NC(12–53), Vif or Tat were added at the final protein to nucleotide molar ratios indicated in the figure legends. Incubation was for 20–30 min at 37 °C. Reactions were stopped by adding 20 μl of the stop solution (0.3% SDS, 15 mM EDTA), and extracted with 30 μl of phenol and 15 μl of chloroform. The aqueous phase was precipitated with ethanol and the pellet

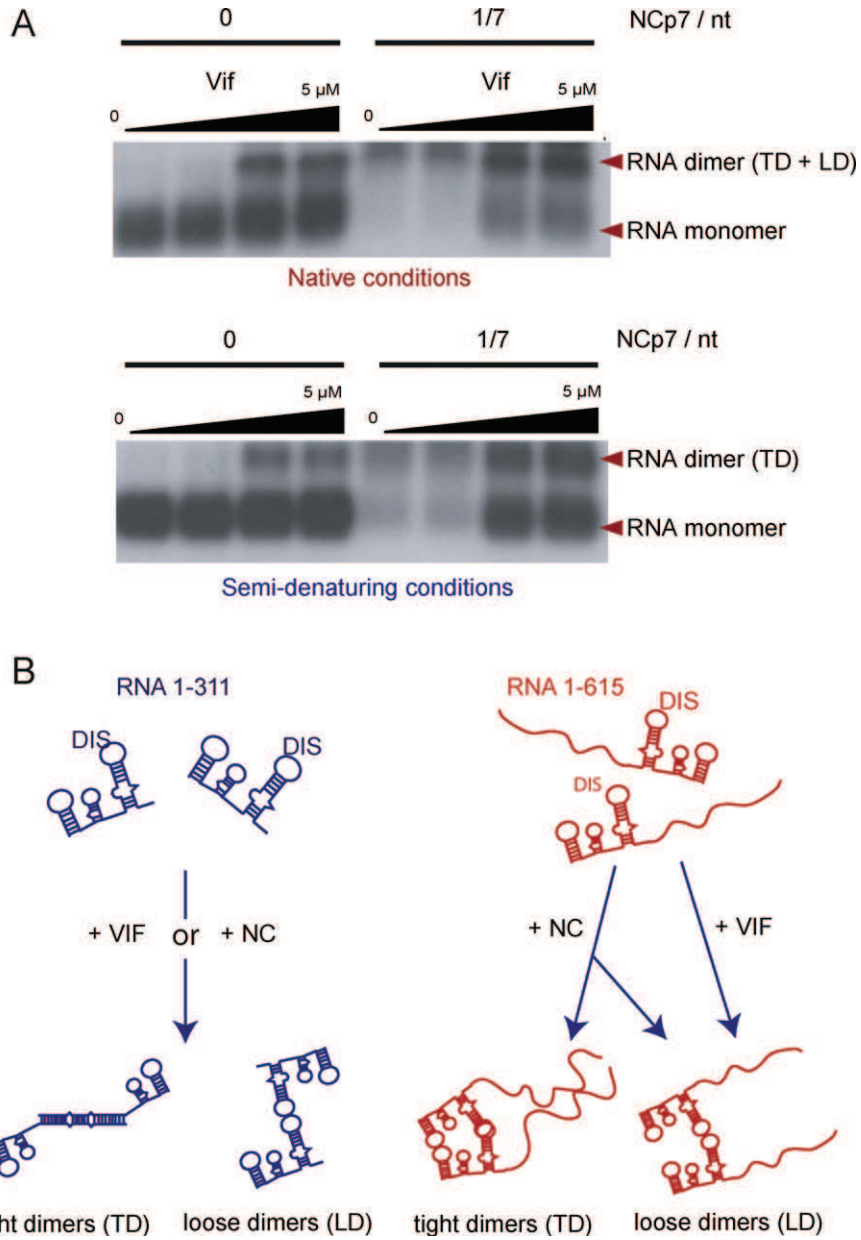

Fig. 5. RNA dimerization induced by Vif and NCp7. (A) HIV RNA 1–311 was allowed to dimerize in the presence of increasing concentration of Vif (0, 0.2, 2.0 and 5.0 µM), in the absence or in presence of NCp7 at a protein/nt molar ratio of 1/7. After protein removal, RNA was visualized under native and semi-denaturing electrophoresis conditions. (B) Schematic representation of Vif and NCp-induced RNA dimerization under native and semi-denaturing conditions.

re-suspended in 45% formamide, 0.5× TBE and 0.1% dyes. ^{32}P-labeled RNAs were analyzed on 8% PAGE in 7 M urea and 0.5× TBE. After electrophoresis, gels were autoradiographed and the efficiency of RNA cleavage was analyzed by phosphorimaging.

6.1.6. RNA dimerization assay

RNA dimerization was performed as described previously (Henriet et al., 2007). Briefly, 100 nM of unlabeled HIV-1 1–311 RNA fragment were diluted in 10 µl of water together with the corresponding labeled RNA (5000 cpm, 3–5 nM). Samples were denatured for 2 min at 90 °C, and snap-cooled on ice for 2 min. Dimerization was initiated by addition of Vif and/or NCp7 under conditions disfavoring salt-induced RNA dimerization (50 mM sodium cacodylate pH 7.5, 50 mM NaCl, 0.1 mM $MgCl_2$). When both proteins were present in the same reaction, the order of addition of the two proteins did not influence the final result. RNA samples were incubated 30 min at 37 °C and deproteinized as above, then resuspended in glycerol-containing loading buffer, split in two equal volumes and analyzed on a 0.8% agarose gel in native (Tris–Borate 0.5×, $MgCl_2$ 0.1 mM, run at 4 °C) or semi-denaturating (TBE 1×, and run at 20 °C) electrophoresis conditions. These two electrophoresis conditions have been tested in order to discriminate loose/unstable RNA dimers (only visible on native conditions) from tight/stable RNA dimers (visible under both electrophoresis conditions). Gels were fixed in 10% trichloroacetic acid for 10 min and dried for 1 h under vacuum at room temperature. Radioactive bands corresponding to monomeric and dimeric species were visualized and quantified using a FLA 5000 (Fuji).

6.2. Results and discussion

6.2.1. HIV-1 Vif activates TAR(+)/TAR(−) annealing

The annealing of the complementary TAR sequences is essential to achieve (−) strand DNA transfer. To better understand

Vif-induced (−) strand DNA transfer, we compared the ability of Vif to promote the annealing of two complementary TAR sequences with that of NCp7 and Tat. In the absence of protein, TAR(+)/TAR(−) annealing occurred at 65 °C in high salt conditions in the positive control (Fig. 3A, Ct+). No TAR(+)/TAR(−) annealing was observed at 37 °C in the negative control (Fig. 3A, Ct−). Incubation with NCp7 or Tat at 37 °C for 5 min favored TAR(+)/TAR(−) annealing at protein to nucleotide molar ratios of 1/20, 1/10 and 1/5 (Fig. 3A, lanes 3–8). In the presence of Vif, TAR(+)/TAR(−) annealing was also observed, but at higher protein to nucleotide molar ratios of 1/30, 1/15 and 1/10 (Fig. 3A, lanes 11–13), indicating that Vif annealing activity was slightly less efficient than that observed for NCp7 or Tat.

6.2.2. Inhibition of Vif-mediated TAR(+)/TAR(−) annealing by 2′O-methylated ODNs

In an attempt to characterize molecules capable of inhibiting the chaperoning activity of Vif, we used methylated oligonucleotides (mODN) found to bind to NCp7 and extensively impair its chaperoning activity *in vitro* and virus replication in T-cells and macrophages (Grigorov et al., 2011). To this end, we monitored the effect of mODNs on Vif-mediated *TAR(+)/TAR(−) annealing* as previously reported for NCp7 (Fig. 3B) (Grigorov et al., 2011). In the positive control of Vif-mediated TAR(+)/TAR(−) annealing, Vif was used at a protein to nucleotide molar ratio of 1/30 (Fig. 3B, line 3). We observed no effect on the TAR(+)/TAR(−) annealing by Vif after addition of increasing concentrations (100–400 μM) of mODN-11 and mODN-9UU (Fig. 3B, lanes 4–6 and 10–12, respectively). However, addition of mODN-9 GU drastically reduced TAR(+)/TAR(−) annealing by Vif (Fig. 3B, lanes 7–9). This result suggests that mODNs could be used to inhibit not only the nucleic RNA chaperone activity of NCp7 (Grigorov et al., 2011) but also that of Vif.

6.2.3. Vif activates hammerhead ribozyme-directed RNA cleavage

The hammerhead ribozyme cleavage assay was used to monitor two RNA chaperone properties: the annealing of the RNA substrate to the ribozyme, and the subsequent dissociation of the RNA products (Fig. 4A) (Cristofari and Darlix, 2002). We observed enhanced ribozyme-directed cleavage of RNA S14 after addition of increasing concentrations of Vif at protein to nucleotide molar ratios between 1/50 and 1/3 (Fig. 4B, lanes 3–7). As expected, we observed the same effect with NCp7 (Fig. 4B, lanes 8–10). No hammerhead ribozyme-directed RNA cleavage was detected using NC(12–53) which has only little nucleic acid chaperone activity (Fig. 4B, lanes 11–13) (Cristofari and Darlix, 2002; Darlix et al., 2011; Kuciak et al., 2008).

6.2.4. Vif induces the formation of HIV-1 RNA loose and tight dimers

Previously, we reported that Vif is able to induce the formation of loose RNA dimers in a RNA dimerization assay using RNA fragments containing the first 615 nts of the HIV-1 genomic RNA (Henriet et al., 2007). Moreover, in the presence of NCp7, Vif was able to inhibit NC-induced tight RNA dimer formation (Henriet et al., 2007). We now report that Vif is able to form both loose and tight RNA dimers when dimerization assays were carried out with an RNA corresponding to the first 311 nts of the HIV-1 genome (Fig. 5A). The dimerization experiment was carried out with increasing concentrations of Vif (0–5 μM) and in the absence or presence of NCp7 (NCp7/nucleotide ratio of 1/7). We analyzed RNA dimerization using two different electrophoresis conditions: (1) native conditions in which both loose and tight dimers are stable (Fig. 5A, upper panel) and (2) semi-denaturing conditions in which only tight dimers are preserved (Fig. 5A, lower panel). In the absence of NCp7, Vif stimulated both loose and tight RNA dimers formation, as observed by the presence of RNA dimers under both electrophoresis conditions, with a dimerization yield of ∼40% at 5 μM Vif (Fig. 5A). In the absence of Vif (Fig. 5A, lane 5), NCp7 induced >90% RNA dimer under both electrophoresis conditions. When increasing concentrations of Vif were added, we observed a reduction of the NCp7-induced tight RNA dimer formation (Fig. 5A, lanes 5–8), indicating a competition between Vif and NCp7, as previously observed (Henriet et al., 2007). These observations suggest that Vif favors the formation of tight RNA 1–311 dimers (Fig. 5B), contrary to what was observed for RNA 1–615 (Henriet et al., 2007). Indeed, in the RNA 1–311 context, the dimerization initiation site (DIS), responsible for RNA dimerization, is located directly at the 3′-end of the molecule, which probably induced a reduction of topological constraints and could thus allow the formation of an extended duplex (Fig. 5B). Conversely, the DIS of RNA 1–615 is located in the middle of the sequence, and in this context, Vif and/or NCp7 may stabilize the RNA dimer *via* different loop-loop interactions. It is thus likely that the tight dimers formed by RNA 1–311 differ from those formed by RNA 1–615, and presumably by full length genomic RNA.

7. Conclusion and future directions

Results presented here (Figs. 3–5) indicate that Vif is an authentic nucleic acid chaperone that may be required at various stages of the HIV-1 replication cycle (Fig. 1). As a matter of fact, Vif may balance the potent RNA chaperoning activities of NC in order to regulate genomic RNA dimerization and maturation (Fig. 5). Through interactions with Gag (125), Vif would at the same time regulate assembly and Gag processing, in turn preventing premature initiation of reverse transcription by RT (90) during virus formation. Work is presently in progress in our laboratories to characterize domains, notably the disordered C-terminal region, involved in the RNA chaperone activity of Vif and evaluate their implications in virus replication.

HIV-1 Vif and the cellular APOBEC3 proteins have been extensively studied in the past 10 years and the understanding on mechanisms restricting viral replication largely benefited to the scientific community. We are just starting to decipher the multiple functions of Vif associated with its biochemical and biophysical properties and the next step will be the resolution of its tridimensional structure, either alone, or most probably in complex with A3G and the E3 ubiquitine ligase (Jager et al., 2012). The discovery and the development of new drug candidates that would inhibit Vif functions and restore the innate cellular restriction will then become an attractive possibility.

Funding

This work was supported by a grant from the French National Agency for Research on AIDS and Viral Hepatitis (ANRS) to JCP, and by post-doctoral and doctoral fellowships from SIDACTION and ANRS to JB and SG, respectively.

Acknowledgements

Authors wish to thank G. Mirambeau, S. Lyonnais and the meeting committee for the organization of the 8th International Retroviral NC Symposium (2011, Barcelona, Spain). We are also indebted to former members of the Marquet/Paillart laboratory who contributed to the work on Vif: Dr. S. Henriet, Dr. G. Mercenne, Dr. L. Sinck, Dr. V. Goldschmidt, C. Tournaire and A. Mariotte. The authors thank Dr. R. Smyth (UPR9002-CNRS) for critical reading of the manuscript.

References

Akari, H., Yoshida, A., Fukumori, T., Adachi, A., 2000. Host cell-dependent replication of HIV-1 mutants with deletions in gp41 cytoplasmic tail region is independent of the function of Vif. Microbes and Infection 2 (9), 1019–1023.

Akari, H., Fujita, M., Kao, S., Khan, M.A., Shehu-Xhilaga, M., Adachi, A., Strebel, K., 2004. High level expression of human immunodeficiency virus type-1 Vif inhibits viral infectivity by modulating proteolytic processing of the Gag precursor at the p2/nucleocapsid processing site. Journal of Biological Chemistry 279 (13), 12355–12362.

Albin, J.S., Harris, R.S., 2010. Interactions of host APOBEC3 restriction factors with HIV-1 in vivo: implications for therapeutics. Expert Reviews in Molecular Medicine 12, e4.

Anderson, J.L., Hope, T.J., 2008. APOBEC3G restricts early HIV-1 replication in the cytoplasm of target cells. Virology 375 (1), 1–12.

Apolloni, A., Meredith, L.W., Suhrbier, A., Kiernan, R., Harrich, D., 2007. The HIV-1 Tat protein stimulates reverse transcription in vitro. Current HIV Research 5 (5), 473–483.

Balaji, S., Kalpana, R., Shapshak, P., 2006. Paradigm development: comparative and predictive 3D modeling of HIV-1 virion infectivity factor (Vif). Bioinformation 1 (8), 290–309.

Bampi, C., Bibillo, A., Wendeler, M., Divita, G., Gorelick, R.J., Le Grice, S.F., Darlix, J.L., 2006. Nucleotide excision repair and template-independent addition by HIV-1 reverse transcriptase in the presence of nucleocapsid protein. Journal of Biological Chemistry 281 (17), 11736–11743.

Baraz, L., Hutoran, M., Blumenzweig, I., Katzenellenbogen, M., Friedler, A., Gilon, C., Steinitz, M., Kotler, M., 2002. Human immunodeficiency virus type 1 Vif binds the viral protease by interaction with its N-terminal region. Journal of General Virology 83 (Pt 9), 2225–2230.

Bardy, M., Gay, B., Pebernard, S., Chazal, N., Courcoul, M., Vigne, R., Decroly, E., Boulanger, P., 2001. Interaction of human immunodeficiency virus type 1 Vif with Gag and Gag-Pol precursors: co-encapsidation and interference with viral protease-mediated Gag processing. Journal of General Virology 82 (Pt 11), 2719–2733.

Barraud, P., Gaudin, C., Dardel, F., Tisné, C., 2007. New insights into the formation of HIV-1 reverse transcription initiation complex. Biochimie 89 (10), 1204–1210.

Barraud, P., Paillart, J.C., Marquet, R., Tisné, C., 2008. Advances in the structural understanding of Vif proteins. Current HIV Research 6 (2), 91–99.

Basu, V.P., Song, M., Gao, L., Rigby, S.T., Hanson, M.N., Bambara, R.A., 2008. Strand transfer events during HIV-1 reverse transcription. Virus Research 134 (1–2), 19–38.

Beltz, H., Azoulay, J., Bernacchi, S., Clamme, J.P., Ficheux, D., Roques, B., Darlix, J.L., Mely, Y., 2003. Impact of the terminal bulges of HIV-1 cTAR DNA on its stability and the destabilizing activity of the nucleocapsid protein NCp7. Journal of Molecular Biology 328 (1), 95–108.

Berger, G., Durand, S., Fargier, G., Nguyen, X.N., Cordeil, S., Bouaziz, S., Muriaux, D., Darlix, J.L., Cimarelli, A., 2011. APOBEC3A is a specific inhibitor of the early phases of HIV-1 infection in myeloid cells. PLoS Pathogens 7 (9), e1002221.

Bergeron, J.R., Huthoff, H., Veselkov, D.A., Beavil, R.L., Simpson, P.J., Matthews, S.J., Malim, M.H., Sanderson, M.R., 2010. The SOCS-box of HIV-1 Vif interacts with Elongin BC by induced-folding to recruit its Cul5-containing ubiquitin ligase complex. PLoS Pathogens 6 (6), e1000925.

Bernacchi, S., Henriet, S., Dumas, P., Paillart, J.C., Marquet, R., 2007. RNA and DNA binding properties of HIV-1 Vif protein: a fluorescence study. Journal of Biological Chemistry 282 (36), 26361–26368.

Bernacchi, S., Mercenne, G., Tournaire, C., Marquet, R., Paillart, J.C., 2011. Importance of the proline-rich multimerization domain on the oligomerization and nucleic acid binding properties of HIV-1 Vif. Nucleic Acids Research 39 (6), 2404–2415.

Binka, M., Ooms, M., Steward, M., Simon, V., 2012. The activity spectrum of Vif from multiple HIV-1 subtypes against APOBEC3G, APOBEC3F, and APOBEC3H. Journal of Virology 86 (1), 49–59.

Bishop, K.N., Holmes, R.K., Malim, M.H., 2006. Antiviral potency of APOBEC proteins does not correlate with cytidine deamination. Journal of Virology 80 (17), 8450–8458.

Bishop, K.N., Verma, M., Kim, E.Y., Wolinsky, S.M., Malim, M.H., 2008. APOBEC3G inhibits elongation of HIV-1 reverse transcripts. PLoS Pathogens 4 (12), e1000231.

Borman, A.M., Quillent, C., Charneau, P., Dauguet, C., Clavel, F., 1995. Human immunodeficiency virus type 1 Vif-mutant particles from restrictive cells: role of Vif in correct particle assembly and infectivity. Journal of Virology 69 (4), 2058–2067.

Boudier, C., Storchak, R., Sharma, K.K., Didier, P., Follenius-Wund, A., Muller, S., Darlix, J.L., Mely, Y., 2010. The mechanism of HIV-1 Tat-directed nucleic acid annealing supports its role in reverse transcription. Journal of Molecular Biology 400 (3), 487–501.

Bouyac, M., Courcoul, M., Bertoia, G., Baudat, Y., Gabuzda, D., Blanc, D., Chazal, N., Boulanger, P., Sire, J., Vigne, R., Spire, B., 1997. Human immunodeficiency virus type 1 Vif protein binds to the Pr55Gag precursor. Journal of Virology 71 (12), 9358–9365.

Brule, F., Marquet, R., Rong, L., Wainberg, M.A., Roques, B.P., Le Grice, S.F., Ehresmann, B., Ehresmann, C., 2002. Structural and functional properties of the HIV-1 RNA-tRNA(Lys)3 primer complex annealed by the nucleocapsid protein: comparison with the heat-annealed complex. RNA 8 (1), 8–15.

Burnett, A., Spearman, P., 2007. APOBEC3G multimers are recruited to the plasma membrane for packaging into human immunodeficiency virus type 1 virus-like particles in an RNA-dependent process requiring the NC basic linker. Journal of Virology 81 (10), 5000–5013.

Carr, J.M., Davis, A.J., Coolen, C., Cheney, K., Burrell, C.J., Li, P., 2006. Vif-deficient HIV reverse transcription complexes (RTCs) are subject to structural changes and mutation of RTC-associated reverse transcription products. Virology 351 (1), 80–91.

Carr, J.M., Coolen, C., Davis, A.J., Burrell, C.J., Li, P., 2008. Human immunodeficiency virus 1 (HIV-1) virion infectivity factor (Vif) is part of reverse transcription complexes and acts as an accessory factor for reverse transcription. Virology 372 (1), 147–156.

Chen, J., Nikolaitchik, O., Singh, J., Wright, A., Bencsics, C.E., Coffin, J.M., Ni, N., Lockett, S., Pathak, V.K., Hu, W.S., 2009. High efficiency of HIV-1 genomic RNA packaging and heterozygote formation revealed by single virion analysis. Proceedings of the National Academy of Sciences of the United States of America 106 (32), 13535–13540.

Chertova, E., Chertov, O., Coren, L.V., Roser, J.D., Trubey, C.M., Bess Jr., J.W., Sowder II, R.C., Barsov, E., Hood, B.L., Fisher, R.J., Nagashima, K., Conrads, T.P., Veenstra, T.D., Lifson, J.D., Ott, D.E., 2006. Proteomic and biochemical analysis of purified human immunodeficiency virus type 1 produced from infected monocyte-derived macrophages. Journal of Virology 80 (18), 9039–9052.

Cimarelli, A., Darlix, J.L., 2002. Assembling the human immunodeficiency virus type 1. Cellular and Molecular Life Sciences 59 (7), 1166–1184.

Clodi, E., Semrad, K., Schroeder, R., 1999. Assaying RNA chaperone activity in vivo using a novel RNA folding trap. EMBO Journal 18 (13), 3776–3782.

Conticello, S.G., Harris, R.S., Neuberger, M.S., 2003. The Vif protein of HIV triggers degradation of the human antiretroviral DNA deaminase APOBEC3G. Current Biology 13 (22), 2009–2013.

Courcoul, M., Patience, C., Rey, F., Blanc, D., Harmache, A., Sire, J., Vigne, R., Spire, B., 1995. Peripheral blood mononuclear cells produce normal amounts of defective Vif-human immunodeficiency virus type 1 particles which are restricted for the preretrotranscription steps. Journal of Virology 69 (4), 2068–2074.

Cristofari, G., Darlix, J.L., 2002. The ubiquitous nature of RNA chaperone proteins. Progress in Nucleic Acid Research and Molecular Biology 72, 223–268.

Dafonseca, S., Coric, P., Gay, B., Hong, S.S., Bouaziz, S., Boulanger, P., 2008. The inhibition of assembly of HIV-1 virus-like particles by 3-O-(3′,3′-dimethylsuccinyl) betulinic acid (DSB) is counteracted by Vif and requires its zinc-binding domain. Virology Journal 5, 162.

Darlix, J.L., Godet, J., Ivanyi-Nagy, R., Fosse, P., Mauffret, O., Mely, Y., 2011. Flexible nature and specific functions of the HIV-1 nucleocapsid protein. Journal of Molecular Biology 410 (4), 565–581.

Dettenhofer, M., Cen, S., Carlson, B.A., Kleiman, L., Yu, X.F., 2000. Association of human immunodeficiency virus type 1 Vif with RNA and its role in reverse transcription. Journal of Virology 74 (19), 8938–8945.

Didierlaurent, L., Houzet, L., Morichaud, Z., Darlix, J.L., Mougel, M., 2008. The conserved N-terminal basic residues and zinc-finger motifs of HIV-1 nucleocapsid restrict the viral cDNA synthesis during virus formation and maturation. Nucleic Acids Research 36 (14), 4745–4753.

Donahue, J.P., Vetter, M.L., Mukhtar, N.A., D'Aquila, R.T., 2008. The HIV-1 Vif PPLP motif is necessary for human APOBEC3G binding and degradation. Virology 377 (1), 49–53.

Douaisi, M., Dussart, S., Courcoul, M., Bessou, G., Lerner, E.C., Decroly, E., Vigne, R., 2005. The tyrosine kinases Fyn and Hck favor the recruitment of tyrosine-phosphorylated APOBEC3G into Vif-defective HIV-1 particles. Biochemical and Biophysical Research Communications 329 (3), 917–924.

Driscoll, M.D., Hughes, S.H., 2000. Human immunodeficiency virus type 1 nucleocapsid protein can prevent self-priming of minus-strand strong stop DNA by promoting the annealing of short oligonucleotides to hairpin sequences. Journal of Virology 74 (19), 8785–8792.

Fan, L., Peden, K., 1992. Cell-free transmission of Vif mutants of HIV-1. Virology 190 (1), 19–29.

Fisher, A.G., Ensoli, B., Ivanoff, L., Chamberlain, M., Petteway, S., Ratner, L., Gallo, R.C., Wong-Staal, F., 1987. The sor gene of HIV-1 is required for efficient virus transmission in vitro. Science 237 (4817), 888–893.

Fouchier, R.A., Simon, J.H., Jaffe, A.B., Malim, M.H., 1996. Human immunodeficiency virus type 1 Vif does not influence expression or virion incorporation of gag-, pol-, and env-encoded proteins. Journal of Virology 70 (12), 8263–8269.

Fujita, M., Sakurai, A., Yoshida, A., Miyaura, M., Koyama, A.H., Sakai, K., Adachi, A., 2003. Amino acid residues 88 and 89 in the central hydrophilic region of human immunodeficiency virus type 1 Vif are critical for viral infectivity by enhancing the steady-state expression of Vif. Journal of Virology 77 (2), 1626–1632.

Gabuzda, D.H., Lawrence, K., Langhoff, E., Terwilliger, E., Dorfman, T., Haseltine, W.A., Sodroski, J., 1992. Role of Vif in replication of human immunodeficiency virus type 1 in $CD4^+$ T lymphocytes. Journal of Virology 66 (11), 6489–6495.

Goncalves, J., Shi, B., Yang, X., Gabuzda, D., 1995. Biological activity of human immunodeficiency virus type 1 Vif requires membrane targeting by C-terminal basic domains. Journal of Virology 69 (11), 7196–7204.

Grigorov, B., Bocquin, A., Gabus, C., Avilov, S., Mely, Y., Agopian, A., Divita, G., Gottikh, M., Witvrouw, M., Darlix, J.L., 2011. Identification of a methylated oligoribonucleotide as a potent inhibitor of HIV-1 reverse transcription complex. Nucleic Acids Research 39 (13), 5586–5596.

Guo, J., Henderson, L.E., Bess, J., Kane, B., Levin, J.G., 1997. Human immunodeficiency virus type 1 nucleocapsid protein promotes efficient strand transfer and specific viral DNA synthesis by inhibiting TAR-dependent self-priming from minus-strand strong-stop DNA. Journal of Virology 71 (7), 5178–5188.

Guo, F., Cen, S., Niu, M., Yang, Y., Gorelick, R.J., Kleiman, L., 2007. The interaction of APOBEC3G with human immunodeficiency virus type 1 nucleocapsid inhibits tRNA3Lys annealing to viral RNA. Journal of Virology 81 (20), 11322–11331.

Hargittai, M.R., Gorelick, R.J., Rouzina, I., Musier-Forsyth, K., 2004. Mechanistic insights into the kinetics of HIV-1 nucleocapsid protein-facilitated tRNA annealing to the primer binding site. Journal of Molecular Biology 337 (4), 951–968.

Harris, R.S., Petersen-Mahrt, S.K., Neuberger, M.S., 2002. RNA editing enzyme APOBEC1 and some of its homologs can act as DNA mutators. Molecular Cell 10 (5), 1247–1253.
Harris, R.S., Bishop, K.N., Sheehy, A.M., Craig, H.M., Petersen-Mahrt, S.K., Watt, I.N., Neuberger, M.S., Malim, M.H., 2003. DNA deamination mediates innate immunity to retroviral infection. Cell 113 (6), 803–809.
Hassaine, G., Courcoul, M., Bessou, G., Barthalay, Y., Picard, C., Olive, D., Collette, Y., Vigne, R., Decroly, E., 2001. The tyrosine kinase Hck is an inhibitor of HIV-1 replication counteracted by the viral Vif protein. Journal of Biological Chemistry 276 (20), 16885–16893.
He, B., Wang, K., Liu, Y., Xue, B., Uversky, V.N., Dunker, A.K., 2009. Predicting intrinsic disorder in proteins: an overview. Cell Research 19 (8), 929–949.
Henriet, S., Richer, D., Bernacchi, S., Decroly, E., Vigne, R., Ehresmann, B., Ehresmann, C., Paillart, J.C., Marquet, R., 2005. Cooperative and specific binding of Vif to the 5′ region of HIV-1 genomic RNA. Journal of Molecular Biology 354 (1), 55–72.
Henriet, S., Sinck, L., Bec, G., Gorelick, R.J., Marquet, R., Paillart, J.C., 2007. Vif is a RNA chaperone that could temporally regulate RNA dimerization and the early steps of HIV-1 reverse transcription. Nucleic Acids Research 35 (15), 5141–5153.
Henriet, S., Mercenne, G., Bernacchi, S., Paillart, J.C., Marquet, R., 2009. Tumultuous relationship between the human immunodeficiency virus type 1 viral infectivity factor (Vif) and the human APOBEC-3G and APOBEC-3F restriction factors. Microbiology and Molecular Biology Reviews 73 (2), 211–232.
Herschlag, D., 1995. RNA chaperones and the RNA folding problem. Journal of Biological Chemistry 270, 20871–20874.
Hoglund, S., Ohagen, A., Lawrence, K., Gabuzda, D., 1994. Role of Vif during packing of the core of HIV-1. Virology 201 (2), 349–355.
Holmes, R.K., Koning, F.A., Bishop, K.N., Malim, M.H., 2007. APOBEC3F can inhibit the accumulation of HIV-1 reverse transcription products in the absence of hypermutation. Comparisons with APOBEC3G. Journal of Biological Chemistry 282 (4), 2587–2595.
Housset, V., de Rocquigny, H., Roques, B.P., Darlix, J.L., 1993. Basic amino acids flanking the zinc finger of Moloney murine leukemia virus nucleocapsid protein NCp10 are critical for virus infectivity. Journal of Virology 67 (5), 2537–2545.
Houzet, L., Morichaud, Z., Didierlaurent, L., Muriaux, D., Darlix, J.L., Mougel, M., 2008. Nucleocapsid mutations turn HIV-1 into a DNA-containing virus. Nucleic Acids Research 36 (7), 2311–2319.
Hultquist, J.F., Binka, M., Larue, R.S., Simon, V., Harris, R.S., 2011a. Vif proteins of human and simian immunodeficiency viruses require cellular CBFbeta to degrade APOBEC3 restriction factors. Journal of Virology.
Hultquist, J.F., Lengyel, J.A., Refsland, E.W., LaRue, R.S., Lackey, L., Brown, W.L., Harris, R.S., 2011b. Human and rhesus APOBEC3D, APOBEC3F, APOBEC3G, and APOBEC3H demonstrate a conserved capacity to restrict Vif-deficient HIV-1. Journal of Virology 85 (21), 11220–11234.
Hultquist, J.F., Binka, M., LaRue, R.S., Simon, V., Harris, R.S., 2012. Vif proteins of human and simian immunodeficiency viruses require cellular CBFbeta to degrade APOBEC3 restriction factors. Journal of Virology 86 (5), 2874–2877.
Isel, C., Ehresmann, C., Keith, G., Ehresmann, B., Marquet, R., 1995. Initiation of reverse transcription of HIV-1: secondary structure of the HIV-1 RNA/tRNA(3Lys) (template/primer). Journal of Molecular Biology 247 (2), 236–250.
Isel, C., Ehresmann, C., Marquet, R., 2010. Initiation of HIV reverse transcription. Viruses 2 (1), 213–243.
Ivanyi-Nagy, R., Lavergne, J.P., Gabus, C., Ficheux, D., Darlix, J.L., 2008. RNA chaperoning and intrinsic disorder in the core proteins of Flaviviridae. Nucleic Acids Research 36 (3), 712–725.
Iwai, K., Yamanaka, K., Kamura, T., Minato, N., Conaway, R.C., Conaway, J.W., Klausner, R.D., Pause, A., 1999. Identification of the von Hippel-lindau tumor-suppressor protein as part of an active E3 ubiquitin ligase complex. Proceedings of the National Academy of Sciences of United States of America 96 (22), 12436–12441.
Iwatani, Y., Chan, D.S., Wang, F., Maynard, K.S., Sugiura, W., Gronenborn, A.M., Rouzina, I., Williams, M.C., Musier-Forsyth, K., Levin, J.G., 2007. Deaminase-independent inhibition of HIV-1 reverse transcription by APOBEC3G. Nucleic Acids Research 35, 7096–7108.
Izumi, T., Takaori-Kondo, A., Shirakawa, K., Higashitsuji, H., Itoh, K., Io, K., Matsui, M., Iwai, K., Kondoh, H., Sato, T., Tomonaga, M., Ikeda, S., Akari, H., Koyanagi, Y., Fujita, J., Uchiyama, T., 2009. MDM2 is a novel E3 ligase for HIV-1 Vif. Retrovirology 6, 1.
Jager, S., Kim, D.Y., Hultquist, J.F., Shindo, K., Larue, R.S., Kwon, E., Li, M., Anderson, B.D., Yen, L., Stanley, D., Mahon, C., Kane, J., Franks-Skiba, K., Cimermancic, P., Burlingame, A., Sali, A., Craik, C.S., Harris, R.S., Gross, J.D., Krogan, N.J., 2011. Vif hijacks CBF-beta to degrade APOBEC3G and promote HIV-1 infection. Nature.
Jager, S., Cimermancic, P., Gulbahce, N., Johnson, J.R., McGovern, K.E., Clarke, S.C., Shales, M., Mercenne, G., Pache, L., Li, K., Hernandez, H., Jang, G.M., Roth, S.L., Akiva, E., Marlett, J., Stephens, M., D'Orso, I., Fernandes, J., Fahey, M., Mahon, C., O'Donoghue, A.J., Todorovic, A., Morris, J.H., Maltby, D.A., Alber, T., Cagney, G., Bushman, F.D., Young, J.A., Chanda, S.K., Sundquist, W.I., Kortemme, T., Hernandez, R.D., Craik, C.S., Burlingame, A., Sali, A., Frankel, A.D., Krogan, N.J., 2012. Global landscape of HIV-human protein complexes. Nature 481 (7381), 365–370.
Jarmuz, A., Chester, A., Bayliss, J., Gisbourne, J., Dunham, I., Scott, J., Navaratnam, N., 2002. An anthropoid-specific locus of orphan C to U RNA-editing enzymes on chromosome 22. Genomics 79 (3), 285–296.
Ji, X., Klarmann, G.J., Preston, B.D., 1996. Effect of human immunodeficiency virus type 1 (HIV-1) nucleocapsid protein on HIV-1 reverse transcriptase activity *in vitro*. Biochemistry 35, 132–143.
Kameoka, M., Rong, L., Gotte, M., Liang, C., Russell, R.S., Wainberg, M.A., 2001. Role for human immunodeficiency virus type 1 Tat protein in suppression of viral reverse transcriptase activity during late stages of viral replication. Journal of Virology 75 (6), 2675–2683.
Kameoka, M., Morgan, M., Binette, M., Russell, R.S., Rong, L., Guo, X., Mouland, A., Kleiman, L., Liang, C., Wainberg, M.A., 2002. The Tat protein of human immunodeficiency virus type 1 (HIV-1) can promote placement of tRNA primer onto viral RNA and suppress later DNA polymerization in HIV-1 reverse transcription. Journal of Virology 76 (8), 3637–3645.
Kao, S., Khan, M.A., Miyagi, E., Plishka, R., Buckler-White, A., Strebel, K., 2003. The human immunodeficiency virus type 1 Vif protein reduces intracellular expression and inhibits packaging of APOBEC3G (CEM15), a cellular inhibitor of virus infectivity. Journal of Virology 77 (21), 11398–11407.
Kataropoulou, A., Bovolenta, C., Belfiore, A., Trabatti, S., Garbelli, A., Porcellini, S., Lupo, R., Maga, G., 2009. Mutational analysis of the HIV-1 auxiliary protein Vif identifies independent domains important for the physical and functional interaction with HIV-1 reverse transcriptase. Nucleic Acids Research 37 (11), 3660–3669.
Khan, M.A., Aberham, C., Kao, S., Akari, H., Gorelick, R., Bour, S., Strebel, K., 2001. Human immunodeficiency virus type 1 Vif protein is packaged into the nucleoprotein complex through an interaction with viral genomic RNA. Journal of Virology 75 (16), 7252–7265.
Khan, M.A., Akari, H., Kao, S., Aberham, C., Davis, D., Buckler-White, A., Strebel, K., 2002. Intravirion processing of the human immunodeficiency virus type 1 Vif protein by the viral protease may be correlated with Vif function. Journal of Virology 76 (18), 9112–9123.
Khan, M.A., Kao, S., Miyagi, E., Takeuchi, H., Goila-Gaur, R., Opi, S., Gipson, C.L., Parslow, T.G., Ly, H., Strebel, K., 2005. Viral RNA is required for the association of APOBEC3G with human immunodeficiency virus type 1 nucleoprotein complexes. Journal of Virology 79 (9), 5870–5874.
Kitamura, S., Ode, H., Iwatani, Y., 2011. Structural features of antiviral APOBEC3 proteins are linked to their functional activities. Frontiers in Microbiology 2, 258.
Kotler, M., Simm, M., Zhao, Y.S., Sova, P., Chao, W., Ohnona, S.F., Roller, R., Krachmarov, C., Potash, M.J., Volsky, D.J., 1997. Human immunodeficiency virus type 1 (HIV-1) protein Vif inhibits the activity of HIV-1 protease in bacteria and in vitro. Journal of Virology 71 (8), 5774–5781.
Kovacs, D., Rakacs, M., Agoston, B., Lenkey, K., Semrad, K., Schroeder, R., Tompa, P., 2009. Janus chaperones: assistance of both RNA- and protein-folding by ribosomal proteins. FEBS Letters 583 (1), 88–92.
Kuciak, M., Gabus, C., Ivanyi-Nagy, R., Semrad, K., Storchak, R., Chaloin, O., Muller, S., Mely, Y., Darlix, J.L., 2008. The HIV-1 transcriptional activator Tat has potent nucleic acid chaperoning activities in vitro. Nucleic Acids Research 36 (10), 3389–3400.
Lecossier, D., Bouchonnet, F., Clavel, F., Hance, A.J., 2003. Hypermutation of HIV-1 DNA in the absence of the Vif protein. Science 300 (5622), 1112.
Lee, Y.M., Liu, B., Yu, X.F., 1999. Formation of virus assembly intermediate complexes in the cytoplasm by wild-type and assembly-defective mutant human immunodeficiency virus type 1 and their association with membranes. Journal of Virology 73 (7), 5654–5662.
Li, X., Quan, Y., Arts, E.J., Li, Z., Preston, B.D., de Rocquigny, H., Roques, B.P., Darlix, J.-L., Kleinman, L., Parniak, M.A., Wainberg, M.A., 1996. Human immunodeficiency virus type 1 nucleocapsid protein (NCp7) directs specific initiation of minus-strand DNA synthesis primed by human $tRNA^{3,lys}$ *in vitro*: studies of viral RNA molecules mutated in regions that flank the primer binding site. Journal of Virology 70, 4996–5004.
Li, X.Y., Guo, F., Zhang, L., Kleiman, L., Cen, S., 2007. APOBEC3G inhibits DNA strand transfer during HIV-1 reverse transcription. Journal of Biological Chemistry 282 (44), 32065–32074.
Liddament, M.T., Brown, W.L., Schumacher, A.J., Harris, R.S., 2004. APOBEC3F properties and hypermutation preferences indicate activity against HIV-1 in vivo. Current Biology 14 (15), 1385–1391.
Liu, B., Sarkis, P.T., Luo, K., Yu, Y., Yu, X.F., 2005. Regulation of Apobec3F and human immunodeficiency virus type 1 Vif by Vif-Cul5-ElonB/C E3 ubiquitin ligase. Journal of Virology 79 (15), 9579–9587.
Lu, K., Heng, X., Summers, M.F., 2011. Structural determinants and mechanism of HIV-1 genome packaging. Journal of Molecular Biology 410 (4), 609–633.
Luo, K., Liu, B., Xiao, Z., Yu, Y., Yu, X., Gorelick, R., Yu, X.F., 2004. Amino-terminal region of the human immunodeficiency virus type 1 nucleocapsid is required for human APOBEC3G packaging. Journal of Virology 78 (21), 11841–11852.
Luo, K., Xiao, Z., Ehrlich, E., Yu, Y., Liu, B., Zheng, S., Yu, X.F., 2005. Primate lentiviral virion infectivity factors are substrate receptors that assemble with cullin 5-E3 ligase through a HCCH motif to suppress APOBEC3G. Proceedings of the National Academy of Sciences of United States of America 102 (32), 11444–11449.
Luo, K., Wang, T., Liu, B., Tian, C., Xiao, Z., Kappes, J., Yu, X.F., 2007. Cytidine deaminases APOBEC3G and APOBEC3F interact with human immunodeficiency virus type 1 integrase and inhibit proviral DNA formation. Journal of Virology 81 (13), 7238–7248.
Lv, W., Liu, Z., Jin, H., Yu, X., Zhang, L., Zhang, L., 2007. Three-dimensional structure of HIV-1 Vif constructed by comparative modeling and the function characterization analyzed by molecular dynamics simulation. Organic & Biomolecular Chemistry 5 (4), 617–626.
Madani, N., Kabat, D., 1998. An endogenous inhibitor of human immunodeficiency virus in human lymphocytes is overcome by the viral Vif protein. Journal of Virology 72 (12), 10251–10255.

Malim, M.H., Emerman, M., 2008. HIV-1 accessory proteins—ensuring viral survival in a hostile environment. Cell Host & Microbe 3 (6), 388–398.
Mandal, D., Exline, C.M., Feng, Z., Stoltzfus, C.M., 2009. Regulation of Vif mRNA splicing by human immunodeficiency virus type 1 requires 5′ splice site D2 and an exonic splicing enhancer to counteract cellular restriction factor APOBEC3G. Journal of Virology 83 (12), 6067–6078.
Mangeat, B., Turelli, P., Caron, G., Friedli, M., Perrin, L., Trono, D., 2003. Broad antiretroviral defence by human APOBEC3G through lethal editing of nascent reverse transcripts. Nature 424 (6944), 99–103.
Marcsisin, S.R., Engen, J.R., 2010. Molecular insight into the conformational dynamics of the Elongin BC complex and its interaction with HIV-1 Vif. Journal of Molecular Biology 402 (5), 892–904.
Marcsisin, S.R., Narute, P.S., Emert-Sedlak, L.A., Kloczewiak, M., Smithgall, T.E., Engen, J.R., 2011. On the solution conformation and dynamics of the HIV-1 viral infectivity factor. Journal of Molecular Biology 410 (5), 1008–1022.
Mariani, R., Chen, D., Schrofelbauer, B., Navarro, F., Konig, R., Bollman, B., Munk, C., Nymark-McMahon, H., Landau, N.R., 2003. Species-specific exclusion of APOBEC3G from HIV-1 virions by Vif. Cell 114 (1), 21–31.
Marin, M., Rose, K.M., Kozak, S.L., Kabat, D., 2003. HIV-1 Vif protein binds the editing enzyme APOBEC3G and induces its degradation. Nature Medicine 9 (11), 1398–1403.
Mbisa, J.L., Barr, R., Thomas, J.A., Vandegraaff, N., Dorweiler, I.J., Svarovskaia, E.S., Brown, W.L., Mansky, L.M., Gorelick, R.J., Harris, R.S., Engelman, A., Pathak, V.K., 2007. Human immunodeficiency virus type 1 cDNAs produced in the presence of APOBEC3G exhibit defects in plus-strand DNA transfer and integration. Journal of Virology 81 (13), 7099–7110.
McGuffin, L.J., Bryson, K., Jones, D.T., 2000. The PSIPRED protein structure prediction server. Bioinformatics 16 (4), 404–405.
Mehle, A., Goncalves, J., Santa-Marta, M., McPike, M., Gabuzda, D., 2004a. Phosphorylation of a novel SOCS-box regulates assembly of the HIV-1 Vif-Cul5 complex that promotes APOBEC3G degradation. Genes and Development 18 (23), 2861–2866.
Mehle, A., Strack, B., Ancuta, P., Zhang, C., McPike, M., Gabuzda, D., 2004b. Vif overcomes the innate antiviral activity of APOBEC3G by promoting its degradation in the ubiquitin-proteasome pathway. Journal of Biological Chemistry 279 (9), 7792–7798.
Mehle, A., Thomas, E.R., Rajendran, K.S., Gabuzda, D., 2006. A zinc-binding region in Vif binds Cul5 and determines cullin selection. Journal of Biological Chemistry 281 (25), 17259–17265.
Mehle, A., Wilson, H., Zhang, C., Brazier, A.J., McPike, M., Pery, E., Gabuzda, D., 2007. Identification of an APOBEC3G binding site in human immunodeficiency virus type 1 Vif and inhibitors of Vif-APOBEC3G binding. Journal of Virology 81 (23), 13235–13241.
Mercenne, G., Bernacchi, S., Richer, D., Bec, G., Henriet, S., Paillart, J.C., Marquet, R., 2010. HIV-1 Vif binds to APOBEC3G mRNA and inhibits its translation. Nucleic Acids Research 38 (2), 633–646.
Miller, J.H., Presnyak, V., Smith, H.C., 2007. The dimerization domain of HIV-1 viral infectivity factor Vif is required to block APOBEC3G incorporation with virions. Retrovirology 4, 81.
Miyagi, E., Opi, S., Takeuchi, H., Khan, M., Goila-Gaur, R., Kao, S., Strebel, K., 2007. Enzymatically active APOBEC3G is required for efficient inhibition of HIV-1. Journal of Virology 81, 13346–13353.
Mougel, M., Houzet, L., Darlix, J.L., 2009. When is it time for reverse transcription to start and go? Retrovirology 6, 24.
Muriaux, D., Darlix, J.L., 2010. Properties and functions of the nucleocapsid protein in virus assembly. RNA Biology 7 (6), 744–753.
Muriaux, D., De, R.H., Roques, B.P., Paoletti, J., 1996. NCp7 activates HIV-1Lai RNA dimerization by converting a transient loop–loop complex into a stable dimer. Journal of Biological Chemistry 271 (52), 33686–33692.
Newman, E.N., Holmes, R.K., Craig, H.M., Klein, K.C., Lingappa, J.R., Malim, M.H., Sheehy, A.M., 2005. Antiviral function of APOBEC3G can be dissociated from cytidine deaminase activity. Current Biology 15 (2), 166–170.
Ohagen, A., Gabuzda, D., 2000. Role of Vif in stability of the human immunodeficiency virus type 1 core. Journal of Virology 74 (23), 11055–11066.
Opi, S., Kao, S., Goila-Gaur, R., Khan, M.A., Miyagi, E., Takeuchi, H., Strebel, K., 2007. Human immunodeficiency virus type 1 Vif inhibits packaging and antiviral activity of a degradation-resistant APOBEC3G variant. Journal of Virology 81 (15), 8236–8246.
Paillart, J.-C., Marquet, R., Skripkin, E., Ehresmann, C., Ehresmann, B., 1996. Dimerization of retroviral genomic RNAs: structural and functional implications. Biochimie 78 (7), 639–653.
Paillart, J.-C., Shehu-Xhilaga, M., Marquet, R., Mak, J., 2004. Dimerization of retroviral RNA genomes: an inseparable pair. Nature Reviews Microbiology 2, 461–472.
Paul, I., Cui, J., Maynard, E.L., 2006. Zinc binding to the HCCH motif of HIV-1 virion infectivity factor induces a conformational change that mediates protein–protein interactions. Proceedings of the National Academy of Sciences of United States of America 103 (49), 18475–18480.
Pery, E., Rajendran, K.S., Brazier, A.J., Gabuzda, D., 2009. Regulation of APOBEC3 proteins by a novel YXXL motif in human immunodeficiency virus type 1 Vif and simian immunodeficiency virus SIVagm Vif. Journal of Virology 83 (5), 2374–2381.
Prats, A.C., Sarih, L., Gabus, C., Litvak, S., Keith, G., Darlix, J.L., 1988. Small finger protein of avian and murine retroviruses has nucleic acid annealing activity and positions the replication primer tRNA onto genomic RNA. EMBO Journal 7 (6), 1777–1783.
Rajkowitsch, L., Chen, D., Stampfl, S., Semrad, K., Waldsich, C., Mayer, O., Jantsch, M.F., Konrat, R., Blasi, U., Schroeder, R., 2007. RNA chaperones, RNA annealers and RNA helicases. RNA Biology 4 (3), 118–130.
Reddy, T.R., Kraus, G., Yamada, O., Looney, D.J., Suhasini, M., Wong-Staal, F., 1995. Comparative analyses of human immunodeficiency virus type 1 (HIV-1) and HIV-2 Vif mutants. Journal of Virology 69 (6), 3549–3553.
Rein, A., 2010. Nucleic acid chaperone activity of retroviral Gag proteins. RNA Biology 7 (6), 700–705.
Reingewertz, T.H., Benyamini, H., Lebendiker, M., Shalev, D.E., Friedler, A., 2009. The C-terminal domain of the HIV-1 Vif protein is natively unfolded in its unbound state. Protein Engineering, Design Selection 22 (5), 281–287.
Reingewertz, T.H., Shalev, D.E., Friedler, A., 2010. Structural disorder in the HIV-1 Vif protein and interaction-dependent gain of structure. Protein and Peptide Letters 17 (8), 988–998.
Russell, R.A., Pathak, V.K., 2007. Identification of two distinct human immunodeficiency virus type 1 Vif determinants critical for interactions with human APOBEC3G and APOBEC3F. Journal of Virology 81 (15), 8201–8210.
Russell, R.S., Liang, C., Wainberg, M.A., 2004. Is HIV-1 RNA dimerization a prerequisite for packaging? Yes, no, probably? Retrovirology 1 (1), 23.
Sakai, H., Shibata, R., Sakuragi, J., Sakuragi, S., Kawamura, M., Adachi, A., 1993. Cell-dependent requirement of human immunodeficiency virus type 1 Vif protein for maturation of virus particles. Journal of Virology 67 (3), 1663–1666.
Santa-Marta, M., Aires da Silva, F., Fonseca, A., Goncalves, J., 2005. HIV-1 Vif can directly inhibit APOBEC3G-mediated cytidine deamination by using a single amino acid interaction and without protein degradation. Journal of Biological Chemistry 280, 8765–8775.
Schafer, A., Bogerd, H.P., Cullen, B.R., 2004. Specific packaging of APOBEC3G into HIV-1 virions is mediated by the nucleocapsid domain of the gag polyprotein precursor. Virology 328 (2), 163–168.
Schmitt, K., Hill, M.S., Ruiz, A., Culley, N., Pinson, D.M., Wong, S.W., Stephens, E.B., 2009. Mutations in the highly conserved SLQYLA motif of Vif in a simian-human immunodeficiency virus result in a less pathogenic virus and are associated with G-to-A mutations in the viral genome. Virology 383 (2), 362–372.
Schrofelbauer, B., Senger, T., Manning, G., Landau, N.R., 2006. Mutational alteration of human immunodeficiency virus type 1 Vif allows for functional interaction with nonhuman primate APOBEC3G. Journal of Virology 80 (12), 5984–5991.
Semrad, K., 2011. Proteins with RNA chaperone activity: a world of diverse proteins with a common task-impediment of RNA misfolding. Biochemistry Research International 2011, 532908.
Sheehy, A.M., Gaddis, N.C., Choi, J.D., Malim, M.H., 2002. Isolation of a human gene that inhibits HIV-1 infection and is suppressed by the viral Vif protein. Nature 418 (6898), 646–650.
Sheehy, A.M., Gaddis, N.C., Malim, M.H., 2003. The antiretroviral enzyme APOBEC3G is degraded by the proteasome in response to HIV-1 Vif. Nature Medicine 9 (11), 1404–1407.
Shen, N., Jette, L., Liang, C., Wainberg, M.A., Laughrea, M., 2000. Impact of human immunodeficiency virus type 1 RNA dimerization on viral infectivity and of stem-loop B on RNA dimerization and reverse transcription and dissociation of dimerization from packaging. Journal of Virology 74 (12), 5729–5735.
Shindo, K., Takaori-Kondo, A., Kobayashi, M., Abudu, A., Fukunaga, K., Uchiyama, T., 2003. The enzymatic activity of CEM15/Apobec-3G is essential for the regulation of the infectivity of HIV-1 virion but not a sole determinant of its antiviral activity. Journal of Biological Chemistry 278 (45), 44412–44416.
Simon, J.H., Gaddis, N.C., Fouchier, R.A., Malim, M.H., 1998. Evidence for a newly discovered cellular anti-HIV-1 phenotype. Nature Medicine 4 (12), 1397–1400.
Simon, J.H., Carpenter, E.A., Fouchier, R.A., Malim, M.H., 1999. Vif and the p55(Gag) polyprotein of human immunodeficiency virus type 1 are present in colocalizing membrane-free cytoplasmic complexes. Journal of Virology 73 (4), 2667–2674.
Simon, V., Zennou, V., Murray, D., Huang, Y., Ho, D.D., Bieniasz, P.D., 2005. Natural variation in Vif: differential impact on APOBEC3G/3F and a potential role in HIV-1 diversification. PLoS Pathogens 1 (1), e6.
Smith, J.L., Bu, W., Burdick, R.C., Pathak, V.K., 2009. Multiple ways of targeting APOBEC3-virion infectivity factor interactions for anti-HIV-1 drug development. Trends in Pharmacological Sciences 30 (12), 638–646.
Sova, P., Volsky, D.J., 1993. Efficiency of viral DNA synthesis during infection of permissive and nonpermissive cells with Vif-negative human immunodeficiency virus type 1. Journal of Virology 67 (10), 6322–6326.
Stanley, B.J., Ehrlich, E.S., Short, L., Yu, Y., Xiao, Z., Yu, X.F., Xiong, Y., 2008. Structural insight into the human immunodeficiency virus Vif SOCS box and its role in human E3 ubiquitin ligase assembly. Journal of Virology 82 (17), 8656–8663.
Stopak, K., de Noronha, C., Yonemoto, W., Greene, W.C., 2003. HIV-1 Vif blocks the antiviral activity of APOBEC3G by impairing both its translation and intracellular stability. Molecular Cell 12 (3), 591–601.
Strebel, K., Daugherty, D., Clouse, K., Cohen, D., Folks, T., Martin, M.A., 1987. The HIV 'A' (sor) gene product is essential for virus infectivity. Nature 328 (6132), 728–730.
Suspene, R., Rusniok, C., Vartanian, J.P., Wain-Hobson, S., 2006. Twin gradients in APOBEC3 edited HIV-1 DNA reflect the dynamics of lentiviral replication. Nucleic Acids Research 34, 4677–4684.
Svarovskaia, E.S., Xu, H., Mbisa, J.L., Barr, R., Gorelick, R.J., Ono, A., Freed, E.O., Hu, W.S., Pathak, V.K., 2004. Human apolipoprotein B mRNA-editing enzyme-catalytic polypeptide-like 3G (APOBEC3G) is incorporated into HIV-1 virions through interactions with viral and nonviral RNAs. Journal of Biological Chemistry 279 (34), 35822–35828.

Syed, F., McCrae, M.A., 2009. Interactions in vivo between the Vif protein of HIV-1 and the precursor (Pr55(GAG)) of the virion nucleocapsid proteins. Archives of Virology 154 (11), 1797–1805.
Techtmann, S.M., Ghirlando, R., Kao, S., Strebel, K., Maynard, E.L., 2012. Hydrodynamic and functional analysis of HIV-1 Vif oligomerization. Biochemistry 51 (10), 2078–2086.
Teng, B., Burant, C.F., Davidson, N.O., 1993. Molecular cloning of an apolipoprotein B messenger RNA editing protein. Science 260 (5115), 1816–1819.
Tian, C., Yu, X., Zhang, W., Wang, T., Xu, R., Yu, X.F., 2006. Differential requirement for conserved tryptophans in human immunodeficiency virus type 1 Vif for the selective suppression of APOBEC3G and APOBEC3F. Journal of Virology 80 (6), 3112–3115.
Tisné, C., 2005. Structural bases of the annealing of primer tRNA(3Lys) to the HIV-1 viral RNA. Current HIV Research 3 (2), 147–156.
Tisné, C., Roques, B.P., Dardel, F., 2004. The annealing mechanism of HIV-1 reverse transcription primer onto the viral genome. Journal of Biological Chemistry 279 (5), 3588–3595.
Tompa, P., Csermely, P., 2004. The role of structural disorder in the function of RNA and protein chaperones. FASEB Journal 18 (11), 1169–1175.
Tompa, P., Kovacs, D., 2010. Intrinsically disordered chaperones in plants and animals. Biochemistry and Cell Biology 88 (2), 167–174.
Tsuchihashi, Z., Brown, P.O., 1994. DNA strand exchange and selective DNA annealing promoted by the human immunodeficiency virus type 1 nucleocapsid protein. Journal of Virology 68, 5863–5870.
Tsuchihashi, Z., Khosla, M., Herschlag, D., 1993. Protein enhancement of hammerhead ribozyme catalysis. Science 262, 99–102.
von Schwedler, U., Song, J., Aiken, C., Trono, D., 1993. Vif is crucial for human immunodeficiency virus type 1 proviral DNA synthesis in infected cells. Journal of Virology 67 (8), 4945–4955.
Wichroski, M.J., Ichiyama, K., Rana, T., 2005. Analysis of HIV-1 Vif-mediated proteasome-dependent depletion of APOBEC3G: correlating function and subcellular localization. Journal of Biological Chemistry 280, 8387–8396.
Wiegand, H.L., Doehle, B.P., Bogerd, H.P., Cullen, B.R., 2004. A second human antiretroviral factor, APOBEC3F, is suppressed by the HIV-1 and HIV-2 Vif proteins. EMBO Journal 23 (12), 2451–2458.
Wolfe, L.S., Stanley, B.J., Liu, C., Eliason, W.K., Xiong, Y., 2010. Dissection of the HIV Vif interaction with human E3 ubiquitin ligase. Journal of Virology 84 (14), 7135–7139.
Wu, W., Henderson, L.E., Copeland, T.D., Gorelick, R.J., Bosche, W.J., Rein, A., Levin, J.G., 1996. Human immunodeficiency virus type 1 nucleocapsid protein reduces reverse transcription pausing at a secondary structure near the murine leukemia virus polypurine tract. Journal of Virology 70, 7132–7142.
Xiao, Z., Ehrlich, E., Yu, Y., Luo, K., Wang, T., Tian, C., Yu, X.F., 2006. Assembly of HIV-1 Vif-Cul5 E3 ubiquitin ligase through a novel zinc-binding domain-stabilized hydrophobic interface in Vif. Virology 349 (2), 290–299.
Xiao, Z., Ehrlich, E., Luo, K., Xiong, Y., Yu, X.F., 2007. Zinc chelation inhibits HIV Vif activity and liberates antiviral function of the cytidine deaminase APOBEC3G. FASEB Journal 21 (1), 217–222.
Xue, B., Mizianty, M.J., Kurgan, L., Uversky, V.N., 2011. Protein intrinsic disorder as a flexible armor and a weapon of HIV-1. Cellular and Molecular Life Sciences.
Yamamoto, Y., Saito, Y., Iida, S., Asano, J., Sone, S., Adachi, A., 1997. Functional analysis of Vif genes derived from various primate immunodeficiency viruses. Virus Genes 14 (3), 195–200.
Yang, X., Gabuzda, D., 1998. Mitogen-activated protein kinase phosphorylates and regulates the HIV-1 Vif protein. Journal of Biological Chemistry 273 (45), 29879–29887.
Yang, X., Goncalves, J., Gabuzda, D., 1996. Phosphorylation of Vif and its role in HIV-1 replication. Journal of Biological Chemistry 271 (17), 10121–10129.
Yang, S., Sun, Y., Zhang, H., 2001. The multimerization of human immunodeficiency virus type I Vif protein: a requirement for Vif function in the viral life cycle. Journal of Biological Chemistry 276 (7), 4889–4893.
Yang, B., Gao, L., Li, L., Lu, Z., Fan, X., Patel, C.A., Pomerantz, R.J., DuBois, G.C., Zhang, H., 2003. Potent suppression of viral infectivity by the peptides that inhibit multimerization of human immunodeficiency virus Type 1 (HIV-1) Vif proteins. Journal of Biological Chemistry 278 (8), 6596–6602.
Yang, Y., Guo, F., Cen, S., Kleiman, L., 2007. Inhibition of initiation of reverse transcription in HIV-1 by human APOBEC3F. Virology 365 (1), 92–100.
Yu, X., Yu, Y., Liu, B., Luo, K., Kong, W., Mao, P., Yu, X.F., 2003. Induction of APOBEC3G ubiquitination and degradation by an HIV-1 Vif-Cul5-SCF complex. Science 302 (5647), 1056–1060.
Yu, Q., Konig, R., Pillai, S., Chiles, K., Kearney, M., Palmer, S., Richman, D., Coffin, J.M., Landau, N.R., 2004a. Single-strand specificity of APOBEC3G accounts for minus-strand deamination of the HIV genome. Nature Structural & Molecular Biology 11 (5), 435–442.
Yu, Y., Xiao, Z., Ehrlich, E.S., Yu, X., Yu, X.F., 2004b. Selective assembly of HIV-1 Vif-Cul5-Elongin B-Elongin C E3 ubiquitin ligase complex through a novel SOCS box and upstream cysteines. Genes and Development 18 (23), 2867–2872.
Zennou, V., Perez-Caballero, D., Gottlinger, H., Bieniasz, P.D., 2004. APOBEC3G incorporation into human immunodeficiency virus type 1 particles. Journal of Virology 78 (21), 12058–12061.
Zhang, H., Pomerantz, R.J., Dornadula, G., Sun, Y., 2000. Human immunodeficiency virus type 1 Vif protein is an integral component of an mRNP complex of viral RNA and could be involved in the viral RNA folding and packaging process. Journal of Virology 74 (18), 8252–8261.
Zhang, H., Yang, B., Pomerantz, R.J., Zhang, C., Arunachalam, S.C., Gao, L., 2003. The cytidine deaminase CEM15 induces hypermutation in newly synthesized HIV-1 DNA. Nature 424 (6944), 94–98.
Zhang, W., Chen, G., Niewiadomska, A.M., Xu, R., Yu, X.F., 2008. Distinct determinants in HIV-1 Vif and human APOBEC3 proteins are required for the suppression of diverse host anti-viral proteins. PLoS ONE 3 (12), e3963.
Zhang, W., Du, J., Evans, S.L., Yu, Y., Yu, X.F., 2011. T-cell differentiation factor CBF-beta regulates HIV-1 Vif-mediated evasion of host restriction. Nature.
Zhen, A., Wang, T., Zhao, K., Xiong, Y., Yu, X.F., 2010. A single amino acid difference in human APOBEC3H variants determines HIV-1 Vif sensitivity. Journal of Virology 84 (4), 1902–1911.
Zheng, Y.H., Irwin, D., Kurosu, T., Tokunaga, K., Sata, T., Peterlin, B.M., 2004. Human APOBEC3F is another host factor that blocks human immunodeficiency virus type 1 replication. Journal of Virology 78 (11), 6073–6076.
Zou, J.X., Luciw, P.A., 1996. The requirement for Vif of SIVmac is cell-type dependent. Journal of General Virology 77 (Pt 3), 427–434.

Article 4: APOBEC3G Impairs the Multimerization of the HIV-1 Vif Protein in Living Cells

This article describes the role of Vif multimerization in viral assembly and A3G repression. My contribution in this study was to identify whether another PPLP-binding protein could also compete and perturb Vif oligomerization. To this aim, we investigated the cellular Hck kinase because it has been previously observed that this protein interacts with a large domain containing the PPLP motif of Vif. Thus, I transfected HeLa cells with unlabeled or eGFP-Vif proteins together with A3G in the presence or absence of Hck and I analyzed A3G degradation using immunoblotting. Moreover, I also contributed in the plasmid construction process.

Journal of Virology

APOBEC3G Impairs the Multimerization of the HIV-1 Vif Protein in Living Cells

Julien Batisse, Santiago Xavier Guerrero, Serena Bernacchi, Ludovic Richert, Julien Godet, Valérie Goldschmidt, Yves Mély, Roland Marquet, Hugues de Rocquigny and Jean-Christophe Paillart

J. Virol. **2013, 87(11):6492. DOI: 10.1128/JVI.03494-12. Published Ahead of Print 10 April 2013.**

JVI
Journals.ASM.org

APOBEC3G Impairs the Multimerization of the HIV-1 Vif Protein in Living Cells

Julien Batisse,[a] Santiago Xavier Guerrero,[a] Serena Bernacchi,[a] Ludovic Richert,[b] Julien Godet,[b] Valérie Goldschmidt,[b]† Yves Mély,[b] Roland Marquet,[a] Hugues de Rocquigny,[b] Jean-Christophe Paillart[a]

Architecture et Réactivité de l'ARN, Université de Strasbourg, CNRS, Institut de Biologie Moléculaire et Cellulaire, Strasbourg Cedex, France[a]; Laboratoire de Biophotonique et Pharmacologie, UMR 7213 CNRS, Faculté de Pharmacie, Université de Strasbourg, Illkirch Cedex, France[b]

The HIV-1 viral infectivity factor (Vif) is a small basic protein essential for viral fitness and pathogenicity. Vif allows productive infection in nonpermissive cells, including most natural HIV-1 target cells, by counteracting the cellular cytosine deaminases APOBEC3G (apolipoprotein B mRNA-editing enzyme catalytic polypeptide-like 3G [A3G]) and A3F. Vif is also associated with the viral assembly complex and packaged into viral particles through interactions with the viral genomic RNA and the nucleocapsid domain of Pr55^{Gag}. Recently, we showed that oligomerization of Vif into high-molecular-mass complexes induces Vif folding and influences its binding to high-affinity RNA binding sites present in the HIV genomic RNA. To get further insight into the role of Vif multimerization in viral assembly and A3G repression, we used fluorescence lifetime imaging microscopy (FLIM)- and fluorescence resonance energy transfer (FRET)-based assays to investigate Vif-Vif interactions in living cells. By using two N-terminally tagged Vif proteins, we show that Vif-Vif interactions occur in living cells. This oligomerization is strongly reduced when the putative Vif multimerization domain (^{161}PPLP^{164}) is mutated, indicating that this domain is crucial, but that regions outside this motif also participate in Vif oligomerization. When coexpressed together with Pr55^{Gag}, Vif is largely relocated to the cell membrane, where Vif oligomerization also occurs. Interestingly, wild-type A3G strongly interferes with Vif multimerization, contrary to an A3G mutant that does not bind to Vif. These findings confirm that Vif oligomerization occurs in living cells partly through its C-terminal motif and suggest that A3G may target and perturb the Vif oligomerization state to limit its functions in the cell.

The human immunodeficiency virus type 1 (HIV-1) infects primary T cells, macrophages, and monocytes, ultimately leading to the destruction of the immune system, infection by opportunistic pathogens, and death, if viral propagation cannot be inhibited. However, these cell lineages express two related cytidine deaminases of the APOBEC (apolipoprotein B mRNA-editing enzyme catalytic polypeptide-like) family, named APOBEC3G (A3G) and A3F, that efficiently restrict HIV-1 replication (1–5). If incorporated into budding virions, A3G and -F cause lethal mutagenesis by cytidine deamination during negative-strand DNA synthesis (4, 6, 7). Moreover, A3G and -F impair HIV-1 DNA synthesis and integration independently of their catalytic activity, suggesting that deamination is not the only determinant for antiviral activity (1, 8–10). This innate defense system most likely evolved from a mechanism initially dedicated to target retrotransposons and retroelements (11, 12).

In order to infect nonpermissive cells containing A3G or -F, HIV-1 has evolved the HIV-1 viral infectivity factor (Vif), a 23-kDa basic protein (13) required for *in vivo* viral propagation and pathogenesis (14–16). Vif has been shown to efficiently counteract the antiviral activity of A3G and -F by various mechanisms (1, 17). Vif targets A3G and -F for degradation via the proteasome by recruiting an E3 ubiquitin ligase cellular complex composed of elongin B (EloB), elongin C (EloC), cullin 5 (Cul5), and RING-box protein 2 (Rbx2) (1, 17–21). Recently, CBF-β, the transcriptional core binding factor-β, has been shown to be an integral component of this complex, directly interacting with Vif and favoring the specific polyubiquitination and degradation of the A3G protein (22, 23). Vif has also been shown to inhibit the antiretroviral activity of A3G and -F by interfering their packaging (24, 25) and intracellular expression (26, 27). Importantly, the use of proteasome inhibitors (24) showed that degradation and inhibition of A3G translation are two independent pathways utilized by Vif to reduce the expression of A3G (26, 27). In this context, we recently showed that Vif downregulates A3G translation by binding to the 5′ untranslated region (UTR) of A3G mRNA (28).

In addition to its well-documented anti-A3G activity, Vif possesses RNA binding and chaperone properties (29, 30). Indeed, Vif has been shown to bind specifically and cooperatively to the 5′-end region of HIV-1 genomic RNA *in vitro* (31, 32) in infected cells (33, 34) and to the A3G mRNA (28). Vif also promotes several steps involving RNA refolding during reverse transcription and RNA dimerization (29, 35). Although the complete structure of Vif is still unresolved, many studies have investigated the biochemical and biophysical properties of this protein. *In vitro*, Vif has been shown to self-associate and to form dimers, trimers, and tetramers (36, 37). The region from positions 151 to 164, which encompasses the conserved proline-rich region ^{161}PPLP^{164}, has been shown to govern Vif multimerization (37, 38). This short domain was found to be crucial for Vif function and viral infectivity (37–39). Moreover, it can interact with A3G (40, 41), cullin

Received 22 December 2012 **Accepted** 25 March 2013
Published ahead of print 10 April 2013
Address correspondence to Jean-Christophe Paillart, jc.paillart@ibmc-cnrs.unistra.fr.
† Deceased.
This article is dedicated to the memory of Valérie Goldschmidt.

doi:10.1128/JVI.03494-12

5 (42), and the HIV-1 reverse transcriptase (35), and it was also observed that an intact PPLP motif is required for interaction between Vif and elongin B (43, 44). Considering the involvement of the PPLP motif in Vif oligomerization, it is conceivable that all of these binding functions could be linked to the multimerization state of Vif. Indeed, we recently reported that alanine substitutions in the Vif PPLP motif do not significantly affect the overall secondary structure of the protein, but impair its oligomerization state *in vitro*, leading to decreasing binding affinity and specificity for nucleic acids (45). Moreover, it seems that the oligomerization and RNA binding properties of Vif are required to form high-molecular-mass complexes composed of Vif and the HIV-1 transactivation response (TAR) element (45).

To investigate the multimerization properties of HIV-1 Vif in a more physiological context, we characterized the interaction of two Vif fusion proteins expressing enhanced green fluorescent protein and mCherry (eGFP-Vif and mCherry-Vif, respectively) in living cells by using a fluorescence resonance energy transfer (FRET) approach analyzed by fluorescence lifetime imaging microscopy (FLIM) and fluorescence correlation spectroscopy (FCS). We provide direct evidence that Vif multimerization occurs in living cells and highlight the role of the PPLP motif in this property. Moreover, in the presence of the $Pr55^{Gag}$ precursor, Vif was largely relocalized to the cell membrane, where Vif multimerization also occurred. However, Vif oligomerization was not required for $Pr55^{Gag}$-induced relocalization to the cell membrane. Finally, we showed that the interaction of A3G with Vif strongly impairs Vif multimerization, most likely by a competition mechanism involving the Vif-binding domain of A3G and the PPLP motif of Vif or by an A3G-induced conformational change in Vif that prevents oligomerization.

MATERIALS AND METHODS

Plasmid construction. Vif-fusion expression plasmids were constructed by two-step PCR and cloning into the pcDNA3.1 (Invitrogen) vector. A first PCR amplification of eGFP and mCherry sequences was performed from vectors expressing mCherry- and eGFP-Vpr (Vpr accession no. ABN49562) (46). The forward primer (primer 1) 5′-CCCAAGCTT**GCCGCCACC**ATGGTGAGCAAGGGCGAG3′ contains a HindIII restriction site (underlined) upstream of a Kozak consensus sequence (boldface). The reverse primer (primer 2) 5′-**GAGAGAGGCGACATCGCCTCC**CTTGTACAGCTCGTCCATGC-3′ contains a linker (boldface) coding for the polypeptide GGDVASL to avoid quenching of the fluorophore by Vif. The Vif sequence (codon optimized for expression in mammalian cells) was amplified from pcDNA-hVif (accession no. AAB60573, codon optimized [47]) (kindly provided by K. Strebel, NIH, Bethesda, MD) with forward primer (primer 3) 5′-**GGAGGCGATGTCGCCTCTCTC**ATGGAGAACCGGTGGCAGGTG-3′ containing a linker sequence (boldface), and reverse primer (primer 4) 5′-CCCGAATTC**TTA**GTGTCCATTCATTGTATGGCTCCCTC-3′ containing an EcoRI restriction site (underlined) and a stop codon (boldface). After purification of PCR products (Macherey-Nagel), a second PCR was performed using both PCR products as the templates, together with primers 1 and 4. Full-length PCR products were then purified, digested with HindIII and EcoRI, and cloned into pcDNA3.1. Substitution of AALA for the ^{164}PPLP^{169} motif was performed by site-directed mutagenesis using Quick-Change mutagenesis (Stratagene) as previously described (28).

The hVif coding sequence, excluding the first ATG, was also amplified using forward primer 5 (5′-CGGGGATCCGAGAACCGGTGGCAGGTGATG-3′), containing a BamHI site (underlined), and reverse primer 4 and cloned into pSA1B (48) previously digested by BamHI and EcoRI. The resulting plasmid, pSA1B-Vif, expresses a hemagglutinin (HA)-tagged Vif protein suitable for immunoprecipitation. Wild-type (WT) and mutant A3G proteins were respectively expressed from pCMV-A3G (accession no. NP_068594) and pCMV-A3G D128K (28). The Gag protein was expressed from the human codon-optimized $Pr55^{Gag\text{-}TC}$ expression vector (accession no. AAB50258) (49) and the kinase Hck was expressed from pcDNA3.1-Hck (kindly provided by E. Decroly, UMR-6098-AFMB, Marseille, France). The integrity of all constructs was confirmed by DNA sequencing (GATC Biotech, Germany).

Cell culture and transfection. HeLa cells were grown at 37°C in 5% CO_2 in Dulbecco's modified Eagle's medium supplemented with 10% fetal calf serum and penicillin and streptomycin antibiotics (Invitrogen). For FLIM and FCS analyses, 2.10^5 cells were cultured on 35-mm μ-dishes (IBIDI-Biovalley, Strasbourg France). For fluorescence imaging and Western blot analysis, 5.10^5 cells were cultured in 6-well plates, with or without glass coverslips. HeLa cells were transfected with 0.5 μg of each plasmid using JetPEI (PolyPlus transfection; Illkirch, France) or X-tremeGENE-9 HD (Roche) according to the supplier's instructions.

Western blot analysis. Twenty-four hours posttransfection, cells were washed with 1× concentrated phosphate-buffered saline (PBS) (140 mM NaCl, 8 mM NaH_2PO_4, 2 mM Na_2HPO_4) and lysed in radioimmunoprecipitation assay (RIPA) buffer (1× PBS, 1% NP-40, 0.5% sodium deoxycholate, 0.05% SDS) supplemented with protease inhibitors (complete EDTA free cocktail; Roche). After centrifugation, total protein concentration was assessed by Bradford analysis (Bio-Rad), and 25 μg of total protein was loaded on a 4 to 12% NuPAGE Bis-Tris gel (Invitrogen). Proteins were then transferred onto polyvinylidene difluoride (PVDF) membrane (0.45-μm pore; Millipore) for 1 h 30 min at 30 V and detected by Western blotting using antibodies directed against Vif (NIH Research and Reference Reagent Program, no. 319, from M. H. Malim) (with full-length 6His-Vif used as an immunogen to produce this antibody [50]), A3G (NIH Research and Reference Reagent Program, no. 9906, from W. Greene), GFP (sc-9996; Santa Cruz Biotechnology, Santa Cruz, CA), mCherry (GTX59788; GeneTex), Hck (no. 610277; BD Transduction Laboratory) (a gift from E. Decroly [51]), and β-actin (AC-74; Sigma-Aldrich, St. Louis, MO), followed by horseradish peroxidase-conjugated anti-mouse or anti-rabbit antibodies (Bio-Rad), revealed by the chemiluminescent ECL Prime system (GE Healthcare).

Immunoprecipitation. HeLa cells were cotransfected with HA-Vif and eGFP-Vif (wild-type or AALA mutant), and 24 h posttransfection, cells were washed in 1× PBS and lysed in 1× RIPA buffer supplemented with protease inhibitors. After centrifugation, an input fraction (50 μl) was kept to check the protein expression level, and the rest was split into two fractions: one-half was incubated 2 h at 4°C with 1 μg of HA antibody (sc-805; Santa Cruz, CA) on a rotating wheel, and the second half was incubated without antibody and used as a negative control. After equilibration, protein A beads were added and the mixture was incubated for 1.5 h at 4°C. Beads were washed 5 times with cold 1× RIPA buffer, resuspended in Laemmli sample buffer, boiled for 5 min, and analyzed by Western blotting. In a similar experiment, HeLa cells were transfected with vectors expressing eGFP-Vif, mCherry-Vif, and either wild-type or D128K mutant A3G.

Confocal microscopy for fluorescence and IF analyses. For confocal microscopy, HeLa cells were seeded onto a 20- by 20-mm glass coverslip, and 24 h posttransfection, cells were washed with 1× PBS and fixed for 5 min in 100% methanol. For the immunofluorescence (IF) assay, the cells were permeabilized for 5 min with 0.1% Triton X-100 in 1× PBS before blocking of nonspecific sites with PBS–3% bovine serum albumin (BSA) for 1 h at 20°C. Cells were stained with mouse monoclonal antibodies (MAbs) against Vif (NIH Research and Reference Reagent Program, no. 319), used in 1× PBS–3% BSA (1/500) for an overnight incubation at 4°C. After several washes in 1× PBS, cells were incubated with anti-mouse antibody labeled with Alexa Fluor 488 (Molecular Probes) for 1 h at 20°C. Coverslips were then mounted on a glass slide in mounting medium containing DAPI (4′,6-diamidino-2-phenylindole) (Slowfade reagent; Molecular Probes). Images were acquired on a Zeiss LSM700 confocal micro-

TABLE 1 Average lifetimes and FRET efficiencies of eGFP-Vif proteins in cytoplasm[a]

Transfection(s)	Avg lifetime, ns (95% CI)	No. of cells	FRET efficiency, % (95% CI)
eGFP-Vif	2.53 (2.52–2.54)	71	
eGFP-Vif + mCherry	2.48 (2.46–2.49)	61	2.0 (−3.0–6.8)
eGFP-Vif + mCherry-Vif	**2.21 (2.19–2.25)**	**71**	**12.2 (2.6–21.7)**
eGFP-Vif AALA + mCherry-Vif AALA	2.35 (2.34–2.38)	74	6.6 (−0.5–13.5)
eGFP-Vif AALA + mCherry-Vif	2.35 (2.33–2.37)	14	6.6
eGFP-Vif + mCherry-Vif AALA	2.35 (2.34–2.36)	12	6.6
eGFP-Vif + A3G	2.52 (2.51–2.53)	38	0.3 (−4.7–5.1)
eGFP-Vif + mCherry + A3G	2.49 (2.47–2.51)	29	1.4 (−3.8–6.4)
eGFP-Vif + mCherry-Vif + A3G	2.38 (2.36–2.40)	54	5.7 (−2.2–13.5)
eGFP-Vif + mCherry-Vif + A3G D128K	2.26 (2.23–2.29)	73	10.4 (−0.9–21.4)
eGFP-Vif AALA + mCherry-Vif AALA +A3G	2.40 (2.37–2.42)	52	5.1 (−2.5–12.4)
eGFP-Vif + mCh-Vif + Hck	2.33 (2.32–2.35)	33	7.6 (−2.4–12.3)

[a] Results in boldface represent the highest FRET efficiency.

scope (Strasbourg-Esplanade Cellular Imaging Facility—IBMP) with a 63× 1.4NA Plan-Apochromat oil objective. Images were processed (contrast, brightness, and merges) with ImageJ 1.43m software (W. J. Rasband, ImageJ [1997 to 2012], National Institutes of Health, Bethesda, MD; http://imagej.nih.gov/ij/).

FRET and FLIM analyses. Time-correlated single-photon-counting (TCSPC) FLIM was performed on a custom two-photon system laser-scanning setup based on an Olympus IX70 inverted microscope (Olympus, Japan) with an Olympus 60× 1.2NA water immersion objective as previously described (46). Two-photon excitation at 900 nm was provided by a mode-locked titanium-sapphire laser (Tsunami; Spectra Physics, CA), and the laser power was adjusted to give count rates with peaks up to 10^6 photons · s^{-1}, so that the pileup effect can be neglected. Imaging was carried out with a laser-scanning system using two fast galvanometer mirrors (model 6210; Cambridge Technology, MA), operating in the descanned fluorescence collection mode. Photons were collected using a set of two filters: a two-photon short-pass filter with a cutoff wavelength of 680 nm (F75-680; AHF, Germany), and a band-pass filter of 520 ± 17 nm (F37-520; AHF, Germany). The fluorescence was directed to a fiber-coupled Avalanche photodetector (APD) (SPCM-AQR-14-FC; PerkinElmer, Canada), which was connected to a time-correlated single-photon-counting module (SPC830; Becker and Hickl, Germany), which operates in the reversed start-stop mode. Typically, the samples were scanned continuously for about 60 s to achieve appropriate photon statistics to analyze the fluorescence decays. Data were analyzed with a commercial software package (SPCImage V3.2; Becker and Hickl, Germany), which uses an iterative reconvolution method to recover the lifetimes from the fluorescence decays. In fluorescence resonance energy transfer (FRET) experiments, when coexpressing donor and acceptor proteins, the FRET efficiency reflecting the distance between the two chromophores was calculated according to

$$E = \frac{R_0^6}{R_0^6 + R^6} = 1 - \frac{\tau_{DA}}{\tau_D}$$

where R_0 is the Förster radius, R is the distance between donor and acceptor, τ_{DA} is the lifetime of the donor in the presence of the acceptor, and τ_D is the lifetime of the donor in the absence of the acceptor.

FCS analysis. FCS was performed using the same core as the system described for FLIM measurements, as previously described (52). The normalized autocorrelation function was calculated online with a hardware correlator (ALV5000; ALV GmbH, Germany). Due to the inherent heterogeneity of the cellular medium, the FCS data were interpreted in terms of anomalous diffusion. Therefore, curves were fitted according to

$$G(\tau) = \frac{1}{N}\left[1 - \left(\frac{\tau}{\tau_A}\right)^a\right]^{-1} \cdot \left[1 + \left(\frac{\tau}{\tau_A}\right)^a \cdot \frac{1}{S^2}\right]^{-1/2}$$

where N is the average number of fluorescent species in the focal volume, τ is the lag time, τ_A is the average residence time in the focal volume, α is the anomalous diffusion coefficient, and S is a structural parameter defined as the ratio between the axial and lateral radii of the beam waist. The molecular brightness (η) of the fluorescent species diffusing through the excitation volume is obtained by dividing the average fluorescence intensity $\langle F \rangle$ by N. In free lateral diffusion ($\alpha = 1$), the mean-square displacement of the diffusing species is proportional to time ($\langle r^2 \rangle \sim t$). This is no more valid for anomalous diffusion ($\alpha < 1$) that takes place in systems containing obstacles. In that case, the mean-square displacement is described by a power law ($\langle r^2 \rangle \sim t^\alpha$) with coefficient α depending on the concentration, size, mobility, and reactivity of the obstacles. Moreover, in living cells, there is no real steady state for the fluorescence intensity fluctuations. For this reason, FCS measurements were sequentially repeated, typically 100× for 6 s. Each FCS curve was then fitted independently. A Labview program was written to automatically process the data. The results represented only the brightness parameter, which is the most relevant in terms of protein oligomerization and was calculated for each curve in order to provide a population distribution curve.

Statistical analysis. Statistical analyses were performed using R version 2.14.0 (http://www.R-project.org/). Fluorescence mean lifetimes and bias-corrected bootstrapped confidence intervals (CI) were calculated based on 50 to 70 cells from at least three independent experiments (Table 1). Posterior FRET distributions and 95% CI estimates were computed using Markov chain Monte Carlo (MCMC) algorithms implemented in OpenBugs version 3.2.1 (http://www.openbugs.info), assuming poorly informative Gaussian priors. The level of statistical significance was set at 5%.

RESULTS

Expression of eGFP- and mCherry-Vif fusion proteins. To investigate Vif multimerization in living cells by FRET or FLIM, we first labeled the Vif protein with two fluorophores compatible with FRET analysis: eGFP and mCherry. As a donor, eGFP presents the advantage of possessing a high quantum yield (0.8), and its time-resolved fluorescence decay is monoexponential, with a lifetime of about 2.6 ns (53). The mCherry tag was used as an acceptor due to the strong overlap between its absorption spectrum and the emission spectrum of eGFP, resulting in a large Förster distance, R_0 (about 54 Å) (54). The other advantage of using mCherry as an acceptor was its monomeric and fully mature state, which enables the protein to conserve its spectroscopic properties when it is fused to a target protein (55). Moreover, several studies have already successfully used the eGFP-mCherry fluorophore pair to investigate protein-protein interactions and

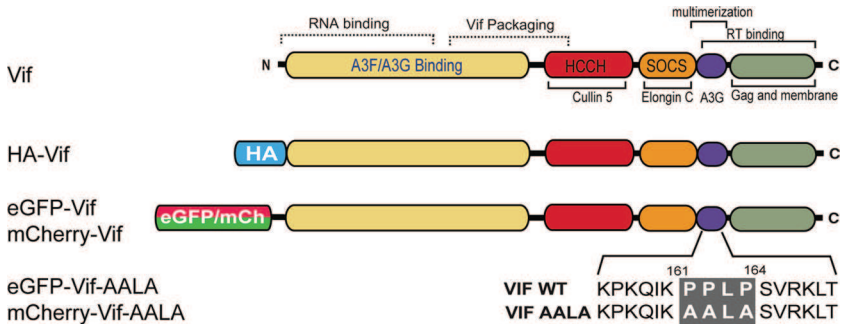

FIG 1 Structural and functional organization of Vif proteins. Vif functional domains are indicated. For eGFP or mCherry fusion proteins, a small linker coding for 7 amino acids (GGDVASL) was added to avoid quenching of the fluorophore. The sequences of the multimerization domains of WT and mutant Vif proteins are indicated.

protein oligomerization by FRET analysis, further validating our selection (46).

These two fluorophores were therefore fused to the N or C terminus of the Vif protein. To avoid quenching of the fluorophores, a short linker (7 amino acids) was inserted between the fluorophore and the Vif coding sequence (Fig. 1). Western blot analysis showed that both N-terminus-tagged proteins were expressed in HeLa cells (Fig. 2A, lanes 5 and 7) at a level comparable to that of the wild-type Vif protein (Fig. 2A, lane 3), but with a slight degradation of the chimeric proteins (a light slower band is visible on the blots with a Vif or GFP antibody). On the contrary, the C-terminus-tagged Vif proteins were expressed at a low level (data not shown). Hence, we carried out the rest of our study using only the N-terminus-tagged Vif proteins. We next checked that the Vif fusion proteins were fully functional and could reduce the expression of A3G. As shown in Fig. 2A, A3G expression was affected by all Vif constructs (lanes 3, 5, and 7), but the effect was a slightly more pronounced with the wild-type Vif protein than the chimeric Vif proteins (80% inhibition versus 60%) (Fig. 2B). This difference most probably results from the steric hindrance of the tag proteins. To investigate Vif multimerization, the same expression vectors were constructed using a mutant of Vif in which the 160PPLP164 motif was substituted for an oligomerization-defective AALA motif (Fig. 1). Although we detected a lower yield of Vif AALA compared to wild-type Vif fusion proteins using a Vif-specific antibody (Fig. 2A, lanes 6 and 8), this is probably due to a defect in the antibody recognition motif (56). Indeed, eGFP-Vif and eGFP-Vif AALA were detected at the same level using an antibody directed against the GFP- or mCherry-tagged proteins (Fig. 2A, middle panels, lanes 5 and 6 and 7 and 8, respectively). Thus, these two proteins were also efficiently expressed in HeLa cells. As previously observed (40, 57), these Vif AALA mutants were inefficient in counteracting A3G (Fig. 2A, lanes 4, 6, and 8, and B), confirming the importance of the PPLP motif in the A3G regulation. These control analyses confirmed the mechanism of Vif function and established that our fusion proteins reliably monitor the effects of Vif on A3G in cells.

Biochemical characterization of Vif oligomerization. To investigate Vif-Vif interaction in HeLa cells, we first coexpressed the different eGFP fusion proteins (eGFP-Vif and eGFP-Vif AALA) together with an HA-tagged Vif protein (HA-Vif). If chimeric Vif proteins are still able to form multimers, we should be able to coimmunoprecipitate eGFP-Vif proteins using an antibody directed against the HA tag. As we previously showed that anti-Vif antibody did not efficiently recognize Vif AALA (Fig. 2A, lane 6 and 8), detection was also performed with an antibody directed against the eGFP moiety (Fig. 3). Under these conditions, we observed that eGFP-Vif and eGFP-Vif AALA were similarly expressed in HeLa cells (Fig. 3A, lanes 3 and 4). In the presence of HA antibody, we showed that eGFP-Vif coprecipitates with the HA-Vif protein (Fig. 3B, lane 3), suggesting that Vif-Vif interaction occurs in HeLa cells. When using the eGFP-Vif AALA, we observed a significant 2-fold reduction (0.48) in protein immunoprecipitated with HA-Vif (Fig. 3B, middle panel, compare lanes 4 and 3), suggesting the Vif AALA protein partially lost its capacity to form multimers. This result is consistent with previous observations indicating that regions outside the PPLP motif also participate in Vif oligomerization (58). Indeed, although the AALA mutation impaired oligomerization (36, 44, 45; this study), dimerization of the protein was still observed *in vitro* (45) and could be sufficient to be detected by immunoprecipitation. Alternatively, cell lysis treatment may have induced conformational changes in the Vif protein that could have exposed secondary interaction domains and induced binding. To further clarify the role of the PPLP motif, we analyzed Vif multimerization directly in living cells by using fluorescence microscopy techniques.

Vif oligomerizes in living cells through its PPLP motif. As a prerequisite for fluorescence assays and because eGFP and mCherry are large with respect to Vif, we also checked whether they affect the intracellular localization of Vif. To this end, we analyzed by confocal microscopy at 24 h posttransfection the expression of eGFP- and mCherry-Vif (wild-type and mutant) fusion proteins in HeLa cells. As shown in Fig. 4A, both eGFP- and mCherry-Vif proteins were mainly localized in the cytoplasm of transfected cells (80 to 90%) but were also present in the nucleus (10 to 20%), in agreement with previous observations (59–61). This localization is not due to the eGFP and mCherry since both fluorescent proteins were found throughout the cell when expressed in their free form (Fig. 4B). Interestingly, a nearly complete colocalization of the two Vif fusion proteins in the same cellular compartments was further evidenced by the overlap of their emissions (Fig. 4A, panels c). Similar results were obtained with the Vif AALA mutants (Fig. 4A, lower panel), demonstrating that mutation in the PPLP motif did not alter Vif localization. Localization of wild-type Vif in an expression (pcDNA-hVif) or proviral (pNL4.3-Env1) vector context by immunofluorescence (IF) confirmed that these proteins were predominantly localized in the cytoplasm with some nuclear localization (Fig. 5). Thus, the

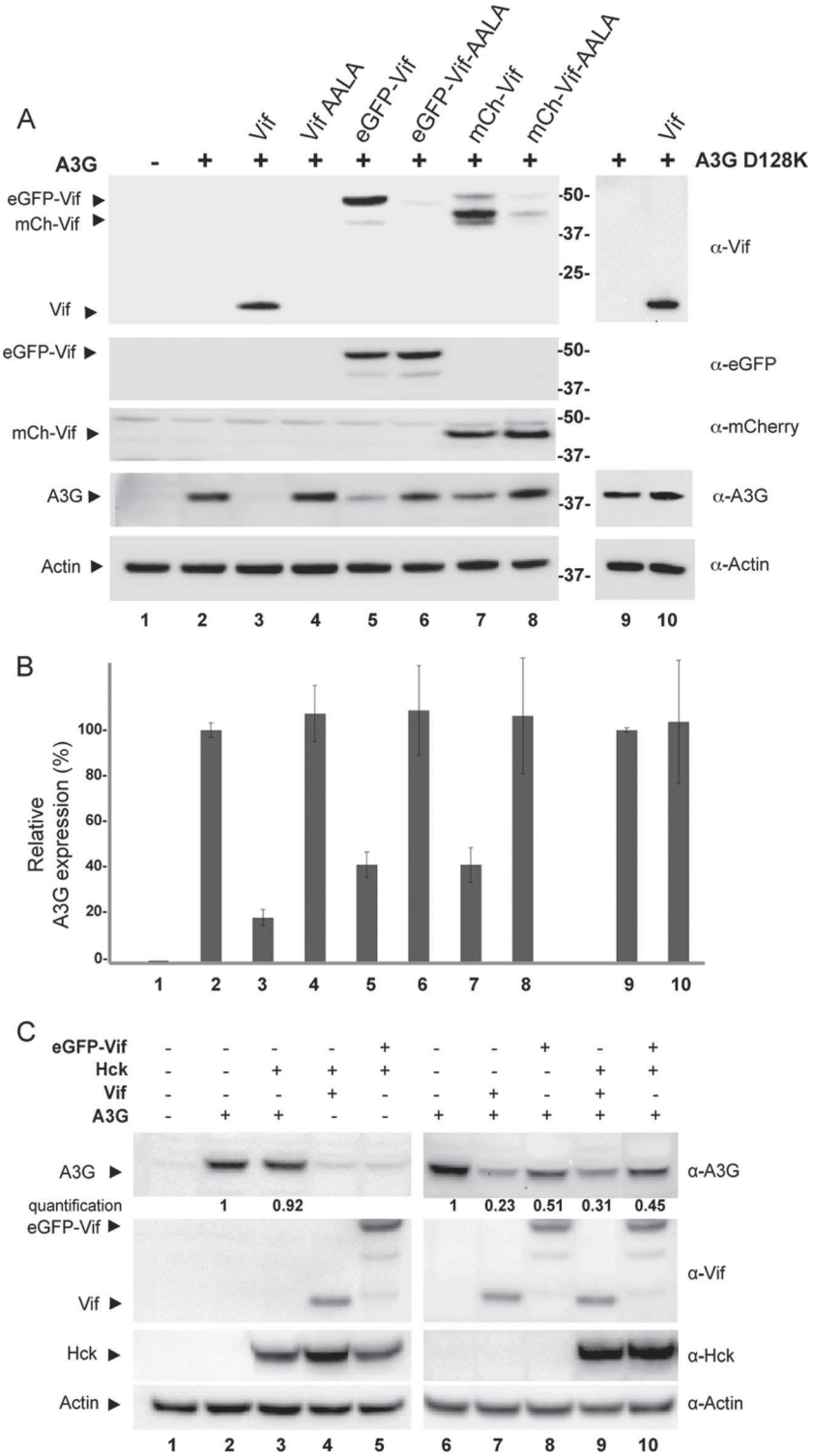

FIG 2 Activity of Vif fusion proteins against A3G. (A) Cells were transfected with 0.5 μg of each plasmid, and total cell extracts were harvested 24 h posttransfection. The Vif (wild-type and AALA mutant) or Vif fusion proteins A3G and A3G D128K were detected by Western blotting (antibody 319 for Vif [α-Vif], 9906 for A3G [α-A3G], sc-9996 for GFP [α-eGFP], GTX59788 for mCherry [α-mCherry], and AC-74 for β-actin [α-Actin]). β-Actin was used as a loading control. (B) A3G degradation efficiency of the different Vif proteins. A3G signals (from panel A) were quantified (A3G/β-actin ratio), and the lane without Vif (lane 2) was set at 100%. Error bars represent standard deviations from three independent experiments. (C) Cells were transfected with vectors expressing Vif (lanes 4, 7, and 9) or eGFP-Vif (lanes 5, 8, and 10) together with A3G (lanes 2 and 3 and 6 to 10) and/or Hck (lanes 3, 4, 5, 9, and 10). Total cell extracts were harvested 24 h posttransfection and analyzed by immunoblotting using antibodies directed against A3G, Vif, and Hck (610277). β-Actin was used as an internal control. In all panels, proteins are identified on the left and the antibody used for the detection is indicated on the right-hand side.

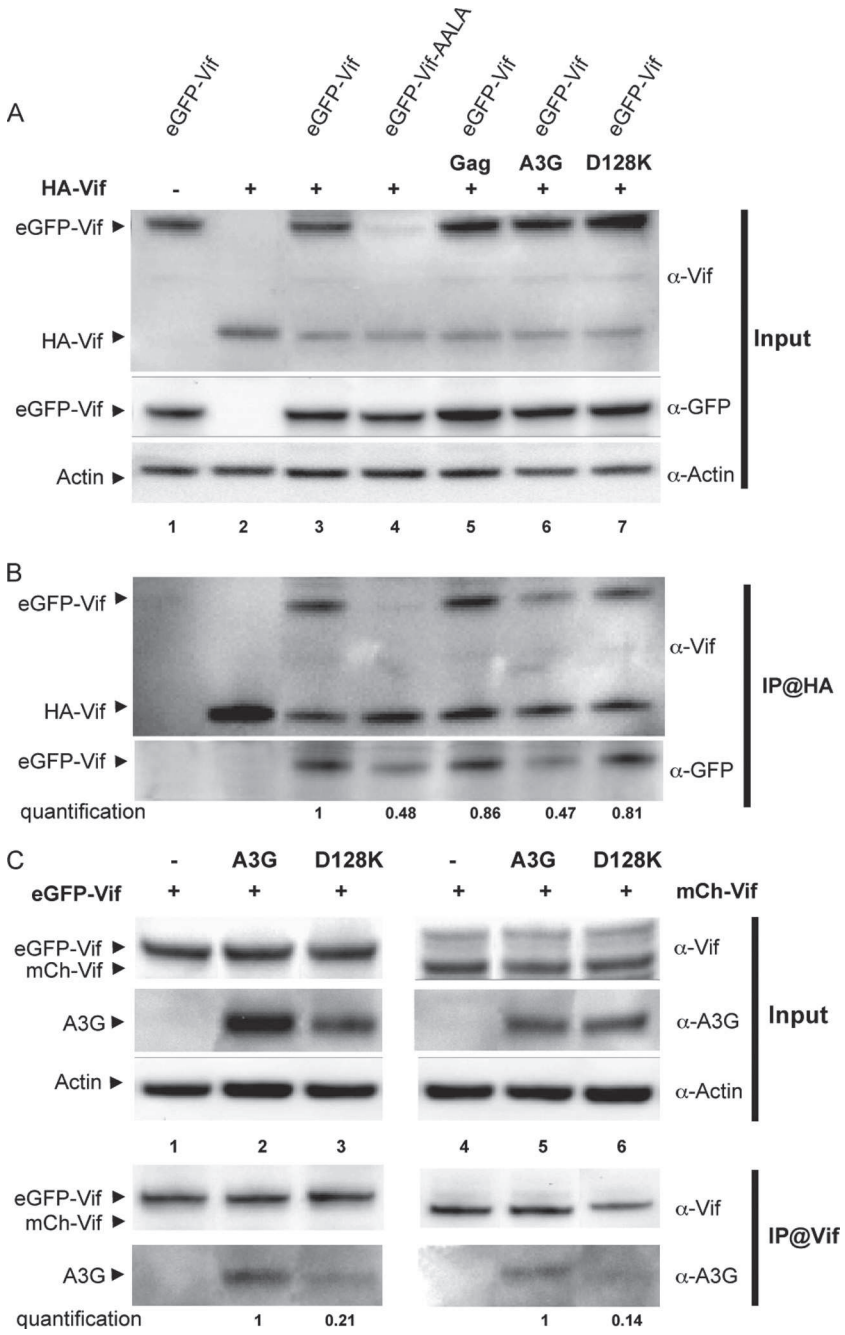

FIG 3 Vif fusion proteins interact in cells. Cells were transfected with 1 μg of each Vif expression vector. Total cell extracts were harvested 24 h posttransfection. (A) The input fractions were revealed by anti-Vif (319) and anti-eGFP (sc-9996) antibodies. The latter was used to allow the detection of the Vif AALA mutant (as observed in Fig. 2A, lane 6). β-Actin was used as an internal control (AC-74). (B) Immunoprecipitation assays were performed using an anti-HA antibody (sc-805) directed against the HA-Vif protein. A negative control without HA-Vif (lane 1) and a specificity control without eGFP-Vif (lane 2) were also included. The fraction of Vif fusion proteins interacting with HA-Vif is indicated. (C) Immunoprecipitation of eGFP-Vif and mCherry-Vif (mCh-Vif) with A3G and A3G D128K proteins. The input fractions were revealed by anti-Vif (antibody 319) and anti-A3G (antibody 9906) antibodies. Immunoprecipitation assays were performed using an anti-Vif antibody directed against the eGFP- and mCherry-Vif proteins. The fraction of A3G proteins interacting with eGFP- and mCherry-Vif is indicated.

fusion of either mCherry or eGFP to the N terminus of Vif has a limited effect on Vif localization in the cell.

Although confocal microscopy showed that fusion Vif proteins colocalized in the cells, a direct Vif-Vif interaction cannot be proven by this technique. We thus measured the FRET efficiency between the two fluorophores, by using FLIM. FRET is a potent tool to investigate interactions in living cells as it only occurs between eGFP- and mCherry-tagged proteins when the two fluorophores are less than 10 nm apart (62, 63). In living cells, FRET can be imaged by monitoring the fluorescence lifetime decrease of the

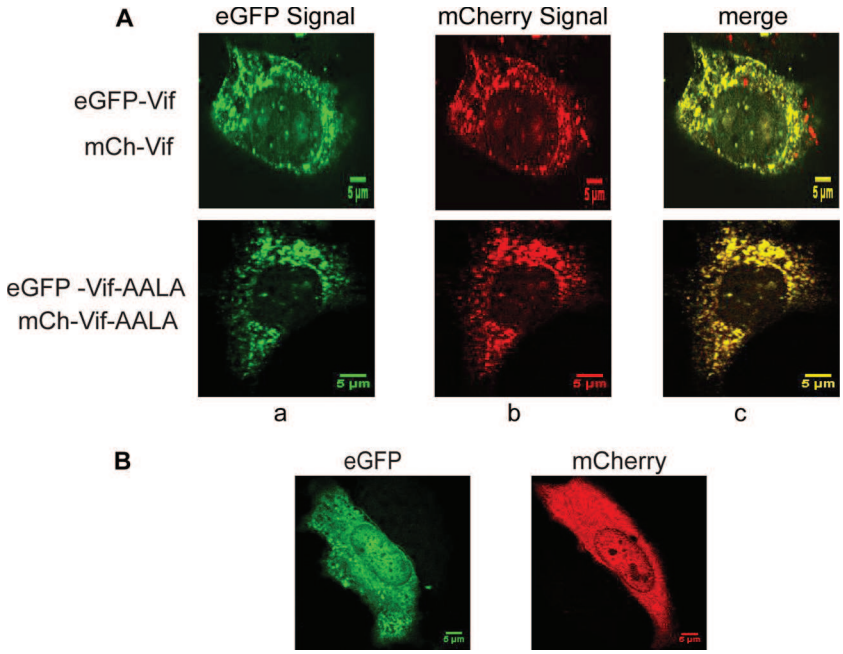

FIG 4 Localization of eGFP- and mCherry-Vif fusion proteins. HeLa cells were transfected with 0.5 μg of each plasmid. Twenty-four hours posttransfection, cells were fixed with methanol and analyzed by confocal microscopy. (A) Colocalization of wild-type (upper panel) and AALA mutant (lower panel) eGFP-Vif (a) and mCherry-Vif (mCh-Vif) proteins (b). Merged images are shown in panels c. Colocalization of the two proteins is indicated by the color yellow. (B) Localization of free eGFP and mCherry proteins.

eGFP donor with the FLIM technique. This lifetime (i.e., the average time that molecules stay in their excited state) is an intrinsic and specific parameter for each fluorophore. In contrast to fluorescence intensity, fluorescence lifetime depends neither on instrumentation setup nor on local concentration of the fluorescent molecules and is not affected by photobleaching. A threshold value of 5% for FRET efficiency is commonly required to define a bona fide interaction between two partners (for a review, see reference 62).

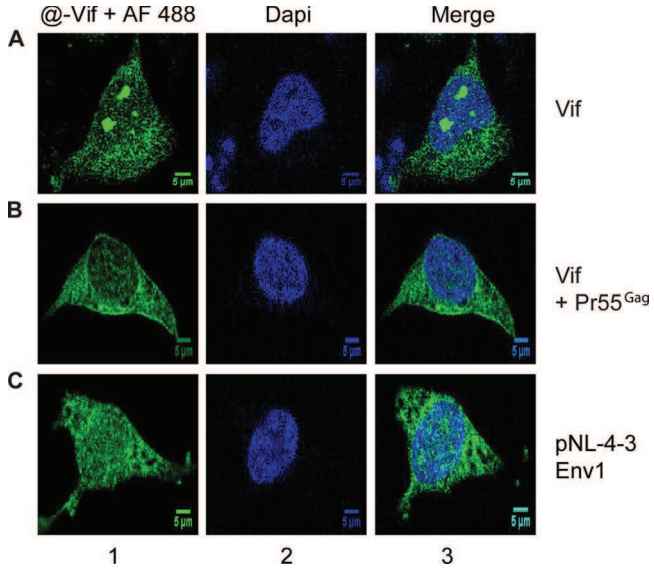

FIG 5 Immunolocalization of Vif in cells. Vif proteins were expressed in transfected HeLa cells from either pcDNA-hVif in the absence (A) or presence (B) of $Pr55^{Gag}$ or from pNL4-3-Env1 plasmid (C). After methanol fixation, cells were permeabilized in 0.1% Triton X-100 in 1× PBS, and Alexa Fluor 488 (AF 488)-coupled anti-rabbit secondary antibody (Molecular Probes) was used to detect primary Vif antibody (panel column 1) (antibody 319). Cell nuclei were stained with DAPI (panel column 2) contained in the mounting reagent (Slowfade reagent; Molecular Probes) (panel column 3 [merged images]).

FLIM measurements were monitored 24 h posttransfection and reported using an arbitrary color scale from blue to red, illustrating short to long lifetimes. Using this scale, an absence of energy transfer will appear in yellow (free eGFP-Vif lifetime, 2.53 ± 0.01 ns), whereas significant efficient transfer will appear in blue (lifetime, <2.30 ns). We first measured eGFP-Vif fluorescence in the nuclear, cytoplasmic, and cell membrane compartments (Fig. 6). As the eGFP lifetimes in these different cell compartments did not show any significant differences (data not shown), for the rest of our article we focus on the average lifetimes of eGFP-Vif in the cytoplasm, except when otherwise mentioned. Control FLIM experiments were performed with HeLa cells transfected either with eGFP-Vif alone or together with free mCherry (Fig. 6A). As shown in Fig. 6C (green dots), the average lifetimes of eGFP-Vif expressed alone (2.53 ± 0.04 ns) or coexpressed with mCherry (2.48 ± 0.05 ns) were similar to the expected lifetime of eGFP alone (46, 53), indicating that the eGFP fluorescence was not altered when fused to Vif and no interaction takes place between eGFP-Vif and free mCherry (Table 1).

In contrast, when eGFP-Vif was coexpressed with mCherry-Vif (Fig. 6B), the eGFP-Vif fluorescence lifetime dropped to 2.21 ± 0.11 ns (Table 1). The distribution of eGFP-Vif fluorescence lifetimes in the presence of mCherry-Vif was found to be clearly different from that in the presence of mCherry (Fig. 6C, blue dots). This fluorescence lifetime decrease was measured on more than 70 cells from at least 3 independent transfections and corresponded to a transfer efficiency of 12.2% (Fig. 6D), indicat-

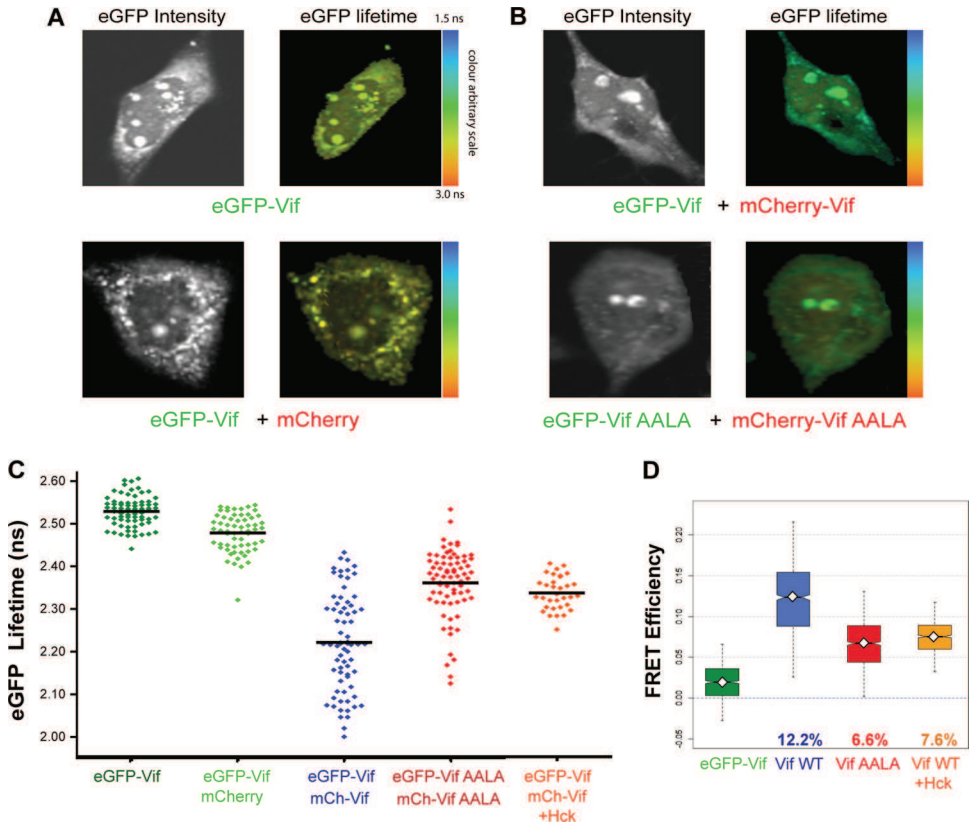

FIG 6 FLIM analyses of the eGFP- and mCherry-Vif WT and AALA mutant. HeLa cells were transfected with 0.5 μg of each plasmid and were observed 24 h posttransfection by confocal microscopy or by FLIM using a two-photon microscope. (A and B) Images are representative of cells expressing eGFP by fluorescence microscopy (left; grayscale) or by FLIM using an arbitrary color scale for the lifetimes expressed in nanoseconds. (C) Lifetime distribution of all analyzed cells under each condition. Controls in the absence of acceptor are depicted in green, the Vif WT in blue, the Vif AALA mutant in red, and the Hck in orange. Black bars indicate the mean values. (D) Box plots depicting the posterior FRET efficiencies distributions. The mean FRET efficiency is represented by the white diamonds. Whiskers (vertical dotted lines) represent the interval containing 95% of the FRET efficiencies.

ing a direct interaction between the two Vif fusion proteins in living cells. In order to confirm this interaction, FRET and FLIM experiments were further performed on the Vif AALA mutant (Fig. 6B). Interestingly, eGFP-Vif AALA displayed an intermediate fluorescence lifetime of 2.35 ± 0.08 ns (Fig. 6C and Table 1), resulting in a lower transfer efficiency of 6.6% (Fig. 6D), suggesting a modification in the Vif interaction and reduced oligomerization of this mutant. Note that the residual FRET efficiency is close to the commonly considered lowest value (5%) for a bona fide interaction (62). Interestingly, mutation of the PPLP motif of only one of the Vif species was sufficient to prevent oligomerization, as the FRET efficiencies observed with the eGFP-Vif AALA–mCherry-Vif and eGFP-Vif–mCherry-Vif AALA combinations were similar to the one observed when the mutation was present on both Vif partners (FRET efficiency of 6.6%) (Table 1). Besides, the nuclear foci observed in our different experiments could mainly be explained by the shuttling of Vif between the cytoplasm and the nucleus and by interactions with nucleolar proteins (59–61). Nevertheless, the Vif lifetime measured in these specific foci did not significantly differ from the lifetimes in other cellular compartments.

Bayesian analyses (see Materials and Methods) of fluorescence lifetimes showed a 20 to 25% reduction of Vif oligomerization when the PPLP motif was substituted for AALA. Moreover, the distribution of the fluorescence lifetime of eGFP-Vif or mCherry-Vif was more dispersed than the one observed for eGFP-Vif alone or eGFP-Vif AALA or mCherry-Vif AALA (Fig. 6C), suggesting that wild-type Vif oligomers may be heterogeneous in the cell.

Taken together, these data indicate that Vif-Vif interactions occur in living cells and that the PPLP motif, located at the C terminus of the protein, is involved in Vif oligomerization. Nevertheless, and as previously observed *in vitro*, other domains in Vif may also participate in this property (46, 53), as oligomerization was not completely abrogated by mutation of the PPLP motif.

Vif multimerization monitored by FCS in living cells. To further characterize Vif oligomerization in cells, fluorescence correlation spectroscopy (FCS) was performed. This technique is based on the measurement of the fluctuations of the fluorescence intensity in the femtoliter volume defined by the two-photon laser excitation. These fluctuations mainly characterize the translational dynamics of the fluorescent molecules that diffuse through the excitation volume. FCS can be performed in any liquid environment such as the cell cytoplasm and allows the determination of several physical parameters, such as diffusion time, local concentration, and molecular brightness. The last parameter corresponds to the average number of photons emitted by a diffusing particle per second and is therefore the most relevant to analyze Vif oligomerization in cells. That is, the brightness of a particle increases

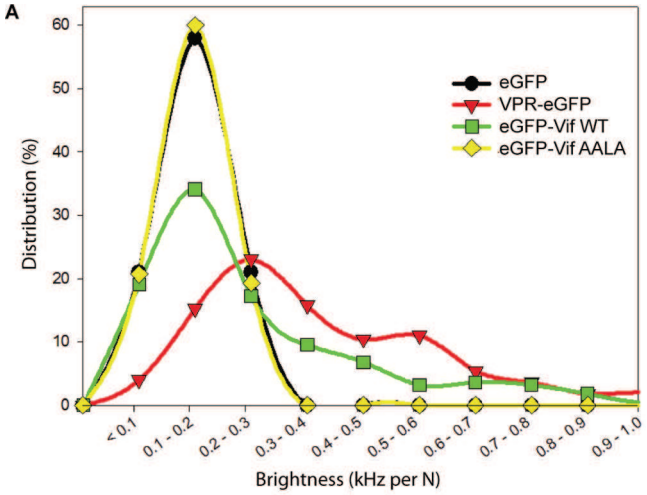

B

Group		eGFP	VPR-eGFP	eGFP-Vif WT	eGFP-Vif AALA
Brightness	Median	0.16	0.35	0.19	0.15
	25%	0.11	0.23	0.12	0.12
	75%	0.20	0.56	0.34	0.20

FIG 7 FCS analysis of eGFP-Vif WT and AALA mutant. (A) Brightness distribution of free eGFP (black circles), Vpr-eGFP (red triangles), eGFP-Vif WT (green squares), and eGFP-Vif AALA (yellow diamonds). The FCS measurements were performed 24 h posttransfection in HeLa cells with 0.5 μg of the appropriate expression vector. Distributions were calculated according to fluorescence fluctuations (FCS) calculated from 100 autocorrelation curves individually fitted with the appropriate model (see Materials and Methods). (B) Table with the brightness median for each condition, together with the values at the two quartiles.

proportionally with the number of fluorescent molecules inside it. First, we monitored the brightness distribution of free eGFP in the cytoplasm of transfected HeLa cells. As expected, the brightness distribution of eGFP followed a Gaussian distribution centered at 0.16 kHz per particle, reflecting the presence of only one, most likely monomeric (63), protein population (Fig. 7, solid black circles). As a positive control, HeLa cells were transfected with a Vpr-eGFP expression vector. Two main Vpr-eGFP populations were observed: a major one presenting a 2-fold-higher brightness than free eGFP (0.35 kHz per particle) and a minor one showing a 4-fold higher brightness (about 0.55 kHz per particle), confirming that Vpr was able to form dimers and multimers in cells (Fig. 7, red triangles) (46). A different behavior was observed when eGFP-Vif was transfected. The distribution curve of eGFP-Vif showed a broad distribution with a main population centered at 0.20 kHz per particle (as free eGFP) (Fig. 7, green squares) and two minor populations centered at ~0.4 kHz per particle and ~0.8 kHz per particle, indicating that Vif exists as a mix of monomers and oligomers in cells (Fig. 7). This result may reflect the large distribution of eGFP-Vif lifetimes observed by FLIM (Fig. 6C). Moreover, when eGFP-Vif AALA was analyzed, a single population, similar to the one obtained for free and monomeric eGFP was obtained (Fig. 7, yellow diamonds), suggesting that this mutant remains largely monomeric. Together, these results confirm that Vif forms oligomers in cells, as observed by FLIM, and validate the PPLP motif as part of an oligomerization domain.

Vif oligomerization is not a prerequisite to induce its relocalization at the plasma membrane by Pr55^{gag}. Since Vif and Pr55^{Gag} have been shown to interact in cells through their C-terminal and nucleocapsid domains, respectively (64, 65), we asked whether Vif oligomerization was required for its interaction with Pr55^{Gag}. To test this hypothesis, we first performed confocal microscopy on HeLa cells transfected with eGFP- and mCherry-Vif (wild type or AALA mutant) and with unlabeled Pr55^{Gag} protein (Fig. 8). As expected, expression of eGFP-Vif and mCherry-Vif was not affected by Pr55^{Gag} (Fig. 8A). However, Pr55^{Gag} partially relocalized Vif to the cell membrane, irrespective of the presence of the wild-type PPLP motif, suggesting that oligomerization of Vif, or the motif by itself, is not involved in Pr55^{Gag} recognition.

It is, however, possible that Vif-Pr55^{Gag} interaction affected the multimerization of Vif. We therefore carried out FLIM acquisitions on HeLa cells transfected with Vif fusion proteins and Pr55^{Gag} (Fig. 8B, left panels). Since the transfer efficiency measured for eGFP-Vif in the presence of Pr55^{Gag} was 10.7% (Fig. 8C and D), a value very similar to the one observed in the absence of Pr55^{Gag} (12.2%) (Fig. 6D), we confirmed that Vif binding to Pr55^{Gag} did not significantly affect its multimerization capacity. Consistent with the presence of Vif at the cell membrane, the eGFP-Vif transfer efficiency measured at this location was somewhat more efficient (13.4%), suggesting that Pr55^{Gag} promoted a closer proximity between the Vif molecules or, alternatively, a higher degree of oligomerization (Table 2). The same experiments were performed using the eGFP-Vif AALA and mCherry-Vif AALA mutants in the presence of Pr55^{Gag} (Fig. 8B, right panels, and C). As previously observed, eGFP-Vif AALA presented a very low transfer efficiency of 4.2% (Fig. 8D), and Bayesian analyses of fluorescence lifetimes showed a 20 to 25% reduction of Vif oligomerization when the PPLP motif was substituted, thus confirming its defect in oligomerization. Similarly, in the presence of Pr55^{Gag}, the FRET efficiency of Vif AALA at the plasma membrane was decreased compared to that of wild-type Vif (6.1% versus 13.4%) (Table 2). Interestingly, as observed in the absence of Pr55^{Gag}, the distribution of the fluorescence lifetime of eGFP-Vif or mCherry-Vif was more dispersed than the one observed for eGFP-Vif alone or eGFP-Vif AALA or mCherry-Vif AALA (Fig. 8C), suggesting again that wild-type Vif oligomers are heterogeneous in cells.

Taken together, these results show that Pr55^{Gag} interacts with Vif proteins, independently of its oligomerization state, and promotes their redistribution at the plasma membrane. This interaction is probably at the origin of Vif incorporation into nascent virions.

Interaction of APOBEC3G with Vif affects its oligomerization state in living cells. The A3G protein is a potent innate antiviral factor, and Vif has been shown to restrict its activity by inducing its degradation through the proteasome, inhibiting its translation and its incorporation into viral particles (for reviews, see references 1 and 5). Most of these activities involve physical interactions between Vif and A3G, and interacting motifs have been previously defined, mostly in the N terminus of each protein (66), but discrete motifs in the C terminus of Vif, such as the PPLP motif, have also been shown to bind A3G (40, 57). To investigate whether the binding of A3G to Vif affects its oligomerization, we transfected HeLa cells with the eGFP- and mCherry-Vif constructs together with an A3G expression vector and analyzed the eGFP-Vif lifetime 24 h posttransfection (Fig. 9). A3G constructs were previously checked for their correct expression and behavior in HeLa cells (Fig. 2A). The results were compared to those obtained with cells expressing an A3G D128K mutant that has been

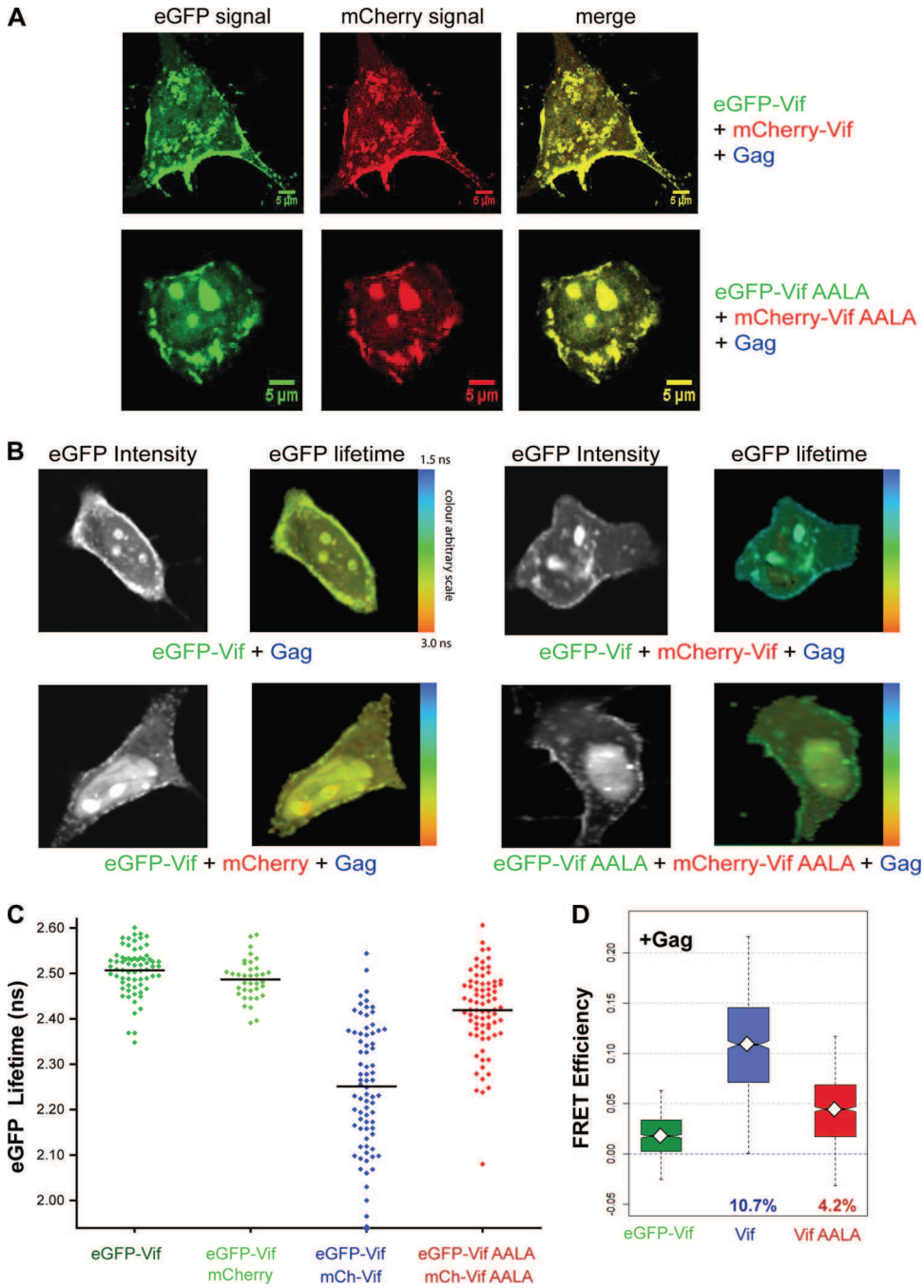

FIG 8 FLIM analyses of Vif proteins in the presence of $Pr55^{Gag}$ protein. (A) Confocal microscopy showing the localization of Vif fusion proteins coexpressed with $Pr55^{Gag}$ in HeLa cells. (B) eGFP fluorescence intensity (greyscale) and eGFP lifetime (arbitrary color scale) are indicated. (C) Lifetime distribution of all analyzed cells. The horizontal black bars indicate mean values. Controls in the absence of acceptor are depicted in green, the Vif WT in blue, and the Vif AALA mutant in red. (D) Box plots depicting the FRET efficiency distributions. The mean FRET efficiency is represented by the white diamonds. Whiskers (vertical dotted lines) represent the interval containing 95% of the FRET efficiencies.

shown to be defective in Vif interaction (67–69). As expected, A3G D128K protein is insensitive to Vif-induced proteasomal degradation (Fig. 2A, right panel, and B). It also does not interact with our eGFP-Vif and mCherry-Vif constructs (Fig. 3C, lanes 3 and 6) nor does it significantly impair the coimmunoprecipitation of eGFP-Vif with HA-Vif (Fig. 3B, lane 7), contrary to the wild-type A3G, which interacts with eGFP- and mCherry-Vif proteins (Fig. 3C, lanes 2 and 5) and leads to a 2-fold reduction (0.47) of Vif multimerization (Fig. 3B, lane 6). Next, as a negative control, A3G was transfected with eGFP-Vif in presence or absence of the mCherry fluorophore. In this case, no difference was observed, with an average fluorescence lifetime of 2.49 ± 0.02 ns (Table 1). However, in the presence of wild-type A3G, the FRET efficiency between eGFP-Vif and mCherry-Vif dropped from 12.2% to 5.7%

TABLE 2 Average lifetimes and FRET efficiencies of eGFP-Vif proteins in the presence of Gag[a]

Transfection(s)	Cytoplasm			Membrane		
	Avg lifetime, ns (95% CI)	No. of cells	FRET efficiency, % (95% CI)	Avg lifetime, ns (95% CI)	No. of cells	FRET efficiency, % (95% CI)
eGFP-Vif	2.51 (2.49–2.52)	69		2.47 (2.46–2.48)	64	
eGFP-Vif + mCherry	2.48 (2.47–2.49)	36	0.8 (−3.7–6.4)	2.47 (2.46–2.48)	36	0.0 (−5.1–5.2)
eGFP-Vif + mCherry-Vif	**2.25 (2.22–2.28)**	**75**	**10.7 (2.7–21.5)**	**2.14 (2.12–2.17)**	**72**	**13.4 (3.9–23.2)**
eGFP-Vif AALA + mCherry-Vif AALA	2.42 (2.39–2.44)	76	4.2 (−3.4–11.7)	2.31 (2.29–2.34)	73	6.1 (−2.1–13.0)
eGFP-Vif + mCherry + A3G	2.53 (2.52–2.54)	36	−0.3 (−4.8–4.1)	2.49 (2.5–2.53)	36	−0.7 (−6.1–5.3)
eGFP-Vif + mCherry-Vif + A3G	2.36 (2.33–2.38)	52	6.5 (−0.2–13.1)	2.23 (2.21–2.26)	52	9.7 (1.3–18.6)
eGFP-Vif + mCherry-Vif + A3G D128K	2.30 (2.27–2.33)	43	8.8 (0.8–16.7)	2.18 (2.16–2.20)	42	11.8 (4.8–19.4)
eGFP-Vif AALA + mCherry-Vif AALA + A3G	2.39 (2.37–2.40)	38	5.5 (0.5–10.3)	2.30 (2.28–2.32)	37	7.0 (0.8–13.7)

[a] Results in boldface represent the highest FRET efficiencies.

(Fig. 9B and Table 1). In contrast, the fluorescence lifetime of eGFP-Vif in the presence of A3G D128K was similar to that observed in the absence of A3G (2.26 ± 0.13 ns) (Table 1), corresponding to a transfer efficiency of 10.4% (Fig. 9B). These results clearly indicate that the binding of A3G affects the capacity of Vif to oligomerize.

Next, we tested whether another PPLP-binding protein could also compete and perturb Vif oligomerization. To this aim, we tested the cellular Hck kinase as it has previously been shown to interact, through its SH3 domain, with a large domain containing the PPLP motif of Vif (51). In a first set of experiments, we transfected HeLa cells with unlabeled or eGFP-Vif proteins together with A3G in the presence or absence of Hck and analyzed A3G degradation (Fig. 2C). Western blot analyses showed that Hck altered neither A3G and Vif (untagged and eGFP-tagged) expression (Fig. 2C, left panel) nor A3G degradation (Fig. 2C, right panel). The relative expression of A3G was in the same order of magnitude as that observed in Fig. 2A, suggesting that Hck did not influence A3G degradation. Next, we investigated whether the binding of Hck to Vif affects its oligomerization. We transfected

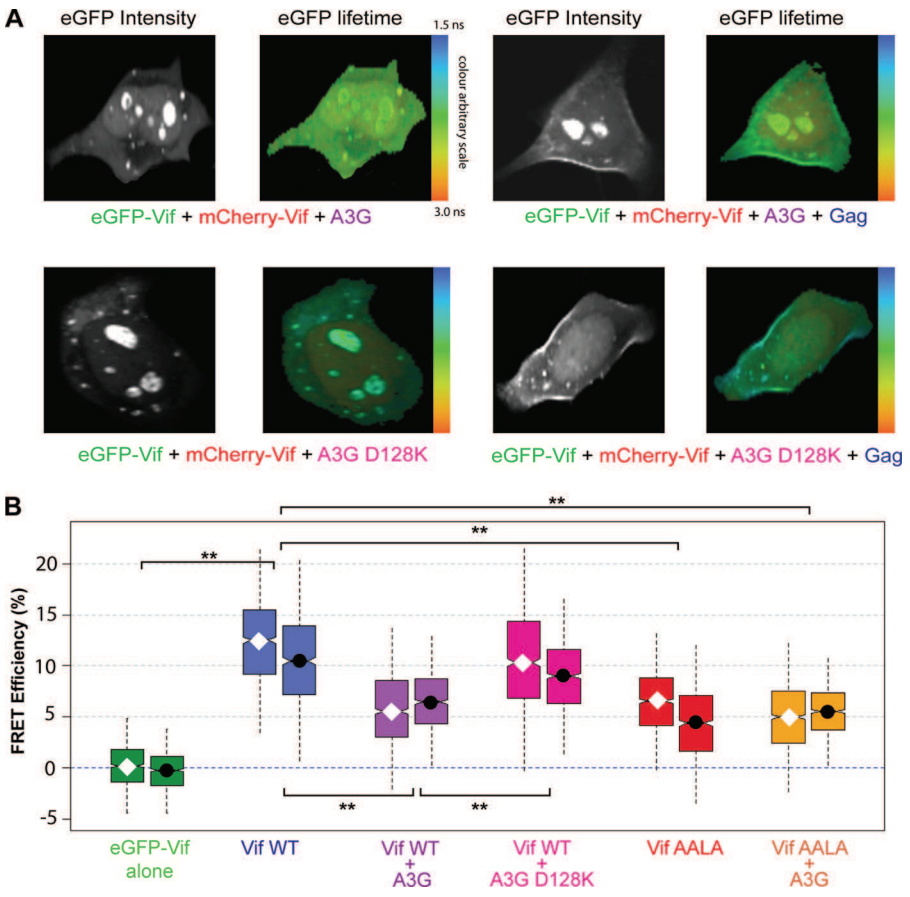

FIG 9 FLIM analyses of Vif in the presence of A3G protein. (A) eGFP fluorescence intensity (greyscale) and eGFP lifetime (arbitrary color scale) are indicated. (B) Box plots depicting the FRET efficiency distributions in the absence (white diamonds) or presence (black dots) of $Pr55^{Gag}$. Whiskers (vertical dotted lines) represent the interval containing 95% of the FRET efficiencies. *P* values for the different assays are indicated. **, <0.01.

HeLa cells with the eGFP-Vif and mCherry-Vif constructs together with Hck and analyzed the eGFP-Vif lifetime 24 h posttransfection (Table 1 and Fig. 6C and D). We observed an intermediate but reproducible decrease of the FRET efficiency in the presence of Hck (7.6% versus 5.7% in the presence of A3G and 12.2% for Vif alone), suggesting that Hck, like A3G, is able to reduce multimerization of Vif in cells.

Finally, in order to establish a relationship between the binding of A3G to $Pr55^{Gag}$ and its interaction with Vif, the same FRET and FLIM approach was repeated in the presence of unlabeled $Pr55^{Gag}$ (Fig. 9A, right panel). As previously observed (Fig. 8C and D and Table 2), the oligomerization of Vif was not affected by the presence of $Pr55^{Gag}$, with a transfer efficiency of 10.7% (versus 12.2% without $Pr55^{Gag}$) (Fig. 8B and Table 2). When wild-type A3G was added, a decrease of FRET efficiency was observed (6.5%), similar to the one obtained without $Pr55^{Gag}$ (5.7%) (Fig. 9B and Table 2). When mutant A3G D128K was used, the transfer efficiency was not significantly affected (8.8% versus 10.4% in the absence of $Pr55^{Gag}$), confirming the absence of interaction with Vif oligomers (Fig. 9B). Concerning the Vif AALA mutant, we did not observe any effect of A3G on the FRET efficiency in the absence (5.1%) or in the presence (5.5%) of $Pr55^{Gag}$. In the presence of $Pr55^{Gag}$, FRET efficiency was also measured at the cell membrane (Table 2). The values obtained in this case were always higher than the ones determined in the cytoplasm and may reflect structural constraints of Vif at this site due to its relocation by $Pr55^{Gag}$. Altogether, these results show that A3G strongly affects the oligomerization of Vif, at a level very similar to that of a mutation in the PPLP motif of Vif, and this effect is not dependent on the presence of $Pr55^{Gag}$.

DISCUSSION

Most HIV-1 proteins have been shown to form dimers or multimers *in vitro* and *in cellulo*, and this characteristic is crucial for their function. Concerning Vif, the oligomerization sequence has been mapped between residues 151 and 164 in the C-terminal domain and more specifically to the ^{161}PPLP^{164} motif (37, 38, 45). The PPLP motif was found to be required for the assembly of an active E3 ubiquitin ligase complex (43, 44), and mutation of this sequence or the use of antagonist peptides has been shown to result in an important loss of viral infectivity (57), one of the reasons being an increased incorporation of A3G into viral particles as a consequence of the inhibition of its degradation (37, 40, 41, 57).

In this study, we used fluorescence confocal microscopy, two-photon FCS, and FLIM approaches to compare the oligomerization properties of wild-type protein and a mutant Vif protein with a substitution in its multimerization motif. Although previous studies have documented the oligomerization status of Vif *in vitro* (36, 37, 44, 45) and in cell culture by coimmunoprecipitation (co-IP) and a mammalian two-hybrid system (37), to our knowledge, the present study constitutes the first report in which Vif oligomerization is directly visualized in living cells and a relationship to its $Pr55^{Gag}$ and A3G binding is established. To this end, we generated wild-type and Vif AALA mutant proteins tagged at their N termini with two FRET-compatible fluorophores, eGFP and mCherry (Fig. 1). To gain insight into the oligomerization status of these chimeric Vif proteins, we performed immunoprecipitation and showed that eGFP-Vif is able to copurify with an HA-Vif protein (Fig. 3B) and that an A3G mutant (D128K) that does not interact with Vif does not perturb this interaction (Fig. 3C). This interaction was further validated by FLIM-based FRET analyses (Fig. 6), where we observed an energy transfer of 12.2% between eGFP- and mCherry-tagged Vif proteins. Interestingly, the FRET efficiency was reduced to 6.6% when the PPLP motif of one or of the two tagged Vif proteins was mutated, confirming the implication of the PPLP sequence in the oligomerization of Vif in living cells. This result suggests that even if oligomerization is considerably diminished (2-fold), it is not completely abolished and that regions outside the PPLP domain are also involved in protein-protein association. This interpretation would be consistent with previous studies using purified Vif protein (45); however, it has to be taken with caution as the residual FRET efficiency is rather close to the significance limit (62). On one hand, a very recent study also pointed out the involvement of domains such as the HCCH motif, the BC box, and downstream residues (S165 and V166) in the oligomerization property of Vif (58). This could explain the interaction observed by co-IP between the eGFP-Vif AALA mutant and wild-type HA-Vif (Fig. 3B). On the other hand, FCS indicated that Vif AALA proteins behaved as a single population of monomeric molecules (Fig. 7), reinforcing the observations that the PPLP motif is one of the key domains involved in oligomerization. The origin of the discrepancy between FLIM and FCS techniques regarding a potential residual oligomerization of Vif AALA is still unclear. However, FCS experiments showed that wild-type Vif could form at least two populations of particles in the cell, a main population consisting of monomers and a second one composed of a larger number of molecules (Fig. 7). The fact that only 30% of the Vif population is multimeric may explain the lower FRET efficiency measured in comparison to Vpr (46). The heterogeneity of Vif oligomers is in agreement with biochemical data showing that the oligomerization state of Vif could vary from 1 to 9 (36, 45).

Although Vif protein oligomerizes *in vitro* (36, 37, 45) and in cells (37; this study), the functional role of Vif oligomerization remains elusive. Indeed, the coexpression of eGFP- and mCherry-Vif proteins with unlabeled $Pr55^{Gag}$ clearly showed that $Pr55^{Gag}$ redistributes the fluorescently tagged Vif proteins to the cell membrane (Fig. 8A). Moreover, Vif oligomerization still occurred at this site, as indicated by the high FRET efficiency (13.4%) (Fig. 8B and Table 2). It is likely that Vif follows the intracellular trafficking of $Pr55^{Gag}$, as its recruitment by $Pr55^{Gag}$ was found to be independent of the anchoring of $Pr55^{Gag}$ to the plasma membrane (70), emphasizing that $Pr55^{Gag}$-mediated packaging of cofactors is not the result of a simple colocalization at the plasma membrane, but probably takes place at the site of their synthesis. Moreover, the fact that Vif was not observed at the plasma membrane in the absence of $Pr55^{Gag}$ indicates that the C terminus of Vif (residues 171 to 192) is not a specific domain required for its targeting to the plasma membrane through electrostatic interactions (71). We showed that the redistribution of Vif to the plasma membrane is independent of its multimerization state since the Vif AALA mutant was also relocated at the membrane in the presence of $Pr55^{Gag}$ (Fig. 8B). Thus, even if the oligomerization domain is adjacent to and overlaps the putative $Pr55^{Gag}$ binding site (through the NC domain), located around residues 157 to 179 (64), its mutation does not seem to perturb its binding to $Pr55^{Gag}$. This suggests that other motifs in Vif may interact with $Pr55^{Gag}$ protein.

Besides its interaction with $Pr55^{Gag}$, it has been shown that the PPLP motif of Vif is necessary for binding to A3G (40, 57) and

could influence the binding to proteins containing an SH3 domain, such as Hck (51). Interestingly, we found that A3G significantly impaired Vif multimerization (Fig. 9). In contrast, an A3G mutant (A3G D128K) that does not interact with Vif (Fig. 3C) (67–69) has no effect, indicating that the inhibition of Vif multimerization by wild-type A3G is likely a consequence of the direct interaction between these two proteins. Altogether, these results demonstrate that the binding of A3G to the N terminus and/or the PPLP motif of Vif affects the capacity of Vif to form oligomers. As previously mentioned, this could be explained by the partial overlap of the A3G binding site and the PPLP motif of Vif (40, 41, 57). Indeed, the Hck kinase significantly reduced the oligomerization of Vif (Fig. 6D), strengthening the fact that the PPLP motif is crucial for Vif multimerization. These data corroborate size exclusion chromatography studies in which the addition of cullin 5 to Vif results in the formation of monomeric complexes due the occlusion of the PPLP dimerization site (44). However, as previously proposed by Walker et al. (57), it could be that substitution of the PPLP motif instead imposes conformational constraints, thus preventing proper folding of Vif and thereby indirectly precluding A3G interaction. This hypothesis is unlikely, as we showed by circular dichroism that the PPLP-to-AALA substitution does not perturb the overall conformation of the protein (45). Consequently, the oligomerization of Vif may be functionally relevant not only to allow its correct conformation but also to interact with A3G and induce its degradation. Indeed, the Vif AALA mutant does not interact with A3G anymore and is defective in inducing its degradation (40, 57) (Fig. 2); this is likely to result in a higher capacity for A3G to be incorporated into viral particles (40).

Although it is known that Vif and A3G interact with the same domain of $Pr55^{Gag}$ (70, 72–76), their relationship relative to Vif multimerization has never been investigated. Here, we found that in the presence of $Pr55^{Gag}$, A3G preserves its ability to affect the multimerization of Vif (Fig. 9B), suggesting that $Pr55^{Gag}$ and A3G interact with different domains of Vif. However, this result may reflect a direct competition between A3G and Vif and explain how Vif might prevent the packaging of A3G into viral particles independently of A3G degradation (77), in addition to a competitive process resulting from the binding of Vif and A3G to a common packaging signal on the viral genomic RNA (29, 32, 78, 79).

In conclusion, we used fluorescent approaches to show for the first time that Vif oligomerizes in living cells. Our results confirmed the importance of the PPLP motif in Vif oligomerization, and this property most probably facilitates A3G binding and degradation. Moreover, A3G was able to impair the multimerization of Vif, at a level similar to that of a mutant (Vif AALA) disrupting Vif oligomerization. Finally, $Pr55^{Gag}$ relocated Vif oligomers to the plasma membrane without preventing A3G from impairing Vif oligomerization. Altogether, our results suggest that disruption of the Vif oligomer interface may affect the overall Vif/A3G complexes (and their interactions), thus likely promoting an increase in A3G packaging and reduced viral infectivity. Further studies will be required to understand how A3G or other binding partners affect the oligomerization state of Vif. Validation of these conclusions awaits the determination of the tridimensional structures of Vif and Vif/A3G complexes.

ACKNOWLEDGMENTS

We are grateful to Hala El Mekdad for technical assistance and Redmond Smyth for critical reading of the manuscript. We thank Magali Frugier (UPR-9002 CNRS, Strasbourg, France) for anti-GFP antibody, Etienne Decroly (UMR-6098-AFMB Marseille, France) for Hck expression vector and antibody, and Jérome Mutterer for confocal microscopy (Strasbourg-Esplanade Cellular Imaging Facility—IBMP, sponsored by the CNRS, University of Strasbourg, and Region Alsace). We further thank Klaus Strebel (NIH, Bethesda, MD) for pNL4.3 Env1 constructs. The following reagents were obtained through the AIDS Research and Reference Reagent Program, Division of AIDS, NIAID, NIH: A3G polyclonal antibody 9906 from Warner Greene and Vif monoclonal antibody 319 from Michael H. Malim.

This work was supported by a grant from the French National Agency for Research on AIDS and Viral Hepatitis (ANRS) to J.C.P. and by postdoctoral and doctoral fellowships from SIDACTION and ANRS to J.B. and S.G., respectively.

REFERENCES

1. **Henriet S, Mercenne G, Bernacchi S, Paillart JC, Marquet R.** 2009. Tumultuous relationship between the human immunodeficiency virus type 1 viral infectivity factor (Vif) and the human APOBEC-3G and APOBEC-3F restriction factors. Microbiol. Mol. Biol. Rev. **73**:211–232.
2. **Sheehy AM, Gaddis NC, Choi JD, Malim MH.** 2002. Isolation of a human gene that inhibits HIV-1 infection and is suppressed by the viral Vif protein. Nature **418**:646–650.
3. **Wiegand HL, Doehle BP, Bogerd HP, Cullen BR.** 2004. A second human antiretroviral factor, APOBEC3F, is suppressed by the HIV-1 and HIV-2 Vif proteins. EMBO J. **23**:2451–2458.
4. **Zhang H, Yang B, Pomerantz RJ, Zhang C, Arunachalam SC, Gao L.** 2003. The cytidine deaminase CEM15 induces hypermutation in newly synthesized HIV-1 DNA. Nature **424**:94–98.
5. **Blanco-Melo D, Venkatesh S, Bieniasz PD.** 2012. Intrinsic cellular defenses against human immunodeficiency viruses. Immunity **37**:399–411.
6. **Harris RS, Bishop KN, Sheehy AM, Craig HM, Petersen-Mahrt SK, Watt IN, Neuberger MS, Malim MH.** 2003. DNA deamination mediates innate immunity to retroviral infection. Cell **113**:803–809.
7. **Mangeat B, Turelli P, Caron G, Friedli M, Perrin L, Trono D.** 2003. Broad antiretroviral defence by human APOBEC3G through lethal editing of nascent reverse transcripts. Nature **424**:99–103.
8. **Guo F, Cen S, Niu M, Saadatmand J, Kleiman L.** 2006. The inhibition of tRNALys3-primed reverse transcription by human APOBEC3G during HIV-1 replication. J. Virol. **80**:11710–11722.
9. **Holmes RK, Malim MH, Bishop KN.** 2007. APOBEC-mediated viral restriction: not simply editing? Trends Biochem. Sci. **32**:118–128.
10. **Mbisa JL, Bu W, Pathak VK.** 2010. APOBEC3F and APOBEC3G inhibit HIV-1 DNA integration by different mechanisms. J. Virol. **84**:5250–5259.
11. **Chiu YL, Greene WC.** 2008. The APOBEC3 cytidine deaminases: an innate defensive network opposing exogenous retroviruses and endogenous retroelements. Annu. Rev. Immunol. **26**:317–353.
12. **Jarmuz A, Chester A, Bayliss J, Gisbourne J, Dunham I, Scott J, Navaratnam N.** 2002. An anthropoid-specific locus of orphan C to U RNA-editing enzymes on chromosome 22. Genomics **79**:285–296.
13. **Sodroski J, Goh WC, Rosen C, Tartar A, Portetelle D, Burny A, Haseltine W.** 1986. Replicative and cytopathic potential of HTLV-III/LAV with sor gene deletions. Science **231**:1549–1553.
14. **Borman AM, Quillent C, Charneau P, Dauguet C, Clavel F.** 1995. Human immunodeficiency virus type 1 Vif^- mutant particles from restrictive cells: role of Vif in correct particle assembly and infectivity. J. Virol. **69**:2058–2067.
15. **Gabuzda DH, Lawrence K, Langhoff E, Terwilliger E, Dorfman T, Haseltine WA, Sodroski J.** 1992. Role of vif in replication of human immunodeficiency virus type 1 in $CD4^+$ T lymphocytes. J. Virol. **66**:6489–6495.
16. **Malim MH, Emerman M.** 2008. HIV-1 accessory proteins—ensuring viral survival in a hostile environment. Cell Host Microbe **3**:388–398.
17. **Wissing S, Galloway NL, Greene WC.** 2010. HIV-1 Vif versus the APOBEC3 cytidine deaminases: an intracellular duel between pathogen and host restriction factors. Mol. Aspects Med. **31**:383–397.
18. **Liu B, Sarkis PT, Luo K, Yu Y, Yu XF.** 2005. Regulation of Apobec3F and human immunodeficiency virus type 1 Vif by Vif-Cul5-ElonB/C E3 ubiquitin ligase. J. Virol. **79**:9579–9587.
19. **Marin M, Rose KM, Kozak SL, Kabat D.** 2003. HIV-1 Vif protein binds

the editing enzyme APOBEC3G and induces its degradation. Nat. Med. **9**:1398–1403.
20. **Mehle A, Goncalves J, Santa-Marta M, McPike M, Gabuzda D.** 2004. Phosphorylation of a novel SOCS-box regulates assembly of the HIV-1 Vif-Cul5 complex that promotes APOBEC3G degradation. Genes Dev. **18**:2861–2866.
21. **Yu X, Yu Y, Liu B, Luo K, Kong W, Mao P, Yu XF.** 2003. Induction of APOBEC3G ubiquitination and degradation by an HIV-1 Vif-Cul5-SCF complex. Science **302**:1056–1060.
22. **Jager S, Kim DY, Hultquist JF, Shindo K, Larue RS, Kwon E, Li M, Anderson BD, Yen L, Stanley D, Mahon C, Kane J, Franks-Skiba K, Cimermancic P, Burlingame A, Sali A, Craik CS, Harris RS, Gross JD, Krogan NJ.** 2011. Vif hijacks CBF-β to degrade APOBEC3G and promote HIV-1 infection. Nature **481**:371–375.
23. **Zhang W, Du J, Evans SL, Yu Y, Yu XF.** 2011. T-cell differentiation factor CBF-β regulates HIV-1 Vif-mediated evasion of host restriction. Nature **481**:376–379.
24. **Mariani R, Chen D, Schrofelbauer B, Navarro F, Konig R, Bollman B, Munk C, Nymark-McMahon H, Landau NR.** 2003. Species-specific exclusion of APOBEC3G from HIV-1 virions by Vif. Cell **114**:21–31.
25. **Opi S, Kao S, Goila-Gaur R, Khan MA, Miyagi E, Takeuchi H, Strebel K.** 2007. Human immunodeficiency virus type 1 Vif inhibits packaging and antiviral activity of a degradation-resistant APOBEC3G variant. J. Virol. **81**:8236–8246.
26. **Kao S, Khan MA, Miyagi E, Plishka R, Buckler-White A, Strebel K.** 2003. The human immunodeficiency virus type 1 Vif protein reduces intracellular expression and inhibits packaging of APOBEC3G (CEM15), a cellular inhibitor of virus infectivity. J. Virol. **77**:11398–11407.
27. **Stopak K, de Noronha C, Yonemoto W, Greene WC.** 2003. HIV-1 Vif blocks the antiviral activity of APOBEC3G by impairing both its translation and intracellular stability. Mol. Cell **12**:591–601.
28. **Mercenne G, Bernacchi S, Richer D, Bec G, Henriet S, Paillart JC, Marquet R.** 2010. HIV-1 Vif binds to APOBEC3G mRNA and inhibits its translation. Nucleic Acids Res. **38**:633–646.
29. **Henriet S, Sinck L, Bec G, Gorelick RJ, Marquet R, Paillart JC.** 2007. Vif is a RNA chaperone that could temporally regulate RNA dimerization and the early steps of HIV-1 reverse transcription. Nucleic Acids Res. **35**:5141–5153.
30. **Batisse J, Guerrero S, Bernacchi S, Sleiman D, Gabus C, Darlix JL, Marquet R, Tisne C, Paillart JC.** 2012. The role of Vif oligomerization and RNA chaperone activity in HIV-1 replication. Virus Res. **169**:361–376.
31. **Bernacchi S, Henriet S, Dumas P, Paillart JC, Marquet R.** 2007. RNA and DNA binding properties of HIV-1 Vif protein: a fluorescence study. J. Biol. Chem. **282**:26361–26368.
32. **Henriet S, Richer D, Bernacchi S, Decroly E, Vigne R, Ehresmann B, Ehresmann C, Paillart JC, Marquet R.** 2005. Cooperative and specific binding of Vif to the 5′ region of HIV-1 genomic RNA. J. Mol. Biol. **354**:55–72.
33. **Dettenhofer M, Cen S, Carlson BA, Kleiman L, Yu XF.** 2000. Association of human immunodeficiency virus type 1 Vif with RNA and its role in reverse transcription. J. Virol. **74**:8938–8945.
34. **Zhang H, Pomerantz RJ, Dornadula G, Sun Y.** 2000. Human immunodeficiency virus type 1 Vif protein is an integral component of an mRNP complex of viral RNA and could be involved in the viral RNA folding and packaging process. J. Virol. **74**:8252–8261.
35. **Kataropoulou A, Bovolenta C, Belfiore A, Trabatti S, Garbelli A, Porcellini S, Lupo R, Maga G.** 2009. Mutational analysis of the HIV-1 auxiliary protein Vif identifies independent domains important for the physical and functional interaction with HIV-1 reverse transcriptase. Nucleic Acids Res. **37**:3660–3669.
36. **Auclair JR, Green KM, Shandilya S, Evans JE, Somasundaran M, Schiffer CA.** 2007. Mass spectrometry analysis of HIV-1 Vif reveals an increase in ordered structure upon oligomerization in regions necessary for viral infectivity. Proteins **69**:270–284.
37. **Yang S, Sun Y, Zhang H.** 2001. The multimerization of human immunodeficiency virus type I Vif protein: a requirement for Vif function in the viral life cycle. J. Biol. Chem. **276**:4889–4893.
38. **Yang B, Gao L, Li L, Lu Z, Fan X, Patel CA, Pomerantz RJ, DuBois GC, Zhang H.** 2003. Potent suppression of viral infectivity by the peptides that inhibit multimerization of human immunodeficiency virus type 1 (HIV-1) Vif proteins. J. Biol. Chem. **278**:6596–6602.
39. **Simon JH, Fouchier RA, Southerling TE, Guerra CB, Grant CK, Malim MH.** 1997. The Vif and Gag proteins of human immunodeficiency virus type 1 colocalize in infected human T cells. J. Virol. **71**:5259–5267.
40. **Donahue JP, Vetter ML, Mukhtar NA, D'Aquila RT.** 2008. The HIV-1 Vif PPLP motif is necessary for human APOBEC3G binding and degradation. Virology **377**:49–53.
41. **Miller JH, Presnyak V, Smith HC.** 2007. The dimerization domain of HIV-1 viral infectivity factor Vif is required to block APOBEC3G incorporation with virions. Retrovirology **4**:81. doi:10.1186/1742-4690-4-81.
42. **Yu Y, Xiao Z, Ehrlich ES, Yu X, Yu XF.** 2004. Selective assembly of HIV-1 Vif-Cul5-ElonginB-ElonginC E3 ubiquitin ligase complex through a novel SOCS box and upstream cysteines. Genes Dev. **18**:2867–2872.
43. **Bergeron JR, Huthoff H, Veselkov DA, Beavil RL, Simpson PJ, Matthews SJ, Malim MH, Sanderson MR.** 2010. The SOCS-box of HIV-1 Vif interacts with ElonginBC by induced-folding to recruit its Cul5-containing ubiquitin ligase complex. PLoS Pathog. **6**:e1000925. doi:10.1371/journal.ppat.1000925.
44. **Wolfe LS, Stanley BJ, Liu C, Eliason WK, Xiong Y.** 2010. Dissection of the HIV Vif interaction with human E3 ubiquitin ligase. J. Virol. **84**:7135–7139.
45. **Bernacchi S, Mercenne G, Tournaire C, Marquet R, Paillart JC.** 2011. Importance of the proline-rich multimerization domain on the oligomerization and nucleic acid binding properties of HIV-1 Vif. Nucleic Acids Res. **39**:2404–2415.
46. **Fritz JV, Didier P, Clamme JP, Schaub E, Muriaux D, Cabanne C, Morellet N, Bouaziz S, Darlix JL, Mely Y, de Rocquigny H.** 2008. Direct Vpr-Vpr interaction in cells monitored by two photon fluorescence correlation spectroscopy and fluorescence lifetime imaging. Retrovirology **5**:87. doi:10.1186/1742-4690-5-87.
47. **Nguyen KL, Llano M, Akari H, Miyagi E, Poeschla EM, Strebel K, Bour S.** 2004. Codon optimization of the HIV-1 vpu and vif genes stabilizes their mRNA and allows for highly efficient Rev-independent expression. Virology **319**:163–175.
48. **Selig L, Pages JC, Tanchou V, Preveral S, Berlioz-Torrent C, Liu LX, Erdtmann L, Darlix J, Benarous R, Benichou S.** 1999. Interaction with the p6 domain of the Gag precursor mediates incorporation into virions of Vpr and Vpx proteins from primate lentiviruses. J. Virol. **73**:592–600.
49. **Rudner L, Nydegger S, Coren LV, Nagashima K, Thali M, Ott DE.** 2005. Dynamic fluorescent imaging of human immunodeficiency virus type 1 Gag in live cells by biarsenical labeling. J. Virol. **79**:4055–4065.
50. **Simon JH, Southerling TE, Peterson JC, Meyer BE, Malim MH.** 1995. Complementation of *vif*-defective human immunodeficiency virus type 1 by primate, but not nonprimate, lentivirus *vif* genes. J. Virol. **69**:4166–4172.
51. **Hassaine G, Courcoul M, Bessou G, Barthalay Y, Picard C, Olive D, Collette Y, Vigne R, Decroly E.** 2001. The tyrosine kinase Hck is an inhibitor of HIV-1 replication counteracted by the viral vif protein. J. Biol. Chem. **276**:16885–16893.
52. **Clamme JP, Azoulay J, Mely Y.** 2003. Monitoring of the formation and dissociation of polyethylenimine/DNA complexes by two photon fluorescence correlation spectroscopy. Biophys. J. **84**:1960–1968.
53. **Pepperkok R, Squire A, Geley S, Bastiaens PI.** 1999. Simultaneous detection of multiple green fluorescent proteins in live cells by fluorescence lifetime imaging microscopy. Curr. Biol. **9**:269–272.
54. **Merzlyak EM, Goedhart J, Shcherbo D, Bulina ME, Shcheglov AS, Fradkov AF, Gaintzeva A, Lukyanov KA, Lukyanov S, Gadella TW, Chudakov DM.** 2007. Bright monomeric red fluorescent protein with an extended fluorescence lifetime. Nat. Methods **4**:555–557.
55. **Shaner NC, Steinbach PA, Tsien RY.** 2005. A guide to choosing fluorescent proteins. Nat. Methods **2**:905–909.
56. **Simon JH, Malim MH.** 1996. The human immunodeficiency virus type 1 Vif protein modulates the postpenetration stability of viral nucleoprotein complexes. J. Virol. **70**:5297–5305.
57. **Walker RC, Jr, Khan MA, Kao S, Goila-Gaur R, Miyagi E, Strebel K.** 2010. Identification of dominant negative human immunodeficiency virus type 1 Vif mutants that interfere with the functional inactivation of APOBEC3G by virus-encoded Vif. J. Virol. **84**:5201–5211.
58. **Techtmann SM, Ghirlando R, Kao S, Strebel K, Maynard EL.** 2012. Hydrodynamic and functional analysis of HIV-1 Vif oligomerization. Biochemistry **51**:2078–2086.
59. **Farrow MA, Somasundaran M, Zhang C, Gabuzda D, Sullivan JL, Greenough TC.** 2005. Nuclear localization of HIV type 1 Vif isolated from a long-term asymptomatic individual and potential role in virus attenuation. AIDS Res. Hum. Retroviruses **21**:565–574.

60. **Wichroski MJ, Ichiyama K, Rana T.** 2005. Analysis of HIV-1 Vif-mediated proteasome-dependent depletion of APOBEC3G: correlating function and subcellular localization. J. Biol. Chem. **280**:8387–8396.
61. **Huvent I, Hong SS, Fournier C, Gay B, Tournier J, Carriere C, Courcoul M, Vigne R, Spire B, Boulanger P.** 1998. Interaction and co-encapsidation of human immunodeficiency virus type 1 Gag and Vif recombinant proteins. J. Gen. Virol. **79**:1069–1081.
62. **Voss TC, Demarco IA, Day RN.** 2005. Quantitative imaging of protein interactions in the cell nucleus. Biotechniques **38**:413–424.
63. **Day RN, Periasamy A, Schaufele F.** 2001. Fluorescence resonance energy transfer microscopy of localized protein interactions in the living cell nucleus. Methods **25**:4–18.
64. **Bouyac M, Courcoul M, Bertoia G, Baudat Y, Gabuzda D, Blanc D, Chazal N, Boulanger P, Sire J, Vigne R, Spire B.** 1997. Human immunodeficiency virus type 1 Vif protein binds to the $Pr55^{Gag}$ precursor. J. Virol. **71**:9358–9365.
65. **Simon JH, Carpenter EA, Fouchier RA, Malim MH.** 1999. Vif and the $p55^{Gag}$ polyprotein of human immunodeficiency virus type 1 are present in colocalizing membrane-free cytoplasmic complexes. J. Virol. **73**:2667–2674.
66. **Barraud P, Paillart JC, Marquet R, Tisne C.** 2008. Advances in the structural understanding of Vif proteins. Curr. HIV Res. **6**:91–99.
67. **Xu H, Svarovskaia ES, Barr R, Zhang Y, Khan MA, Strebel K, Pathak VK.** 2004. A single amino acid substitution in human APOBEC3G antiretroviral enzyme confers resistance to HIV-1 virion infectivity factor-induced depletion. Proc. Natl. Acad. Sci. U. S. A. **101**:5652–5657.
68. **Bogerd HP, Doehle BP, Wiegand HL, Cullen BR.** 2004. A single amino acid difference in the host APOBEC3G protein controls the primate species specificity of HIV type 1 virion infectivity factor. Proc. Natl. Acad. Sci. U. S. A. **101**:3770–3774.
69. **Schrofelbauer B, Chen D, Landau NR.** 2004. A single amino acid of APOBEC3G controls its species-specific interaction with virion infectivity factor (Vif). Proc. Natl. Acad. Sci. U. S. A. **101**:3927–3932.
70. **Bardy M, Gay B, Pebernard S, Chazal N, Courcoul M, Vigne R, Decroly E, Boulanger P.** 2001. Interaction of human immunodeficiency virus type 1 Vif with Gag and Gag-Pol precursors: co-encapsidation and interference with viral protease-mediated Gag processing. J. Gen. Virol. **82**:2719–2733.
71. **Goncalves J, Jallepalli P, Gabuzda DH.** 1994. Subcellular localization of the Vif protein of human immunodeficiency virus type 1. J. Virol. **68**:704–712.
72. **Alce TM, Popik W.** 2004. APOBEC3G is incorporated into virus-like particles by a direct interaction with HIV-1 Gag nucleocapsid protein. J. Biol. Chem. **279**:34083–34086.
73. **Cen S, Guo F, Niu M, Saadatmand J, Deflassieux J, Kleiman L.** 2004. The interaction between HIV-1 Gag and APOBEC3G. J. Biol. Chem. **279**:33177–33184.
74. **Luo K, Liu B, Xiao Z, Yu Y, Yu X, Gorelick R, Yu XF.** 2004. Amino-terminal region of the human immunodeficiency virus type 1 nucleocapsid is required for human APOBEC3G packaging. J. Virol. **78**:11841–11852.
75. **Schafer A, Bogerd HP, Cullen BR.** 2004. Specific packaging of APOBEC3G into HIV-1 virions is mediated by the nucleocapsid domain of the gag polyprotein precursor. Virology **328**:163–168.
76. **Syed F, McCrae MA.** 2009. Interactions in vivo between the Vif protein of HIV-1 and the precursor ($Pr55^{GAG}$) of the virion nucleocapsid proteins. Arch. Virol. **154**:1797–1805.
77. **Kao S, Miyagi E, Khan MA, Takeuchi H, Opi S, Goila-Gaur R, Strebel K.** 2004. Production of infectious human immunodeficiency virus type 1 does not require depletion of APOBEC3G from virus-producing cells. Retrovirology **1**:27. doi:10.1186/1742-4690-1-27.
78. **Khan MA, Aberham C, Kao S, Akari H, Gorelick R, Bour S, Strebel K.** 2001. Human immunodeficiency virus type 1 Vif protein is packaged into the nucleoprotein complex through an interaction with viral genomic RNA. J. Virol. **75**:7252–7265.
79. **Khan MA, Kao S, Miyagi E, Takeuchi H, Goila-Gaur R, Opi S, Gipson CL, Parslow TG, Ly H, Strebel K.** 2005. Viral RNA is required for the association of APOBEC3G with human immunodeficiency virus type 1 nucleoprotein complexes. J. Virol. **79**:5870–5874.

Article 5: Un facteur de transcription se fait complice du VIH-1 pour détruire les défenses cellulaires

Un facteur de transcription se fait complice du VIH-1 pour détruire les défenses cellulaires

Roland Marquet, Santiago Guerrero, Serena Bernacchi, Sophie Pernot, Julien Batisse, Jean-Christophe Paillart

Architecture et réactivité de l'ARN, Université de Strasbourg, CNRS, Institut de biologie moléculaire et cellulaire, 15, rue René Descartes, 67084 Strasbourg cedex, France.
r.marquet@ibmc-cnrs.unistra.fr

> Les éléments génétiques mobiles représentent une fraction considérable de notre génome et les mammifères ont développé plusieurs facteurs cellulaires restreignant l'expansion des transposons, rétrotransposons et rétrovirus. Plusieurs facteurs de restriction inhibant la réplication des rétrovirus, dont les virus de l'immunodéficience humaine de types 1 et 2 (VIH-1, VIH-2), ont ainsi été identifiés : TRIM5α (*tripartite motif-containing protein 5α*), la téthérine, SAMHD1 (*SAM domain and HD domain 1*), et plusieurs membres de la famille des cytidines désaminases APOBEC-3 (*apolipoprotein B mRNA-editing, enzyme-catalytic, polypeptide-like 3*) [1-3]. Parmi ces derniers, A-3G et A-3F, qui sont exprimés dans les cellules cibles naturelles des VIH-1 et VIH-2, sont les plus importants [1, 3]. Les rétrovirus ont cependant acquis la capacité de contourner ces facteurs de restriction. Certains ont développé des protéines dites accessoires dans ce seul but : c'est le cas du facteur d'infectiosité viral (Vif) et de la protéine virale U (Vpu) des VIH-1 et VIH-2, ainsi que de la protéine virale X (Vpx) du VIH-2, qui contrecarrent respectivement A-3C/3DE/3F/3G/3H [1, 3], la téthérine [1] et SAMHD1 [2]. La neutralisation des facteurs de restriction par les rétrovirus implique très souvent le détournement de la voie de dégradation des protéines cellulaires par le protéasome en réponse à leur polyubiquitination.

Ubiquitinylation des facteurs de restriction par la protéine virale Vif

L'ubiquitinylation des protéines eucaryotes fait tout d'abord intervenir une des deux enzymes activatrices, E1, qui transfère l'ubiquitine à l'une des enzymes de conjugaison, E2 ; enfin, une ubiquitine ligase (E3, il en existe plusieurs centaines), transfère l'ubiquitine aux substrats spécifiques. Trois protéines accessoires du VIH-1, Vif, Vpu et Vpr sont connues pour détourner trois ubiquitine ligases E3 différentes appartenant à la famille des cullin-RING E3 ligases. La protéine Vif du VIH-1 possède en son centre un motif HCCH liant le zinc et une boîte culline qui permettent le recrutement de la culline 5 (Cul-5), Cul-5 étant capable de lier Rbx-2, une protéine possédant un domaine RING. Vif possède en outre dans sa région carboxy-terminale un motif appelé SOCS (*suppressor of cytokine signaling*) *box* qui recrute l'élongine C (Elo-C) qui forme un hétérodimère avec l'élongine B (Elo-B) *(Figure 1, voie B)*. Le complexe Cul-5/Rbx2/Elo-B/Elo-C ainsi recruté par la protéine Vif permet l'ubiquitinylation d'A-3G/A-3F, orientant ainsi ces protéines vers la dégradation par le protéasome *(Figure 1, voie B)*.

CBF-β : un nouveau ligand de Vif impliqué dans l'infectiosité des VIH/VIS chez les primates

Deux articles publiés récemment dans la revue *Nature* [4, 5] ont identifié un nouveau ligand de Vif impliqué dans la dégradation d'A-3G, qui fait également l'objet d'une publication récente dans *Journal of Virology* [6]. En effet, Krogan *et al.* [7] ont entrepris l'identification systématique des ligands des protéines du VIH-1, dont Vif, en combinant purification d'affinité et spectrométrie de masse. Chacune des protéines du VIH-1 a été exprimée avec deux étiquettes différentes (*Strep* ou *Flag*) soit par transfection transitoire de cellules humaines d'épithélium rénal embryonnaire (HEK-293), soit par expression stable et inductible à partir de cellules lymphoïdes Jurkat. Les auteurs se sont focalisés sur les protéines identifiées indépendamment du type cellulaire et de l'étiquette utilisée pour la purification [5, 7]. Par cette approche, sept protéines humaines ont été identifiées comme des ligands directs ou indirects de Vif dans les deux types cellulaires : l'une intervient dans l'autophagie (MARA1), cinq sont les constituants de l'ubiquitine ligase E3 (Elo-B, Elo-C, Cul-5, Rbx-2, et Cul-2 qui interagit avec Cul-5) et la dernière est CBF-β (*core binding factor-β*). Zhang *et al.* [4] ont, quant à eux, employé Vif munie d'une étiquette HA (hémaglutinine) pour immunoprécipiter ses partenaires dans les cellules H9, une lignée cellulaire T. Ils ont ensuite identifié par spectrométrie de masse Cul-5, Elo-B, Elo-C et CBF-β. L'interaction entre Vif et CBF-β a été validée par des études de colocalisation et de transfert d'énergie de fluorescence (FRET) dans des cellules HEK 293T transfectées [4].

m/s n° 4, vol. 28, avril 2012
DOI : 10.1051/medsci/2012284007

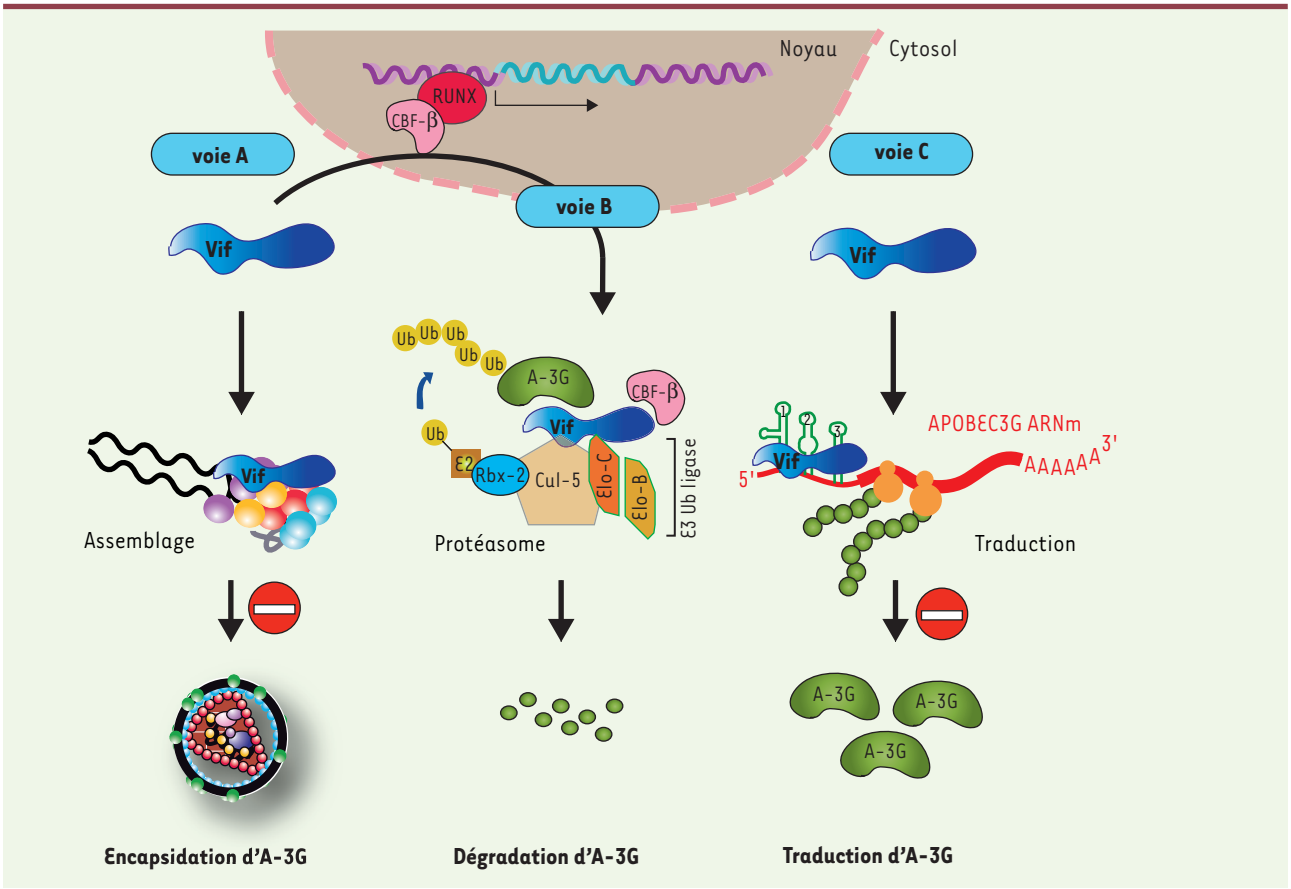

Figure 1. ***Mécanismes d'action de Vif.*** Vif contrecarre le facteur de restriction A3-G par au moins trois mécanismes distincts : (1) compétition avec A-3G lors de l'assemblage viral (voie A), (2) induction de sa dégradation par le protéasome (voie B), et (3) inhibition de sa traduction (voie C).

CBF-β est un cofacteur de transcription impliqué dans le développement et la différenciation de plusieurs types cellulaires, dont les lymphocytes T. Il ne lie pas l'ADN mais interagit avec les protéines de la famille RUNX (*Runt-related transcription factor 1*), dont il module le repliement et les propriétés de fixation à l'ADN *(Figure 1)*. Zhang *et al.* ont déterminé que la région amino-terminale de Vif est cruciale pour sa liaison à CBF-β et que cette liaison n'entre pas en compétition avec le recrutement des protéines RUNX dont Vif n'affecte pas l'activité transcriptionnelle [4]. Les deux publications parues dans *Nature* [4, 5] démontrent que CBF-β fait partie du complexe E3 ubiquitine ligase comprenant la Cul-5, Rbx2, Elo-C et Elo-B. Cependant, la fixation de CBF-β à ce complexe requiert Vif, ce qui indique que CBF-β n'est pas un constituant général des Cul-5 E3 ubiquitine ligases [4, 5]. Vif forme un complexe soluble et monodisperse avec CBF-β, Elo-B et Elo-C qui lie A-3G et s'associe à Cul-5/Rxb-2 [5], CBF-β facilitant le recrutement de Cul-5 [4]. La réciproque n'est cependant pas vraie : Cul-5 n'influence pas la fixation de CBF-β à Vif [4]. En outre, Jäger *et al.* ont démontré que le complexe Cul-5/Rxb-2/Elo-B/Elo-C/Vif/CBF-β reconstitué *in vitro* à partir de protéines recombinantes est capable de polyubiquitiner A-3G [5].

Les deux études [4, 5] ont démontré également que lorsque l'expression de CBF-β est diminuée par l'utilisation de siARN ou de shARN, la concentration intracellulaire d'A-3G et son incorporation dans les particules virales - nécessaire à son activité de restriction - augmentent, tandis que l'infectiosité du VIH-1 diminue. Comme attendu, CBF-β n'affecte pas l'infectiosité virale en l'absence d'A-3G. L'étude de Hulquist *et al.* étend la portée de ces résultats, puisqu'elle les généralise aux deux isoformes de CBF-β, à un grand nombre d'isolats du VIH-1 de sous-types différents et à l'ensemble des cytidines désaminases de la famille APOBEC-3 sensibles à la dégradation induite par Vif (A-3C/3DE/3F/3G/3H) [6]. De façon similaire, CBF-β lie la protéine Vif du virus d'immunodéficience des macaques rhésus (VISmac), favorisant la dégradation des APOBEC-3 sensibles à Vif chez cet animal et leur exclusion des particules virales dont elle augmente l'infectiosité [4-6]. Cependant, la dégradation de l'unique protéine APOBEC-3 bovine induite par Vif du virus de l'immunodéficience bovine (VIB) n'est pas affectée par CBF-β [4], suggérant que

l'implication de cette protéine dans la dégradation des protéines de la famille APOBEC-3 se limite aux primates.

Perspectives thérapeutiques antivirales

L'identification d'un facteur humain intervenant spécifiquement dans la dégradation des protéines de la famille APOBEC-3 ouvre la voie à de nouvelles stratégies antivirales dirigées contre les VIH-1 et 2. En effet, des molécules perturbant l'interaction entre Vif et CBF-β devraient inhiber la dégradation de ces facteurs de résistance sans perturber la fonction des autres ubiquitine ligases. La mise en évidence du complexe stable et soluble CBF-β /Vif/Elo-C/Elo-B et la reconstitution *in vitro* d'un complexe E3 ubiquitine ligase actif [5] permettent d'envisager le criblage à haut flux d'inhibiteurs ou leur conception rationnelle lorsque la structure cristallographique de ces complexes aura été obtenue. La dégradation d'A-3G par la voie du protéasome n'est pas le seul mécanisme par lequel Vif contrecarre ce facteur de restriction : Vif réduit également l'expression d'A-3G en inhibant sa traduction [8] *(Figure 1, voie C)* et agit de façon directe pour inhiber son incorporation dans les particules virales, sans doute par compétition [3] *(Figure 1, voie A)*. Ces deux derniers mécanismes restent encore mal connus et pourraient, eux-aussi, déboucher sur de nouvelles stratégies d'inhibition du VIH-1. ◊

A transcription factor acts as a HIV-1 accomplice to destroy the cellular defences

RÉFÉRENCES

1. Strebel K, Luban J, Jeang KT. Human cellular restriction factors that target HIV-1 replication. *BMC Med* 2009 ; 7 : 48.
2. Laguette N, Sobhian B, Casartelli N, *et al.* SAMHD1 is the dendritic- and myeloid-cell-specific HIV-1 restriction factor counteracted by Vpx. *Nature* 2011 ; 474 : 654-7.
3. Henriet S, Mercenne G, Bernacchi S, *et al.* Tumultuous relationship between the human immunodeficiency virus type 1 viral infectivity factor (Vif) and the human APOBEC-3G and APOBEC-3F restriction factors. *Microbiol Mol Biol Rev* 2009 ; 73 : 211-32.
4. Zhang W, Du J, Evans SL, *et al.* T-cell differentiation factor CBF-beta regulates HIV-1 Vif-mediated evasion of host restriction. *Nature* 2012 ; 481 : 376-9.
5. Jager S, Kim DY, Hultquist JF, *et al.* Vif hijacks CBF-beta to degrade APOBEC3G and promote HIV-1 infection. *Nature* 2012 ; 481 : 371-5.
6. Hultquist JF, Binka M, LaRue RS, *et al.* Vif proteins of human and simian immunodeficiency viruses require cellular CBF-β to degrade APOBEC3 restriction factors. *J Virol* 2012 ; 86 : 2874-7.
7. Jager S, Cimermancic P, Gulbahce N, *et al.* Global landscape of HIV-human protein complexes. *Nature* 2012 ; 481 : 365-70.
8. Mercenne G, Bernacchi S, Richer D, *et al.* HIV-1 Vif binds to APOBEC3G mRNA and inhibits its translation. *Nucleic Acids Res* 2010 ; 38 : 633-46.

NOUVELLE

Rôle des fibrilles amyloïdes dans la transmission du VIH

Nadia R. Roan, Marielle Cavrois, Warner C. Greene

Gladstone Institute of Virology and Immunology, University of California at San Francisco, San Francisco, CA 94158, États-Unis.
nroan@gladstone.ucsf.edu

› Comme en témoignent les 34 millions de personnes infectées en 2010, le VIH/Sida demeure un problème de santé publique majeur [1]. Une grande partie des infections mondiales se concentrent en Afrique sub-saharienne où la transmission lors de rapports hétérosexuels est le mode de propagation le plus courant. Comme cette transmission se produit quasiment toujours en présence de sperme, il est essentiel d'élucider l'effet du sperme sur la transmission du virus.

Le sperme, un facteur facilitateur de l'infection VIH

Loin d'être un véhicule passif pour le VIH, le sperme peut grandement augmenter l'infection par le VIH *in vitro*. Plusieurs groupes ont publié que la présence de sperme augmente dramatiquement l'infection de lignées cellulaires et de cellules primaires par le VIH [2-6]. Quels sont les facteurs présents dans le sperme responsables de cet effet ? Un certain nombre de composants du liquide séminal, dont la fonction physiologique est de protéger les spermatozoïdes lors de leur voyage vers l'ovule, peuvent protéger également les virions. C'est le cas des amines basiques comme la spermine, la spermidine, putrescine, cadavérine, etc., qui évitent la dénaturation des spermatozoïdes dans l'environnement acide de l'appareil vaginal et qui, malheureusement, empêchent aussi l'inactivation du virus [7-9]. D'autres composants du sperme, plus récemment identifiés par Munch *et al.* forment des fibrilles amyloïdes capables d'augmenter l'infectivité du VIH [2]. Ces fibrilles ont été nommées SEVI pour *semen-derived enhancer of viral infection*. L'augmentation du pouvoir infectieux du VIH conférée par SEVI est plus marquée lorsque l'inoculum viral est limité, une situation qui semble survenir lors de la transmission du VIH. Des expériences de dilution limite du virus ont montré que les fibrilles de SEVI peuvent augmenter l'infection par un facteur de 100 000 [2]. Une dose de VIH qui serait donc insuffisante pour être infectieuse pourrait devenir, dans ce contexte, hautement infectieuse.

Les fibrilles amyloïdes du sperme

Les fibrilles amyloïdes sont des polymères de feuillets β et ont été déjà associées à des maladies neurologiques, maladies d'Alzheimer et de Huntington par exemple. SEVI est constitué de

Posters and oral presentations

1. **Guerrero, S.**, Batisse, J., Mercenne, G., Richer, D., Laumond, G., Decoville, T., Moog, C., Marquet, R. & Paillart, J.-C. Inhibition of APOBEC3G translation by Vif restores HIV-1 infectivity. Présentation orale au «Retroviruses meeting at Cold Spring Harbor Laboratory», New York, **États-Unis**, Mai **2013**

2. **Guerrero, S.**, Mercenne, G., Batisse, J., Richer, D., Marquet, R. & Paillart, J.-C. Importance of the 5'-Untranslated Region in the Translational Regulation of APOBEC3G mRNA by the HIV-1 Vif Protein. Poster présenté au «19th Conference on Retroviruses and Opportunistic Infections», Seattle, **États-Unis**, Mars **2012**

3. **Guerrero, S.**, Mercenne, G., Batisse, J., Bernacchi, S., Richer, D., Marquet, R. & Paillart, J.-C. Translational inhibition of APOBEC3G antiviral factor by HIV-1 Vif protein. Poster présenté au « Université des jeunes Chercheurs, SIDACTION », Marseille, **France**, Septembre **2011**

4. **Guerrero, S.**, Mercenne, G., Batisse, J., Bernacchi, S., Richer, D., Marquet, R. & Paillart, J.-C. Translational inhibition of APOBEC3G antiviral factor by HIV-1 Vif protein. Poster présenté au « XI Congreso Nacional di Virologia », Granade, **Espagne**, 29 Mai-1er Juin **2011**

A-107

Importance of the 5'-Untranslated Region in the Translational Regulation of APOBEC3G mRNA by the HIV-1 Vif Protein

Santiago GUERRERO, Gaëlle MERCENNE, Julien BATISSE, Delphine RICHER, Roland MARQUET & Jean-Christophe PAILLART

Architecture & Réactivité de l'ARN - Université de Strasbourg, CNRS, IBMC, Strasbourg, France

Contact:
Santiago Guerrero
Institut de Biologie Moléculaire et Cellulaire
15 rue René Descartes
F-67084 STRASBOURG CEDEX- FRANCE
Tél : 00 33 (0)3 88 41 70 91
Fax : 00 33 (0)3 88 60 22 18
E-mail: s.guerrero@ibmc-cnrs.unistra.fr
sxguerrero@gmail.com
http://www-ibmc.u-strasbg.fr/arn/Marquet/

ABSTRACT

Background: The HIV-1 viral infectivity factor (Vif) is a small basic protein essential for viral fitness and pathogenicity. Vif targets cellular cytosine deaminases, APOBEC3G (hA3G) and hA3F, which inhibit HIV-1 replication by inducing extensive mutation (G to A) in (-) strand DNA during reverse transcription and by reducing the efficiency of reverse transcription and integration. Vif counteracts hA3G/3F (1) by inducing its degradation through the ubiquitin-proteasome pathway, (2) by preventing its incorporation into viral particles and (3) by repressing its translation at the mRNA level.

Methods: To address the role of Vif in the translational regulation of hA3G, we first characterized Vif binding sites on the full-length hA3G mRNA and on fragments corresponding to its coding or untranslated regions (UTRs) using RNase footprinting. Secondly, we analyzed the effect of Vif on hA3G translation in an in vitro transcription/translation assay and in HEK 293T cells using different hA3G mRNA constructs containing or not the UTRs. In order to discriminate between the proteasome degradation pathway and translational inhibition, we used proteasome inhibitors (MG132 and ALLN) as well as a dominant-negative mutant form of Cullin 5. Finally, to determine the motifs of the 5'-UTR involved in the translational inhibition of hA3G by Vif, we performed the same experiments using different hA3G 5'-UTR mutants according to our previously published structural model of the 5'-UTR.

Results: RNase footprinting revealed 3 to 4 Vif binding sites in the 5'-UTR and 3 to 6 Vif binding sites in the 3'-UTR. Vif binding affinity is higher for the 3'-UTR than for the 5'-UTR, even though 5'-UTR contains at least one high affinity Vif binding site (Kd = 27±6 nM). In vitro transcription/translation assays and cotransfections in HEK 293T using different hA3G mRNA constructs identified the 5'-UTR as a major element for the translational inhibition by Vif. Preliminary results using different hA3G 5'-UTR mutants show that the entire 5'-UTR structure is require for this repression and no specific motif is necessary.

Conclusions: Experiments are in progress to determine, with precision the Vif protein domains involved in translational regulation of A3G and to clarify the impact of this translational repression in viral infectivity.

BACKGROUND

The genome of HIV-1 encodes several auxiliary proteins that are generally not found in other retroviruses. Among them, Vif (Viral Infectivity Factor) is essential in the formation of infectious viral particles in cells named "non-permissives" (T lymphocytes, monocytes, macrophages), whereas ΔVif viruses efficiently replicate in T cell lines termed "permissive" (Jurkat, CEM-SS...). Non-permissive cells specifically express APOBEC3G (A3G) and A3F proteins, two cytidine deaminases that act on the (-) strand DNA during reverse transcription of the viral genomic RNA. In response to this mechanism of defense, HIV-1 co-evolved by expressing the Vif protein. Vif strongly reduces expression level of A3G by (1) recruiting an E3 ubiquitin ligase, Vif induces A3G degradation by the proteasome, (2) Vif negatively reduces A3G mRNA translation by an unknown mechanism and (3) by direct competition with A3G packaging sites on HIV-1 genomic RNA and NC domain of Pr55Gag.

RESULTS

In vitro probing and footprint assays

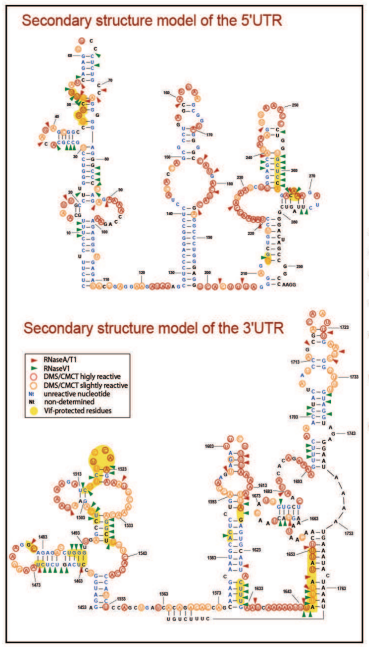

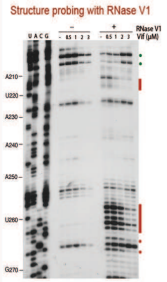

- 5' & 3'-UTRs of A3G fold into three structured domains separated by single-stranded junctions.
- RNase footprinting revealed 3-4 and 3-6 Vif binding sites in the 5'UTR and in the 3'UTR, respectively.

APOBEC3G inhibits HIV-1 replication

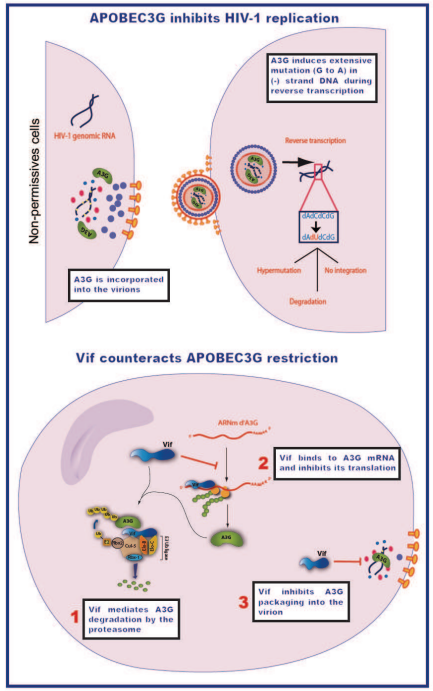

Vif counteracts APOBEC3G restriction

Translation of hA3G in HEK293 T

Identification of hA3G mRNA UTR regions involved in Vif regulation

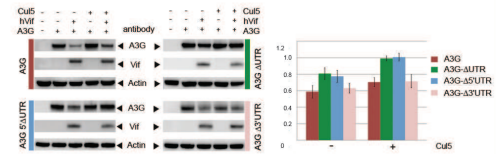

- Cotransfections in HEK 293T using different hA3G mRNA constructs identified the 5'-UTR as a major element for the translational inhibition by Vif.

Identification of hA3G mRNA 5'UTR regions involved in Vif regulation

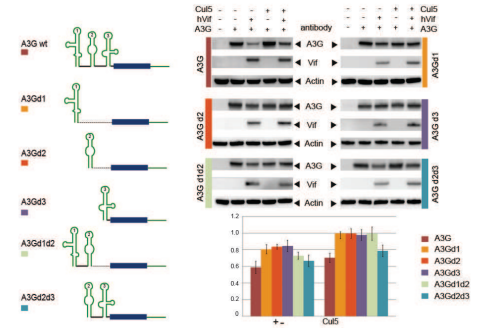

- Cotransfections in HEK 293T using different different hA3G 5'-UTR mutants show that the entire 5'-UTR structure is require for this repression and no specific motif is necessary.

CONCLUSIONS

In parallel to its effect on proteasomal degradation of hA3G, Vif inhibits hA3G translation by binding to its mRNA and particularly to its 5'UTR. Within the 5'UTR, no specific motif is necessary in Vif regulation. Experiments are in progress to determine, with precision the Vif protein domains involved in translational regulation of A3G and to clarify the impact of this translational repression in viral infectivity. Comprehension of these processes is of importance for therapeutic because its inhibition would allow an increase of A3G packaging and a strong decrease of virus infectivity.

We acknowledge K. Strebel for providing Vif expressing vector (pcDNA hVif) and the NIH AIDS Research & Reference Reagent Program: APOBEC3G antiserum (ApoC17) from K. Strebel, and Vif monoclonal antibody from M. Malim.

This work is supported by Sidaction and anrs Agence nationale de recherches sur le sida et les hépatites virales

La protéine Vif du VIH-1 se lie à l'ARNm d'APOBEC3G et inhibe sa traduction

Santiago GUERRERO, Gaëlle MERCENNE, Julien BATISSE, Serena BERNACCHI,
Delphine RICHER, Roland MARQUET & Jean-Christophe PAILLART
Architecture & Réactivité de l'ARN - Université de Strasbourg, CNRS, IBMC, Strasbourg, France
s.guerrero@ibmc-cnrs.unistra.fr

INTRODUCTION

Le génome du VIH-1 code pour plusieurs protéines dites « auxiliaires » qui ne sont pas retrouvées chez les rétrovirus simples. Initialement considérées comme accessoires, ces protéines sont essentielles à la propagation de l'infection et au développement de la pathogenèse in vivo. Parmi elles, Vif (Viral Infectivity Factor), est essentielle à la formation de particules virales infectieuses dans les cellules dites « non-permissives » (lymphocytes T CD4+, monocytes, macrophages), alors que des virus qui ne contiennent pas la protéine Vif se répliquent efficacement dans des lignées cellulaires T dites « permissives » (Jurkat, CEM-SS…). Les travaux récents de plusieurs laboratoires ont montré que les cellules non-permissives expriment de façon spécifique les protéines APOBEC3G (A3G) et A3F, deux cytidine désaminases dont l'action hypermutatrice lors de la synthèse du brin (-) d'ADN est létale pour le virus. En réponse à ce mécanisme de défense, le VIH-1 a co-évolué en exprimant la protéine Vif qui contrecarre l'activité du facteur antiviral APOBEC3G en induisant sa dégradation par le protéasome et en inhibant sa traduction. Vif régule négativement la traduction de l'ARNm d'A3G par un mécanisme encore inconnu, mais il est vraisemblable qu'il implique les propriétés de fixation aux ARN de Vif. L'objetif de ce projet est de caractériser les mécanismes d'inhibition traductionnelle d'A3G par Vif.

RÉSULTATS

1- Vif se fixe aux régions non traduites de l'ARNm d'A3G et inhibe sa traduction

Empreintes enzymatiques de Vif sur l'ARNm

Modèle de la region 5'UTR

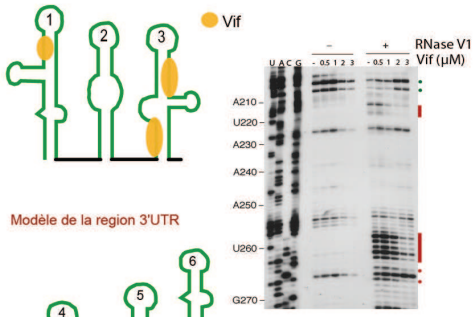

Modèle de la region 3'UTR

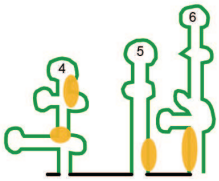

A3G possède une action hypermutatrice

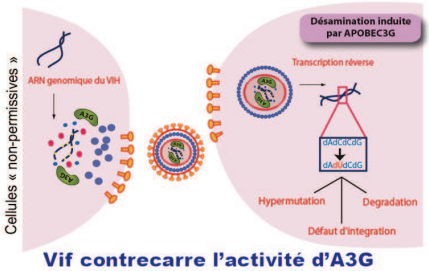

Vif contrecarre l'activité d'A3G

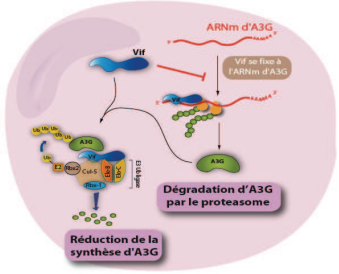

Traduction d'A3G dans des cellules HEK293T

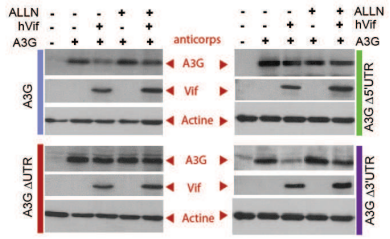

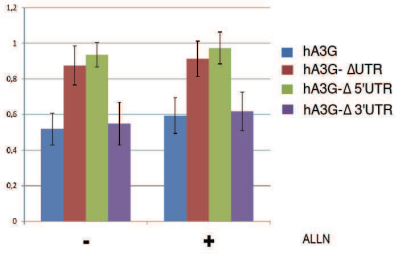

- Les régions 5' et 3' UTR se structurent formant des tiges-boucles en 3 domaines structurés, séparés par des jonctions simples brins
- Les expériences d'empreintes enzymatiques révèlent plusieurs sites de fixation de Vif sur les régions 5'UTR et 3'UTR de l'ARNm d'A3G
- La traduction d'A3G dans les cellules HEK293 en présence ou en absence d'ALLN, un inhibiteur du proteasome, révèle L'importance de la région 5'UTR dans l'inhibition de la traduction

PERSPECTIVES

1- Interaction entre Vif et l'ARNm d'A3G

- Identification des domaines de la région 5'UTR de l'ARNm d'A3G impliquées dans la régulation par Vif

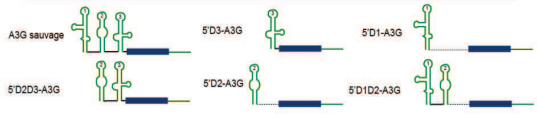

- Identification des domaines de Vif impliqués dans la régulation traductionnelle d'A3G

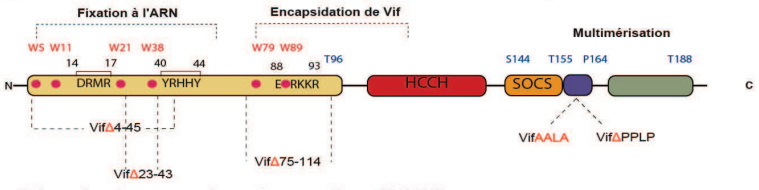

2- Infectivité virale

- Co-transfection avec pNL4-3 ou pNL4-3Δvif et les différents constructions d'A3G

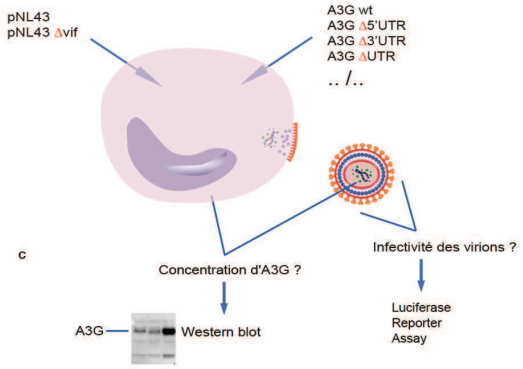

3- Régulation traductionnelle d'A3G

- Composition des complexes d'initiation de la traduction

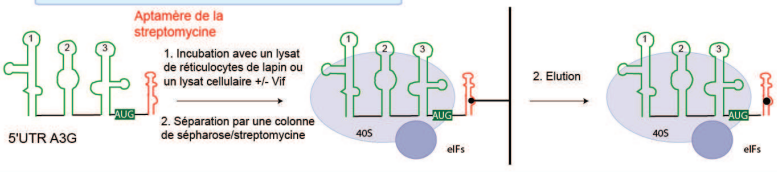

- Présence d'un élément IRES (Internal Ribosome Entry Site) dans la région 5'UTR de l'ARNm d' A3G

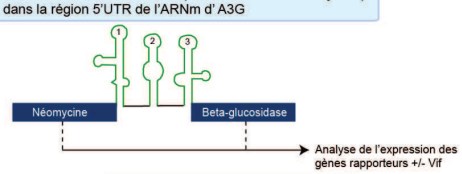

CONCLUSIONS

Les expériences d'empreinte enzymatique ainsi que la traduction d'A3G dans des cellules HEK293T ont permis d'identifier la région 5'UTR comme un élément majeur dans la régulation traductionnelle d'A3G par Vif. Des expériences sont en cours pour déterminer avec précision les motifs de la 5'-UTR impliqués dans l'inhibition traductionnelle d'A3G et clarifier l'impact de cette répression traductionnelle dans le cycle de réplication virale. La compréhension de ces différents processus est importante d'un point de vue thérapeutique car leur inhibition permettrait une encapsidation accrue des protéines A3G/3F et une baisse importante de l'infectivité virale.

Mercenne, G., Bernacchi, S., Richer, D., Bec, G., Henriet S, Paillart J, Marquet R. HIV-1 Vif binds to APOBEC3G mRNA and inhibits its translation. Nucleic Acids Res 2010 38(2):633-646. We acknowledge K. Strebel for providing Vif expressing vector (pcDNA hVif) and the NIH AIDS Research & Reference Reagent Program: APOBEC3G antiserum (ApoC17) from K. Strebel, and Vif monoclonal antibody from M. Malim.
This work is supported by

HIV-1 Vif binds to APOBEC3G mRNA and inhibits its translation

Santiago GUERRERO, Gaëlle MERCENNE, Julien BATISSE, Serena BERNACCHI,
Delphine RICHER, Roland MARQUET & Jean-Christophe PAILLART
Architecture & Réactivité de l'ARN - Université de Strasbourg, CNRS, IBMC, Strasbourg, France
s.guerrero@ibmc-cnrs.unistra.fr

INTRODUCTION

The HIV-1 viral infectivity factor (Vif) is a small basic protein that is essential to viral fitness and pathogenicity. Vif allows productive infection of non-permissive cells (including most natural HIV-1 targets) by counteracting the cellular cytosine deaminases APOBEC3G (hA3G) and hA3F. The Vif-induced degradation of these restriction factors by the proteasome has been extensively studied, but little is known about the translational repression of hA3G and hA3F by Vif, which has also been proposed to participate in Vif function.

RESULTS

1- Vif binds to the A3G mRNA unstranslated regions (UTRs) and inhibits its translation

In vitro probing and footprint assays

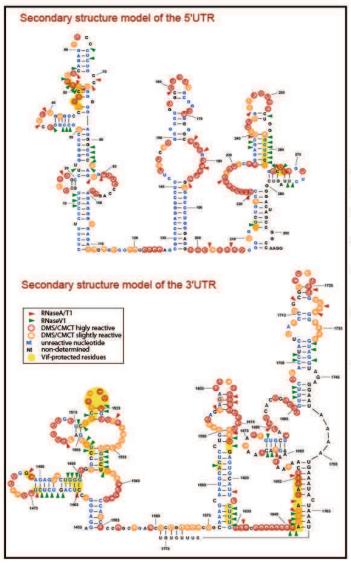

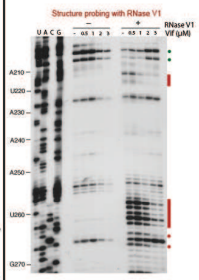

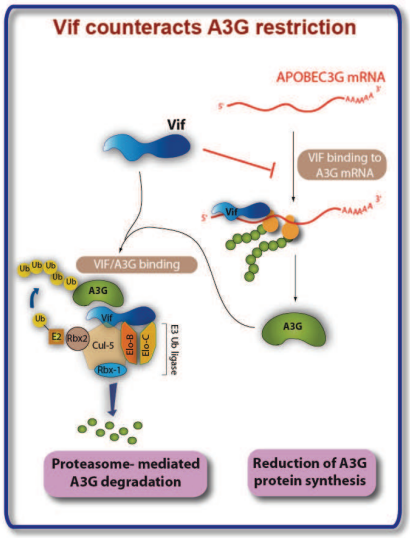

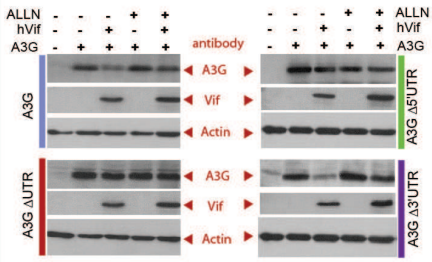

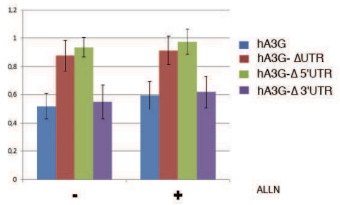

- 5' & 3'-UTRs of A3G fold into three structured domains separated by single-stranded junctions.
- RNase footprinting revealed 3-4 and 3-6 Vif binding sites in the 5'UTR and in the 3'UTR, respectively.
- The 5'UTR is necessary to allow Vif-mediated repression of hA3G.

PERSPECTIVES

1- Vif-A3G mRNA interaction

- Identification of A3G mRNA 5'UTR regions involved in Vif regulation

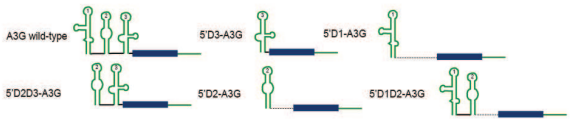

- Identification of Vif domains involved in translational regulation of A3G

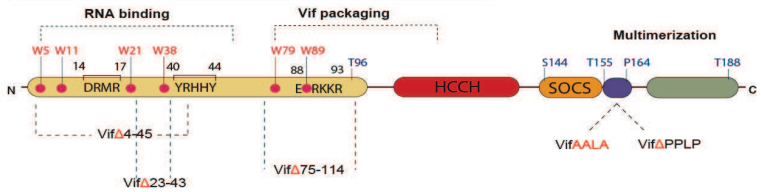

2- Viral infectivity

- Co-transfection with pNL4-3 or pNL4-3Δvif and different constructions of A3G

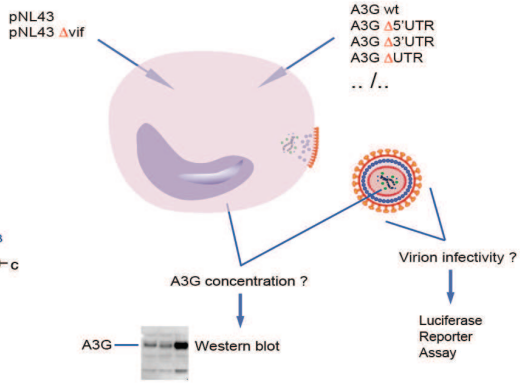

3- Translational regulation of A3G

- Composition of the translation Initiation complexes

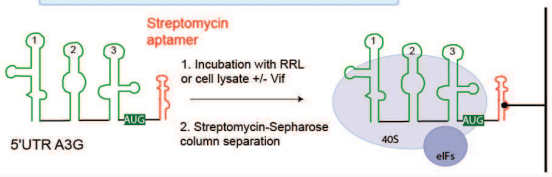

- Presence of IRES element in the 5'UTR of A3G mRNA

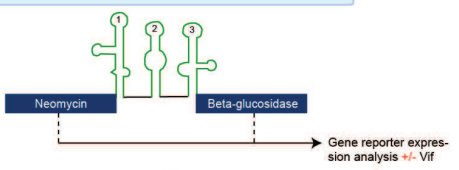

CONCLUSIONS

In parallel to its effect on proteasomal degradation of hA3G, Vif inhibits hA3G translation by binding to its mRNA and particularly to its 5'UTR. However, we did not see any correlation between the relative binding affinity of Vif to the 5' and 3'UTRs and their role in Vif-mediated translational repression. Experiments are in progress to determine with precision the motifs of the 5'-UTR involved in the translational inhibition of hA3G and clarify the impact of this translational repression in the viral replication cycle.

Mercenne, G., Bernacchi, S., Richer, D., Bec, G., Henriet S, Paillart J, Marquet R. HIV-1 Vif binds to APOBEC3G mRNA and inhibits its translation. Nucleic Acids Res 2010 38(2):633-646. We acknowledge K. Strebel for providing Vif expressing vector (pcDNA hVif) and the NIH AIDS Research & Reference Reagent Program: APOBEC3G anti-serum (ApoC17) from K. Strebel, and Vif monoclonal antibody from M. Malim.
This work is supported by

VII. REFERENCES

Abbas, W., Khan, K.A., Tripathy, M.K., Dichamp, I., Keita, M., Rohr, O., and Herbein, G. (2012). Inhibition of ER stress-mediated apoptosis in macrophages by nuclear-cytoplasmic relocalization of eEF1A by the HIV-1 Nef protein. Cell Death Dis. *3*, e292.

Adams, R.L., and Wente, S.R. (2013). Uncovering nuclear pore complexity with innovation. Cell *152*, 1218–1221.

Aitken, C.E., and Lorsch, J.R. (2012). A mechanistic overview of translation initiation in eukaryotes. Nat. Struct. Mol. Biol. *19*, 568–576.

Albin, J.S., and Harris, R.S. (2010). Interactions of host APOBEC3 restriction factors with HIV-1 in vivo: implications for therapeutics. Expert Rev. Mol. Med. *12*, e4.

Alce, T.M., and Popik, W. (2004). APOBEC3G is incorporated into virus-like particles by a direct interaction with HIV-1 Gag nucleocapsid protein. J. Biol. Chem. *279*, 34083–34086.

Algire, M.A., Maag, D., and Lorsch, J.R. (2005). Pi release from eIF2, not GTP hydrolysis, is the step controlled by start-site selection during eukaryotic translation initiation. Mol. Cell *20*, 251–262.

Alkhatib, G., Combadiere, C., Broder, C.C., Feng, Y., Kennedy, P.E., Murphy, P.M., and Berger, E.A. (1996). CC CKR5: a RANTES, MIP-1alpha, MIP-1beta receptor as a fusion cofactor for macrophage-tropic HIV-1. Science *272*, 1955–1958.

Allen, I.C., Scull, M.A., Moore, C.B., Holl, E.K., McElvania-TeKippe, E., Taxman, D.J., Guthrie, E.H., Pickles, R.J., and Ting, J.P.-Y. (2009). The NLRP3 inflammasome mediates in vivo innate immunity to influenza A virus through recognition of viral RNA. Immunity *30*, 556–565.

Allouch, A., Di Primio, C., Alpi, E., Lusic, M., Arosio, D., Giacca, M., and Cereseto, A. (2011). The TRIM family protein KAP1 inhibits HIV-1 integration. Cell Host Microbe *9*, 484–495.

Alvarez, E., Castelló, A., Menéndez-Arias, L., and Carrasco, L. (2006). HIV protease cleaves poly(A)-binding protein. Biochem. J. *396*, 219–226.

Aravind, L., and Koonin, E.V. (1998). The HD domain defines a new superfamily of metal-dependent phosphohydrolases. Trends Biochem. Sci. *23*, 469–472.

Arhel, N. (2010). Revisiting HIV-1 uncoating. Retrovirology *7*, 96.

Arhel, N.J., Souquere-Besse, S., Munier, S., Souque, P., Guadagnini, S., Rutherford, S., Prévost, M.-C., Allen, T.D., and Charneau, P. (2007). HIV-1 DNA Flap formation promotes uncoating of the pre-integration complex at the nuclear pore. EMBO J. *26*, 3025–3037.

Ashur-Fabian, O., Har-Zahav, A., Shaish, A., Wiener Amram, H., Margalit, O., Weizer-Stern, O., Dominissini, D., Harats, D., Amariglio, N., and Rechavi, G. (2010). apoB and apobec1, two genes key to lipid metabolism, are transcriptionally regulated by p53. Cell Cycle Georget. Tex *9*, 3761–3770.

Balasubramaniam, M., and Freed, E.O. (2011). New insights into HIV assembly and trafficking. Physiol. Bethesda Md *26*, 236–251.

Baldauf, H.-M., Pan, X., Erikson, E., Schmidt, S., Daddacha, W., Burggraf, M., Schenkova, K., Ambiel, I., Wabnitz, G., Gramberg, T., et al. (2012). SAMHD1 restricts HIV-1 infection in resting CD4(+) T cells. Nat. Med. *18*, 1682–1687.

Balvay, L., Soto Rifo, R., Ricci, E.P., Decimo, D., and Ohlmann, T. (2009). Structural and functional diversity of viral IRESes. Biochim. Biophys. Acta *1789*, 542–557.

Barré-Sinoussi, F., Chermann, J.C., Rey, F., Nugeyre, M.T., Chamaret, S., Gruest, J., Dauguet, C., Axler-Blin, C., Vézinet-Brun, F., Rouzioux, C., et al. (1983). Isolation of a T-lymphotropic retrovirus from a patient at risk for acquired immune deficiency syndrome (AIDS). Science *220*, 868–871.

Basu, V.P., Song, M., Gao, L., Rigby, S.T., Hanson, M.N., and Bambara, R.A. (2008). Strand transfer events during HIV-1 reverse transcription. Virus Res. *134*, 19–38.

Batisse, J., Guerrero, S., Bernacchi, S., Sleiman, D., Gabus, C., Darlix, J.-L., Marquet, R., Tisné, C., and Paillart, J.-C. (2012). The role of Vif oligomerization and RNA chaperone activity in HIV-1 replication. Virus Res. *169*, 361–376.

Bauby, H., Lopez-Verges, S., and Berlioz-Torrent, C. (2008). TIP47: a cellular factor required for envelope glycoproteins incorporation into HIV particles. Virologie *12*, 201–213.

Bell, T.A., Casa-Esperón, E. de la, Doherty, H.E., Ideraabdullah, F., Kim, K., Wang, Y., Lange, L.A., Wilhemsen, K., Lange, E.M., Sapienza, C., et al. (2006). The Paternal Gene of the DDK Syndrome Maps to the Schlafen Gene Cluster on Mouse Chromosome 11. Genetics *172*, 411–423.

Berger, A., Sommer, A.F.R., Zwarg, J., Hamdorf, M., Welzel, K., Esly, N., Panitz, S., Reuter, A., Ramos, I., Jatiani, A., et al. (2011a). SAMHD1-deficient CD14+ cells from individuals with Aicardi-Goutières syndrome are highly susceptible to HIV-1 infection. PLoS Pathog. *7*, e1002425.

Berger, G., Durand, S., Fargier, G., Nguyen, X.-N., Cordeil, S., Bouaziz, S., Muriaux, D., Darlix, J.-L., and Cimarelli, A. (2011b). APOBEC3A Is a Specific Inhibitor of the Early Phases of HIV-1 Infection in Myeloid Cells. PLoS Pathog *7*, e1002221.

Berger, G., Turpin, J., Cordeil, S., Tartour, K., Nguyen, X.-N., Mahieux, R., and Cimarelli, A. (2012). Functional Analysis of the Relationship between Vpx and the Restriction Factor SAMHD1. J. Biol. Chem. *287*, 41210–41217.

Berger, M., Krebs, P., Crozat, K., Li, X., Croker, B.A., Siggs, O.M., Popkin, D., Du, X., Lawson, B.R., Theofilopoulos, A.N., et al. (2010). An Slfn2 mutation causes

lymphoid and myeloid immunodeficiency due to loss of immune cell quiescence. Nat. Immunol. *11*, 335–343.

Berkhout, B., Arts, K., and Abbink, T.E.M. (2011). Ribosomal scanning on the 5'-untranslated region of the human immunodeficiency virus RNA genome. Nucleic Acids Res. *39*, 5232–5244.

Bernacchi, S., Henriet, S., Dumas, P., Paillart, J.-C., and Marquet, R. (2007). RNA and DNA binding properties of HIV-1 Vif protein: a fluorescence study. J. Biol. Chem. *282*, 26361–26368.

Berthelot, K., Muldoon, M., Rajkowitsch, L., Hughes, J., and McCarthy, J.E.G. (2004). Dynamics and processivity of 40S ribosome scanning on mRNA in yeast. Mol. Microbiol. *51*, 987–1001.

Bishop, K.N., Holmes, R.K., and Malim, M.H. (2006). Antiviral potency of APOBEC proteins does not correlate with cytidine deamination. J. Virol. *80*, 8450–8458.

Bogerd, H.P., Wiegand, H.L., Doehle, B.P., and Cullen, B.R. (2007). The intrinsic antiretroviral factor APOBEC3B contains two enzymatically active cytidine deaminase domains. Virology *364*, 486–493.

Bohn, M.-F., Shandilya, S.M.D., Albin, J.S., Somasundaran, M., Harris, R.S., and Schiffer, C.A. (2013). Interfaces determined from the crystal structure of the catalytic domain of APOBEC3F reveal determinants for solution behavior. Meet. Retroviruses - Cold Spring Harb. Lab. 2013.

Bourara, K., Liegler, T.J., and Grant, R.M. (2007). Target cell APOBEC3C can induce limited G-to-A mutation in HIV-1. PLoS Pathog. *3*, 1477–1485.

Brandariz-Nuñez, A., Valle-Casuso, J.C., White, T.E., Laguette, N., Benkirane, M., Brojatsch, J., and Diaz-Griffero, F. (2012). Role of SAMHD1 nuclear localization in restriction of HIV-1 and SIVmac. Retrovirology *9*, 49.

Brasey, A., Lopez-Lastra, M., Ohlmann, T., Beerens, N., Berkhout, B., Darlix, J.-L., and Sonenberg, N. (2003). The leader of human immunodeficiency virus type 1 genomic RNA harbors an internal ribosome entry segment that is active during the G2/M phase of the cell cycle. J. Virol. *77*, 3939–3949.

Brennan, G., Kozyrev, Y., and Hu, S.-L. (2008). TRIMCyp expression in Old World primates Macaca nemestrina and Macaca fascicularis. Proc. Natl. Acad. Sci. *105*, 3569–3574.

De Breyne, S., Soto-Rifo, R., López-Lastra, M., and Ohlmann, T. (2013). Translation initiation is driven by different mechanisms on the HIV-1 and HIV-2 genomic RNAs. Virus Res. *171*, 366–381.

Browne, E.P., Allers, C., and Landau, N.R. (2009). Restriction of HIV-1 by APOBEC3G is cytidine deaminase-dependent. Virology *387*, 313–321.

Buck, C.B., Shen, X., Egan, M.A., Pierson, T.C., Walker, C.M., and Siliciano, R.F. (2001). The human immunodeficiency virus type 1 gag gene encodes an internal ribosome entry site. J. Virol. *75*, 181–191.

Burdick, R., Smith, J.L., Chaipan, C., Friew, Y., Chen, J., Venkatachari, N.J., Delviks-Frankenberry, K.A., Hu, W.-S., and Pathak, V.K. (2010). P body-associated protein Mov10 inhibits HIV-1 replication at multiple stages. J. Virol. *84*, 10241–10253.

Burdick, R.C., Hu, W.-S., and Pathak, V.K. (2013). Tracking APOBEC3-labeled HIV-1 during infection reveals dramatic differences in behavior among virally incorporated APOBEC3 proteins. Meet. Retroviruses - Cold Spring Harb. Lab. 2013.

Burnett, A., and Spearman, P. (2007). APOBEC3G multimers are recruited to the plasma membrane for packaging into human immunodeficiency virus type 1 virus-like particles in an RNA-dependent process requiring the NC basic linker. J. Virol. *81*, 5000–5013.

Bustos, O., Naik, S., Ayers, G., Casola, C., Perez-Lamigueiro, M.A., Chippindale, P.T., Pritham, E.J., and de la Casa-Esperón, E. (2009). Evolution of the Schlafen genes, a gene family associated with embryonic lethality, meiotic drive, immune processes and orthopoxvirus virulence. Gene *447*, 1–11.

Calvo, S.E., Pagliarini, D.J., and Mootha, V.K. (2009). Upstream open reading frames cause widespread reduction of protein expression and are polymorphic among humans. Proc. Natl. Acad. Sci. U. S. A. *106*, 7507–7512.

Cao, J., and Geballe, A.P. (1996). Coding sequence-dependent ribosomal arrest at termination of translation. Mol. Cell. Biol. *16*, 603–608.

Carrington, M., and Alter, G. (2012). Innate immune control of HIV. Cold Spring Harb. Perspect. Med. *2*, a007070.

Castelló, A., Franco, D., Moral-López, P., Berlanga, J.J., Alvarez, E., Wimmer, E., and Carrasco, L. (2009). HIV- 1 protease inhibits Cap- and poly(A)-dependent translation upon eIF4GI and PABP cleavage. PloS One *4*, e7997.

Centers for Disease Control (CDC) (1981). Kaposi's sarcoma and Pneumocystis pneumonia among homosexual men--New York City and California. MMWR Morb. Mortal. Wkly. Rep. *30*, 305–308.

Centers for Disease Control (CDC) (1982). A cluster of Kaposi's sarcoma and Pneumocystis carinii pneumonia among homosexual male residents of Los Angeles and Orange Counties, California. MMWR Morb. Mortal. Wkly. Rep. *31*, 305–307.

Chaipan, C., Smith, J.L., Hu, W.-S., and Pathak, V.K. (2013). APOBEC3G restricts HIV-1 to a greater extent than APOBEC3F and APOBEC3DE in human primary CD4+ T cells and macrophages. J. Virol. *87*, 444–453.

Chakrabarti, L., Guyader, M., Alizon, M., Daniel, M.D., Desrosiers, R.C., Tiollais, P., and Sonigo, P. (1987). Sequence of simian immunodeficiency virus from macaque and its relationship to other human and simian retroviruses. Nature *328*, 543–547.

Chamond, N., Locker, N., and Sargueil, B. (2010). The different pathways of HIV genomic RNA translation. Biochem. Soc. Trans. *38*, 1548–1552.

Chang, T.-H., Huang, H.-Y., Hsu, J.B.-K., Weng, S.-L., Horng, J.-T., and Huang, H.-D. (2013). An enhanced computational platform for investigating the roles of regulatory RNA and for identifying functional RNA motifs. BMC Bioinformatics *14 Suppl 2*, S4.

Chen, K.-M., Harjes, E., Gross, P.J., Fahmy, A., Lu, Y., Shindo, K., Harris, R.S., and Matsuo, H. (2008). Structure of the DNA deaminase domain of the HIV-1 restriction factor APOBEC3G. Nature *452*, 116–119.

Child, S.J., Miller, M.K., and Geballe, A.P. (1999). Translational control by an upstream open reading frame in the HER-2/neu transcript. J. Biol. Chem. *274*, 24335–24341.

Chuang, R.Y., Weaver, P.L., Liu, Z., and Chang, T.H. (1997). Requirement of the DEAD-Box protein ded1p for messenger RNA translation. Science *275*, 1468–1471.

Cimarelli, A., and Luban, J. (1999). Translation elongation factor 1-alpha interacts specifically with the human immunodeficiency virus type 1 Gag polyprotein. J. Virol. *73*, 5388–5401.

Ciuffi, A. (2008). Mechanisms governing lentivirus integration site selection. Curr. Gene Ther. *8*, 419–429.

Clavel, F., Guétard, D., Brun-Vézinet, F., Chamaret, S., Rey, M.A., Santos-Ferreira, M.O., Laurent, A.G., Dauguet, C., Katlama, C., and Rouzioux, C. (1986). Isolation of a new human retrovirus from West African patients with AIDS. Science *233*, 343–346.

Clerzius, G., Gélinas, J.-F., and Gatignol, A. (2011). Multiple levels of PKR inhibition during HIV-1 replication. Rev. Med. Virol. *21*, 42–53.

Collins, J.E., Wright, C.L., Edwards, C.A., Davis, M.P., Grinham, J.A., Cole, C.G., Goward, M.E., Aguado, B., Mallya, M., Mokrab, Y., et al. (2004). A genome annotation-driven approach to cloning the human ORFeome. Genome Biol. *5*, R84.

Cooper, A., García, M., Petrovas, C., Yamamoto, T., Koup, R.A., and Nabel, G.J. (2013). HIV-1 causes CD4 cell death through DNA-dependent protein kinase during viral integration. Nature *advance online publication*.

Cuchalová, L., Kouba, T., Herrmannová, A., Dányi, I., Chiu, W.-L., and Valásek, L. (2010). The RNA recognition motif of eukaryotic translation initiation factor 3g (eIF3g) is required for resumption of scanning of posttermination ribosomes for reinitiation on GCN4 and together with eIF3i stimulates linear scanning. Mol. Cell. Biol. *30*, 4671–4686.

Cullen, B.R. (2003a). Nuclear RNA export. J. Cell Sci. *116*, 587–597.

Cullen, B.R. (2003b). Nuclear mRNA export: insights from virology. Trends Biochem. Sci. *28*, 419–424.

Van Damme, N., Goff, D., Katsura, C., Jorgenson, R.L., Mitchell, R., Johnson, M.C., Stephens, E.B., and Guatelli, J. (2008). The interferon-induced protein BST-2 restricts HIV-1 release and is downregulated from the cell surface by the viral Vpu protein. Cell Host Microbe *3*, 245–252.

Dang, Y., Wang, X., Esselman, W.J., and Zheng, Y.-H. (2006). Identification of APOBEC3DE as another antiretroviral factor from the human APOBEC family. J. Virol. *80*, 10522–10533.

Dang, Y., Siew, L.M., Wang, X., Han, Y., Lampen, R., and Zheng, Y.-H. (2008). Human cytidine deaminase APOBEC3H restricts HIV-1 replication. J. Biol. Chem. *283*, 11606–11614.

Das, K., and Arnold, E. (2013). HIV-1 reverse transcriptase and antiviral drug resistance. Part 1. Curr. Opin. Virol.

Das, S., Ghosh, R., and Maitra, U. (2001). Eukaryotic translation initiation factor 5 functions as a GTPase-activating protein. J. Biol. Chem. *276*, 6720–6726.

Delaloye, J., Roger, T., Steiner-Tardivel, Q.-G., Le Roy, D., Knaup Reymond, M., Akira, S., Petrilli, V., Gomez, C.E., Perdiguero, B., Tschopp, J., et al. (2009). Innate immune sensing of modified vaccinia virus Ankara (MVA) is mediated by TLR2-TLR6, MDA-5 and the NALP3 inflammasome. PLoS Pathog. *5*, e1000480.

Descours, B., Cribier, A., Chable-Bessia, C., Ayinde, D., Rice, G., Crow, Y., Yatim, A., Schwartz, O., Laguette, N., and Benkirane, M. (2012). SAMHD1 restricts HIV-1 reverse transcription in quiescent CD4(+) T-cells. Retrovirology *9*, 87.

Dixit, E., and Kagan, J.C. (2013). Intracellular Pathogen Detection by RIG-I-Like Receptors. Adv. Immunol. *117*, 99–125.

Doehle, B.P., Schäfer, A., and Cullen, B.R. (2005). Human APOBEC3B is a potent inhibitor of HIV-1 infectivity and is resistant to HIV-1 Vif. Virology *339*, 281–288.

Dordor, A., Poudevigne, E., Göttlinger, H., and Weissenhorn, W. (2011). Essential and supporting host cell factors for HIV-1 budding. Future Microbiol. *6*, 1159–1170.

Dragin, L., Nguyen, L.A., Lahouassa, H., Sourisce, A., Kim, B., Ramirez, B.C., and Margottin-Goguet, F. (2013). Interferon block to HIV-1 transduction in macrophages despite SAMHD1 degradation and high deoxynucleoside triphosphates supply. Retrovirology *10*, 30.

Dubé, M., Roy, B.B., Guiot-Guillain, P., Binette, J., Mercier, J., Chiasson, A., and Cohen, E.A. (2010). Antagonism of tetherin restriction of HIV-1 release by Vpu involves binding and sequestration of the restriction factor in a perinuclear compartment. PLoS Pathog. *6*, e1000856.

Duncan, C.J.A., and Sattentau, Q.J. (2011). Viral determinants of HIV-1 macrophage tropism. Viruses *3*, 2255–2279.

Eisenächer, K., and Krug, A. (2012). Regulation of RLR-mediated innate immune signaling--it is all about keeping the balance. Eur. J. Cell Biol. *91*, 36–47.

Fang, J., Acheampong, E., Dave, R., Wang, F., Mukhtar, M., and Pomerantz, R.J. (2005). The RNA helicase DDX1 is involved in restricted HIV-1 Rev function in human astrocytes. Virology *336*, 299–307.

Fang, P., Spevak, C.C., Wu, C., and Sachs, M.S. (2004). A nascent polypeptide domain that can regulate translation elongation. Proc. Natl. Acad. Sci. U. S. A. *101*, 4059–4064.

Fassati, A., Görlich, D., Harrison, I., Zaytseva, L., and Mingot, J.-M. (2003). Nuclear import of HIV-1 intracellular reverse transcription complexes is mediated by importin 7. EMBO J. *22*, 3675–3685.

Fehrholz, M., Kendl, S., Prifert, C., Weissbrich, B., Lemon, K., Rennick, L., Duprex, P.W., Rima, B.K., Koning, F.A., Holmes, R.K., et al. (2012). The innate antiviral factor APOBEC3G targets replication of measles, mumps and respiratory syncytial viruses. J. Gen. Virol. *93*, 565–576.

Fernandes, J., Jayaraman, B., and Frankel, A. (2012). The HIV-1 Rev response element: an RNA scaffold that directs the cooperative assembly of a homo-oligomeric ribonucleoprotein complex. RNA Biol. *9*, 6–11.

Fitzpatrick, K., Skasko, M., Deerinck, T.J., Crum, J., Ellisman, M.H., and Guatelli, J. (2010). Direct restriction of virus release and incorporation of the interferon-induced protein BST-2 into HIV-1 particles. PLoS Pathog. *6*, e1000701.

Franca, R., Spadari, S., and Maga, G. (2006). APOBEC deaminases as cellular antiviral factors: a novel natural host defense mechanism. Med. Sci. Monit. Int. Med. J. Exp. Clin. Res. *12*, RA92–98.

Franchi, L., Warner, N., Viani, K., and Nuñez, G. (2009). Function of Nod-like receptors in microbial recognition and host defense. Immunol. Rev. *227*, 106–128.

Fritz, C.C., Zapp, M.L., and Green, M.R. (1995). A human nucleoporin-like protein that specifically interacts with HIV Rev. Nature *376*, 530–533.

Fullam, A., and Schröder, M. (2013). DExD/H-box RNA helicases as mediators of anti-viral innate immunity and essential host factors for viral replication. Biochim. Biophys. Acta *1829*, 854–865.

Galão, R.P., Le Tortorec, A., Pickering, S., Kueck, T., and Neil, S.J.D. (2012). Innate sensing of HIV-1 assembly by Tetherin induces NFκB-dependent proinflammatory responses. Cell Host Microbe *12*, 633–644.

Gallo, R.C., Salahuddin, S.Z., Popovic, M., Shearer, G.M., Kaplan, M., Haynes, B.F., Palker, T.J., Redfield, R., Oleske, J., and Safai, B. (1984). Frequent detection and isolation of cytopathic retroviruses (HTLV-III) from patients with AIDS and at risk for AIDS. Science *224*, 500–503.

Ganser-Pornillos, B.K., Chandrasekaran, V., Pornillos, O., Sodroski, J.G., Sundquist, W.I., and Yeager, M. (2011). Hexagonal assembly of a restricting TRIM5alpha protein. Proc. Natl. Acad. Sci. U. S. A. *108*, 534–539.

Gendron, K., Ferbeyre, G., Heveker, N., and Brakier-Gingras, L. (2011). The activity of the HIV-1 IRES is stimulated by oxidative stress and controlled by a negative regulatory element. Nucleic Acids Res. *39*, 902–912.

Geraghty, R.J., Talbot, K.J., Callahan, M., Harper, W., and Panganiban, A.T. (1994). Cell type-dependence for Vpu function. J. Med. Primatol. *23*, 146–150.

Geserick, P., Kaiser, F., Klemm, U., Kaufmann, S.H.E., and Zerrahn, J. (2004). Modulation of T cell development and activation by novel members of the Schlafen (slfn) gene family harbouring an RNA helicase-like motif. Int. Immunol. *16*, 1535–1548.

Gillick, K., Pollpeter, D., Phalora, P., Kim, E.-Y., Wolinsky, S.M., and Malim, M.H. (2013). Suppression of HIV-1 infection by APOBEC3 proteins in primary human CD4(+) T cells is associated with inhibition of processive reverse transcription as well as excessive cytidine deamination. J. Virol. *87*, 1508–1517.

Glazkova, D.V., Bogoslovskaia, E.V., Markelov, M.L., Shipulin, G.A., and Pokrovskiĭ, V.V. (2012). [Treatment of HIV-infection by means of gene therapy]. Vestn. Ross. Akad. Meditsinskikh Nauk Ross. Akad. Meditsinskikh Nauk 16–23.

Goila-Gaur, R., Khan, M.A., Miyagi, E., Kao, S., and Strebel, K. (2007). Targeting APOBEC3A to the viral nucleoprotein complex confers antiviral activity. Retrovirology *4*, 61.

Goldstone, D.C., Ennis-Adeniran, V., Hedden, J.J., Groom, H.C.T., Rice, G.I., Christodoulou, E., Walker, P.A., Kelly, G., Haire, L.F., Yap, M.W., et al. (2011). HIV-1 restriction factor SAMHD1 is a deoxynucleoside triphosphate triphosphohydrolase. Nature *480*, 379–382.

Goujon, C., Moncorgé, O., Bauby, H., Doyle, T., Ward, C.C., Schaller, T., Hué, S., Barclay, W.S., Schulz, R., and Malim, M.H. (2013). Human MX2 is an interferon-induced post-entry inhibitor of HIV-1 infection. Nature *502*, 559–562.

Greatorex, J., Gallego, J., Varani, G., and Lever, A. (2002). Structure and stability of wild-type and mutant RNA internal loops from the SL-1 domain of the HIV-1 packaging signal. J. Mol. Biol. *322*, 543–557.

Greijer, A.E., and van der Wall, E. (2004). The role of hypoxia inducible factor 1 (HIF-1) in hypoxia induced apoptosis. J. Clin. Pathol. *57*, 1009–1014.

Le Grice, S.F.J. (2012). Human immunodeficiency virus reverse transcriptase: 25 years of research, drug discovery, and promise. J. Biol. Chem. *287*, 40850–40857.

Griffiths, D.J. (2001). Endogenous retroviruses in the human genome sequence. Genome Biol. *2*, reviews1017.

Gringhuis, S.I., van der Vlist, M., van den Berg, L.M., den Dunnen, J., Litjens, M., and Geijtenbeek, T.B.H. (2010). HIV-1 exploits innate signaling by TLR8 and DC-SIGN for productive infection of dendritic cells. Nat. Immunol. *11*, 419–426.

Groom, H.C.T., Anderson, E.C., Dangerfield, J.A., and Lever, A.M.L. (2009). Rev regulates translation of human immunodeficiency virus type 1 RNAs. J. Gen. Virol. *90*, 1141–1147.

Groppo, R., and Richter, J.D. (2009). Translational control from head to tail. Curr. Opin. Cell Biol. *21*, 444–451.

Grütter, M.G., and Luban, J. (2012). TRIM5 structure, HIV-1 capsid recognition, and innate immune signaling. Curr. Opin. Virol. *2*, 142–150.

Guo, F., Cen, S., Niu, M., Saadatmand, J., and Kleiman, L. (2006). Inhibition of formula-primed reverse transcription by human APOBEC3G during human immunodeficiency virus type 1 replication. J. Virol. *80*, 11710–11722.

Gupta, R.K., Mlcochova, P., Pelchen-Matthews, A., Petit, S.J., Mattiuzzo, G., Pillay, D., Takeuchi, Y., Marsh, M., and Towers, G.J. (2009). Simian immunodeficiency virus envelope glycoprotein counteracts tetherin/BST-2/CD317 by intracellular sequestration. Proc. Natl. Acad. Sci. *106*, 20889–20894.

Guyader, M., Emerman, M., Sonigo, P., Clavel, F., Montagnier, L., and Alizon, M. (1987). Genome organization and transactivation of the human immunodeficiency virus type 2. Nature *326*, 662–669.

Guyader, M., Emerman, M., Montagnier, L., and Peden, K. (1989). VPX mutants of HIV-2 are infectious in established cell lines but display a severe defect in peripheral blood lymphocytes. EMBO J. *8*, 1169–1175.

Hallenberger, S., Bosch, V., Angliker, H., Shaw, E., Klenk, H.D., and Garten, W. (1992). Inhibition of furin-mediated cleavage activation of HIV-1 glycoprotein gp160. Nature *360*, 358–361.

Harari, A., Ooms, M., Mulder, L.C.F., and Simon, V. (2009). Polymorphisms and splice variants influence the antiretroviral activity of human APOBEC3H. J. Virol. *83*, 295–303.

Hardy, A.W., Graham, D.R., Shearer, G.M., and Herbeuval, J.-P. (2007). HIV turns plasmacytoid dendritic cells (pDC) into TRAIL-expressing killer pDC and down-regulates HIV coreceptors by Toll-like receptor 7-induced IFN-alpha. Proc. Natl. Acad. Sci. U. S. A. *104*, 17453–17458.

Harjes, E., Gross, P.J., Chen, K.-M., Lu, Y., Shindo, K., Nowarski, R., Gross, J.D., Kotler, M., Harris, R.S., and Matsuo, H. (2009). An extended structure of the APOBEC3G catalytic domain suggests a unique holoenzyme model. J. Mol. Biol. *389*, 819–832.

Harris, R.S., and Liddament, M.T. (2004). Retroviral restriction by APOBEC proteins. Nat. Rev. Immunol. *4*, 868–877.

Harris, R.S., Bishop, K.N., Sheehy, A.M., Craig, H.M., Petersen-Mahrt, S.K., Watt, I.N., Neuberger, M.S., and Malim, M.H. (2003). DNA deamination mediates innate immunity to retroviral infection. Cell *113*, 803–809.

Harris, R.S., Hultquist, J.F., and Evans, D.T. (2012). The restriction factors of human immunodeficiency virus. J. Biol. Chem. *287*, 40875–40883.

Hatziioannou, T., Perez-Caballero, D., Yang, A., Cowan, S., and Bieniasz, P.D. (2004). Retrovirus resistance factors Ref1 and Lv1 are species-specific variants of TRIM5α. Proc. Natl. Acad. Sci. U. S. A. *101*, 10774–10779.

Hauser, H., Lopez, L.A., Yang, S.J., Oldenburg, J.E., Exline, C.M., Guatelli, J.C., and Cannon, P.M. (2010). HIV-1 Vpu and HIV-2 Env counteract BST-2/tetherin by sequestration in a perinuclear compartment. Retrovirology *7*, 51.

Heil, F., Hemmi, H., Hochrein, H., Ampenberger, F., Kirschning, C., Akira, S., Lipford, G., Wagner, H., and Bauer, S. (2004). Species-specific recognition of single-stranded RNA via toll-like receptor 7 and 8. Science *303*, 1526–1529.

Henriet, S., Richer, D., Bernacchi, S., Decroly, E., Vigne, R., Ehresmann, B., Ehresmann, C., Paillart, J.-C., and Marquet, R. (2005). Cooperative and specific binding of Vif to the 5' region of HIV-1 genomic RNA. J. Mol. Biol. *354*, 55–72.

Henriet, S., Sinck, L., Bec, G., Gorelick, R.J., Marquet, R., and Paillart, J.-C. (2007). Vif is a RNA chaperone that could temporally regulate RNA dimerization and the early steps of HIV-1 reverse transcription. Nucleic Acids Res. *35*, 5141–5153.

Henriet, S., Mercenne, G., Bernacchi, S., Paillart, J.-C., and Marquet, R. (2009). Tumultuous Relationship between the Human Immunodeficiency Virus Type 1 Viral Infectivity Factor (Vif) and the Human APOBEC-3G and APOBEC-3F Restriction Factors. Microbiol. Mol. Biol. Rev. *73*, 211–232.

Hilbert, M., Kebbel, F., Gubaev, A., and Klostermeier, D. (2011). eIF4G stimulates the activity of the DEAD box protein eIF4A by a conformational guidance mechanism. Nucleic Acids Res. *39*, 2260–2270.

Hinnebusch, A.G., and Lorsch, J.R. (2012). The mechanism of eukaryotic translation initiation: new insights and challenges. Cold Spring Harb. Perspect. Biol. *4*.

Hinz, A., Miguet, N., Natrajan, G., Usami, Y., Yamanaka, H., Renesto, P., Hartlieb, B., McCarthy, A.A., Simorre, J.-P., Göttlinger, H., et al. (2010). Structural basis of HIV-1 tethering to membranes by the BST-2/tetherin ectodomain. Cell Host Microbe *7*, 314–323.

Hirsch, V.M., Olmsted, R.A., Murphey-Corb, M., Purcell, R.H., and Johnson, P.R. (1989). An African primate lentivirus (SIVsm) closely related to HIV-2. Nature *339*, 389–392.

Hoffmann, J.A. (2003). The immune response of Drosophila. Nature *426*, 33–38.

Hofmann, W., Reichart, B., Ewald, A., Müller, E., Schmitt, I., Stauber, R.H., Lottspeich, F., Jockusch, B.M., Scheer, U., Hauber, J., et al. (2001). Cofactor requirements for nuclear export of Rev response element (RRE)- and constitutive transport element (CTE)-containing retroviral RNAs. An unexpected role for actin. J. Cell Biol. *152*, 895–910.

Holcik, M., and Korneluk, R.G. (2000). Functional characterization of the X-linked inhibitor of apoptosis (XIAP) internal ribosome entry site element: role of La autoantigen in XIAP translation. Mol. Cell. Biol. *20*, 4648–4657.

Holden, L.G., Prochnow, C., Chang, Y.P., Bransteitter, R., Chelico, L., Sen, U., Stevens, R.C., Goodman, M.F., and Chen, X.S. (2008). Crystal structure of the anti-viral APOBEC3G catalytic domain and functional implications. Nature *456*, 121–124.

Holloway, A.F., Occhiodoro, F., Mittler, G., Meisterernst, M., and Shannon, M.F. (2000). Functional interaction between the HIV transactivator Tat and the transcriptional coactivator PC4 in T cells. J. Biol. Chem. *275*, 21668–21677.

Holmes, R.K., Koning, F.A., Bishop, K.N., and Malim, M.H. (2007). APOBEC3F can inhibit the accumulation of HIV-1 reverse transcription products in the absence of hypermutation. Comparisons with APOBEC3G. J. Biol. Chem. *282*, 2587–2595.

Holtz, C.M., Sadler, H.A., and Mansky, L.M. (2013). APOBEC3G cytosine deamination hotspots are defined by both sequence context and single-stranded DNA secondary structure. Nucleic Acids Res.

Hornung, V., Ellegast, J., Kim, S., Brzózka, K., Jung, A., Kato, H., Poeck, H., Akira, S., Conzelmann, K.-K., Schlee, M., et al. (2006). 5’-Triphosphate RNA Is the Ligand for RIG-I. Science *314*, 994–997.

Horos, R., Ijspeert, H., Pospisilova, D., Sendtner, R., Andrieu-Soler, C., Taskesen, E., Nieradka, A., Cmejla, R., Sendtner, M., Touw, I.P., et al. (2012). Ribosomal deficiencies in Diamond-Blackfan anemia impair translation of transcripts essential for differentiation of murine and human erythroblasts. Blood *119*, 262–272.

Hoxie, J.A., and June, C.H. (2012). Novel cell and gene therapies for HIV. Cold Spring Harb. Perspect. Med. *2*.

Hrecka, K., Hao, C., Gierszewska, M., Swanson, S.K., Kesik-Brodacka, M., Srivastava, S., Florens, L., Washburn, M.P., and Skowronski, J. (2011). Vpx relieves inhibition of HIV-1 infection of macrophages mediated by the SAMHD1 protein. Nature *474*, 658–661.

Huang, W., Zuo, T., Luo, X., Jin, H., Liu, Z., Yang, Z., Yu, X., Zhang, L., and Zhang, L. (2013). Indolizine derivatives as HIV-1 VIF-ElonginC interaction inhibitors. Chem. Biol. Drug Des. *81*, 730–741.

Huet, T., Cheynier, R., Meyerhans, A., Roelants, G., and Wain-Hobson, S. (1990). Genetic organization of a chimpanzee lentivirus related to HIV-1. Nature *345*, 356–359.

Hultquist, J.F., and Harris, R.S. (2013). APOBEC3B restricts HIV-1 in a cell type dependent manner. Meet. Retroviruses - Cold Spring Harb. Lab. 2013.

Ilina, T., Labarge, K., Sarafianos, S.G., Ishima, R., and Parniak, M.A. (2012). Inhibitors of HIV-1 Reverse Transcriptase-Associated Ribonuclease H Activity. Biology *1*, 521–541.

Ingolia, N.T., Ghaemmaghami, S., Newman, J.R.S., and Weissman, J.S. (2009). Genome-wide analysis in vivo of translation with nucleotide resolution using ribosome profiling. Science *324*, 218–223.

Isogai, T., and Yamamoto, J. (2008). NEDO functional analysis of protein and research application project.

Ivanov, I.P., Loughran, G., Sachs, M.S., and Atkins, J.F. (2010). Initiation context modulates autoregulation of eukaryotic translation initiation factor 1 (eIF1). Proc. Natl. Acad. Sci. U. S. A. *107*, 18056–18060.

Iwasaki, A. (2012). Innate immune recognition of HIV-1. Immunity *37*, 389–398.

Izaurralde, E., Lewis, J., McGuigan, C., Jankowska, M., Darzynkiewicz, E., and Mattaj, I.W. (1994). A nuclear cap binding protein complex involved in pre-mRNA splicing. Cell *78*, 657–668.

Jackson, R.J., Hellen, C.U.T., and Pestova, T.V. (2010). The mechanism of eukaryotic translation initiation and principles of its regulation. Nat. Rev. Mol. Cell Biol. *11*, 113–127.

Jackson, R.J., Hellen, C.U.T., and Pestova, T.V. (2012). Termination and post-termination events in eukaryotic translation. Adv. Protein Chem. Struct. Biol. *86*, 45–93.

Jacobs, S.R., and Damania, B. (2012). NLRs, inflammasomes, and viral infection. J. Leukoc. Biol. *92*, 469–477.

Jäger, S., Cimermancic, P., Gulbahce, N., Johnson, J.R., McGovern, K.E., Clarke, S.C., Shales, M., Mercenne, G., Pache, L., Li, K., et al. (2012). Global landscape of HIV-human protein complexes. Nature *481*, 365–370.

Janvier, K., Pelchen-Matthews, A., Renaud, J.-B., Caillet, M., Marsh, M., and Berlioz-Torrent, C. (2011). The ESCRT-0 component HRS is required for HIV-1 Vpu-mediated BST-2/tetherin down-regulation. PLoS Pathog. *7*, e1001265.

Jern, P., Russell, R.A., Pathak, V.K., and Coffin, J.M. (2009). Likely role of APOBEC3G-mediated G-to-A mutations in HIV-1 evolution and drug resistance. PLoS Pathog. *5*, e1000367.

Jolicoeur, P., and Rassart, E. (1980). Effect of Fv-1 gene product on synthesis of linear and supercoiled viral DNA in cells infected with murine leukemia virus. J. Virol. *33*, 183–195.

Jolly, C. (2011). Cell-to-cell transmission of retroviruses: Innate immunity and interferon-induced restriction factors. Virology *411*, 251–259.

Jouvenet, N., Neil, S.J.D., Zhadina, M., Zang, T., Kratovac, Z., Lee, Y., McNatt, M., Hatziioannou, T., and Bieniasz, P.D. (2009). Broad-spectrum inhibition of retroviral and filoviral particle release by tetherin. J. Virol. *83*, 1837–1844.

Kajaste-Rudnitski, A., Marelli, S.S., Pultrone, C., Pertel, T., Uchil, P.D., Mechti, N., Mothes, W., Poli, G., Luban, J., and Vicenzi, E. (2011). TRIM22 inhibits HIV-1 transcription independently of its E3 ubiquitin ligase activity, Tat, and NF-kappaB-responsive long terminal repeat elements. J. Virol. *85*, 5183–5196.

Kalpana, G.V., Marmon, S., Wang, W., Crabtree, G.R., and Goff, S.P. (1994). Binding and stimulation of HIV-1 integrase by a human homolog of yeast transcription factor SNF5. Science *266*, 2002–2006.

Kane, M., Yadav, S.S., Bitzegeio, J., Kutluay, S.B., Zang, T., Wilson, S.J., Schoggins, J.W., Rice, C.M., Yamashita, M., Hatziioannou, T., et al. (2013). MX2 is an interferon-induced inhibitor of HIV-1 infection. Nature *502*, 563–566.

Kanneganti, T.-D. (2010). Central roles of NLRs and inflammasomes in viral infection. Nat. Rev. Immunol. *10*, 688–698.

Kao, S., Khan, M.A., Miyagi, E., Plishka, R., Buckler-White, A., and Strebel, K. (2003). The human immunodeficiency virus type 1 Vif protein reduces intracellular expression and inhibits packaging of APOBEC3G (CEM15), a cellular inhibitor of virus infectivity. J. Virol. *77*, 11398–11407.

Kapp, L.D., and Lorsch, J.R. (2004). The molecular mechanics of eukaryotic translation. Annu. Rev. Biochem. *73*, 657–704.

Kato, H., Takeuchi, O., and Akira, S. (2006). [Cell type specific involvement of RIG-I in antiviral responses]. Nihon Rinsho Jpn. J. Clin. Med. *64*, 1244–1247.

Katsoulidis, E., Mavrommatis, E., Woodard, J., Shields, M.A., Sassano, A., Carayol, N., Sawicki, K.T., Munshi, H.G., and Platanias, L.C. (2010). Role of interferon {alpha} (IFN{alpha})-inducible Schlafen-5 in regulation of anchorage-independent growth and invasion of malignant melanoma cells. J. Biol. Chem. *285*, 40333–40341.

Kaushik, R., Zhu, X., Stranska, R., Wu, Y., and Stevenson, M. (2009). A cellular restriction dictates the permissivity of nondividing monocytes/macrophages to lentivirus and gammaretrovirus infection. Cell Host Microbe *6*, 68–80.

Kawai, T., Takahashi, K., Sato, S., Coban, C., Kumar, H., Kato, H., Ishii, K.J., Takeuchi, O., and Akira, S. (2005). IPS-1, an adaptor triggering RIG-I- and Mda5-mediated type I interferon induction. Nat. Immunol. *6*, 981–988.

Khamsri, B., Murao, F., Yoshida, A., Sakurai, A., Uchiyama, T., Shirai, H., Matsuo, Y., Fujita, M., and Adachi, A. (2006). Comparative study on the structure and cytopathogenic activity of HIV Vpr/Vpx proteins. Microbes Infect. *8*, 10–15.

Khan, R., and Giedroc, D.P. (1992). Recombinant human immunodeficiency virus type 1 nucleocapsid (NCp7) protein unwinds tRNA. J. Biol. Chem. *267*, 6689–6695.

Khan, M.A., Kao, S., Miyagi, E., Takeuchi, H., Goila-Gaur, R., Opi, S., Gipson, C.L., Parslow, T.G., Ly, H., and Strebel, K. (2005). Viral RNA is required for the association of APOBEC3G with human immunodeficiency virus type 1 nucleoprotein complexes. J. Virol. *79*, 5870–5874.

King, M.C., Raposo, G., and Lemmon, M.A. (2004). Inhibition of nuclear import and cell-cycle progression by mutated forms of the dynamin-like GTPase MxB. Proc. Natl. Acad. Sci. U. S. A. *101*, 8957–8962.

Kitamura, S., Ode, H., Nakashima, M., Imahashi, M., Naganawa, Y., Kurosawa, T., Yokomaku, Y., Yamane, T., Watanabe, N., Suzuki, A., et al. (2012). The APOBEC3C crystal structure and the interface for HIV-1 Vif binding. Nat. Struct. Mol. Biol. *19*, 1005–1010.

Kozak, M. (1984). Point mutations close to the AUG initiator codon affect the efficiency of translation of rat preproinsulin in vivo. Nature *308*, 241–246.

Kozak, M. (1986). Point mutations define a sequence flanking the AUG initiator codon that modulates translation by eukaryotic ribosomes. Cell *44*, 283–292.

Kozak, M. (1990). Downstream secondary structure facilitates recognition of initiator codons by eukaryotic ribosomes. Proc. Natl. Acad. Sci. U. S. A. *87*, 8301–8305.

Kozak, M. (2005). Regulation of translation via mRNA structure in prokaryotes and eukaryotes. Gene *361*, 13–37.

Kozak, C.A., and Chakraborti, A. (1996). Single amino acid changes in the murine leukemia virus capsid protein gene define the target of Fv1 resistance. Virology *225*, 300–305.

Krishnan, L., and Engelman, A. (2012). Retroviral integrase proteins and HIV-1 DNA integration. J. Biol. Chem. *287*, 40858–40866.

Kronja, I., and Orr-Weaver, T.L. (2011). Translational regulation of the cell cycle: when, where, how and why? Philos. Trans. R. Soc. Lond. B. Biol. Sci. *366*, 3638–3652.

Kuhl, B.D., Cheng, V., Wainberg, M.A., and Liang, C. (2011). Tetherin and its viral antagonists. J. Neuroimmune Pharmacol. Off. J. Soc. NeuroImmune Pharmacol. *6*, 188–201.

Kula, A., Guerra, J., Knezevich, A., Kleva, D., Myers, M.P., and Marcello, A. (2011). Characterization of the HIV-1 RNA associated proteome identifies Matrin 3 as a nuclear cofactor of Rev function. Retrovirology *8*, 60.

Kula, A., Gharu, L., and Marcello, A. (2013). HIV-1 pre-mRNA commitment to Rev mediated export through PSF and Matrin 3. Virology *435*, 329–340.

Labban, M., and Sossin, W.S. (2011). Translation of 5’ terminal oligopyrimidine tract (5’TOP) mRNAs in Aplysia Californica is regulated by the target of rapamycin (TOR). Biochem. Biophys. Res. Commun. *404*, 816–821.

Laguette, N., Sobhian, B., Casartelli, N., Ringeard, M., Chable-Bessia, C., Ségéral, E., Yatim, A., Emiliani, S., Schwartz, O., and Benkirane, M. (2011). SAMHD1 is the dendritic- and myeloid-cell-specific HIV-1 restriction factor counteracted by Vpx. Nature *474*, 654–657.

Landry, D.M., Hertz, M.I., and Thompson, S.R. (2009). RPS25 is essential for translation initiation by the Dicistroviridae and hepatitis C viral IRESs. Genes Dev. *23*, 2753–2764.

Lange, J.M.A., and van Leeuwen, R. (2002). Antiretroviral therapy and resistance to antiretroviral drugs. Ethiop. Med. J. *40 Suppl 1*, 51–75.

Langlois, M.-A., and Neuberger, M.S. (2008). Human APOBEC3G can restrict retroviral infection in avian cells and acts independently of both UNG and SMUG1. J. Virol. *82*, 4660–4664.

LaRue, R.S., Jónsson, S.R., Silverstein, K.A., Lajoie, M., Bertrand, D., El-Mabrouk, N., Hötzel, I., Andrésdóttir, V., Smith, T.P., and Harris, R.S. (2008). The artiodactyl APOBEC3 innate immune repertoire shows evidence for a multi-functional domain organization that existed in the ancestor of placental mammals. BMC Mol. Biol. *9*, 104.

LaRue, R.S., Andrésdóttir, V., Blanchard, Y., Conticello, S.G., Derse, D., Emerman, M., Greene, W.C., Jónsson, S.R., Landau, N.R., Löchelt, M., et al. (2009). Guidelines for naming nonprimate APOBEC3 genes and proteins. J. Virol. *83*, 494–497.

Law, G.L., Raney, A., Heusner, C., and Morris, D.R. (2001). Polyamine regulation of ribosome pausing at the upstream open reading frame of S-adenosylmethionine decarboxylase. J. Biol. Chem. *276*, 38036–38043.

Leblanc, J., Weil, J., and Beemon, K. (2013). Posttranscriptional regulation of retroviral gene expression: primary RNA transcripts play three roles as pre-mRNA, mRNA, and genomic RNA. Wiley Interdiscip. Rev. RNA.

LeFebvre, A.K., Korneeva, N.L., Trutschl, M., Cvek, U., Duzan, R.D., Bradley, C.A., Hershey, J.W.B., and Rhoads, R.E. (2006). Translation initiation factor eIF4G-1 binds to eIF3 through the eIF3e subunit. J. Biol. Chem. *281*, 22917–22932.

Lemaire, P.A., Anderson, E., Lary, J., and Cole, J.L. (2008). Mechanism of PKR Activation by dsRNA. J. Mol. Biol. *381*, 351–360.

Lemaitre, B., Nicolas, E., Michaut, L., Reichhart, J.M., and Hoffmann, J.A. (1996). The dorsoventral regulatory gene cassette spätzle/Toll/cactus controls the potent antifungal response in Drosophila adults. Cell *86*, 973–983.

Li, D., Wei, T., Abbott, C.M., and Harrich, D. (2013). The unexpected roles of eukaryotic translation elongation factors in RNA virus replication and pathogenesis. Microbiol. Mol. Biol. Rev. MMBR *77*, 253–266.

Li, J., Liu, Y., Kim, B.O., and He, J.J. (2002). Direct participation of Sam68, the 68-kilodalton Src-associated protein in mitosis, in the CRM1-mediated Rev nuclear export pathway. J. Virol. *76*, 8374–8382.

Li, J., Potash, M.J., and Volsky, D.J. (2004). Functional domains of APOBEC3G required for antiviral activity. J. Cell. Biochem. *92*, 560–572.

Li, L., Yoder, K., Hansen, M.S., Olvera, J., Miller, M.D., and Bushman, F.D. (2000a). Retroviral cDNA integration: stimulation by HMG I family proteins. J. Virol. *74*, 10965–10974.

Li, M., Kao, E., Gao, X., Sandig, H., Limmer, K., Pavon-Eternod, M., Jones, T.E., Landry, S., Pan, T., Weitzman, M.D., et al. (2012a). Codon-usage-based inhibition of HIV protein synthesis by human schlafen 11. Nature *491*, 125–128.

Li, N., Zhang, W., and Cao, X. (2000b). Identification of human homologue of mouse IFN-gamma induced protein from human dendritic cells. Immunol. Lett. *74*, 221–224.

Li, S., Wang, L., Berman, M., Kong, Y.-Y., and Dorf, M.E. (2011). Mapping a dynamic innate immunity protein interaction network regulating type I interferon production. Immunity *35*, 426–440.

Li, X.-Y., Guo, F., Zhang, L., Kleiman, L., and Cen, S. (2007). APOBEC3G inhibits DNA strand transfer during HIV-1 reverse transcription. J. Biol. Chem. *282*, 32065–32074.

Li, Z., Wu, S., Wang, J., Li, W., Lin, Y., Ji, C., Xue, J., and Chen, J. (2012b). Evaluation of the interactions of HIV-1 integrase with small ubiquitin-like modifiers and their conjugation enzyme Ubc9. Int. J. Mol. Med. *30*, 1053–1060.

Liddament, M.T., Brown, W.L., Schumacher, A.J., and Harris, R.S. (2004). APOBEC3F properties and hypermutation preferences indicate activity against HIV-1 in vivo. Curr. Biol. CB *14*, 1385–1391.

Lilly, F. (1967). Susceptibility to two strains of Friend leukemia virus in mice. Science *155*, 461–462.

Lim, E.S., Fregoso, O.I., McCoy, C.O., Matsen, F.A., Malik, H.S., and Emerman, M. (2012). The ability of primate lentiviruses to degrade the monocyte restriction factor SAMHD1 preceded the birth of the viral accessory protein Vpx. Cell Host Microbe *11*, 194–204.

Lincoln, A.J., Monczak, Y., Williams, S.C., and Johnson, P.F. (1998). Inhibition of CCAAT/enhancer-binding protein alpha and beta translation by upstream open reading frames. J. Biol. Chem. *273*, 9552–9560.

Liu, J., Henao-Mejia, J., Liu, H., Zhao, Y., and He, J.J. (2011). Translational Regulation of HIV-1 Replication by HIV-1 Rev Cellular Cofactors Sam68, eIF5A, hRIP, and DDX3. J. Neuroimmune Pharmacol. *6*, 308–321.

Liu, Z., Pan, Q., Ding, S., Qian, J., Xu, F., Zhou, J., Cen, S., Guo, F., and Liang, C. (2013). The Interferon-Inducible MxB Protein Inhibits HIV-1 Infection. Cell Host Microbe *14*, 398–410.

Llano, M., Saenz, D.T., Meehan, A., Wongthida, P., Peretz, M., Walker, W.H., Teo, W., and Poeschla, E.M. (2006). An essential role for LEDGF/p75 in HIV integration. Science *314*, 461–464.

Locker, N., Chamond, N., and Sargueil, B. (2011). A conserved structure within the HIV gag open reading frame that controls translation initiation directly recruits the 40S subunit and eIF3. Nucleic Acids Res. *39*, 2367–2377.

Lorgeoux, R.-P., Guo, F., and Liang, C. (2012). From promoting to inhibiting: diverse roles of helicases in HIV-1 Replication. Retrovirology *9*, 79.

Luban, J. (2012). TRIM5 and the Regulation of HIV-1 Infectivity. Mol. Biol. Int. *2012*, 426840.

Lukic, Z., and Campbell, E.M. (2012). The cell biology of TRIM5α. Curr. HIV/AIDS Rep. *9*, 73–80.

Lukic, Z., Hausmann, S., Sebastian, S., Rucci, J., Sastri, J., Robia, S.L., Luban, J., and Campbell, E.M. (2011). TRIM5α associates with proteasomal subunits in cells while in complex with HIV-1 virions. Retrovirology *8*, 93.

Luo, K., Wang, T., Liu, B., Tian, C., Xiao, Z., Kappes, J., and Yu, X.-F. (2007). Cytidine deaminases APOBEC3G and APOBEC3F interact with human immunodeficiency virus type 1 integrase and inhibit proviral DNA formation. J. Virol. *81*, 7238–7248.

Maag, D., Fekete, C.A., Gryczynski, Z., and Lorsch, J.R. (2005). A conformational change in the eukaryotic translation preinitiation complex and release of eIF1 signal recognition of the start codon. Mol. Cell *17*, 265–275.

MacMillan, A.L., Kohli, R.M., and Ross, S.R. (2013). APOBEC3 inhibition of mouse mammary tumor virus infection: the role of cytidine deamination versus inhibition of reverse transcription. J. Virol. *87*, 4808–4817.

Madani, N., and Kabat, D. (1998). An endogenous inhibitor of human immunodeficiency virus in human lymphocytes is overcome by the viral Vif protein. J. Virol. *72*, 10251–10255.

Majumdar, R., Bandyopadhyay, A., and Maitra, U. (2003). Mammalian translation initiation factor eIF1 functions with eIF1A and eIF3 in the formation of a stable 40 S preinitiation complex. J. Biol. Chem. *278*, 6580–6587.

Mangeat, B., Turelli, P., Caron, G., Friedli, M., Perrin, L., and Trono, D. (2003). Broad antiretroviral defence by human APOBEC3G through lethal editing of nascent reverse transcripts. Nature *424*, 99–103.

Maquat, L.E., Tarn, W.-Y., and Isken, O. (2010). The pioneer round of translation: features and functions. Cell *142*, 368–374.

De Marco, A., Heuser, A.-M., Glass, B., Kräusslich, H.-G., Müller, B., and Briggs, J.A.G. (2012). Role of the SP2 domain and its proteolytic cleavage in HIV-1 structural maturation and infectivity. J. Virol. *86*, 13708–13716.

Mariani, R., Chen, D., Schröfelbauer, B., Navarro, F., König, R., Bollman, B., Münk, C., Nymark-McMahon, H., and Landau, N.R. (2003). Species-specific exclusion of APOBEC3G from HIV-1 virions by Vif. Cell *114*, 21–31.

Markou, T., Marshall, A.K., Cullingford, T.E., Tham, E.L., Sugden, P.H., and Clerk, A. (2010). Regulation of the cardiomyocyte transcriptome vs translatome by endothelin-1 and insulin: translational regulation of 5' terminal oligopyrimidine tract (TOP) mRNAs by insulin. BMC Genomics *11*, 343.

Martin-Marcos, P., Cheung, Y.-N., and Hinnebusch, A.G. (2011). Functional elements in initiation factors 1, 1A, and 2β discriminate against poor AUG context and non-AUG start codons. Mol. Cell. Biol. *31*, 4814–4831.

Martin-Serrano, J., and Neil, S.J.D. (2011). Host factors involved in retroviral budding and release. Nat. Rev. Microbiol. *9*, 519–531.

Mavrommatis, E., Fish, E.N., and Platanias, L.C. (2013). The schlafen family of proteins and their regulation by interferons. J. Interferon Cytokine Res. Off. J. Int. Soc. Interferon Cytokine Res. *33*, 206–210.

Mbisa, J.L., Barr, R., Thomas, J.A., Vandegraaff, N., Dorweiler, I.J., Svarovskaia, E.S., Brown, W.L., Mansky, L.M., Gorelick, R.J., Harris, R.S., et al. (2007). Human immunodeficiency virus type 1 cDNAs produced in the presence of APOBEC3G exhibit defects in plus-strand DNA transfer and integration. J. Virol. *81*, 7099–7110.

Mbisa, J.L., Bu, W., and Pathak, V.K. (2010). APOBEC3F and APOBEC3G inhibit HIV-1 DNA integration by different mechanisms. J. Virol. *84*, 5250–5259.

McCoy, L.E., and Weiss, R.A. (2013). Neutralizing antibodies to HIV-1 induced by immunization. J. Exp. Med. *210*, 209–223.

McMillan, N.A., Chun, R.F., Siderovski, D.P., Galabru, J., Toone, W.M., Samuel, C.E., Mak, T.W., Hovanessian, A.G., Jeang, K.T., and Williams, B.R. (1995). HIV-1 Tat directly interacts with the interferon-induced, double-stranded RNA-dependent kinase, PKR. Virology *213*, 413–424.

Medzhitov, R., Schneider, D.S., and Soares, M.P. (2012). Disease Tolerance as a Defense Strategy. Science *335*, 936–941.

Melén, K., Keskinen, P., Ronni, T., Sareneva, T., Lounatmaa, K., and Julkunen, I. (1996). Human MxB protein, an interferon-alpha-inducible GTPase, contains a nuclear targeting signal and is localized in the heterochromatin region beneath the nuclear envelope. J. Biol. Chem. *271*, 23478–23486.

Mercenne, G., Bernacchi, S., Richer, D., Bec, G., Henriet, S., Paillart, J.-C., and Marquet, R. (2010). HIV-1 Vif binds to APOBEC3G mRNA and inhibits its translation. Nucleic Acids Res. *38*, 633–646.

Merrick, W.C. (2010). Eukaryotic Protein Synthesis: Still a Mystery. J. Biol. Chem. *285*, 21197–21201.

Merson, M.H., O'Malley, J., Serwadda, D., and Apisuk, C. (2008). The history and challenge of HIV prevention. The Lancet *372*, 475–488.

Meyuhas, O. (2000). Synthesis of the translational apparatus is regulated at the translational level. Eur. J. Biochem. FEBS *267*, 6321–6330.

Miller, M.D., Farnet, C.M., and Bushman, F.D. (1997). Human immunodeficiency virus type 1 preintegration complexes: studies of organization and composition. J. Virol. *71*, 5382–5390.

Miyagi, E., Opi, S., Takeuchi, H., Khan, M., Goila-Gaur, R., Kao, S., and Strebel, K. (2007). Enzymatically active APOBEC3G is required for efficient inhibition of human immunodeficiency virus type 1. J. Virol. *81*, 13346–13353.

Monette, A., Ajamian, L., López-Lastra, M., and Mouland, A.J. (2009). Human immunodeficiency virus type 1 (HIV-1) induces the cytoplasmic retention of heterogeneous nuclear ribonucleoprotein A1 by disrupting nuclear import: implications for HIV-1 gene expression. J. Biol. Chem. *284*, 31350–31362.

Monie, T.P. (2013). NLR activation takes a direct route. Trends Biochem. Sci. *38*, 131–139.

Moore, M.J., and Proudfoot, N.J. (2009). Pre-mRNA processing reaches back to transcription and ahead to translation. Cell *136*, 688–700.

Muckenfuss, H., Kaiser, J.K., Krebil, E., Battenberg, M., Schwer, C., Cichutek, K., Münk, C., and Flory, E. (2007). Sp1 and Sp3 regulate basal transcription of the human APOBEC3G gene. Nucleic Acids Res. *35*, 3784–3796.

Müller-McNicoll, M., and Neugebauer, K.M. (2013). How cells get the message: dynamic assembly and function of mRNA-protein complexes. Nat. Rev. Genet. *14*, 275–287.

Munzarová, V., Pánek, J., Gunišová, S., Dányi, I., Szamecz, B., and Valášek, L.S. (2011). Translation reinitiation relies on the interaction between eIF3a/TIF32 and progressively folded cis-acting mRNA elements preceding short uORFs. PLoS Genet. *7*, e1002137.

Nanda, J.S., Cheung, Y.-N., Takacs, J.E., Martin-Marcos, P., Saini, A.K., Hinnebusch, A.G., and Lorsch, J.R. (2009). eIF1 controls multiple steps in start codon recognition during eukaryotic translation initiation. J. Mol. Biol. *394*, 268–285.

Nathans, R., Cao, H., Sharova, N., Ali, A., Sharkey, M., Stranska, R., Stevenson, M., and Rana, T.M. (2008). Small-molecule inhibition of HIV-1 Vif. Nat. Biotechnol. *26*, 1187–1192.

Naveau, M., Lazennec-Schurdevin, C., Panvert, M., Mechulam, Y., and Schmitt, E. (2010). tRNA binding properties of eukaryotic translation initiation factor 2 from Encephalitozoon cuniculi. Biochemistry (Mosc.) *49*, 8680–8688.

Navratilova, Z. (2006). Polymorphisms in CCL2&CCL5 chemokines/chemokine receptors genes and their association with diseases. Biomed. Pap. Med. Fac. Univ. Palacký Olomouc Czechoslov. *150*, 191–204.

Neil, S.J.D., Zang, T., and Bieniasz, P.D. (2008). Tetherin inhibits retrovirus release and is antagonized by HIV-1 Vpu. Nature *451*, 425–430.

Neumann, B., Zhao, L., Murphy, K., and Gonda, T.J. (2008). Subcellular localization of the Schlafen protein family. Biochem. Biophys. Res. Commun. *370*, 62–66.

Newman, E.N.C., Holmes, R.K., Craig, H.M., Klein, K.C., Lingappa, J.R., Malim, M.H., and Sheehy, A.M. (2005). Antiviral function of APOBEC3G can be dissociated from cytidine deaminase activity. Curr. Biol. CB *15*, 166–170.

Nishitsuji, H., Hayashi, T., Takahashi, T., Miyano, M., Kannagi, M., and Masuda, T. (2009). Augmentation of reverse transcription by integrase through an interaction with host factor, SIP1/Gemin2 Is critical for HIV-1 infection. PloS One *4*, e7825.

O'Connor, C., Pertel, T., Gray, S., Robia, S.L., Bakowska, J.C., Luban, J., and Campbell, E.M. (2010). p62/Sequestosome-1 Associates with and Sustains the Expression of Retroviral Restriction Factor TRIM5? J. Virol. *84*, 5997–6006.

Ocwieja, K.E. (2012). Patterns of HIV Integration and Splicing: Windows on Mechanism (University of Pennsylvania).

OhAinle, M., Kerns, J.A., Malik, H.S., and Emerman, M. (2006). Adaptive evolution and antiviral activity of the conserved mammalian cytidine deaminase APOBEC3H. J. Virol. *80*, 3853–3862.

Ohlmann, T., Prévôt, D., Décimo, D., Roux, F., Garin, J., Morley, S.J., and Darlix, J.-L. (2002). In vitro cleavage of eIF4GI but not eIF4GII by HIV-1 protease and its effects on translation in the rabbit reticulocyte lysate system. J. Mol. Biol. *318*, 9–20.

Ooms, M., Letko, M., Binka, M., and Simon, V. (2013). The Resistance of Human APOBEC3H to HIV-1 NL4-3 Molecular Clone Is Determined by a Single Amino Acid in Vif. Plos One *8*.

Oshiumi, H., Sakai, K., Matsumoto, M., and Seya, T. (2010). DEAD/H BOX 3 (DDX3) helicase binds the RIG-I adaptor IPS-1 to up-regulate IFN-beta-inducing potential. Eur. J. Immunol. *40*, 940–948.

Ott, D.E. (2008). Cellular proteins detected in HIV-1. Rev. Med. Virol. *18*, 159–175.

Ott, D.E., Coren, L.V., Johnson, D.G., Kane, B.P., Sowder, R.C., 2nd, Kim, Y.D., Fisher, R.J., Zhou, X.Z., Lu, K.P., and Henderson, L.E. (2000). Actin-binding cellular proteins inside human immunodeficiency virus type 1. Virology *266*, 42–51.

Özeş, A.R., Feoktistova, K., Avanzino, B.C., and Fraser, C.S. (2011). Duplex unwinding and ATPase activities of the DEAD-box helicase eIF4A are coupled by eIF4G and eIF4B. J. Mol. Biol. *412*, 674–687.

Paillart, J.-C., Shehu-Xhilaga, M., Marquet, R., and Mak, J. (2004). Dimerization of retroviral RNA genomes: an inseparable pair. Nat. Rev. Microbiol. *2*, 461–472.

Pan, X.-B., Qu, X.-W., Jiang, D., Zhao, X.-L., Han, J.-C., and Wei, L. (2013). BST2/Tetherin inhibits hepatitis C virus production in human hepatoma cells. Antiviral Res. *98*, 54–60.

Panté, N., and Kann, M. (2002). Nuclear pore complex is able to transport macromolecules with diameters of about 39 nm. Mol. Biol. Cell *13*, 425–434.

Passmore, L.A., Schmeing, T.M., Maag, D., Applefield, D.J., Acker, M.G., Algire, M.A., Lorsch, J.R., and Ramakrishnan, V. (2007). The Eukaryotic Translation Initiation Factors eIF1 and eIF1A Induce an Open Conformation of the 40S Ribosome. Mol. Cell *26*, 41–50.

Paxton, W., Connor, R.I., and Landau, N.R. (1993). Incorporation of Vpr into human immunodeficiency virus type 1 virions: requirement for the p6 region of gag and mutational analysis. J. Virol. *67*, 7229–7237.

Pelechano, V., Wei, W., and Steinmetz, L.M. (2013). Extensive transcriptional heterogeneity revealed by isoform profiling. Nature *497*, 127–131.

Perez-Caballero, D., Hatziioannou, T., Zhang, F., Cowan, S., and Bieniasz, P.D. (2005). Restriction of human immunodeficiency virus type 1 by TRIM-CypA occurs with rapid kinetics and independently of cytoplasmic bodies, ubiquitin, and proteasome activity. J. Virol. *79*, 15567–15572.

Pertel, T., Hausmann, S., Morger, D., Züger, S., Guerra, J., Lascano, J., Reinhard, C., Santoni, F.A., Uchil, P.D., Chatel, L., et al. (2011). TRIM5 is an innate immune sensor for the retrovirus capsid lattice. Nature *472*, 361–365.

Pestova, T.V., and Kolupaeva, V.G. (2002). The roles of individual eukaryotic translation initiation factors in ribosomal scanning and initiation codon selection. Genes Dev. *16*, 2906–2922.

Pestova, T.V., Lomakin, I.B., Lee, J.H., Choi, S.K., Dever, T.E., and Hellen, C.U. (2000). The joining of ribosomal subunits in eukaryotes requires eIF5B. Nature *403*, 332–335.

Philpott, D.J., and Girardin, S.E. (2010). Nod-like receptors: sentinels at host membranes. Curr. Opin. Immunol. *22*, 428–434.

Pichlmair, A., Schulz, O., Tan, C.P., Näslund, T.I., Liljeström, P., Weber, F., and Reis e Sousa, C. (2006). RIG-I-mediated antiviral responses to single-stranded RNA bearing 5'-phosphates. Science *314*, 997–1001.

Pisarev, A.V., Kolupaeva, V.G., Pisareva, V.P., Merrick, W.C., Hellen, C.U.T., and Pestova, T.V. (2006). Specific functional interactions of nucleotides at key -3 and +4 positions flanking the initiation codon with components of the mammalian 48S translation initiation complex. Genes Dev. *20*, 624–636.

Pisarev, A.V., Hellen, C.U.T., and Pestova, T.V. (2007). Recycling of eukaryotic posttermination ribosomal complexes. Cell *131*, 286–299.

Pisarev, A.V., Skabkin, M.A., Pisareva, V.P., Skabkina, O.V., Rakotondrafara, A.M., Hentze, M.W., Hellen, C.U.T., and Pestova, T.V. (2010). The role of ABCE1 in eukaryotic posttermination ribosomal recycling. Mol. Cell *37*, 196–210.

Pisareva, V.P., Pisarev, A.V., Komar, A.A., Hellen, C.U.T., and Pestova, T.V. (2008). Translation Initiation on Mammalian mRNAs with Structured 5′UTRs Requires DExH-Box Protein DHX29. Cell *135*, 1237–1250.

Planelles, V., and Barker, E. (2010). Roles of Vpr and Vpx in modulating the virus-host cell relationship. Mol. Aspects Med. *31*, 398–406.

Planelles, V., and Benichou, S. (2009). Vpr and Its Interactions with Cellular Proteins. In HIV Interactions with Host Cell Proteins, P. Spearman, and E.O. Freed, eds. (Springer Berlin Heidelberg), pp. 177–200.

Poeck, H., Bscheider, M., Gross, O., Finger, K., Roth, S., Rebsamen, M., Hannesschläger, N., Schlee, M., Rothenfusser, S., Barchet, W., et al. (2010). Recognition of RNA virus by RIG-I results in activation of CARD9 and inflammasome signaling for interleukin 1 beta production. Nat. Immunol. *11*, 63–69.

Pontillo, A., Brandão, L.A., Guimarães, R.L., Segat, L., Athanasakis, E., and Crovella, S. (2010). A 3'UTR SNP in NLRP3 gene is associated with susceptibility to HIV-1 infection. J. Acquir. Immune Defic. Syndr. 1999 *54*, 236–240.

Pontillo, A., Oshiro, T.M., Girardelli, M., Kamada, A.J., Crovella, S., and Duarte, A.J.S. (2012). Polymorphisms in inflammasome' genes and susceptibility to HIV-1 infection. J. Acquir. Immune Defic. Syndr. 1999 *59*, 121–125.

Poovassery, J.S., and Bishop, G.A. (2012). Type I IFN receptor and the B cell antigen receptor regulate TLR7 responses via distinct molecular mechanisms. J. Immunol. Baltim. Md 1950 *189*, 1757–1764.

Prévôt, D., Décimo, D., Herbreteau, C.H., Roux, F., Garin, J., Darlix, J.-L., and Ohlmann, T. (2003). Characterization of a novel RNA-binding region of eIF4GI critical for ribosomal scanning. EMBO J. *22*, 1909–1921.

Purcell, D.F., and Martin, M.A. (1993). Alternative splicing of human immunodeficiency virus type 1 mRNA modulates viral protein expression, replication, and infectivity. J. Virol. *67*, 6365–6378.

Qiao, F., and Bowie, J.U. (2005). The many faces of SAM. Sci. STKE Signal Transduct. Knowl. Environ. *2005*, re7.

Radoshitzky, S.R., Dong, L., Chi, X., Clester, J.C., Retterer, C., Spurgers, K., Kuhn, J.H., Sandwick, S., Ruthel, G., Kota, K., et al. (2010). Infectious Lassa virus, but not filoviruses, is restricted by BST-2/tetherin. J. Virol. *84*, 10569–10580.

Reeves, J.D., Hibbitts, S., Simmons, G., McKnight, A., Azevedo-Pereira, J.M., Moniz-Pereira, J., and Clapham, P.R. (1999). Primary human immunodeficiency virus type 2 (HIV-2) isolates infect CD4-negative cells via CCR5 and CXCR4: comparison with HIV-1 and simian immunodeficiency virus and relevance to cell tropism in vivo. J. Virol. *73*, 7795–7804.

Refsland, E.W., Hultquist, J.F., and Harris, R.S. (2012). Endogenous origins of HIV-1 G-to-A hypermutation and restriction in the nonpermissive T cell line CEM2n. PLoS Pathog. *8*, e1002800.

Rice, G.I., Bond, J., Asipu, A., Brunette, R.L., Manfield, I.W., Carr, I.M., Fuller, J.C., Jackson, R.M., Lamb, T., Briggs, T.A., et al. (2009). Mutations involved in Aicardi-Goutières syndrome implicate SAMHD1 as regulator of the innate immune response. Nat. Genet. *41*, 829–832.

Richter, J.D., and Sonenberg, N. (2005). Regulation of cap-dependent translation by eIF4E inhibitory proteins. Nature *433*, 477–480.

Rivas-Aravena, A., Ramdohr, P., Vallejos, M., Valiente-Echeverría, F., Dormoy-Raclet, V., Rodríguez, F., Pino, K., Holzmann, C., Huidobro-Toro, J.P., Gallouzi, I.-E., et al. (2009). The Elav-like protein HuR exerts translational control of viral internal ribosome entry sites. Virology *392*, 178–185.

Rogers, G.W., Jr, Richter, N.J., Lima, W.F., and Merrick, W.C. (2001). Modulation of the helicase activity of eIF4A by eIF4B, eIF4H, and eIF4F. J. Biol. Chem. *276*, 30914–30922.

Rogozin, I.B., Basu, M.K., Jordan, I.K., Pavlov, Y.I., and Koonin, E.V. (2005). APOBEC4, a new member of the AID/APOBEC family of polynucleotide (deoxy)cytidine deaminases predicted by computational analysis. Cell Cycle Georget. Tex *4*, 1281–1285.

Ruhl, M., Himmelspach, M., Bahr, G.M., Hammerschmid, F., Jaksche, H., Wolff, B., Aschauer, H., Farrington, G.K., Probst, H., and Bevec, D. (1993). Eukaryotic initiation factor 5A is a cellular target of the human immunodeficiency virus type 1 Rev activation domain mediating trans-activation. J. Cell Biol. *123*, 1309–1320.

Sadler, A.J., and Williams, B.R.G. (2007). Structure and function of the protein kinase R. Curr. Top. Microbiol. Immunol. *316*, 253–292.

Sakuma, R., Mael, A.A., and Ikeda, Y. (2007). Alpha Interferon Enhances TRIM5?-Mediated Antiviral Activities in Human and Rhesus Monkey Cells. J. Virol. *81*, 10201–10206.

Sánchez-Velar, N., Udofia, E.B., Yu, Z., and Zapp, M.L. (2004). hRIP, a cellular cofactor for Rev function, promotes release of HIV RNAs from the perinuclear region. Genes Dev. *18*, 23–34.

Santana-de Anda, K., Gómez-Martín, D., Soto-Solís, R., and Alcocer-Varela, J. (2013). Plasmacytoid dendritic cells: Key players in viral infections and autoimmune diseases. Semin. Arthritis Rheum.

Sato, Y., Probst, H.C., Tatsumi, R., Ikeuchi, Y., Neuberger, M.S., and Rada, C. (2010). Deficiency in APOBEC2 leads to a shift in muscle fiber type, diminished body mass, and myopathy. J. Biol. Chem. *285*, 7111–7118.

Satoh, T., Kato, H., Kumagai, Y., Yoneyama, M., Sato, S., Matsushita, K., Tsujimura, T., Fujita, T., Akira, S., and Takeuchi, O. (2010). LGP2 is a positive regulator of RIG-I- and MDA5-mediated antiviral responses. Proc. Natl. Acad. Sci. U. S. A. *107*, 1512–1517.

Sayah, D.M., Sokolskaja, E., Berthoux, L., and Luban, J. (2004). Cyclophilin A retrotransposition into TRIM5 explains owl monkey resistance to HIV-1. Nature *430*, 569–573.

Schäfer, A., Bogerd, H.P., and Cullen, B.R. (2004). Specific packaging of APOBEC3G into HIV-1 virions is mediated by the nucleocapsid domain of the gag polyprotein precursor. Virology *328*, 163–168.

Schoggins, J.W., Wilson, S.J., Panis, M., Murphy, M.Y., Jones, C.T., Bieniasz, P., and Rice, C.M. (2011). A diverse range of gene products are effectors of the type I interferon antiviral response. Nature *472*, 481–485.

Schwarz, D.A., Katayama, C.D., and Hedrick, S.M. (1998). Schlafen, a new family of growth regulatory genes that affect thymocyte development. Immunity *9*, 657–668.

Selig, L., Pages, J.C., Tanchou, V., Prévéral, S., Berlioz-Torrent, C., Liu, L.X., Erdtmann, L., Darlix, J., Benarous, R., and Benichou, S. (1999). Interaction with the p6 domain of the gag precursor mediates incorporation into virions of Vpr and Vpx proteins from primate lentiviruses. J. Virol. *73*, 592–600.

Shandilya, S.M.D., Nalam, M.N.L., Nalivaika, E.A., Gross, P.J., Valesano, J.C., Shindo, K., Li, M., Munson, M., Royer, W.E., Harjes, E., et al. (2010). Crystal Structure of the APOBEC3G Catalytic Domain Reveals Potential Oligomerization Interfaces. Structure *18*, 28–38.

Shandilya, S.M.D., Bohn, M.-F., Albin, J.S., Somasundaran, M., Harris, R.S., and Schiffer, C.A. (2013). Crystal structure of the catalytic domain of APOBEC3F reveals novel interaction surface with implications for inhibitor design and HIV-1 Vif binding. Meet. Retroviruses - Cold Spring Harb. Lab. 2013.

Sharma, A., Yilmaz, A., Marsh, K., Cochrane, A., and Boris-Lawrie, K. (2012). Thriving under stress: selective translation of HIV-1 structural protein mRNA during Vpr-mediated impairment of eIF4E translation activity. PLoS Pathog. *8*, e1002612.

Sharp, P.M., and Hahn, B.H. (2011). Origins of HIV and the AIDS Pandemic. Cold Spring Harb. Perspect. Med. *1*.

Sharp, P.M., Rayner, J.C., and Hahn, B.H. (2013). Great Apes and Zoonoses. Science *340*, 284–286.

Sheehy, A.M., Gaddis, N.C., Choi, J.D., and Malim, M.H. (2002). Isolation of a human gene that inhibits HIV-1 infection and is suppressed by the viral Vif protein. Nature *418*, 646–650.

Shindo, K., Takaori-Kondo, A., Kobayashi, M., Abudu, A., Fukunaga, K., and Uchiyama, T. (2003). The enzymatic activity of CEM15/Apobec-3G is essential for the regulation of the infectivity of HIV-1 virion but not a sole determinant of its antiviral activity. J. Biol. Chem. *278*, 44412–44416.

Sigrist, C.J.A., Cerutti, L., Hulo, N., Gattiker, A., Falquet, L., Pagni, M., Bairoch, A., and Bucher, P. (2002). PROSITE: a documented database using patterns and profiles as motif descriptors. Brief. Bioinform. *3*, 265–274.

Silvin, A., and Manel, N. (2013). Interactions between HIV-1 and innate immunity in dendritic cells. Adv. Exp. Med. Biol. *762*, 183–200.

Simon, J.H.M., Gaddis, N.C., Fouchier, R.A.M., and Malim, M.H. (1998). Evidence for a newly discovered cellular anti-HIV-1 phenotype. Nat. Med. *4*, 1397–1400.

Skabkin, M.A., Skabkina, O.V., Dhote, V., Komar, A.A., Hellen, C.U.T., and Pestova, T.V. (2010). Activities of Ligatin and MCT-1/DENR in eukaryotic translation initiation and ribosomal recycling. Genes Dev. *24*, 1787–1801.

Skabkin, M.A., Skabkina, O.V., Hellen, C.U.T., and Pestova, T.V. (2013). Reinitiation and Other Unconventional Posttermination Events during Eukaryotic Translation. Mol. Cell *51*, 249–264.

Smigielski, E.M., Sirotkin, K., Ward, M., and Sherry, S.T. (2000). dbSNP: a database of single nucleotide polymorphisms. Nucleic Acids Res. *28*, 352–355.

Smith, H.C. (2011). APOBEC3G: a double agent in defense. Trends Biochem. Sci. *36*, 239–244.

Smith, H.C., Bennett, R.P., Kizilyer, A., McDougall, W.M., and Prohaska, K.M. (2012). Functions and regulation of the APOBEC family of proteins. Semin. Cell Dev. Biol. *23*, 258–268.

Sohn, W.-J., Kim, D., Lee, K.-W., Kim, M.-S., Kwon, S., Lee, Y., Kim, D.-S., and Kwon, H.-J. (2007). Novel transcriptional regulation of the schlafen-2 gene in macrophages in response to TLR-triggered stimulation. Mol. Immunol. *44*, 3273–3282.

Solis, M., Nakhaei, P., Jalalirad, M., Lacoste, J., Douville, R., Arguello, M., Zhao, T., Laughrea, M., Wainberg, M.A., and Hiscott, J. (2011). RIG-I-mediated antiviral signaling is inhibited in HIV-1 infection by a protease-mediated sequestration of RIG-I. J. Virol. *85*, 1224–1236.

Solomon, W.C., Harjes, S., Li, M., Chen, K.-M., Harjes, E., Harris, R.S., and Matsuo, H. (2013). Impact of histidine 216 on DNA binding and catalytic activity of APOBEC3G. Meet. Retroviruses - Cold Spring Harb. Lab. 2013.

Soto-Rifo, R., and Ohlmann, T. (2013). The role of the DEAD-box RNA helicase DDX3 in mRNA metabolism. Wiley Interdiscip. Rev. RNA *4*, 369–385.

Soto-Rifo, R., Rubilar, P.S., Limousin, T., de Breyne, S., Décimo, D., and Ohlmann, T. (2012). DEAD-box protein DDX3 associates with eIF4F to promote translation of selected mRNAs. EMBO J. *31*, 3745–3756.

Soto-Rifo, R., Rubilar, P.S., and Ohlmann, T. (2013). The DEAD-box helicase DDX3 substitutes for the cap-binding protein eIF4E to promote compartmentalized translation initiation of the HIV-1 genomic RNA. Nucleic Acids Res. *41*, 6286–6299.

Spriggs, K.A., Stoneley, M., Bushell, M., and Willis, A.E. (2008). Re-programming of translation following cell stress allows IRES-mediated translation to predominate. Biol. Cell Auspices Eur. Cell Biol. Organ. *100*, 27–38.

St Gelais, C., de Silva, S., Amie, S.M., Coleman, C.M., Hoy, H., Hollenbaugh, J.A., Kim, B., and Wu, L. (2012). SAMHD1 restricts HIV-1 infection in dendritic cells (DCs) by dNTP depletion, but its expression in DCs and primary CD4+ T-lymphocytes cannot be upregulated by interferons. Retrovirology *9*, 105.

Stopak, K., de Noronha, C., Yonemoto, W., and Greene, W.C. (2003). HIV-1 Vif blocks the antiviral activity of APOBEC3G by impairing both its translation and intracellular stability. Mol. Cell *12*, 591–601.

Strausberg, R.L., Feingold, E.A., Grouse, L.H., Derge, J.G., Klausner, R.D., Collins, F.S., Wagner, L., Shenmen, C.M., Schuler, G.D., Altschul, S.F., et al. (2002). Generation and initial analysis of more than 15,000 full-length human and mouse cDNA sequences. Proc. Natl. Acad. Sci. U. S. A. *99*, 16899–16903.

Strebel, K., Klimkait, T., and Martin, M.A. (1988). A novel gene of HIV-1, vpu, and its 16-kilodalton product. Science *241*, 1221–1223.

Sundquist, W.I., and Kräusslich, H.-G. (2012). HIV-1 assembly, budding, and maturation. Cold Spring Harb. Perspect. Med. *2*, a006924.

Suzuki, Y., and Craigie, R. (2007). The road to chromatin - nuclear entry of retroviruses. Nat. Rev. Microbiol. *5*, 187–196.

Suzuki, Y., Ishihara, D., Sasaki, M., Nakagawa, H., Hata, H., Tsunoda, T., Watanabe, M., Komatsu, T., Ota, T., Isogai, T., et al. (2000). Statistical analysis of the 5' untranslated region of human mRNA using "Oligo-Capped" cDNA libraries. Genomics *64*, 286–297.

Swanstrom, R., and Coffin, J. (2012). HIV-1 pathogenesis: the virus. Cold Spring Harb. Perspect. Med. *2*, a007443.

Szamecz, B., Rutkai, E., Cuchalová, L., Munzarová, V., Herrmannová, A., Nielsen, K.H., Burela, L., Hinnebusch, A.G., and Valásek, L. (2008). eIF3a cooperates with sequences 5' of uORF1 to promote resumption of scanning by post-termination ribosomes for reinitiation on GCN4 mRNA. Genes Dev. *22*, 2414–2425.

Takemura, R., Takeiwa, T., Taniguchi, I., McCloskey, A., and Ohno, M. (2011). Multiple factors in the early splicing complex are involved in the nuclear retention of pre-mRNAs in mammalian cells. Genes Cells Devoted Mol. Cell. Mech. *16*, 1035–1049.

Tarn, W.-Y., and Chang, T.-H. (2009). The current understanding of Ded1p/DDX3 homologs from yeast to human. RNA Biol. *6*, 17–20.

Tazi, J., Bakkour, N., Marchand, V., Ayadi, L., Aboufirassi, A., and Branlant, C. (2010). Alternative splicing: regulation of HIV-1 multiplication as a target for therapeutic action. FEBS J. *277*, 867–876.

Thielen, B.K., McNevin, J.P., McElrath, M.J., Hunt, B.V.S., Klein, K.C., and Lingappa, J.R. (2010). Innate Immune Signaling Induces High Levels of TC-specific Deaminase Activity in Primary Monocyte-derived Cells through Expression of APOBEC3A Isoforms. J. Biol. Chem. *285*, 27753–27766.

Thomas, D.C., Voronin, Y.A., Nikolenko, G.N., Chen, J., Hu, W.-S., and Pathak, V.K. (2007). Determination of the ex vivo rates of human immunodeficiency virus type 1 reverse transcription by using novel strand-specific amplification analysis. J. Virol. *81*, 4798–4807.

Thompson, S.R. (2012). Tricks an IRES uses to enslave ribosomes. Trends Microbiol. *20*, 558–566.

Travassos, L.H., Carneiro, L.A.M., Ramjeet, M., Hussey, S., Kim, Y.-G., Magalhães, J.G., Yuan, L., Soares, F., Chea, E., Le Bourhis, L., et al. (2010). Nod1 and Nod2 direct autophagy by recruiting ATG16L1 to the plasma membrane at the site of bacterial entry. Nat. Immunol. *11*, 55–62.

Tremblay, M.J. (2010). HIV-1 and pattern-recognition receptors: a marriage of convenience. Nat. Immunol. *11*, 363–365.

Turelli, P., Mangeat, B., Jost, S., Vianin, S., and Trono, D. (2004). Inhibition of hepatitis B virus replication by APOBEC3G. Science *303*, 1829.

Uchida, N., Hoshino, S.-I., Imataka, H., Sonenberg, N., and Katada, T. (2002). A novel role of the mammalian GSPT/eRF3 associating with poly(A)-binding protein in Cap/Poly(A)-dependent translation. J. Biol. Chem. *277*, 50286–50292.

Uchil, P.D., Quinlan, B.D., Chan, W.-T., Luna, J.M., and Mothes, W. (2008). TRIM E3 ligases interfere with early and late stages of the retroviral life cycle. PLoS Pathog. *4*, e16.

Uyttendaele, I., Lavens, D., Catteeuw, D., Lemmens, I., Bovijn, C., Tavernier, J., and Peelman, F. (2012). Random Mutagenesis MAPPIT Analysis Identifies Binding Sites for Vif and Gag in Both Cytidine Deaminase Domains of Apobec3G. PLoS ONE *7*, e44143.

Valiente-Echeverría, F., Vallejos, M., Monette, A., Pino, K., Letelier, A., Huidobro-Toro, J.P., Mouland, A.J., and López-Lastra, M. (2013). A cis-acting element present within the Gag open reading frame negatively impacts on the activity of the HIV-1 IRES. PloS One *8*, e56962.

Valle-Casuso, J.C., and Diaz-Griffero, F. (2013). Endogenously Expressed TRIM5α Proteins Block Retroviral Infection After Reverse Transcription. Meet. Retroviruses - Cold Spring Harb. Lab. 2013.

Vallejos, M., Deforges, J., Plank, T.-D.M., Letelier, A., Ramdohr, P., Abraham, C.G., Valiente-Echeverría, F., Kieft, J.S., Sargueil, B., and López-Lastra, M. (2011). Activity of the human immunodeficiency virus type 1 cell cycle-dependent internal ribosomal entry site is modulated by IRES trans-acting factors. Nucleic Acids Res. *39*, 6186–6200.

Vallejos, M., Carvajal, F., Pino, K., Navarrete, C., Ferres, M., Huidobro-Toro, J.P., Sargueil, B., and López-Lastra, M. (2012). Functional and Structural Analysis of the Internal Ribosome Entry Site Present in the mRNA of Natural Variants of the HIV-1. PLoS ONE *7*, e35031.

Varthakavi, V., Smith, R.M., Bour, S.P., Strebel, K., and Spearman, P. (2003). Viral protein U counteracts a human host cell restriction that inhibits HIV-1 particle production. Proc. Natl. Acad. Sci. U. S. A. *100*, 15154–15159.

Ventoso, I., Blanco, R., Perales, C., and Carrasco, L. (2001). HIV-1 protease cleaves eukaryotic initiation factor 4G and inhibits cap-dependent translation. Proc. Natl. Acad. Sci. *98*, 12966–12971.

Virgen, C.A., Kratovac, Z., Bieniasz, P.D., and Hatziioannou, T. (2008). Independent genesis of chimeric TRIM5-cyclophilin proteins in two primate species. Proc. Natl. Acad. Sci. U. S. A. *105*, 3563–3568.

Wagschal, A., Rousset, E., Basavarajaiah, P., Contreras, X., Harwig, A., Laurent-Chabalier, S., Nakamura, M., Chen, X., Zhang, K., Meziane, O., et al. (2012). Microprocessor, Setx, Xrn2, and Rrp6 co-operate to induce premature termination of transcription by RNAPII. Cell *150*, 1147–1157.

Walsh, M.F., Hermann, R., Sun, K., and Basson, M.D. (2012). Schlafen 3 changes during rat intestinal maturation. Am. J. Surg. *204*, 598–601.

Wang, X.-Q., and Rothnagel, J.A. (2004). 5′-Untranslated regions with multiple upstream AUG codons can support low-level translation via leaky scanning and reinitiation. Nucleic Acids Res. *32*, 1382–1391.

Wang, T., Tian, C., Zhang, W., Luo, K., Sarkis, P.T.N., Yu, L., Liu, B., Yu, Y., and Yu, X.-F. (2007). 7SL RNA mediates virion packaging of the antiviral cytidine deaminase APOBEC3G. J. Virol. *81*, 13112–13124.

Wang, X., Han, Y., Dang, Y., Fu, W., Zhou, T., Ptak, R.G., and Zheng, Y.-H. (2010). Moloney leukemia virus 10 (MOV10) protein inhibits retrovirus replication. J. Biol. Chem. *285*, 14346–14355.

Wang, X., Ao, Z., Chen, L., Kobinger, G., Peng, J., and Yao, X. (2012a). The Cellular Antiviral Protein APOBEC3G Interacts with HIV-1 Reverse Transcriptase and Inhibits Its Function during Viral Replication. J. Virol. *86*, 3777–3786.

Wang, Y., Whittall, T., Rahman, D., Bunnik, E.M., Vaughan, R., Schøller, J., Bergmeier, L.A., Montefiori, D., Singh, M., Schuitemaker, H., et al. (2012b). The role of innate APOBEC3G and adaptive AID immune responses in HLA-HIV/SIV immunized SHIV infected macaques. PloS One *7*, e34433.

Warren, K., Wei, T., Li, D., Qin, F., Warrilow, D., Lin, M.-H., Sivakumaran, H., Apolloni, A., Abbott, C.M., Jones, A., et al. (2012). Eukaryotic elongation factor 1 complex subunits are critical HIV-1 reverse transcription cofactors. Proc. Natl. Acad. Sci. U. S. A. *109*, 9587–9592.

Warrilow, D., Tachedjian, G., and Harrich, D. (2009). Maturation of the HIV reverse transcription complex: putting the jigsaw together. Rev. Med. Virol. *19*, 324–337.

Watanabe, R., Murai, M.J., Singh, C.R., Fox, S., Ii, M., and Asano, K. (2010). The eukaryotic initiation factor (eIF) 4G HEAT domain promotes translation re-initiation in

yeast both dependent on and independent of eIF4A mRNA helicase. J. Biol. Chem. *285*, 21922–21933.

Wei, J., Wu, C., and Sachs, M.S. (2012). The arginine attenuator peptide interferes with the ribosome peptidyl transferase center. Mol. Cell. Biol. *32*, 2396–2406.

Weidner, J.M., Jiang, D., Pan, X.-B., Chang, J., Block, T.M., and Guo, J.-T. (2010). Interferon-induced cell membrane proteins, IFITM3 and tetherin, inhibit vesicular stomatitis virus infection via distinct mechanisms. J. Virol. *84*, 12646–12657.

Weill, L., James, L., Ulryck, N., Chamond, N., Herbreteau, C.H., Ohlmann, T., and Sargueil, B. (2010). A new type of IRES within gag coding region recruits three initiation complexes on HIV-2 genomic RNA. Nucleic Acids Res. *38*, 1367–1381.

Van Weringh, A., Ragonnet-Cronin, M., Pranckeviciene, E., Pavon-Eternod, M., Kleiman, L., and Xia, X. (2011). HIV-1 modulates the tRNA pool to improve translation efficiency. Mol. Biol. Evol. *28*, 1827–1834.

Wiegand, H.L., Doehle, B.P., Bogerd, H.P., and Cullen, B.R. (2004). A second human antiretroviral factor, APOBEC3F, is suppressed by the HIV-1 and HIV-2 Vif proteins. EMBO J. *23*, 2451–2458.

Wissing, S., Galloway, N.L.K., and Greene, W.C. (2010). HIV-1 Vif versus the APOBEC3 cytidine deaminases: an intracellular duel between pathogen and host restriction factors. Mol. Aspects Med. *31*, 383–397.

Xu, H., Svarovskaia, E.S., Barr, R., Zhang, Y., Khan, M.A., Strebel, K., and Pathak, V.K. (2004). A single amino acid substitution in human APOBEC3G antiretroviral enzyme confers resistance to HIV-1 virion infectivity factor-induced depletion. Proc. Natl. Acad. Sci. U. S. A. *101*, 5652–5657.

Xu, H., Chertova, E., Chen, J., Ott, D.E., Roser, J.D., Hu, W.-S., and Pathak, V.K. (2007). Stoichiometry of the antiviral protein APOBEC3G in HIV-1 virions. Virology *360*, 247–256.

Xue, S., and Barna, M. (2012). Specialized ribosomes: a new frontier in gene regulation and organismal biology. Nat. Rev. Mol. Cell Biol. *13*, 355–369.

Yamashita, R., Suzuki, Y., Takeuchi, N., Wakaguri, H., Ueda, T., Sugano, S., and Nakai, K. (2008). Comprehensive detection of human terminal oligo-pyrimidine (TOP) genes and analysis of their characteristics. Nucleic Acids Res. *36*, 3707–3715.

Yan, J., Kaur, S., DeLucia, M., Hao, C., Mehrens, J., Wang, C., Golczak, M., Palczewski, K., Gronenborn, A.M., Ahn, J., et al. (2013). Tetramerization of SAMHD1 is required for biological activity and inhibition of HIV infection. J. Biol. Chem. *288*, 10406–10417.

Yang, Y., Guo, F., Cen, S., and Kleiman, L. (2007). Inhibition of initiation of reverse transcription in HIV-1 by human APOBEC3F. Virology *365*, 92–100.

Yap, M.W., Nisole, S., Lynch, C., and Stoye, J.P. (2004). Trim5alpha protein restricts both HIV-1 and murine leukemia virus. Proc. Natl. Acad. Sci. U. S. A. *101*, 10786–10791.

Yasuda-Inoue, M., Kuroki, M., and Ariumi, Y. (2013). Distinct DDX DEAD-box RNA helicases cooperate to modulate the HIV-1 Rev function. Biochem. Biophys. Res. Commun. *434*, 803–808.

Yedavalli, V.S.R.K., Neuveut, C., Chi, Y.-H., Kleiman, L., and Jeang, K.-T. (2004). Requirement of DDX3 DEAD box RNA helicase for HIV-1 Rev-RRE export function. Cell *119*, 381–392.

Yu, M., and Levine, S.J. (2011). Toll-like Receptor 3, RIG-I-like Receptors and the NLRP3 Inflammasome: Key Modulators of Innate Immune Responses to Double-stranded RNA Viruses. Cytokine Growth Factor Rev. *22*, 63–72.

Yu, Q., König, R., Pillai, S., Chiles, K., Kearney, M., Palmer, S., Richman, D., Coffin, J.M., and Landau, N.R. (2004). Single-strand specificity of APOBEC3G accounts for minus-strand deamination of the HIV genome. Nat. Struct. Mol. Biol. *11*, 435–442.

Yu, X.F., Yu, Q.C., Essex, M., and Lee, T.H. (1991). The vpx gene of simian immunodeficiency virus facilitates efficient viral replication in fresh lymphocytes and macrophage. J. Virol. *65*, 5088–5091.

Yu, Y., Marintchev, A., Kolupaeva, V.G., Unbehaun, A., Veryasova, T., Lai, S.-C., Hong, P., Wagner, G., Hellen, C.U.T., and Pestova, T.V. (2009). Position of eukaryotic translation initiation factor eIF1A on the 40S ribosomal subunit mapped by directed hydroxyl radical probing. Nucleic Acids Res. *37*, 5167–5182.

Zennou, V., Perez-Caballero, D., Göttlinger, H., and Bieniasz, P.D. (2004). APOBEC3G incorporation into human immunodeficiency virus type 1 particles. J. Virol. *78*, 12058–12061.

Zhang, H., Yang, B., Pomerantz, R.J., Zhang, C., Arunachalam, S.C., and Gao, L. (2003). The cytidine deaminase CEM15 induces hypermutation in newly synthesized HIV-1 DNA. Nature *424*, 94–98.

Zheng, Y.-H., Irwin, D., Kurosu, T., Tokunaga, K., Sata, T., and Peterlin, B.M. (2004). Human APOBEC3F is another host factor that blocks human immunodeficiency virus type 1 replication. J. Virol. *78*, 6073–6076.

Zheng, Y.-H., Jeang, K.-T., and Tokunaga, K. (2012). Host restriction factors in retroviral infection: promises in virus-host interaction. Retrovirology *9*, 112.

Zhou, W., and Song, W. (2006). Leaky Scanning and Reinitiation Regulate BACE1 Gene Expression. Mol. Cell. Biol. *26*, 3353–3364.

Zhu, P., Liu, J., Bess, J., Jr, Chertova, E., Lifson, J.D., Grisé, H., Ofek, G.A., Taylor, K.A., and Roux, K.H. (2006). Distribution and three-dimensional structure of AIDS virus envelope spikes. Nature *441*, 847–852.

Zoppoli, G., Regairaz, M., Leo, E., Reinhold, W.C., Varma, S., Ballestrero, A., Doroshow, J.H., and Pommier, Y. (2012). Putative DNA/RNA helicase Schlafen-11 (SLFN11) sensitizes cancer cells to DNA-damaging agents. Proc. Natl. Acad. Sci. U. S. A. *109*, 15030–15035.

Zuo, T., Liu, D., Lv, W., Wang, X., Wang, J., Lv, M., Huang, W., Wu, J., Zhang, H., Jin, H., et al. (2012). Small-molecule inhibition of human immunodeficiency virus type 1 replication by targeting the interaction between Vif and ElonginC. J. Virol. *86*, 5497–5507.

Zur, H., and Tuller, T. (2013). New Universal Rules of Eukaryotic Translation Initiation Fidelity. PLoS Comput Biol *9*, e1003136.

Rôle de la protéine Vif dans la réplication du VIH-1 : régulation traductionnelle du facteur de restriction APOBEC3G et activité chaperonnes d'ARN

Vif (Viral Infectivity Factor) est une protéine auxiliaire qui augmente le «fitness» viral dans l'hôte infecté. Vif est essentielle à la formation de particules virales infectieuses dans les cellules dites «non-permissives», alors que des virus ΔVif se répliquent efficacement dans des lignées cellulaires T dites « permissives ». Les cellules non-permissives expriment les facteurs de restriction APOBEC3G (APOlipoprotein B mRNA-Editing enzyme Catalytic polypeptide 3G ou A3G) et A3F, deux cytidine désaminases dont l'action hypermutatrice est létale pour le virus. Vif réduit de façon considérable le taux d'expression des protéines A3G/3F par deux mécanismes principaux : (1) en recrutant une E3 ubiquitine ligase, Vif induit la dégradation d'A3G par le protéasome et (2) en se fixant sur l'ARNm, Vif régulant négativement la traduction d'A3G par un mécanisme dépendent de la région 5'-UTR. L'objectif de mon projet a été de déterminer le rôle et le mécanisme de la régulation traductionnelle du facteur de restriction A3G par la protéine Vif du VIH-1 *ex vivo*. En parallèle, nous nous sommes intéressés à déterminer les domaines de la protéine Vif impliqués dans l'activité chaperonne d'ARN. Par l'analyse des « westerns blots » issus de co-transfections de différents vecteurs d'expression d'A3G en présence ou absence de Vif et d'un dominant négative de la Cullin 5, nous avons démontré *ex vivo* que Vif requiert les tiges boucles 2 et 3 de la région 5'UTR (de façon simultanée) pour inhiber la traduction d'A3G. La régulation traductionnelle d'A3G par Vif cause 50% de la réduction total d'A3G en présence de Vif. Ensuite, nous avons observé qu'une une petite uORF (Upstream Open Reading Frame), contenue entre ces deux tiges-boucles est nécessaire pour l'inhibition d'A3G par Vif. Les uORFs, présents dans 50 % des gènes eucaryotes, interviennent principalement dans des mécanismes de régulation traductionnelle. Ainsi, nous avons observé *in vitro* et *ex vivo* que l'uORF régule négativement la traduction de l'ORF majeure d'A3G. Par l'analyse de l'expression de différents mutants de l'uORF, nous avons démontré *ex vivo* que 60% des complexes d'initiation de la traduction synthétisent A3G par « leaky scanning » et 40 % sont recrutés dans la traduction de l'uORF, en inhibant ainsi l'expression d'A3G. A partir de ces résultats nous proposons un modèle de l'inhibition d'A3G par Vif. Dans ce modèle, Vif pourrais inhiber l'étape de terminaison de la traduction de l'uORF en causant un « stalling » des ribosomes en empêchant ainsi à des nouveaux complexes d'initiation d'attendre l'ORF majeur. Nous avons aussi déterminé l'impact de la régulation traductionnelle d'A3G par Vif sur l'incorporation d'A3G dans les particules virales et sur l'infectivité virale. Nous avons alors observé que l'inhibition traductionnel d'A3G par Vif réduit l'incorporation d'A3G dans les particules virales avec un profil de diminution d'A3G similaire à celui observé dans les cellules. En utilisant des cellules indicatrices TZM-bl, nous avons ensuite observé que l'inhibition traductionnelle d'A3G par Vif augmente l'infectivité virale de 50%. Finalement, nous avons déterminé les domaines de la protéine Vif impliqués dans l'activité chaperonnes d'ARN. En utilisant des essaies de dimerisation des fragments d'ARN du VIH-1, nous avons pu mettre en évidence que le domaine C-terminal de la protéine Vif était impliqué dans cette activité. Ces résultats nous ont permis de mieux comprendre ce phénomène de restriction cellulaire et pourraient être importants dans le développement de nouvelles stratégies d'inhibition de la réplication virale qui ciblerait spécifiquement l'interaction de Vif avec l'ARNm d'A3G.